

Knowledge Base for the Effect of Debris on Pressurized Water Reactor Emergency Core Cooling Sump Performance

Los Alamos National Laboratory

**U.S. Nuclear Regulatory Commission
Office of Nuclear Regulatory Research
Washington, DC 20555-0001**



NUREG/CR-6808
LA-UR-03-0880

Knowledge Base for the Effect of Debris on Pressurized Water Reactor Emergency Core Cooling Sump Performance

Manuscript Completed: February 2003
Date Published: February 2003

Prepared by
D.V. Rao, Principal Investigator

C.J. Shaffer,* D.V. Rao,
M.T. Leonard,** K.W. Ross***

Los Alamos National Laboratory
Los Alamos, NM 87545

Subcontractors:

*ARES Corporation
851 University Blvd. S.E., Suite 100
Albuquerque, NM 87106

**dycoda, LLC
70 Andres Sanchez Blvd.
Belen, NM 87002

***Innovative Technology Solutions Corporation
6000 Uptown Blvd. N.E., Suite 300
Albuquerque, NM 87110

B.P. Jain, NRC Project Manager

Prepared for
Division of Engineering Technology
Office of Nuclear Regulatory Research
U.S. Nuclear Regulatory Commission
Washington, DC 20555-0001
NRC Job Code Y6041



ABSTRACT

This report describes the substantial base of knowledge that has been amassed as a result of the research on boiling-water reactor (BWR) suction-strainer and pressurized-water reactor (PWR) sump-screen clogging issues. These issues deal with the potential insulation and other debris generated in the event of a postulated loss-of-coolant accident within the containment of a light-water reactor and subsequently transport to and accumulation on the recirculation sump screens. This debris accumulation could potentially challenge the plant's capability to provide adequate long-term cooling water to the emergency core cooling system (ECCS) and the containment spray system pumps.

This report describes analytical and experimental approaches that have been used to assess the different aspects of sump and strainer blockage and to identify the strengths, limitations, important parameters and plant features, and appropriateness of the different approaches. The report is organized in the same order that an evaluation of the potential of sump screen blockage would be performed. The report provides background information on the issues, including significant United States regulatory developments regarding the resolution of the issue. The report is designed to serve as a reference for plant-specific analyses with regard to whether a sump or strainer would perform its function without preventing the operation of the ECCS pumps.

CONTENTS

	<i>Page</i>
Abstract.....	iii
Executive Summary.....	xiii
Acknowledgements	xv
Abbreviations	xvii
Units Conversion Table	xix
1.0 Introduction	1-1
1.1 Historical Overview	1-1
1.2 Description of Safety Concern	1-8
1.3 Criteria for Evaluating Sump Failure	1-9
1.3.1 Fully Submerged Sump Screens	1-10
1.3.2 Partially Submerged Sump Screens.....	1-10
1.4 Description of Postulated Pressurized-Water Reactor Accidents.....	1-11
1.4.1 Overview	1-11
1.4.2 Large Loss-of-Coolant Accident	1-15
1.4.2.1 Reactor Coolant System Blowdown Phase.....	1-15
1.4.2.2 Emergency Core Cooling System Injection Phase.....	1-20
1.4.2.3 Recirculation Phase.....	1-21
1.4.3 Medium Loss-of-Coolant Accident.....	1-21
1.4.3.1 Reactor Coolant System Blowdown Phase.....	1-21
1.4.3.2 Emergency Core Cooling System Injection Phase.....	1-21
1.4.3.3 Recirculation Phase.....	1-21
1.4.4 Small Loss-of Coolant Accident.....	1-25
1.4.4.1 Reactor Coolant System Blowdown Phase.....	1-25
1.4.4.2 Emergency Core Cooling System Injection Phase.....	1-25
1.4.4.3 Recirculation Phase.....	1-25
1.4.5 Other Plant Design Features that Influence Accident Progression	1-25
1.5 Description of Relevant Plant Features that Influence Accident Progression	1-30
1.6 Regulatory Considerations.....	1-31
1.6.1 Code of Federal Regulations	1-32
1.6.2 Regulatory Guidance	1-34
1.7 Report Outline.....	1-35
1.8 References.....	1-35
2.0 Debris Sources	2-1
2.1 Actual Debris Found During Inspections	2-1
2.2 Loss-of-Coolant-Accident-Generated Debris.....	2-2
2.3 Loss-of-Coolant-Accident Exposure-Generated Debris	2-3
2.4 Operational Debris	2-4
2.5 Aging Effects on Mineral Fiber Thermal Insulation.....	2-5
2.6 Relative Timing and Debris Bed Composition	2-5
2.7 References.....	2-6
3.0 Debris Generation.....	3-1
3.1 Overview of the Mechanics of Debris Generation	3-1
3.1.1 Break-Jet Phenomena	3-4
3.1.1.1 Size/Configuration of Pipe Rupture	3-4
3.1.1.2 Break Effluent	3-4

3.1.1.3	Obstacles.....	3-5
3.1.2	Debris Classification	3-5
3.1.2.1	Size Classification of Fibrous Debris	3-6
3.1.2.2	Size Classification of RMI Debris	3-6
3.2	Debris-Generation Testing.....	3-6
3.2.1	Air-Jet Testing.....	3-9
3.2.1.1	NRC BWR Drywell Inertial Capture Tests	3-9
3.2.1.2	BWROG Air-Jet Impact Testing (AJIT).....	3-10
3.2.2	Steam and Two-Phase Jet Testing.....	3-12
3.2.2.1	Marviken Full-Scale Containment Experiments	3-12
3.2.2.2	HDR Tests	3-12
3.2.2.3	Karlshamn Caposil and Newtherm Tests	3-13
3.2.2.4	Siemens Metallic Insulation Jet Tests (MIJITs).....	3-14
3.2.2.5	Ontario Power Generation Test.....	3-15
3.2.2.6	Battelle/KAEFER Tests	3-19
3.3	Debris-Generation Models and Analytical Approaches	3-22
3.3.1	Cone Models.....	3-23
3.3.1.1	ANSI/ANS Standard	3-23
3.3.1.2	Three-Region Conical Jet.....	3-25
3.3.2	Spherical Models	3-26
3.3.2.1	Three-Region Spherical Model.....	3-26
3.3.2.2	Equivalent-Volume Sphere Model.....	3-27
3.3.3	Debris-Size Distribution as a Function of Local Jet Pressure.....	3-28
3.4	References.....	3-29
4.0	Airborne/Washdown Debris Transport in Containment.....	4-1
4.1	Overview on Mechanics.....	4-2
4.1.1	Accident Characterization Relevant to Debris Transport.....	4-2
4.1.2	Plant Features Affecting Debris Transport.....	4-3
4.1.3	Physical Processes and Phenomena Affecting Debris Transport	4-4
4.1.4	Debris Characteristics Affecting Transport	4-8
4.2	Airborne/Washdown Debris-Transport Testing.....	4-8
4.2.1	Airborne Phase Debris-Transport Testing	4-8
4.2.1.1	Separate-Effects Debris-Transport Tests	4-8
4.2.1.2	Integrated-Effects Debris-Transport Tests	4-13
4.2.1.3	Blowdown Experiments at Heissdampfreaktor (HDR) Facility	4-17
4.2.1.4	Karlshamn Steam Blast Tests	4-18
4.2.2	Airborne/Washdown Combined Phase Debris-Transport Testing.....	4-20
4.2.2.1	BWROG Testing of Debris Transport Through Downcomers/Vents	4-20
4.2.3	Washdown-Phase Debris-Transport Testing.....	4-23
4.2.3.1	Separate-Effects Insulation Debris Washdown Tests	4-23
4.2.3.2	Oskarshamn Nuclear Power Plant Containment Washdown Tests	4-25
4.3	Airborne/Washdown Debris-Transport Analyses.....	4-25
4.3.1	Evaluations of Operational Incidents	4-27
4.3.1.1	Evaluation of Incident at Gundremmingen-1	4-27
4.3.1.2	Evaluation of Incident at Barsebäck-2	4-27
4.3.2	Phenomena Identification and Ranking Tables	4-31
4.3.2.1	BWR PIRT	4-31
4.3.2.2	PWR PIRT	4-31
4.3.3	Airborne/Washdown Debris-Transport Evaluations.....	4-33
4.3.3.1	MELCOR Simulation of Karlshamn Tests	4-33
4.3.3.2	BWR Drywell Debris Transport Study (DDTS)	4-34
4.3.3.3	PWR Volunteer Plant Analysis	4-41
4.3.4	Generalized Debris-Transport Guidance	4-44
4.3.4.1	BWR URG Guidance for Drywell Debris Transport and the NRC Review	4-44

4.3.4.2	Transport Fractions for Parametric Evaluation	4-48
4.4	Types of Analytical Approaches	4-49
4.5	Rules of Thumb.....	4-50
4.6	References.....	4-50
5.0	Sump Pool Debris Transport	5-1
5.1	Overview of Mechanics.....	5-1
5.1.1	Accident Characterization	5-2
5.1.2	Plant Features.....	5-3
5.1.3	Physical Processes/Phenomena	5-4
5.1.4	Debris Characteristics.....	5-7
5.2	Debris Transport in Pooled Water Testing.....	5-7
5.2.1	Alden Research Laboratory Buoyancy and Transport Testing on Fibrous Insulation Debris	5-7
5.2.2	Pennsylvania Power and Light Debris Transport Tests.....	5-10
5.2.3	Alden Research Laboratory Suppression Pool Debris Sedimentation Testing	5-11
5.2.3.1	Fibrous Debris Sedimentation Testing	5-12
5.2.3.2	Reflective Metal Insulation Debris Sedimentation Testing	5-15
5.2.4	Alden Research Laboratory Reflective Metallic Insulation Materials Transport Testing	5-15
5.2.5	University of New Mexico Separate Effects Debris Transport Testing	5-17
5.2.6	University of New Mexico Integrated Debris Transport Testing	5-24
5.2.7	Bremen Polytechnic Testing of KAEFER Insulation Systems	5-29
5.2.8	Alden Research Laboratory Testing of Owens-Corning Fiberglass (NUKON) Insulation.....	5-32
5.2.9	STUK Metallic Insulation Transport and Clogging Tests	5-33
5.3	Debris Transport in Pooled Water Analysis	5-34
5.3.1	Phenomena Identification and Ranking Tables	5-34
5.3.1.1	Boiling-Water Reactor Phenomena Identification and Ranking Table	5-34
5.3.1.2	Pressurized-Water Reactor Phenomena Ranking and Identification Table.....	5-34
5.3.2	Boiling-Water Reactor Drywell Floor Pool Debris Transport Study	5-36
5.3.3	Boiling-Water Reactor Suppression-Pool Debris-Transport Analysis	5-37
5.3.4	Pressurized-Water Reactor Volunteer Plant Pool Debris Transport Analysis	5-38
5.3.5	Nuclear Regulatory Commission Review of Licensee Experimental Approach to Sump Blockage Potential.....	5-38
5.3.6	Computational Fluid Dynamic Simulations of UNM Integrated Debris-Transport Testing	5-41
5.4	Summary of Approaches to Modeling Containment Pool Transport	5-41
5.5	Guidance.....	5-43
5.6	References.....	5-44
6.0	Debris Accumulation.....	6-1
6.1	Locations of Concern	6-1
6.1.1	Sump Screens	6-1
6.1.2	Containment Flow Restrictions	6-3
6.2	Accumulation Patterns	6-3
6.3	Parameters Affecting Debris Accumulation	6-8
6.3.1	Local Flow Field	6-8
6.3.2	Local Geometry.....	6-9
6.3.3	Submergence.....	6-9
6.3.4	Debris Characteristics.....	6-10
6.4	Test Data.....	6-10
6.4.1	BWR Strainer Tests	6-10
6.4.2	Test Results for Vertical PWR Sump Screen Configurations	6-11
6.5	References.....	6-14

7.0	Debris Head Loss	7-1
7.1	Factors Affecting Debris-Bed Build-Up and Head Loss	7-1
7.1.1	Fibrous Debris Beds	7-1
7.1.2	Mixed Particulate and Fiber Beds	7-4
7.1.3	Reflective Metallic Insulation	7-6
7.1.4	Mixed Fiber and RMI Debris Beds	7-8
7.2	Review of Experimental Programs	7-9
7.2.1	Flat-Plate Strainers	7-11
7.2.2	Flat-Plate Strainers in Flumes	7-18
7.2.3	Prototype Module Strainer Testing	7-20
7.2.4	Semi-Scale Installed Strainer Testing	7-28
7.3	Analysis of Test Data	7-29
7.3.1	United States Nuclear Regulatory Commission Characterization of Head Loss Data	7-29
7.3.1.1	Fiberglass and Particulate Debris	7-29
7.3.1.2	Reflective Metallic Insulation	7-29
7.3.2	Analysis of Non-Flat-Plate Strainer Data	7-35
7.3.2.1	Phenomena of Debris Build-Up on Stacked-Disk Strainers	7-37
7.3.2.2	Application of the NUREG/CR-6224 Correlation to the PCI Strainer	7-37
7.4	Ongoing Research on Outstanding Issues	7-41
7.4.1	Long-Term Fibrous Debris Bed Stability	7-41
7.4.2	Calcium Silicate Debris Head Loss	7-42
7.4.3	Vertically Oriented Screens	7-42
7.5	References	7-42
8.0	Resolution Options	8-1
8.1	Overview of Resolution Options	8-1
8.2	Replacement Strainer Designs	8-2
8.2.1	Passive Strainer Designs Installed in U.S. Nuclear Power Plants	8-2
8.2.1.1	PCI Stacked-Disk Strainers	8-4
8.2.1.2	General Electric Stacked-Disk Strainers	8-6
8.2.1.3	ABB Combustion Engineering Strainers	8-6
8.2.1.4	Mark III Strainers	8-7
8.2.2	Active Strainer Designs	8-8
8.2.2.1	BWROG Research Into Active Strainer Concepts	8-8
8.3	Overview of U.S. BWR Plant Implementation	8-9
8.3.1	NRC Review of U.S. Plant Implementation	8-9
8.3.2	Onsite Plant Audits	8-10
8.4	Special Considerations for PWR Resolution Options	8-12
8.4.1	Flow Path Blocking	8-12
8.4.2	Strainer Penetration	8-12
8.4.2.1	Spray Nozzles	8-13
8.4.2.2	Fuel Bundles	8-13
8.4.3	LOCA Jet and Missile Considerations	8-15
8.4.4	Feasibility and Efficiency of Backflushing	8-15
8.4.5	Debris Induced Mechanical Structural Loadings	8-15
8.5	References	8-16
9.0	Significant Events	9-1
9.1	LOCA Debris Generation Events	9-1
9.2	Events Rendering a System Inoperable	9-2
9.3	Debris-Found-in-Containment Events	9-5
9.4	Inadequate Maintenance Leading to Potential Sources of Debris	9-8
9.5	Sump-Screen Inadequacies	9-10
9.6	References	9-12

10.0	Summary and Conclusions.....	10-1
10.1	Summary of Knowledge Base	10-1
10.2	Conclusions	10-13

Figures

1-1	Illustration of Sump Features and Parameters.....	1-9
1-2	Sump-Screen Schematics.....	1-10
1-3	Flow Chart of Analysis Process.....	1-12
1-4	PWR LLOCA Accident Progression in a Large Dry Containment.....	1-19
1-5	PWR MLOCA Accident Progression in a Large Dry Containment.....	1-24
1-6	PWR SLOCA Accident Progression in a Large Dry Containment	1-29
3-1	Example ZOI at a Postulated Break Location	3-2
3-2	Variation in the ZOI Shape with DEGB Separation and Offset.....	3-5
3-3	Fiberglass Insulation Debris of Two Example Size Classes	3-7
3-4	Inner Construction and Installation of a Typical RMI Cassette	3-8
3-5	RMI Foil Before/After "Crumpling" (Left) and Crumpled RMI Foil Debris (Right).....	3-8
3-6	Configuration of the CEESI Test Facility for the NRC/SEA BWR Drywell Debris-Transport Tests	3-10
3-7	Typical RMI Debris Generated by Large Pipe Break	3-15
3-8	RMI Debris Observed in Siemens Steam-Jet Impact Tests.....	3-15
3-9	Insulation Target Mounting Configuration in OPG Test (Longitudinal Seam at 45°, Circumferential Seam Offset).....	3-17
3-10	Typical Calcium-Silicate Debris Collected from an OPG Two-Phase Jet Test.....	3-18
3-11	Test Configuration of Aluminum-Clad Calcium-Silicate Insulation (Distance from Break of 9D and Longitudinal Seam at 45°).....	3-19
3-12	Post-Test Configuration of Aluminum-Clad Fiberglass Insulation (Distance from Break of 10D and Longitudinal Seam at 45°)	3-20
3-13	Configuration of the Target Field in the Battelle/KAEFER Tests	3-20
3-14	Typical View of Target Destruction in Battelle/KAEFER Tests	3-22
3-15	ANSI/ANS Standard Free-Expanding Jet Model.....	3-24
3-16	Isobar of Damage Pressure P_x within a Fixed, Free-Expanding Jet	3-24
3-17	Illustration of the Three-Region, Two-Phase Conical-Jet ZOI Model.....	3-26
3-18	Illustration of the Three-Region, Two-Phase Spherical ZOI Model.....	3-27
3-19	Debris Size as a Function of Local Jet Pressure	3-30
4-1	Separate-Effects Insulation Debris-Transport/Capture Test Apparatus.....	4-12
4-2	Typical Fibrous Debris Capture by a Wetted Pipe	4-13
4-3	CEESI Air-Jet Test Facility	4-14
4-4	Samples of Debris Generated in the CEESI Tests	4-16
4-5	Typical Debris Deposition on a Grating in CEESI Tests	4-16
4-6	Capture of Small Debris by Grating.....	4-17
4-7	ABB-Atom Containment Experimental Arrangement	4-19
4-8	Schematic of 1/8-Scale Mark I Configuration Test Apparatus	4-21
4-9	Schematic of 1/8-Scale Mark II Configuration Test Apparatus	4-22
4-10	Schematic of Washdown Test Apparatus	4-24
4-11	Time-Dependency of 1-in. Insulation Blanket Material Under Break-Flow Conditions	4-26
4-12	Typical Condition of Debris After Exposure to Water.....	4-26
4-13	Schematic Illustrating the Complexity of Drywell Debris Transport	4-36
4-14	Sample Drywell Debris Transport Logic Chart.....	4-37
5-1	Suppression Pool Sedimentation Test Apparatus.....	5-13
5-2	Fibrous Debris Classifications	5-14
5-3	Fibrous Debris Terminal Settling Velocities.....	5-14
5-4	Typical Large (6-in.) RMI Debris in Suspension During Chugging	5-16
5-5	Photo of Large UNM Flume Test Apparatus	5-19
5-6	Diagram of Large UNM Flume Test Apparatus.....	5-19

5-7	Photo of Large UNM Flume Inlet Flow Conditioning Apparatus	5-20
5-8	Typical Test Sample of LDFG Insulation Debris	5-20
5-9	Typical Test Sample of Aluminum RMI Insulation Debris	5-21
5-10	Typical Test Sample of Paint-Chip Debris	5-21
5-11	Comparison of Terminal Settling Velocities	5-22
5-12	Comparison of Incipient and Bulk Tumbling Velocities	5-23
5-13	Comparison of Incipient Lift Velocities to Incipient Tumbling Velocities	5-23
5-14	Steel Tank Used in Integrated Testing	5-26
5-15	Integrated Test Tank Outlet Box	5-26
5-16	Test Configuration A.....	5-27
5-17	Test Configuration B.....	5-27
5-18	Test Configuration C.....	5-27
5-19	Test Configuration D.....	5-27
5-20	Samples of KAEFER Insulation Systems Tested.....	5-31
5-21	Bremen Buoyancy Test Illustration.....	5-32
5-22	Typical Fibrous Debris Transport in the Suppression Pool.....	5-39
5-23	Configuration of Millstone-2 Debris-Transport Experiment.....	5-39
5-24	Sample CFD Prediction of Flow Velocities for One Test Configuration	5-42
6-1	Examples of Various Recirculation Sump Configurations in PWRs.....	6-2
6-2	Example of Containment Floor Flow Restriction that Might Result in Diversion of Flow From the Recirculation Sump.....	6-3
6-3	Debris Accumulation Profiles Observed in Linear Flume Experiments.....	6-6
6-4	Photographs of Debris Accumulation on a 1-ft X 1-ft Vertical Screen in a Large Linear Flume ..	6-7
6-5	Typical Buildup of Fine Fibrous Debris that Easily Remains Suspended	6-8
6-6	Example Installation of a BWR Stacked-Disk ECCS Recirculation Suction Strainer.....	6-12
6-7	Fibrous Debris Accumulation on a Stacked-Disk Strainer	6-12
6-8	RMI Debris Accumulation on a Stacked-Disk Strainer.....	6-13
7-1(a)	High-Resolution Scanning Electron Microscope Image of Fibrous Debris	7-2
7-1(b)	Low-Resolution Scanning Electron Microscope Image of Fibrous Debris	7-2
7-2	Head Losses vs Fiber Volume for Fixed Quantities of Particulate.....	7-5
7-3	Aluminum RMI Accumulation on a Stacked Disk Strainer	7-8
7-4(a)	RMI/Fiber/Sludge Post Head Loss Test Debris Bed	7-10
7-4(b)	RMI and Fiber Accumulation on a Strainer	7-10
7-5	Equivalency Between a Truncated Cone Strainer Debris Accumulation and Flat-Plate Strainer Simulation	7-12
7-6	Vertical Flat-Plate Strainer Head Loss Facility at Alden Research Laboratory.....	7-13
7-7(a)	Flat-Plate-Strainer Head Loss Facility Used in KKL Test.....	7-16
7-7(b)	Gravity Head Loss Test Setup Used in the BWROG Tests	7-17
7-8(a)	Schematic of the Horizontal Flume Used in NRC-Sponsored ARL-Conducted PWR Sump Screen Tests).....	7-19
7-8(b)	Picture of Large RMI Foil Accumulation on the Vertical Screen	7-19
7-9(a)	Flume Test Setup Used in the CDI Experiments for Millstone 2.....	7-21
7-9(b)	Test Setup Used for Transport and Head Loss Measurement in the KKB Plant-Specific Tests	7-22
7-10	STUK RMI Head Loss Test Setup for Prototype Strainer	7-23
7-11	BWROG Prototype Strainer Module Test Setup	7-25
7-12	Measured Head Loss as Function of Strainer Debris Loading for Specialty Strainers	7-26
7-13	Semi-Scale Test Facility Used in Grand Gulf Quarter-Scale Testing	7-29
7-14	Prototype Strainer Module Test Setup Used in Grand Gulf Prototype Tests.....	7-30
7-15	Idealized View of Flow Through an RMI Bed	7-32
7-16	Comparison of NRC/ARL Test Data with LANL Correlation	7-34
7-17	Comparison of BWROG Test Data for Truncated Cone Strainer with LANL RMI Correlation....	7-34
7-18	Comparison of LANL RMI Correlation Predictions for Truncated Cone Strainer with the Experimental Data Obtained from LaSalle Tests	7-36
7-19	Comparison of LANL RMI Predictions with the STUK Head Loss Data	7-36
7-20	Schematic Representation of Debris Build-Up on a Stacked-Disk Strainer.....	7-38

7-21	Point-by-Point Comparison of Correlation Predictions with PCI Head Loss Data	7-39
7-22	Dimensionless Representation of Stacked-Disk Strainer Effective Area as a Function of Debris Volume	7-40
7-23	Example of Long Term Head Loss for a NUKON™ Debris Bed	7-41
8-1	BWROG Prototype Module Test Program	8-3
8-2	Measured Head Loss as a Function of Strainer Debris Loading for Typical Advanced Passive Strainers.....	8-3
8-3	PCI Stacked-Disk Strainer Being Installed at Pilgrim Nuclear Power Plant.....	8-5
8-4	The Core Tube Used in the PCI Stacked-Disk Strainers	8-5

Tables

1-1	Important Parameters Tracked and Their Relevance	1-13
1-2	Debris Generation and Transport Parameters: LLOCA-Large Dry Containment	1-16
1-3	Debris Generation and Transport Parameters: LLOCA-Ice Condenser Containment.....	1-17
1-4	PWR LLOCA Sequences	1-18
1-5	Debris Generation and Transport Parameters: MLOCA-Large Dry Containment	1-22
1-6	Debris Generation and Transport Parameters: MLOCA-Ice Condenser Containment.....	1-23
1-7	Debris Generation and Transport Parameters: SLOCA-Large Dry Containment	1-26
1-8	Debris Generation and Transport Parameters: SLOCA-Ice Condenser Containment	1-27
1-9	Debris Generation and Transport Parameters: SLOCA-Sub-Atmospheric Containment	1-28
3-1	Damage Pressures for Insulation Materials Found in U.S. PWRs	3-4
3-2	Size Classification Scheme for Fibrous Debris	3-7
3-3	Typical Size Characteristics of RMI Debris	3-9
3-4	Measured Particle-Size Distribution from Newtherm 1000 (Calcium-Silicate) Erosion Tests.....	3-14
3-5	Test Matrix for the OPG Calcium-Silicate Jet Impact Tests	3-17
3-6	Size Distribution of Calcium-Silicate Debris in Tests Where Insulation Was Liberated	3-18
3-7	Size Distribution of Fiberglass Debris in Tests Where Insulation Was Liberated	3-20
4-1	Physical Processes and Phenomena Affecting Airborne/Washdown Debris Transport	4-4
4-2	Thermal-Hydraulic Airborne Processes and Phenomena	4-5
4-3	Airborne Debris-Transport Mechanisms.....	4-6
4-4	Thermal-Hydraulic Processes and Phenomena.....	4-7
4-5	Washdown Debris-Transport Mechanisms	4-7
4-6	Airborne/Washdown Debris Transport Testing	4-9
4-7	Small Fibrous Debris Capture Fractions	4-18
4-8	Airborne/Washdown Debris-Transport Analyses	4-28
4-9	Highly Ranked Phenomenon from BWR Drywell Transport PIRT Table	4-32
4-10	Processes and Phenomena Ranked as High	4-33
4-11	Highly Ranked Processes and Phenomena for the Containment Above the Sump Pool.....	4-34
4-12	Study Transport Fractions for Main-Steam-Line Breaks	4-40
4-13	Study Transport Fractions for Recirculation Line Breaks.....	4-40
4-14	Study Transport Fractions for All Insulation Located in ZOI.....	4-41
4-15	Debris Size Categories and Their Capture and Retention Properties	4-43
4-16	Fractions of Blanket Material with Low Transport Efficiency.....	4-45
4-17	URG Drywell Transport Fractions	4-46
4-18	URG Combined Debris-Generation and Transport Fractions for Mark I, III.....	4-47
4-19	Debris-Transport Fractions Estimates Used in Parametric Evaluation	4-50
5-1	Summary Data for Diffused Flow Entry Inlet Conditions	5-22
5-2	Water Chemical Conditions in KAEFER Insulation Buoyancy Tests	5-31
5-3	Flow Velocity Needed to Initiated Motion of NUKON Insulation Fragments	5-33
5-4	Highly Ranked Phenomena from BWR Drywell Floor Pool Debris Transport PIRT Table	5-35
5-5	Highly Ranked Processes and Phenomena for the Debris Transport in a PWR Containment Sump Pool	5-35
6-1	Minimum Screen Approach Velocity for Debris to “Flip Up” or be Hydraulically “Lifted” Onto a Sump Screen.....	6-13
7-1	Head Loss Test Data for Mixtures of Calcium-Silicate and Fiberglass Insulation Debris	7-6

7-2	Characteristic Parameters for RMI Debris Beds	7-32
7-3	Geometric Details of the Portion of the Strainer Tested in the LaSalle Test Program.....	7-35
8-1	Total Strainer Area and Vendor for Each BWR Plant Responding to NRCB 96-03	8-10
8-2	Issue Resolution Summary for Audited Plants.....	8-11
8-3	Fibre Penetration, 4-mm Perforated Plate	8-14
8-4	Fibre Penetration, 4-mm Perforated Plate	8-14
9-1	Events With LOCA Generated Insulation Debris	9-2
9-2	Events Rendering a System Inoperable.....	9-3
9-3	Events With Debris Found Inside Containment	9-6
9-4	Events of Inadequate Maintenance Potentially Leading to Sources of Debris	9-9
9-5	Events Where Inadequacies Found in Sump Screens.....	9-11

EXECUTIVE SUMMARY

In the event of a loss-of-coolant accident (LOCA) within the containment of a light-water reactor, piping thermal insulation and other materials in the vicinity of the break will be dislodged by the pipe break and steam/water-jet impingement. A fraction of this fragmented and dislodged insulation and other materials, such as paint chips, paint particulates, and concrete dust, will be transported to the containment floor by the steam/water flows induced by the break and by the containment sprays. Some of this debris eventually will be transported to and accumulated on the recirculation-sump suction screens in pressurized-water reactor (PWR) containments or on the pump-suction strainer in boiling-water reactor (BWR) containments. Debris accumulation on the sump screen or strainers could challenge the plant's capability to provide adequate, long-term cooling water to the emergency core cooling system (ECCS) and the containment spray system pumps.

As a result of the research on the BWR suction-strainer and PWR sump-screen clogging issues, a substantial base of knowledge has been amassed that covers all aspects of the issues from the generation of debris to the head loss associated with a debris bed on a strainer or screen. This report describes the different analytical and experimental approaches that have been used to assess the various aspects of sump and strainer blockage and identify the strengths, limitations, important parameters and plant features, and appropriateness of the different approaches. The report also discusses significant United States (U.S.) Nuclear Regulatory Commission (NRC) regulatory actions regarding resolution of this issue. In essence, the report is designed to serve as a reference for plant-specific analyses in regard to whether the sump or strainer would perform its function without preventing the operation of the ECCS pumps.

This report is intended primarily for analyzing PWR sump-screen clogging issues, largely because the BWR issue had been resolved at the time the report was written. Nevertheless, the report also will be valuable in the review of any additional analyses for BWR plants as well. A majority of the strainer blockage research to date was conducted specifically for the resolution of the BWR issue; however, most of this research is also directly applicable to the

resolution of the PWR issue. Therefore, both BWR and PWR research and analytical approaches are discussed, and the applicability of that research, i.e., BWR vs PWR, is stated.

The report provides background information (Section 1) regarding the PWR containment sump and the BWR suction-strainer debris clogging issues. This background information includes a brief historical overview of the resolution of the BWR issue with a lead into the PWR issue, a description of the safety concern relative to PWR reactors, the criteria for evaluating sump failure, descriptions of postulated accidents, descriptions of relevant plant features that influence accident progression, and a discussion of the regulatory considerations.

The purpose of a sump screen is to prevent debris that may damage or clog components downstream of the sump from entering the ECCS and reactor coolant system. Debris accumulation across a sump screen would create a pressure drop across that screen that potentially could cause insufficient flow to reach the pump inlet. The knowledge-base report is organized in the same manner that an evaluation of the potential of sump screen blockage would be performed. These steps are the identification of sources of potential debris (Section 2); the potential generation of insulation debris by the effluences from a postulated LOCA (Section 3); the potential transport of the LOCA-generated debris to the containment sump (Section 4); the potential transport of debris within the sump pool to the recirculation sump screen (Section 5); the potential accumulation of the debris on the sump screen, specifically the uniformity and composition of the bed of debris (Section 6); and the potential head loss associated with the accumulated debris (Section 7). The report also summarizes the resolution options available to BWR plant licensees to resolve the BWR suction-strainer clogging issue and the advanced features of the new replacement strainers that were implemented in the BWR plants so that the strainers can accumulate the potential debris loading without the associated debris-bed head loss (Section 8). Domestic and foreign plant events relevant to the PWR sump-screen clogging issue are discussed (Section 9). Finally, an overall summary of the knowledge base is provided in Section 10.

ACKNOWLEDGMENTS

The U.S. Nuclear Regulatory Commission (NRC) Office of Nuclear Regulatory Research (RES) sponsored the work reported here. Dr. B. P. Jain is the Technical Monitor for this task. He provided technical direction and actively participated in reviewing the report and provided valuable comments. The authors would also like to acknowledge R. E. Architzel and J. Lehning of the NRC, Dr. J. Hyvarinen of Radiation and Nuclear Safety Authority (STUK), Finland, and Dr. M. Maqua of Gesellschaft fuer Anlagen- und Reaktorsicherheit (GRS) mbH, Germany, for their timely technical review of the report and

Gordon Hart of Performance Contracting Inc. for the information he supplied regarding the aging of insulation during normal plant operations.

The authors would like to acknowledge the contributions of Mrs. N. Butner. Nancy was primarily responsible for producing this document, from developing the project plan through incorporating the review comments. Ms. M. Timmers, J. Lujan, and J. Snyder, LANL, spent numerous hours editing and generally fixing the document.

ABBREVIATIONS

ABB	ABB Atom/Combustion Engineering
AJIT	Air-Jet Impact Testing
ANS	American Nuclear Society
ANSI	American National Standards Institute
ARL	Alden Research Laboratory
BWR	Boiling-Water Reactor
BWROG	Boiling Water Reactor Owners' Group
CCW	Component Cooling Water
CDF	Core-Damage Frequency
CDI	Continuum Dynamics Inc.
CE	Combustion Engineering
CEESI	Colorado Engineering Experiment Station, Inc.
CFD	Computational Fluid Dynamics
CFR	Code of Federal Regulations
CS	Containment Spray
CSNI	Committee on the Safety of Nuclear Installations
CSS	Containment Spray System
DBA	Design-Basis Accident
DB-LOCA	Design-Basis Loss-of-Coolant Accident
DDTS	Drywell Debris Transport Study
DEGB	Double-Ended Guillotine Break
DPSC	Diamond Power Specialty Company
ECCS	Emergency Core Cooling System
EOP	Emergency Operating Procedures
EPRI	Electric Power Research Institute
ESF	Engineered Safeguard Feature
FME	Foreign Material Exclusion
FSAR	Final Safety Analysis Report
GDC	General Design Criteria
GE	General Electric Nuclear Energy
GGNS	Grand Gulf Nuclear Station
GL	Generic Letter
GSI	Generic Safety Issue
HDFG	High-Density Fiberglass
HDR	Heisdampfreaktor
HELB	High Energy Line Break
HEPA	High-Efficiency Particulate Air
HPSI	High-Pressure Safety Injection
IN	Information Notice
ITS	Innovative Technology Solutions, Inc.
IVO	Imatran Voima Oy
KKL	Kernkraftwerk, Liebstadt
KWU	Siemens AG Power Generation Group
LDFG	Low-Density Fiberglass
LOCA	Loss-of-Coolant Accident
LLOC	Large Loss-of-Coolant Accident
LPCI	Low-Pressure Coolant Injection
LPCS	Low-Pressure Core Spray
LPSI	Low-Pressure Safety Injection
LTP	Licensing Topical Report
LWR	Light-Water Reactor
MIJIT	Metallic Insulation Jet Impact Testing Facility
MLOCA	Medium Loss-of-Coolant Accident

MSL	Main Steam Line
MSLB	Main-Steam-Line Break
NDE	Non Destructive Evaluation
NEA	Nuclear Energy Agency
NEI	Nuclear Energy Institute
NPSH	Net Positive Suction Head
NRC	Nuclear Regulatory Commission
NRCB	NRC Bulletin
OECD	Organization for Economic Cooperation and Development
OPG	Ontario Power Generating
PCI	Performance Contracting Inc.
PIRT	Phenomena Identification and Ranking Table
PORV	Power-Operated Relief Valve
PVC	Polyvinyl Chloride
PWR	Pressurized-Water Reactor
RCP	Reactor Coolant Pump
RCS	Reactor Coolant System
RG	Regulatory Guide
RHR	Residual Heat Removal
RL	Recirculation Line
RLB	Recirculation-Line Break
RMI	Reflective Metal Insulation
RWST	Refueling Water Storage Tank
SAT	Spray Additive Tank
SEA	Science and Engineering Associates, Inc.
SER	Safety Evaluation Report
SI	Safety Injection
SKI	Statens Kärnkraftenspektion
SLOCA	Small Loss-of-Coolant Accident
SRP	Standard Review Plan
SRV	Safety Relief Valve
SSC	System, Structure, and Component
STUK	Finnish Centre for Radiation and Nuclear Safety
TPI	Transco Products, Inc.
TVO	Teollisuuden Voima Oy
UNM	University of New Mexico
URG	Utility Resolution Guidance
US	United States
USI	Unreviewed Safety Issue
ZOI	Zone of Influence

UNITS CONVERSION TABLE

Convert From	Convert To	Multiply By
<i>Length</i>		
in.	m	0.02540
mil*	m	2.540E-5
ft	m	0.3048
<i>Area</i>		
in. ²	m ²	6.452E-4
ft ²	m ²	0.09290
<i>Volume</i>		
ft ³	m ³	0.02832
gal.	m ³	0.003785
gpm	m ³ /s	6.308E-5
<i>Pressure</i>		
psi	Pa	6895
<i>Mass</i>		
lbm**	kg	0.4536
<i>Density</i>		
lbm/ft ³	kg/m ³	16.02
<i>Velocity</i>		
ft/s	m/s	0.3048
<i>Temperature</i>		
°F***	°C	0.5556

* mil = one-thousandth of an inch

** lbm is often simply given as lb

*** Subtract 32 before multiplying

1.0 INTRODUCTION

In the event of a loss-of-coolant accident (LOCA)¹ within the containment of a light-water reactor (LWR), piping thermal insulation and other materials in the vicinity of the break will be dislodged by the pipe break and the ensuing steam/water-jet impingement. A fraction of this fragmented and dislodged insulation and other materials, such as chips of paint, paint particulates, and concrete dust, will be transported to the containment floor by the steam/water flows induced by the break and by the containment sprays. Some of this debris will eventually be transported to and accumulate on the recirculation-sump suction screens in pressurized water reactor (PWR) containments or a pump suction strainer in boiling water reactor (BWR) containments. Debris accumulation on the sump screen or strainers could challenge the plant's capability to provide adequate, long-term cooling water to the emergency core cooling system (ECCS) and to the containment spray system (CSS) pumps.

As a result of the research on the BWR suction-strainer and PWR sump-screen clogging issues, a substantial base of knowledge has been amassed that covers all aspects of the issues, from the generation of debris to the head loss associated with a debris bed on a strainer or screen. This report describes the different analytical and experimental approaches that have been used to assess the various aspects of sump and strainer blockage and identifies the strengths, limitations, important parameters, and plant features and the appropriateness of the different approaches. The report also discusses significant U.S. Nuclear Regulatory Commission (NRC) regulatory actions regarding resolution of the issue. In essence, the report is designed to serve as a reference for plant-specific analyses with regard to whether the sump or strainer would perform its function without preventing the operation of the ECCS pumps.

This report is intended for use in resolving the PWR issue because the BWR issue had been resolved. Nevertheless, the report will serve the review of any additional analyses for BWR

plants, as well. A majority of the strainer blockage research to date was conducted specifically for the resolution of the BWR issue; however, most of this research is also directly applicable to the resolution of the PWR issue. Therefore, both BWR and PWR research and analytical approaches are discussed, and the applicability of that research, i.e., BWR vs PWR, is stated.

The following background information is presented as preparation to understanding the discussions of the current state of knowledge in the succeeding sections.

- A brief historical overview of the resolution of the BWR issue with a lead into the PWR issue
- A description of the safety concerns relative to PWR reactors
- Criteria for evaluating sump failure
- Descriptions of postulated PWR accidents
- Relevant plant features that influence accident progression
- The regulatory considerations

1.1 Historical Overview

In January 1979, the NRC originally declared sump-screen blockage to be an Unresolved Safety Issue, USI A-43,¹⁻¹ titled "Containment Emergency Sump Performance" and published the concerns identified in the USI in NUREG-0510, "Identification of Unresolved Safety Issues Relating to Nuclear Power Plants."¹⁻² USI A-43 dealt with concerns regarding the availability of adequate long-term recirculation cooling water following a LOCA. This cooling water must be sufficiently free of debris so that pump performance is not impaired and long-term recirculation flow capability is not degraded.

Although USI A-43 was derived principally from concerns regarding PWR containment emergency sump performance, these concerns applied to BWR ECCS suction, as well. The BWR residual heat removal (RHR) system performs the low-pressure coolant injection (LPCI) function of the ECCS and the safety-related CSS. In addition, BWR designs incorporate a low-pressure core spray (LPCS) system as part of the ECCS. The suction

¹ The focus of this safety issue is on LOCAs, but the issue may also apply to other high-energy line breaks (HELBs) within the design basis that would require long-term recirculation cooling.

strainers located in the BWR suppression pool are analogous to the PWR sump debris screen.

Substantial experimental and analytical research was conducted to support the resolution of USI A-43. In 1985, the regulatory analysis results and the technical findings of research related to resolving USI A-43 were reported in NUREG-0869¹⁻³ and NUREG-0897,¹⁻⁴ respectively. The bases for these findings were documented in a series of NRC contractor reports, which are listed in the NUREG-0897 reference section.¹⁻⁴ In NUREG-0897,¹⁻⁴ the NRC concluded the following.

- The formation of an air-core vortex that would result in unacceptable levels of air ingestion that potentially could severely degrade pump performance was a concern. This concern was more applicable to PWRs but was still relevant to BWRs. Hydraulic tests showed that the potential for air ingestion was less severe than previously hypothesized. In addition, under normal flow conditions and in the absence of cavitation effects, pump performance is only slightly degraded when air ingestion is less than 2%.
- The effects of LOCA-generated insulation debris on RHR recirculation requirements depend on:
 1. the types and quantities of insulation,
 2. the potential of a high-pressure break to severely damage large quantities of insulation,
 3. the transport of debris to the sump screen or strainer,
 4. the blockage potential of the transported debris, and
 5. the impact on available net positive suction head (NPSH).
- The effects of debris blockage on the NPSH margin must be dealt with on a plant-specific basis. Insulation debris transport tests showed that severely damaged or fragmented insulation readily transported at relatively low velocities (0.2 to 0.5 ft/s). Therefore, the level of damage near the postulated break location became a dominant consideration. The level of damage to insulation was correlated with distance between the insulation and the break, in terms of L/Ds (distance divided by the pipe-break diameter). Data showed that jet load pressures would inflict severe damage to insulation within 3 L/Ds, and

substantial damage in the 3- to 5-L/D range with damage occurring out to about 7 L/D.

- The types and quantities of debris small enough to pass through screens or suction strainers and reach the pump impeller should not impair long-term hydraulic performance. In pumps with mechanical shaft seals, debris could cause clogging or excessive wear, leading to increased seal leakage. However, catastrophic failure of a shaft seal as a result of debris ingestion was considered unlikely. If the seal did fail, pump leakage would be restricted.
- Nineteen nuclear power plants were surveyed in 1982 to identify the insulation types used, the quantities and distribution of insulation, the methods of attachment, the components and piping insulated, the variability of plant layouts, and the sump designs and locations. The types of insulation found were categorized into two major groups: reflective metallic insulation (RMI) and fibrous insulations. The RMI was manufactured by at least four different manufacturers. The fibrous insulation included NUKON™ fiberglass blankets, fiberglass molded blocks, mineral wool fiber blocks, calcium-silicate molded blocks, and expanded perlite-molded blocks. Insulations sometimes were enclosed in an outer shell or jacket or cloth cover.

USI A-43 was declared resolved in 1985. The NRC resolution of USI A-43 was presented to the Commission in October 1985.¹⁻⁵ The resolution consisted of:

1. publishing NUREG-0897¹⁻⁴ as a summary of the key technical findings for use as an information source by applicants, licensees, and the staff;
2. revising the Standard Review Plan (SRP), Section 6.2.2,¹⁻⁶ and Regulatory Guide (RG) 1.82,¹⁻⁷ "Water Sources for Long-Term Recirculation Cooling Following a Loss-of-Coolant Accident," to reflect the staff's technical findings; and
3. issuing Generic Letter (GL) 85-22,¹⁻³³ "Potential for Loss of Post-LOCA Recirculation Capability Due to Insulation Debris Blockage," to all holders of an operating license or construction permit outlining safety concerns and recommending the use of Regulatory Guide (RG) 1.82, Revision 1¹⁻⁷ as guidance for

conducting 10 Code of Federal Regulations (CFR) 50.59 analyses.¹⁻⁸

In addition, a regulatory analysis was performed (see NUREG-0869¹⁻³) to serve as a basis for the final resolution of USI A-43.

The regulatory analysis did not support a generic backfit action because plant-specific design features and post-LOCA recirculation flow requirements govern debris blockage effects. As a result, the analysis conclusion was that the issue must be resolved on a plant-specific basis. The staff recommended that RG 1.82, Revision 1,¹⁻⁷ be used as guidance for the evaluation (10 CFR 50.59)¹⁻⁸ of plant modifications involving replacement and/or modification of thermal insulation installed on the primary coolant system piping and components. The 50% blockage criterion of Revision 0 of RG 1.82¹⁻⁷ was considered inadequate to address this issue.

After the closure of USI A-43,¹⁻¹ several ECCS strainer and foreign material discovery events prompted a review of the strainer blockage issue for BWRs. (These events are described in more detail in Section 9.) Perhaps the most notable of these events occurred on July 28, 1992, during the startup of Barsebäck, Unit 2, in Sweden. This is discussed in NRC Information Notice (IN) 92-71, "Partial Blockage of Suppression Pool Strainers at a Foreign BWR," September 30, 1992.¹⁻⁹ In this event, a spurious opening of a safety valve while the reactor was pressurized discharged steam into the drywell, dislodging mineral wool insulation that subsequently transported to the suppression pool, resulting in suction-strainer blockage and pump cavitation. The Barsebäck-2 event demonstrated that larger quantities of fibrous debris could reach the strainers than had been predicted by models and analysis methods developed for the resolution of USI A-43.¹⁻¹

ECCS suction-strainer clogging events also occurred at U.S. plants. These included the following.

- Two events (1992 and 1993) occurred at the Mark III Perry Nuclear Power Plant.¹⁻¹⁰ Debris was found on the suppression pool floor and on the RHR suction strainers during a refueling outage inspection. In addition, the buildup of debris on the strainer caused an excessive differential pressure,

which deformed the strainers. After the damaged strainers were replaced and the suppression pool was cleaned, the strainers were again found to be fouled by debris such that the pump suction pressure dropped to 0 during a test. The debris consisted of glass fibers, corrosion products, and other materials. Fibrous material acted as a filter for suspended particles—a phenomenon not previously recognized by either the NRC or industry.

- An event occurred at Limerick Generating Station Unit 1 in 1995¹⁻¹¹ in which a safety relief valve (SRV) opened while Unit 1 was at 100% power. Subsequently, a thin mat of fibrous material and sludge covering the RHR pump suction strainers in the suppression pool caused fluctuating motor current and flow, indicating pump cavitation was occurring. Limerick subsequently removed about 635 kg of debris from the pool.
- In 1988 and 1989, the Grand Gulf Nuclear Station experienced strainer blockage events during testing of the RHR pumps. Pump suction pressures fell below the in-service inspection acceptance criteria.¹⁻¹⁰
- In 1994, divers discovered numerous pieces of cloth-like material on the bottom of the torus and on the ECCS strainers at Browns Ferry Nuclear Plant Unit 2.¹⁻¹² This debris had partially blocked the strainers.

Substantial quantities of debris were discovered in suppression pools on other occasions. In other cases, plant inspections have found deteriorated insulation that would render these materials more likely to form debris following a LOCA. In other plant inspections, previously unidentified unqualified coatings that could form debris following a LOCA have been found.

All of these events occurred despite existing NRC regulations and regulatory guidance. Foreign materials, degraded coatings inside the containment that detach from their substrate, ECCS components not consistent with their design basis, and LOCA-generated debris are potential common-cause failure mechanisms for the ECCS and containment spray system (CSS). Debris may clog suction strainers, sump screens, filters, nozzles, and small-clearance flow paths in the ECCS and safety-related CSS and interfere with the long-term cooling function, source-term reduction and/or pressure-reduction capabilities of the plant. The NRC has

consistently emphasized the need to minimize the presence of foreign material in the containment [e.g., a strong foreign material exclusion (FME) program].

The string of operational events described above demonstrated that

- larger quantities of debris could reach the ECCS strainers than had been predicted by models and analysis methods developed during the resolution of USI A-43;¹⁻¹
- fibrous material acts as a filter for suspended particles, a phenomenon not previously recognized by the NRC or industry;
- head loss correlations developed during the resolution of USI A-43¹⁻¹ under-predicted strainer head losses for combined fiber/particulate debris beds; and
- Extensive quantities of foreign materials were being found in suppression pools despite ongoing FME programs.

The ECCS strainer and foreign material discovery events prompted a review of the strainer blockage issue; hence, the NRC sponsored research to estimate possible shortcomings of existing suction strainer designs in U.S. BWR plants and to evaluate the actions taken by the nuclear power industry to ensure the availability of long-term recirculation of cooling water in BWR plants.

Concerns generated by these strainer-blockage events prompted the NRC to issue Bulletin 93-02,¹⁻¹³ "Debris Plugging of Emergency Core Cooling Suction Strainers," on May 11, 1993, to both BWR and PWR licensees. Licensees were requested to:

- identify fibrous air filters and other temporary sources of fibrous material in the primary containment not designed to withstand a LOCA,
- take prompt action to remove the identified material, and
- take any other immediate compensatory measures necessary to ensure the functional capability of the ECCS.

The NRC sponsored research to evaluate the adequacy of existing suction strainer designs in U.S. BWR plants by initiating a detailed plant-specific study in September 1993 using a

reference BWR/4 reactor with a Mark I containment. The results were published in NUREG/CR-6224¹⁻¹⁴ in 1995. This plant-specific analysis developed analytical models applicable to the reference BWR that considered debris generation, drywell debris transport, suppression-pool debris transport, and strainer blockage. The NUREG/CR-6224 study identified a lack of critical data needed to complete the study.¹⁻¹⁴ As a result, the NRC sponsored a series of small-scale experiments designed to gain insights into the behavior of debris in the suppression pool and acquire mixed debris bed head loss data. A computer program called BLOCKAGE was developed to calculate debris generation, debris transport, fiber/particulate debris bed head losses and the effect of the debris on the available ECC NPSH.^{1-15,1-16} Probabilistic analyses were performed that focused on evaluating the likelihood of ECCS strainer blockage and blockage-related core damage from large loss of coolant accident (LLOCA) initiators. The final results of the reference plant study, which is documented in NUREG/CR-6224,¹⁻¹⁴ demonstrated that for the reference plant, there was a high probability that the available NPSH margin for the ECCS pumps would be inadequate if insulation and other debris caused by a LOCA transported to the suction strainers. In addition, the study calculated that the loss of NPSH could occur quickly (less than 10 min into the event). The study also concluded that determining the adequacy of the NPSH margin for a given ECCS system is highly plant-specific because of the large variations in such plant characteristics as containment type, ECCS flow rates, insulation types, plant layout, plant cleanliness, and available NPSH margin.

The NRC also exchanged information and experience with the international community. The Swedish nuclear power inspectorate, Statens Kärnkraftinspektion (SKI), hosted a workshop to study the strainer blockage issue in 1994. The workshop revealed a confusing picture of the available knowledge base, including examples of conflicting information and a variety of interpretations of the regulatory guidance in the NRC's RG 1.82, Rev. 1.¹⁻⁷ Following this workshop, SKI requested the formation of an international working group to establish an internationally agreed-upon knowledge base for assessing the reliability of emergency core cooling water recirculation systems. The NRC compiled a source book of

available knowledge for the CSNI of the Organization for Economic Cooperation and Development (OECD) Nuclear Energy Agency.¹⁻¹⁷

Based on the NRC's preliminary research and information learned at the OECD/Nuclear Energy Agency (NEA) workshop, the NRC issued Supplement 1 to Bulletin 93-02 on February 18, 1994, requesting BWR licensees to take further interim actions pending final resolution.¹⁻¹³ These actions involved implementing operating procedures and conducting training and briefings designed to enhance the capability to prevent or mitigate loss of ECCS following a LOCA as a result of strainer clogging. The purpose of these interim actions was to ensure the reliability of the ECCS so that the staff and industry would have sufficient time to develop a permanent resolution.

To provide time to conduct research to resolve the strainer clogging issue, the NRC first ensured that public health and safety were protected adequately. In responding to NRC Bulletin 93-02¹⁻¹³ and its supplement, BWR licensees implemented interim measures to ensure adequate protection of public health and safety. Specifically, licensees ensured that:

1. alternate water sources (both safety- and non-safety-related sources) to mitigate a strainer clogging event were available,
2. emergency operating procedures (EOPs) provided adequate guidance on mitigating a strainer-clogging event,
3. operators were trained adequately to mitigate a strainer-clogging event, and
4. loose and temporary fibrous materials stored in the containment were removed.

The responses to NRC Bulletin 93-02¹⁻¹³ showed that most suppression pools had already been cleaned recently and that those licensees who had not cleaned their suppression pools recently were scheduled to do so during their next refueling outage. In addition, a generic safety assessment conducted by the Boiling Water Reactor Owners' Group (BWROG) concluded that operators would have adequate time to make use of alternate water sources (25–35 min) if needed during a LOCA and that the probability of the initiating event is low. For these reasons, the NRC allowed continued operation by BWR licensees until the final

resolution to the strainer clogging issue was developed and implemented. The NRC initiated the final resolution to the strainer issue with the issuance of NRC Bulletin 96-03.¹⁻¹⁸ Satisfactory implementation of the requested actions in NRC Bulletin 96-03 ensured that the ECCS can perform its safety function and minimize the need for operator action to mitigate a LOCA.

The NRC issued RG 1.82, Revision 2, in May 1996.¹⁻⁷ This regulatory guide describes acceptable methods for implementing applicable design requirements for sumps and suppression pools functioning as water sources for emergency core cooling, containment heat removal, or containment atmosphere cleanup. In addition, guidelines for evaluating the adequacy of the sump and suppression pool for long-term recirculation cooling following a LOCA are provided. This regulatory guide was revised to update the BWR debris-blockage evaluation guidance because operational events, analyses, and research work that have occurred since the issuance of Revision 1 indicated that the previous guidance was not comprehensive enough to evaluate a BWR plant's susceptibility to the detrimental effects caused by suction-strainer debris blockage adequately.

An essential aspect of predicting the potential for strainer clogging is estimating the amount of debris that is likely to transport from the drywell into the wetwell. The transport processes are complex in that they involve transport during both the reactor blowdown phase (i.e., entrainment in steam/gas flows) and the post-blowdown phase (i.e., via water flowing out of the break and/or containment sprays). In Revision 2 of RG 1.82,¹⁻⁷ the NRC recommended assuming 100% debris transport unless analyses or experiments justified lower transport fractions. To facilitate a better understanding of debris transport, the NRC initiated a study in September 1996, referred to as the drywell debris transport study (DDTS), to investigate debris transport in BWR drywells using a bounding analysis approach. The focus of the DDTS was to provide a description of the important phenomena and plant features that control and/or dominate debris transport and the relative importance of each phenomenon as a function of the debris size. The results of the DDTS, which are documented in NUREG/CR-6369,¹⁻¹⁹ provide reasonable engineering insights that can be used to evaluate the

adequacy of the debris-transport factors used in plant-specific strainer-blockage analyses.

The NRC staff issued NRC Bulletin 96-03,¹⁻¹⁸ "Potential Plugging of Emergency Core Cooling Suction Strainers by Debris in Boiling-Water Reactors," on May 6, 1996. All BWR licensees were requested to implement appropriate measures to ensure the capability of the ECCS to perform its safety function following a LOCA. The staff had identified three potential resolution options but allowed licensees to propose others that provided an equivalent level of assurance. The three options identified by the staff were to install:

1. a large-capacity passive strainer designed with sufficient capacity to ensure that debris loadings equivalent to a scenario calculated in accordance with Section C.2.2 of RG 1.82, Revision 2¹⁻⁷ do not cause a loss of NPSH for the ECCS;
2. a self-cleaning strainer that automatically prevents strainer clogging by providing continuous cleaning of the strainer surface with a scraper blade or brush; and
3. a backflush system that relies on operator action to remove debris from the surface of the strainer to prevent it from clogging.

All licensees were requested to implement these actions by the end of the first refueling outage starting after January 1, 1997.

The staff closely followed the BWROG's efforts to resolve this issue. The BWROG evaluated several potential solutions, and completed testing on three new strainer designs: two passive designs and one self-cleaning design. The BWROG effort was consistent with the options proposed in NRCB 96-03¹⁻¹⁸ for resolution of the potential ECCS strainer clogging issue. The BWROG then developed topical report NEDO-32686,¹⁻²⁰ "Utility Resolution Guidance for ECCS Suction Strainer Blockage," November 1996 [the Utility Resolution Guidance (URG)], to provide utilities with:

1. guidance on evaluation of the potential ECCS strainer clogging issue for their plant;
2. a technically sound, standard industry approach to resolution of the issue; and
3. guidance that is consistent with the requested actions in NRCB 96-03¹⁻¹⁸ for

demonstrating compliance with 10 CFR 50.46.¹⁻⁸

The URG includes guidance on calculational methodologies for performing plant-specific evaluations. The BWROG and the industry conducted several small-scale tests to obtain the data needed to develop the URG and to qualify plant-specific strainer designs. The URG included substantial portions of these data.

The NRC reviewed the URG and issued its Safety Evaluation Report (SER) on August 20, 1998.¹⁻²¹ In the SER, the staff noted that the issue of potential strainer blockage is complex in that head loss across suction strainers is not only a function of the amount of debris but also of the types of debris (e.g., fibrous insulation, paint, reflective metallic insulation, dirt, corrosion products, etc.) and characteristics of the debris (size, shape, etc.). The analyst must evaluate the worst case for potential strainer debris loadings; consider the potential for foreign material to be introduced during normal plant evolutions such as refueling and maintenance outages; and evaluate maintenance practices, including the maintenance of qualified coatings in the drywell and wetwell.

The staff found the URG to be comprehensive, providing general guidance on resolution options and detailed guidance on performing plant specific analyses to estimate potential worst-case debris loadings on ECCS suction strainers during a LOCA. However, the URG lacked complete guidance and/or adequate supporting analysis in several areas. Because insufficient detail and supporting justification on the "resolution options," were included in the URG, further supporting justification from a licensee or the BWROG was required for the staff to reach a conclusion on their acceptability.

The NRC staff issued GL 97-04, "Assurance of Sufficient Net Positive Suction Head for Emergency Core Cooling and Containment Heat Removal Pumps," to all holders of operating licenses for nuclear power plants on October 7, 1997.¹⁻²² The staff wanted to ensure that the NPSH available for ECCS and containment heat-removal pumps would be adequate under all design-basis accident (DBA) scenarios. The staff was concerned that changes to plant configuration, operating procedures, environmental conditions, or other operating parameters over the life of the plant could result

in inadequate NPSH. Some licensees discovered that they needed to have their licensing basis include credit for containment overpressure to meet the NPSH requirements of the ECCS and containment heat-removal pumps. Some licensees were assuming containment overpressure credit inconsistent with the plant's licensing basis. GL 97-04 requested addressees to provide current information regarding their NPSH analyses.

The staff evaluated its position on the use of containment overpressure in calculating NPSH margin as part of its review of industry responses to GL 97-04.¹⁻²² The concerns that led to the issuance of GL 97-04 illustrated an existing uncertainty and variability in the application of the methods used to calculate the NPSH margin. These concerns were confirmed by the review of the industry submittals.¹⁻²³ Crediting containment overpressure in the NPSH margin requires supporting analyses. "Overpressure analyses" are detailed and comprehensive analyses performed to conservatively predict the minimum containment pressure available during a DBA. All means of removing heat from the containment are considered, including all installed pressure-reducing systems and processes. These systems and processes include heat transfer to structures, containment leakage, containment sprays, pool-surface heat and mass transfer, fan coolers, RHR heat exchangers, and power conversion systems. Because the NPSH is strongly dependent on the accident scenario, a comprehensive range of accident scenarios is evaluated to ensure that the minimum pressure is determined conservatively for the purpose of granting an overpressure credit. Because there is substantial uncertainty associated with the strainer clogging issue, the staff did not recommend licensing basis changes as a "resolution option."

The NRC issued GL 98-04,¹⁻²⁴ "Potential for Degradation of the Emergency Core Cooling System and the Containment Spray System After Loss-of-Coolant Accident Because of Construction and Protective Coating Deficiencies and Foreign Material in Containment," on July 14, 1998, to all holders of operating licenses for operating nuclear power reactors. GL 98-04¹⁻²⁴ alerted addressees of additional strainer-blockage concerns, including problems associated with:

1. the material condition of Service Level 1 protective coatings inside the containment,
2. foreign material found inside operating nuclear power plant containments, and
3. design and construction deficiencies with the material condition of ECCS systems, structures, and components inside the containment.

The NRC expected addressees to ensure that the ECCS and the safety-related CSS remain capable of performing their intended safety functions.

The industry addressed the requirements of NRC Bulletin 96-03¹⁻¹⁸ by installing large capacity passive strainers in each plant (NRCB 96-03 Option 1) with sufficient capacity to ensure that debris loadings equivalent to a scenario calculated in accordance with Section C.2.2 of RG 1.82, Revision 2,¹⁻⁷ do not cause a loss of NPSH for the ECCS. Four BWR plants were chosen for detailed audits by the NRC staff: Limerick (BWR/4 Mark II), Dresden (BWR/3 Mark I), Duane Arnold (BWR/4 Mark I), and Grand Gulf (BWR/6 Mark III).

The research and regulatory developments associated with the resolution of the strainer-blockage issue for the U.S. BWR plants were summarized in Los Alamos National Laboratory report LA-UR-01-1595.¹⁻²⁵ This report contains a more thorough history of events and developments than was just presented in this introduction. The report also includes brief summaries of the various experiments and analyses conducted to support the issue resolution.

As a result of research findings related to resolving the BWR ECCS strainer blockage safety issue, the NRC conducted further research into the PWR sump-screen blockage issue to determine if further action was needed beyond the original resolution of USI A-43.¹⁻¹ The Generic Safety Issue (GSI)-191, "PWR Sump Blockage," study was established to determine if the transport and accumulation of debris in a containment following a LOCA would impede the operation of the ECCS in operating PWRs.

A parametric evaluation¹⁻²⁶ was performed as part of the GSI-191 study to demonstrate the credibility of recirculation-sump clogging for operating PWRs. Each of the 69 domestic

PWRs was modeled in the evaluation using a mixture of generic and plant-specific data. The minimum amount of debris accumulation on the sump screen needed to exceed the required NPSH margin for the ECCS and CSS pumps was determined for each of the 69 representative models. Further, both completed and ongoing GSI-191 PWR research, as well as existing BWR research, were used to support the development of these models and the input to these models.¹⁻²⁶⁻¹⁻²⁹ The evaluation considered small, medium, and large LOCAs using both favorable and unfavorable assumptions, relative to the plant, to a number of parameters. The results of the parametric evaluation formed a credible technical basis for making the determination that sump blockage was a credible concern.

A risk study that supported the parametric evaluation¹⁻³⁰ was performed to estimate the amount by which the core damage frequency (CDF) would increase if failure of PWR ECCS recirculation cooling resulting from debris accumulation on the sump screen were accounted for in a manner that reflects the results of recent experimental and analytical work. Further, the estimate was made in a manner that reflected the total population of U.S. PWR plants. Results suggest that the conditional probability of recirculation sump failure, given a demand for recirculation cooling, is sufficiently high at many U.S. plants to cause an increase in the total CDF of an order of magnitude or more.

However, the parametric evaluation had a number of limitations; the most notable were attributed to the extremely limited plant-specific data available to the study. The need for more accurate plant-specific assessments of the adequacy of the recirculation function of the ECCS and CSS to be performed for each operating PWR was indicated clearly. The Nuclear Energy Institute (NEI) also recognized this need and has since initiated a program to develop evaluation guidance for the industry, a program being closely monitored by the NRC.

1.2 Description of Safety Concern

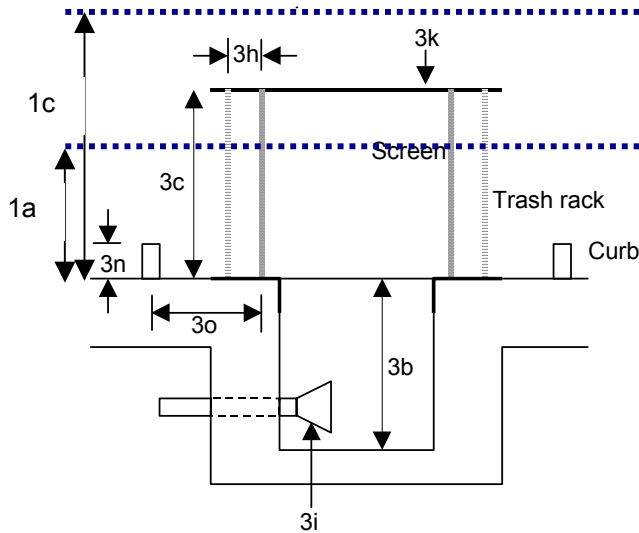
In the event of a LOCA within the containment of a PWR, piping thermal insulation and other materials in the vicinity of the break will be dislodged by break-jet impingement. A fraction of this fragmented and dislodged insulation and

other materials such as paint chips, paint particulates, and concrete dust will be transported to the containment floor by the steam/water flows induced by the break and the containment sprays. Some of this debris eventually will be transported to and accumulated on the recirculation sump suction screens. Debris accumulation on the sump screen may challenge the sump's capability to provide adequate, long-term cooling water to the ECCS and the containment spray (CS) pumps.

Generally speaking, the sump is the space enclosed by the trash rack; the space enclosed by the sump screen is referred to as the sump pit or sump region. Figure 1-1 illustrates the general features of a PWR sump layout generically; the parameters indicated were those queried of the industry during a survey conducted as part of the GSI-191 study.¹⁻²⁶ Actual sump designs vary significantly from this figure, but all share similar geometric features. The purpose of the trash rack and sump screen is to prevent debris that may damage or clog components downstream of the sump from entering the ECCS and reactor coolant system (RCS). The area outside of the sump is referred to as the containment floor or pool.

An examination of plant drawings, preliminary analyses, and ongoing tests suggests that a prominent mechanism for recirculation sump failure involves pressure drop across the sump screen induced by debris accumulation. However, sump-screen failure through other mechanisms is also possible for some configurations. Three failure mechanisms were considered as part of the GSI-191 study.

1. Loss of NPSH margin caused by excess pressure drop across the screen resulting from debris buildup. This concern applies to all plant units having sump screens that are completely submerged in the containment pool in combination with other plant features that permit generation and accumulation of debris on the sump screen.
2. Loss of the static head necessary to drive recirculation flow through a screen because of excess pressure drop across the screen resulting from debris buildup. This concern applies to all plant units having sump screens that are not completely submerged in combination with other plant features that permit generation and accumulation of debris on the sump screen.



Symbol

3b	Sump depth
3c	Height above floor
3h	Distance between trash rack and screen
3i	Vortex suppressor
3k	Solid plate
3n	Debris curb height
3o	Distance between debris curb and screen
1a	Height of water pool on containment floor at time of switchover
1c	Max. Height of water pool on containment floor

Figure 1-1 Illustration of Sump Features and Parameters

3. Blockage of water-flow paths could (a) cause buildup (and retention) of water in some regions of the containment and result in lower water levels near the sump and thus a lower NPSH margin than estimated by the licensees, or (b) altogether prevent adequate water flow through these openings.

Realistically, an analysis of the likelihood of any of the above three recirculation-flow failure mechanisms required plant-specific data that only the licensee has in sufficient quantity to perform a definitive analysis. The parametric evaluation discussed in the preceding section²⁶ attempted to evaluate the likelihood, but those results were not definitive. Rather, the objective of that study, which was conducted using a mixture of generic and plant-specific data, was simply to demonstrate the credibility of recirculation-sump clogging for operating PWRs. For each of the 69 representative models, the minimum amount of debris accumulation on the sump screen needed to exceed the required NPSH margin for the ECCS and CSS pumps was determined and then compared with the potential for generating debris within the containment. The sump-clogging credibility was demonstrated effectively.

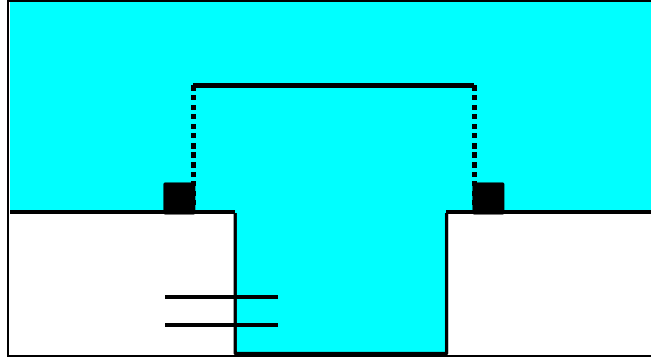
Other concerns related to debris generated during postulated accidents include:

- the potential for debris to pass through the sump screen, enter the RCS, and damage or block ECCS or RCS components and
- structural failure of the sump screens as a result of loads from debris or direct jet impingement.

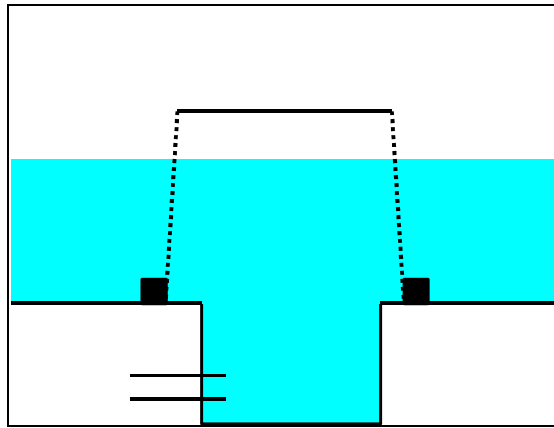
These concerns were considered beyond the scope of the GSI-191 study and the parametric evaluation.

1.3 Criteria for Evaluating Sump Failure

The sump-failure criterion applicable to each plant is determined primarily by sump submergence. Figure 1-2 illustrates the two basic sump configurations of fully and partially submerged screens. Although only vertical sump configurations are shown here, the same designations are applicable for inclined-screen designs. The key distinction between the fully and partially submerged configurations is that partially submerged screens allow equal pressure above both the pit and the pool, which are potentially separated by a debris bed. Fully submerged screens have a complete seal of water between the pump inlet and the containment atmosphere along all water paths passing through the sump screen. The effect of this difference in evaluation of the sump-failure criterion is described below.



(a) Fully submerged screen configuration showing solid water from pump inlet to containment atmosphere.



(b) Partially submerged screen configuration showing containment atmosphere over both the external pool and the internal sump pit with water on lower portion of screen.

Figure 1-2 Sump-Screen Schematics

1.3.1 Fully Submerged Sump Screens

Figure 1-2(a) is a schematic of a sump screen that is fully submerged at the time of switchover to ECCS from the injection phase to the recirculation phase. The most likely mode of failure for sumps in this configuration would be cavitation within the pump housing if the head loss caused by debris accumulation exceeds the NPSH margin. The NPSH margin is the excess in the available NPSH over that required by the pump per the manufacturer's specifications. The excess or margin is determined with the sump screens clean, i.e., no debris. The available NPSH is a function of the water level in the containment sump, the temperature of the sump water, the containment pressure, and the piping friction losses between sump and pump inlet. Because the NPSH margin is higher at the

maximum sump pool level than at the switchover pool level, the evaluation of sump blockage must consider the margin at the time of switchover. The accumulation of debris on the screen also would be transient; however, accurately determining the timing of debris accumulation on the screens would be a very difficult analysis. Conservatively, the head loss associated with the maximum accumulation of debris usually is compared with the minimum NPSH margin, which usually would occur at the time of switchover rather than the time of maximum debris loading.

1.3.2 Partially Submerged Sump Screens

Figure 1-2(b) is a schematic of a sump that is partially submerged at the time of switchover. Failure can occur for sumps in this configuration

in one of two ways: by pump cavitation as explained above or when head loss caused by debris buildup prevents sufficient water from entering the sump. As debris accumulates on the screen and causes a drop in pressure across it, the water level behind the screen would drop somewhat lower than the water level in front of the screen. In other words, this additional hydrostatic head resulting from the differing water levels compensates for the added head loss of the debris to maintain the volumetric demands of the pump, which remains relatively constant. Because the pit and the pool are at equal atmospheric overpressure, the only force available to move water through a debris bed is the static pressure head in the pool. After the pool level behind the screen drops to the bottom of the screen, the maximum hydrostatic pressure head will have been reached and the subsequent volumetric flow will decrease below the required pump flow, causing pump cavitation.

The effective maximum hydrostatic head loss actually would be less than the difference between the sump-pool level and the bottom of the sump screen. The pressure differential across the debris bed on the screen increases from 0 at the top of the debris bed to the maximum head at the bottom of the screen. Numeric simulations have confirmed that the effective maximum hydrostatic head loss across a debris bed is approximately equal to one-half of the height of the sump pool. To summarize, after the head loss across the sump screen resulting from debris accumulation exceeds the hydrostatic head corresponding to one-half the height of the sump pool, the volumetric flow to the pump decreases below the required flow to the pump and the pump will fail.

In some plants, the sump could be partially submerged at pump switchover but be totally submerged later as the sump reached its full level. This can occur for a number of reasons, including accumulation of CS water, continued melting of ice-condenser reservoirs, and continued addition of refueling water storage tank (RWST) inventory to the containment pool. As the pool depth changes during recirculation, the wetted or submerged area of the sump screens also would change. The depth of the pool also determines the average velocity of water approaching the screen, which, in turn, affects both debris transport to the screen and the pressure drop across the debris bed.

1.4 Description of Postulated Pressurized-Water Reactor Accidents

1.4.1 Overview

This section presents the results of thermal-hydraulic simulations performed to achieve three objectives.²

1. Identify important RCS and containment thermal-hydraulic parameters that influence the generation and/or transport of debris in PWR containments.
2. Determine time-dependent values for these parameters as a function of the assumed system's response (where applicable) by performing plant simulations using NRC-approved computer codes.
3. Use the calculated plant-response information to construct accident progression sequences that form the basis for strainer-blockage evaluations and probabilistic risk evaluations.

Evaluations were made for seven accident scenarios:

1. an LLOCA (cold- and hot-leg breaks),
2. a medium loss-of-coolant accident (MLOCA) (6-in. cold-leg break),
3. a small loss-of-coolant accident (SLOCA) (2-in. cold-leg break),
4. a small-small LOCA (1/4-in. cold-leg break),
5. a pressurizer surge line break,
6. a loss of offsite power with simultaneous failure of feedwater, and
7. inadvertent opening and stuck-open power-operated relief valve (PORV).

Figure 1-3 shows the major steps involved in the calculational effort. These include the following.

- RELAP5/MOD3.2¹⁻³¹ was used for simulating the RCS response to each of the postulated accident sequences. The RELAP5 simulations incorporated realistic initial and boundary conditions and a full representation of a Westinghouse four-loop RCS design. Selected simulations were also performed for Combustion Engineering (CE) plants.

² These results are documented in more detail in Ref. 1-27.

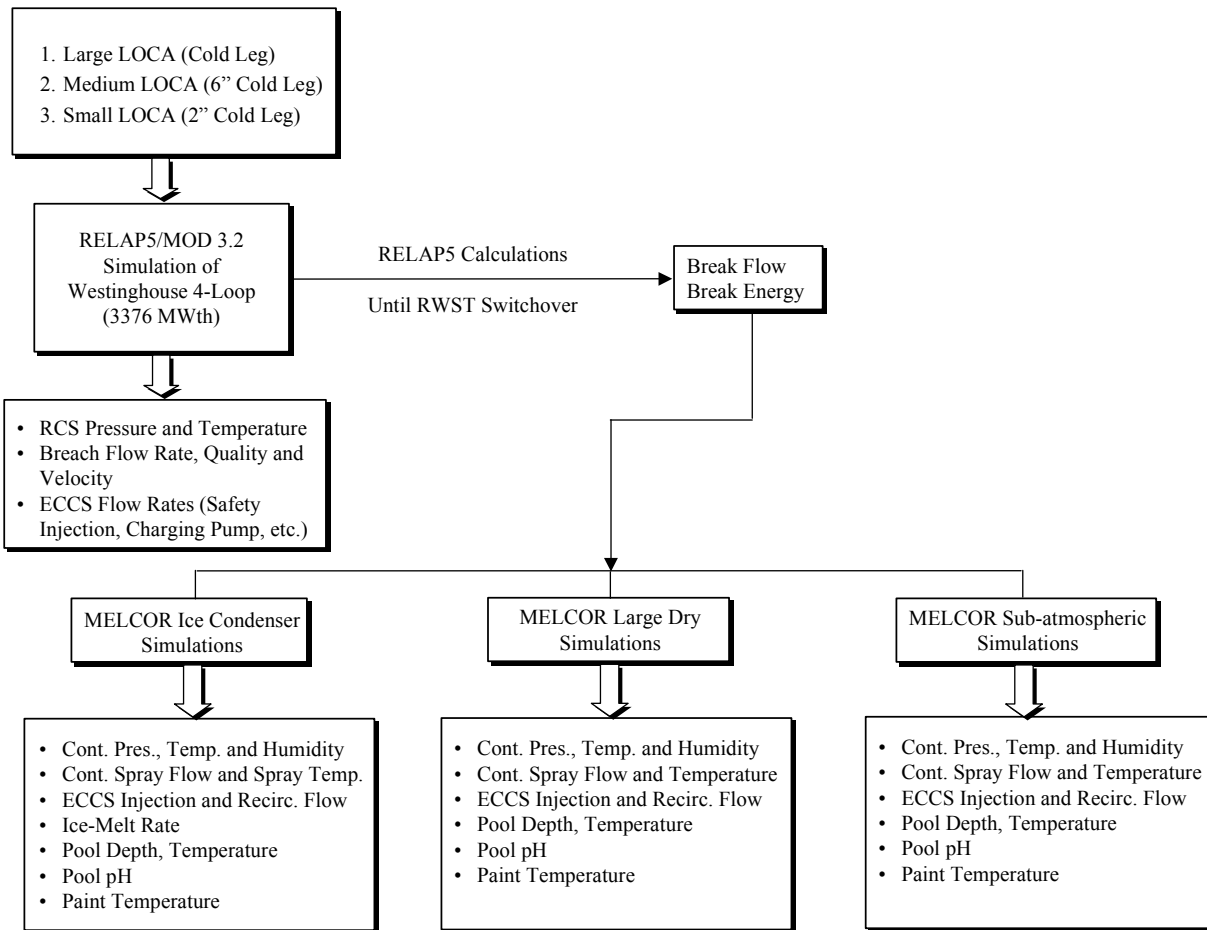


Figure 1-3 Flow Chart of Analysis Process

- MELCOR Version 1.8.2¹⁻³² was used for simulating the response of the ice condenser, large dry, and sub-atmospheric containments to a release of steam/water into the containment as a result of each accident sequence (as predicted by RELAP5).

The parameters tracked for each code simulation are shown in Figure 1-3. These parameters were limited to those that could influence debris generation and transport following a LOCA. A brief description of each of the important parameters and their potential effects is provided in Table 1-1.

Brief discussions of the simulation results are provided in Sections 1.4.2 through 1.4.4 for an LLOCA, an MLOCA, and an SLOCA, respectively. An examination of the data summarized in these sections reveals that

accident progression differs markedly with event type and containment type. The important differences are as follows.

- Time at which blowdown commences and the duration over which blowdown occurs varies considerably with accident type.* In one extreme, the RCS blowdown following an LLOCA commences immediately and terminates within 30 s. The stagnation pressure at the break plane over that time period varies between 2000 and 300 psia. On the other extreme, blowdown following the SLOCA occurs over the first hour of the transient; even after 1 h, it is possible that the pressure vessel remains at pressures as high as 500 psi. Debris-generation estimates must account for these differences, especially for those insulations for which generation is driven by erosion. It is possible that a small-break zone of

Table 1-1 Important Parameters Tracked and Their Relevance

RCS PRESSURE AND TEMPERATURE: The flow through an RCS breach would be choked as long as the RCS temperature (and hence pressure) remains elevated. The critical (choked) flow rate through the breach would depend strongly on upstream pressure and temperature, which define the thermodynamic state of the fluid. The state of the fluid largely determines the expansion characteristics of a two-phase flashing jet.

BREACH FLOW CONDITIONS (FLOW RATE, VELOCITY, AND QUALITY): The destructive potential of a break jet depends strongly on break flow conditions. The velocities of both phases (liquid and vapor) are important here. The values calculated are the velocities at the choke plane. The moisture content of the fluid exiting the breach influences the damage potential of the jet. The quantity calculated here is the ratio of vapor mass flow rate to total mass flow rate at the choke plane.

ECCS SAFETY INJECTION FLOW: The rates of ECCS safety injection determine when the inventory of the RWST would be depleted, requiring switchover to ECCS recirculation through the emergency sump. The timing of switchover is important with regard to debris settling opportunities. Flow patterns in the water pool formed on the floor of the containment would be influenced by injection rates. Injection rates determine accident progression as related to the rate at which the RCS is cooled down.

ECCS RECIRCULATION FLOW: The rate at which flow is recirculated through the emergency sump will determine the flow patterns, velocities, and turbulence levels in the containment pool. The potential for debris transport is governed by these traits.

CONTAINMENT SPRAY FLOW: Containment sprays have the potential to wash settled debris from containment structures and suspended debris from the containment atmosphere down to the containment pool. Whether the sprays are operating or not largely determines the time at which the RWST inventory is expended and the magnitude of the recirculation flow through the emergency sump. The flow patterns and turbulence levels in the containment pool may be affected by where and how the sprays drain.

The potential for containment sprays to influence debris transport is thought to be considerable. As such, it is important to note the large variability in spray activation logic that exists from plant to plant, e.g., containment high-high pressure set points. Additionally, actions taken by the operators to shut containment sprays down would influence debris transport.

CONTAINMENT SPRAY TEMPERATURE: In some plants, recirculated spray water passes through heat exchangers. The heat removal would influence containment pressure and temperature trends. This phenomenon is of particular interest in ice-condenser containments. Therefore, special emphasis was put on modeling RHR heat exchangers and determining spray temperatures as close to reality as possible.

POOL DEPTH AND TEMPERATURE: The available NPSH at the recirculation pumps depends on the depth of the containment pool and its temperature. The velocities, flow patterns, and turbulence levels (and hence debris transport potential) in the pool depend on pool depth.

POOL PH: Basic or acidic tendencies in recirculating water may change the corrosion, dissolution, or precipitation characteristics of metal or degraded metal-based paints in containment. A specific concern is the possible precipitation of ZnOH formed from chemical interaction between zinc (in the zinc-based paints) and water at high temperature. The dissolution/precipitation of ZnOH in water is influenced by the degree of boration.

CONTAINMENT ATMOSPHERIC VELOCITY: The atmospheric velocities generated in the containment in response to an RCS breach determine to what degree generated debris initially disperses within the containment. These are the velocities developed as containment is subjected to the shock and pressurizing effects of the flashing break jet.

PAINT TEMPERATURE: Sustained elevated temperatures may degrade containment paints. An elaborate paint representation model was included in the MELCOR input model.

influence (ZOI) may be characterized by a larger L/D compared with large or medium breaks.³

2. *The magnitude of the ECCS recirculation flow through the emergency sump varies between events.* In the case of an SLOCA, the maximum ECCS flow through the sump during recirculation corresponds to the make-up flow for the high-pressure safety injection (HPSI) and charging pump discharge into the RCS (at about 500 psi) and subsequently leaking into the containment through the breach. On the other hand, following a LLOCA or a MLOCA, the maximum ECCS flow approaches the design flow (which is approximately 11,000 gpm for the cases simulated). The implication is that the potential for debris transport would be higher following an LLOCA than for the SLOCA analyzed. The plant-specific estimates for ECCS recirculation flow for each case can be obtained as follows.

- A generic value⁴ of 10,000 gpm (large break) could be used for most plants, or alternately, the plant response to NRC GL 97-04¹⁻²² may be used.
- A generic value of 2500 gpm (small break) could be used for most plants. A survey of plant data suggests that actual ECCS flow following a SLOCA could vary between 1800 gpm and 4800 gpm, with a median value of 2500 gpm (Ref. 1-26, Volume 2).

3. *A CS actuation is accident-specific and plant-specific.* In an accident where containment fan coolers sufficiently managed containment pressure and temperature to below the engineered safeguard feature (ESF) actuation set point, sprays would not actuate. If the sprays were not used or were used only sparingly, the

length of time that ECCS injection could draw from the RWST would be increased largely. This also would minimize the potential for debris washdown by the cascading spray water. Note that for SLOCA events, sprays were not required for large dry containments whose actuation set points are higher than 10 psi, thereby limiting the maximum flow expected through the sump. Sprays were required for the ice condenser containment, resulting in sump flow rates nearly 4 times that required for the large dry plants. Sprays also are required for many large dry plants (including, but not limited to, sub-atmospheric containments) whose actuation set points are equal to or lower than 10 psi.⁵ This is because of the following:

- In several plants, the chilled water supply to the fan coolers is isolated following the LOCA, which reduces the efficiency of the fan coolers for removing containment heat. [The ultimate heat sink is via the component cooling water (CCW), which may not be sufficiently sized to handle such heat loads.]
- Degradations in fan coolers also may be possible if LOCA debris reaches or deposits on the fan cooler heat exchangers.
- Fan coolers are not safety-class equipment in most PWRs.⁶ For those plants, it is not clear that such fan coolers can be relied on for pressure control for a variety of reasons ranging from the fact that their functionality is not tested for these conditions to the fact that the heat removal source for fan coolers may be isolated as a result of a hi-hi or hi containment pressure set point (differs from containment to containment). However, for plants with safety-class fan coolers, those coolers can be relied upon to cool the containment, e.g., the fan coolers at

³ The ZOI is defined as the zone within which the break jet would have sufficient energy to generate debris of transportable size and form. L/D is a unitless measure of the size of the ZOI, where L is the maximum linear distance from the location of the break to the outer boundary of the ZOI and D is the diameter of the broken pipe.

⁴ The generic values presented here originally were developed for use in the parametric evaluation where plant-specific data were lacking. In plant-specific analyses, plant-specific values should be used where possible.

⁵ A SLOCA simulation was performed assuming fan coolers were not operational. The maximum containment pressure for this calculation was estimated to be approximately 18 psi, as opposed to 6 psi (see Table 1-7) for the case where fan coolers are assumed to operate.¹⁻²⁷

⁶ In the thermal-hydraulic simulations discussed in this section, all plant systems including the fan coolers were assumed to operate as designed.

Combustion Engineering (CE) plants with safety related CCW and safety related power to low speed fans.

The plant estimates for CS recirculation flow for each plant can be obtained as follows.

- A generic value of 6000 gpm can be used for most PWRs or preferably one can use appropriate flow rates applicable to each plant. Individual plant flow is generally not significantly different and thus will not influence the accident outcome.

1.4.2 Large Loss-of-Coolant Accident

The LLOCA simulated was a cold-leg, pump-discharge, double-ended guillotine break (DEGB). The RCS pressure and average temperature before the break were 2250 psia and 570°F. The cold-leg inside diameter was 27.5 in., corresponding to a cross-section area of 4.12 ft². The break was assumed to be instantaneous with a discharge coefficient of unity. A cold-leg break was chosen as the LLOCA event because design-basis accidents typically are cold-leg breaks. With respect to debris generation and transport, any differences between a cold-leg and hot-leg break likely would be small. This is not the case for core response, but with respect to emergency sump blockage, differences between large hot-leg and large cold-leg breaks are probably negligible. This assumption is supported by the results (not presented here) of a supplementary RELAP5 large-hot-leg-break calculation that compares closely with the results of the large-cold-leg-break calculation with respect to break-flow characteristics.

The calculated results for the LLOCA events in large dry and ice condenser containments are provided in Tables 1-2 and 1-3, respectively.⁷ These simulations were used to develop a generic description of LLOCA accident progression in a PWR, both in terms of the system's response and its implications on debris generation and transport. Table 1-4 provides a

⁷Large dry containment LLOCA results are representative of those expected for sub-atmospheric containments as well, with the exception that inside recirculation pump flow for the sub-atmospheric containment would have to be added.

general chronology of events for a PWR LLOCA sequence. Figure 1-4 summarizes key findings to supplement the tabulated results, with further explanation as follows.

1.4.2.1 Reactor Coolant System Blowdown Phase

In this report, the RCS blowdown refers to the event (or process) by which elevated energy in the RCS inventory is vented to the containment as the RCS vents through the breach. Blowdown and the subsequent flashing⁸ in the containment cause rapid decay in the RCS pressure and rapid buildup of containment pressure. Either of these initiates reactor scram.⁹ With delay built-in, it is expected that reactor scram would occur within the first 2 s. It is during RCS blowdown that flow from the break occurs and the highest (and most destructive) energy is released. Therefore, debris generation by jet impingement would be greatest during this time. Also, debris could be displaced from the vicinity of the break as the flashing two-phase break jet expands into the containment. Large atmospheric velocities may develop in the containment, approaching 200 ft/s in the ice condenser containment and 300 ft/s in the large dry containment, as breach effluent quickly expands to all regions of the containment. In the vicinity of the breach, containment structures would be drenched by water flowing from it. Increase in containment pressure also causes immediate automatic actuation of containment sprays, for all plant types, condensing steam and washing structures throughout containment. Spray water drains over and down containment walls and equipment, carrying both insulation and particulate (e.g., dirt and dust) debris to a growing water pool on the containment floor. In most containments, NaOH liquid stored in the spray additive tank (SAT) will be added to the boric acid water to facilitate absorption of iodine that may be released to the containment. Therefore, a secondary CS effect is a potential

⁸Flashing refers to the phenomenon by which the mainly liquid inventory of the RCS turns into a steam and liquid mixture as it is expelled into the containment atmosphere, which is at a significantly lower pressure.

⁹The accident progression in sequences in which scram does not occur is significantly different and will not be discussed in this document.

Table 1-2 Debris Generation and Transport Parameters: LLOCA—Large Dry Containment												
Parameter	Blowdown Phase			Injection Phase			Recirculation Phase					
	0+	20 s	45 s	45 s	15 min	27 min	27 min	2 h	24 h			
RCS pressure at break (psia)	2250	393	55									
RCS temperature at break (°F)	531	291	250	250	173	144	144					
Break flow (lb/s)	7.97e4	1.28e4	4.89e3									
Break flow velocity (ft/s)	296	930	100									
Break flow quality	0	0.25	0.3	0.3	0							
Safety injection (gpm)				11500	11500	11500						
Recirculation flow (gpm)						17500	11800	11800	11800			
Spray flow (gpm)				0	5700	5700	5700	0				
Spray temperature (°F)					105	190	190					
Containment pressure (psig)	0	36	33	33	11.5	7	7	1.5	0			
Containment temperature (°F)	110	305	250	250	190	163	163	115	95			
Pool depth (ft)					2	3.5	3.5	3.5	3.5			
Pool temperature (°F)					212	187	187	125	100			
Pool pH												
Containment atmosphere velocity (ft/s)	282		7									
Containment relative humidity (%)	50	100	100	100	100	90	90	100	100			
Paint temperature (°F)	100			215	240	220	220	145	112			
Peak break flow: 7.97e4 lb/s at 0+ s	Peak break flow velocity: 930 ft/s at 21 s											
Quality at peak break flow: 0	Quality at peak break flow velocity: 0.25											
Peak containment pressure: 36 psig at 20 s	Peak containment atmosphere velocity: 282 ft/s at 0+ s											

Table 1-3 Debris Generation and Transport Parameters: LLOCA—Ice Condenser Containment												
Parameter	Blowdown Phase			Injection Phase			Recirculation Phase					
	0+	20 s	45 s	45 s	10 min	17 min	17 min	2 h	24 h			
RCS pressure at break (psia)	2250	393	55									
RCS temperature at break (°F)	531	291	250	250	200	160	160					
Break flow (lb/s)	7.97e4	1.28e4	4.89e3									
Break flow velocity (ft/s)	296	930	100									
Break flow quality	0	0.25	0.3	0.3	0							
Safety injection (gpm)				11500	11500	11500						
Recirculation flow (gpm)						18000	18000	18000	18000			
Spray flow (gpm)				6400	6400	6400	6400	6400	6400			
Spray temperature (°F)				105	105	97	95	89				
Containment pressure (psig)	0+	14	10.1	10.1	4.5	4.5	3	2				
Containment temperature (°F)	100	168	160	160	103	105	98	100				
Pool depth (ft)				4	8.5	10.75	10.8	10.1				
Pool temperature (°F)				180	157	159	148	126				
Pool pH												
Containment atmosphere velocity (ft/s)	184	18	1									
Containment relative humidity (%)	0	50	100	100	80	96	97	98				
Paint temperature (°F)	100	106	112	112	113	112	90	90				
Peak break flow: 7.97e4 lb/s at 0+ s	Peak break flow velocity: 930 ft/s at 21 s											
Quality at peak break flow: 0	Quality at peak break flow velocity: 0.25											
Peak containment pressure: 14.4 psig at 15 s	Peak containment atmosphere velocity: 184 ft/s at 0+ s											

Table 1-4 PWR LLOCA Sequences					
Time after LOCA (s)	Accum. (SI Tanks)	HPSI	LPSI	CS	Comments
0-1	Reactor scram. Initially high containment pressure. Followed by low pressure in the pressurizer. Debris generation commences caused by the initial pressure wave, followed by jet impingement. The blowdown flow rate is large. But mostly saturated water. Quality ≤ 0.05 . Saturated jet-models are appropriate. SNL/ANSI Models suggest wider jets, but pressures decay rapidly with distance				
2		Initiation signal	Initiation signal	Initiation signal	Initiation signal from low pressurizer pressure or high containment pressure/temp
5	Accumulator injection begins	Pumps start to inject into vessel (bypass flow out)	Pumps start (RCS P > pump dead head)	Pump start and sprays on	In cold-leg break, ECCS bypass is caused by counter-current injection in the downcomer. Hot-leg does not have this problem.
10	The blowdown flow rate decreases steadily from $\sim 20,000$ lb/s to 5000 lb/s. Cold-leg pressure falls considerably to about 1000 psia. At the same time, effluent quality increases from 0.1 to 0.5 (especially that from steam generator side of the break). Flow is vapor continuum with water droplets suspended in it. Saturated water or steam jet-models are appropriate. At these conditions, SNL/ANSI models show that jet expansion induces high pressures far from the break location.				
25		End of bypass; HPSI injection			
25-30	Break velocity reaches a maximum > 1000 ft/s. Quality in excess of 0.6. Steam flow at less than 500 lb/s. Highly energetic blowdown is probably complete. However, blowdown continues as residual steam continues to be vented.				
35	Accumulators empty		Vessel LPSI ramps to design flow.		
40	Blowdown is terminated, and therefore, debris generation is complete. Blowdown pressure at the nozzle less than 150 psi. Debris would be distributed throughout the containment. Pool is somewhat turbulent. Height < 1 ft.				
55-200	Reflood and quenching of the fuel rods ($T_{max} \sim 1036$ °F). In cold-leg break, quenching occurs between 125 and 150 s. In the case of hot-leg break, quenching occurs between 45 and 60 s ($T_{max} \sim 950$ °F).				
200-1200	Debris added to lower containment pool by spray washdown drainage and break washdown. The containment floor keeps filling. No directionality to the flow. Heavy debris may settle down.				
1200	RWST low level indication received by the operator. Operator prepares to turn on ECCS in sump recirculation mode. Actual switchover when the RWST low-low level signal is received.				
1500		Switch suction to sump	Switch suction to sump	Terminate or to sump	Many plants have containment fan coolers for long-term cooling.
1500-18000	Debris may be brought to the sump screen. Buildup of debris on the sump screen may cause excessive head loss. Containment sprays may be terminated in large dry containments at the 2-h mark.				
>36000		Switch to hot-leg recirculation.	Switch to hot-leg recirculation		

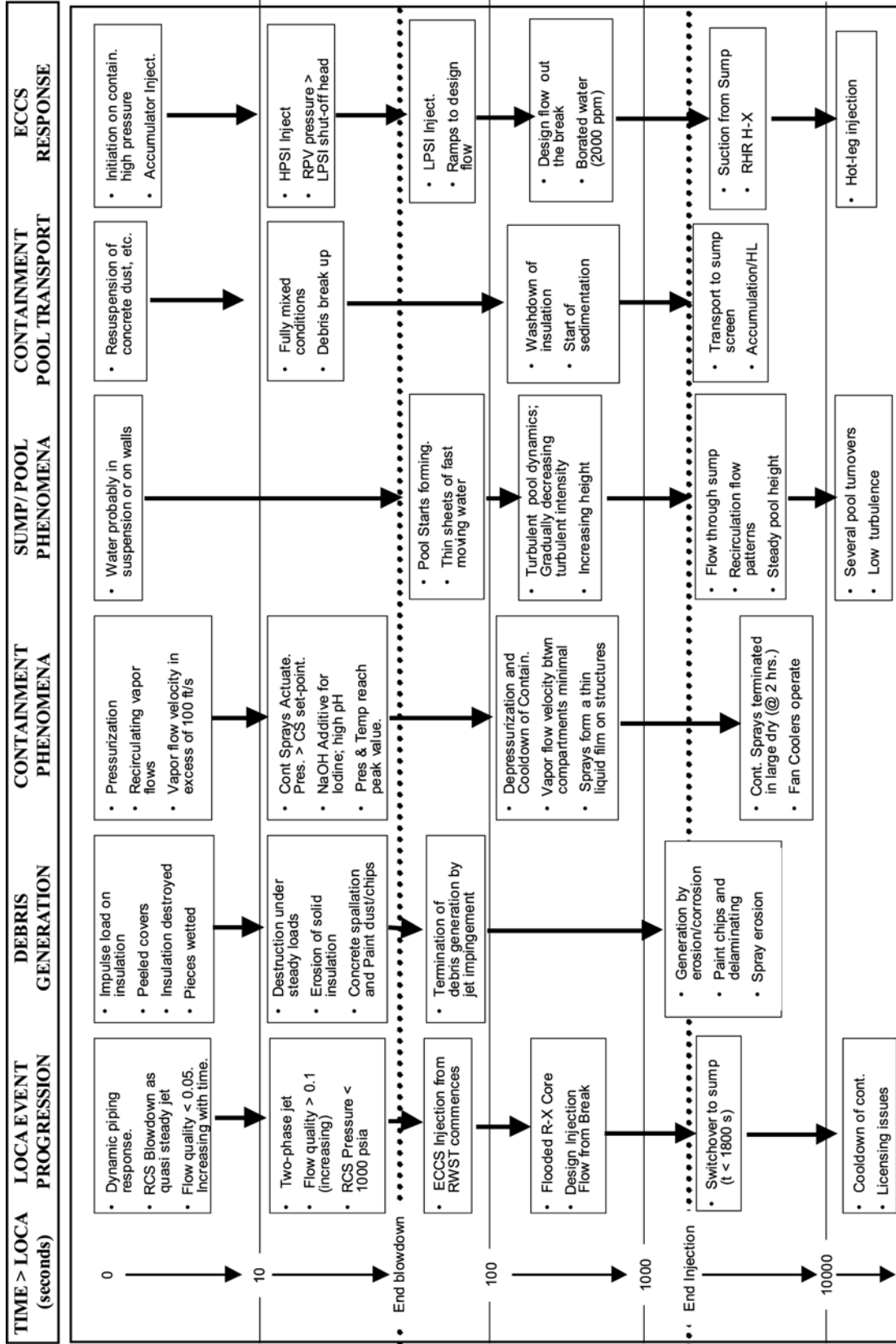


Figure 1-4 PWR LLOCA Accident Progression in a Large Dry Containment

increase in pool pH, which in turn, could play a role in particulate debris precipitation caused by the interaction of hot, borated, high-pH water with zinc and aluminum surfaces. The rates of these reactions are used in many Final Safety Analysis Reports (FSARs) to estimate the hydrogen source term and evaluate the potential for hydrogen accumulation in the containment.

Accurate characterizations of conditions that exist during the blowdown phase are important for estimating debris generation and, to some degree, debris transport. For LLOCA events, RCS blowdown occurs over a period of approximately 30 s, during which vessel pressure goes from 2250 psia to near containment pressure. During this time, the reactor pressure vessel thermodynamic conditions undergo a rapid change. Initially, the break flow is subcooled at the break plane and flashes as it expands into the containment. Within 2 s, the vessel pressure drops below 2000 psi and the flow in the pipes and the vessel becomes saturated. Thereafter, the break flow quality is equal to or higher than 10%. On the other hand, the void fraction increases to approximately 1.0, clearly indicating that the water content would be dispersed in the vapor continuum in the form of small droplets. The corresponding flow velocity at the break plane reaches a maximum of about 930 ft/s. This clearly indicates that jets would reach supersonic conditions during their expansion upon exiting the break. Based on these simulations, the energetic blowdown terminates within 25–30 s as the vessel pressure decreases to near 150 psig. Although steam at high velocities continues to exit, the stagnation pressure is not sufficient to induce very high pressures at distances far from the break. Thus, it is reasonable to assume that debris generation following an LLOCA occurs within the first minute. (Note: Debris generation by non-jet-related phenomena may occur over a prolonged period of time as a result of high temperature, humidity, and sprays.) The RCS blowdown continues until the vessel pressure falls below the shut-off head for the accumulator tank,¹⁰ the HPSI, and the low-pressure safety injection (LPSI). This causes increasingly large quantities of cooler, borated RWST water to quench the core and terminate blowdown.

¹⁰The accumulators are also known as safety injection tanks in some designs.

1.4.2.2 Emergency Core Cooling System Injection Phase

The injection phase refers to the period during which the RCS relies on safety injection, drawing on the RWST for decay heat removal. In the case of an LLOCA, the injection phase immediately succeeds the initial RCS blowdown. During this phase, core reflood is accomplished and quasi-steady conditions are arrived at in the reactor, where decay heat is removed continually by injection flow. In ice condenser containments, the ice condenser compartment doors open and the recirculation fans move the containment atmosphere through the ice condensers. Opportunities would exist for debris to settle in the pool during this relatively quiescent time before ECCS recirculation. Containment pressure would decrease from its maximum value (reached in the blowdown phase). The injection phase is considered to be over when the RWST inventory is expended and switchover to sump recirculation is initiated.

Accurate characterization of conditions that exist during injection phase may be important for estimating the quantity of debris transported from the upper containment to the pool and for estimating the quantity of debris that may remain in suspension. Following the initial break, safety injection (SI) begins immediately with the combined operation of the accumulators, the charging pumps, the HPSI pumps, and the LPSI (RHR) pumps. The SI flow approaches the design value (which is 11,500 gpm in the plant simulated) in about a minute and continues at that rate until switchover. Current simulations did not take credit for potential reduction in the injection flow (e.g., system-failure scenarios). Containment sprays continue to operate; spray water and water exiting the break will cause washdown of debris from the upper portions of the containment to the pool on the containment floor.

It has been determined that large quantities of water would be introduced into the containment within a few minutes following an LLOCA. As a result, the water-pool depth on the containment floor increases steadily. In the case of a large dry containment, the peak pool height is reached at the end of the injection phase; in an ice-condenser containment, the peak value is reached several hours into the accident after all the ice has melted.

1.4.2.3 Recirculation Phase

After the RWST inventory is expended, the ECCS pumps would be realigned to take suction from the emergency sump in the containment floor. This would begin the ECCS recirculation phase, in which water would be pulled from the containment pool, passed through heat exchangers, and delivered to the RCS, where it would pick up decay heat from the reactor core, flow out the breach, and return to the containment pool. Pool depth would reach a steady state during the recirculation phase, and containment pressure and temperature would be decreasing gradually. It would be during this accident phase that the potential would exist for debris resulting from an RCS breach (or residing in containment beforehand) to continue to be transported to the containment emergency sump. Because of the suction from the sump, this pool debris may accumulate on the sump screens, restrict flow, and either reduce available NPSH or starve the ECCS recirculation pumps.

The primary observation regarding the RCS and containment conditions during the recirculation phase is that the sump flow rate reaches the design capacity of all the pumps, which in the plants analyzed is 17,500 gpm for the large dry and sub-atmospheric containments and 18,000 gpm for the ice condenser containment.

1.4.3 Medium Loss-of-Coolant Accident

The MLOCA simulated was 6-in. in diameter circular hole, corresponding to a cross-section area of 0.1963-ft², in a cold leg downstream of the reactor coolant pump (RCP). The hole became full-sized instantaneously. It was situated on the side of the cold leg and centered halfway up. A discharge coefficient of unity was used, which made these simulations very conservative. The cold-leg location of the hole was chosen arbitrarily and is not expected to be a determining factor in the simulation results.

The calculated results for the MLOCA events in large dry and ice condenser containments are provided in Tables 1-5 and 1-6, respectively. Figure 1-5 presents the time scales associated with the occurrence of some of the events. The following sections highlight the differences between the MLOCA event and the LLOCA event described above.

1.4.3.1 Reactor Coolant System Blowdown Phase

In the case of an MLOCA, RCS blowdown occurs over a prolonged period (3 min) compared with that in an LLOCA. Blowdown starts at 0 s when the vessel is at 2250 psia and terminates as the RCS pressure and liquid subcooling decrease. Peak break flow for the MLOCA is at least a factor of 15 less than that observed for the LLOCA. In addition, the resulting vapor velocity in the containment peaks around 30 ft/s, as opposed to 200–300 ft/s for the LLOCA. These observations suggest less severe debris generation and transport caused by the LOCA jet itself. Another significant observation is that after MLOCAs, the exit flow at the break plane remains subcooled throughout the blowdown, at least until the vessel pressure falls to a point where blowdown would have little effect on debris generation. This may affect the ZOI over which debris would be generated.

1.4.3.2 Emergency Core Cooling System Injection Phase

There are three fundamental differences between an MLOCA and an LLOCA.

- ECCS injection begins before termination of the RCS blowdown. Initiation of injection occurs after 20–60 s, whereas the blowdown phase is not terminated until approximately 180 s.
- The LPSI does not inject significant quantities of water into the core in the short term. The LPSI (or RHR) pumps start injecting into the core at about 15 min.
- In the plants analyzed, spray actuation occurs shortly after ECCS injection begins (approximately 3 min, right around the termination of the RCS blowdown).

1.4.3.3 Recirculation Phase

The recirculation-phase accident characteristics for the MLOCA are similar to those described in Sec. 1.4.2.3 for the LLOCA. The sump recirculation flow rate for each plant analyzed was approximately half of that for the LLOCA simulation. The containment pressure and temperature increased following the ECCS switchover to the recirculation mode at 57 min. due to an increase in the spray water temperature, from approximately 105° to 150°F.

Table 1-5 Debris Generation and Transport Parameters: MLOCA—Large Dry Containment										
Parameter	Blowdown Phase			Injection Phase			Recirculation Phase			
	0+	30 s	180 s	20 s	15 min	57 min	57 min	2 h	24 h	
RCS pressure at break (psia)	2250	900	508							
RCS temperature at break (°F)	537	521	392		330	274	274			
Break flow (lb/s)	4940	1670	1000							
Break flow velocity (ft/s)	510	190	108							
Break flow quality	0	0	0		0.03	0.03	0.03	0	0	
Safety injection (gpm)				885	2500	2500				
Recirculation flow (gpm)							8250	2550	2550	
Spray flow (gpm)		0	5700		5700	5700	5700	0		
Spray temperature (°F)			105		105	150	150	150		
Containment pressure (psig)	0	6	9.5		5	3	3	4.2	1.5	
Containment temperature (°F)	110	170	182		160	140	140	148	120	
Pool depth (ft)					0.9	3.3	3.3	3.3	3.3	
Pool temperature (°F)					170	145	145	147	125	
Pool pH										
Containment atmosphere velocity (ft/s)	35	10	5							
Containment relative humidity (%)	50	100	100		98	98	98	98	100	
Paint temperature (°F)	110		160		175	160	160	155	121	
Peak break flow:	4940 lb/s at 0+ s									
Quality at peak break flow:	0									
Peak containment pressure:	10.2 psig at 2 min									
Peak break flow velocity:	510 ft/s at 0+ s									
Quality at peak break flow velocity:	0									
Peak containment atmosphere velocity:	35 ft/s at 0+ s									

Table 1-6 Debris Generation and Transport Parameters: MLOCA—Ice Condenser Containment											
Parameter	Blowdown Phase			Injection Phase			Recirculation Phase				
	0+	30 s	180 s	20 s	15 min	34 min	34 min	2 h	24 h		
RCS pressure at break (psia)	2250	900	508								
RCS temperature at break (°F)	537	521	392		330	300					
Break flow (lb/s)	4940	1670	1000								
Break flow velocity (ft/s)	510	190	108								
Break flow quality	0	0	0		0.03	0.03		0			
Safety injection (gpm)				885	2500	2500					
Recirculation flow (gpm)							9000	9000	9000		
Spray flow (gpm)		0	6400		6400	6400	6400	6400	6400		
Spray temperature (°F)			105		105	105	86.5	84			
Containment pressure (psig)	0+	9.8	7.8		4	4	1.8	1.4			
Containment temperature (°F)	100	145	151		110	110	87	90			
Pool depth (ft)					4	7.9	8	9.6			
Pool temperature (°F)					150	146	117	104			
Pool pH											
Containment atmosphere velocity (ft/s)	30	2.5	1.25								
Containment relative humidity (%)	0	10	40		80	97	97	98			
Paint temperature (°F)	100	101	125		130	125	125	95	90		
Peak break flow: 4940 lb/s at 0+ s Quality at peak break flow: 0 Peak containment pressure: 11 psig at 55 s Peak break flow velocity: 510 ft/s at 0+ s Quality at peak break flow velocity: 0 Peak containment atmosphere velocity: 30 ft/s at 0+ s											

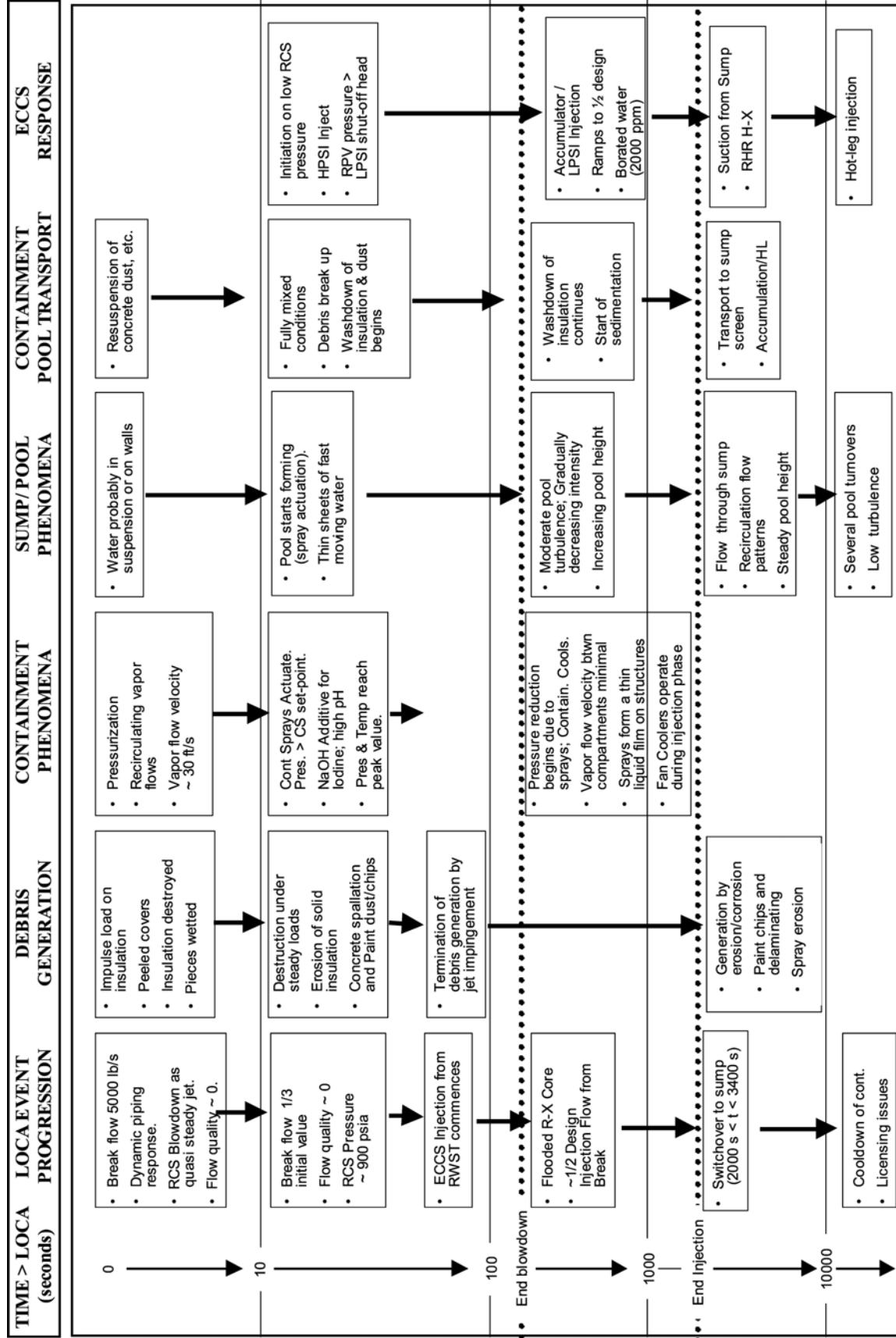


Figure 1-5 PWR MLOCA Progression in a Large Dry Containment

1.4.4 Small Loss-of-Coolant Accident

The SLOCA studied was a 2-in. diameter, circular hole in a cold leg, corresponding to a cross-section area of 0.0218-ft², downstream of the RCP.¹¹ The hole became full-sized instantaneously. It was situated on the side of the cold leg and centered halfway up. A conservative discharge coefficient of unity was defined. The cold-leg location of the hole was chosen arbitrarily and is not expected to be a determining factor in the simulation results. The 2-in. specification of this hole was made with the expectation that the RCS pressure would stabilize above the accumulator pressure such that the accumulators would not inject.

The calculated results for the SLOCA events in large dry, ice condenser, and sub-atmospheric containments are provided in Tables 1-7 through 1-9, respectively. Figure 1-6 presents the time scales associated with the occurrence of some of the events.

1.4.4.1 Reactor Coolant System Blowdown Phase

RCS blowdown in the case of an SLOCA occurs over a prolonged period (60 min). Blowdown starts at 0 s when the vessel is at 2000 psia and terminates mainly as the RCS pressure and liquid subcooling decrease. Peak break-flow velocities for the SLOCAs are a factor of 30 less than those for the LLOCA and a factor of 2 less than those for the MLOCA. Containment atmosphere velocities are a factor of 30–60 less than those for the LLOCA and a factor of 2 less than those for the MLOCA. Another significant observation is that following SLOCAs, the exit flow at the break plane remains subcooled throughout the blowdown (at least until the vessel pressure falls to a point where blowdown would have little effect on debris generation). This may affect the ZOI over which debris would be generated.

1.4.4.2 Emergency Core Cooling System Injection Phase

There are fundamental differences between an SLOCA and an LLOCA.

¹¹The study also simulated a 1.75-in. break. The results were found to be very similar to the 2-in. break.

- The LPSI does not inject into the core at all; the HPSI and charging pumps are sufficient to make up for lost inventory.
- Actuation of containment sprays is highly plant-specific and may not be needed at all. In the large dry containment plant analyzed (which has a CS actuation set point of 9.5 psig), spray operation is not required.¹² Spray actuation is seen after 30 min in the ice condenser simulation and after 15 min in the sub-atmospheric plant. Even then, the operator may terminate sprays during the SLOCA event to prolong RWST availability and rely on fan coolers (or the ice condenser) for decay heat removal from the containment. Note that washdown of debris from the upper containment to the floor pool may be limited to more localized areas (near the break) for plants in which containment sprays are not required. As noted in Section 1.4.1, some plants, such as CE plants, have containment heat removal capability that can be relied upon to cool the containment indirectly without spray cooling.
- Paint is exposed to significantly higher peak temperatures following a LLOCA than it would be following a SLOCA.

1.4.4.3 Recirculation Phase

The recirculation-phase accident characteristics for the SLOCA are similar to those described in Sec. 1.4.2.3 for the LLOCA. The primary difference is that the required flow rates for the SLOCA are significantly less than those for the LLOCA (as low as 2500 gpm for plants in which containment sprays do not actuate). The paint temperatures for paint on thin steel remains a few degrees hotter in the long-term for a SLOCA compared with a LLOCA, but the paint temperatures would be about the same for paint on concrete surfaces.

1.4.5 Other Plant Design Features That Influence Accident Progression

Other plant design features (beyond those previously discussed) may influence the debris-

¹²Again, the results presented here are for an accident scenario in which fan coolers operate. Other calculations suggest a peak containment pressure during an SLOCA in a large-dry containment could reach values nearing 18 psig if fan coolers fail to operate.¹⁻²⁷

Table 1-7 Debris Generation and Transport Parameters: SLOCA—Large Dry Containment

Parameter	Blowdown Phase			Injection Phase			Recirculation Phase		
	0+	30 min	1 h	60 s	2 h	3 h	3 h	12 h	24 h
RCS pressure at break (psia)	2250	605	512						
RCS temperature at break (°F)	538	354	371		270	236	236		
Break flow (lb/s)	550	343	300						
Break flow velocity (ft/s)	320	320	320						
Break flow quality	0	0	0						
Safety injection (gpm)				1500	2500	2500	2500	2500	2500
Recirculation flow (gpm)									
Spray flow (gpm)	Sprays not required								
Spray temperature (°F)									
Containment pressure (psig)	0	5	5		4	3	3	1	0.75
Containment temperature (°F)	110	160	160		150	140	140	115	110
Pool depth (ft)			0.8		1.5	2.25	2.25	3	3
Pool temperature (°F)			157		157	150	150	125	118
Pool pH									
Containment atmosphere velocity (ft/s)	9	4	4						
Containment relative humidity (%)	50	100	100		100	100	100	100	100
Paint temperature (°F)	100	160	160		157	153	153	127	117
Peak break flow: 550 lb/s at 0+ s Quality at peak break flow: 0 Peak containment pressure: 6 psig at 38 min Peak break flow velocity: 320 ft/s at 0+ Quality at peak break flow velocity: 0 Peak containment atmosphere velocity: 9 ft/s at 20 s									

Table 1-8 Debris Generation and Transport Parameters: SLOCA—Ice Condenser Containment

Parameter	Blowdown Phase			Injection Phase			Recirculation Phase		
	0+	30 min	1 h	60 s	15 min	35 min	35 min	5 h	24 h
RCS pressure at break (psia)	2250	605	512						
RCS temperature at break (°F)	538	354	371		391	362			
Break flow (lb/s)	550	343	300						
Break flow velocity (ft/s)	320	320	320						
Break flow quality	0	0	0						
Safety injection (gpm)				1500	2500	2500			
Recirculation flow (gpm)							9000	9000	9000
Spray flow (gpm)		6400	6400	0	6400	6400	6400	6400	6400
Spray temperature (°F)		105	91		105	105	91	87.5	86
Containment pressure (psig)	0+	4.1	3.6	3.4	4.4	4.2		2.25	1.8
Containment temperature (°F)	100	111	96.5	94	112	110	110	92	95
Pool depth (ft)		5.5	6.75		2.5	6.5	6.5	9	8.9
Pool temperature (°F)		137	132		137	137	137	120	114
Pool pH									
Containment atmosphere velocity (ft/s)	2.9	0.7	0.7						
Containment relative humidity (%)	0	97	97	6	100	97	97	97	97
Paint temperature (°F)	100	110	104	100	106	110	110	92	96
Peak break flow: 550 lb/s at 0+ s	Peak break flow velocity: 320 ft/s at 0+								
Quality at peak break flow: 0	Quality at peak break flow velocity: 0								
Peak containment pressure: 4.4 psig at 15 min	Peak containment atmosphere velocity: 2.9 ft/s at 23 s								

Table 1-9 Debris Generation and Transport Parameters: SLOCA—Sub-Atmospheric Containment

Parameter	Blowdown Phase			Injection Phase			Recirculation Phase		
	0+	30 min	1 h	60 s	1 h	3 h	3 h	12 h	24 h
RCS pressure at break (psia)	2250	605	512						
RCS temperature at break (°F)	538	354	371		270	236	236		
Break flow (lb/s)	550	343	300						
Break flow velocity (ft/s)	320	320	320						
Break flow quality	0	0	0						
Safety injection (gpm)				1500	2500	2500			
Recirculation flow (gpm)							2500	2500	2500
Spray flow (gpm)					9000	9000	9000	9000	9000
Spray temperature (°F)					105	150	150	125	120
Containment pressure (psig)	0	5	5		4	3	3	1	0.75
Containment temperature (°F)	110	160	160		150	140	140	115	110
Pool depth (ft)			0.8		1.5	2.25	2.25	3	3
Pool temperature (°F)			157		157	150	150	125	118
Pool pH									
Containment atmosphere velocity (ft/s)	9	4	4						
Containment relative humidity (%)	50	100	100		100	100	100	100	100
Paint temperature (°F)	100	160	160		157	153	153	127	117
Peak break flow: 550 lb/s at 0+ s	Peak break flow velocity: 320 ft/s at 0+								
Quality at peak break flow: 0	Quality at peak break flow velocity: 0								
Peak containment pressure: 6 psig at 38 min	Peak containment atmosphere velocity: 9 ft/s at 20 s								

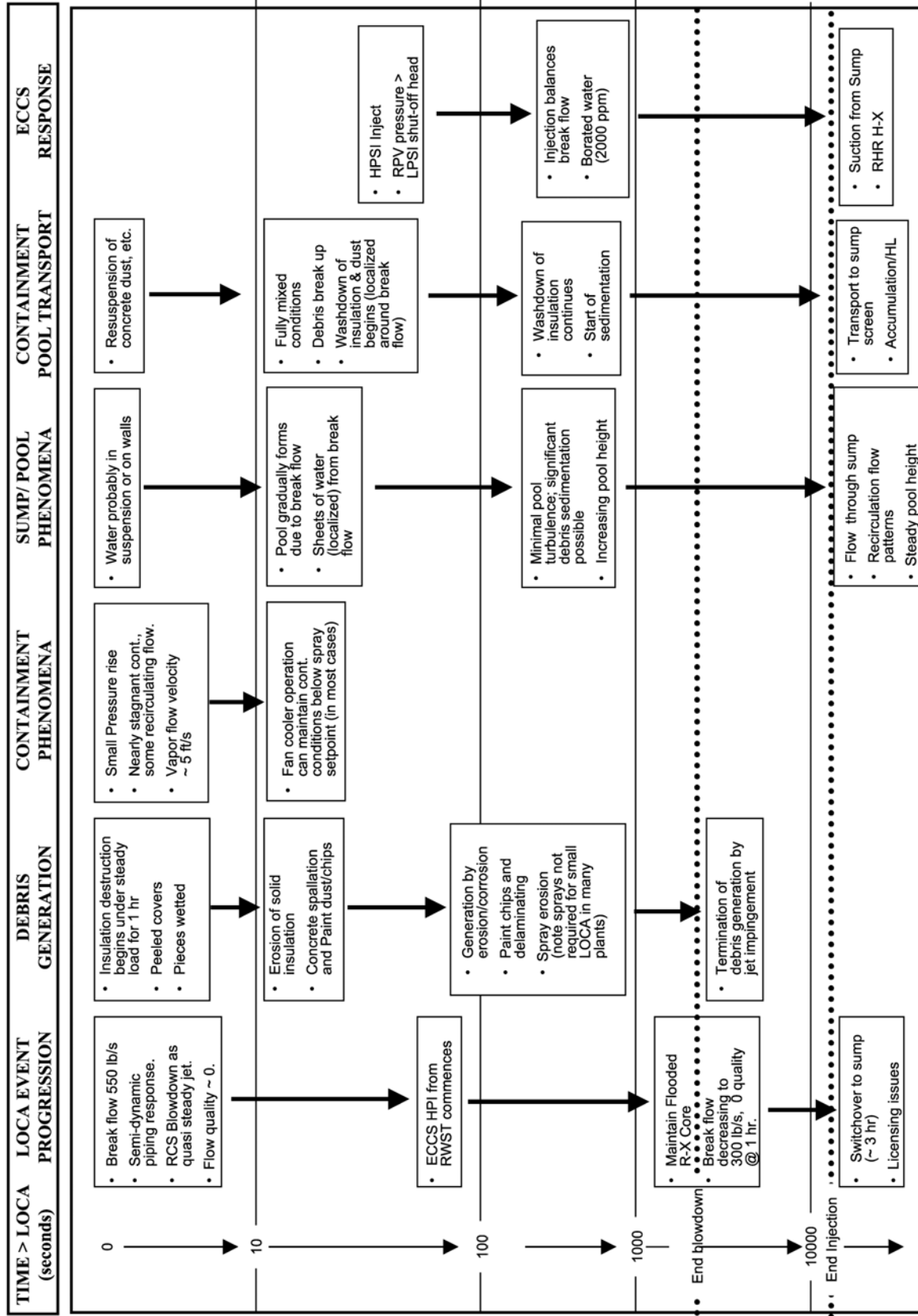


Figure 1-6. PWR SLOCA Accident Progression in a Large Dry Containment

related accident progression. For example, in many plants, heat exchangers are installed directly in the core-cooling recirculation flow paths to ensure that the water is cooled before it is returned to the core. However, in some plants, the core cooling recirculation systems do not have dedicated heat exchangers and instead make indirect use of heat exchangers from other systems (i.e., CS) to ensure that heat is removed from the reactor coolant. Examples of plants where core cooling makes indirect use of heat exchangers from CS includes the plants with sub-atmospheric containments and CE plants. For these types of plants, successful core cooling during recirculation may require (1) direct sump flow from the core cooling system and (2) sump recirculation cooling from the CS system.

For plants with sub-atmospheric containments, switchover for the set of “inside” recirculation spray pumps is performed quickly (approximately 2 min), whereas the switchover for ECCS pumps and CS pumps is considerably longer (on the order of 30 min or more depending on LOCA type). The relatively quick switchover of the inside recirculation spray pumps is accomplished to minimize containment pressure and temperature. The inside recirculation spray system is equipped with a heat exchanger, and it appears that its actuation is credited in estimating the NPSH margin for the ECCS and CS system during the recirculation phase.

Recovery from a stuck-open PORV may be possible at many plants through operator actions to close the associated block valve. The need for sump recirculation could be avoided by this action.

The containment structures are sufficiently robust that failure of CS is not expected to cause containment failure from overpressure.

1.5 Description of Relevant Plant Features that Influence Accident Progression

Some general conclusions regarding important plant features that influence accident outcome

are listed below. The primary source for this information is the PWR plant survey published in 2002.¹⁻²⁶

Sump Design and Configurations

- The ECCS and/or CSS pumps in nearly one-third of the PWR plants surveyed have an NPSH margin less than 2 ft-water, and another one-third have an NPSH margin between 2-ft water and 4-ft water. In general, PWR sumps have low NPSH margins compared with the head loss effects of debris accumulation on the sump screen.
- PWR sump designs vary significantly, ranging from horizontal screens located below the floor elevation to vertical screens located on pedestals. The sump-screen surface areas vary significantly from unit to unit, ranging from 11 ft² to 700 ft² (the median value is approximately 125 ft²). Some plants employ curb-like features to prevent heavier debris from accumulating on the sump screen, and some do not have any noticeable curbs.
- In 19 PWR units, the sump screen would not be completely submerged at the time that ECCS recirculation starts. The mode of failure is strongly influenced by sump submergence.
- Sump-screen clearance size varies considerably. A majority of the plants used a sump-screen opening size of 0.125 in., reportedly to ensure that the maximum size of the debris that can pass through the sump screen is less than the smallest clearance in the RCS and the CSS. However, 26 PWR units indicated that sump-screen clearance is higher than 0.125 in., reaching up to 1 in. Two units reported not having fine screens, other than the standard industrial grating used to filter out very large debris.

Sources and Locations of Debris

- U.S. PWRs employ a variety of types of insulation and modes of encapsulation, ranging from non-encapsulated fiberglass to fully encapsulated stainless steel RMI. A significant majority of PWRs have fiberglass and calcium-silicate insulations in the containment, either on primary piping or on

supporting systems.¹³ The types of fibrous insulation varied significantly, but much of it is in the form of generic low-density fiberglass (LDFG) and mineral wool. It appears that many of the newer plants (or plants replacing steam generators) have been replacing RMI insulation on the primary systems with “high-performance” fiberglass. In general, the smaller pipes and steam generators are more likely to be insulated with fiberglass and calcium-silicate than the reactor pressure vessel or the hot leg or cold leg. Other sources of fibrous materials in the containment for some plants include up to approximately 13,000 ft³ of filter media on the air-handling units and up to 1500 ft³ of fibrous insulation (e.g., Kaowool) used as fire barrier materials. Given that (a) very small quantities of fibrous insulation would be necessary to induce large pressure drops across the sump screens (less than 10 ft³) and (b) most plants have comparatively very large inventories of fibrous insulation, it is clear that plant-specific analyses are necessary before the recirculation sumps of any particular plant can be declared safe with respect to screen blockage.

- Other sources of debris in the PWR containments include cement dust and dirt (either present in the containment *a priori* or generated by a LOCA), particulate insulations used on the fire barriers (e.g., Marinite), failed containment coatings (a medium-sized PWR has approximately 650,000 ft² of coated surfaces in the containment), and precipitants (zinc and aluminum precipitation by-products).¹⁴ Estimates for this type of debris range from 100 lb to several 1000 lb; either of these bounds would result in very large head losses when combined with fibrous material.

¹³About 40 PWR units have in excess of 10% of the plant insulation in the form of fiberglass and another 5–10% in the form of calcium-silicate. A typical plant has approximately 7500 ft³ of insulation on the primary pipes and supporting systems pipes that are in close proximity to the primary pipes.

¹⁴PWR DBAs evaluate the potential for precipitation of aluminum and zinc when they are subjected to high-pH, hot, borated water because these chemical reactions generate H₂.

Containment Features Affecting Debris Transport

- CS set points typically are defined based on LLOCA and equipment qualification considerations. Consequently, sprays may not (automatically) actuate during SLOCAs¹⁵ because of the lower peak containment pressures associated with SLOCAs. CS actuation following an SLOCA event plays an important role in the transport of debris to the sump, and at the same time, it affects the timing of sump failure.¹⁶ Set points for CS actuation vary considerably and span a wide range: 2.8 psig to 30 psig. Consistently lower values are observed in sub-atmospheric and ice condenser containment designs, as would be expected. Nevertheless, values at or below 10 psig¹⁷ are observed for large dry containments, as well.

1.6 Regulatory Considerations

Federal regulations were established to govern the design and operational aspects of nuclear power reactors that affect the safety of those plants. These regulations are codified in the CFR. Title 10¹⁻⁸ of the CFR deals with energy and Part 50 of Title 10¹⁻⁸ consists of regulations promulgated by the NRC to provide for the licensing of production and use of facilities. The NRC published RG documents to guide the nuclear power industry to compliance with the regulations. Regulations and regulatory guidance applicable to the strainer blockage

¹⁵Fan cooler response to LOCAs also plays a vital role in determining spray actuation following SLOCA. These concerns are not applicable to LLOCAs or MLOCAs, where automatic actuation of sprays is expected in every plant.

¹⁶The drainage of the spray water from the upper reaches of the containment down to the containment sump could transport substantial quantities of debris to the sump that otherwise would likely remain where deposited following the RCS depressurization (i.e., the containment sprays would substantially increase the fraction of debris transported to the sump screens over the fraction that would be transported without spray operation).

¹⁷The 10-psig set point is important because MELCOR simulations showed that if both fan coolers in a large dry containment are not operating at full capacity, containment pressure could exceed 10 psig for breaks ≥ 2 in.¹⁻²⁷

issue are summarized in Sections 1.6.1 and 1.6.2, respectively.

1.6.1 Code of Federal Regulations

This section provides a description of the regulations that apply to the strainer blockage issue. Title 10 of the CFR¹⁻⁸ provides the authority to the NRC to regulate nuclear power plants. Section 50.46, "Acceptance Criteria for Emergency Core Cooling Systems for Light-Water Nuclear Power Reactors," of 10 CFR¹⁻⁸ requires that licensees of a BWR or PWR design their ECCS systems to meet five criteria. Specifically, the rule provides acceptance criteria for peak cladding temperature, maximum cladding oxidation, maximum hydrogen generation, coolable core geometry, and long-term cooling. The long-term cooling criterion states, "After any calculated successful initial operation of the ECCS, the calculated core temperature shall be maintained at an acceptably low value and decay heat shall be removed for the extended period of time required by the long-lived radioactivity remaining in the core." Licensees are required to demonstrate this capability while assuming the most conservative (worst) single failure. Some licensees may credit CSSs in the licensing basis for radioactive source-term and pressure reduction. The capability of the ECCS and safety-related CSS pumps to fulfill the criteria of limiting the peak cladding temperature and to provide long-term cooling over the duration of the postulated accident could be seriously compromised by the loss of adequate NPSH and the resulting cavitation. Operational experience and detailed analysis demonstrated that excessive buildup of debris from thermal insulation, corrosion products, and other particulates on ECCS pump strainers is highly likely to cause a common-cause failure of the ECCS thereby preventing the ECCS from providing long-term cooling following a LOCA. Therefore, Section 50.46 clearly applies to the strainer blockage issue, and licensees must resolve this issue for their respective plants in order to ensure compliance with the regulations.

General Design Criteria (GDC) 35, 36, 37, 38, 39, and 40 in Appendix A to 10 CFR Part 50¹⁻⁸ require appropriate design, inspectability, and testability of the ECCS and the containment heat

removal systems.¹⁸ These GDC establish minimum requirements for the principal design criteria for water-cooled nuclear power plants similar in design and location to plants for which the NRC has issued construction permits. The GDC also are considered to be generally applicable to other types of nuclear power units and are intended to provide guidance in establishing the principal design criteria for such other units. Specifically, these criteria state the following.

Criterion 35 – Emergency core cooling. A system to provide abundant emergency core cooling shall be provided. The system safety function shall be to transfer heat from the reactor core following any loss of reactor coolant at a rate such that (1) fuel and clad damage that could interfere with continued effective core cooling is prevented and (2) clad metal-water reaction is limited to negligible amounts. Suitable redundancy in components and features, and suitable interconnections, leak detection, isolation, and containment capabilities shall be provided to assure that for onsite electric power system operation (assuming offsite power is not available) and for offsite electric power system operation (assuming onsite power is not available) the system safety function can be accomplished, assuming a single failure.

Criterion 36 – Inspection of emergency core cooling system. The emergency core cooling system shall be designed to permit appropriate periodic inspection of important components, such as spray rings in the reactor pressure vessel, water injection nozzles, and piping, to assure the integrity and capability of the system.

¹⁸ GDC 41, 42, and 43, which define criteria for containment atmosphere cleanup, apply in regards to the availability of containment spray systems to remove fission products from the containment atmosphere. In addition, Section 50.67 of 10 CFR Part 50, which addresses accident source terms, would be affected should ECCS be lost due to sump blockage. Further, 10 CFR Part 100 details reactor site criteria including factors considered when evaluating reactor sites such as the expectation those reactors will reflect through their design, construction, and operation an extremely low probability for accidents that could result in release of significant quantities of radioactive fission products.

Criterion 37 – Testing of emergency core cooling system. The emergency core cooling system shall be designed to permit appropriate periodic pressure and functional testing to assure (1) the structural and leaktight integrity of its components, (2) the operability and performance of the active components of the system, and (3) the operability of the system as a whole and, under conditions as close to design as practical, the performance of the full operational sequence that brings the system into operation, including operation of applicable portions of the protection system, the transfer between normal and emergency power sources, and the operation of the associated cooling water system.

Criterion 38 -- Containment heat removal. A system to remove heat from the reactor containment shall be provided. The system safety function shall be to reduce rapidly, consistent with the functioning of other associated systems, the containment pressure and temperature following any loss-of-coolant accident and maintain them at acceptably low levels. Suitable redundancy in components and features, and suitable interconnections, leak detection, isolation, and containment capabilities shall be provided to assure that for onsite electric power system operation (assuming offsite power is not available) and for offsite electric power system operation (assuming onsite power is not available) the system safety function can be accomplished, assuming a single failure.

Criterion 39 -- Inspection of containment heat removal system. The containment heat removal system shall be designed to permit appropriate periodic inspection of important components, such as the torus, sumps, spray nozzles, and piping to assure the integrity and capability of the system.

Criterion 40 -- Testing of containment heat removal system. The containment heat removal system shall be designed to permit appropriate periodic pressure and functional testing to assure (1) the structural and leaktight integrity of its components, (2) the operability and performance of the active components of the system, and (3) the operability of the system as a whole, and under conditions as close to the design as practical the performance of the full operational sequence that brings the system into operation, including operation of applicable portions of the protection system, the transfer

between normal and emergency power sources, and the operation of the associated cooling water system.

Section 50.65 of 10 CFR Part 50, "Requirements for monitoring the effectiveness of maintenance at nuclear power plants"¹⁻⁸ (referred to hereafter as the Maintenance Rule) provides the requirements for monitoring and maintenance of plant structures, systems, and components (SSCs). The maintenance rule requires the licensee of a nuclear power plant to monitor the performance or condition of SSCs in a manner sufficient to provide reasonable assurance that the SSCs are capable of fulfilling their intended functions. When the performance or condition of an SSC does not meet its established goals, appropriate action shall be taken. Based on the criteria in the rule, the maintenance rule includes in its scope BWR suction strainers, all safety-related CSSs, and those non-safety-related CSSs that fall into the following categories.

1. Those that are relied on to mitigate accidents or transients or are used in plant emergency operating procedures
2. Those whose failure could prevent safety-related CSSs from fulfilling their safety-related function
3. Those whose failure could cause a reactor scram or an actuation of a safety-related system.

Protective coatings also are covered by the Maintenance Rule to the extent that coating activities can affect safety-related equipment, e.g., suction strainers. On the basis of the guidelines in the rule, the maintenance rule requires that licensees monitor the effectiveness of maintenance for these protective coatings. The staff also considers the requirements of 10 CFR Part 50, Appendix B, "Quality Assurance Criteria for Nuclear Power Plants and Fuel Reprocessing Plants,"¹⁻⁸ to be applicable to safety-related containment coatings. Criterion IX of Appendix B, "Control of Special Processes," is especially relevant requiring that "Measures shall be established to assure that special processes are controlled and accomplished by qualified personnel using qualified procedures in accordance with applicable codes, standards, specifications, criteria, and other special requirements."

Appendix K of 10 CFR Part 50,¹⁻⁸ "ECCS Evaluation Models," establishes requirements

for analytical determinations that impact aspects of the strainer blockage issue. These analytical requirements include:

1. fission product decay heat generation rate (affects the calculated suppression pool temperature),
2. break flow characteristics and discharge model (affects the estimated amounts of debris),
3. post-blowdown phenomena and heat removal by the ECCS, and
4. required ECCS model documentation.

Appendix K also specifies that single failures be considered and the containment pressure to be used for evaluating cooling effectiveness.

1.6.2 Regulatory Guidance

This section provides a description of regulatory guidance that applies to the strainer/sump blockage issue. The NRC provided guidance on ensuring adequate long-term recirculation cooling following a LOCA in RG 1.82, "Water Sources for Long-Term Recirculation Cooling Following a Loss-of-Coolant Accident."¹⁻⁷ The guide describes acceptable methods for implementing applicable GDC requirements with respect to the sumps and suppression pools functioning as water sources for emergency core cooling, containment heat removal, or containment atmosphere cleanup. Guidelines for evaluating availability of the sump and suppression pool for long-term recirculation cooling following a LOCA are included in the RG 1.82.¹⁻⁷

Revisions 1 and 2 of RG 1.82 were issued in November 1985 and May 1996, respectively; Revision 3 is scheduled for September 2003. The first revision, Revision 1, reflected the staff's technical findings related to USI A-43¹⁻¹ that were reported in NUREG-0897.¹⁻⁴ A key aspect of the revision was the staff's recognition that the 50% strainer blockage criterion of Revision 0 did not address the issue adequately and was inconsistent with the technical findings developed for the resolution of USI A-43.¹⁻¹ It was assumed in Revision 0 that the minimum NPSH margin could be computed by assuming that 50% of the screen area was blocked by debris. GL 85-22¹⁻³³ recommended use of RG 1.82 Revision 1¹⁻⁷ for changeout and/or modifications of thermal insulation installed on primary coolant system piping and components. Revision 2 altered the strainer blockage

guidance for BWRs because operational events, analyses, and research following Revision 1 indicated that the previous guidance was not comprehensive enough to adequately evaluate a BWR plant's susceptibility to the detrimental effects caused by debris blockage of the suction strainers.

RG 1.82 Revision 2¹⁻⁷ guidance addressed operational debris, as well as debris generated by a postulated LOCA. Specifically, the Regulatory Guide stated that all potential debris sources should be evaluated, including, but not limited to, insulation materials (e.g., fibrous, ceramic, and metallic), filters, corrosion material, foreign materials, and paints/coatings. Operational debris included corrosion products (such as BWR suppression pool sludge), and foreign materials (FME procedures were not specifically introduced into Rev. 2). Revision 2 also noted that debris could be generated and transported by the washdown process, as well as, the blowdown process. Other important aspects of Revision 2 included: the use of debris interceptors (i.e., suction strainers) in BWR designs to protect pump inlets and NPSH margins; the design of passive and/or active strainers; instrumentation, in-service inspections; suppression pool cleanliness; the evaluation of alternate water sources, analytical methods for debris generation, transport, and strainer blockage head loss, and the need for appropriate supporting test data. Revision 2 references provide further detailed technical guidance for the evaluation of potential strainer clogging. Guidance for the evaluation of potential sump clogging for PWR plants will be provided in Revision 3 of RG 1.82.

RG 1.82 Revision 2¹⁻⁷ cited RG 1.1,¹⁻³⁴ "Net Positive Suction Head for Emergency Core Cooling and Containment Heat Removal System Pumps," for specific conditions to be used in determining the available NPSH for ECCS pumps in a BWR plant's licensing basis. RG 1.1¹⁻³⁴ considered the potential for degraded pump performance for ECCS and containment heat removal, which could be caused by a number of factors, including inadequate NPSH. If the available NPSH to a pump is not sufficient, cavitation of the pumped fluid can occur, thereby significantly reducing the capability of the system to accomplish its safety functions. It is important that the proper performance of the ECCS and containment heat removal systems be independent of calculated increases in

containment pressure caused by postulated LOCAs to ensure reliable operation under a variety of postulated accident conditions. The NRC's regulatory position is that the ECCS and containment heat removal systems should be designed with adequate NPSH margin assuming the maximum expected temperatures of the pumped fluids and no increase in containment pressure above atmospheric.

The NRC issued Revision 1 of RG 1.54, "Quality Assurance Requirements for Protective Coatings Applied to Water-Cooled Nuclear Power Plants," in July 2000¹⁻³⁵ to provide guidance regarding compliance with quality assurance requirements related to protective coating systems applied to ferritic steel, aluminum, stainless steel, zinc-coated (galvanized) steel, and masonry surfaces. The revision encourages industry to develop codes, standards, and guide that can be endorsed by the NRC and carried out by industry. With noted exceptions, the ASTM standards cited in the Regulatory Position of Revision 1 for the selection, qualification, application, and maintenance of protective coatings in nuclear power plants have been reviewed by the NRC staff and found acceptable.

Additional guidance is found in the applicable sections of the NRC SRP.¹⁻⁶ These sections include:

1. Section 6.2.2, "Containment Heat Removal Systems,"
2. Section 6.1.2, "Protective Coating Systems (Paints) – Organic Materials," and
3. Section 6.2.1.5, "Minimum Containment Pressure Analysis for Emergency Core Cooling System Performance Capability Studies."

1.7 Report Outline

This report is organized in the order that screen blockage analyses are usually performed. The analysis is usually decomposed into several steps as listed below.

- Section 2 discusses the identification of the potential sources of debris at the plant under evaluation.
- Section 3 discusses the testing and analytical models associated with estimating

the volumes of debris that could potentially be generated.

- Section 4 discusses the testing and analytical models associated with the transport of the debris within the upper containment, i.e., blowdown debris transport and subsequent washdown debris transport by the containment sprays.
- Section 5 discusses the testing and analytical models associated with the transport of the debris within the sump pool.
- Section 6 discusses the accumulation of debris on a sump screen or a pump suction strainer.
- Section 7 discusses the estimation of the head loss associated with a particular debris bed on a sump screen or a pump suction strainer.
- Section 8 discusses the redesigns of sump screens or pump suction strainers that have occurred during the resolutions of strainer blockage issue.
- Section 9 discusses the related significant events that have occurred both in the U.S. and internationally.
- Section 10 discusses the summary and conclusions of the report.

1.8 References

- 1-1. NUREG-0933, R. Emrit, R. Riggs, W. Milstead, J. Pittman, "A Prioritization of Generic Safety Issues," U.S. Nuclear Regulatory Commission, Revision 16, November 1993.
- 1-2. NUREG-0510, "Identification of Unresolved Safety Issues Relating to Nuclear Power Plants," U.S. Nuclear Regulatory Commission, January 1979.
- 1-3. NUREG-0869, Revision 1, A. W. Serkiz. "USI A-43 Regulatory Analysis," U.S. Nuclear Regulatory Commission, October 1985.
- 1-4. NUREG-0897, Revision 1, A. W. Serkiz, "Containment Emergency Sump Performance," U.S. Nuclear Regulatory Commission, October 1985.
- 1-5. SECY-85-349, "Resolution of Unresolved Safety Issue A-43, 'Containment Emergency Sump Performance,'" October 31, 1985.
- 1.6. NUREG-0800, Revision 4, "Standard Review Plan for the Review of Safety

- Analysis Reports for Nuclear Power Plants," LWR Edition, Section 6.2.2: Containment Heat Removal Systems, U.S. Nuclear Regulatory Commission, June 1987.
- 1-7. RG-1.82, Regulatory Guide 1.82, Revision 1, "Water Sources for Long-Term Recirculation Cooling Following a Loss-of-Coolant Accident," U.S. Nuclear Regulatory Commission, Revision 1, November 1985 and Revision 2, May 1996.
 - 1-8. 10 CFR Part 50, Title 10, Code of Federal Regulations, published by the Office of the Federal Register, National Archives and Records Administration, U.S. Government Printing Office, January 1, 1997.
 - 1-9. NRC Information Notice, IN-92-71, "Partial Blockage of Suppression Pool Strainers at a Foreign BWR," NRC Information Notice, September 30, 1992.
 - 1-10. NRC Information Notice, IN-93-34, "Potential for Loss of Emergency Cooling Function Due to a Combination of Operational and Post-LOCA Debris in Containment," NRC Information Notice, April 26, 1993.
Supplement 1, "Potential for Loss of Emergency Cooling Function Due to a Combination of Operational and Post-LOCA Debris in Containment," NRC Information Notice, May 6, 1993.
 - 1-11. NRC Information Notice, IN-95-47, Revision 1, "Unexpected Opening of a Safety/Relief Valve and Complications Involving Suppression Pool Cooling Strainer Blockage," NRC Information Notice, November 30, 1995.
 - 1-12. NRC Information Notice, IN-95-06, "Potential Blockage of Safety-Related Strainers by Material Brought inside Containment," NRC Information Notice, January 25, 1995.
 - 1-13. NRC Bulletin 93-02, "Debris Plugging of Emergency Core Cooling Suction Strainers," NRC Bulletin to Licensees, May 11, 1993, and Supplement 1, February 18, 1994.
 - 1-14. NUREG/CR-6224, G. Zigler, J. Brideau, D. V. Rao, C. Shaffer, F. Souto, W. Thomas, "Parametric Study of the Potential for BWR ECCS Strainer Blockage Due to LOCA Generated Debris," Final Report, U.S. Nuclear Regulatory Commission, October 1995.
 - 1-15. NUREG/CR-6370, D. V. Rao, W. Bernahl, J. Brideau, C. Shaffer and F. Souto, "BLOCKAGE 2.5 User's Manual," SEA96-3104-A:3, December 1996.
 - 1-16. NUREG/CR-6371, C. Shaffer, W. Bernahl, J. Brideau, and D. V. Rao, "BLOCKAGE 2.5 Reference Manual," SEA96-3104-A:4, December 1996.
 - 1-17. NEA/CSNI/R (95) 11, "Knowledge Base for Emergency Core Cooling System Recirculation Reliability," Prepared by U.S. Nuclear Regulatory Commission for the Principal Working Group 1 (PWG-1), International Task Group, Committee on the Safety of Nuclear Installations, Organization for Economic Cooperation and development (OECD) Nuclear Energy Agency (NEA), February 1996.
 - 1-18. NRC Bulletin 96-03, "Potential Plugging of Emergency Core Cooling Suction Strainers by Debris in Boiling-Water Reactors," NRC Bulletin to BWR Licensees, May 6, 1996.
 - 1-19. NUREG/CR-6369, Volume 1, D. V. Rao, C. Shaffer, and E. Haskin, "Drywell Debris Transport Study," U.S. Nuclear Regulatory Commission, SEA97-3501-A:14, September 1999.
NUREG/CR-6369, Volume 2, D. V. Rao, C. Shaffer, B. Carpenter, D. Cremer, J. Brideau, G. Hecker, M. Padmanabhan, and P. Stacey, "Drywell Debris Transport Study: Experimental Work," SEA97-3501-A:15, September 1999.
NUREG/CR-6369, Volume 3, C. Shaffer, D. V. Rao, and J. Brideau, "Drywell Debris Transport Study: Computational Work," SEA97-3501-A:17, September 1999.
 - 1-20. NEDO-32686, Rev. 0, "Utility Resolution Guidance for ECCS Suction Strainer Blockage," BWROG, November 1996.
 - 1-21. NRC-SER-URG, "Safety Evaluation by the Office of Nuclear Reactor Regulation Related to NRC Bulletin 96-03 Boiling Water Reactor Owners Group Topical Report NEDO-32686, 'Utility Resolution Guidance for ECCS Suction Strainer Blockage,'" Docket No. PROJ0691, August 20, 1998.

- 1-22. GL-97-04, "Assurance of Sufficient Net Positive Suction Head for Emergency Core Cooling and Containment Heat Removal Pumps," NRC Generic Letter to All Holders of Operating Licenses for Nuclear Power Plants, October 7, 1997.
- 1-23. SEA97-3705, Clint Shaffer and Willard Thomas, "Reliance on Containment Overpressure for Ensuring Appropriate NPSH," Technical Evaluation Report to U.S. NRC, SEA97-3705-A:5, April 29, 1998.
- 1-24. GL-98-04, "Potential for Degradation of the Emergency Core Cooling System and the Containment Spray System After Loss-of-Coolant Accident Because of Construction and Protective Coating Deficiencies and Foreign Material in Containment," NRC Generic Letter to All Holders of Operating Licenses for Nuclear Power Plants, July 14, 1998.
- 1-25. LA-UR-01-1595, D. V. Rao, Clinton J. Shaffer, and Robert Elliott, "BWR ECCS Strainer Blockage Issue: Summary of Research and Resolution Actions," Prepared for U.S. Nuclear Regulatory Commission, Los Alamos National Laboratory, LA-UR-01-1595, March 21, 2001.
- 1-26. NUREG/CR-6762, "GSI-191 Technical Assessment," U.S. Nuclear Regulatory Commission (2002).
 Volume 1: D. V. Rao, B. Letellier, C. Shaffer, S. Ashbaugh, and L. Bartlein, "GSI-191 Technical Assessment: Parametric Evaluation for Pressurized Water Reactor Recirculation Sump Performance," LA-UR-01-4083, 2002.
 Volume 2: D. V. Rao, B. Letellier, K. W. Ross, L. Bartlein, and M. T. Leonard, "GSI-191 Technical Assessment: Summary and Analysis of U.S. Pressurized Water Reactor Industry Survey Responses and Responses to GL 97-04," LA-UR-01-1800, 2002.
 Volume 3: C. J. Shaffer, D. V. Rao, and S. G. Ashbaugh, "GSI-191 Technical Assessment: Development of Debris-Generation Quantities in Support of the Parametric Evaluation," LA-UR-01-6640, 2002.
 Volume 4: S. G. Ashbaugh, and D. V. Rao, "GSI-191 Technical Assessment: Development of Debris Transport Fractions in Support of the Parametric Evaluation," LA-UR-01-5965, 2002.
- 1-27. NUREG/CR-6770, K. W. Ross, D. V. Rao, and S. G. Ashbaugh, "GSI-191: Thermal-Hydraulic Response of PWR Reactor Coolant System and Containments to Selected Accident Sequences," NUREG/CR-6770, LA-UR-01-5561, 2002.
- 1-28. NUREG/CR-6772, D. V. Rao, B. C. Letellier, A. K. Maji, and B. Marshall, "GSI-191: Separate-Effects Characterization of Debris Transport in Water," NUREG/CR-6772, LA-UR-01-6882, 2002.
- 1-29. NUREG/CR-6773, D. V. Rao, C. J. Shaffer, B. C. Letellier, A. K. Maji, and L. Bartlein, "GSI-191: Integrated Debris-Transport Tests in Water Using Simulated Containment Floor Geometries," NUREG/CR-6773, LA-UR-02-6786, 2002.
- 1-30. NUREG/CR-6771, J. L. Darby, W. Thomas, D. V. Rao, B. C. Letellier, S. G. Ashbaugh, and M. T. Leonard, "GSI-191: The Impact of Debris-Induced Loss of ECCS Recirculation on PWR Core Damage Frequency," NUREG/CR-6771, LA-UR-02-0279, 2002.
- 1-31. NUREG/CR-5535, Lockheed Idaho Technologies Co., "RELAP5/MOD3 Code Manual," Volumes I through VII, NUREG/CR-5535, Rev. 1, Idaho National Engineering Laboratory, June 1995.
- 1-32. NUREG/CR-6119, Summers, R. M., et al., "MELCOR Computer Code Manuals," Volumes 1 and 2, NUREG/CR-6119, SAND93-1285, Sandia National Laboratories, September 1994.
- 1-33. GL-85-22, "Potential for Loss of Post-LOCA Recirculation Capability Due to Insulation Debris Blockage," NRC Generic Letter to All Licensees of Operating Reactors, Applicants for Operating Licenses, and Holders of Construction Permits, December 3, 1985.
- 1-34. RG-1.1, Regulatory Guide 1.1, "Net Positive Suction Head for Emergency Core Cooling and Containment Heat Removal System Pumps," U.S. Nuclear Regulatory Commission, November 2, 1970.

1-35. RG-1.54, Regulatory Guide 1.54, "Quality Assurance Requirements for Protective Coatings Applied to Water-Cooled Nuclear Power Plants," Rev. 1, July 2000.

2.0 DEBRIS SOURCES

Sources of debris that could contribute to the potential clogging of a strainer or sump screen include LOCA-generated debris, exposure-generated debris, and operational debris.

- LOCA-generated debris would be any materials damaged or destroyed by the effluents of a primary-system depressurization such that these materials subsequently could transport from their original location (e.g., piping insulation).
- Exposure-generated debris would be any materials damaged by prolonged exposure to the LOCA environment that subsequently could transport (e.g., failed unqualified coatings).
- Operational debris would be any resident material that normally is not considered permanently part of the plant (e.g., dust/dirt, rags, and plastic bags).

Each of these types of debris has been found following operational events and/or plant inspections.

The NEI conducted a survey on PWR sump design and operations for PWR reactors operating within the US in 1999 and forwarded the survey results to the US NRC. The NRC reviewed the survey results and published their findings in Volume 2 of NUREG/CR-6762.²⁻¹ In addition, an earlier survey was conducted in 1982.²⁻² These two surveys provide an overview of the types of insulation used by nuclear power plants in the US.

This section describes

- the debris actually found inside plant containments,
- the types of debris formed by LOCA depressurization effluents,
- the types of debris formed by prolonged exposure to a LOCA environment, and
- the types of debris formed by operational processes.

2.1 Actual Debris Found During Inspections

A wide variety of debris has been found inside the containments of operating nuclear power

plants. In some cases, the debris has rendered systems inoperable. The associated event reports are described in Section 9. Operational debris has included materials left over from the actual construction of the containment and materials left inside the containment during maintenance, repairs, and modifications. The operational and/or potential debris also includes such materials as equipment covers intended for removal before operation, tools, rope, and dust/dirt. Many event reports simply stated that miscellaneous operational debris was found without specifying the content of that debris. Failed coatings have been found where the coating pieces had or could have formed debris. The types of debris found are now listed by very general screen-blockage characteristics.

Fibrous Debris

Fibrous debris from sources such as temporary cooling filters used during an outage has been found inside the containment. In the most notable events, the fibers were found in suppression pools after excessive strainer head loss rendered a system inoperable.

Particulate Debris

Operational particulate debris has included corrosion products, construction/maintenance residues, and operational accumulations.

- Sludge buildup in suppression pools resulted from the continuous corrosion of structural steel.
- Dirt, dust, and pebble accumulations found in sumps were the result of insufficient housekeeping.
- Weld slag found in sumps was the result of insufficient cleanup following construction or modifications.

Transportable Sheet-Like Materials

Numerous miscellaneous, relatively transportable materials were found that would essentially behave like a solid sheet of material when they were on a strainer/screen, i.e., totally blocking a small section of the screen. These included the following.

- Sheets of thin plastic, e.g., bags or wraps
- Cloth-like materials

- Oil cloth
- Coveralls
- Nylon bags
- Duct tape
- Downcomer cleanliness covers
- Rubber mats
- Step-off pads
- Gasket materials
- Foam rubber plug

Relatively Non-Transportable Materials

Numerous miscellaneous materials were found that were relatively nontransportable and therefore less likely to contribute to significant strainer/sump-screen blockage, including the following.

- Tools
 - Hammer
 - Slugging wrench
 - Socket
 - Grinder wheel
 - Flashlight
- Miscellaneous hardware
 - Nuts and bolts
 - Scaffold knuckle
 - Antenna
 - Metal sheeting
 - Welding rod
 - Hoses and hose clamps
 - Tygon tubing
 - Tie wraps
 - Rope
 - Hardhats
 - Pens/Pencils

Although these materials are less likely to transport or cause strainer/sump-screen blockage, these types of debris can render a system inoperable under certain circumstances and have done so. Certainly, if the debris were left inside a sump screen, a pump could ingest it. For example, in 1980, a welding rod was found jammed between the impeller and the casing ring of an RHR system at the Trojan plant.

Failed Coatings

Several incidences of failed coatings and of the identification of unqualified coatings where only qualified coating should have been used were found during inspections. For example, in 1993 at North Anna Unit 1, most of the unqualified silicon-aluminum paint covering the steam

generators and pressurizer had detached from those surfaces and was held in place only by the surrounding insulation jackets.

Adherence to the FME and other housekeeping programs by the licensees will limit the extent of operational debris within the containment.

These include periodic inspections and cleanings to minimize the amount of foreign material and suppression-pool sludge. However, despite the ongoing FME programs, extensive quantities of foreign materials still were being found in suppression pools.

2.2 Loss-of-Coolant-Accident-Generated Debris

The break effluent following a LOCA would generate substantial quantities of debris within the containment, mostly within the vicinity of the break. The majority of the destruction to materials near the break would occur within the region generally designated as the ZOI. The size of the ZOI (refer to Section 3), which usually is considered to be spherical, depends on the type of material, i.e., the region of destruction could extend further for some materials than for others. However, some debris could be generated well beyond the ZOI. As the containment pressurizes, equipment covers, loose coatings, etc., could be blown free to become debris. A rapid pressurization could burst light bulbs anywhere within the containment. All of these sources of debris should be considered.

The debris generated within the ZOI would almost certainly be the largest source of transportable debris. Sources of debris within the ZOI generally include

- insulation materials and their respective jacketing,
- fire barrier materials,
- surface coatings, and
- concrete erosion.

The largest source of debris within the ZOI usually would be destroyed or damaged insulation. There are several types of insulation materials (as well as manufacturers of insulation), and each has unique destruction and transport characteristics. The types of insulation include those listed below.

- Fibrous insulation
 - LDFG
 - High-density fiberglass (HDFG)
 - Mineral wool
 - Miscellaneous other types
- RMI
 - Aluminum RMI
 - Stainless-steel RMI
- Particulate insulation
 - Calcium silicate
 - Asbestos
 - Unibestos
 - Microtherm
 - Min-K
 - Gypsum board
- Foam insulation
 - Foamglass
 - Foamed plastic
 - Armaflex
 - Vinyl cell
 - Neoprene

A number of different types of fire-barrier materials is used inside containments, but the volume of debris generated from fire-barrier materials tends to be substantially less than that of insulation, primarily because there usually would be much less fire-barrier material inside the ZOI. The pieces of failed coatings, ranging from powder to large chips of paint, would contribute to the buildup of particulate on the strainer/screen, as would the by-product of concrete erosion.

Beyond the ZOI, the LOCA-generated debris could include such materials as cloth used in equipment covers, permanent tags and stickers, and glass from broken light bulbs. The various filters located within containment potentially could contribute to the generation of debris, even though these filters are usually considered sufficiently protected that the LOCA flows (beyond the ZOI) would not damage the filter sufficiently to form debris. These filter materials could include filter paper, fiberglass, high-efficiency particulate air (HEPA) filters, and charcoal.

2.3 Loss-of-Coolant-Accident Exposure-Generated Debris

After the primary system depressurization is complete, the materials inside the containment would be subject to the high temperatures and

humidity resulting from the depressurization. In addition, the containment sprays, if activated, would impact and wet surfaces throughout the containment continuously. Prolonged exposure to the LOCA environment (both during depressurization and afterward) could cause some materials to fail, thereby generating additional debris.

One concern is that protective coatings within containments would have the potential to detach from their substrate as a result of prolonged exposure to a LOCA environment. Qualified protective coatings are expected to adhere to their substrates during a design-basis LOCA (DB-LOCA), except those coatings directly impacted by the break jet. A research program conducted at the Savannah River Technology Center to investigate the performance and potential for debris formation of coating systems used in nuclear power plant containments²⁻³ concluded that qualified, properly applied coatings that have not been subjected to irradiation of 10^9 rads can be expected to remain fully adhered to and intact on a steel substrate following exposure to all simulated DB-LOCA conditions. However, coatings that have been subjected to irradiation of 10^9 rads exhibited profound blistering, even when properly applied, leading to disbondment of a near-surface coating layer (1–2 mils of the 10-mil thickness) when exposed to elevated temperatures and moisture conditions within the range of DBA conditions. This phenomenon likely would produce a coating-debris source term.

All coatings inside the containment are not qualified,²⁻⁴ and therefore, the amount of unqualified coatings must be controlled because the unqualified coatings are assumed to detach from their substrates during a DB-LOCA and may be transported to the emergency sump screens or suction strainers. Several instances have been reported to the NRC in which protective coatings either have not been applied/maintained properly or have not been qualified adequately for their intended use.²⁻⁵

The characteristics of failed coating debris have been examined by the BWROG for selected types of coatings and test conditions.²⁻⁶ Test samples were prepared by first exposing the coating to a minimum radiation dose of 10^9 rads at an average dose rate of 1.65 Mrads/h at the University of Massachusetts Lowell Radiation Laboratory. The specimens next were subjected

to a series of three LOCA tests at the Testing Department of the Carboline Company to investigate the post-LOCA failure mechanisms and the failure timing of the coating systems. A scanning electron microscope was used to perform a detailed examination of pieces of debris. Microhardness measurements also were taken and compared for selected coating types. The coating debris examined ranged from powder residues to large, slightly curved pieces.

The LOCA environment, especially with the containment sprays operating, also could fail the adhesive intended to attach tags or labels permanently to walls and equipment. This type of debris material could well transport to the sump screens or suction strainers.

The exposure of the LOCA environment would likely cause oxidation of metallic surfaces that could generate transportable particulate debris.¹ There are unpainted metallic surfaces (steel, zinc, and aluminum) in all PWR containments that would be exposed in an accident environment to hot and highly borated water. The borated water would react with those surfaces, generating particulates.²⁻¹ Estimating the potential quantity of these particulates is difficult because the oxidation rates depend on a variety of parameters, such as the type of chemistry, the water temperature, the pH of the water, and the aeration of the water. The investigation of this phenomenon is only cursory at this time, and the current estimates vary greatly, depending on the values of the assumed parameters.

In addition to generating certain types of debris, exposure to the LOCA environment can degrade previously generated debris further. For example, individual fibers from pieces of relatively nontransportable or trapped fibrous debris likely would break free, at least to some extent, forming transportable debris. In the case of calcium-silicate debris, small particles likely would break free from the larger pieces. This issue needs to be addressed in debris-transport calculations.

¹Ongoing research is studying the importance of this potential source of debris, but it likely is negligible in the short term.

2.4 Operational Debris

Operational debris is debris formed from the operational erosion of containment materials or from materials that normally would not be left inside the containment during operation. A tool would be an example of a material left inside the containment following a period of maintenance. The location of debris such as a tool would be important to whether that tool could have an adverse affect. An example of operational erosion would be the iron oxide sludge that forms continuously in a BWR wetwell. Some of this sludge likely would always be found in the wetwell, but it should be kept to a minimum by cleaning of the wetwell during outages. Good general housekeeping is needed to limit debris such as dirt/dust that can accumulate throughout the containment. Even if an area of the containment looks clean, small quantities of dirt/duct could be located out of sight in and around equipment where the containment sprays would transport that debris to the sump. Operational debris has included (but is not limited to) the following.

- Wetwell sludge
- Dirt and dust
- Rust on unpainted surfaces
- Products of wear and tear (e.g., paint chips)
- Temporary air treatment filters
- Tools
- Rags
- Sheeting of various materials
- Plastic products (e.g., plastic bags)
- Paper products
- Rope
- Tape
- Wire ties
- Fire hoses

The quantities of operational debris present inside containment are plant-specific. The FME and other housekeeping programs might well be able to reasonably ensure that certain operational debris is not present, at least in places where the debris can transport to the sump screens or suction strainers. Much of the history of foreign materials inside containment predates the FME program. However, foreign material continues to be found inside containment.²⁻⁴

2.5 Aging Effects on Mineral Fiber Thermal Insulation

The effects of aging on mineral fiber thermal insulation would affect, at least to some extent, the generation of insulation debris, its subsequent transport to a PWR sump screen or a BWR suction strainer, and the resultant head loss across a bed of debris on that screen/strainer. The aging effects could include exposure to high temperatures, exposure to radiation, and operational damage. Of these types of aging or damage, the exposure to high temperature is the most significant effect. Insulation damaged significantly during normal operational of the plant normally would be replaced because of its reduced ability to perform its function. Although gamma and neutron radiation at sufficient intensity would decompose organic binders, operational observations do not indicate a significant aging resulting from exposure to radiation.

Mineral fiber insulation consists of either of two different types of material: fiberglass insulation and mineral or rock wool insulation. Fiberglass insulation is made from melted glass that is spun into fibers about 2 in.-long and, for mechanical products, with a 5- to 7-micron fiber diameter and a product bulk density of 2 to 3 lbs/ft³. These fibers are very flexible and resilient and essentially are free of "shot" or inorganic particles and short fibers. In contrast, mineral wool insulation is made from melted rock and/or slag and spun into fibers about ½ in. long and 3 to 10 microns in diameter. Typical bulk densities for mechanical mineral wool products are 6 to 10 lb/ft³. Mineral wool insulation products typically have a significant "shot," or particle and short fiber content, of 15 to 30% by weight.

The important aging effect appears to be the degradation of fiber insulation as a result of exposure to the high temperatures of the piping being insulated. Mineral fiber insulations all use a binder to essentially adhere the fibers to one another, thereby forming a fiber matrix that creates the pack of fibers. Binders are usually made from a phenolic resin and typically constitute about 3% by weight²⁻⁷ for LDFG insulation. These binders are hydrophobic in nature but decompose chemically (into gases) at temperatures greater than about 450°F.²⁻⁸ Typical RCS coolant temperatures range from

about 560°F at the vessel inlet to about 620°F at the vessel outlet, well above the fibrous insulation decomposition temperature. Because of the temperature gradient through the fiber pack, only part of the binder decomposes; i.e., only the portion where the insulation temperature exceeds 450°F. On a 600°F surface, this decomposed portion is typically about 1/3 of the total binder content.

A reduction in the binder that cements the fibers together could increase the generation of the very fine debris during a LOCA, which in turn would enhance debris transport to the sump screen or suction strainer. Less binder in the fibrous debris bed could allow the fiber to compact tighter with a corresponding reduction in bed porosity and increase in head loss across the bed. The aging effect would vary with the type insulation (e.g., LDFG insulation compared with mineral wool insulation). Head-loss testing has included tests using fibrous insulation artificially aged by heat-treating the test specimens. A typical heat treatment has been to place the specimen on a 650°F hot plate for a few days (4 days per ASTM C411), thereby heating only one side of the specimen as would occur to insulation installed around a pipe.²⁻⁹ Definitive data regarding the effects of aging on debris generation, transport, and head loss are scarce. Realistically, at this time, it can be said only that the effect could be significant and perhaps substantial for specific types of fibrous insulation.

2.6 Relative Timing and Debris Bed Composition

The relative arrival time of debris onto the sump screens or suction strainers can affect the composition of the accumulated debris and the associated head loss. The head loss also would depend on the timing of the recirculation pump operation and the pool height at activation. The initial formation of a bed of debris on the screens after the activation of recirculation pumping likely would consist of debris located in the sump at the time of the accident and debris transported to the sump in the short term. Debris initially located in the sump could consist of operational debris left in the sump area and LOCA generated debris deposited in the sump during blowdown debris transport. During the period of short-term transport (the first few hours following the break), a majority of the transportable debris

likely would be transported to the sump by the containment sprays (assuming the containment spray systems were activated). In the longer term, debris transport would consist primarily of exposure-generated debris and the erosion of larger non-transportable debris.

2.7 References

- 2-1. NUREG/CR-6762, D. V. Rao, B. C. Letellier, C. Shaffer, S. Ashbaugh, and L. Bartlein, "GSI-191: Parametric Evaluations for Pressurized Water Reactor Recirculation Sump Performance," NUREG/CR-6762, Volume 1, 2002.
- 2-2. NUREG/CR-2403, Reyer, R., E. Gahan, and J. W. Riddington, "Survey of Insulation Used in Nuclear Power Plants and the Potential for Debris Generation," NUREG/CR-2403, Burns and Roe, Inc. and Sandia National Laboratories, October 1981, and Supplement No. 1, July 1982.
- 2-3. WSRC-TR-2001-00067, M. E. Dupont, et al., "Degradation and Failure Characteristics of NPP Containment Protective Coating Systems (U) Interim Report No. 3," Westinghouse Savannah River Company, WSRC-TR-2001-00067, February 2001.
- 2-4. GL-98-04, "Potential for Degradation of the Emergency Core Cooling System and the Containment Spray System After Loss-of-Coolant Accident Because of Construction and Protective Coating Deficiencies and Foreign Material in Containment," NRC Generic Letter to All Holders of Operating Licenses for Nuclear Power Plants, July 14, 1998.
- 2-5. IN-97-13, "Deficient Conditions Associated with Protective Coatings at Nuclear Power Plants," NRC Information Notice, March 24, 1997.
- 2-6. ITS-DDES, J. Bostelman, G. Zigler, and G. Ashley, "Failed Coating Debris Characterization," Prepared for: BWROG Containment Coating Committee, ITS Corporation and Duke Engineering Services, July 21, 1998.
- 2-7. Gordon Hart, "Tests for Long Term Head Loss Across Fiberglass Insulation Debris Using Warm, Alkaline Water," Paper presented to the OECD/NEA Workshop on Sump Screen Clogging, Stockholm, May 10-11, 1999.
- 2-8. "Knowledge Base for Emergency Core Cooling System Recirculation Reliability," Prepared by U.S. Nuclear Regulatory Commission for the Principal Working Group 1 (PWG-1), International Task Group, Committee on the Safety of Nuclear Installations, Organization for Economic Cooperation and development (OECD) Nuclear Energy Agency (NEA), Restricted, NEA/CSNI/R (95) 11, February 1996.
- 2-9. James B. Nystrom, "Extended Head Loss Testing in Alkaline Water of Thermal Insulation used in Nuclear Containments," Alden Research Laboratory, Inc., 72-92/M670F, May 1992.

3.0. DEBRIS GENERATION

This section describes the mechanisms by which the hydrodynamic forces created during a LOCA destroy insulation on neighboring piping and other components, creating debris available for transport to the containment sump. Experimental measurements of the quantities of debris generated when insulation is subjected to these forces also are summarized. Finally, analytical models for estimating the quantity of debris generated during postulated LOCAs of various sizes and locations within the containment are described.

Critical locations within a PWR containment where the accumulation of debris would adversely affect recirculation performance also are described. What is currently known about the effect of parameters such as insulation type and debris size on the spatial distribution of debris fragments on the surface of the screen is discussed as well. This information was gathered primarily from experimental observations of debris accumulation on simulated PWR sump screens.

Various mechanisms have been postulated for generating debris as a consequence of a postulated LOCA in a PWR. Analysis performed to resolve USI A-43 indicated that dynamic (shock) forces and mechanical erosion caused by impingement of the steam/water jet from the broken pipe on neighboring pipe insulation, equipment coatings, and other structures would be the dominant mechanism for LOCA-generated debris.¹ This finding was retained in the subsequent re-evaluation of LOCA-generated debris in US BWR plants.²

The physical processes that govern debris generation by this mechanism, particularly as it relates to the damage or destruction of piping and component insulation, are described in Section 3.1. Published data on this subject are summarized in Section 3.2. As is often the case, much of the data collected in US and international research programs were collected in well-instrumented, but idealized, laboratory conditions. Therefore, an analytical method is required to apply the data to the more complex conditions associated with reactor/containment designs with varying configurations and potential debris sources. Useful models and methods for estimating the quantities of debris generated by a postulated LOCA are described in Section 3.3.

3.1 Overview of the Mechanics of Debris Generation

Component insulation is destroyed initially by the blast effects of a shock wave that expands away from the break in the RCS piping when it first opens.³ The strength of the shock wave decays rapidly as it expands away from the break plane because of the increased volume (decreased density) of the expanding steam/water mixture. This initial shock wave may cause substantial damage to even the most heavily reinforced insulating constructions (e.g., steel-jacketed RMI or fiber) if they are located sufficiently close to the break. After the shock wave passes, shear forces and consequential erosion of piping insulation, paint, coatings, and other materials in the wake of the break jet result in additional debris generation.⁴

In an ideal (unobstructed) environment, the shock wave expands away from the break in a spherical pattern. The steam/water jet expands

¹ Other mechanisms include acceleration forces associated with pipe whip and mechanical damage caused by the impact of the broken pipe on neighboring structures. The potential for debris generation by these mechanisms was examined in support of the resolution to USI A-43.³⁻¹ This assessment concluded that "jet impingement is by far the most significant of the insulation debris generation mechanisms." Consequently, debris generation from pipe whip and pipe impact is not discussed further in this document.

² This includes the NRC contractor analyses summarized in NUREG/CR-6224³⁻² and Utility Resolution Guidance (URG) prepared by the BWR Owners' Group (BWROG).³⁻³ The NRC issued a Safety Evaluation Report (SER) regarding the BWROG URG.³⁻⁴

³ Analysis performed by General Electric for BWR coolant system pressures (1000 psia or 70 bar) suggests a shock wave might not be generated if the break opening time were sufficiently long, as might occur if the "leak-before-break" assumption were adopted [BWROG, 1996].

⁴ The current understanding of debris-generation phenomena is that the initial blast (shock) accompanying rupture of a high-pressure steam- or water-filled pipe does not have a significant effect on such debris sources as equipment or containment surface coatings. However, it would cause substantial resuspension of dirt, dust and other loose particulate material in the area.

away from the break plane in the shape of a cone. Experimental measurements and analytical studies have allowed the pressure distribution within a conical jet to be characterized with reasonable accuracy (see Section 3.1.1.). Unfortunately, the current state of knowledge regarding the specific mechanisms for the damage or destruction of component insulation is not sufficiently complete to discern how near-field shock dynamics and far-field jet erosion combine to dislodge insulation from its initial location and break it apart into debris fragments of various sizes. This is in part because experiments simulating the damage or destruction of piping insulation by impingement of a high-pressure steam/water jet are able to “measure” only the end-state of the insulation material, i.e., the amount of material dislodged from a target location, and the size distribution of fragmented debris (see Section 3.2.) It is not reasonably possible to determine accurately specifically how the fragments were generated.

Another factor that complicates an evaluation of debris generation is the high degree of congestion in close proximity to many candidate break locations in a typical PWR containment. The close proximity of insulated components, containment structures, and other obstacles limits the usefulness of break-jet pressure distributions measured in an idealized,

unobstructed environment. Rarefaction and reflected expansion waves are generated as the shock front encounters obstacles in its path. The steam/water jet also may impact neighboring obstacles, redirecting flow from portions of the jet and possibly dissipating some of its energy.

These complications, combined with the possibility that the break plane can move in space because of the motion of the ruptured pipe, cause the set of potential insulation “targets” to be rather large. Various analytical methods for characterizing the ZOI within which insulation might be damaged have been proposed as described in Section 3.3. These methods each attempt to correlate the energy contained in the steam/water jet to a region in space within which the jet pressure would be large enough to cause damage to various types of insulation material. In all cases, the extent of damage becomes less severe with distance from the break location. As shown in Figure 3-1, these factors lead to a damage pattern resembling concentric rings emanating from the postulated break location. The boundaries of these rings can be either conical or spherical, depending on the specific modeling assumptions used to define the ZOI. Alternative models for estimating the shapes and dimensions of these rings are described in Section 3.3.

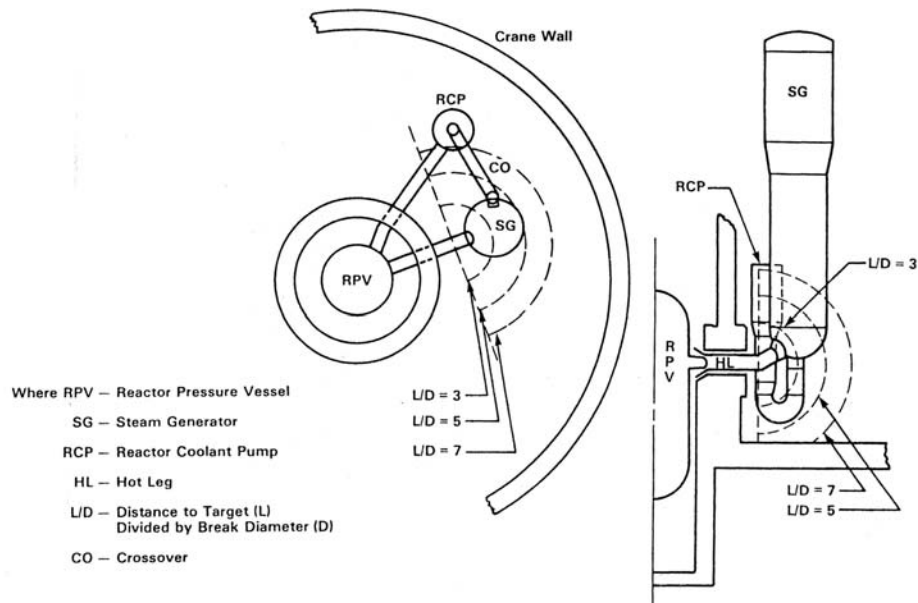


Figure 3-1 Example ZOI at a Postulated Break Location³⁻⁵

The extent of damage to insulation positioned at a given distance from the break depends on the following.

- The physical properties of the insulation component and its installation hardware
 - The material used to form the core of the insulation component (e.g., fiberglass with a blanket, layered metal sheeting within a cassette)
 - The composition and thickness of the insulation enclosure [e.g., steel jacket(s), woven fiber matting]
 - The construction and mechanical properties of the component installation hardware (e.g., banding, closure clasps, wire retainers)
- The orientation of the insulation relative to the jet⁵
- The exposure history of the insulation (thermal and radiation environment)⁶

These factors combine to affect the “damage pressure” for a particular insulating construction. “Damage pressure” is a characteristic of a particular insulating material and method of installation. It represents the maximum distance from the break plane at which an insulation blanket (if fiber) or cassette (if RMI) has been observed in controlled experiments to be dislodged from piping and break into smaller fragments (i.e., the distance where the jet pressure drops below the minimum pressure that can cause damage to the insulation).

In some analyses, this characteristic is measured simply in terms of the maximum number of pipe diameters away from the break plane where damage has been observed

⁵ Orientation has often been ignored in characterizing debris generation; however, as described in Section 3.2, the orientation of the seams of steel jacketing on fiber or calcium-silicate insulation can affect the extent of damage significantly.

⁶ Exposure of some forms of insulation to sustained high temperatures and/or radiation fields can cause the base insulation materials to become brittle. For example, the binding compounds used in some types of insulation can break down under sustained heating. The resulting changes in the mechanical properties of the insulation can lead to a decrease in its characteristic damage pressure and increase the proportion of small debris fragments.

experimentally.⁷ Another method for expressing the threshold for damage is to correlate the distance from the break to the stagnation pressure of the jet at that location (thus, the term damage “pressure”). Analytical models for associating the distance at which insulation damage is measured to stagnation pressure are described in Section 3.3. Damage pressures for various types of insulation are summarized in Table 3-1.

The term “destruction” pressure has been used interchangeably in the past (specifically during the BWR resolution studies) with “damage” pressure but herein the term “damage” pressure has been preferred to acknowledge that this pressure is a threshold pressure and that the destruction of insulation is incomplete at this pressure. The extent of damage increases as local pressures increase. The extent of damage within a ZOI is very dependent upon the type of insulation. Some more fragile types of insulations (e.g., calcium silicate) would likely be more extensively damaged than a less fragile type (e.g., RMI) in term of the fraction of the ZOI insulation turned into very fine or small debris. This subject is discussed further in Section 3.3.3.

The damage pressure also depends on (1) whether the insulation is jacketed, (2) the material and number of layers of jacketing, and (3) the orientation of the jacket seams relative to the axis of the break. The insulation jacket may provide some protection to the insulation (but not in all cases), which would be reflected in an increase in the damage pressure. The orientation of the jacket seam relative to the jet has been found to affect the damage pressure profoundly. At a seam orientation of 45°, the jacket can be opened up at the seam much more easily than if the seam was on opposite side from the jet (180°). In reality, the damage to insulation within the ZOI could be rather chaotic because the jet would impact insulation at a variety of seam and pipe orientations. Insulation closer to the jet but with its jacket seam opposite the jet might survive, whereas insulation further out was destroyed because its seam was oriented toward the jet.

⁷ Distance is expressed in terms of L/D, where L/D is the number of pipe diameters (D) away from the (guillotine) break plane where the insulating construction is positioned.

Table 3-1 Damage Pressures for Insulation Materials Found in U.S. PWRs*

Insulating Construction (Fibrous)	Damage Pressure (psi)	Insulating Construction (RMI)	Damage Pressure (psi)
Min-K	4	Mirror [®] /std bands	4
Koolphen-K	6	Mirror [®] /Sure-hold [®] band	150
Unjacketed Nukon [®]	10	Transco RMI	190
Jacketed Nukon [®] /std bands	10	Darchem DARMET	190
Knaupf	10		
Temp-Mat/SS wire retainer	17		
K-wool	40		
Jacketed Nukon [®] /Sure-hold [®] bands	150	Insulating Construction (Other) Calcium-silicate/aluminum jacketing	Damage Pressure (psi) 20

*The listing of insulating materials, with the exception of the calcium-silicate pressure, was derived from responses to an NEI survey³⁻⁶ and industry responses to GL 97-04;³⁻⁷ information obtained from these sources is summarized in Ref. 3-10. The listed values for damage pressure are the minimum of those reported by the BWROG in its URG documents³⁻³ and the results of confirmatory analysis performed by NRC and documented in Appendix B of Ref. 3-4. These data were based on air-jet testing. The aluminum-jacketed calcium-silicate pressure of 20 psi was determined from the OPG two-phase (steam with droplets) jet test data (Section 3.2.2.5), which is considerably lower than the BWROG air-jet test result of 160 psi. The OPG test data indicate lower damage pressures when the jet is a two-phase jet rather than an air jet. Further, the damage pressure for the jacketed calcium-silicate depended on the seam angle, and the 20-psi value was based on the optimum seam angle for damage.

Finally, the hardware used to mount an insulation blanket or cassette to piping can affect its resistance to jet forces significantly. For example, tests performed by the BWROG indicated that Sure-hold[®] bands had significantly better mechanical properties than standard bands with common closure clasps. As indicated in Table 3-1, application of the Sure-hold[®] bands resulted in an approximately 30-fold increase in the damage pressure for Nukon[®] fiberglass blankets and DPSC Mirror[®] RMI.

A common way to measure the extent of damage inflicted on component insulation during jet impact tests is to sort the resulting debris into various sizes. Increasing local pressure causes the base insulation material to fragment into smaller pieces. The resulting size distribution of debris fragments is important for evaluating the efficiency of debris transport to the recirculation sump (see Sections 4 and 5), debris accumulation profiles on the sump screen (see Section 6), and finally, screen head loss (see Section 7). Standard schemes for classifying debris sizes and shapes are described in Section 3.1.2. The available data on debris-size distributions for various insulating material are summarized in Section 3.2

3.1.1 Break-Jet Phenomena

The shape of the break jet and its orientation in space depend on several factors. The most important factors are

- the size and configuration of the pipe rupture,
- the break effluent (steam, water or a two-phase mixture), and
- the size and orientation of neighboring obstacles.

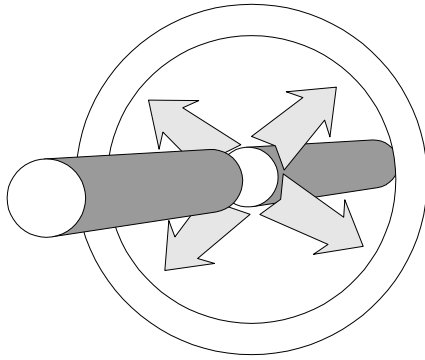
The effects of these factors on a free-expanding jet can be summarized as follows.

3.1.1.1 Size/Configuration of Pipe Rupture

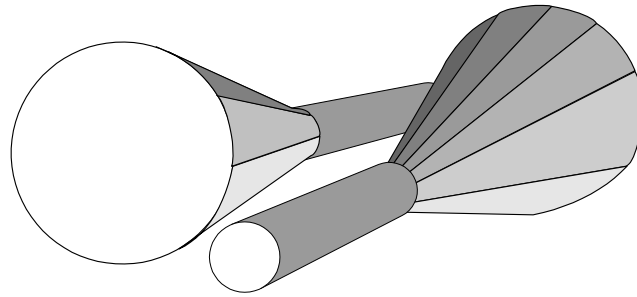
The total volume and shape of the jet emerging from a ruptured pipe depends on the size of the ruptured pipe, the shape and area of the opening in the pipe, and (for DEGBs) the relative positions of the opposing pipe ends. Two examples are shown in Figure 3-2.

3.1.1.2 Break Effluent

The thermodynamic state of the break effluent has been found to have an important effect on the rate at which jet pressure decays with distance from the break plane and the extent to which the jet expands in the radial direction. At any location along the jet centerline (beyond one pipe diameter), the local pressure for a two-phase jet (i.e., a steam/water mixture) is less than that for a steam-only jet with the same initial stagnation pressure.³⁻⁸ Further, the cross-sectional area of the jet is larger for a steam-only jet than for a two-phase jet with the same initial stagnation pressure.³⁻⁹



100% pipe separation, 0% offset



100% pipe separation, and 100% offset

Figure 3-2 Variation in the ZOI Shape with DEGB Separation and Offset

3.1.1.3 Obstacles

Postulated breaks in the coolant system piping are not likely to occur at locations in the containment where there is an unobstructed, clean, line-of-sight view of insulation on neighboring components. Walls, floors, catwalks, and other structures may interfere with the trajectory of fluid emerging from a ruptured pipe. Structures close to the break can cause the standing shock wave at the break exit to be reflected, increasing local pressures. Large structures further away from the break can divert subsonic jet flow significantly, changing the overall volume and shape of the area impacted by the break effluent. A large obstacle such as a floor, wall, or large vessel (e.g., steam generator) can cast a large “shadow,” preventing jet forces from affecting insulation on components on its opposite side. These factors, combined with the high degree of congestion in many locations of the containment, cause the overall region of space affected by a ruptured pipe to be much different in terms of the impacted volume shape and size than the volume swept out by an imaginary cone protruding from the break plane. These factors are taken into account in developing models to characterize the shape and dimension of the ZOI surrounding a postulated break (see Section 3.3.)

3.1.2 Debris Classification

To handle the differences in generation and transport effectively, LOCA-generated debris is classified into distinct debris groups: fibrous insulation debris, RMI insulation debris,

particulate insulation debris,⁸ foam or rubber insulation debris, failed coatings debris, miscellaneous particulate, and miscellaneous operational material debris (examples are given in Section 2). Each of these groups generates debris of various sizes because of the variability in the break jet, the installed configuration of material, and other factors described above.⁹ The size distributions of these debris species, as well as other characteristics, play an important role in transport efficiency and sump-screen accumulation patterns (see Sections 4, 5, and 6, respectively) and therefore directly affect sump performance. This effect can be illustrated by contrasting the two very different sizes of fibrous debris: fine fibers (or fines) and large fibrous mat fragments.

Fines are transported easily to the containment floor and tend to remain suspended in the pool of water for prolonged periods of time. These characteristics greatly increase the potential for fines to be transported to, and collect on, the sump screen. Large fibrous fragments can

⁸ Calcium-silicate insulation is a common type of a particulate insulation; other types include asbestos, Unibestos, Min-K, Microtherm, and gypsum board.³⁻¹⁰

⁹ The size distribution of particulate matter may not be a concern in the assessment of sump-screen blockage, and this type of debris has often been treated as simply “particulate.” However, the size of individual particles can vary considerably—from common dirt/dust with characteristic diameters on the order of micro-meters to granules of ablated concrete with diameters on the order of millimeters. The size distribution could be important in a transport analysis performed to reduce the assumed compete transport of the particulate to the sump screen.

become attached to structures or captured by floor grating at upper elevations of the containment and therefore may not be transported easily to the containment floor. If these fragments reach the floor, they tend to either float or (if saturated with water) sink to the floor of the pool of water. Relatively high local pool velocities are required to move large fragments to the screen, where they tend to collect near the base of a vertical screen, leaving the upper portions of the screen free of debris (of similar size). Additionally, fines tend to form more compact and uniform beds on the screen, resulting in larger pressure drops than beds of similar thickness formed by larger fragments.

3.1.2.1 Size Classification of Fibrous Debris

The results of debris-generation experiments involving fibrous insulating materials demonstrate that impingement of a high-pressure jet onto fibrous insulation (jacketed or not) generates debris that spans a wide range of sizes—from individual fibers to intact or nearly intact pillows. A scheme for classifying the size of fibrous debris was developed in the NRC's evaluation of debris generation for BWRs.¹⁰ Because the transport and head loss properties of fibrous debris depend on the debris shape and size, these physical characteristics are used to describe the various "classes" of debris generated when fibrous insulation is subjected to jet blasts of variable intensity. The size classification scheme is summarized in Table 3-2. Photographs of fibrous debris in Classes 3 and 5 are shown in Figure 3-3.

3.1.2.2 Size Classification of RMI Debris

The internal construction of a typical RMI cassette is shown in Figure 3-4. Transportable debris generated from this type of construction typically consists of small crumpled sheets of

the internal foil, which resembles shrapnel. Figure 3-5 is a photograph of cut pieces of RMI foil (roughly 2 in. square) and crumpled "debris."

The spectrum of debris sizes typically observed in blast tests involving this type of insulation is more limited than that observed with fibrous insulation. A structured RMI debris-size classification was not developed in the NRC study of BWR strainer performance. However, four broad classes can be suggested based on observations of RMI debris generation tests (see Section 3.2) and are described in Table 3-3.






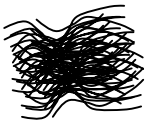
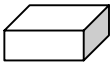
As described in the next section, the size distribution of RMI debris depends on the material used (aluminum vs stainless steel) and the cassette construction (banding, type of closure clasps, etc.).

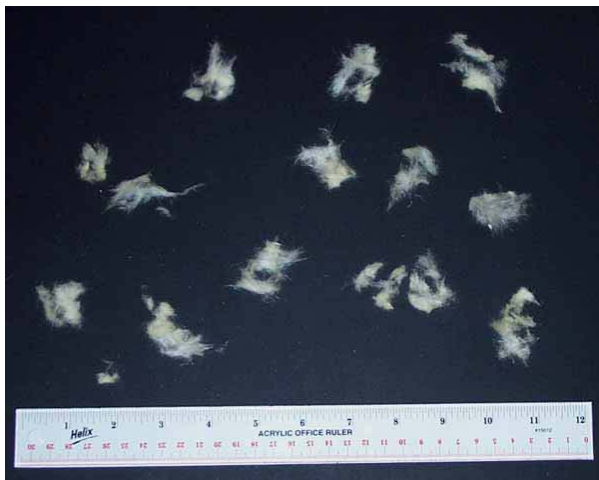
3.2 Debris-Generation Testing

Investigators in several countries have performed experimental simulations of jet-blast impingement onto RCS insulation of various shapes, materials, and construction. One distinguishing feature of these tests is the jet effluent (air or steam/water). For reasons of economy, many early experimental studies of the destructive forces on RCS insulation materials were performed using high-pressure air jets rather than two-phase (steam/water) jets. However, analysis performed in support of a parametric evaluation of PWR recirculation sump performance³⁻²⁴ indicates that the ZOI associated with prototypic two-phase (steam/water) jets is larger than the ZOI indicated by air-jet simulant tests¹¹ and that the debris generated would be somewhat finer.³⁻¹¹ The specific cause of these differences is not well understood. Further work in this area is needed to fully explain the observed effects. Nevertheless, it is generally agreed that some adjustment should be made to the results of the air-jet tests to interpret the results properly for use in reactor containment conditions. The following summaries of debris-generation testing separate the results obtained from air jets and those obtained with more prototypic steam/water jets.

¹⁰ Actually, a number of classification schemes have been devised through the years to meet the particular needs of a test program or analysis; they range from two general groupings (fines and everything else) to the NRC seven-group scheme. Some translating between the size classification schemes may have to be done while comparing studies on the base of knowledge. For example, fine debris has been used to describe everything in the NRC classification from Classes 1 through 6, but in other analyses, the fines only cover debris that would always remain suspended. For PWR analyses, it is important to distinguish between suspended and nonsuspended debris.

¹¹ The radius of the ZOI in the parametric study was increased to 12D from the BWROG radius of 10.4D, corresponding to a lowering of the damage pressure from 6 to 4 psi. This increase in the ZOI radius increased the volume of the spherical ZOI by 50%.

Table 3-2 Size Classification Scheme for Fibrous Debris ³⁻²		
No.	Description	
1		Very small pieces of fiberglass material; "microscopic" fines that appear to be cylinders of varying L/D.
2		Single, flexible strands of fiberglass; essentially acts as a suspending strand.
3		Multiple attached or interwoven strands that exhibit considerable flexibility and that, because of random orientations induced by turbulent drag, can exhibit low settling velocities.
4		Fiber clusters that have more rigidity than Class 3 debris and that react to drag forces as a semi-rigid body.
5		Clumps of fibrous debris that have been noted to sink when saturated with water. Generated by different methods by various researchers but easily created by manual shredding of fiber matting.
6		Larger clumps of fibers lying between Classes 5 and 7.
7		Fragments of fiber that retain some aspects of the original rectangular construction of the fiber matting. Typically pre-cut pieces of a large blanket to simulate moderate-size segments of original blanket.



Fiberglass shreds in size Class 3



Fiberglass shreds in size Class 5

Figure 3-3. Fiberglass Insulation Debris of Two Example Size Classes

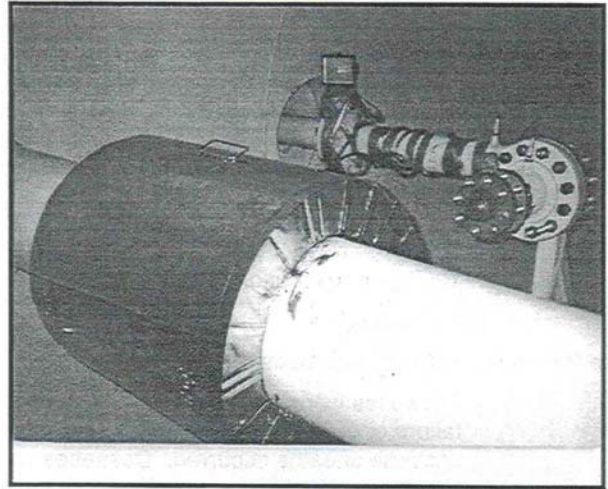
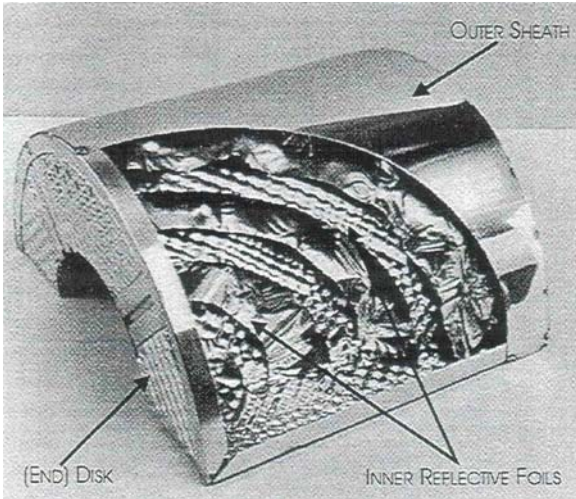




Figure 3-4 Inner Construction and Installation of a Typical RMI Cassette³⁻³



Figure 3-5 RMI Foil Before/After "Crumpling" (Left) and Crumpled RMI Foil Debris (Right)

No.	Description	
1		Small crumpled pieces of RMI foil typically 0.5 to 1.0 in. across. The crumpled foils transport more readily than flat foils and tend to “roll” along the floor of moving pool of water.
2		Small flat pieces of RMI foil typically 2 in. across.
3	Photo not available for this type of debris	Large wrapped or crumpled pieces of RMI foil or crushed sections of the outer casing of the original cassette.
4	Photo not available for this type of debris	Large flat sheets of RMI foil.

3.2.1 Air-Jet Testing

3.2.1.1 NRC BWR Drywell Inertial Capture Tests³⁻¹²

The NRC commissioned Science and Engineering Associates, Inc. (SEA) to perform a series of tests designed to measure the extent to which LOCA-generated debris would be captured on structures internal to the drywell of a BWR during the blowdown period of a LOCA. One portion of these tests involved measurements of debris generation, transport, and inertial capture of typical BWR piping insulation materials. The tests were performed at the Colorado Engineering Experiment Station, Inc. (CEESI), which has an 11,000-ft³ air-storage tank and air-blast test chamber that can be used to simulate jet impingement (and debris-transport) conditions. Exhaust air exiting the far end of the test chamber passed through a fine mesh screen (1/8-in. mesh) to capture debris that was not collected on the simulated typical drywell structures placed downstream of the target pipe. Debris-generation and transport tests were conducted at nozzle stagnation pressures of approximately 1000 psig. The test facility is shown in Figure 3-6.

Although the primary objective of these tests was to study inertial capture of debris on drywell structures, data also were collected that provide insights into the amount and size distribution of

fibrous debris.¹² The target material in the NRC/SEA tests conducted at CEESI was Transco fiberglass insulation encased in a tough canvas bag and designed to wrap around a pipe. Each blanket was 3 ft long and approximately 3 in. thick. The blankets were held in place by canvas straps and supported by three stainless-steel bands and two end supports to prevent axial movement along the target assembly. The Transco blankets each had two seams (i.e., each blanket was formed from two half-sections) that were arranged so that the seams were aligned with the top and bottom of the pipe 90° from the jet centerline.

Debris fragments found dispersed through the test apparatus were collected and sorted according to their size and material composition. Seven debris classes were collected.

- A. Canvassed insulation consisting of large sections of canvas covers encapsulating insulation (protecting insulation)
- B. Insulation attached to Class A debris but extruding from the canvas (unprotected insulation)
- C. Large (greater than hand-size) pieces of exposed insulation
- D. Medium (less than hand-size but smaller than grating mesh) pieces of exposed insulation

¹² These tests did not examine jet impingement on RMI cassettes.

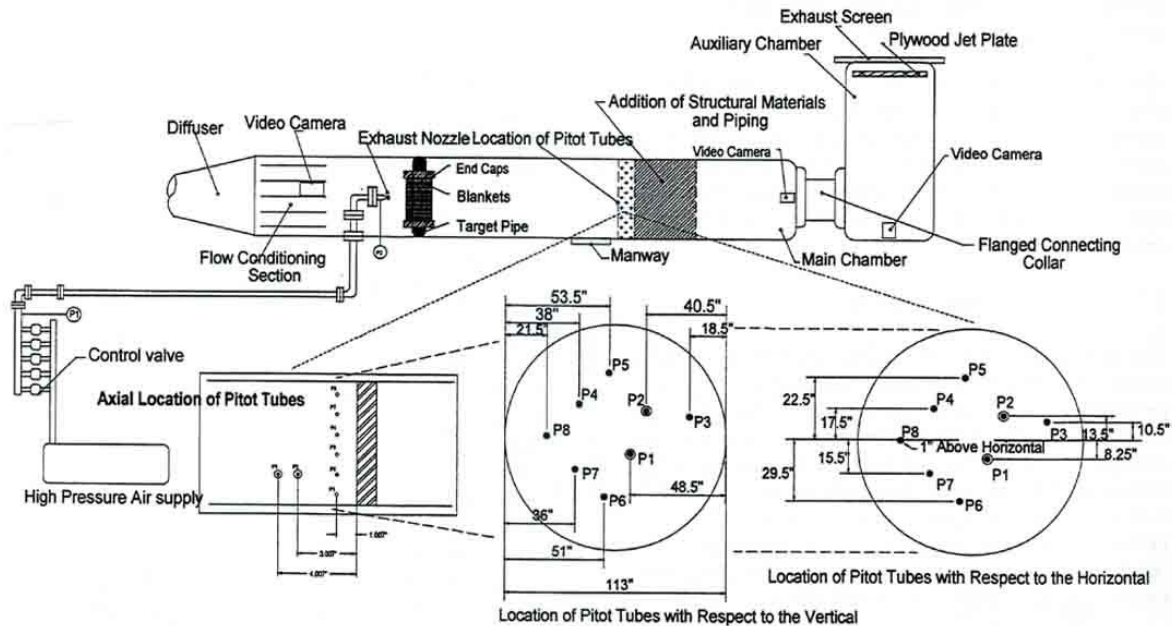


Figure 3-6 Configuration of the CEESI Test Facility for the NRC/SEA BWR Drywell Debris-Transport Tests

- E. Small (smaller than grating mesh) pieces of exposed insulation
- F. Pieces of shredded canvas without insulation
- G. Agglomerated debris consisting of a tangled mix of canvas and insulation

The findings related to fibrous-debris generation are summarized in the following paragraphs.

The target blankets were destroyed completely or nearly completely by the air blast, and the degree of destruction was generally similar among the various tests.¹³ From 15 to 25% of the original blanket insulation mass was

classified as nonrecoverable mass; i.e., the fibrous debris either exited the test chamber through a fine mesh screen or was too fine to collect by hand. This nonrecoverable mass translates into a generation of debris fine enough to remain suspended in a pool of water indefinitely that averages about 20% of the insulation in a totally destroyed blanket. Usually one relatively large section of canvas was found on the floor near the target or hanging on the continuous grating downstream of the target mounting). This section of canvas sometimes had a substantial quantity of fiberglass attached to it (45% of the total in one test). However, in some tests, this canvas was empty of fiberglass.

¹³ Because the main test objective was the study of debris transport, the blankets were positioned and oriented to maximize destruction, thereby creating more debris for transport. Positioning an insulation target blanket closer to the jet nozzle increased the pressure that the air jet applied to the target, hence increasing the damage to the insulation. However, if the blanket were placed too close, the ends of the target would extend beyond the flow of air from the jet so that some of the target would escape serious damage, e.g., placing the target directly in front of the jet and very close to the jet would destroy the center of the blanket but not the entire blanket. A distance was found that allowed each blanket to be essentially totally destroyed.

3.2.1.2 BWROG Air-Jet Impact Testing (AJIT)³⁻³

General Electric Nuclear Energy (GE) conducted tests at CEESI to examine the failure characteristics of fibrous insulation and RMI when they are subjected to jet impingement forces. The tests also provided data on the size distribution of the resulting debris. CEESI has compressed air facilities with 11,000 ft³ of storage at 2500 psia. Insulation samples were mounted inside a wind tunnel with a perforated plate (containing 1/8-in. holes) covering an 86-in. man-way at its exit, thus allowing air to be

discharged from the facility but keeping most of the insulation debris within the test chamber. Debris-generation tests were conducted under conditions that resulted in a choked-flow stagnation pressure at the 3-in. exhaust nozzle of 1110 psig (+25/-100), simulating coolant circuit conditions in a BWR.

A total of 77 tests were performed involving four broad classes of insulation: aluminum RMI, stainless-steel RMI, fibrous insulation, and lead shielding. Four of the tests were designed to measure target pipe stagnation pressure at various distances from the jet nozzle. The insulating materials used, as well as their construction and installation, conformed to vendor standards. The following vendors and product names were examined.

RMI

Transco Products, Inc. (TPI)
 Diamond Power Specialty Company (DPSC)
 Mirror®
 Darchem Engineering, Ltd. DARMET

Fiber

NUKON® blankets (jacketed and unjacketed)
 Min-K (unjacketed)
 Temp-Mat™ (unjacketed)
 K-Wool (unjacketed)
 Knau® (jacketed and unjacketed)

Other

Calcium-silicate
 Koolphen-K® closed-cell phenolic with anti-sweat jacketing

The distances from the break nozzle ranged from an L/D of 2.5 to an L/D of 116.3. The general test conclusions were summarized as follows.³⁻³

Throughout the AJIT Program testing, the inner and outer sheaths of reflective metallic insulation and stainless steel jacketing used on fibrous insulation did not fail in a manner, which would contribute to transportable debris. Tests of RMI conducted at distances of 2.4 L/D (7.25 in.) resulted in deformation of the cassette outer sheath but did not cause the stainless steel to be penetrated. In tests that did generate transportable reflective foil debris, the debris occurred due to the separation of the outer sheath

of the RMI cassette from the cassette side and/or (end) disk panels. The tests that generated the largest amounts of transportable debris resulted when the outer sheath or jacketing material was completely separated from the internal or jacketed insulation.

Debris generation resulting from an RMI assembly or jacketed fibrous insulation material was typically due to failure of the fastening mechanism of the assembly. Latch and strike mechanism failures occurred in 76% of the tests conducted which used latch and strike attachment mechanisms (32 of 42 tests). The latch and strike failures included straightening of the “J” hook on the strike, failure of the latch assembly (i.e., the locking clip and articulated latch hook breaking into component parts), and compression of the outer sheath or jacket to dimensions where the latch and strike were capable of release without damage to the latch and strike.

With the exception of the testing performed on Darchem DARMET® RMI (with Cam-Lock® latches and strikes) and aluminum jacketed calcium-silicate insulation, failure of the latch and strikes occurred out to distances of 100 L/D (300 in.). This corresponds to a target pipe stagnation pressure of approximately 4 psig. In the case of fibrous insulation materials, the use of jacketing as a means of reducing debris generation does not appear to be effective without the use of an additional banding material, which better secures the jacketing to the insulation assembly and the pipe.

The following values for damage pressure were recommended for fibrous and other (non-RMI) insulation materials.

Calcium-Silicate	160 psig
K-Wool	40 psig
Temp-Mat™	17 psig
Knau® Fiberglass	10 psig
NUKON® Fiberglass (jacketed and unjacketed)	10 psig
Koolphen-K®	6 psig
Min-K	4 psig

3.2.2 Steam and Two-Phase Jet Testing

A large body of experimental work related to debris generation has been performed in facilities using steam or two-phase (steam/water) jets. These facilities are located in the U.S., Germany, Sweden, and Canada. The published test data are summarized in the following sections.

3.2.2.1 Marviken Full-Scale Containment Experiments³⁻¹³

The Marviken Power Plant originally was designed and built as a boiling, heavy-water, direct-cycle reactor with natural circulation and provisions for nuclear superheating of steam. It was constructed and tested up to light-water commissioning tests but was never charged with nuclear fuel. The facility subsequently was used for a wide range of containment safety experiments, among which were several high-pressure blowdown experiments in which damage to equipment paint, containment (concrete) coatings, and component insulation was examined.

A series of blowdown experiments was performed between 1972 and 1973 to examine the (BWR) pressure suppression containment response and iodine transport within the containment during a simulated pipe break. These experiments also provided useful information on the extent to which containment paint and thermal insulation materials were damaged from the resulting break flow.

Components inside the containment were insulated with jacketed and unjacketed rockwool and calcium-silicate. The locations and orientations of the insulation relative to the break were not measured quantitatively; rather, the initial conditions were described in qualitative terms and with schematic (isometric) layout diagrams. The simulated pipe break also was not configured in a manner that created a coherent jet. Rather, the break plane was oriented vertically, and the break effluent impacted a horizontal deflector plate to disperse flow throughout the containment atmosphere. As noted above, the primary purpose of these tests was to examine containment thermodynamic response and bulk transport of iodine; the evaluation of insulation damage was a secondary consideration.

Qualitative observations and photographs of the extent of damage to insulation were recorded. The major findings include the following.

- Significant damage was observed to all forms of insulation in close proximity to the break location (within a few meters). In some locations, material was completely removed from its original mounted positions, and large amounts of insulation debris were found large distances from the break.
- Sheets of aluminum jacketing were stripped from some locations and were found crumpled at large distances from their initial locations.
- Test pieces shielded from the break by large concrete structures were not destroyed.

3.2.2.2 HDR Tests³⁻⁵

The Heissdampfreaktor (HDR) facility is a decommissioned BWR nuclear facility in Karlsruhe, Germany, that was refit in the late 1970s for light-water-reactor research. The reactor internals were removed, and the facility was decontaminated. New equipment was installed specifically for reactor blowdown simulations in a small, but authentic, reactor containment facility. The initial thermodynamic state developed in the test vessel for blowdown simulations is 110 bar (~1600 psia) and 310°C (323°F).

Among the tests performed in the HDR (and documented in NUREG-0897³⁻⁵) were blowdown simulations specifically designed to evaluate the extent of damage to RMI and fiberglass blanket insulation during blowdown. One test (described in Appendix C of NUREG-0897) involved four specimens of stainless-steel Mirror[®] cassettes with fasteners installed according to manufacturer specifications. In a second series of two tests, NUKON[®] blankets were installed.¹⁴

The test specimens were installed on target piping or rectangular steel struts located at various positions in the HDR containment. The distance from the break nozzle and insulation samples spanned a wide range but was generally less than 7D.

¹⁴ Jacketed and unjacketed samples were used in the NUKON[®] tests.

It is important to note that a deflection plate was positioned approximately 4 ft away from the break nozzle (450 mm inner diameter nozzle with break initiated using rupture disks) in the HDR tests to protect the containment wall. Therefore, the deflection plate distributed the break flow to the surrounding area, rather than the flow bearing down upon target material as a coherent jet.

The major observations made from these tests can be summarized as follows.

- The stainless-steel Mirror[®] insulation remained essentially intact when it was installed at distances greater than 7D from the break. The single sample installed closer to the break (approximately 2D) was torn apart. The outer casing was heavily damaged and compressed against neighboring structures. The inner stainless-steel foils were ripped from the casing and crumpled into relatively small pieces.
- Unjacketed NUKON[®] blankets positioned within 7D of the break were destroyed, with weight losses of the internal wool of 85 to 100%. Blankets jacketed with 22-gage stainless steel and installed at similar positions experienced less damage, with weight losses ranging from 7% to 75%.
- Flat NUKON[®] blankets covered with a metal mesh jacketing and placed above the impingement plate at a distance of 7.4D were totally destroyed.

3.2.2.3 Karlshamn Caposil and Newtherm Tests^{3-14,3-15,3-16}

A series of steam-jet impact tests was conducted by Studsvik in 1993 to determine the extent to which blocks of calcium-silicate insulation material would be eroded at various distances from a postulated steam-line break. The specific material examined in these tests was Caposil HT1 and Newtherm 1000. The Caposil HT1 material was supplied by the Ringhals and Oskarshamn nuclear power plants; the Newtherm 1000 material was provided by Ringhals and ABB-Atom. The materials were tested in both aged and unaged (new installation) conditions. The aged insulation had been in service at one of the power plants at temperatures of 290°C (553°F) for approximately 15 yr.

Samples of material were cut and mounted into a firm steel casing and then mounted downstream of a steam jet. Tests were conducted in which the jet impacted the samples at 90° (i.e., perpendicular) to the sample and 45° from the sample surface. Erosion patterns on the samples were noted, and debris stripped from the sample blocks was collected for analysis. Tests were conducted with the jet positioned between 2 and 10 break-diameters from the sample. All tests involved steam jets delivered from a high-pressure storage tank at 80 bar (1160 psia) and 280°C (535°F).

Observations made from these tests included the following.

- The radius of the eroded zone was found to be roughly equal to the distance of the break plane from the material surface. This observation is consistent with the conceptual picture of an expanding 90° conical free jet.
- The stagnation pressure at the “erosion limit” (i.e., the maximum distance from the break where significant erosion was observed) was found to be 1.67 bar (24 psia).
- The extent of material erosion increased with decreasing distance from the break plane. The sample blocks were destroyed or broken into several pieces at distances of less than 5 nozzle diameters.
- The wear loss of Caposil HT1 was found to be less than that of unaged Newtherm 1000 for the same exposure time.

A series of four tests was conducted in a closed container with a filtered exhaust so that debris fragments could be collected and analyzed. After these tests, collected debris was sorted into three size bins for subsequent processing.

- Pieces picked up by hand
- Slurry separated using a 2-mm net
- “Fines” suspended in water.

ABB analyzed the particles for four cases as summarized in Table 3-4.

The “flow density” (steam mass flux) was higher in Tests 1 and 2 compared with Tests 3 and 4. This difference is cited as the reason for the lower fraction of large particle sizes in Tests 3 and 4. A deficit of approximately 10% of the

Table 3-4 Measured Particle-Size Distribution from Newtherm 1000 (Calcium-Silicate) Erosion Tests³⁻¹⁶						
Test No.	Mass of Material (g)					
	Particle Size (µm)			Total	Quantity Before Test	Per Cent Lost
	> 850	20–850	< 20			
1	1135.3	43.8	71.1	1250.2	1475.4	15.3
2	1002.4	77.6	73.6	1153.6	1404.5	17.9
3	775.	148.5	165.0	1088.5	1407.8	22.7
4	841.4	94.0	198.7	1134.1	1402.8	19.2

original insulating material mass was found in the total mass of debris collected in these experiments. This “mass” was ejected from the experimental facility (in spite of the exhaust filter) and is assumed to be “fine” particles.

3.2.2.4 Siemens Metallic Insulation Jet Impact Tests (MIJITs)^{3-17,3-18}

Between October 1994 and February 1995, the Swedish Nuclear Utilities conducted metallic insulation jet impact tests (MIJITs) at the Siemens AG Power Generation Group (KWU) test facility in Karlstein am Main, Germany. Although the Swedish tests were reasonably extensive, only a general summary of the test results was released. Specific test data from the RMI debris generation tests were not made publicly available. In addition, the data are not directly applicable to US power plants because the European RMI design was substantially different from the RMI currently installed in US power plants.

In 1995, the NRC conducted a single debris-generation test to generate representative RMI debris to obtain insights and data on the effects of RMI relative to US plants. These tests were contracted to Siemens AG/KWU in Karlstein, Germany.

Each of the Swedish tests examined the performance of RMI used in European nuclear stations, which was manufactured by Grünzweig and Hartmann or Darchem Engineering. The NRC test was performed using RMI cassettes frequently found in US nuclear plants. The NRC samples were provided by DPSC, the manufacturer of Mirror[®] RMI cassettes. The tests were performed with high-pressure, saturated water and (separately) saturated steam. The facility consisted of a tall vessel and a blowdown line with a double rupture disk and orifice (break plane) mounted at its end. Target insulation materials were installed on a 10-in.

pipe that was positioned downstream of the simulated break at distances up to 25 break-pipe diameters. The orientation and position of the target pipe relative to the jet centerline could be changed to examine the effects of an asymmetric jet impingement.

A total of seven saturated water tests and nine saturated steam tests were performed in the Swedish test program. The following observations were recorded in publicly distributed reports.

- All insulation panels directly impacted by the steam jet (up to L/D = 25) were destroyed.
- Insulation outside the core of the steam jet was not fragmented.
- The degree of destruction caused by saturated water jets was much less than that caused by saturated steam jets. Damage tended to take the form of crumpling the RMI panels rather than fragmenting them into small pieces. Panel disintegration was observed (with a water jet) only when the target became stuck in the mounting trestle and remained in the core of the jet during the 30-s blowdown. In this case, a small percentage of the panel was fragmented.

The NRC test was conducted on May 31, 1995. Most of the RMI debris was recovered and categorized by the location where it was found. Approximately 91% of the debris was recovered as loose foil pieces; the remainder was found wedged in place among the structures. The debris was analyzed with respect to size distribution. The overall size distribution for the total recovered debris mass is shown in Figure 3-7. A photograph of the RMI debris generated by this test where the RMI panel was positioned directly over the break is shown in Figure 3-8.

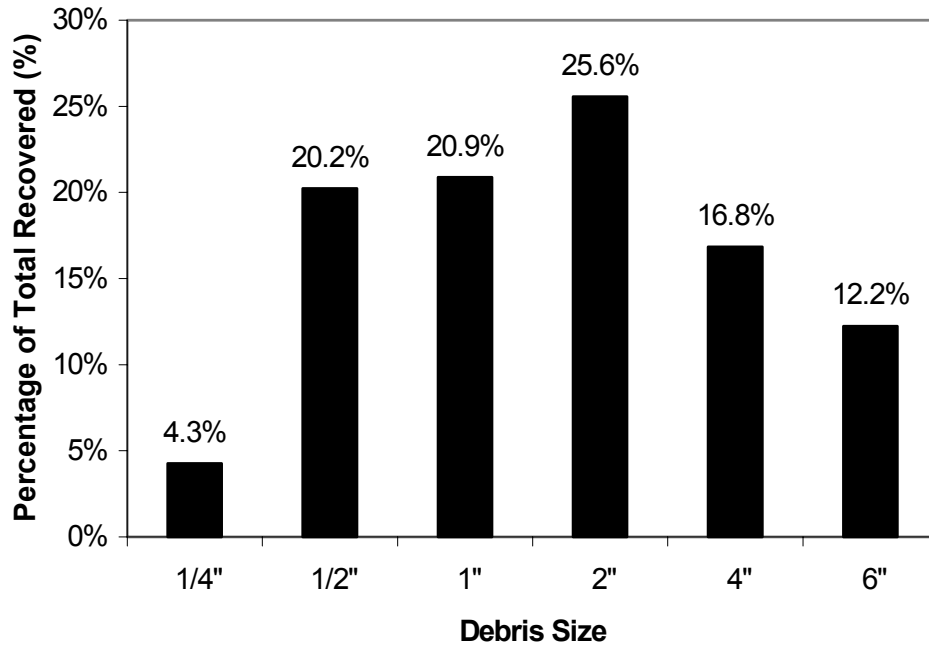


Figure 3-7 Typical RMI Debris Generated by Large Pipe Break



Figure 3-8 RMI Debris Observed in Siemens Steam-Jet Impact Tests

3.2.2.5 Ontario Power Generation Tests³⁻¹⁹

The OPG testing program was designed to address debris generation by two-phase jets created during a PWR blowdown through postulated breaks. The principal insulation of concern was aluminum-clad calcium-silicate; however, data from a single test performed with jacketed fiberglass also was made available to the NRC. In addition to broad objectives to collect data related to debris generation, an

additional (NRC) objective¹⁵ was to compare the insulation damage behaviors between the two-phase OPG tests and the BWROG AJIT tests.

The OPG jet-impact test rig consisted of a tank with a capacity of approximately 2.2 m³ filled with heated, pressurized water. A 3-in. schedule-160 nozzle was connected to the tank by a rupture-disk triggering mechanism,

¹⁵ The NRC contributed funding to the OPG tests.

associated piping, and instrumentation. A robust sample-holding frame held the insulation in front of the nozzle at a predetermined position and orientation. A debris catch cage approximately 12 ft³ in volume surrounded the nozzle and target to capture insulation debris for analysis.

With the 3-in. nozzle, the duration of the blowdown was approximately 10 s when the tank was filled initially with saturated water at a pressure of 10 MPa (1450 psia). Typical initial conditions for the tests were 324°F and 1417 psig.

Calcium-Silicate Tests

The target insulation was mounted on two 2-in. schedule-160 pipes. Figure 3-9 is a photograph of a typical mounting configuration. The insulation targets were 48 in. long and 1 in. thick; thus, the target outer diameter was 4.375 in. A 0.016-in.-thick aluminum cladding surrounded the insulation. The cladding and banding specifications were based on large-scale piping used in OPG's (CANDU) nuclear plants. Two or three sections of cladding (depending on the test) were required because the standard cladding length was 24 in. Thus, each target had one or two circumferential seams in addition to a longitudinal seam running its length. For calcium-silicate targets, the bands were stainless steel with a thickness of 0.020 in. and standard crimp connectors. For the single fiberglass test, the bands were 0.5 in. wide and 0.05 in. thick. The average spacing between bands¹⁶ was 6.5 in.

The longitudinal seam was oriented at an angle relative to the jet centerline. The targets were always mounted with their centerlines perpendicular to the jet centerline. The convention used was 0° at the front, 90° on the top, 180° at the rear, and 270° at the bottom. Most tests were conducted at an angle of 45°.

Because clad failure was found to be sensitive to the angle of the longitudinal seam, a few tests were performed in which a second layer of cladding was added to the target with the longitudinal seam of the outer clad positioned 45° from the jet and the seam of the inner clad positioned 180° from the outer clad.

¹⁶ For tests in which the jet was centered between the bands (circumferential seam offset from the jet center), the spacing was 8 in.

In addition to orientation of the longitudinal seam of cladding, test variables included the distance of the target from the jet and the position of the circumferential seam relative to the jet centerline. One test also was performed in which the target was positioned with a radial offset relative to the jet centerline. A summary of the specific test conditions examined (for calcium-silicate insulation) is shown in Table 3-5. Note that some test conditions were repeated to examine the reproducibility of the results (e.g., tests 1, 2, and 4).

For test conditions in which insulation was liberated, debris was collected by hand and sorted into three size classes: over 3 in., between 3 in. and 1 in., and under 1 in. Substantial quantities of debris were too small to be collected, and this debris was termed "dust;" its mass was calculated by subtracting the collected mass from the initial target insulation mass. The results are shown in Table 3-6. Photographs of debris in each of the collectable size classes are shown in Figure 3-10.

In addition to the measured debris size distributions, the following observations were made.

- When failure occurred, the mode of failure was tearing of the cladding caused by pressure acting on the edge of the (longitudinal) seam, thus exposing insulating material to the jet. The failure mode was such that a large fraction of calcium-silicate remained on the piping, protected from the jet by cladding on the front of the pipe. However, rapid disintegration and/or erosion of the calcium-silicate on the back side of the pipe caused a substantial fraction of the initial insulation mass to be converted to dust.
- The fraction of calcium-silicate converted to dust was found to be as high as 46% at target distances between 5D and 11D from the break. The level of material disintegration remained significant but reduced to 14% at 20D.
- The position of the longitudinal seam of the aluminum cladding was an important factor in determining whether insulation damage occurred.
 - When the longitudinal seam of over-clad calcium-silicate insulation was directly in line with the jet (at 0°), damage was observed at distances up to 7D.



Figure 3-9 Insulation Target Mounting Configuration in OPG Test (Longitudinal Seam at 45°, Circumferential Seam Offset)

Table 3-5 Test Matrix for the OPG Calcium-Silicate Jet Impact Tests					
TEST	Target Distance from Break	Over-cladding?	Orientation of Longitudinal Seam	Position of Circumferential Seam	RESULTS Insulation Liberated?
1	7D	No	0°	Jet center	Yes (small amount)
2	7D	No	0°	Jet center	No
3	5D	No	0°	Jet center	Yes
4	7D	No	0°	Jet center	No
5	5D	No	0°	Jet center	Yes
6	5D	No	180°	Jet center	No
7	5D, 2D radial offset	No	0°	Jet center	No
8	7D	No	45°	Offset	Yes
9	4D	Yes	45°	Offset	No
10	3D	Yes	45°	Offset	No
11	4D	Yes	45°	Offset	No
12	9D	No	45°	Offset	Yes
13	11D	No	45°	Offset	Yes
14	13D	No	45°	Offset	Yes
15	20D	No	45°	Offset	Yes

Table 3-6 Size Distribution of Calcium-Silicate Debris in Tests Where Insulation Was Liberated							
TEST	Target Distance	Initial Weight (g)	Remaining on Target (g)	Debris Size Classes			
				Over 3 in. (g)	1 to 3 in. (g)	Under 1 in. (g)	Dust (g)
5	5D	2109	1112	238	247	31	481
7	5D, offset 2D	2074	1325	75	160	49	465
8	7D	2116	1578	52	118	34	334
12	9D	2089	1263	48	136	55	587
13	11D	2090	1252	114	120	37	567
14	13D	2143	1700	53	61	23	306
15	20D	2130	1654	98	60	17	301



Figure 3-10 Typical Calcium-Silicate Debris Collected from an OPG Two-Phase Jet Test

- When the seam was oriented 45° away from the jet, damage occurred out to 20D, the furthest distance tested.¹⁷
- When the longitudinal seam was rotated away from the jet (180°), no damage was found at 5D.
- Application of a second layer of cladding (over-clad) successfully prevented damage with the insulation positioned as close as 3D from the break.

¹⁷ The jet centerline pressure at 20D estimated using the American National Standards Institute/American Nuclear Society (ANSI/ANS) 58.2 model (Section 3.3.1.1) was about 24 psi (Ref. 3-11, Volume 3). Because tests were not conducted at distances beyond 20D and damage could occur at distance somewhat greater than 20D, the minimum or onset pressure for damage would be somewhat less than 24 psi. When the jacket seam was oriented at 45°, the estimated minimum pressure for the onset of damage to the insulation was judged to be about 20 psi. Note that at distances of 20D, the analytical model used

Photographs of the end state of the calcium-silicate target insulation for one of the OPG tests that resulted in insulation damage are shown in Figure 3-11.

to estimate the pressure could have significant uncertainty associated with the estimate.



Front view



Back view

Figure 3-11 Post-Test Configuration of Aluminum-Clad Calcium-Silicate Insulation (Distance from Break of 9D and Longitudinal Seam at 45°)

Low-Density Fiberglass Test

The results of a single OPG test involving LDFG were available to the NRC. The general construction of the target insulation was similar to that described above for calcium-silicate: 0.016-in. aluminum cladding and the 0.5-in.-wide, 0.05-in.-thick stainless-steel bands. The target was positioned 10D away from the break nozzle, and the longitudinal seam of the cladding was oriented at 45°.

Extensive damage was observed along the full length of the insulation target. Fiberglass on the back side of the target pipe was removed completely; fiberglass on the front side was compressed and remained trapped by dented (but not perforated) cladding.

Shreds of the dislodged fiberglass were collected and sorted into three size classes: over 3 in., between 3 in. and 1 in., and under 1 in. As with the calcium-silicate, substantial quantities of debris were too small to be collected; however, the debris mass was calculated by subtracting the collected mass from the initial target insulation mass. The results are shown in Table 3-7.

Photographs of the fiberglass target insulation at the conclusion of an OPG test are shown in Figure 3-12.

3.2.2.6 Battelle/KAEFER Tests³⁻²⁰

Battelle Ingenieurtechnik conducted a series of debris generation experiments in 1995 for a German manufacturer of insulating systems—KAEFER Isoliertechnik GmbH. The experiments were performed in a facility constructed at an earlier time for simulations of high-pressure, two-phase vessel blowdown. The facility consisted of an electrically heated pressure vessel and appended piping that were isolated from the environment by a fast-opening burst-disk assembly designed to not discharge any fragments that might interfere with downstream insulation targets. The burst-disk assembly was set to open at an internal pressure of approximately 140 bar (2030 psia). Therefore, debris-generation measurements could be performed at pressures close to those of typical PWR systems.

A unique feature of these experiments is the arrangement of target insulating systems downstream of the break orifice. In contrast to debris-generation experiments performed by other investigators, which positioned a single target in the wake of the jet, the Battelle/KAEFER tests were conducted using an array of targets as shown in Figure 3-13. The array included four insulated 80-mm (3.2-in.)-diameter pipes positioned at different distances and orientations from the break plane. Two of

Table 3-7 Size Distribution of Fiberglass Debris in Tests Where Insulation Was Liberated							
TEST	Target Distance	Initial Dry Weight (g)	Dry Weight Remaining on Target (g)	Debris Size Classes			
				Dry Weight Over 3 in. (g)	Dry Weight 1 to 3 in. (g)	Dry Weight Under 1 in. (g)	Dry Weight of Unaccounted "fines" (g)
22	10D	530	250	6	21	4	249



Back side of target pipe



Collected debris

Figure 3-12 Post-Test Configuration of Aluminum-Clad Fiberglass Insulation (Distance from Break of 10D and Longitudinal Seam at 45°)

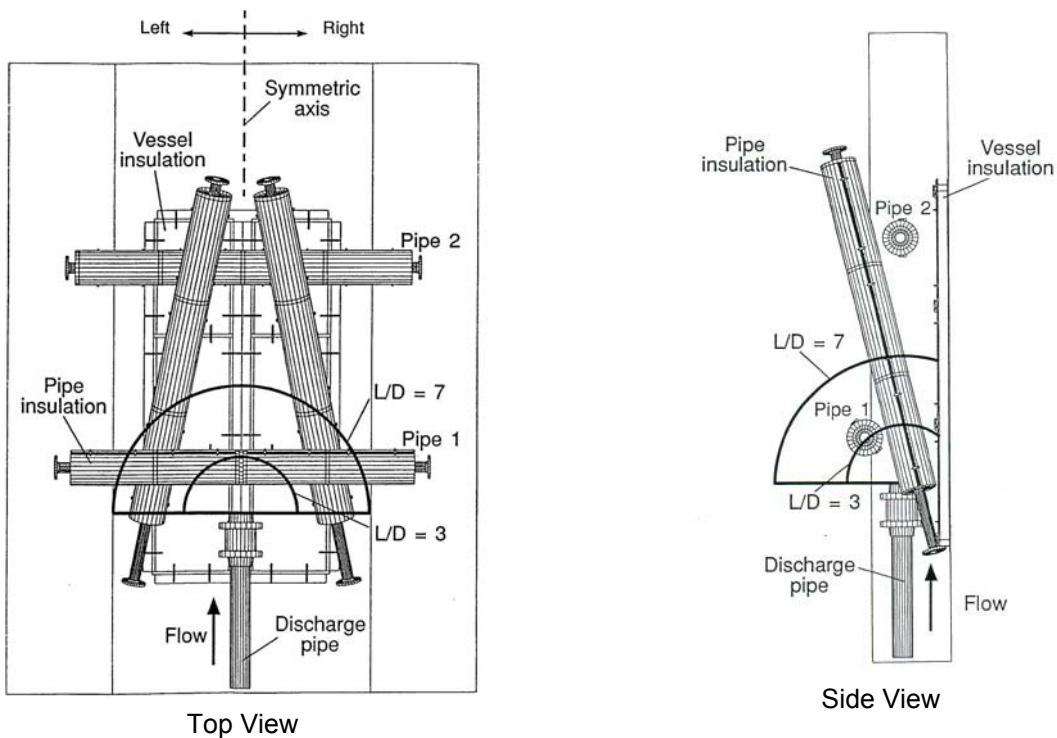


Figure 3-13 Configuration of the Target Field in the Battelle/KAEFER Tests³⁻²⁰

the pipes were oriented perpendicular to the jet (one close to the break plane, the other farther away). The other two pipes were mounted at a slight angle to, and laterally offset from the jet centerline. The four target pipes were positioned so that insulation response could be observed at distances covering three ranges: $L/D = 0$ to 3, $L/D = 3$ to 7, and $L/D > 7$. The test field also included an array of flat insulation that was located beneath the piping targets and installed flush onto the base of the test field. These flat insulation components were designed to represent vessel insulation assemblies. They were installed in two sections: one on the left-hand side of the test field and the other on the right hand side.

A total of four tests was performed with this arrangement. Each test involved a different combination of six types of insulating constructions on the piping and flat panel targets. The types of insulation studied were

- a stainless-steel RMI cassette,
- calcium-silicate in a steel cassette,
- a steel-jacketed Min-Wool blanket,
- steel-jacketed fiberglass,
- Min-Wool in a steel cassette, and
- fiberglass in a steel cassette.

In each test, a single type of insulating construction was installed on target locations on the left-hand side of the test field; a different type was installed on targets on the right-hand side. KAEFER Isoliertechnik GmbH manufactured all of the insulation.

The primary objective of the Battelle/KAEFER tests was to evaluate KAEFER insulation performance against the criteria described in US NRC Regulatory Guide 1.82,³⁻²¹ not to study the amount or characteristics of resultant debris. As a result, the Battelle/KAEFER test report describes the experimental findings in terms of the extent of damage to installed insulation rather than describing the shape, size or other characteristics of the debris generated (i.e., the complement of “debris generation” data.) Figure 3-14 shows the damage to the test specimens typical of these experiments. Specifically, the post-test condition of the insulation target field is described in terms of two quantities.

- Per cent remaining in “as-fabricated” or as-installed condition
- Per cent destroyed or fragmented

These quantities are estimated for each piece of insulation installed in the various target locations and are expressed simply in terms of per cent of the original installed target component. The data sheets for each test also recorded qualitative observations of target insulation conditions. For example, the surface conditions of partially damaged components were noted (e.g., dented or punctured), the size of fissures (if any) in weld seams on the outer cassette structure were estimated, and the fraction of the component’s core insulating material lost was estimated.

The following general observations were made from the data collected in these tests.

- The insulating construction with the poorest overall performance was the jacketed fiberglass blanket, with 68% of the target material in the field destroyed or severely damaged. The jacketed Min-Wool construction performed slightly better with ~44% damaged. All types of insulation encased in steel cassettes had lower levels of destruction than these two types.
- The extent of damage to targets in the test field was generally higher at locations close to the break plane (i.e., $3 < L/D < 5$) than at locations distant from the break plane ($L/D > 5$). However, significant exceptions were noted. Tests with targets manufactured as steel cassettes often showed damage patterns in which the damage to near-field targets was lower than damage to targets at the mid- or far-field. One possible explanation for this unusual observation is collateral damage. That is, material stripped from targets near- or mid-field became projectiles that struck other targets downstream.
- The orientation of weld seams in steel cassettes relative to the axis of the steam jet was found to influence the amount of damage inflicted on this type of insulation. The cases in which damage levels to cassettes were high often correlated to conditions in which the jet impacted a weld seam and ripped open the cassette.
- The overall levels of damage observed for the flat-panel insulation installed at the base of the test field were not significantly different from those observed for pipe insulation (i.e., the same trends noted above

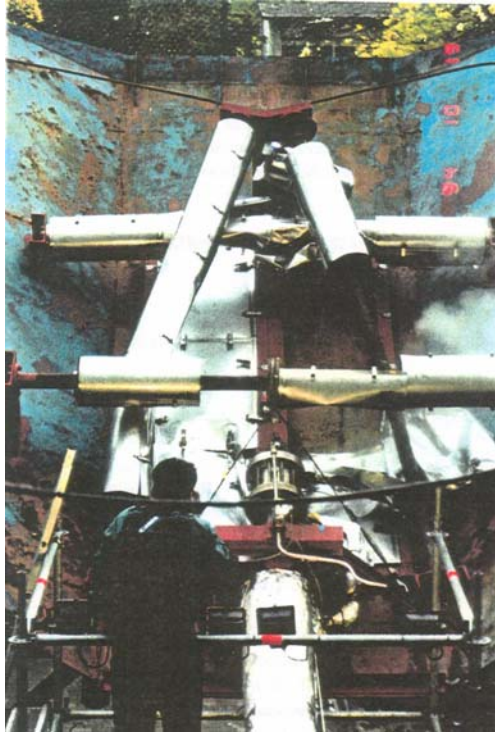


Figure 3-14 Typical View of Target Destruction in Battelle/KAEFER Tests³⁻²⁰

apply equally well to piping and flat-panel installations.) However, after a flat-panel target located near the jet was damaged (i.e., ripped from its initial location), the damage appeared to propagate upward, removing subsequent pieces of insulation from the base of the target field. As a result, the flat targets either tended to remain intact or be removed completely.

3.3 Debris-Generation Models and Analytical Approaches

In Section 3.2, the test data described the minimum pressure at which various forms of insulation material would be dislodged from their installed locations and, to a lesser extent, the physical forms (shape and size) that the resulting debris would take. To use this information to characterize debris generation in a reactor containment, one must be able to first determine the forces (i.e., pressure field) surrounding a postulated break location.

Jet impingement forces resulting from stationary breaks in high-pressure piping have been measured experimentally³⁻²² and calculated using models for isentropic expansion and flow

across shock discontinuities.^{3-8,3-9} This information subsequently was used as a basis for designing piping systems and other structures within reactor containments to survive mechanical loads created by the two-phase effluent from postulated RCS piping breaks.³⁻²³ Another important application of this information was the development of a conceptual picture of the ZOI within which piping insulation might be affected by jet forces emerging from a postulated pipe break. The ZOI was described by a right-angle cone projected along the axis of the ruptured pipe, which was assumed to expand freely into unobstructed space. This model for characterizing the region of space where pressures would be higher than ambient and sufficient to inflict damage on component insulation is reviewed in Section 3.3.1.

Unfortunately, the idealized pipe-break configurations examined in experimental studies do not address the effects of pipe movement or jet deflection in a congested area. As a result, an alternative approach to defining the ZOI for estimating debris generation was developed in the evaluations of BWR suppression-pool strainer performance.³⁻² This model, which is referred to as the “spherical debris-generation

model” accounts for the effects of jet reflection and pipe motion by transforming the total energy within an idealized conical jet into an equivalent sphere that surrounds the break location. This model also has the advantage of not requiring information about the angular orientation of the rupture pipe in space to map out the volume within which insulation of a particular material/construction would be damaged. This model is described in Section 3.3.2.

3.3.1 Cone Models

3.3.1.1 ANSI/ANS Standard

ANSI/ANS-58.2-1988³⁻²³ describes an analytical method for evaluating the geometry of a free-expanding jet. In addition to its basic purpose, which is to describe fluid forces on structures at various distances from a postulated pipe break, the basic mathematical model is the foundation of the conical ZOI used in Ref. 3-5.¹⁸

The model represents the free-expanding jet as a series of three regions, as shown in Figure 3-15. Region 1, which is described as the “jet core,” represents the region of space immediately downstream of the break within which fluid striking an intervening object (target) would experience full recovery of the fluid stagnation pressure. This region is significant only for jets involving subcooled stagnation conditions. Region 2 extends from the end of the jet core to a distance downstream of the break, where the jet has expanded (in free, unimpeded space) to its asymptotic limit, i.e., isentropic expansion to near-ambient conditions. In practice, this means that the jet centerline pressure has decreased to less than twice the ambient pressure. In Region 3, the jet expands at a reduced rate and at an assumed angle of 10° to become fully equilibrated with ambient conditions.

The distance to the asymptotic plane from the break (L_a) and the cross-sectional area of the jet at the asymptotic plane (A_a) are calculated relative to the equivalent dimensions at the break plane; i.e., the break diameter D_e and

break area A_a with the formulas listed in the right-hand side of Figure 3-15.

The diameters of the jet in Regions 2 and 3 (relative to the break diameter D_e) are calculated as follows.

Region 2:

$$\frac{D_j}{D_e} = \sqrt{C_T \left[1 + \frac{L}{L_a} \left(\frac{A}{C_T A_e} - 1 \right) \right]}$$

and

Region 3:

$$\frac{D_j}{D_e} = \sqrt{\frac{A_j}{A_e}} = \sqrt{\frac{A_j A_a}{A_a A_e}} = \left[1 + \frac{2(L - L_a)}{D_a} \tan 10^\circ \right] \sqrt{\frac{A_a}{A_e}},$$

where L = distance away from the break place at which the jet diameter is D_j .

In addition to determining the overall dimensions of the jet, applying the ANSI/ANS model to estimate debris generation requires information regarding the geometry of the isobar within the jet that encloses the region of space where pressures exceed a particular damage pressure. This region of space is shown in Figure 3-16 and is described by the following expressions.

The pressure at any distance downstream of the break plane (L) and distance away from the jet centerline (D_x) is calculated as follows.

Region 2:

$$\frac{P_x}{P_{jc}} = \left(1 - \frac{D_x}{D_j} \right) \left\{ 1 - 2 \frac{D_x}{D_j} \left[1 - 3C_T \left(\frac{D_e}{D_j} \right)^2 \left(\frac{P_o}{P_{jc}} \right) \right] \right\}$$

and

Region 3:

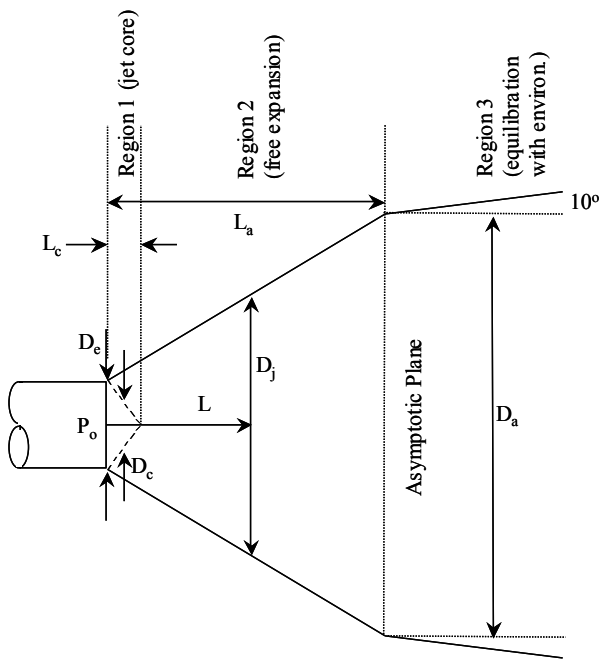
$$\frac{P_x}{P_{jc}} = 1 - \frac{D_x}{D_j},$$

where the pressure along the jet centerline (P_{jc}) is

Region 2:

$$\frac{P_{jc}}{P_o} = F_c - \left[F_c - 3C_{Te} \left(\frac{D_e}{D_a} \right)^2 \right] \frac{\left(1 - \frac{L_c L_a}{L_a L_L} \right)}{\left(1 - \frac{L_c}{L_a} \right)},$$

¹⁸ A number of experimentally based empirical correlations for jet expansion exist in the literature. Although these correlations may predict the data on which the correlations are based adequately, extreme care must be taken in extrapolating those correlations to other pipe-break configurations, sizes, pressures, etc.



$$\frac{L_a}{D_e} = \frac{1}{2} \left(\sqrt{\frac{A_a}{A_e}} - 1 \right)$$

$$\frac{A_a}{A_e} = \left(\frac{G_{crit}^2}{g_c \rho_{ma} C_T P_0} \right)$$

$$\rho_{ma} = \frac{1}{\frac{\chi_a}{\rho_g} + \frac{(1-\chi_a)}{\rho_f}}$$

where; $\rho_{f/g}, \chi$ are evaluated at P_a

$$\frac{P_a}{P_{amb}} = 1 - 0.5 \left(1 - \frac{2P_{amb}}{P_0} \right) f(h_o)$$

$$f(h_o) = \begin{cases} \sqrt{0.1 + \left(\frac{h_o - h_f}{h_{fg}} \right)} & \text{for } \left(\frac{h_o - h_f}{h_{fg}} \right) > -0.1 \\ 0.0 & \text{for } \left(\frac{h_o - h_f}{h_{fg}} \right) < -0.1 \end{cases}$$

where: G_{crit} = break flow rate (mass flux)
 ρ_{ma} = mixture density at asymptotic plane
 ρ_g, ρ_f = saturated vapor, liquid density
 C_T = thrust coefficient
 P_0 = stagnation pressure
 χ = mixture vapor mass fraction (quality)
 h_o, h_f = stagnation, saturation liquid enthalpy

Figure 3-15 ANSI/ANS Standard Free-Expanding Jet Model

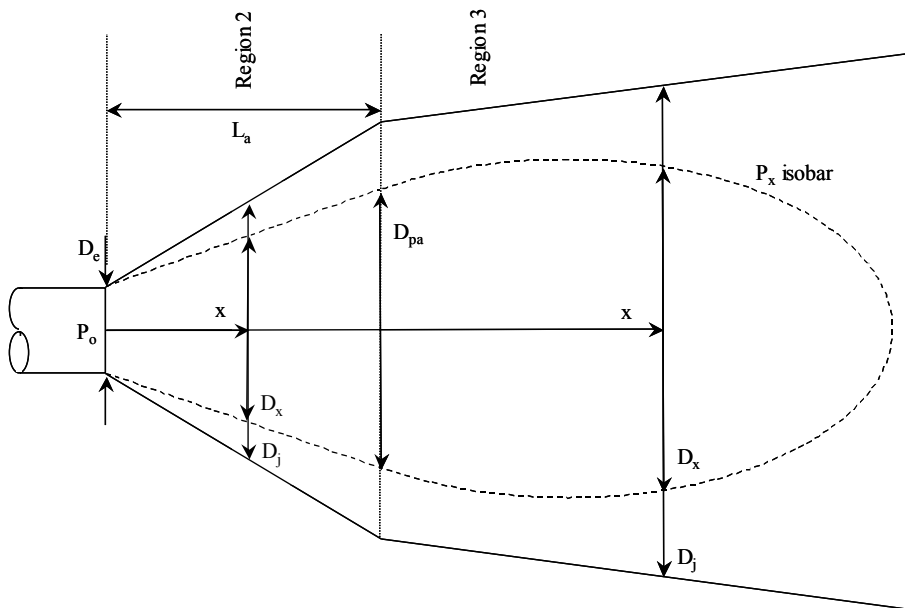


Figure 3-16 Isobar of Damage Pressure P_x within a Fixed, Free-Expanding Jet

where

$$F_c = \begin{cases} 1.0 & \text{for } \left(\frac{D_j}{D_e}\right)^2 \leq 6C_T \text{ at } L = L_c \\ 6C_T \left(\frac{D_e}{D_j}\right)^2 & \text{for } \left(\frac{D_j}{D_e}\right)^2 > 6C_T \text{ at } L = L_c \end{cases}$$

Region 3:

$$P_{jc} = 3P_o \frac{A_j}{A_e}$$

At any distance away from the break plane, the diameter of the volume defined by an isobar of a fixed pressure (P_x) can be calculated by solving the above equations for D_x . The result is

Region 2:

$$\frac{D_x}{D_j} = \frac{1}{4A} \left[(2A+1) - \sqrt{(2A+1)^2 - 8A \left(1 - \frac{P_x}{P_{jc}}\right)} \right]$$

where

$$A = \left[1 - 3C_{Te} \left(\frac{D_e}{D_j}\right)^2 \left(\frac{P_{oe}}{P_{jc}}\right) \right]$$

Region 3:

$$\frac{D_x}{D_j} = 1 - \frac{P_x}{P_{jc}}$$

3.3.1.2 Three-Region Conical Jet³⁻⁵

A variant of the three-region conical-jet expansion model was proposed in NUREG-0897 to describe the varying degrees of damage inflicted on insulation material, with distance away from the break, by the initial shock wave and subsequent mechanical erosion. The model did not calculate the pressure distribution within the free-expanding jet explicitly but described the distance downstream of the break plane at which the level of material damage decreased from "total destruction" (Region 1) to "high levels of destruction" (Region 2) to "dislodged, as-fabricated pieces" (Region 3). The distance away from the break plane at the interface between these regions was described in terms of the number of break diameters (L/D) as shown in Figure 3-17.

The boundaries of the three regions represented in this model were based on calculations of two-dimensional pressure distributions (similar to those described for the ANSI/ANS standard). The following significant findings were derived from the calculations and reported.³⁻⁵

1. "Target pressure loadings increase asymptotically at L/D's less than 3.0 to break exit pressures. At L/D's less than 3, survivability of insulation materials is highly unlikely.
2. At L/D's from 5 to 7, the centerline stagnation pressure becomes essentially constant at approximately 2 ± 1 bars.
3. The multidimensional pressure field loads the target over a large region; this region may be approximated by a 90° jet cone expansion model. A hemispherical expansion model could be another approximation for this expanding pressure field. These two-dimensional calculations do not support the use of the Moody jet model (a narrow cone) for targets close to the break locations."

Experiments performed in the HDR facility (see Section 3.2.2.2) formed the primary basis for connecting the two-phase pressure distributions calculated with the conical jet expansion model to observation of insulation damage. Sufficient experimental data were not available at the time that NUREG-0897³⁻⁵ was published to quantitatively distinguish "high levels of destruction" in Region 2 from either of its two neighbors. However, the following qualitative description of damage was offered.

... it appears that [in Region 2] the RMI debris could consist of damaged inner foils and damage assemblies or components that were the result of further LOCA damage. Experimental data available for fibrous insulations indicate that shredding and damage can extend into Region 2, with such damage decreasing with distance from the jet. However, if the 'inner core' of fibrous insulation is exposed to the break jet (as would occur if the cover blanket were breached), blowdown transport of this material would be expected to extend for distances much greater than 7 L/D's.

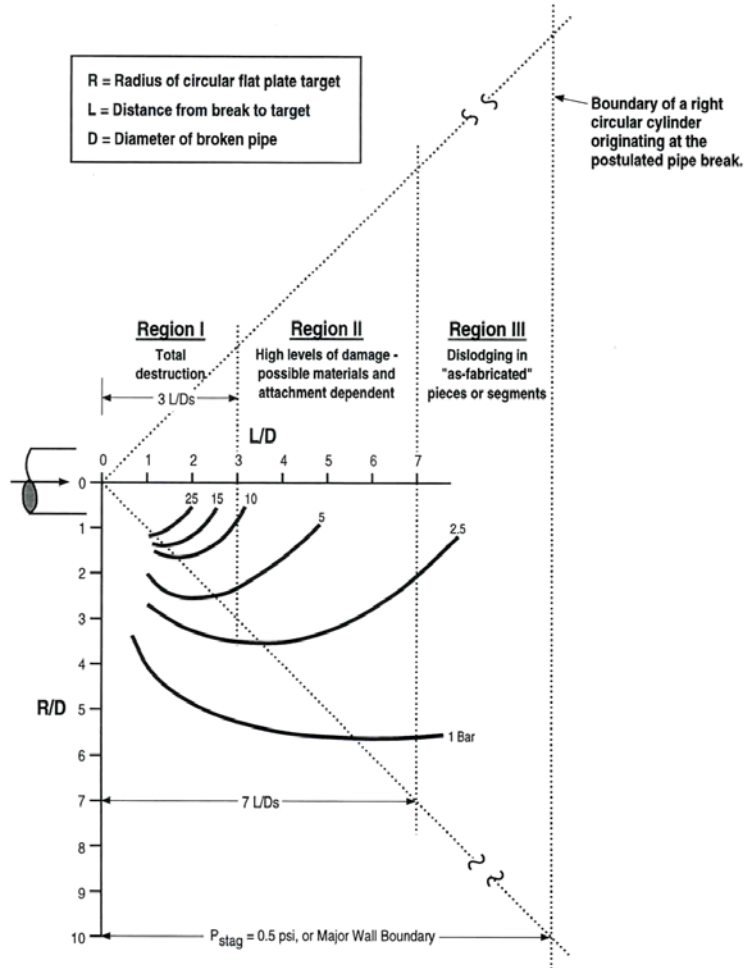


Figure 3-17 Illustration of the Three-Region, Two-Phase Conical-Jet ZOI Model³⁻⁹

3.3.2 Spherical Models

3.3.2.1 Three-Region Spherical Model³⁻²

A major limitation of the conical model is the inherent assumption that pipe separation and offset at the location of the break are fixed in space. That is, movement of the break plane(s) is not taken into account explicitly. The ANSI/ANS standard³⁻²³ acknowledges this limitation by stating that adjustments to the model are necessary to properly account for movement of the break plane(s) and/or reflection of the jet by intervening structures. In particular, the ANSI/ANS Standard states:

“Regardless of the fluid jet model used to determine affected structures and components, engineering judgment shall be applied in determining whether the jet will impinge upon a given target. The geometry

of the jet cannot be perfectly defined for all of the various fluid conditions under today’s state of the art ... Neither can the movement of the ruptured pipe, thus the jet centerline, be defined with complete accuracy.”

Also,

“The movement of the jet centerline due to pipe whip shall be taken into account in the characterization of jet impingement loads on a target.”

The so-called “three-region, spherical model” for characterizing the ZOI at a particular break location was developed to address uncertainties in break-plane movement and jet reflection.³⁻² The three-region, spherical model is illustrated in Figure 3-18.

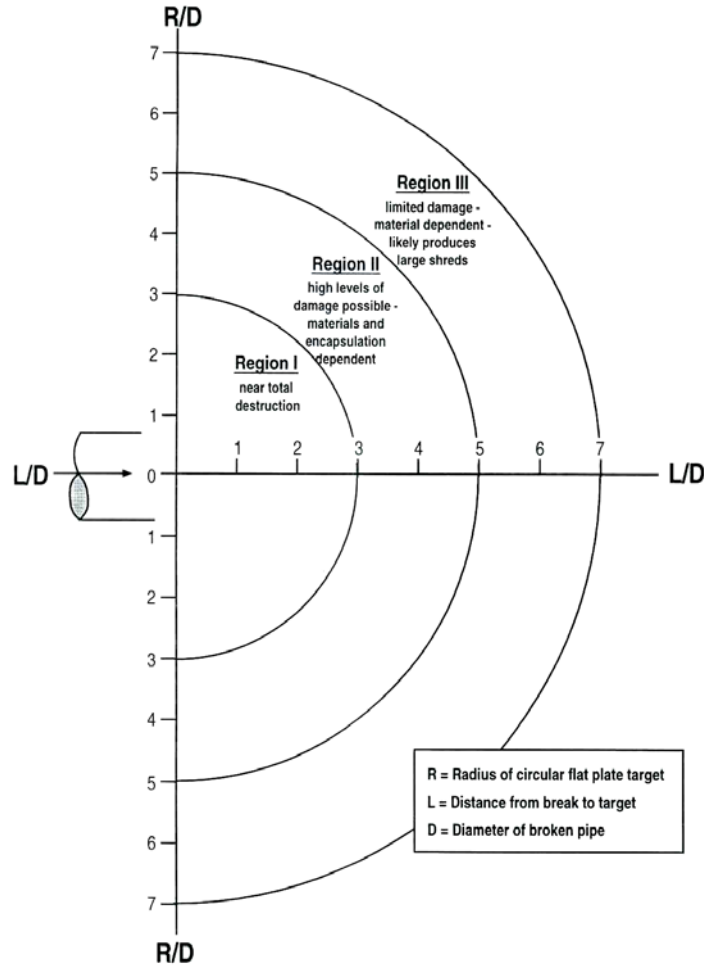


Figure 3-18 Illustration of the Three-Region, Two-Phase Spherical ZOI Model³⁻²

As in the three-region cone model, the degree of damage decreases from Region 1 to Region 2 to Region 3. The extent of damage (i.e., the size distribution of insulation fragments) is based on experimental observations of target material impacted by stationary jets at varying distances from the break plane. For example, the experimental observations summarized in Section 3.2 clearly indicate that the fraction of insulation reduced to small fragments is much less for steel-jacketed fibrous pillows than for unjacketed fiber blankets. In the NRC's evaluation of BWR suppression-pool strainers,³⁻² such differences were handled through the use of "destruction factors." For example, destruction factors of 0.75, 0.60, and 0.40 were used to represent the fraction of steel-jacketed Nukon[®] reduced to a sufficiently small size to be transported by blowdown forces from the drywell

to the wetwell of a BWR Mark I containment. Different values were used for other types of insulation.

3.3.2.2 Equivalent-Volume Sphere Model

An alternative approach to distorting the conical ZOI sphere is the so-called "equivalent-volume" sphere model. This model couples the ideas (from Section 3.3.1.1) of a conical isobar within which pressures exceed a particular damage pressure with a spherical shape to capture the major effects of break-plane movement and jet reflection. A version of this model initially was proposed by the BWROG as one of three possible methods for estimating quantities of debris generation.³⁻³ The basic approach has five essential steps.

1. Determine the damage or destruction pressure (P_{dest}) for an insulating construction of interest.
2. Determine the total volume of space swept out by the conical isobar defined by the damage pressure (i.e., $P_x = P_{dest}$ in Section 3.3.1.1).
3. Convert the total volume within the isobar to a sphere of radius R .
4. Place the origin of the sphere at a specific, postulated break location and determine the total quantity of insulation of the selected type that is within the sphere.
5. Move the origin of the sphere to all other candidate break locations and repeat the exercise.¹⁹

The radius of the equivalent sphere is a function of the damage pressure (unique to each type of insulating construction), the diameter of the pipe where the break is assumed to occur, and the fluid medium within the pipe (i.e., steam vs water).

In the BWROG method, multipliers or correction factors were applied to this basic method to account for destruction factors less than 1.0. The NRC's evaluation of this method determined the general approach to be acceptable for insulating construction with low characteristic damage pressure (Ref. 3-4, Appendices B, C, D, F, G, and K). However, for insulations with high damage pressure, the staff recommended that licensees develop the equivalent sphere on the basis of target-area-average pressures instead of the jet centerline pressures.

¹⁹ Computer programs have been developed to calculate the volume of insulation inside the ZOI for all potential break locations within a containment systematically. For example, the volunteer plant assessments performed as part of the NRC's parametric evaluation of recirculation sump performance used the CASINOVA program to perform these computations.³⁻¹¹ This program has the ability to vary the ZOI for each type of material near a particular weld (i.e., the ZOI associated with the damage pressure for a particular material) and to evaluate all high-energy welds systematically. The systematic analysis provides a spectrum of potential insulation debris volumes by insulation type that can be used to determine the size a screen capable of handling the potential debris load to the recirculation sump screens.

3.3.3 Debris-Size Distribution as a Function of Local Jet Pressure

All insulation located within the ZOI generally is assumed to be damaged to some extent. The extent of damage could range from the total destruction of a blanket (or RMI cassette) with all of its insulation turned into debris of very small dimensions to the blanket/cassette being only slightly damaged and even remaining attached to its piping. Available debris-generation tests clearly indicate that the extent of damage (i.e., the size distribution of resulting debris fragments) depends strongly on the magnitude of the jet forces in the immediate proximity to individual insulation components. Qualitatively, increasing the local jet forces (i.e., increasing local stagnation pressures) tends to produce higher fractions of small debris fragments.

The size distribution of debris formed from insulation targets located within the ZOI can be determined only by combining measurements of debris-size distribution with measurements (or analytical estimates) of local stagnation pressure. Unfortunately, the quantitative relationship between the distribution of debris fragment size and local jet pressure has not been investigated thoroughly. Most reports of experimental work on debris generation document the size distribution of resultant debris fragments along with the initial location of the insulation target but do not measure, or estimate, the local jet stagnation pressure. This extension of test data is left to others to develop by applying one of the models described in Section 3.3.1 or 3.3.2. This gap in the published knowledge base on debris generation is being addressed in an ongoing NRC study of PWR recirculation sump performance for a "volunteer plant." The results of this work are anticipated in early 2003. The general method being used to correlate debris size(s) to local jet pressure in the volunteer plant analysis is summarized below.

Using the spherical ZOI damage model, the fraction of insulation of type- i that is reduced to debris within a particular size bin is given by the following integration:

$$F_i = \frac{3}{r_{ZOI}^3} \int_0^{r_{ZOI}} g_i(r) r^2 dr \quad ,$$

where

- F_i = the fraction of debris of type- i within a particular size bin,
- $g_i(r)$ = the damage distribution for of debris type- i ,
- r = the radius from the break in the spherical ZOI model, and
- r_{ZOI} = the outer radius of the ZOI.

The volume associated with a particular level of damage is determined by estimating the volume within a particular isobar within the jet (i.e., any insulation located within this isobar would be damaged to the extent, or greater, associated with that pressure). As described in Section 3.3.2.2, the equivalent-volume sphere model can be used to convert this volume to an equivalent spherical volume with an origin at the break plane. Hence, the debris-size distribution can be associated with a particular spherical radius [i.e., $g_i(r)$]. The distribution would be specific to a particular kind of insulation, jacketing, jacketing seam orientation, and banding.

The difficulty associated with this evaluation is the limited database for insulation debris generation. Examples of debris generation data that include debris-size information that can be correlated to local jet pressure include the BWROG AJIT tests (Section 3.2.1.2) and the OPG steam/water debris generation tests (Section 3.2.2.5). However, when these data are subjected to the above integration, sufficient data points are not available to fully characterize the damage distribution function [$g_i(r)$]. For example, the BWROG data for DPSC Mirror[®] stainless-steel RMI, which was found to be damaged at jet pressures as low as 4 psi, indicates the size distribution shown in Figure 3-19 when the insulation is installed with standard bands.²⁰

Although these data may be suitable for describing the extent of cassette damage in the outer reaches of the ZOI, they do not describe debris generated at locations closer to the break, where the cassette would be subject to substantially higher local stagnation pressures. Information at very high local pressures can be gleaned from limited data collected in the Siemens-Karlstein tests (Section 3.2.2.4).

These tests included measurements of RMI destruction when a cassette was mounted directly in front of the break plane. Under such conditions, the cassette was reduced to small shreds, with a majority of the pieces characterized as smaller than 2-in. (see Figure 3-7.) Unfortunately, no data are available for the damage of this type of insulation at local pressures between 120 psi and approximately 1000 psi. Given the combined body of data, the ZOI integration for small (< 2-in.) debris fragments of stainless-steel RMI can be made by conservatively assuming that insulation of this type subjected to jet pressures greater than 120 psi becomes debris smaller than 2 in.

Similar exercises can be performed for other types of insulation. However, there are gaps in quantitative measurements of debris size with variable local pressure (i.e., position relative to the break plane) for all types of debris. Consequently, conservative assumptions regarding debris size often are used to characterize quantities of transportable debris.

3.4 References

- 3-1. Wysocki, J., and R., Kolbe, "Methodology for Evaluation of Insulation Debris Effects," NUREG/CR-2791, SAND82-7067, Burns and Roe, Inc. and Sandia National Laboratories, September 1982.
- 3-2. Zigler, G., J. Brideau, D. V. Rao, C. Shaffer, F. Souto, and W. Thomas, "Parametric Study of the Potential for BWR ECCS Strainer Blockage Due to LOCA Generated Debris," NUREG/CR-6224, SEA 93-554-06-A:1, Science and Engineering Associates, Inc., October 1995.
- 3-3. BWR Owners' Group, "Technical Support Documentation: Utility Resolution Guidance (URG) for ECCS Suction Strainer Blockage, 4 Vols., Doc. Control 96-266, November 1996.
- 3-4. "Safety Evaluation by the Office of Nuclear Reactor Regulation Related to NRC Bulletin 96-03 Boiling Water Reactor Owners Group Topical Report NEDO-32686, 'Utility Resolution Guidance for ECCS Suction Strainer Blockage,'" Docket No. PROJ0691, August 20, 1998.

²⁰Distributions developed using most conservative applicable data points.

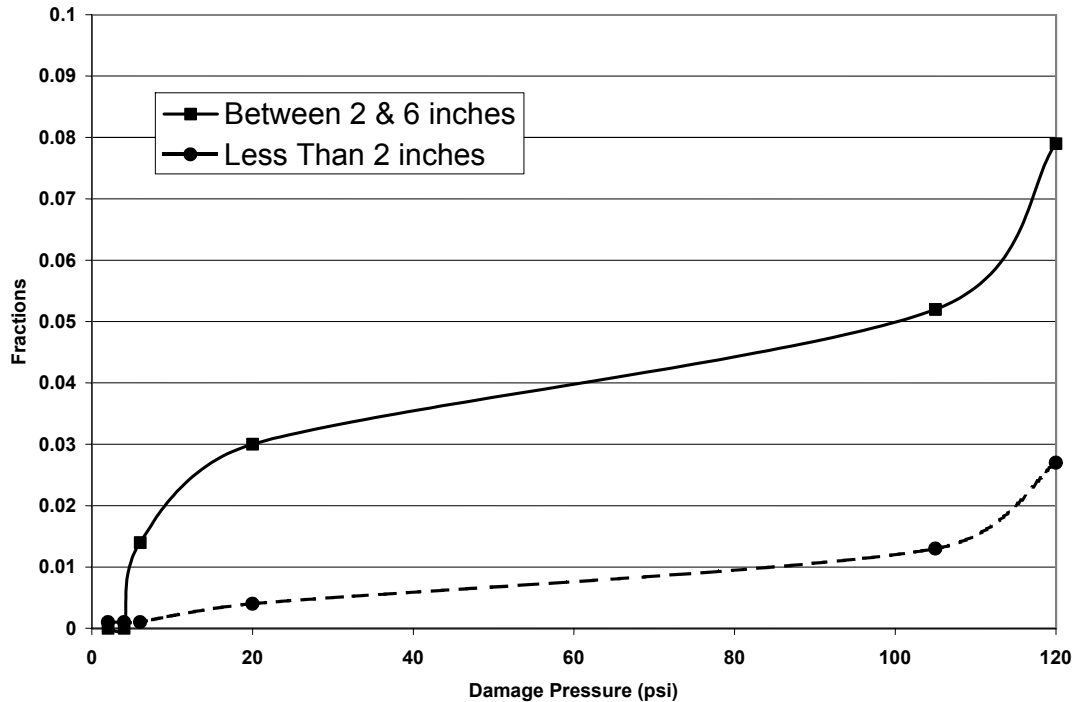


Figure 3-19 Debris Size as a Function of Local Jet Pressure
 (Applicable Only to DPSC SS Mirror® Insulation Based on Available Data)

- 3-5. U.S. Nuclear Regulatory Commission, "Containment Emergency Sump Performance," NUREG-0897, Rev. 1, Nuclear Regulatory Commission, October 1985.
- 3-6. Nuclear Energy Institute (NEI), "Results of Industry Survey on PWR Sump Design and Operations," June 7, 1999
- 3-7. U.S. Nuclear Regulatory Commission, "Assurance of Sufficient Net Positive Suction Head for Emergency Core Cooling and Containment Heat Removal Pumps," Generic Letter 97-04, October 1997.
- 3-8. Moody, F. J., "Prediction of Blowdown Thrust and Jet Forces," Paper 69-HT-31, American Society of Mechanical Engineers, 1969,
- 3-9. Weigand, G., et al., "Two Phase Jet Loads," NUREG/CR-2913 Rev. 4, Sandia National Laboratories, January 1983.
- 3-10. Rao, D. V., B. C. Letellier, K. W. Ross, L. S. Bartlein, and M. T. Leonard, "GSI-191 Technical Assessment: Summary and Analysis of U.S. Pressurized Water Reactor Industry Survey Responses to GL 97-04," NUREG/CR-6762, Volume 2, LA-UR-01-1800, August 2002.
- 3-11. Rao, D. V., C. J. Shaffer, and S. G. Ashbaugh, "GSI-191 Technical Assessment: Development of Debris-Generation Quantities in Support of the Parametric Evaluation," NUREG/CR-6762, Vol. 3, LA-UR-01-6640, Los Alamos National Laboratory, November 2001.
- 3-12. Rao, D. V., C. Shaffer, and E. Haskin, "Drywell Debris Transport Study," NUREG/CR-6369, SEA 97-3105-A:14, 3 Vols., Science and Engineering Associated, Inc., September 1999.
- 3-13. Studsvik Energiteknik, "Component Tests: Paint and Heat Insulation," MXA-4-206, Marviken Power Station, Sweden, September 1997.
- 3-14. Studsvik Material AB, "Steam Jet Dislodgement Tests of Thermal Insulating Material of Type Newtherm 1000 and Caposil HT1," M-93/41, April 1993.

- 3-15. Studsvik Material AB, "Steam Jet Dislodgement Tests of Two Thermal Insulating Materials," M-93-60, May 1993.
- 3-16. Blomqvist, M. and M Delby, ABB-Atom, "Report from Tests Concerning the Effect of Steam Jet on Copsil Insulation at Karlshamn, Carried Out on April 22-23, 1993, and May 6, 1993," SDC 93-1174, June 1993.
- 3-17. Vattenfall Energiesystem, "Metallic Insulation Jet Impact Tests (MIJIT)," GEK 77/95, June 1995.
- 3-18. Zigler, G., et al., "Experimental Investigation of Head Loss and Sedimentation Characteristics of Reflective Metallic Insulation Debris," SEA-95-970-01-A:2 (1996), and NT34/95/e32, "RMI Debris Generation Testing: Pilot Steam Test with a Target Bobbin of Diamond Power Panels."
- 3-19. Ontario Power Generation, "Jet Impact Tests—Preliminary Results and Their Applications," N-REP-34320-10000-R00, April 2001.
- 3-20. Wenzel, H. H., et al., "Blow-down Investigations on the Performance of Insulating Systems—Taking into Account the Regulatory Guide 1.82," B.I.G. V-32.608, Battelle Ingenieurtechnik GmbH, Germany, August 1995.
- 3-21. Regulatory Guide 1.82, Revision 1, "Water Sources for Long-Term Recirculation Cooling Following a Loss-of-Coolant Accident," U.S. Nuclear Regulatory Commission, Revision 1, November 1985, and Revision 2, May 1996.
- 3-22. Studsvik Energiteknik, "The Marviken Full Scale Jet Impingement Tests—Summary Report," MXD-301, September 1982.
- 3-23. American Nuclear Society, "Design Basis for Protection of Light Water Nuclear Power Plants Against the Effects of Postulated Pipe Rupture," ANSI/ANS-58.2-1988, October 1988.
- 3-24. Rao, D. V., B. C. Letellier, C. Shaffer, S. Ashbaugh, and L. S. Bartlein, "GSI-191 Technical Assessment: Parametric Evaluations for Pressurized Water Reactor Recirculation Sump Performance," NUREG/CR-6762, Vol. 1, LA-UR-01-4083, Los Alamos National Laboratory, August 2002.

4.0 AIRBORNE/WASHDOWN DEBRIS TRANSPORT IN CONTAINMENT

Section 4 summarizes the available knowledge regarding transport of insulation debris within the containment from its location of origin to the containment sump pool. The transport of insulation debris would be caused first by the effluences from a high-energy pipe break that would not only destroy insulation near the break, but also would transport that debris throughout the containment, i.e., airborne debris transport. If the break effluences were to pressurize the containment sufficiently to activate¹ the containment spray system to suppress pressurization, the transport of insulation debris would also be driven by the drainage of spray water from the spray heads to the recirculation sump, i.e., washdown debris transport. The knowledge base associated with insulation debris transport is organized in the following subsections.

- Section 4.1 presents an overview of the mechanics associated with airborne/washdown debris transport, including the characteristics of an accident relevant to debris transport, the relevant plant features, the physical processes and phenomena, and the debris characteristics affecting transport.
- Section 4.2 describes the testing relevant to airborne/washdown debris transport that has been performed.
- Section 4.3 describes the analyses relevant to airborne/washdown debris transport that have been performed.
- Section 4.4 summarizes the analytical approaches developed to predict the transport of insulation debris.
- Section 4.5 discusses the basic “rules of thumb” observed during testing and analytical studies.

The phenomena associated with airborne and washdown debris transport is also discussed. These phenomena include the following:

- How substantial quantities of airborne debris in motion would come into contact with

¹The spray system would activate if the containment pressure exceeded the system-activation setpoint. The pressurization of the containment is plant- and accident-scenario-dependent (e.g., the size of the break).

containment structures and equipment and be deposited onto these surfaces.

- How debris would settle gravitationally onto equipment and floors as depressurization flows slow down.
- How airborne debris (usually very fine) would be washed out of the air by the spray droplets except in areas not covered by the sprays.
- How the impact of these sprays onto surfaces and the subsequent drainage of the accumulated water would wash deposited debris down toward the sump pool.
- How containment sprays may degrade insulation debris further through the process of erosion, thereby creating even more of the very fine and most transportable debris.
- How the analysis of debris transport in the containment depends on the type and characteristics of the debris generated by the break (discussed in Section 3).

The containment transport analyses (above the sump pool) provide a description of the debris entering the sump pool in terms of the type of debris, where the debris enters the pool, and when the debris enters the pool. Section 5 discusses the transport of debris within the sump pool. A majority of the testing and analysis relevant to airborne/washdown insulation debris transport was performed to support the suction-strainer-clogging issue for BWRs; however, most of this research is also directly applicable to PWRs. The applicability of BWR research to PWRs is discussed as appropriate.

It also should be noted that debris-transport research has tended to focus on the transport characteristics of fibrous insulation debris. Research has also considered other types of insulation debris, notably experimental RMI debris research, but the potential for fibrous insulation debris to clog a strainer generally has been found to be substantially greater for fibrous debris than for RMI debris. Further research has tended to focus on LDFG over the other types, e.g., HDFG or mineral wool fibrous debris. Therefore, there are gaps in the completeness of debris-transport research.

4.1 Overview of Mechanics

The transport of debris within a PWR would be influenced by both the spectrum of physical processes and phenomena and the features of a particular containment design. Because of the violent nature of flows following a LOCA, insulation destruction and subsequent debris transport are chaotic processes. For example, a piece of debris could be deposited near the sump screen directly or it could take a much more tortuous path—first going to the dome and then being washed by the sprays back down to the sump. A piece of debris could also be trapped in any number of locations. Debris-transport analysis includes the characterization of the accident, the design and configuration of the plant, the generation of debris by the break flows, and both airborne and waterborne debris-transport dynamics.

The NRC convened a panel of recognized experts with broad-based knowledge and experience to apply the Phenomena Identification and Ranking Table (PIRT) process to the transport through a PWR containment of debris generated by a high-energy pipe break.⁴⁻¹ The PIRT process was designed to identify processes and phenomena that would dominate debris-transport behavior. Further, these processes and phenomena were prioritized with respect to their contributions to the reactor phenomenological response to the accident scenario. The NRC also convened a PIRT panel to rank transport processes relative to debris transport within a BWR drywell.⁴⁻²

This section specifically discusses:

- the characteristics of postulated accident scenarios relevant to the transport of insulation debris (Section 4.1.1),
- the plant features that would affect transport of insulation debris (Section 4.1.2),
- the physical processes and phenomena that affect transport of insulation debris (Section 4.1.3), and
- the characteristics of insulation debris that affect its transport (Section 4.1.4).

4.1.1 Accident Characterization Relevant to Debris Transport

Long-term recirculation cooling must operate following the range of possible LOCA accident

scenarios and non-LOCA accident scenarios (e.g., a main steam line break). A comprehensive debris-transport study should consider an appropriate selection of these scenarios. The maximum debris transport to the screen likely will be determined by a small subset of accident scenarios, but this scenario subset should be determined systematically. Many important debris-transport parameters will depend on the accident scenarios.

Perhaps the most important aspect of the accident scenario in regard to debris transport in the containment is the size of the break, which is usually specified as a small, medium, or large LOCA. The break size influences the debris transport in a number of ways:

- The size of the break largely determines the dynamics within the containment of the resultant primary system depressurization. The primary system depressurization period usually is referred to as the blowdown phase. Blowdown dynamics determine transport velocities and flow qualities within the containment, which in turn affect the mechanisms for debris deposition onto structures.
- The size of the break also affects the timing of the accident sequence, i.e., the completion of the blowdown phase, the ECCS injection phase, and the time when the recirculation pumps start to pump water from the sump (recirculation phase). The injection phase corresponds to ECCS injection into the primary system that subsequently establishes the sump pool. The recirculation phase refers to long-term ECCS recirculation.
- The size of the break can also determine whether the containment sprays activate. For large breaks, the sprays likely would activate almost immediately, whereas with a smaller break, the containment pressure rise may not be sufficient to initiate the sprays.
- The size of the break would determine the pumping flow rate from the sump in that the pump flow rate would be limited by the rate of flow from the break after the vessel inventory was replaced.

Debris transport would be affected by the location and size of the break. The location of the break, along with the general design of the containment, determines the patterns of flow throughout the containment. It affects flow

dynamics, how and where debris impacts structures, whether debris would be transported away from the sump or toward the sump, etc. The location of the break relative to the piping insulation would affect the type of debris being transported (refer to Section 3). The location of the break would also affect the sump-pool flow dynamics near the recirculation sump (refer to Section 5).

4.1.2 Plant Features Affecting Debris Transport

A number of features in nuclear power plant containments would significantly affect the transport of insulation debris. These features include the containment's engineered safety features and associated plant operating procedures. Perhaps the most significant containment feature is the containment pressure-suppression system. In a BWR plant, the primary pressure suppression system is its suppression pool and the containment sprays. In a PWR plant, the relatively large free volume functions to keep pressure from becoming excessive, thus, the large free volume is essentially a pressure-suppression system. The containment sprays also help keep pressure from becoming excessive. The containment size was reduced in ice-condenser plants because of their banks of ice, which would condense steam effectively, and in sub-atmospheric plants, where the operating pressure inside the containment is below atmospheric pressure. The most significant difference between PWR and BWR containments with respect to debris transport is the pressure-suppression system, other than the sprays, and its location relative to the postulated break. In BWR containments, the break effluences would flow down toward the suppression pool via downcomer vents, i.e., toward the ECCS suction strainers. In PWR containments, the break effluences would tend to flow generally up toward the large free volume of the containment dome, i.e., away from the ECCS sump screens. For example, in ice-condenser containments, the containment was designed to direct the break flows through the ice banks, which exit into the dome. These flows also would carry the insulation into these regions. This means that for PWR plants, substantial quantities of debris would be propelled away from the lower regions of the

containment and toward the higher regions² of the containment. If it were not for the containment sprays washing the debris down toward the recirculation sump, the debris carried aloft likely would remain in the higher reaches of the containment.

The flow propelling debris upward in the containment could be channeled through relatively narrow passageways in some containment designs, such as an ice condenser bank, where substantial portions of the debris entrained within the flow likely would be deposited inertially within the channel. Such an effect could provide a means for analytically determining a quantity of debris that would not likely subsequently transport downward to the sump. Other structural features would capture debris as it was propelled past the structure. These structures include gratings, piping, and beams.

After the airborne debris is dispersed throughout the containment, the washdown of that debris to the recirculation sump would be determined primarily by the design of the containment spray system, including the drainage of the sprayed water. First, the spray droplets would tend to sweep any remaining airborne debris out of the containment atmosphere, and then the falling droplets would wash debris off surfaces (structures, equipment, walls, floors, etc.). As the drainage water worked its way downward, entrained debris would move along with the flow. However, not all debris would be washed off surfaces and entrained, and the containment sprays may not cover substantial areas within the containment.

Containments are designed, in general, to readily drain the spray water to the sump to minimize water holdup and maximize sump water levels. However, the refueling pools could hold up substantial quantities of water if the pool drains are not open or are blocked by debris. Thus, the design of the refueling pools, including the pool drainage system, can be an important containment feature in regard to debris transport.

The locations where spray drainage enters the sump pool relative to the location of the

²This effect would be lessened somewhat when the pipe break was located higher up in the containment, such as in a main steam line.

recirculation sump are also important. Debris deposited into the pool well away from the recirculation sump would be less likely to transport to the sump screen than debris that was deposited near the sump. Debris transport within the sump pool depends on a number of plant features, including the lower compartment geometry that defines the shape and depth of the sump pool, such as the open floor area, ledges, structures, and obstacles within the pool. In addition, the relative locations of the sump, the LOCA break, and the drainage paths from the upper reaches of the compartment to the sump pool are important to determining pool turbulence, which, in turn, determines whether debris can settle in the pool.

4.1.3 Physical Processes and Phenomena Affecting Debris Transport

Of the full spectrum of physical processes and phenomena that would affect the transport of debris from its source to the sump pool, a subset has been identified that should be considered the most important in debris-transport analysis. These include thermal-hydraulic processes that contribute to the transport and/or deposition of the debris and the debris deposition

mechanisms. Further, these processes and phenomena can be grouped according to transport phase, i.e., the airborne dispersion by the depressurization flows and the subsequent washdown of dispersed debris by the containment sprays. These processes and phenomena are listed in Table 4-1 and described in Tables 4-2 through 4-5.

The complete range of thermal-hydraulic processes affect the transport of insulation debris. Furthermore, the containment thermal-hydraulic response to a LOCA includes most forms of thermal-hydraulic processes. Debris transport is affected by a full spectrum of physical processes, including particle deposition and resuspension for airborne transport and both settling and resuspension within calm and turbulent water pools for both buoyant and nonbuoyant debris. The dominant debris-capture mechanism in a rapidly moving flow likely would be inertial capture, but in slower flows, the dominant process likely would be gravitational settling. Much of the debris deposited onto structures likely would be washed off the structures by containment sprays or possibly even by condensate drainage. Other debris on structures could be subject to erosion.

Category	Airborne Debris Transport	Washdown Debris Transport
Thermal-Hydraulic Processes and Phenomena Affecting Debris Transport	Pressure-Driven Flows Localized Flow Fields Turbulence Liquid Flashing Entrained Liquid Liquid Impaction on Surfaces Surface Condensation Condensation on Debris Sheeting Flow Dynamics	Containment Spray Droplet Fallout Spray Droplet Accumulation Floor Drainage of Accumulated Spray Pool Formation (Other than Sump) Spray Drainage Runoff Break Deluge Ice Melting in Ice Condenser Plant
Debris-Transport Mechanisms	Debris Advection Disintegration Debris Entrapment (Deposition) Gravitational Settling Inertial Impaction Turbulent Impaction Diffusiophoresis Adhesion Resuspension	Spray Droplet Sweepout of Debris Surface Reentrainment of Debris Deluge Transport Accumulation of Entrained Debris Drain Blockage by Debris Pool Entrapment of Debris Debris Erosion (Disintegration)

Table 4-2 Thermal-Hydraulic Airborne Processes and Phenomena

Processes and/or Phenomena	Description
Pressure-Driven Flows	The bulk flows, i.e., the net or macroscopic flow characteristics of the containment atmosphere. These flows would be the carriers of the debris. System-level thermal-hydraulic codes can predict these bulk flows reasonably well.
Localized Flow Fields	Flow directions and/or velocities that differ from the bulk atmosphere flow characteristics because of localized geometries. Localized flow fields would be most pronounced in the region near the break, where the depressurization jet is expanding and being redirected by structures, equipment, and walls. The flows can be extremely dynamic in this region. Predictions of these localized flow fields likely would require sophisticated CFD code analyses.
Turbulence	Local fluid vortices or flow eddies created by flow around obstacles. These vortices and flow eddies provide locations where debris potentially could settle even though bulk conditions would not predict settling. However, the locations could be transient such that settled debris could be reentrained.
Liquid Flashing	Liquid-to-vapor phase transformation caused by expansion across a choked break plane.
Entrained Liquid	Flow of break fluid that does not flash but continues as a liquid stream that would wet walls impacted by the stream and form pools as the water accumulates on the floor.
Liquid Impaction on Surfaces	Liquid impacting a surface (either entrained liquid or falling water droplets) that would wet that surface, thereby forming a liquid film on the surface. The liquid film would subsequently enhance debris capture by that surface. Debris-transport testing has shown surface wetting to greatly enhance debris deposition.
Surface Condensation	Formation of a liquid film on structure surfaces as a result of condensation of steam from the atmosphere would also wet surfaces. The rate of condensation depends on the rate of heat transfer into a structure, as well as on the moisture content of the atmosphere.
Condensation on Debris	Steam condensation onto debris in general would increase the weight of the debris, thereby enhancing the gravitational settling of that debris.
Sheeting Flow Dynamics	A dynamic sheet of water could be driven across a surface of any orientation by impaction of a liquid stream. This stream could entrain and transport debris already deposited onto that surface. Sheeting would most likely occur because of flows from the break. Before forming a sump pool, the initial break flows to the sump floor would transport debris already deposited on the sump floor (See Section 5).

Table 4-3 Airborne Debris-Transport Mechanisms	
Processes and/or Phenomena	Description
Debris Advection	Transport of airborne debris within the carrier-gas medium by flows at the spectrum of scales from bulk to turbulent eddies.
Disintegration	<p>Further destruction of debris as a result of debris impacting a structure, debris impacting debris, or liquid impacting debris. The most significant aspect of this secondary destruction is the generation of finer debris, such as individual fibers from fibrous insulation, because fine debris was found to readily transport from both the upper reaches of the containment by the containment sprays and within the sump pool. Further, this fine debris forms a thin uniform layer across the entire sump screen, threatening blockage through what has been called a "thin bed effect." Thus, a relatively small amount of disintegration could have a significant effect on screen blockage. Erosion of fibrous debris by falling water and within a turbulent pool has been seen experimentally.</p> <p>The opposite of disintegration, i.e., agglomeration, where debris pieces combine into larger pieces, was not observed during airborne debris-transport testing.</p>
Debris Entrapment (Deposition)	One mechanism or another would eventually trap debris undergoing airborne advection. Debris could be removed directly from the flow stream or through simple fallout of the atmosphere after depressurization completed. These mechanisms are listed next in this table.
Gravitational Settling	Downward relocation (sedimentation) of debris in the containment atmosphere onto structure surfaces under the force of gravity. Gravitational settling becomes an effective deposition mechanism after the bulk flow slows sufficiently so that gravity causes debris to fall faster than flow turbulence can keep the debris in suspension. Thus, gravitational settling would occur in regions well away from the break, where the break flow has dispersed, and after the depressurization completes (post-blowdown).
Inertial Impaction	Capture of debris particles on structure surfaces because of inertially driven impaction. Airborne-debris transport testing has demonstrated that inertial impaction is an effective form of deposition whenever flows are rapid and surfaces are wetted. Substantial debris was found to be deposited onto a grating whenever test flows passed through wetted grating onto miscellaneous structures such as I-beams and pipes, and onto flat surfaces when the flow was forced through a sharp bend. This type of debris deposition would be most effective in the region of the break or along the flow pathway from the break to the larger upper dome.
Turbulent Impaction	Capture of debris on structural surfaces caused by turbulent eddies. Although this form of debris deposition would occur, its importance is much less than deposition by inertial impaction and by gravitational settling. Also, turbulent impaction would be more effective on very fine debris than on larger debris.
Diffusiophoresis	Transport of debris particles toward deposition surfaces because of the concentration gradients of the atmosphere contents. Following a LOCA, the gradient is dominated by steam concentration gradients created by condensation on containment structures. This form of deposition is also secondary to deposition by inertial impaction and gravitational settling.
Adhesion	Permanent retention of debris particles on a structure surface as a result of mechanical interactions with a rough surface or other forces. The flow velocities would be insufficient to remove the debris from the surface again.
Resuspension	Reentrainment of debris previously deposited on structure surfaces into the atmosphere flow stream because of local fluid/structure shear forces.

Table 4-4 Thermal-Hydraulic Washdown Processes and Phenomena	
Processes and/or Phenomena	Description
Containment Spray Droplet Fallout	Falling containment sprays condense steam and cool the containment atmosphere. The interaction of spray droplets with the atmosphere can induce local fluid vortices, eddies, or fields.
Spray Droplet Accumulation	Spray water would accumulate and run off of surfaces, providing another mechanism for debris transport.
Floor Drainage of Accumulated Spray	Spray water accumulating on a floor, other than the sump floor, would drain from that floor by pathways such as floor drains or an overflow onto a lower level.
Pool Formation (Other than Sump)	In some circumstances, spray water can pool at locations other than the sump. Water could pool in a refueling pool if the pool drains were not open or if the drains were blocked by debris.
Spray Drainage Runoff	The drainage of accumulated spray water from surfaces.
Break Deluge	Large flow rate of liquid effluent from a break in the reactor coolant system onto containment structures.
Ice Melt in Ice Condenser Plant	The water from melting ice would drain from the ice banks and thereby transport debris with the ice melt.

Table 4-5 Washdown Debris-Transport Mechanisms	
Processes and/or Phenomena	Description
Spray Droplet Sweepout of Debris	Transport of airborne debris from the containment atmosphere by containment spray droplets.
Surface Reentrainment of Debris	Reentrainment of debris previously deposited on structure surfaces by containment spray runoff.
Deluge Transport	Relocation of debris from containment structures due to interactions with the deluge of liquid from the ECCS and/or spray system.
Accumulation of Entrained Debris	Debris being transported by containment spray runoff can accumulate together at such locations as floor drains.
Drain Blockage by Debris	Accumulated debris could potentially form a flow blockage at drains, such as floor drains or the refueling pool drains.
Pool Entrapment of Debris	At any location where water could pool, debris could settle to the floor of that pool and remain there.
Debris Erosion (Disintegration)	Further destruction of debris as a result of spray drainage or deluge water impacting the debris. Under these conditions, disintegration is in the form of erosion, where finer debris, such as individual fibers from fibrous insulation, is removed from larger debris. This fine debris tends to transport readily from both the upper reaches of the containment by the containment sprays and within the sump pool. Further, this fine debris forms a thin uniform layer across the entire sump screen, threatening blockage. Thus, a relatively small amount of disintegration could have a significant effect on screen blockage. Erosion of fibrous debris by falling water and within a turbulent pool has been seen experimentally.

4.1.4 Debris Characteristics Affecting Transport

Transport of debris is strongly dependent on the characteristics of the debris formed, including the types of debris (insulation type, coatings, dust, etc.) and the size distribution and form of the debris. Each type of debris has its own set of physical properties, such as density; specific surface area; buoyancy when dry, partially wet, or fully saturated; and settling velocity in water. Several distinct types of insulation are used in PWR plants. The size and form of the debris depend on the method of debris formation, e.g., jet impingement, erosion, aging, operational, etc. The size and form of the debris affect whether it passes through grating or a screen, as well as affecting its transport to the grating or screen. For example, fibrous debris may consist of individual fibers or large sections of an insulation blanket and all sizes between these two extremes.

4.2 Airborne/Washdown Debris-Transport Testing

The NRC, U.S. industry, and international organizations conducted tests to examine different aspects of airborne and washdown debris transport within a nuclear power plant containment experimentally. The results of these tests provided qualitative insights into which physical processes and phenomena were most important and also provided quantitative test data regarding debris characteristics, deposition, and transport. Much of this information was obtained specifically to support the resolution of the BWR strainer-blockage issue; however, the information is also directly applicable to the PWR sump-screen blockage issue, for the most part.

The testing pertinent to airborne/washdown debris transport is listed in Table 4-6. The first four test series pertained to airborne debris transport, but not to washdown debris transport. Conversely, the last two test series in the table pertain to washdown but not airborne debris transport. The single test series sponsored by the BWROG had elements of both airborne and washdown debris transport within the series.

The NRC sponsored three series of small-scale tests designed to examine the transport and capture characteristics of debris within a BWR

drywell caused by steam and water depressurization flows and to examine the transport and erosion characteristics of debris within a drywell by water washdown flows.⁴⁻³ Two test series were designed to study airborne transport of fibrous debris: the separate-effects and the integrated-effects debris-transport tests. In the separate-effects tests, transport characteristics were determined for fibrous debris capture on structures where the test configuration was set up for one type of structure and orientation at a time, e.g., debris transport through a grating. In the integrated-effects testing, a combination of different types of structures was implemented into the test chamber at the same time. A third test series examined the transport and erosion characteristics of debris by water washdown flows within a drywell that impacted fibrous debris with water to determine the extent of transport from a structure and the degree of erosion to the debris that remained on the structure.

To date, only one series of small-scale tests has been performed by U.S. industry that relates to airborne/washdown debris transport. These tests were conducted to provide guidance to utilities for resolution of the BWR strainer-blockage issue, but are qualitatively applicable to the PWR issue as well.

Experiments have been conducted outside the U.S., and the NRC has reviewed data applicable to the resolution of the BWR strainer and PWR sump-screen clogging issues in the U.S. Three of these experiments obtained data that pertain to airborne and/or washdown debris transport. The primary source for this information is a knowledge base report prepared by the NRC for the Organization for Economic Cooperation and Development (OECD).⁴⁻⁴

These tests are summarized in the order listed in Table 4-6.

4.2.1 Airborne Phase Debris-Transport Testing

4.2.1.1 Separate-Effects Debris-Transport Tests

In 1996–1997, the Alden Research Laboratory (ARL) conducted tests for the NRC that were designed to provide a basic understanding of

Table 4-6 Airborne/Washdown Debris-Transport Testing

Test Description	Sponsor, Laboratory, and Date	Debris Source	Transport Medium	Objectives	Significant Limitations	Reference
Airborne-Phase Debris Transport						
Separate-Effects Debris-Transport Tests	NRC ARL 1997	Injection of Prepared LDFG Debris	Fan-Driven Air	Obtain basic data related to inertial capture of small insulation debris generated by a postulated MSLB. Possible degradation and erosion mechanisms by airflow were a secondary objective.	Limited debris sizes and loadings. One-dimensional flow fields. Non-prototypical congestion of structures. Use of airflow rather than steam flow. Only one type of insulation debris tested (LDFG).	NUREG/CR-6369 (Volume 2)
Integrated-Effects Debris-Transport Tests	NRC CEESI 1997	Air-Blasted LDFG Debris	Blowdown Air Jet	Obtain debris-transport data under integrated conditions prototypical of a BWR drywell following a postulated LOCA.	Use of airflow rather than steam flow. Surface wetness applied by spray mist rather than steam condensation. Only one type of insulation debris tested (LDFG).	NUREG/CR-6369 (Volume 2)
HDR Facility Blowdown Experiments (Full-Scale)	Owens-Corning HDR 1985	Steam-Blasted LDFG	Blowdown Steam Jet	Obtain containment thermal-hydraulic blowdown data. Two tests conducted to determine capability of LDFG insulation to withstand impact of high-pressure steam-water blast and to determine debris size distribution.	Limited debris-transport testing and data collection (for most of the test, debris-transport data were a by-product).	NEA/CSNI/R (95) 11 and NUREG-0897, Rev. 1
Karishamn Steam Blast Tests	ABB-Atom Karishamn 1992	Steam-Blasted Aged Mineral Wool	Blowdown Steam Jet	Investigate the dislodgment of insulation and subsequent transport in the containment following a LOCA.	Test scaling was too small to realistically simulate thermal-hydraulic conditions in a BWR drywell. Transport velocities were not typical of conditions expected in a nuclear power plant, i.e., the flows were too slow.	NEA/CSNI/R (95) 11

Table 4-6 Airborne/Washdown Debris-Transport Testing

Test Description	Sponsor, Laboratory, and Date	Debris Source	Transport Medium	Objectives	Significant Limitations	Reference
Airborne/Washdown Combined-Phase Debris Transport						
BWROG Debris-Transport Tests	BWROG CD 1996	Injection of Prepared LDFG and RMI Insulation and Paint Chips	Steam/ Water Jet	Obtain insulation debris-transport data applicable to transport of debris from a BWR drywell to the wetwell through the downcomers and main vents. Specifically, obtain conservative estimates of the transport fractions for both the blowdown and washdown phases.	Test scaling was too small to realistically simulate thermal-hydraulic conditions within a BWR drywell.	NEDO-32686
Washdown-Phase Debris Transport						
Separate-Effects Insulation Debris Washdown Tests	NRC/SEA 1997	Air-Blasted and Prepared LDFG Debris	Sprayed Water	Obtain water-driven debris erosion data for debris captured by floor gratings.	Testing was small-scale. Only one type of insulation debris tested (LDFG).	NUREG/CR-6369 (Volume 2)
Oskarshamn NPP Containment Washdown Tests (Full-Scale)	ABB-Atom Oskarshamn NPP 1994	Old and New Insulation Material (Unknown Type)	Sprayed Water	Investigate the transport of insulation material by the containment spray system in a full-scale plant.	Most test conditions including type of insulation were not reported. Debris preparation and initial distribution may not have been typical of a postulated LOCA.	NEA/CSNI/R (95) 11

LOCA-generated fibrous insulation debris capture on typical BWR containment structures as a result of an inertial capture process. Because these data were obtained for basic structural components that are common to both PWR and BWR containments, the results of these tests are generally applicable to all BWR and PWR containment designs. A complete description of the tests, including apparatus descriptions, procedures, and data, is documented in Volume 2 of Ref. 4-3.

The structural congestion (pipes, gratings, I-beams, and vents) within containments would affect the transport of fibrous debris, and substantial quantities of impacted debris likely would remain stuck (captured) on these structures. The tests were designed to examine the following.

1. The role of debris inertia on the capture during airborne transport of fibrous debris on typical BWR drywell structures (similar structures exist in PWRs). A number of different structures were tested to examine the effects of shape and orientation relative to the direction of flow.
2. The effect of surface wetness on retention of fibrous debris by surfaces impacted by debris. It was suspected that surface wetting resulting from steam condensation would significantly enhance the efficiency of capture.
3. Possible degradation and erosion mechanisms for captured large pieces (e.g., trapped against a grating) during blowdown. Such fibrous debris would be subjected to high-velocity steam flow intermixed with water droplets, thereby potentially further degrading the debris pieces.

A once-through flow tunnel was constructed of plywood panels with a blower at the upstream end of the test section and an air-filtering plenum downstream of the test section. The primary test section had a cross section with inner dimensions of 4 ft by 4 ft and a length of 8 ft. Because airflow velocities within this test section were limited to about 50 ft/s, a smaller 2-ft by 2-ft test section was inserted within the larger test section in selected tests to achieve velocities of up to 150 ft/s. The smaller test section was 5 ft long. The test apparatus is shown in Figure 4-1.

Perforated plates and a honeycomb structure were used to achieve a uniform velocity distribution. In addition, the head loss across this flow-conditioning device was calibrated with respect to tunnel velocities and later used to establish specified test section velocities.

Test obstructions consisted of individual components and combinations of individual components, with the individual components including I-beams, gratings, pipes, and a vent cover. Single-component tests involved mounting one or two objects side by side within the test tunnel with the objects being the same type, having identical cross sections, and being aligned similarly to the flow. In combined-component tests, combinations of components (one or more shapes) were mounted with different orientations, i.e., different alignments to the flow, and sometimes positioned so that front-mounted components partially shielded rear-mounted components. Thus, the effects of component proximity wake effects and shielding were evaluated.

Obstruction surfaces were wetted in most tests by spray injection nozzles located upstream of the test section. The duration of the spray controlled the extent of surface wetness (either 10 s or 30 s). Most tests were conducted with a 10-s prewet time.

The fibrous insulation debris was injected into the tunnel through a rupture disk capping one end of each of two pressurized 4-in. polyvinyl chloride (PVC) pipes. The pipes' sections were suspended from the tunnel ceiling downstream of the flow-conditioning structure and filled with preshredded insulation. Air was pumped into the pipe until the rupture disk failed, so that the jet of escaping air dispersed the insulation debris. The fibrous insulation debris was generated from heat-treated LDFG blankets.

Forty-eight tests were conducted to examine a variety of test conditions. The test parameters included

- the flow velocity (24–150 ft/s),
- the wetness of structure surfaces (dry to draining water film conditions),
- the type of structure (I-beams, piping, gratings, and Mark II vents),
- the approximate debris size, and
- the debris loading (6.3–12.5 g/ft²).

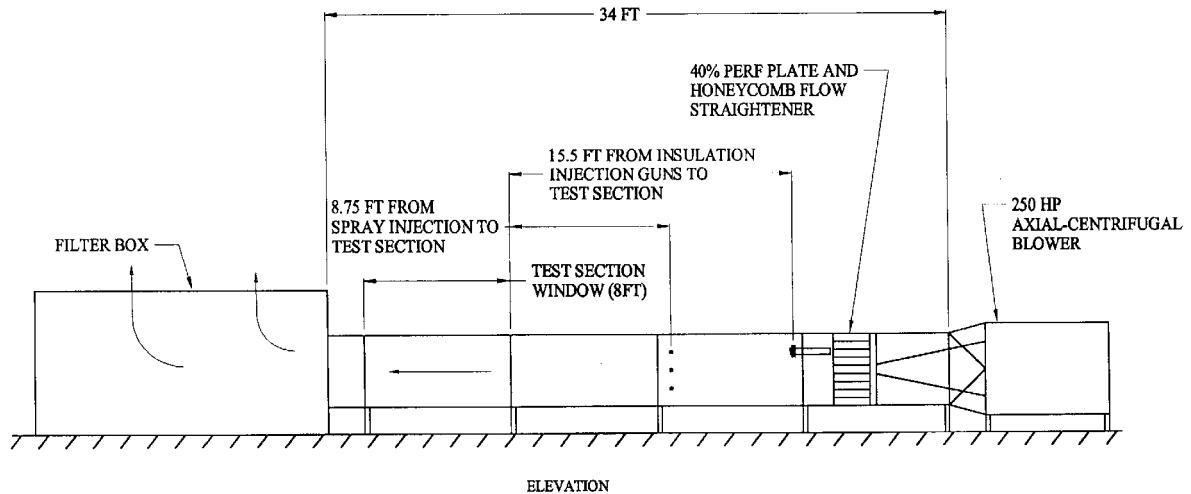


Figure 4-1 Separate-Effects Insulation Debris-Transport/Capture Test Apparatus

Within the ranges of tested parameters, the test data exhibited the following trends.

- Gratings captured more fibrous insulation debris than did other types of structures. For example, in combination-component tests in which the grating was placed downstream of other grating (pipes and I-beams), the grating captured substantially more debris than all other upstream structures combined.
- Surface wetness clearly influenced the extent of debris capture on structures, especially for pipes and I-beams. When pipes and I-beams were dry, these surfaces essentially did not capture debris. Capture on floor gratings was affected by wetness but was less sensitive to the degree of wetness than were other structure types. Typical debris capture by a wetted pipe is shown in Figure 4-2.
- Tests with dual gratings in series showed substantially more debris capture on the upstream grating (averaging about 25%) than on the downstream grating (about 12%), most likely because the largest debris was removed from the flow stream by the upstream grating. Note that the capture percentages reflect the fraction of the mass of debris approaching a particular structure that subsequently was captured by that structure.
- Mark II vents with wetted surfaces captured about 12% of small debris on the cover plate and the simulated drywell floor.

- Break-up or disintegration of fibrous debris captured on a grating was negligible when 6-in. by 6-in. thin pieces (1/8 to 1/2-in. thick) of insulation were subjected to gas velocities approaching 140 ft/s.
- Gravitational settling (i.e., debris settling to the tunnel floor) was negligible for all tests except the Mark II vent geometry (settling was not included in the vent-capture percentage).

These separate-effects tests had the notable limitations of

1. relatively light debris loadings on the structures compared with expected BWR conditions,
2. a modest assortment of debris sizes,
3. nonprototypical congestion of structures, and
4. overly simplified flow fields approaching the structures.

The debris loading approaching a structure refers to the density of debris pieces per unit of cross-sectional flow area. The principal concern was that debris captured on a structure could be knocked free (reentrained) by the impact of additional debris under conditions of heavy debris loading, thereby effectively reducing the capture efficiency for that structure. To ensure conservative estimates for debris capture, additional data were needed for heavier, more prototypical debris loadings. Therefore, additional experiments of a more representative

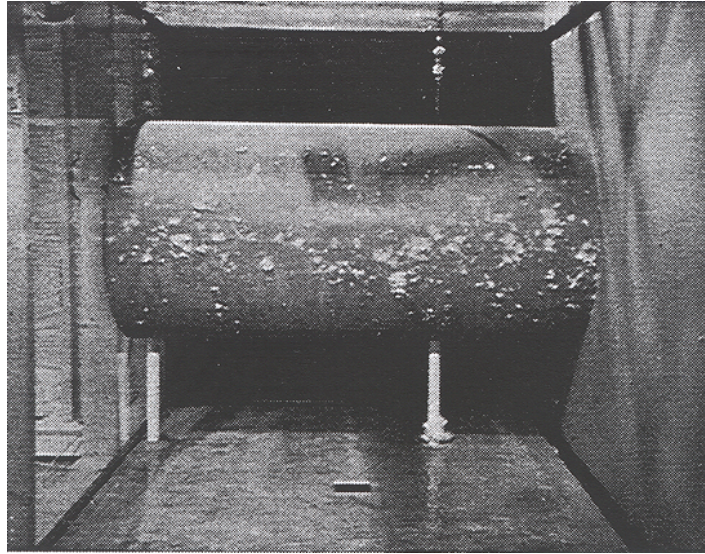


Figure 4-2 Typical Fibrous Debris Capture by a Wetted Pipe

and integrated nature were performed to further understand the role of fibrous insulation debris inertial capture.

4.2.1.2 Integrated-Effects Debris-Transport Tests

Although the separate-effects tests described in Section 4.2.1.1 provided valuable data, those tests still had the notable limitations listed above. The integrated debris-capture tests were designed to minimize the limitations noted for the separate-effects tests. The primary objective of these tests was to provide integrated fibrous-debris-capture data to benchmark analytical models and methods used to predict debris transport within a BWR drywell. The integrated-effects tests also combined debris generation with debris transport. The integrated debris-transport tests were conducted at the CEESI air-blast facility in 1997. A complete description of the tests, including apparatus descriptions, procedures, and data, is documented in Volume 2 of Ref. 3. Because these data were obtained for basic structural components that are common to both PWR and BWR containments, the results of these tests are generally applicable to all BWR and PWR containment designs.

The CEESI facility was capable of storing as much as 11,000 ft³ of air at 2,500 psia. In these tests, a dispersing 1,100-psi air jet was used to destroy insulation blankets and then transport

the debris through test chambers that contained obstructions. The insulation blankets were mounted and restrained in a manner designed to maximize their destruction and therefore maximize the amount of debris impacting the structures. Debris sizes ranged from individual fibers to partially intact blankets. The structures for debris capture were more complex and more prototypical than those used in the separate-effects testing. The flow patterns in the integrated testing were also more complex, (more three-dimensional) than those for the separate-effects testing. The data from these integrated tests were compared with the data from the separate-effects tests for insights into the effects of complex structural arrangements and fluid flows on debris capture.

The main test chamber, which is shown in Figure 4-3, consisted of a large horizontal cylinder with an inner diameter of 9.4 ft and a length of 93 ft. In addition, a 32-ft auxiliary chamber of the same diameter was attached with a flanged collar at the exit end of the main chamber in a horizontal "L" configuration. The upstream end of the main chamber, behind the air-jet nozzle, was blocked almost completely so that only a small portion of the air could exit the chamber in the reverse direction. The purpose of the auxiliary chamber was to investigate fibrous debris capture associated with flows undergoing a change in direction; in this case, a 90° bend.

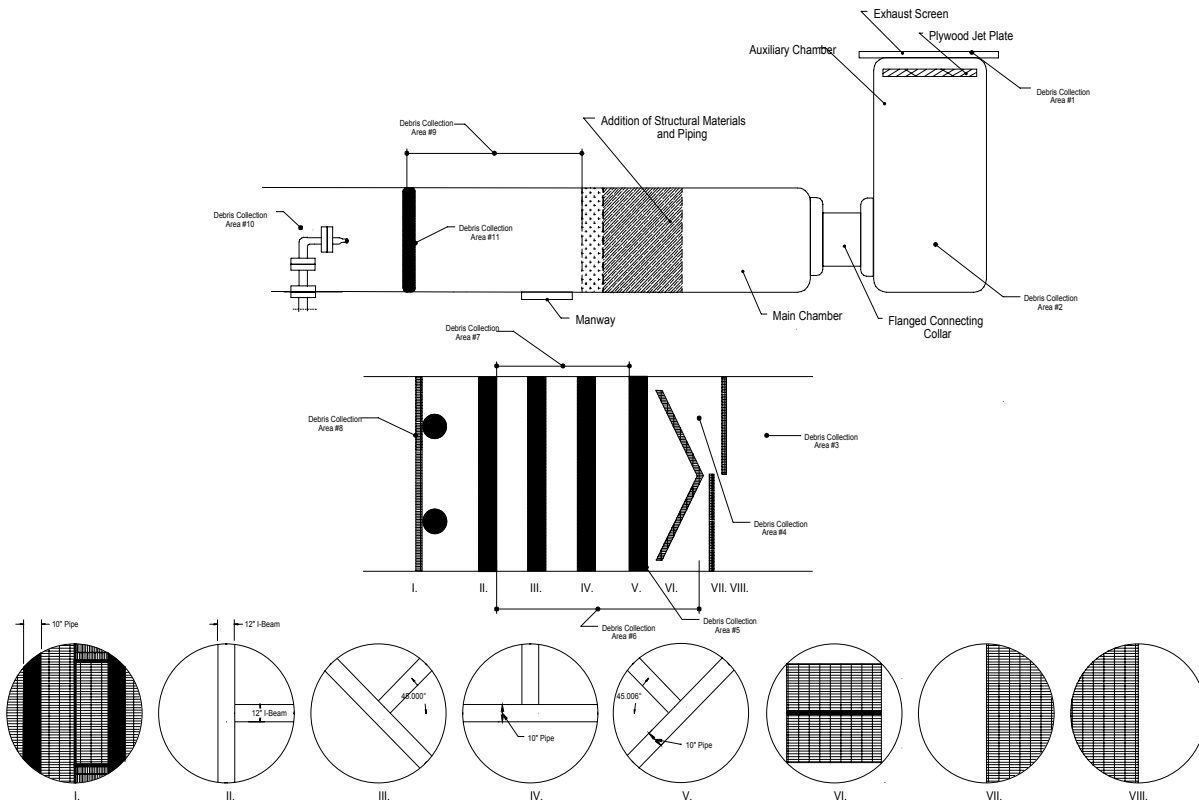


Figure 4-3 CEESI Air-Jet Test Facility

Target insulation blankets were mounted a few feet downstream of the air-jet nozzle. The blankets were mounted on a 12.75-in. outer diameter pipe that extended across the main test chamber at mid-height and positioned directly in front of the air jet nozzle. The target pipe mount was secured to rails so that the target could be positioned any distance from the jet out to 30 ft from the nozzle. The targets consisted of canvas-covered LDFG insulation blankets that were usually 3 ft long with either two or three stainless-steel bands placed around them to hold the blanket in place. Metal jackets were not used to encapsulate the blankets. A 1.5-ft-long blanket was used in one test.

The structural test section contained an assemblage of structural components (gratings, pipes, and I-beams) designed to simulate a prototypical section of a BWR drywell. The design focused on maintaining the same surface-to-volume ratios as found in BWR containments, and, to the extent practical, the structures were oriented in a manner analogous to the orientations found in actual plant

conditions. These structural components are also shown schematically in Figure 4-3.

All I-beams were 12 in. from upper to lower flange, and all pipes were 10 in. in diameter. I-beams were oriented with their web into the direction of airflow. Starting from the front (the flow entrance) of the structural test section, the test section contained the following structural subassemblies.

- A continuous grating with two vertically oriented pipes directly behind it
- I-beams with a full-length beam oriented vertically and a half-beam oriented horizontally
- I-beams with a full-length beam oriented 45° from vertical
- Horizontally oriented pipe with a half I-beam oriented vertically
- A pipe oriented 45° from vertical
- A V-shaped grating (approximately 56°) that obstructed about 57% of the total test-chamber flow area.

- Two half-section gratings separated axially by 22 in., referred as the split grating.

In the separate-effects tests, surface wetness was shown to affect the capture efficiency of structures profoundly. Therefore, surface wetness was a primary concern in the integrated tests. In the CEESI tests, structures were prewet with misters positioned throughout the test section. The mister system, which was constructed from PVC pipe, sprayed warm water as fine droplets from a high-pressure (150-psig) source. The misting system was operated long enough (approximately 10 min) to form a draining water layer.

The size of the jet nozzle was designed to minimize air usage while still allowing the jet to continue long enough for the debris-generation and debris-transport processes to complete (i.e., all debris was either deposited onto a surface or passed through the test chamber). The nozzle discharge was monitored and recorded. Developmental tests determined that at least 10 s were required for a 4-in. diameter nozzle and 12 s were required for a 3-in. diameter nozzle. Facility operators were able to approximate the jet-duration time specified for a particular test. Air-jet discharge was initiated using a rupture disk.

The developmental tests were instrumented with Pitot tubes to monitor and map the flow distributions before the flow entered the congested test section. The airflow velocities entering the area containing the congestion of structural components generally ranged from 25 to 50 ft/s. These velocities were in good agreement with velocities predicted for the tests using a commercially available CFD code. These velocities were also comparable to CFD-predicted velocities for a typical BWR drywell. After the flows dissipate into pressure-driven flows, BWR steam-flow velocities were predicted to generally range from about 30 to 50 ft/s. Therefore, the airflow velocities in the CEESI tests were considered prototypical of steam-flow velocities that would exist in a BWR drywell following a postulated LOCA.

Ten production tests that examined a variety of test conditions regarding debris transport were conducted. In addition, four of the developmental tests also provided useful debris-transport data. The test parameters included:

- the nominal nozzle diameter, either 3 or 4 in.,
- the duration of the air-jet flow (5 to 24 s),
- the surface wetness, and
- the distance between the nozzle and the target.

Most of the tests were conducted using a nominal 4-in. diameter nozzle, a flow duration of 12 to 17 s, and wet surfaces. One of the fibrous-debris transport tests (Test H7) was conducted with all surfaces deliberately maintained dry to illustrate the effect of surface wetness on debris capture. In addition, the mister system partially malfunctioned in two tests, resulting in incomplete surface wetness and a subsequent reduction in debris capture.

The distance between the nozzle and the target was initially adjusted until the optimum distance for maximum target destruction was found; a distance of ~120 in. (L/D of 30) appeared to maximize destruction. Insulation debris consisted of pieces of bare fiberglass insulation of various sizes, pieces of shredded canvas, agglomerated pieces containing both insulation and canvas, and large sections of the canvas cover that remained relatively intact and sometimes contained substantial quantities of insulation. The bare insulation was divided into three general size groups—large, medium, and small. Samples of debris pieces are shown in Figure 4-4.

The tests demonstrated the ability of structural components to capture debris. The average overall transport fraction for small debris in the CEESI was 33% of the total debris generated, i.e. ~2/3 of the generated debris was captured, primarily by inertial impaction, within the test facility.

Once again, gratings were found to be the most effective at catching fibrous debris. The debris captured by the split grating in Test H2 is shown in Figure 4-5. Note that the upstream gratings had captured the large debris already. The capture efficiencies for the split grating and for each test are plotted in Figure 4-6 as a function of debris loading. The corresponding separate-effects data also are shown. This figure clearly shows the effect of surface wetness and debris loading and the general agreement between the separate and integrated effects tests.



Figure 4-4 Samples of Debris Generated in the CEESI Tests

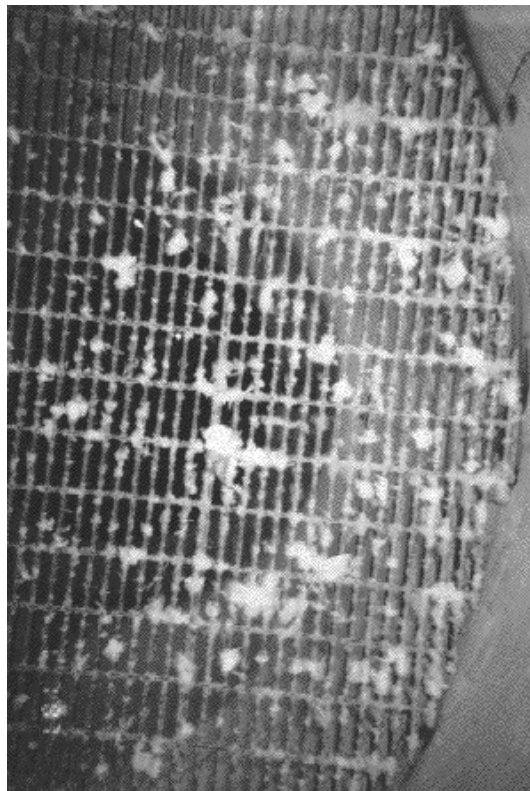


Figure 4-5 Typical Debris Deposition on a Grating in CEESI Tests

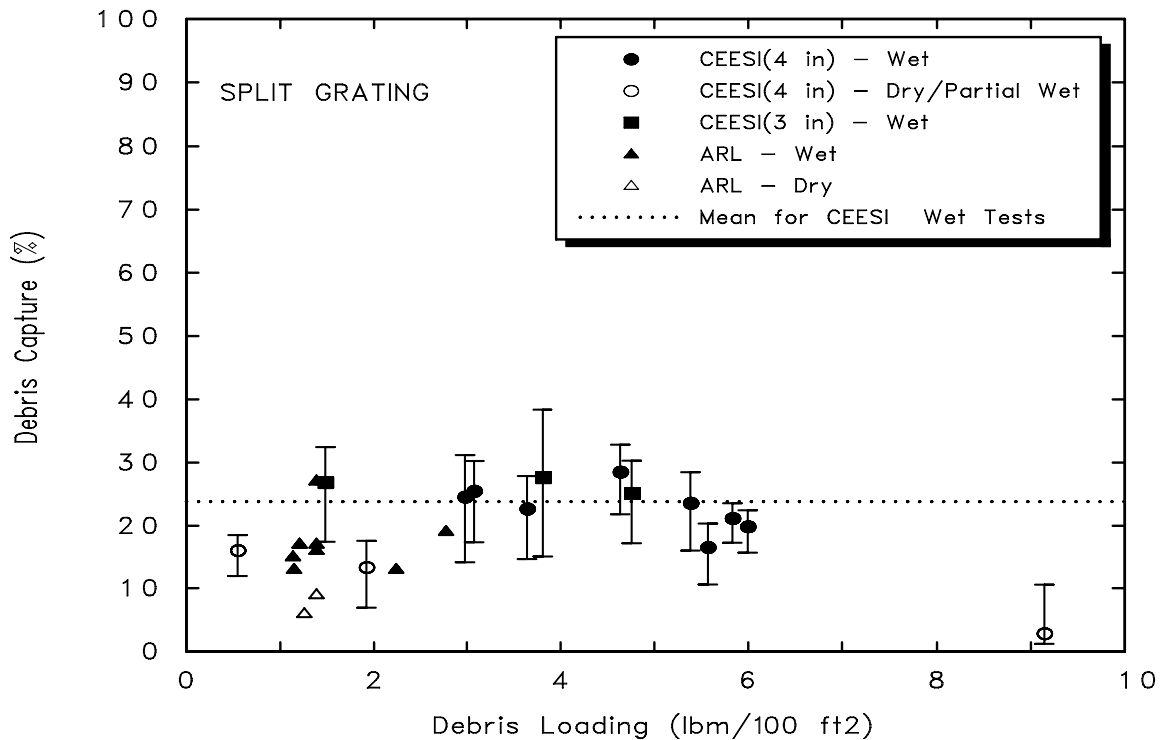


Figure 4-6 Capture of Small Debris by Grating

The average fractions of small debris captured by each test structure component are shown in Table 4-7. Note that the first continuous grating stopped almost all of the larger debris and that the capture fraction for the continuous grating was not obtained. This was because of the failure of the mister system to wet the continuous grating adequately (i.e., this grating illustrated dry behavior).

The 90° bend between the two chambers caused debris to be captured at the bend, which was maintained wet by a mister in the auxiliary chamber. Seventeen percent of the debris entering the auxiliary chamber was trapped on the chamber wall as a direct result of the bend. The I-beams and pipes captured a lesser but still substantial amount.

The capture fractions were found to be relatively independent of the debris mass loading (i.e., lbm/ft²) impacting the structures. The integrated-effects tests' capture data were consistent with the separate-effects tests data, indicating that the finer aspects of the local flow fields (e.g., eddies and wakes) do not influence debris capture significantly. The separate-

effects and integrated-effects tests clearly established that a fraction of the small and large debris would be deposited as the debris transported through the drywell following a blowdown. The most likely locations for the deposition in a BWR are the floor gratings located at different elevations. These captured pieces would potentially be subjected to subsequent washdown water flows.

4.2.1.3 Blowdown Experiments at Heissdampfreaktor (HDR) Facility

A decommissioned 100-MW_{th} superheated steam reactor, HDR, was refitted as a testing facility for LWR safety research.⁴⁻⁴ The reactor vessel, without its internals, was decontaminated and modified for blowdown testing. For a blowdown test, the vessel was typically charged initially to 11 MPa and 310°C. Note that U.S. PWRs typically operate at a pressure of about 15 MPa.

About 40 blowdown tests were performed during the late 1970s and the 1980s. In general, the aim of these experiments was the qualification of equipment under accident conditions. Some of

Structure Type	Debris Capture
I-Beams and Pipes (Prototypical Assembly)	9%
Gratings	
V Shaped Grating	28%
Split Grating	24%
90° Bend in Flow	17%

the tests lasted for less than a second; during others, the content of the pressure vessel was allowed to expand until the vessel pressure dropped to containment pressure. The diameter of the nozzle was 0.45 m, and the break was initiated using a rupture disk. A deflector plate was installed in front of the nozzle to break up the jet. The tests were reviewed in regard to their applicability to debris generation; this review is discussed in Ref. 4-5.

The transport behavior of the insulation debris was not an objective of the experiments; it was only a by-product. Insulation material that was present for operational purposes was damaged badly in the first experiments and replaced by other insulation types in an effort to limit the damage. Different insulation types were used, including jacketed mineral wool (fibrous), foam glass, encapsulated fiberglass, covered glass wool, and RMI.

The HDR containment measures about 20 m (66 ft) in diameter and 60 m (200 ft) high and is subdivided into a number of compartments. The break compartment is situated about 25 m (82 ft) above the sump. The water from the break had to pass down through four floors to reach the sump.

Although debris transport was not an objective of the experiments, three observations were made regarding the transport of insulation debris within the HDR.

- Debris was found in rooms adjacent to the break compartment, as well as in the break compartment, for each type of insulation except RMI, indicating more limited transport for RMI than for other types of debris. However, only one RMI test specimen was used, so this test result may not be representative of the behavior of large amounts of RMI debris.

- The mineral wool insulation originally installed before the first blowdown experiment was torn from the piping during blowdown. This debris was caught in large flocks at railings and at other obstacles, as well as in stagnation areas. This observation provided initial indications of how fibrous debris would be captured.
- Almost no insulation debris was found in the sump, which was four floors beneath the break compartment. However, the post-test investigation did not examine the distribution of individual fibers. The predominant pathway for the blowdown flows would have been toward the larger compartments, i.e., the upper dome. Also note that these tests did not consider washdown debris transport from the operation of containment sprays, which certainly would have washed debris to the sump.

The results from these tests in regard to debris transport were only qualitative; even the distribution of insulation debris collected within the break and adjacent compartments was not quantified. However, insights were gained that supported later debris-transport testing.

4.2.1.4 Karlshamn Steam Blast Tests

Experiments were conducted by ABB-Atom at the Karlshamn fossil-fueled power plant to determine the relative distribution of insulation debris in the containment.⁴⁻⁴ These experiments were conducted in a small-scale test assembly that was subdivided into a few inner volumes. The outer dimensions of the assembly were 3.33 m by 2.56 m, and the assembly was 4.25 m high. The assembly was divided into four levels, as shown in Figure 4-7. Floor gratings connected the upper three levels. The lowest level simulated a wetwell, and the connection between the lowest level and the level above simulated a vent downcomer. The only water

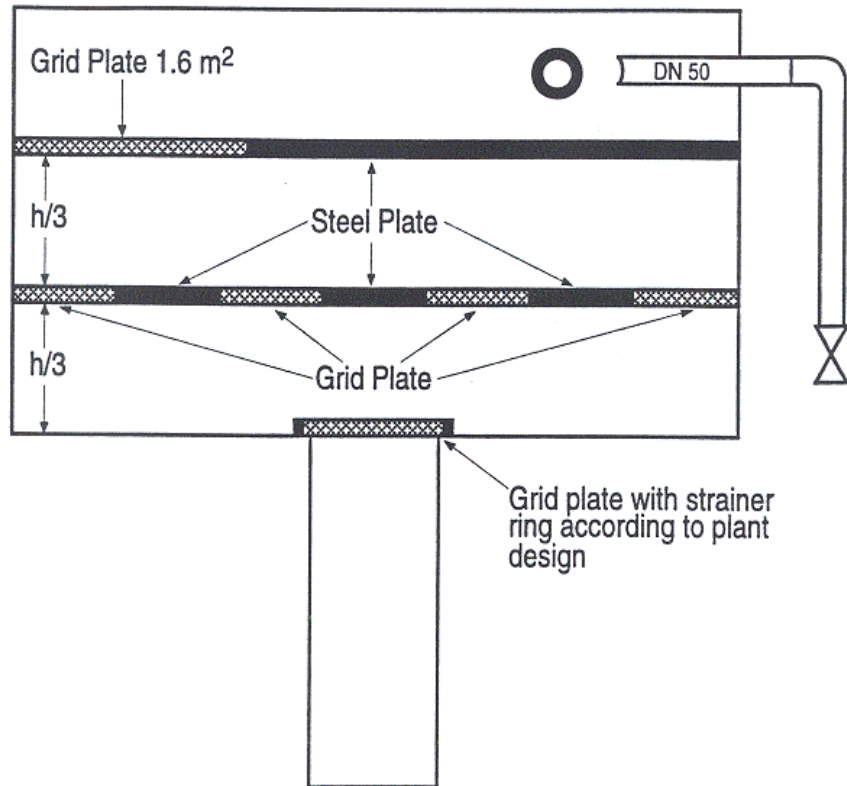


Figure 4-7 ABB-Atom Containment Experimental Arrangement

involved in these tests was condensed steam. Fibrous insulation was attached to a pipe in the upper level of the test apparatus, where it was exposed to a steam jet driven by an 8-MPa steam source.³ The jet fragmented the insulation, and the insulation debris was dispersed within the test apparatus by the steam flow and displaced air.

Most of the fibrous insulation debris was distributed in the upper parts of the test apparatus. The gratings held debris back, debris adhered to walls where steam condensed, and debris accumulated in areas of low flow velocity. Only minor quantities of the debris reached the wetwell level through the downcomer vent. In fact, the quantities reaching the wetwell were about 3% or less of the total quantity of dislodged insulation. As expected, the quantities of debris transported to the wetwell were found to be dependent on the transport velocities.

³An unknown amount of pressure was lost as the steam flowed through 75 m of pipeline from the source to the jet.

These findings are consistent with debris-transport test results from later, more sophisticated testing, even though the later testing showed much more debris transported to the wetwell. The peak bulk flow velocities in the Karlshamn tests were about 1 m/s, whereas the transport velocities were much faster following a postulated LOCA in an actual plant (and in the later, more typical tests conducted by the NRC). In the Karlshamn tests, debris was able to settle gravitationally at all levels, whereas at typical transport velocities, the flow turbulence would generally be much too high to allow settling anywhere near the break. After break flows disperse sufficiently into compartments well away from the break, flow velocities and turbulence can be expected to slow sufficiently to allow gravitational settling, as was seen in the Karlshamn tests. Thus, the Karlshamn tests might be considered representative of debris transport in some areas of PWR containments but not in the region of the break. The Karlshamn results might also be representative of debris transport following very small LOCAs. In general, the Karlshamn tests results have

limited applicability to the U.S. PWR sump-screen-blockage issue because the test scaling was not representative of U.S. containments and the debris transport velocities were not typical of expected velocities.

4.2.2 Airborne/Washdown Combined Phase Debris-Transport Testing

4.2.2.1 BWROG Testing of Debris Transport Through Downcomers/Vents

The NRC issued NRC Bulletin 96-03, "Potential Plugging of Emergency Core Cooling Suction Strainers by Debris in Boiling-Water Reactors," on May 6, 1996. All BWR licensees were requested to implement appropriate measures to ensure the capability of the ECCS to perform its safety function following a LOCA. The bulletin noted that plant-specific analyses to resolve this issue are difficult to perform because a substantial number of uncertainties are involved. These uncertainties included the amount of debris that would be transported to the suppression pool. The BWROG then developed the URG⁴⁻⁶ to provide utilities with:

- guidance on the evaluation of the ECCS potential strainer clogging issue for their plants,
- a standard industry approach to resolution of the issue that is technically sound, and
- guidance consistent with the requested actions in the bulletin for demonstrating compliance with 10 CFR 50.46.

The URG includes guidance on a calculational methodology for performing plant-specific evaluations. The NRC reviewed the BWROG URG document and issued the staff's SER on August 20, 1998.⁴⁻⁷

The BWROG sponsored tests designed to gather data on the transport of insulation debris from a BWR drywell to the wetwell through downcomers and main vents. The overall objective of this test program was to determine conservative estimates for the blowdown and washdown-transport fractions. As described in Ref. 4-6, transport fractions were measured through a 1/8-scale Mark I main vent and a Mark II downcomer for saturated steam, saturated water jets, and coolant water flows. Thus, the dynamics of debris transport were simulated in subscale containment configurations and scaled blowdown rates. A total of 33 tests was

conducted with fibrous insulation, RMI insulation, and paint chips. The tests investigated the effects of

- simulated debris preparation,
- full-scale prototypical gratings,
- blowdown jet orientation and duration,
- duration of debris washdown process,
- flow rate and pipe orientation, and
- debris introduction location.

Drums were used to construct containment vessels configured for the Mark I and Mark II vent designs, as shown schematically in Figures 4-8 and 4-9. The apparatus was simplified in that it did not contain any of the structural congestion typical of reactor containments, e.g., piping, wire trays, etc. A catch basket was attached to the end of the vent to trap the exiting debris. The drums were approximately 30 in. in diameter and 41 in. high (~125 gal.). For the Mark I configuration, prototypically-sized grating was placed at one level to estimate the effect of gratings on transport. Gratings were placed at two levels in the Mark II configuration. The system pressure, washdown flow rates, and debris quantities were measured in the tests.

For fibrous debris transport, it was concluded that

- the transport of all fibrous debris from the lower drywell volume is not a certainty;
- only the finest fiber debris fragments in Mark I containments may be carried from the lower drywell down the main vents;
- for the Mark II configuration, the average transport of fine fibers never exceeded 56%;
- for fiber debris larger than the distance between the bars of a typical grating, the transport fraction from the Mark I lower containment was 33%; and
- debris hang-up on the grating was dependent on grating location relative to the pipe-break location.

For RMI debris transport, it was concluded that

- nearly all of the small stainless-steel RMI foils transport from the lower Mark I containment volumes and
- an average of 10% of the small stainless-steel RMI foils transport from the lower Mark II containment volumes.

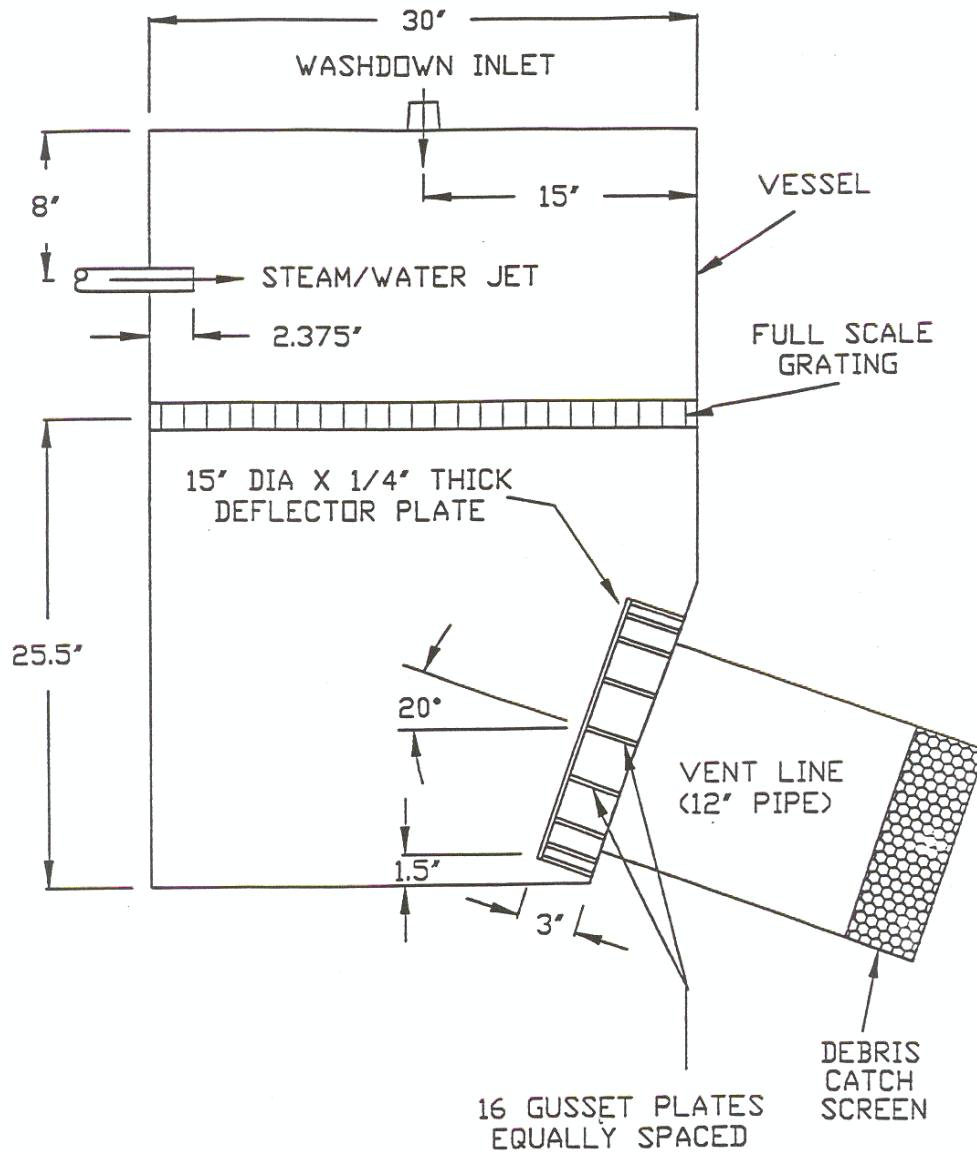


Figure 4-8 Schematic of 1/8-Scale Mark I Configuration Test Apparatus

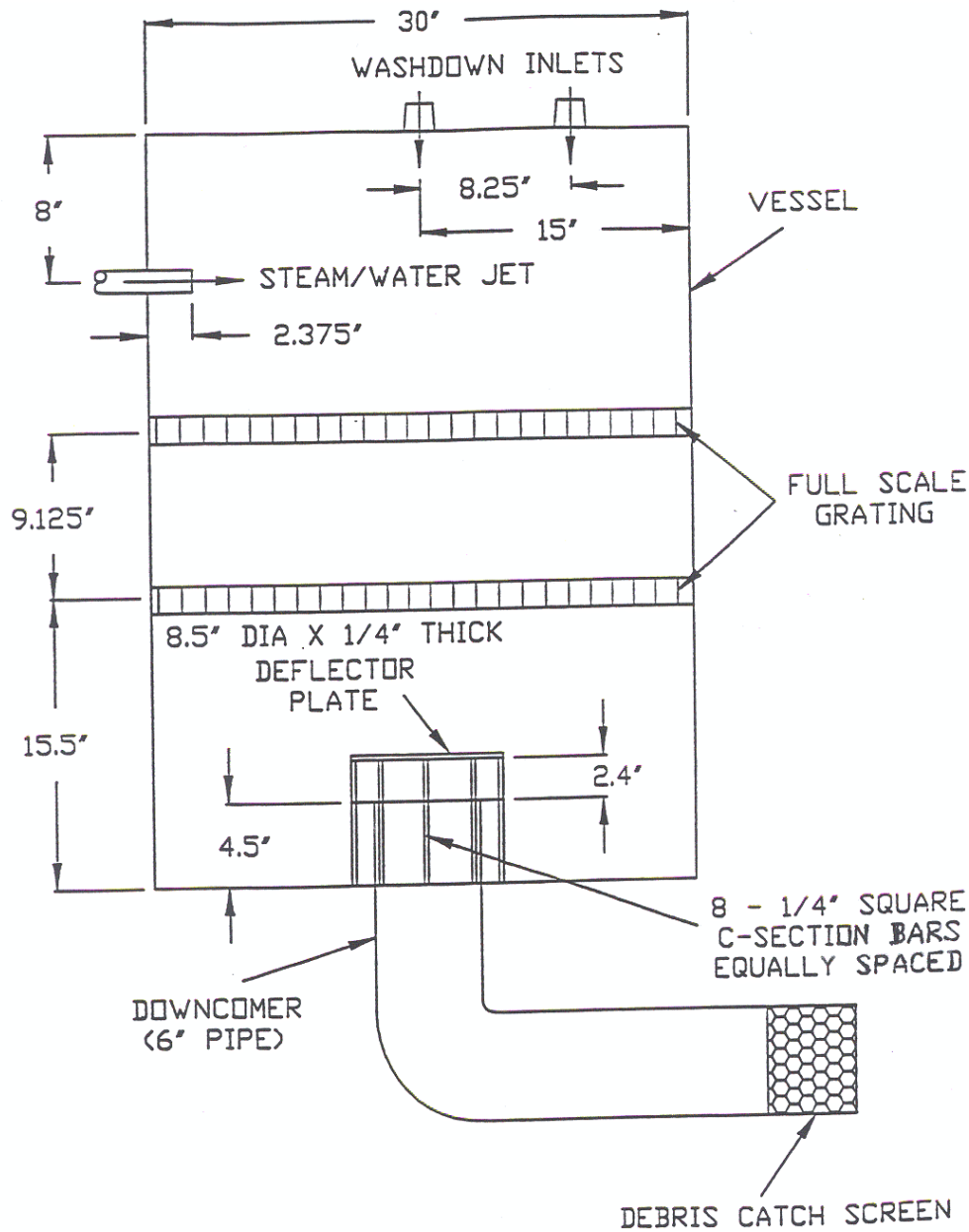


Figure 4-9 Schematic of 1/8-Scale Mark II Configuration Test Apparatus

The BWROG recommended 100% fine-fibrous debris transport through the drywell to the vent downcomers for the Mark I and III containment designs and 56% for the Mark II design. The transport of the large fibrous debris depended on the location of the debris relative to the gratings. For RMI debris, the BWROG again recommended 100% for the Mark I and III designs, but only 10% for the Mark II design. These numbers were for airborne and washdown debris transport combined.

The NRC review of the BWROG URG document⁴⁻⁷ with regard to the drywell debris transport determined that the guidance in the URG was nonconservative for Mark II containments. The NRC staff concluded that the same transport fractions used for the containments of Mark I and Mark III designs should also be used for the Mark II containments, i.e., 100% transport.

The primary criticism of the BWROG drywell debris-transport tests was of the scaling of the tests in that the drums were simply too small to simulate realistically the thermal-hydraulic conditions within a BWR drywell following a postulated LOCA. The test conditions, such as blowdown flow rates through the drum, may not have been prototypical. The BWROG did not perform any separate-effects testing to support the test results, which were for testing where all the effects were integrated. Much of the BWROG's claim of conservative results was based on exclusion of structures (piping, cable trays, etc.), which were not present in the experiments; however, the NRC-sponsored testing determined that the debris deposition on these structures was secondary in importance to the grating that was present in the test.

4.2.3 Washdown-Phase Debris-Transport Testing

4.2.3.1 Separate-Effects Insulation Debris Washdown Tests

Debris captured on structures during the blowdown phase following a LOCA would subsequently be subjected to transport and/or erosion by water flows from long-term recirculation cooling and containment sprays (washdown phase). For a BWR plant, the primary concern is the erosion and waterborne transport of debris captured on a floor grating directly below the broken pipe. In this situation, the debris would be pummeled by recirculation water flow that would cascade from the break to the drywell floor. Pieces of debris continually impacted by falling water could erode, allowing debris to pass through the grating and continue traveling toward the strainers. A series of tests was conducted in 1997 at a facility operated by SEA to examine the potential effect of washdown erosion. A complete description of the tests, including apparatus descriptions, procedures, and data, is documented in Volume 2 of Ref. 4-3.

The primary objective was to obtain experimental data that could be used to estimate the extent and timing of erosion during the washdown phase that would occur to insulation captured by floor gratings. The tests were to study the erosion of fibrous debris of different sizes at a variety of flow rates with the objective of answering two questions.

- What fraction of a piece of debris would erode and subsequently be transported to the drywell floor?
- Does the rate of erosion decrease with time, potentially reaching an asymptotic behavior?

These tests were conducted within a 5-ft-long, 2-ft by 2-ft vertical test chamber constructed of 0.5-in. clear polycarbonate to allow complete visualization of the tests. Figure 4-10 is a schematic of the test apparatus. An aluminum grating with 1-in. by 4-in. cells, which is characteristic of gratings used in BWR drywells, was placed at the bottom of this test chamber to hold the pieces of debris. Water was pumped into the top of the test chamber. Three simulated pipes were positioned to break up the structure of the injected flow before the water reached the debris. The simulated pipes were constructed of Plexiglas and were 2 in. in diameter.

A 400-gal. tank was used as a water reservoir for recirculation purposes. A 250-gpm centrifugal pump pumped water from this tank to the top of the test chamber through a 4-in. diameter PVC pipe. A debris catcher of fine-mesh wire screen was installed below the test chamber to catch insulation debris and erosion products, thereby preventing their recirculation back into the test chamber. A second filter was fitted to the pump suction to guarantee complete filtration of the debris from the pump inlet flow. A valve in the PCV pipe controlled the flow; the flow rate was monitored by a calibrated flow meter.

The simulated pipes conditioned the flow entering at the top of the test chamber; i.e., the bulk flow was broken up in a prototypical fashion. In this manner, water impacting the debris was spread relatively uniformly across the test chamber. In tests simulating spray-induced washdown, a removable spray head was attached to the PVC outlet.

Debris of various sizes was placed on the gratings and pipes and subjected to water flow typical of containment spray nozzles and break flow. Tests were conducted with room-temperature water using pieces of insulation generated by an air-jet impingement.

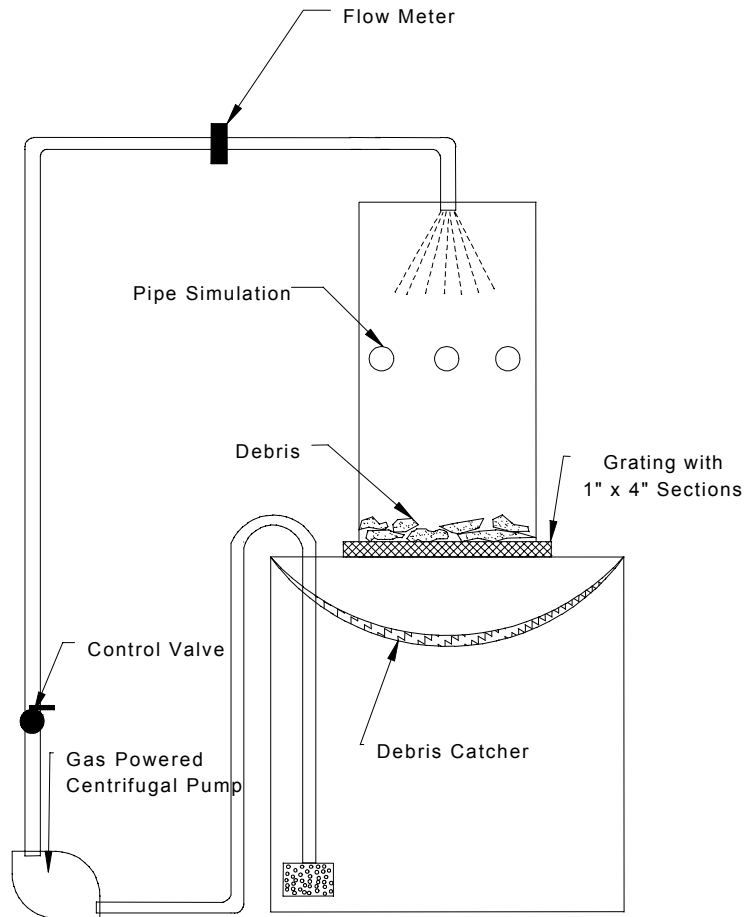


Figure 4-10 Schematic of Washdown Test Apparatus

Both the debris size and the water flow rate were varied to simulate washdown of small debris by containment sprays, as well as erosion and transport of large debris by break flows. Twenty-six parametric tests were conducted that examined a variety of test conditions. The test parameters included

- the water flow rate;
- the type of flow conditioning, i.e., with or without the removable spray head;
- the duration of the flow;
- the size and condition of the debris;
- the mass of the debris; and
- the thickness of the debris bed.

LDFG was tested, and four sizes of debris were tested to represent the range of debris expected following a LOCA:

- Fine Debris. This debris consisted of insulation pieces of loosely attached individual fibers less than an inch long. This debris was obtained directly from the CEESI air-jet transport tests. Such fine debris was typically found attached to wet surfaces such as pipes and gratings.
- Small Debris. This debris was characterized having a light, loose, and well-aerated texture with an average density lower than 0.25 lbf/ft³. The pieces were typically about 1.5 in. in size and possessed little of the insulation's original structure. This debris also was obtained from the CEESI air-jet transport tests and was used primarily in the spray tests.
- Medium Debris. This debris consisted of pieces of insulation typically about 4 in. by 6 in. in size. This debris was formed by one of two methods.

- Generated in the CEESI air jet tests where, although torn, the pieces kept some of the original structure of the insulation
- Intact insulation cut with scissors into medium-sized pieces
- Large Debris. This debris consisted of relatively large pieces of insulation ranging in size from 10 in. by 10 in. to 18 in. by 18 in. This debris was cut into predetermined sizes manually. Note that the air-jet tests clearly demonstrated that large pieces of debris produced by jet impingement tended to retain most of the original insulation structure.

Within the ranges of tested parameters, the data exhibited the following trends.

- Little or no erosion is possible for insulation pieces covered in canvas when they are subjected to washdown flow resulting from either the break overflow or containment spray.
- Most of the small pieces of debris resting on the grating bars will be washed down by water within approximately 15 min, after which the washdown reaches an asymptote.
- A significant fraction of the medium pieces would be eroded and transported.
- Large pieces will not be forced through the grating even at high flows. The pieces will remain on the grating and may erode with time. Erosion also exhibits a relatively constant rate behavior, as shown in Figure 4-11. The typical condition of debris after exposure to water is shown in Figure 4-12.
- The product of the erosion of large debris is fine debris, i.e., individual fibers and small clumps of fibers, that is likely to remain suspended in a pool of water with minimal turbulence.

Test Conclusions

- All finer debris (smaller than the grating cells) captured on the grating as a result of inertial capture would most likely be washed down when it is subjected to break and/or containment spray flows.
- A significant fraction of the medium pieces would be transported. For break overflows, most of the medium pieces likely would

transport. For containment spray flows, perhaps 50% would transport.

- Erosion of large debris is dependent on both time and flow rate. At low flow rates typical of containment sprays, the erosion of large pieces is negligible, especially considering that containment sprays are operated only intermittently. At water flow rates typical of break flow, the rate of erosion is substantial (as high as 25% for a 3-h duration). For such conditions, an erosion rate of 3 lbm/100-ft²/h is recommended.

4.2.3.2 Oskarshamn Nuclear Power Plant Containment Washdown Tests

ABB-Atom conducted experiments at the Oskarshamn BWR nuclear power plant to investigate the transport of insulation material by the containment spray system.⁴⁻⁴ After old and new insulation material was spread out on the diaphragm floor between the drywell and the wetwell, the containment spray system was activated. The distribution of the insulation material was determined after the experiments. In these experiments, a maximum of 5% of the material was transported into the wetwell.

The results of these tests have little value, primarily because the type and condition of the debris were not mentioned in the published report. Debris washdown is highly dependent on the type of insulation, the size of the debris, and the placement of the debris relative to the sprays and the vent downcomers. Based on U.S. NRC-sponsored testing, larger pieces of RMI debris placed well away from the inlet to the downcomer likely would have a very low transport fraction; conversely, fine fibrous debris likely would have a much higher transport fraction. These tests are mentioned here for completeness, but more information is needed for these tests to be useful.

4.3 Airborne/Washdown Debris-Transport Analyses

The NRC, U.S. industry, and international organizations have developed methodologies and performed analyses to estimate the airborne and washdown transport of debris within U.S. nuclear power plant containments. The results of these analyses provided qualitative and quantitative insights into the physical processes

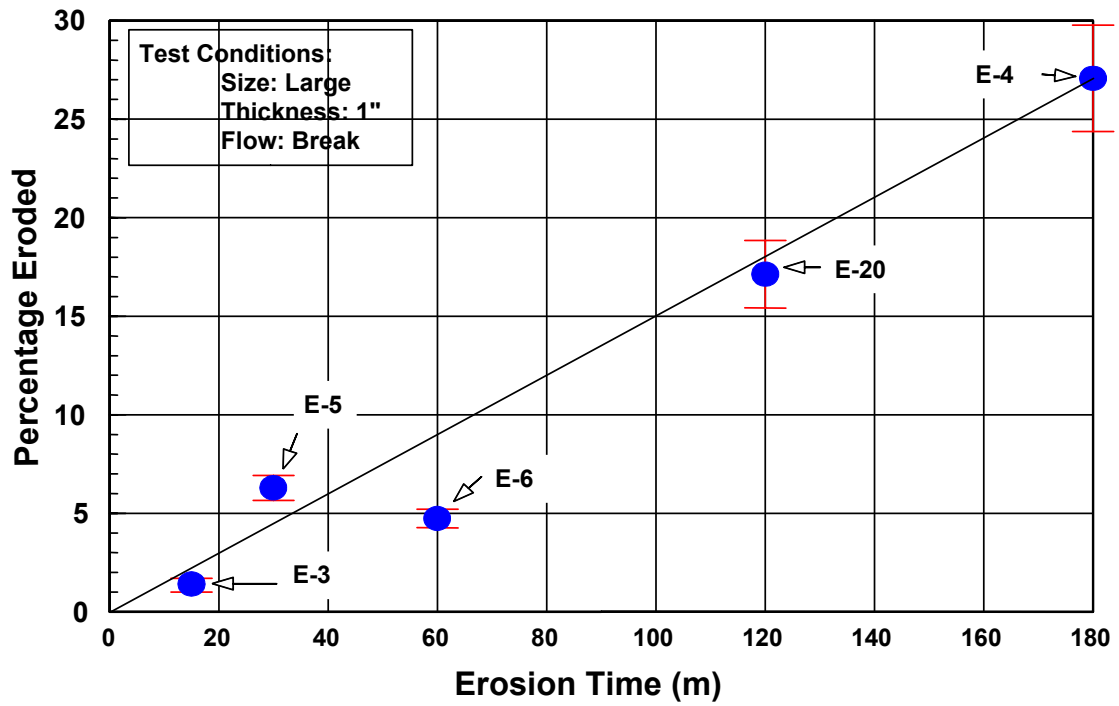


Figure 4-11 Time-Dependency of 1-in. Insulation Blanket Material Under Break-Flow Conditions



Figure 4-12 Typical Condition of Debris After Exposure to Water

and phenomena that govern debris transport. As mentioned earlier, much of this information was obtained specifically to support the resolution of the BWR strainer blockage issue; however, that information also is directly applicable to the PWR sump-screen blockage issue for the most part.

The analyses pertinent to airborne/washdown debris transport are listed in Table 4-8. These analyses include the following.

- Brief evaluations of operational incidents that occurred at the Gundremmingen-1 nuclear power plant (1977) in Germany and at the Barsebäck-2 nuclear power plant (1992) in Sweden in which insulation debris was generated and transported. These incidences both occurred at plants that had similarities to U.S. BWR plants (Section 4.3.1).
- The NRC sponsored the development of debris-transport PIRTs for both BWR and PWR nuclear power plants in the U.S. (Section 4.3.2).
- The Karlshamn debris-transport tests were simulated with the MELCOR code to test the ability of the code to predict the transport of insulation debris (Section 4.3.3.1).
- The NRC sponsored the DDTS to estimate BWR drywell debris-transport fractions using a bounding analysis approach (Section 4.3.3.2).
- The NRC sponsored a detailed analysis of debris generation and transport within a volunteer U.S. PWR nuclear power plant (Section 4.3.3.3).
- The BWROG developed their URG to support utility plant-specific analyses (Section 4.3.4.1).
- The NRC sponsored a parametric evaluation of the potential for sump-screen blockage within operating U.S. PWR plants. The evaluation included a generic estimate of the containment debris-transport fractions (Section 4.3.4.2).

4.3.1 Evaluations of Operational Incidents

4.3.1.1 Evaluation of Incident at Gundremmingen-1

An event occurred at the German BWR reactor Gundremmingen-1 (KRB-1) in 1977 in which the 14 SRVs of the primary circuit opened during a transient.⁴⁻⁴ The SRVs were located inside the

containment at a pipe attached to the main steam line between the reactor pressure vessel and the high-pressure turbine. The valves blew directly into the surrounding containment where the pipes had been insulated with fiberglass insulation reinforced with wire mesh and jacketed with sheet zinc. The piping insulation was extensively damaged.

After the incident, approximately 450 m³ (16,000 ft³) of water was found in the sump; about 240 m³ (8500 ft³) of the water originated in the coolant circuit; the rest was delivered by the CSS. This water transported a substantial quantity of insulation debris into the control drive mechanism compartment directly below the SRVs. The floor was covered with flocks of insulation material, but no larger parts of the insulation, such as sheet metals or textiles, were transported there. A thick layer of fiberglass insulation was found at the strainers installed in front of ducts leading from this compartment into the sump. Because recirculation from the sump was not required, the layer of insulation debris on the strainers had no further consequences. Therefore, it is not known whether recirculation from the sump was possible. No details regarding the quantities of debris generated and transported were made available for further analysis. Nevertheless, the potential for clogging recirculation strainers with insulation debris generated by an operational incident was clearly demonstrated.

4.3.1.2 Evaluation of Incident at Barsebäck-2

An event occurred at the Barsebäck-2 BWR nuclear power plant on July 28, 1992, during a reactor restart procedure after the annual refueling outage.⁴⁻⁴ The reactor power was below 2% of nominal when an SRV opened inadvertently because of a leaking pilot valve. The main valve opened when the reactor pressure had reached 3.0 MPa (435 psig). The steam was released as a jet directly into the containment. The containment is basically an upright cylinder with the drywell in the upper part and the wetwell directly beneath. Vertical pressure-relief pipes connect the drywell and the wetwell, and their openings are flush (covered by gratings) with the drywell floor. The containment was isolated when the drywell pressurized, so the blowdown pipes into the wetwell cleared. The containment vessel spraying system and the ECCS were started automatically.

Table 4-8 Airborne/Washdown Debris-Transport Analyses

Test Description	Sponsor, Analyst, and Date	Debris Source	Transport Medium	Objectives	Evaluation Products	Reference
Evaluation of Operational Incidences						
1977 Incident at Gundremmingen-1	OECD --- 1996	Damage to Operational Fiberglass Insulation	Inadvertent Opening of 14 SRVs and Containment Sprays	Understand debris transport that occurred during an operational incident at a nuclear power plant.	Qualitative information only. No details regarding quantities of debris generated and transported were made available for analysis. However, the potential for clogging recirculation strainers with insulation debris generated by an operational incident was clearly demonstrated.	NEA/CSNI/R (95) 11
1992 Incident at Barsebäck-2	OECD --- 1996	Damage to Operational Fiberglass Insulation	Inadvertent Opening of SRV and Containment Sprays	Understand debris transport that occurred during an operational incident at a nuclear power plant.	The quantities of debris generated and the dispersion of that debris were estimated. However, the relative quantities transported by airborne dispersion vs debris washdown could not be determined.	NEA/CSNI/R (95) 11
Phenomena Identification and Ranking Tables (PIRTs)						
BWR PIRT	NRC PIRT Panel 1997	Postulated LOCA-Generated Insulation Debris	BWR LOCAs	Use PIRT process to identify phenomena and to rank their importance as related to transport of LOCA-generated debris within U.S. BWR drywells and advise the NRC staff regarding debris-transport analyses and experimentation.	PIRT tables identified phenomena that could potentially influence debris transport within BWR drywells and ranked them according to their perceived importance with the highest-ranked phenomena clearly flagged.	INEEL/EXT-97-00894
PWR PIRT	NRC PIRT Panel 1999	Postulated LOCA-Generated Insulation Debris	PWR LOCAs	Use PIRT process to identify phenomena and to rank their importance as related to transport of LOCA-generated debris within U.S. PWR containments and advise the NRC staff regarding debris-transport analyses and experimentation.	PIRT tables identified phenomena that could potentially influence debris transport within PWR containments and ranked them according to their perceived importance with the highest-ranked phenomena clearly flagged.	LA-UR-99-3371, Rev. 2

Table 4-8 Airborne/Washdown Debris-Transport Analyses

Test Description	Sponsor, Analyst, and Date	Debris Source	Transport Medium	Objectives	Evaluation Products	Reference
Airborne/Washdown Debris-Transport Evaluations						
MELCOR Simulation of 1992 ABB-Atom Karlshamn Tests	SEA SEA 1995	Steam-Blasted Fibrous Debris	Blowdown Steam Jet	Test the ability of the MELCOR code to simulate insulation-debris transport.	The MELCOR code predicted results that compared well with the experimental debris-transport results. However, it was determined that the Karlshamn flow velocities were atypically too slow and that the MELCOR code would not likely perform well at typical flow velocities where inertial impaction would be a primary deposition mechanism because MELCOR does not model inertial impaction.	SEA-95-970-01-A:5
Drywell Debris Transport Study (DDTS)	NRC SEA 1997	BWR LOCA-Generated Debris	LOCA Steam- Water and Containment Sprays	Using a bounding analysis approach, the fractions of postulated LOCA-generated debris that subsequently would be transported to the wetwell were estimated. The analysis considered both the blowdown and the washdown phases.	Transport fractions for fibrous insulation debris were estimated using assumptions appropriate for an upper-bound estimate and a less conservative central estimate. In addition, the study provided engineering insights into debris transport processes that were useful when judging appropriateness of utility-generated debris-transport fractions.	NUREG/CR-6369
PWR Volunteer Plant Analysis	NRC LANL 2002	PWR LOCA-Generated Debris	PWR LOCAs	Develop and demonstrate a methodology for estimating the debris-transport fractions within PWR containments.	Generalized methodology was developed and demonstrated by estimating the transport fractions for a specific LOCA in the volunteer plant.	TBD

Table 4-8 Airborne/Washdown Debris-Transport Analyses

Test Description	Sponsor, Analyst, and Date	Debris Source	Transport Medium	Objectives	Evaluation Products	Reference
Generalized Debris-Transport Guidance						
BWROG URG	BWROG BWROG 1996	BWR LOCA- Generated Debris	BWR LOCAs	Provide guidance to the operators of U.S. BWR nuclear power plants regarding the resolution of the BWR strainer blockage issue. This guidance included methodology for estimating the drywell debris transport fractions.	The URG for ECCS Suction Strainer Blockage was developed. (The NRC staff subsequently reviewed the URG; their review comments noted where they agreed or did not agree with the URG.)	NEDO- 32686
Transport Fractions for Parametric Evaluation	NRC LANL 2002	PWR LOCA- Generated Debris	PWR LOCAs	Generic composite debris-transport fractions were estimated to support the parametric evaluation of the potential for sump-screen blockage in U.S. PWR plants.	A set of transport fractions was estimated based on both documented research and on-going research that could be applied in a generic fashion to all U.S. PWR plants for the specific purposes of the parametric evaluation and therefore are not generally applicable to plant-specific analyses. These transport fractions, defined as the fraction of the ZOI insulation subsequently transported to the sump screen, tended to favor the plant situation and thus should not be treated as conservative.	NUREG/CR- 6762

About 200 kg (440 lb) of fibrous insulation debris was generated and about 50% of this debris subsequently reached the wetwell, resulting in a large pressure loss at the strainers about 70 min after the beginning of the event. Gratings in the drywell did not hold back the insulation material effectively. The approximate distribution of insulation debris within the drywell following the event was

- 50% on the beamwork, mainly concentrated in three areas: inside the drywell “gutter,” near the outer containment wall, and on or near the grid plates over the blowdown pipes;
- 20% on the wall next to the affected pipe, from which most of the insulation originated, and on the components around the safety valve;
- 10% on the wall opposite the affected pipe;
- 12% on the walls above the grating lying above the safety valve; and
- 8% on the grating above the safety valve.

The debris was transported by steam and airflow generated by the blowdown and by water from the CSS. It could not be determined how the transport developed with respect to time and whether the blowdown or washdown processes transported the major part of the debris found in the wetwell.

The generation and transport of large amounts of fibrous debris by the simple erroneous opening of a safety valve were observed. The transport included the short-term transport resulting from the steam and air blast and the longer-term washdown transport associated with operation of the containment spray system. The extent of damage and of transport appeared to be remarkably large given the small leak size and low reactor pressure. The locations of debris on such surfaces as the walls suggest the significance of inertial impaction as a deposition mechanism near the location of the break.

4.3.2 Phenomena Identification and Ranking Tables

4.3.2.1 BWR PIRT

The NRC sponsored the formation of a PIRT panel of recognized experts with broad-based knowledge and experience to identify and rank the phenomena and processes associated with the transport of break-generated debris through a BWR containment drywell following the

initiation of one or more accident sequences.⁴⁻² The primary objective of the BWR PIRT was to support the DDTs, which is discussed in Section 4.3.3.2. The PIRT process was designed to enhance the DDTs analysis by identifying processes and phenomena that would dominate debris-transport behavior. Further, these processes and phenomena were prioritized with respect to their contributions to the reactor phenomenological response to the accident scenario. The PIRT panel also evaluated the plans for experimental research, the experimental results, and the analytical results. Their final report was updated to reflect the final results of the DDTs. The phenomena ranked as having the highest importance with respect to debris transport within a BWR drywell are listed in Table 4-9.

4.3.2.2 PWR PIRT

Like the BWR PIRTs discussed in Section 4.3.2.1, the NRC sponsored the formation of a PIRT panel of recognized experts with broad-based knowledge and experience to identify and rank the phenomena and processes associated with the transport of debris in PWR containments following the initiation of one or more accident sequences.⁴⁻¹ The PWR PIRT has been used to support decision-making regarding analytical, experimental, and modeling efforts related to debris transport within PWR containments.

A modest database of experimental and technical results existed to support this PIRT effort. The PIRT panel initially focused on a Westinghouse four-loop PWR with a large dry ambient containment as the base configuration and a double-ended, cold-leg, large-break LOCA for the baseline scenario. Following the initial effort, the PWR PIRT considered the other two existing U.S. PWR containment designs, i.e., the sub-atmospheric and ice condenser containments. The event scenario was divided into three time phases: blowdown between event initiation and 40 s, post-blowdown between 40 s and 30 min, and sump operation between 30 min and 2 days. Each phase was characterized with respect to physical conditions, key phenomena and processes, and equipment operation. The containment was partitioned into three components:

- the containment open areas, excluding the potential pool in the bottom of the

Table 4-9 Highly Ranked Phenomenon from BWR Drywell Transport PIRT Table	
Processes and/or Phenomena	Description
Pressure-Driven Flows	These flows represent the bulk flows, i.e., the net or macroscopic flow characteristics of the containment atmosphere.
Localized Flow Fields	Flow direction and/or velocities that differ from the bulk atmosphere flow characteristics because of localized geometries.
Liquid Flashing	Liquid to vapor phase transformation because of expansion across choked break plane.
Recirculation Deluge (Steaming)	Large flow rate of liquid effluent from a low-elevation break in the reactor coolant system (e.g., recirculation line) onto drywell structures or from sprays when activated.
ECCS Deluge	Large flow rate of liquid effluent from ECCS onto drywell structures.
Drywell Floor Pool Formation, Overflow, and Flow Dynamics Following Recirculation Line Break	Creation of a water pool on the drywell floor sufficiently deep to allow overflow into wetwell transfer piping. Flow dynamics include multi-dimensional flow patterns and velocities, free-surface behavior, and turbulent mixing.
Surface Wetting	Formation of a liquid film on structure surfaces due to condensation of steam from the atmosphere or impaction of water droplets onto structure surfaces.
Structural Congestion (Porosity)	Variations in fluid flow area and flow as related to the density of the structures in the drywell, and due to the tortuousness of the flow paths around these structures.
Debris Advection/Slip	Transport of airborne debris within the carrier gas medium.
Inertial Impaction	Capture of debris on structure surfaces due to inertial impaction.
Adhesion	Permanent retention of debris particles on a structure surface due to mechanical interactions with a rough surface or other forces.
Recirculation Deluge (Steaming) Related Transport	Relocation of debris from drywell structures due to interactions with the deluge of liquid from recirculation pipe breaks, or sprays.
Debris Transport and Deposition within Pool	Relocation of debris in the drywell floor pool towards the wetwell vent pipe entrances.

- containment and the debris-generating ZOI in the vicinity of the break;
- the containment structures; and
- the containment floor upon which a liquid pool forms in the lower containment elevations.

The panel identified a primary evaluation criterion for judging the relative importance of the phenomena and processes important to PWR-containment debris transport. The criterion was the fraction of debris mass generated by the LOCA that is transported to the sump entrance. Each phenomenon or process identified by the panel was ranked relative to its importance with respect to the transportation of debris to the sump entrance. Highly-ranked phenomena and processes were judged to have a dominant effect with respect to the primary evaluation

criterion. Medium-ranked phenomena and processes were judged to have a moderate effect with respect to the primary evaluation criterion. Low-ranked phenomena and processes were judged to have a small effect with respect to the primary evaluation criterion.

The results of the panel's identification and ranking efforts were tabulated, and all processes and phenomena were ranked according to perceived relative level of importance, i.e., high, medium, or low. (See the PWR-PIRT final report for complete tabulation). The processes ranked as high are shown in Table 4-10. In the table, the processes and phenomena are grouped by accident phase and containment location. Most of the high-importance processes dealt with debris transport on the containment floor, where the sump pool was either forming or

Transport Phase	Containment Component		
	Open Areas	Structures	Floor
Blowdown (0–40 s)	Gravitational settling	None	None
Post-Blowdown (40 s–30 min)	Droplet motions Debris sweepout	Surface draining Deluge transport Disintegration Entrapment	<u>Pool Behavior</u> Formation Agitation Flow dynamics Film entry transport Liquid entry transport Disintegration Settling Transport
Sump Operation	None	None	<u>Pool Behavior</u> Agitation Flow dynamics Sump-induced flow Reentrainment Transport Sump-induced overflow

had already formed. (These processes and phenomena are the subject of Section 5.) Only seven processes were listed with high importance for the containment above the sump pool, which is the subject of this section. Definitions of these seven processes are provided in Table 4-11.

During blowdown, gravitational settling of large pieces of debris generated by the break-jet flow was ranked as high. During post-blowdown, the four processes associated with the containment above the sump pool deal with debris washdown by the containment sprays. During the sump-operation phase, no processes were ranked as high except those dealing with sump-floor debris transport.

4.3.3 Airborne/Washdown Debris-Transport Evaluations

4.3.3.1 MELCOR Simulation of Karlshamn Tests

Using the MELCOR code, SEA simulated one of the Karlshamn tests to demonstrate the ability of the code to simulate insulation debris transport.⁴⁻⁸ As discussed in Section 4.2.1.4, these tests were conducted in a small-scale test

assembly, shown schematically in Figure 4-7, that was subdivided into a few inner volumes. A steam jet was used to fragment insulation and disperse its debris within the test apparatus. Most of the fibrous insulation debris was distributed in the upper parts of the test apparatus. The gratings held debris back, debris adhered to walls where steam condensed, and debris accumulated in areas of low flow velocity.

The MELCOR code, which was developed at Sandia National Laboratories for the NRC, is a fully integrated computer code that models the progression of severe accidents in LWR nuclear power plants.⁴⁻⁹ Thermal-hydraulic behavior is modeled with a lumped-parameter approach using control volumes connected by flow paths. Each volume is defined spatially by its volume vs altitude; may contain a gravitationally separated pool of single- or two-phase water; and can have an atmosphere consisting of any combination of water vapor, suspended water droplets, or noncondensable gases. Noncondensable gases are modeled as ideal gases with temperature-dependent specific heat capacities. The flow paths connect volumes and define paths for moving hydrodynamic materials.

Processes and/or Phenomena	Description
Gravitational Settling	Downward relocation (sedimentation) of debris in the containment atmosphere onto structure surfaces under the force of gravity.
Droplet Motions	Movement of droplets introduced into containment by the spray system.
Debris Sweepout	Transport of debris through the containment by liquid droplets from the containment spray system.
Surface Draining	Movement of liquid streams from higher elevations to lower elevations.
Deluge Transport	Relocation of debris from containment structures as a result of interactions with the deluge of liquid from the ECCS and spray system.
Disintegration	Breakup of relatively large pieces of debris into smaller particles that can be reentrained into the flow stream caused by the impact of falling liquid streams from the break, fan coolers, and liquid draining off surfaces.
Entrapment	Capture of debris in local structural "pooling points," i.e., locations that allow the accumulation and storage of draining condensate and associated transported debris.

The governing thermal-hydraulic equations conserve mass, momentum, and energy. The MELCOR code contains models to predict the transport and behavior of aerosols that directly couple to the thermal-hydraulic models. The aerosol deposition processes modeled include gravity, diffusion, thermophoresis, and diffusiophoresis.

The MELCOR code results compared well with the experimental results; however, this high degree of comparability does not extend to the conditions typical of postulated LOCAs. The peak bulk flow velocities in the Karlshamn tests were about 1 m/s, whereas the transport velocities were much faster following a postulated LOCA in an actual plant. The atypically slow flow velocities in the Karlshamn tests allowed the debris to settle gravitationally at all levels, whereas at typical transport velocities, the flow turbulence generally would be much too high to allow settling anywhere near the break. After break flows disperse sufficiently into compartments well away from the break, flow velocities and turbulence can be expected to slow sufficiently to allow gravitational settling as was seen in the Karlshamn tests. Thus, the Karlshamn tests might be considered representative of debris transport in some areas of PWR containments, but not in the region of the break. Alternatively, the Karlshamn results might be representative of debris transport following very small LOCAs.

After a complete review of the Karlshamn simulation, it was concluded that although the MELCOR code did a good job of predicting debris transport within the Karlshamn tests apparatus, the code could not reliably be used to predict debris transport within a containment where the flow velocities and flow turbulence would be too high to allow significant debris settling. Also, it should be noted that the MELCOR code does not model inertial impaction of an aerosol, which would be substantial near the break region of the containment. Therefore, system-level codes such as MELCOR were used to estimate thermal-hydraulic conditions within a containment following a LOCA, but not to predict debris transport.

4.3.3.2 BWR Drywell Debris Transport Study (DDTS)

In September 1996, the NRC initiated a study, referred to as the DDTS, to investigate the transport and capture characteristics of debris in BWR drywells using a bounding analysis approach. Understanding the relatively complex drywell debris-transport processes was an essential aspect of predicting the potential for strainer clogging in the estimation of debris transport in the drywell. These processes involve the transport of debris during both the reactor blowdown phase through entrainment in steam/gas flows and the post-blowdown phase

by water flowing out of the break and/or containment sprays. The erosion characteristics of debris caused by air and water flows must also be considered. The focus of the DDTs was to provide a description of the important phenomena and plant features that control or dominate debris transport and the relative importance of each phenomenon as a function of the debris size. Further, these analyses were to demonstrate calculational methodologies that can be applied to plant-specific debris-transport estimates. It also should be noted that the DDTs focused almost entirely on the transport of LDFG insulation debris.

Because of its complexity, the problem was broken into several individual steps. Each step was studied either experimentally or analytically, and engineering judgment was applied where applicable data were not available. The results of the individual steps were quantified using a logic-chart approach to determine transport fractions for (1) each debris size classification, (2) each BWR containment design, (3) both upper bound and central estimates, and (4) each accident scenario studied. The complexity is illustrated in Figure 4-13 for both the blowdown and washdown phases.

Upper bound estimates provide transport fractions that are extremely unlikely to be exceeded. Because each upper bound estimate represents the compounding of upper bound estimates for each individual step, the overall upper bound transport fractions are highly conservative. The central estimates were developed using a more realistic, yet conservative, representation of each individual step. Although the central-estimate transport fractions were deemed closer to reality, the estimates lacked the assurance of not being exceeded under any accident condition.

Early in the study the thermal and hydraulic conditions that would govern debris transport were analytically assessed by performing end-to-end scoping calculations that encompassed the possible debris-transport and capture processes. These calculations included both a series of hand computations and system-level computer code calculations (i.e., MELCOR, RELAP, and CFD). All calculations were designed to examine selected specific aspects of the overall problem. The calculation results were used to subdivide the problem into several components that could be solved individually

through the separate-effects experiments, analytical modeling, and engineering calculations. The calculations also identified vital database elements necessary to quantify transport.

Experiments and further analytical studies were undertaken to provide a basis for quantifying debris transport during blowdown, washdown of debris by ECCS water flow, and debris sedimentation on the drywell floor. In particular, three sets of experiments, which are discussed in Section 4.2, were designed and conducted as part of this study. Detailed CFD simulations were used to determine likely flow patterns that would exist on the drywell floor during ECCS recirculation and the likelihood of debris sedimentation under these conditions.

Transport fractions were estimated (i.e., Mark I, Mark II, and Mark III) for a spectrum of postulated accident scenarios. Two major types of piping breaks were studied: main steam line (MSL) breaks and recirculation line (RL) breaks. Both throttled and unthrottled ECCS break overflow was considered. Containment sprays were considered to operate intermittently or not at all.

A simplified logic-chart method was chosen to integrate the problem subcomponents into a comprehensive study. An example logic chart is shown in Figure 4-14. A separate logic chart was generated for each scenario and each containment design. Individual steps in the logic charts were solved using available knowledge tempered by conservative engineering judgment. Finally, the logic charts were quantified and the results were tabulated.

The logic chart subdivides the problem into five independent steps: (1) LOCA type, (2) debris classification, (3) debris distribution after blowdown, (4) erosion and washdown, and (5) sedimentation in the drywell floor pool. Because the debris size distribution was not within the scope of this study, a size distribution from a BWROG study⁴⁻⁶ was used in the DDTs to illustrate the computation of overall debris-transport fractions. Four size classifications are shown in the chart: small, large-above, large-below, and canvassed. Because large debris does not pass through floor grating, the large debris classification was subdivided into debris formed above any grating and debris formed below all gratings. Overall transport fractions were applied to all insulation within the ZOI.

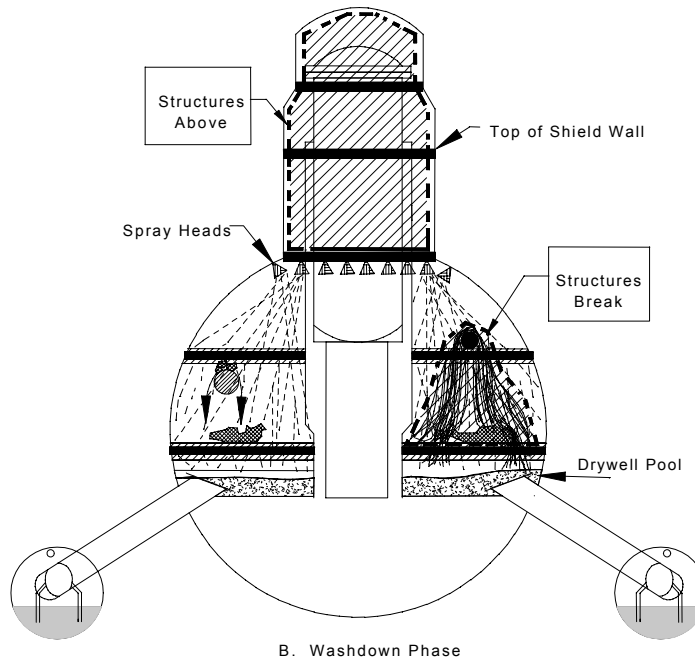
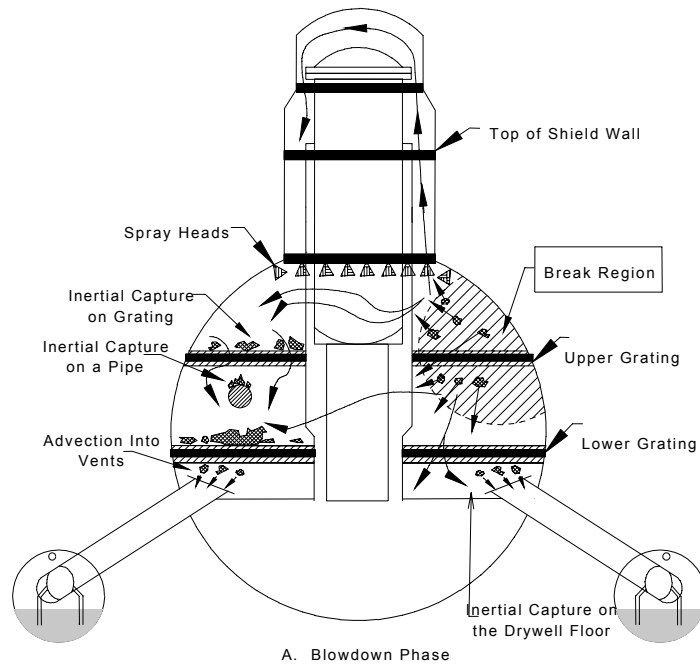


Figure 4-13 Schematic Illustrating the Complexity of Drywell Debris Transport

LOCA Type	Debris Classification	Distribution After Blowdown	Erosion and Washdown	Drywell Floor Pool	Path No.	Fraction	Final Location	
MARK I CENTRAL ESTIMATE MSL BREAK ECCS THROTTLED SPRAYS OPERATED FIBROUS INSULATION	Small Pieces 0.22	Adverted to Vents			1	1.144E-01	Vents	
		0.52 Enclosures			2	2.200E-03	Enclosures	
		0.01			Waterborne	3	0.000E+00	Vents
		Drywell Floor			0.00			
		0.01			Sediment	4	2.200E-03	Floor
					1.00			
					Waterborne	5	8.800E-07	Vents
					0.01			
		Structures-Above			Condensate Drainage	6	8.712E-05	Floor
		0.04			Adheres	7	8.712E-03	Structures-Above
					0.99			
					Waterborne	8	1.100E-04	Vents
					0.01			
		Structures-Break			Sprays/Condensate	9	1.089E-02	Floor
		0.10			Adheres	10	1.100E-02	Structures-Break
					0.50			
					Waterborne	11	3.520E-04	Vents
					0.01			
		Structures-Other			Sprays/Condensate	12	3.485E-02	Floor
		0.32			Adheres	13	3.520E-02	Structures-Other
					0.50			
					Waterborne	14	5.100E-04	Vents
					1.00			
		Structures-Break			Sprays/Condensate	15	0.000E+00	Floor
		0.15			Adheres	16	5.049E-02	Structures-Break
					0.99			
					Waterborne	17	2.890E-03	Vents
					1.00			
		Large-Above			Sprays/Condensate	18	0.000E+00	Floor
		0.34			Adheres	19	2.861E-01	Structures-Other
			0.01					
Structures-Other			Sprays/Condensate	20	3.600E-02	Vents		
0.85			Adheres	21	4.000E-04	Enclosures		
			0.99					
			Waterborne	22	0.000E+00	Vents		
			0.00					
Drywell Floor			Sediment	23	1.600E-03	Floor		
0.04			1.00					
			Waterborne	24	0.000E+00	Vents		
			0.00					
Structures-Break			Sprays/Condensate	25	4.000E-06	Floor		
0.01			Adheres	26	3.960E-04	Structures-Break		
			0.99					
			Waterborne	27	0.000E+00	Vents		
			0.00					
Structures-Other			Sprays/Condensate	28	1.600E-05	Floor		
0.04			Adheres	29	1.584E-03	Structures-Other		
			0.99					
Canvassed				30	4.000E-01	Structures/Floor		
0.40				Total	1.000E+00			

Figure 4-14 Sample Drywell Debris Transport Logic Chart

Accordingly, the canvassed classification included intact blankets located within the ZOI. The third column shows where the debris is expected to reside following the end of blowdown. Drywell structures were divided according to location in the drywell:

- structures located above the containment spray heads (which are not subject to spray flows),
- structures located directly below the break (which can be subjected to recirculation break flows), and
- all other structures subjected to sprays but not to break flows.

Additionally, small debris can be deposited directly onto the floor by mechanisms such as vent capture or entrapment within an enclosure such as the reactor cavity. Large debris generated above any grating was assumed to reside on a grating either below the break or not below the break. Large debris deposited above the spray heads or in enclosures was not considered credible. Each branch in the erosion and washdown column simply calculated the amounts of captured debris that remained on the structures after being subjected to the appropriate washdown flows (i.e., recirculation break flow, containment spray flow, and condensate drainage). Similarly, each branch in the drywell floor pool column asks how much of the debris settles to the floor and remains there.

Analyses supporting the DDTS included a variety of calculations designed to examine selected specific aspects of the overall problem. These included hand calculations, system-level code calculations, and CFD calculations. The computer code calculations that were performed in support of the DDTS are described in the following paragraphs.

MELCOR Code Calculations

The MELCOR computer code was used to examine the thermal-hydraulic conditions within the drywell following a postulated LOCA. The simulations were based on the BWR Mark I reference plant analyzed during the NUREG/CR-6224 strainer-blockage study.⁴⁻¹⁰ Insights were obtained regarding containment pressures and temperatures, bulk flow velocities, the time required to clear the vent downcomer of water, rate of steam condensation on drywell structures and

subsequent thickness of films, rate of accumulation of water on the drywell floor, and transport of noncondensable gases to the wetwell. Several key observations were made of these MELCOR calculations, including those in the following list.

- The drywell pressure increased rapidly to about 3 atm (44 psia) in about 1 s, corresponding to the clearing of the downcomer vents. Further pressurization was prevented by the pressure-suppression system. After a relatively short period of 5 to 10 s, the pressures decreased again.
- The water in the downcomer vent pipes was purged from the pipes in about 1 s.
- Steam immediately condensed upon contact with surface structures until the temperature of the surface equilibrated with the steam environment. For example, the total rate of condensation within the drywell for the high MSL break peaked at 1170 lbm/s at about 2.5 s.
- Water films with a thickness of 200 to 400 μm accumulated on the structures in as little time as 1 s, depending on the location of the surface relative to the pipe break.
- Peak flow velocities as high as 820 ft/s were found near the break, and flow velocities through the vent downcomer pipes exceeded 660 ft/s. Elsewhere in the drywell, the velocities varied considerably from one location to another.
- The majority of the nitrogen gas initially located in the drywell was forced into the wetwell in about 3 s. The residence time for a tracer gas injected into the drywell along with the break source was generally less than 2 s.
- A pool of water accumulated on the drywell floor and in the reactor cavity sumps, as was expected. In the MSL breaks, the pool would not overflow into the downcomer vent pipes because the depth of the water was only about a quarter of the depth required to overflow. In the recirculation line break (RLB), the results were considerably different. The overflow through the downcomer vent began at 5 s for the low RLB. The asymmetrical pressures acting on the drywell floor pool pushed the accumulated water to the backside of the pedestal from the break; after the drywell pressures peaked, the pool became two-phased. The raised water level caused the

water to overflow into the vents at the backside. The drywell pool leveled out again after the primary system was depressurized.

RELAP Code Calculations

Calculations were performed with the RELAP computer code to characterize the break flow, (i.e., rate of flow and thermodynamic state as a function of time). Following a main steam line break (MSLB), essentially dry steam expands into the containment. The steam mass-flow rate falls from an initial value of close to 6000 lbm/s (assuming blowdown from both ends of the broken pipe) to about 1000 lbm/s within a period of 50 s, whereas the steam velocity remains essentially at the sonic velocity of about 700 ft/s. Water enters the drywell in the form of fine droplets (approximately 5 μm) of entrained water, but the water content is not likely to be large enough to completely wet the debris during its generation.

Following an RLB, the initial flow would be mainly water, but after a period of 5 to 10 s, a mixture of water and steam is discharged at high velocities. During this phase, the dynamic pressures far outweigh the corresponding pressures during the initial 5 s after the break. Because the debris generation is proportional to the dynamic pressure, these results suggest that for an RLB, most of the fibrous insulation debris will be produced in the later stages of the accident. The total mass flow rate remains fairly high (approximately 20,000 lbm/s) throughout the blowdown phase of an RLB compared with the flow rate for a similar size MSLB; however, the water content of the exit flow is very large. In these conditions, it is expected that all of the structures located in the path of the jet will be drenched with water, and the insulation materials in the vicinity of the break are likely to be thoroughly wet before the break jet produces significant debris. Additionally, it is likely that the majority of the debris generated will follow the steam component of the break flow rather than the liquid component. The DDTS assumed that 80% of the debris would be transported with the steam and 20% would be transported with the water.

CFD Calculations

Substantial quantities of insulation debris could land on the drywell floor during the primary

system depressurization or be washed down to the drywell floor from drywell structures after being captured during depressurization. From there, the debris could be transported from the floor into the vent downcomers. Therefore, determining the potential for debris to remain captured on the floor was a necessary step in the overall debris-transport study. This determination was made based on simulating the drywell floor pool for a variety of conditions using a commercially available CFD code. The primary objective of this analysis was to evaluate the potential for fibrous debris to settle in drywell pools and to estimate the fractions of the debris that would be transported to the suppression pool. The study considered Mark I, II, and III designs for variations in pool depth and entrance conditions to the pools.

The CFD results needed to be benchmarked to prototypical experimental data to correlate pool turbulence levels with the conditions that allowed debris to settle. This was accomplished by simulating the ARL Pennsylvania Power and Light Company (PP&L) flume tests with the CFD code and then correlating the code-predicted turbulence level for a given test with the PP&L test results that showed whether fibrous debris actually settled in each test. The PP&L flume tests are documented in "Results of Hydraulic Tests on ECCS Strainer Blockage and Material Transport in a BWR Suppression Pool" (1994).⁴⁻¹¹ The maximum levels of turbulence that allowed debris to settle were determined and applied to the drywell floor pool simulation results. Two maximum levels were determined, one for small debris and one for large debris.

The results of each of the drywell floor pool simulations consisted of graphical pictures of pool flow behavior, such as two- and three-dimensional color pictures of flow velocities and flow turbulence in the form of specific kinetic energy. These turbulence levels then were compared with the maximum levels for debris settling determined by the code calibration. If pool turbulence were higher than the levels found to keep debris in suspension, then debris would not likely settle. On the basis of this graphical data, engineering judgment was used to determine the likelihood for debris settling for each pool configuration. With noted design-specific exceptions, drywell floor pools formed by recirculation break flows are considered likely to transport the majority of insulation debris into

the vent downcomers, and pools formed by the containment sprays are likely to retain debris.

Debris Transport Quantification Results

A summary of the upper bound and central estimated transport fractions for a postulated LOCA in the mid-region of the drywell are presented in Tables 4-12 and 4-13 for the MSLBs and the RLBs. As previously noted, the DDTs focused on the transport of LDFG insulation debris. A complete set of results can be found in Ref. 4-3.

The central estimate transport fractions shown in Table 4-12 are the fractions for the MSLB scenarios in which the operators throttle the ECCS back to the steaming mode and the containment sprays are operated intermittently. This scenario was chosen for summary purposes because it is the most likely scenario that operators would follow. Conversely, the upper bound estimate transport fractions in Table 4-12 are the fractions for the MSLB scenarios in which the ECCS is not throttled back to the steaming mode and the sprays are operated. This scenario was chosen for the upper bound estimate because it represents the worst-case scenario in terms of debris transport. Similarly, the transport fractions shown in the Table 4-13 summary for RLB scenarios are those for ECCS throttling and spray operation

for the central estimates and no throttling and spray operation for the upper bound.

Transport fractions corresponding to Tables 4-12 and 4-13 for all of the insulation initially located within the ZOI are provided in Table 4-14. These transport fractions were determined using the BWROG debris-size distribution of 0.22, 0.38, and 0.40 for small, large, and canvassed debris. The large debris was subdivided further into large-above and large-below categories using engineering judgment. These subdivisions were 80% and 90% above the grating for the central and upper bound estimates, respectively.

Several general conclusions can be drawn from these results.

- The total fraction of debris transported depends strongly on the assumed size distribution of the debris and the location of the break.
- Small debris readily transports toward vent entrances with a substantial amount captured, primarily by the gratings.
- A majority of the large debris generated above any grating is not likely to transport to the vents.
- A majority of the large debris generated below all gratings will likely transport into the vents.

Table 4-12 Study Transport Fractions for Main-Steam-Line Breaks						
Plant Design	Central Estimate			Upper Bound Estimate		
	Small Debris	Large Debris		Small Debris	Large Debris	
		Above Any Grating	Below All Gratings		Above Any Grating	Below All Gratings
Mark I	0.52	0.01	0.90	1.0	0.05	1.0
Mark II	0.74	0.01	0.90	1.0	0.05	1.0
Mark III	0.55	0	0.90	0.93	0.03	1.0

Table 4-13 Study Transport Fractions for Recirculation Line Breaks						
Plant Design	Central Estimate			Upper Bound Estimate		
	Small Debris	Large Debris		Small Debris	Large Debris	
		Above Any Grating	Below All Gratings		Above Any Grating	Below All Gratings
Mark I	0.86	0.02	0.94	1.0	0.30	1.0
Mark II	0.89	0.02	0.95	1.0	0.30	1.0
Mark III	0.72	0.01	0.90	1.0	0.30	1.0

Plant Design	Main-Steam-Line Break		Recirculation-Line Break	
	Central	Upper Bound	Central	Upper Bound
Mark I	0.15	0.31	0.23	0.39
Mark II	0.20	0.31	0.24	0.39
Mark III	0.16	0.29	0.20	0.39

The study concluded that the URG-recommended transport fractions for Mark II containments underestimate debris transport. For Mark I and Mark III drywells, the study concluded that the URG appears to provide reasonable estimates, provided the plant contains a continuous lower grating with no large holes. However, although the RG 1.82, Rev. 2 recommended assumption of 100% transport of transportable debris was found to provide a reasonable upper bound for breaks located below the lowest grating, the recommendation greatly overestimates debris transport for breaks located above the lowest grating. Finally, the study concluded that licensees should pay close attention to plant features that are unique to their plant and how they were modeled in this study. If necessary, the logic charts provided in this study can easily be modified to account for plant-specific features, such as number and arrangement of floor gratings. They also are flexible enough to accommodate new evidence and assumptions related to debris size and distribution.

The DDTS is documented in the three-volume NUREG/CR-6369 report.⁴⁻³ The main volume, Volume 1, summarizes the overall study, in particular, the debris-transport quantification and transport fractions. The experiments conducted to support this study are documented in detail in Volume 2. The analyses conducted to support this study are documented in detail in Volume 3. The DDTS reports provide reasonable engineering insights that can be used to evaluate the adequacy of the debris-transport fractions used in the utility strainer-blockage analyses.

4.3.3.3 PWR Volunteer Plant Analysis

The primary objective of this analysis was to develop and demonstrate an effective methodology for estimating containment debris transport that could be used to assess the debris transport within PWR plants. The transport

analysis consisted of airborne debris transport, where the effluences from a high-energy pipe break would destroy insulation near the break and then transport that debris throughout the containment, and washdown debris transport caused by operation of the containment sprays. The airborne/washdown debris-transport analysis provides the source term for the sump-pool debris-transport analysis.

The volunteer plant chosen for detailed analysis has a large, dry cylindrical containment with a hemispherical dome constructed of steel-lined reinforced concrete with a free volume of approximately 3 million cubic feet. The nuclear steam supply system is a Westinghouse reactor with four steam generators. Each of the steam generators is housed in a separate compartment that vents upward into the dome. Approximately 2/3 of the free space within the containment is located in the upper dome region, which is relatively free of equipment. The lower part of the containment is compartmentalized. The internal structures are supported independently so that a circumferential gap exists between the internal structures and the steel containment liner. Numerous pathways, including the circumferential gap, interconnect the lower compartments.

The containment spray system has spray train headers at four different levels, but about 70% of the spray nozzles are located in the upper dome. The compartments in the lower levels are not covered completely by the spray system, including even the compartments containing spray heads. Therefore, significant areas exist where debris washdown by the sprays would not occur. The sprays activate when the containment pressure exceeds 18.2 psig. If the sprays do not activate, debris washdown likely would be minimal.

The insulation composition for the volunteer plant is roughly 13% LDFG, 86% RMI, and 1% Min-K. The volunteer plant analysis focused on

debris transport for LDFG insulation because LDFG insulation debris causes much more head loss on a sump screen than does a comparable amount of RMI insulation debris, and there was relatively little Min-K in the containment. (Although the analysis focused on the transport of LDFG insulation debris, the transport of the RMI and Min-k insulation debris were also estimated.)

The LDFG debris in the volunteer plant analysis was subdivided into four categories; the transport of each category of debris was treated separately. All insulation located within the break-region ZOI is assumed to be damaged to some extent. The damage could range from the total destruction of a blanket, with all of its insulation turned into small or very fine debris, to the blanket being only slightly damaged and even remaining attached to its piping, perhaps with some insulation erosion occurring through a rip in the blanket cover. The four categories and their properties are shown in Table 4-15.

The primary difference between the two smaller categories and the two larger categories was whether the debris was likely to pass through a grating. The fines were then distinguished from the small pieces because the fines would tend to remain in suspension in the sump pool under even relatively quiescent conditions, whereas the small pieces would tend to sink. Further, the fines tend to transport a little more like an aerosol in the containment air/steam flows and are less quick to settle when airflow turbulence drops off than the small pieces. The distinguishing difference between the large and intact debris was whether the blanket covering was still protecting the LDFG insulation. The primary reason for this distinction was whether the containment sprays could erode the insulation material further. Estimates were made for a distribution among the four categories based on available data and previously accepted engineering judgments. (The database for LOCA generated debris size distributions is sparse.)

The debris-transport methodology decomposed the overall transport problem into many smaller problems that were either amenable to solution or could be judged conservatively in a manner similar to that used in the DDTs (see Section 4.3.3.2).⁴⁻³ The volunteer plant PWR debris-transport methodology necessarily differed from the DDTs BWR transport methodology because

of differences in plant designs. Because debris will for the most part travel with the effluences from the break, a majority of the debris not captured in the break region likely would be blown upward into the dome region. Conversely, in the DDTs study, the break effluences flowed predominantly to the suppression pool. Although debris blown into the upper compartment may be washed back down into the lower compartment by the containment sprays, the washdown pathway can be a tortuous one that certainly could result in substantial debris entrapment.

The DDTs methodology of using logic charts to decompose the transport problem in the volunteer plant worked well within the region of the break. However, outside the region of the break, the complexity of the lower region inner compartments made that approach unreasonable. Therefore, in the volunteer plant analysis, debris capture was estimated first in the break region using the logic chart approach, and then a less sophisticated approach was used for the remaining containment.

In the region of the break, the MELCOR code was used to determine the distribution of flows from the region. Based on the reasoning that fine and small debris will disperse relatively uniformly with the flows and, to a lesser extent, the large debris, the MELCOR flow distributions become the dispersion distributions. Debris capture along these flow pathways was estimated using appropriate capture fractions; e.g., the debris capture fractions for debris passing through gratings were measured. (See Sections 4.2.1.1 and 4.2.1.2.) Another example of debris capture that can be readily justified is debris capture at the personnel access doorways between the steam generator compartments and the sump annulus. Here, the flow must make either one or two 90° bends, and it was determined and measured experimentally that debris would be captured onto a wetted surface at a sharp bend in the flow.

Outside the region of the break, the containment free volume was subdivided into a number of regions based on geometry and the locations of the containment sprays. Within each volume region, the surface area was subdivided according to both its orientation and its exposure to wetness. Because debris gravitationally settles onto horizontal surfaces, the floor areas

Table 4-15 Debris Size Categories and Their Capture and Retention Properties

Fraction Variable	Size	Description	Airborne Behavior	Waterborne Behavior	Debris Capture Mechanisms	Requirements for Crediting Retention
D_F	Fines	Individual fibers or small groups of fibers.	Readily moves with airflows and slow to settle out of air even after completion of blowdown.	Easily remains suspended in water, even relatively quiescent water.	Inertial impaction Diffusiophoresis Diffusion Gravitational settling Spray washout	Must be deposited onto surface not subsequently subjected to containment sprays or to spray drainage. Note that natural circulation airflow likely will transport residual airborne debris into a sprayed region. Retention in quiescent pools without significant flow through the pool may be possible.
D_S	Small Pieces	Pieces of debris that easily pass through gratings.	Readily moves with depressurization airflows and tends to settle out when airflows slow.	Readily sinks in hot water, then transports along the floor when flow velocities and pool turbulence are sufficient. Debris subject to subsequent erosion by flow water and turbulent pool agitation.	Inertial impaction Gravitational settling Spray washout	Must be deposited onto surface not subsequently subjected to high rates of containment sprays or to substantial drainage of spray water. Retention in quiescent pools (e.g., reactor cavity). Debris subject to subsequent erosion.
D_L	Large Pieces	Pieces of debris that do not easily pass through gratings.	Transports with dynamic depressurization flows but generally stopped by gratings.	Readily sinks in hot water and can transport along the floor at faster flow velocities. Debris subject to subsequent erosion by flow water and by turbulent pool agitation.	Trapped by structures (e.g., gratings) Gravitational settling	Must be either firmly captured by structure or on a floor where spray drainage and/or pool flow velocities are not sufficient to move the object. Debris subject to subsequent erosion.
D_I	Intact	Damaged but relatively intact pillows.	Transports with dynamic depressurization flows or may remain attached to its piping.	Readily sinks in hot water and can transport along the floor at faster flow velocities. Debris assumed still encased in its cover and thereby not subject to significant subsequent erosion by flow water and turbulent pool agitation.	Trapped by structures (e.g., gratings) Gravitational settling Not detached from piping	Must be firmly captured either by a structure or on a floor where spray drainage and/or pool flow velocities are not sufficient to move the object. Intact debris subsequently would not erode because of its encasement.

were treated separately from the other areas. The exposure to wetness determines the extent of debris washdown; therefore, areas subjected to containment sprays were treated differently than areas simply wetted by steam condensation. As the containment pressurizes following a LOCA, break flows carrying debris would enter all free volumes within the containment. Larger debris would tend to settle out of the break flows as the flow slowed down after leaving the break region. However, the fine and smaller debris more likely would remain entrained so that it would be distributed more uniformly throughout the containment. In the volunteer plant analysis, the fine and small debris was distributed according to free volume. The larger debris was distributed according to where it would fall out of the flow as the flow slowed. After the debris was dispersed to a volume region, it was assumed to have deposited within that region. The surface area distribution fractions were estimated using the areas tempered by engineering judgment.

Debris deposited throughout the containment subsequently would be subject to potential washdown by the containment sprays, the drainage of the spray water to the sump pool, and, to a lesser extent, by the drainage of condensate. Debris on surfaces that is hit directly by containment spray is much more likely to transport with the flow of water than debris on a surface that is merely wetted by condensation. Debris entrained in spray water drainage is less easy to characterize. If the drainage flows are substantial and rapid moving, the debris likely would transport with the water. However, at some locations, the drainage flow could slow and be shallow enough for the debris to remain in place. As drainage water drops from one level to another, as it would through the volunteer plant floor drains, the impact of the water on the next lower level could splatter it sufficiently to transport debris beyond the main flow of the drainage, thereby capturing the debris a second time. In addition, the flow of water could erode the debris further; generating more of the very fine easily transportable debris. The drainage of spray water from the location of the spray heads down to the sump pool was evaluated. This evaluation provided insights for the transport analysis, such as identifying areas not impacted by the containment sprays, the water drainage pathways, likely locations for drainage water to pool, and locations where

drainage water plummets from one level to the next.

The retention of debris during washdown must be estimated for the debris deposited on each surface, i.e., the fraction of debris that remains on each surface. These estimates, which are based on experimental data and engineering judgment, were assigned somewhat generically. For surfaces that would be washed by only condensate drainage, nearly all deposited fine and small debris likely would remain there. For surfaces that were hit directly by sprays, a majority of the fine and small debris likely would transport with the flow. Large and intact debris likely would not be washed down to the sump pool because of the screens or gratings across the floor drains and the size of those drains. For, surfaces that are not sprayed directly but subsequently drain accumulated spray water, such as floors close to spray areas, the retention fractions are much less clear.

4.3.4 Generalized Debris-Transport Guidance

4.3.4.1 BWR URG Guidance for Drywell Debris Transport and the NRC Review

Based on the small-scale testing summarized in Section 4.2.2.1, the BWROG provided guidance regarding options for estimating the fraction of the damaged insulation generated in the drywell that would be transported subsequently to the suppression pool.⁴⁻⁶ It should be noted that the BWROG approach combined debris generation and drywell debris transport into a combined methodology such that the URG recommends fractions of the damaged insulation within the ZOI that should be considered likely to transport to the suppression pool for each type of insulation. The NRC staff reviewed the BWROG guidance to determine its adequacy.⁴⁻⁷

A number of aspects were considered by the BWROG in determining the recommended fractions. First, the debris was categorized into three groups such that the transport of each group could be considered independently of the other groups. Based on the condition of debris recovered in the AJIT tests, the damaged fibrous insulation was categorized as fines, large pieces, and blankets. The damaged RMI debris was categorized as small pieces (<6 in.²), large foils (>6 in.²), and intact assemblies.

The fibrous “fines” and the RMI “small pieces” generally were considered transportable because they would easily pass through a typical grating. A continuous grating would stop virtually all of the other debris categories.

For fibrous debris, the “large pieces” and “blankets” were effectively treated in the BWROG analyses as a combined group referred to as “blanket material.” In both cases, a grating effectively stopped them from transporting, and both were subjected to erosion by break overflow. The insulation within the inner 3 L/D was assumed completely destroyed into transportable debris.

The BWROG used AJIT data to derive the relative fractions of the insulation destroyed into one of three size categories. These fractions depended on the type of insulation and, for some insulation types, on whether the insulation originally was located above or below the lowest elevation grating in the drywell. The BWROG calculated these fractions as integral values averaged over the entire ZOI. These URG fractions are listed in Table 4-16. For example, 77% of the damaged NUKON™ within the ZOI was considered “blanket material” and the remaining 23% was “fines.”

The BWROG estimated the transport fractions for each debris category for both fibrous and RMI debris. These fractions are listed in Table 4-17. The BWROG recommended that 100% of the fibrous fines and the RMI small pieces be considered as transported to the suppression pool for Mark I and Mark III plants as a combined result of both blowdown and washdown processes and for both MSL and RL breaks. However, for Mark II plants, the

BWROG limited the transport of fibrous fine debris to 50% for MSL breaks and 56% for RL breaks and RMI small debris to 10% for MSL breaks and 5% for RL breaks. These estimates were based on small-scale experimental data and the analysis of the water flow on drywell floors.

For larger debris, either fibrous or RMI, no direct transport to the suppression pool was assumed for debris generated above the lowest grating. For larger pieces of fibrous debris generated below the lowest grating, a fraction of this debris was assumed to transport directly to the suppression pool. For Mark I and Mark III plants, this fraction was estimated at 70%, but for Mark II plants, the estimate was reduced to 30%. Larger pieces of RMI (generated either above or below a grating) were not assumed to transport to the suppression pool. The remaining mode of transport applicable to fibrous debris was erosion by break overflow. Here, an assumed 25% of blanket material remaining in the drywell would be located so that it would be plummeted by the break overflow and 25% of this material would be eroded away and transported to the suppression pool, resulting in 6.25% of blanket-material transporting to the suppression pool. Lacking appropriate data, an erosion fraction of 1.0 was assumed for calcium-silicate, Koolphen-K, and Min-K insulations (nonfibrous). The URG did not address breaks that could result in debris being generated both above and below the lowest grating. Further, the URG did not specifically address offset or split gratings where depressurization flows could partially bypass the gratings.

Table 4-16 Fractions of Blanket Material with Low Transport Efficiency

Insulation Material	Fraction of Blanket Material with Low Transport Efficiency
NUKON™	0.77
Temp Mat™	0.84
K-Wool	0.78
Knauf®	0.70
NUKON™ Jacketed with Sure-Hold Bands	0.85
Calcium-Silicate with Aluminum Jacketing	0
Koolphen-K®	0.74

Table 4-17 URG Drywell Transport Fractions			
Fibrous Insulation Debris		RMI Debris	
Size Category	Transport Fraction	Size Category	Transport Fraction
Fines	1.0 for Mark I and III 0.5 for Mark II MSLB 0.56 for Mark II RLB	Small Pieces	1.0 for Mark I and III 0.1 for Mark II MSLB 0.05 for Mark II RLB
Blanket Material Above Grating	No Direct Transport 25% Erosion of 25% of Pieces = 6.25%	Large Foils Above Grating	No Transport No Erosion
Blanket Material Below Grating	70% Direct + 6.25% Erosion of Remaining 30% for Mark I and III 30% Direct + 6.25% Erosion of Remaining 70% for Mark II	Large Foils Below Grating	No Transport No Erosion

These debris-generation and debris-transport fractions were developed further into combined debris-generation and transport fraction for each type of insulation. Unjacketed NUKON™ debris generated above the lowest grating, for example, 23% of the damaged insulation, was turned into fine debris that subsequently transports directly to the suppression pool. Then, 6.25% of the remaining 77% (blanket material) was eroded away and also transported for a total of 28% of the ZOI insulation transported into the suppression pool (i.e., $0.23 + 0.0625 \times 0.77 = 0.28$). Below the lowest grating, the total debris transported would consist of the 23% fines, 70% of the 77% blanket material, and 6.25% of the nontransport blanket-material that subsequently was eroded (i.e., $0.23 + 0.70 \times 0.77 + 0.0625 \times 0.30 \times 0.77 = 0.78$). Combined debris-generation and transport fractions for the Mark I and Mark III plants are listed in Table 4-18.

The BWROG did not develop transport factors for materials other than insulation materials. Where an approved transport factor is not available, licensees should either assume a factor of 1.0 or perform the testing/analysis necessary to justify another factor.

NRC Evaluation

The URG recommendations were based primarily on data from small-scale debris-generation and transport tests conducted by the BWROG. Because the staff had several concerns related to scaling small-scale transport test data to BWR conditions, the staff conducted

confirmatory research to verify the accuracy of guidance provided by the URG. Specific concerns included whether or not the flow rates and flow durations in the small-scale tests were prototypical of conditions that would exist in BWR drywells following a LOCA. The staff's analysis indicated the BWROG test flow velocities were on the order of 50% of prototypical velocities for a postulated large MSL break. It was not clear to the staff in evaluating the BWROG test program whether the test results were reasonable, conservative, or nonconservative if scaled to a full-sized plant. Therefore, the staff concluded that there is inadequate substantiation for the BWROG claim that the use of these test results would conservatively bound the drywell transport fraction. The NRC-sponsored DDTs (see Section 2.2.3)⁴⁻³ demonstrated that a high percentage of fine debris could transport to the suppression pool and that the transport of the debris is both plant-specific and break-specific.

Estimating the erosion of large fibrous debris depends on estimating the quantity of debris subjected to erosion, the rate of erosion, and the duration of the erosion. The URG estimate of 25% of the debris being subjected to erosion was based on engineering judgment and was considered by the BWROG to be sufficient to ensure a conservative estimate of the mass of eroded debris. The staff evaluation of the URG guidance for assuming erosion of large fibrous debris concluded that the guidance is adequate provided that the unthrottled ECCS flow does not continue for more than 3 h. The staff concluded that licensees should determine an

Table 4-18 URG Combined Debris-Generation and Transport Fractions for Mark I, III*		
Material	Above Grating	Below Grating
Darchem DARMET®	0.50	0.50
Transco RMI	0.50	0.50
Jacket NUKON™ with Modified Sure-Hold Bands, Camloc® Strikers, and Latches	0.15	0.15
Diamond Power MIRROR® with Modified Sure-Hold Bands, Camloc® Strikers, and Latches	0.50	0.50
Calcium-Silicate with Aluminum Jacketing	0.10	0.10
K-Wool	0.27	0.78
Temp-Mat™ with Stainless-Steel Wire Retainer	0.21	0.76
Knauf®	0.34	0.80
Jacketed NUKON™ with Standard Bands	0.28	0.78
Unjacketed NUKON™	0.28	0.78
Koolphen-K®	0.45	0.45
Diamond Power MIRROR® with Standard Bands	0.50	0.50
Min-K	1.0	1.0
*Same fractions used for steam and water breaks.		

appropriate fraction for their analysis if unthrottled flow continues for more than 3 h. Note that NRC-sponsored research demonstrated that erosion of NUKON™ occurs at a linear rate (see Section 2.1.1.5), which facilitates scaling NUKON™ erosion. Based on the overall level of conservatism in the URG guidance, the staff concluded that the URG guidance regarding the prediction of the erosion of large fibrous debris by break overflow was acceptable.

The staff reviewed the URG destruction fractions, i.e., the determination of the fractions of the destroyed insulation that would remain in “blanket material” form with low transport efficiency. On the basis of NRC-sponsored research, the staff noted a number of strengths and conservatisms associated with the URG guidance. The blanket arrangement used in the BWROG tests was conservative, (e.g., the orientation of blanket seams and jacket latches relative to the air-jet nozzle). The BWROG tests oriented seams and latches to maximize blanket destruction. In BWR drywells, insulation blankets could be protected by other structures located in the jet pathway, and this protection was not taken into account in the tests. In the BWROG air-jet tests, the insulation blankets were oriented normal to the air jet to maximize destruction, but in BWR drywells, the majority of the piping (>65%) and therefore the insulation

blankets would be located parallel to the jet flow. Thus, much less of the blanket would be subjected to the full jet flow. The weakness of the BWROG test data was that they were very limited for several types of insulation, specifically Temp-Mat, K-wool, and some of the RMI. However, the staff concluded that the URG methods for determining the ZOI and debris generation are sufficiently conservative to outweigh this weakness.

The primary criticism of the URG drywell debris-transport guidance was the substantially reduced transport fractions applied to the Mark II containments relative to the Mark I and III containments. The NRC-sponsored tests of the Mark II geometry did not identify any basis to conclude that the transport fraction for a Mark II containment would be different from that of a Mark I or a Mark III containment. Given the uncertainty associated with estimating the debris transport fraction, which includes the uncertainty associated with estimating size distribution and quantities of insulation damaged, the staff concluded that the BWROG transport fractions for fibrous debris in Mark II containments are both nonconservative and unacceptable and that Mark II containments should use the same transport fractions as the Mark I and Mark III containments.

4.3.4.2 Transport Fractions for Parametric Evaluation

The NRC sponsored a parametric evaluation to demonstrate whether sump failure is a plausible concern for operating PWR plants in the U.S.^{4-12, Vol. 1} The results of the parametric evaluation formed a credible technical basis for decision-making regarding the resolution of the PWR sump-screen issue. Among the limitations of the parametric evaluations was the necessity of assuming and applying generic debris-transport fractions to all PWR plants, knowing that transport fractions are highly plant-specific. The development of these generic transport fractions is discussed in detail in Volume 4 of Ref. 4-12.

A number of simplifying assumptions were necessary to keep the parametric evaluation tractable for each of the 69 operating PWR plants. In addition, the assumptions generally were slanted in favor of sump failure not being a plausible concern. For the purposes of the parametric evaluation, the containment airborne and washdown-transport fractions were combined with the sump-pool transport fraction. That is, the transport fraction used in the parametric evaluation was the fraction of the insulation originally contained within the ZOI that subsequently was transported to the sump screen.

To further simplify the evaluation, one set of transport fractions was applied to all types of insulation debris in the analysis. The insulations types for all the PWRs were categorized for the purposes of this evaluation as either fibrous, reflective metallic, particulate (e.g., calcium-silicate), or foam. The foam insulation was neglected from further analysis on the basis that it would float above the screens and therefore not contribute to head loss.⁴ The generic parametric evaluation transport fractions were used to estimate the transport of fibrous insulation, reflective metallic insulation, and particulate insulation alike.

⁴Note that this assumption was suitable for the purposes of the parametric evaluation but *not* necessarily for plant-specific analyses in that some foam types might not be sufficiently buoyant to float over a sump screen and even buoyant debris would impact, at least to some extent. a sump screen that is not completely submerged.

With respect to sump-screen head loss, the parametric evaluation quickly determined that the head loss associated with fibrous insulation debris would be substantially greater than the head loss associated with the RMI debris. Hence, the study focused on fibrous insulation debris head loss for any plant reporting significant fibrous insulation in the containment. For plants claiming that all or nearly all of their insulation was RMI, the parametric evaluation examined the RMI head loss to determine the likelihood of that plant's sump screen becoming clogged by RMI debris alone.⁵

The head loss associated with calcium-silicate was not evaluated specifically because of the general lack of head loss data for calcium-silicate. The parametric evaluation simply determined the likely quantities of calcium-silicate to transport to the sump screens and added those quantities to the assumed quantity of general particulate transport down from the containment, an approach that definitely is not suitable for plant-specific analyses. Because the presence of calcium-silicate in a fibrous debris bed has been found to substantially enhance the head loss associated with that bed over and above the corresponding head loss without the calcium-silicate present, this approach represents an underestimate (possibly a huge underestimate) of the head loss associated with calcium-silicate. The problems associated with not evaluating the blockage potential associated with calcium-silicate insulation were noted in the evaluation.

It was assumed that 33% of the ZOI insulation was damaged into a form that has been loosely

⁵ It should be noted that in all likelihood no PWR containment would be completely free from fibrous debris. As discussed in Section 2, any containment should be expected to contain a certain amount of miscellaneous dust, which would partially consist of fibers. This type of fibrous debris is referred to as 'latent fibers' and little, if any, data exists at this time to quantify the amount of latent fiber within containment. Latent fibers would be easily washed by the containment sprays to the sump where the fibers would tend to accumulate on the sump screen forming a thin, uniform bed of fibrous debris. In addition, a plant relying primarily on RMI insulation would most likely use other types of insulation in locations where the use of RMI was not practical, and such a plant likely would have other non-insulation materials within the containment that contained fibers, such as fire barrier materials.

referred to as “transportable debris.”^{4-12, Vol. 3} In other words, 67% of the insulation would not likely transport to the sump because the debris pieces would be larger debris or even partially destroyed insulation blankets still attached to their respective piping. However, erosion of the larger pieces as a result of the impact of water flow is known to happen. Therefore, the 33% was enhanced to 40% to account for erosion.⁶ In this manner, the evaluation could neglect further consideration of the transport of the larger debris.

The transport fractions used in the parametric evaluation were based on ongoing NRC-sponsored research into debris transport, including small-scale testing, and on engineering judgment. The results and conclusions from this research had not been completely formulated at the time of the evaluation. The engineering judgment relied on debris-transport research from the corresponding resolution of the strainer-blockage issue for the BWR plants, as well as the ongoing PWR-related research.

The transport fractions used in the parametric evaluation are shown in Table 4-19. In the parametric evaluation, selected parameters were treated using a range of values that were denoted as favorable and unfavorable with respect to the potential for sump blockage. A favorable position was slanted toward not illustrating a credible concern regarding sump blockage. The favorable/unfavorable difference in the transport fractions was a result of the transport fraction associated with transport within the sump pool.

These transport fractions served their purpose in the parametric evaluation but should not be used in detailed PWR debris-transport analyses in lieu of plant-specific debris-transport fractions. As stated, the purpose of the parametric evaluation was simply to demonstrate a plausible concern using very limited plant-specific information. Thus, plant-specific analyses should use plant-specific data. The plant-specific transport fractions could exceed those of the parametric evaluation.

4.4 Types of Analytical Approaches

Analytical work has clearly demonstrated that system-level codes (for example, the MELCOR

code) do not have the capability to realistically simulate debris transport except for limited transport conditions. The same can be said of CFD codes. The aerosol-transport models in these codes do not usually have inertial impaction models. Inertial impaction models exist for specific circumstances, such as at a bend in a pipe, but these models are not generally applicable to the variety of specific flow situations within containments, even if these situations could be modeled thermally-hydraulically. An exception would be the transport of small debris at relatively slow flow velocities, such as the Karlshamn experiments. (See Section 4.3.3.1.) Here the debris deposition was primarily a result of gravitational settling, which was the dominant deposition mechanism in those tests and is modeled in MELCOR. However, these types of codes are very useful for characterizing thermal-hydraulic conditions within the containment. These codes can predict the flow velocities and distributions, rates of condensation, surface film thicknesses, temperatures, pressures, etc., reasonably well.

One method of reducing the debris-transport fractions is to evaluate specific locations where debris is likely to be trapped and not subsequently washed down to the sump pool. For example, debris carried by flow exiting the break region compartment by way of a door that makes one or more 90° bends may likely become trapped where containment sprays would not impact the trapped debris. Debris-transport testing clearly demonstrated inertial debris capture whenever the flow makes a sharp change of direction and the associated surfaces are wetted. Most surfaces within the containment would be wetted quickly by steam condensation. These experimentally justified specific debris-capture locations could conceivably add up to a significant reduction in the debris-transport fraction.

The logic chart approach developed in the DDTs analyses, discussed in Section 4.3.3.2, might be used to decompose the problem, such that individual parts of the overall transport problem can be resolved by adapting experimental data tempered with engineering judgment. This approach works best where there are relatively few flow pathways and substantial inertial capture along those pathways because of sharp bends in the flow or structures such as gratings. For simpler containments, the approach might be applied to the entire

⁶ An assumption that 10% of the large debris was eroded into fines debris ($0.1 \times 0.67 = 0.07$).

Transport Conditions	Favorable Estimate	Unfavorable Estimate
Small LOCA (SLOCA) with Sprays Inactive	0.05	0.10
SLOCA with Sprays Active	0.10	0.25
All Medium LOCAs (MLOCAs) and Large LOCAs (LLOCAs)	0.10	0.25

containment, but the approach likely would be difficult to apply for more complex flow situations. The approach should usually still be applicable to the region of the break, even if the flows in the overall containment are too complex for a logic-chart type of analysis.

It might be appropriate to assume a relatively uniform dispersion for the fine and small debris outside the break region for some analyses. After the inertially impacted deposition is estimated, the remaining airborne debris is distributed according free volume. Outside of the break region, the depressurization flows should slow dramatically as the flows expand. As the flows expand and slow, inertial impaction deposition would become much less important, and as the flow turbulence subsides, gravitational settling would dominate debris capture. Without inertial impaction, the debris would tend to follow the movement of steam and air until settling becomes effective.

The larger debris cannot be dispersed uniformly. Rather, the larger debris would simply fall out after the transport velocities slowed, such as when the depressurization flows entered the containment dome. Large debris ejected into the containment dome would most likely simply fall to the floor of the uppermost levels.

4.5 Rules of Thumb

It is difficult to formulate general rules of thumb appropriate to airborne and washdown debris transport in a PWR containment. Airborne and washdown debris transport are both plant-specific and accident-specific. However, the following general and somewhat simplistic observations apply to airborne and washdown debris transport.

- Fine and small debris transport more readily than does the larger debris.

- Substantial inertial deposition can be expected in the region of the break.
- Outside the region of the break, gravitational settling would dominate debris deposition after the flow turbulence decreased significantly to allow settling.
- If the containment spray system were activated, then substantial quantities (if not most) of fine and small debris impacted by the sprays likely would be washed down to the sump pool.

4.6 References

4-1. B. E. Boyack, T. S. Andreychek, P. Griffith, F. E. Haskin, and J. Tills, "PWR Debris Transport in Dry Ambient Containments – Phenomena Identification and Ranking Tables (PIRTs)," Los Alamos National Laboratory report LA-UR-99-3371, Revision 2, December 14, 1999.

4-2. G. Wilson, et al., "BWR Drywell Debris Transport Phenomena Identification and Ranking Tables (PIRTs)," Final Report, Idaho National Engineering Laboratory report INEL/EXT-97-00894, Lockheed Martin Idaho Technologies Co., Idaho Falls, ID, September 1997.

4-3. D. V. Rao, C. Shaffer, and E. Haskin, "Drywell Debris Transport Study," U.S. Nuclear Regulatory Commission, NUREG/CR-6369, Volume 1, September 1999.

Volume 2, D. V. Rao, C. Shaffer, B. Carpenter, D. Cremer, J. Brideau, G. Hecker, M. Padmanabhan, and P. Stacey, "Drywell Debris Transport Study: Experimental Work," September 1999.

Volume 3, C. Shaffer, D. V. Rao, and J. Brideau, "Drywell Debris Transport Study: Computational Work," September 1999.

- 4-4. "Knowledge Base for Emergency Core Cooling System Recirculation Reliability," NEA/CSNI/R (95) 11, Prepared by U.S. Nuclear Regulatory Commission for the Principal Working Group 1 (PWG-1), International Task Group, Committee on the Safety of Nuclear Installations, Organization for Economic Cooperation and development (OECD) Nuclear Energy Agency (NEA), February 1996.
- 4-5. A. W. Serkiz, "Containment Emergency Sump Performance," U.S. Nuclear Regulatory Commission, NUREG-0897, Revision 1, October 1985.
- 4-6. "Utility Resolution Guidance for ECCS Suction Strainer Blockage," BWROG, NEDO-32686, Rev. 0, November 1996.
- 4-7. "Safety Evaluation by the Office of Nuclear Reactor Regulation Related to NRC Bulletin 96-03 Boiling Water Reactor Owners Group Topical Report NEDO-32686, 'Utility Resolution Guidance for ECCS Suction Strainer Blockage,'" Docket No. PROJ0691, NRC-SER-URG, August 20, 1998.
- 4-8. C. J. Shaffer, "Demonstration of MELCOR Code Capability to Simulate Insulation Debris Transport Within a BWR Drywell," Computational Analysis Report, SEA-95-970-01-A:5, October 23, 1995.
- 4-9. R. O. Gauntt, et al., "MELCOR Computer Code Manuals," Volumes 1 and 2, Revision 2, NUREG/CR-6119, SAND2000-2417, Sandia National Laboratories, October 2000.
- 4-10. G. Zigler, J. Bridaeu, D. V. Rao, C. Shaffer, F. Souto, W. Thomas, "Parametric Study of the Potential for BWR ECCS Strainer Blockage Due to LOCA Generated Debris," Final Report, U.S. Nuclear Regulatory Commission, NUREG/CR-6224, October 1995.
- 4-11. K. W. Brinckman, "Results of Hydraulic Tests on ECCS Strainer Blockage and Material Transport in a BWR Suppression Pool," EC-059-1006, Revision 0, May 1994.
- 4-12. D. V. Rao et al., "GSI-191: Parametric Evaluations for Pressurized Water Reactor Recirculation Sump Performance," NUREG/CR-6762, Volume 1, 2002.
- Volume 2, D. V. Rao, B. C. Letellier, K. W. Ross, L. S. Bartlein, and M. T. Leonard, "Technical Assessment: Summary and Analysis of U.S. Pressurized Water Reactor Industry Survey Responses and Responses to GL 97-04," 2002.
- Volume 3, C. J. Shaffer, D. V. Rao, and S. G. Ashbaugh, "Technical Assessment: Development of Debris-Generation Quantities in Support of the Parametric Evaluation," NUREG/CR-6762, 2002.
- Volume 4, S. G. Ashbaugh and D. V. Rao, "Technical Assessment: Development of Debris Transport Fractions in Support of the Parametric Evaluation," 2002.

5.0 SUMP POOL DEBRIS TRANSPORT

Section 5 summarizes the available knowledge regarding transport of insulation debris within the containment sump pool that would form from the accumulation of water during the injection phase of a LOCA. Debris would accumulate in the sump pool with some deposited in the sump region during the blowdown debris-transport period and other transported into the pool along with the water. The airborne/washdown transport of the debris to the sump pool, including where and when the debris would enter the pool, was discussed in Section 4. The phenomena associated with the transport of debris within the sump pool are discussed in this section. The knowledge base associated with insulation and other debris transport¹ within the sump pool is organized as follows.

- Section 5.1 presents an overview of the mechanics associated with debris transport within the sump pool, including the characteristics of an accident relevant to debris transport, the relevant plant features, the physical processes and phenomena, and the debris characteristics affecting debris transport.
- Section 5.2 describes the tests performed that are relevant to sump-pool debris transport.
- Section 5.3 describes the analyses performed that are relevant to sump-pool debris transport.
- Section 5.4 summarizes the types of analytical approaches developed to predict the transport of insulation debris within a sump pool.
- Section 5.5 discusses the guidance based on insights gained from testing and analytical studies.

A majority of the testing and analysis relevant to sump pool insulation debris transport was done to support the suction-strainer clogging issue for BWRs; however, most of this research is directly applicable to PWRs as well. The applicability of BWR research to PWRs is discussed as appropriate. Further, it also should be noted that debris-transport research tended to focus on the transport characteristics of fibrous insulation debris. Research also has considered other types of

insulation debris, notably RMI debris, but the potential for fibrous insulation debris to clog a strainer generally has been found to be substantially greater for fibrous debris than for RMI debris. Further research has tended to focus on LDFG insulation over the other types of fibrous insulation, i.e., HDFG or mineral wool fibrous debris. Thus, there are gaps in the completeness of debris transport research for all types of insulation debris.

5.1 Overview of Mechanics

The transport of debris within a PWR containment sump pool would be influenced by a variety of physical processes and phenomena and by the features of a particular containment design. These debris transport processes range from debris deposited on the sump floor during blowdown that would subsequently be swept by the spread of water as the sump begins to fill, to debris that later transports into an established sump pool from the upper reaches of the containment by the deluge of containment spray water drainage.

The NRC convened a panel of recognized experts with broad-based knowledge and experience to apply the PIRT process to the transport of debris generated by a high-energy pipe break through a PWR containment.⁵⁻¹ The PIRT process was designed to identify processes and phenomena that would dominate the debris-transport behavior. Further, these processes and phenomena were prioritized with respect to their contributions to the reactor phenomenological response to the accident scenario. The NRC also convened a PIRT panel to rank transport processes relative to debris transport within a BWR drywell.⁵⁻²

This section specifically discusses

- the characteristics of postulated accident scenarios relevant to the transport of insulation debris within a sump pool (Section 5.1.1),
- the plant features that would affect the transport of insulation debris within a sump pool (Section 5.1.2),
- the physical processes and phenomena that affect the transport of insulation debris within a sump pool (Section 5.1.3), and

¹The same physical processes and phenomena that govern the transport of insulation debris also would govern the transport of non-insulation debris. However, most experimental transport research has focused on the transport of insulation debris; exceptions include limited transport data for paint chips, rust flakes, and iron oxide particulate.

- the characteristics of debris that affect the transport of insulation debris within a sump pool (Section 5.1.4).

5.1.1 Accident Characterization

Many aspects of a PWR accident scenario are important in judging the transportability of debris in the water pool formed on the containment floor. Accident aspects recognized as being important are discussed below. These include the characteristics of the debris deposition within the pool (location and timing), the break (location, orientation, and flow rate), the containment sprays (drainage locations and flow rate), the recirculation sump (location, flow rate, and the activation time), and the sump pool (geometric shape, depth, and temperature).

The transport of debris varies with the postulated accident scenario, which would specify such parameters as the LOCA break size and location. Thermal-hydraulics codes can be used to estimate containment, RCS, and CSS conditions such as pressures, temperatures, and flow rates. For example, the predicted containment pressure would determine whether containment sprays would activate automatically on a high-pressure alarm. The operating procedures should determine whether and when containment sprays might be deactivated by operator action.

Fundamental to analyzing the potential for debris transport in a containment pool are the types, sizes, and quantities of debris that could be in the pool and where and when the debris entered the pool. The transport of debris within the sump pool would occur in two very different phases. The first pool transport phase would occur as the sump pool forms where debris that was deposited onto the sump floor during and shortly after RCS depressurization before sump-pool formation (and also before ECCS switchover to the recirculation mode) would be transported with the fill-up water flows.

During the fill-up phase, debris on the floor would transport as the initially shallow and fast-flowing water spread out across the sump floor. This behavior was observed in the integrated tank tests.⁵⁻³ In this mode of transport, debris could be transported a substantial distance from its initial deposition location; the transport could move debris either toward or away from the recirculation sump. Debris could easily be pushed into inner compartments or out of the main flow locations where it likely would remain. These effects would

be lessened with the distance from the inlet and as the sump water level rose.

The second pool transport phase generally covers the period after the ECCS has switched over to recirculation at or near quasi-steady-state pool flow conditions. Debris transport in the steady-state phase would move debris from where the debris was located in the pool following the fill-up. In addition, more debris would enter the pool because of containment spray drainage. This debris could simply drop into an already established pool, where it could sink to the pool floor or float with the water flow.

The complex movement of water through the sump pool would be unique for each postulated accident sequence and for each plant. The geometry of the sump pool affects the complexity of water movement and that geometry is plant-specific. Water would flow from its point of entry to the entrance of the recirculation sump. Water flowing to the sump would come from the pipe break and from the drainage of the containment sprays (if activated). Water from the break would plummet from the break location; therefore, the break location, the orientation of the break, and the rate of flow from the break could affect flow patterns in the pool. Further, the elevation of the break and the congestion of piping and equipment below the break could affect the momentum and structure of the flow entering the pool, which in turn determines pool turbulence near the break. Pool turbulence would further disintegrate the debris to some extent; it also affects whether debris can settle.

Water from containment spray drainage would enter the sump pool at multiple locations, and the drainage pattern would be very plant-specific. Typical water drains into the sump pool include refueling pool drains, floor drains, stairwells, elevator shafts, an annular circumferential gap, and/or openings to the upper containment, such as a steam generator shaft. In some plants, a train of containment sprays may spray directly into the sump pool. The pattern of the spray drainage and the containment spray flow rate would affect the complexity of the flows within the pool and the subsequent transport of debris within the pool.

The locations of the incoming water relative to the location of the recirculation sump would be especially important. The relative locations determine the flow patterns, which in turn determine whether or how many significant quiescent regions would exist in the pool. Debris within quiescent

regions could remain in those regions indefinitely. For example, if incoming water entered the sump pool well away from the recirculation sump inlet, then the water flow could sweep a majority of the pool, thereby enhancing debris transport. Conversely, incoming water could enter near the recirculation inlet so that much of the sump pool was relatively quiescent. Debris would be much more likely to remain suspended in the turbulent regions of the pool than in the more quiescent regions. In addition, it is known that pool turbulence can affect the further disintegration of certain types of debris, e.g., fibrous or calcium silicate insulation debris.

The depth of the pool strongly affects debris transport. Specifically, the deeper the pool, the slower the water flows; a deeper pool would have less turbulence in general. The available water would govern the maximum depth of the pool, but the depth of the pool when the ECCS switches over to the recirculation mode also depends on relative timing (i.e., the depth of the pool at switchover could be substantially less than the maximum pool depth). For example, pool depth would depend on the rate of ice melt in an ice-condenser plant.

The temperature of the water affects water density and viscosity, the rate at which water penetrates dry insulation debris, and, potentially, debris disintegration rates. Density and viscosity affect the water drag on debris and thus the transport of debris within the sump pool to some extent (e.g., the minimum velocity needed to move a piece of debris across the pool floor); however, this effect was not pronounced for the debris types tested. Alternatively, the water density and viscosity do have a significant effect on debris-bed head loss (discussed in Section 7). The pool temperature has a pronounced effect on the rate at which water penetrates the inner spaces of fibrous debris, thereby releasing the trapped air. This, in turn, affects the buoyancy of the debris. When fibrous debris is dropped in colder water, it can float for an extended period of time, whereas when similar debris is dropped in heated water, the debris tends to sink in a reasonably short period of time. Temperature may have an effect on the disintegration rate of certain types of insulation, particularly calcium silicate insulation.

5.1.2 Plant Features

A number of features in nuclear power plant containments would significantly affect the transport of insulation debris within a PWR sump pool.

These features include its engineered safety features and associated plant operating procedures. Plant features recognized as important include the geometric features of the sump pool and features that control water flows into and out of the pool.

Geometric features, such as compartmentalization, free-flowing annuli, flow restrictions, and obstacles, all affect the patterns of flow. There would be areas of relatively high flow velocity and areas of relatively slow or quiescent flow velocities. Debris would transport readily in the high-velocity areas but not in the low-velocity areas. Further, the shape of the sump pool can contribute to rotational flows (vortices), where debris can be trapped within the vortex. The flow would accelerate through narrow pathways, such as an entrance into an interior compartment, and then decelerate beyond the entrance as the flow expands, thereby likely creating regions of rotational flow. Debris that did not transport to the sump screen would have been trapped effectively within a quiescent region, such as an inner compartment that does not receive significant flow, or trapped effectively inside a vortex, or stopped behind an obstacle. The existence of a vortex suppressor in the sump pit or inlet screening structure could influence how flow approaches the sump.

Obstacles to debris transport on the floor of the sump pool include the equipment located there and curbs deliberately placed along the floor in front of the sump screen to retard the transport of debris to it. The equipment located in a sump usually is supported on stands that anchor to the floor, frequently on some sort of small, raised, concrete platform. These obstacles could stop tumbling debris from reaching the screen unless the local flow velocities were sufficient to lift the piece of debris over or around the obstacle. The location, extent, and height of a curb would be important. An example of a miscellaneous structure that could affect debris transport is a closed chain-link gate at a walkway between compartments.

Drainage from the containment sprays ultimately moves from the upper containment levels into the sump pool. The drainage pattern would be very plant-specific and likely would involve a number of features, including refueling pool drains, floor drains, stairwells, elevator shafts, an annular circumferential gap, or openings to the upper containment, such as a steam generator shaft. In some plants, a train of containment sprays may spray directly into the sump pool. The pattern of

the spray drainage and the containment spray flow rate would affect the complexity of the flows within the pool and the subsequent transport of debris within the pool.

Plant features that affect the water level also affect debris transport. These features include the volumes of water injected into the RCS and containment during the injection phase of the accident. For an ice condenser plant, the quantity of ice and the features associated with the melting of the ice would affect the depth of the pool. Features that could potentially hold water in the upper reaches of the containment could reduce pool depth; for example, if the refueling pool drains were to become blocked by debris, the water retained in the refueling pool would effectively reduce the sump pool depth.

The location and design of the recirculation sump affects the transport of debris in the sump pool. The approach velocities of the water entering the sump screen depend on the area of the screen and the pumping flow rate. The turbulence near the sump screen affects the formation of the debris bed, and the level of turbulence would be related directly to the proximity of the sump to the break. Should the break be located near the sump screen, turbulence associated with the falling water could remove previously deposited debris from the screen and the turbulence could negate the effectiveness of debris curbs placed in front of the screens. Conversely, a sump distanced from a break or sheltered from a break by compartment walls would not experience much direct agitation from the break stream.

Some sump designs would mean that the entire screen would be submerged during operation of the recirculation pump, whereas other sump screens would remain partially exposed during the entire accident scenario. The submergence of the sump determines the failure criteria for the screen; that is, the failure of a submerged screen would be a result of the debris-bed head loss exceeding the available NPSH margin, but the failure of a non-submerged sump screen would be a result of the debris-bed head loss exceeding the available hydrostatic head (approximately half of the sump pool depth). The volume of the sump pit could affect debris transport during the fill-up transport phase. As the pit fills with water, the fast moving shallow flow of water across the sump floor would move debris toward the sump screen, as the sump pit filled. Therefore, the larger the pit, the greater the potential for debris

transport toward the screen during the initial filling phase.

5.1.3 Physical Processes/Phenomena

The analysis of debris transport test results identified many processes and phenomena that could significantly affect the transport of debris within the sump pool. These include hydraulic processes that contribute to the transport of debris and the debris transport and entrapment processes.

Hydraulic Processes

Hydraulic processes include the entry of water onto the containment sump floor, the establishment of a pool, the pumping of water from the sump, and the flow through an established pool. The processes include both bulk-flow and localized processes.

Following a LOCA, liquid effluences from the break would drain to the sump, either directly or after flowing off of containment structures, with most of this drainage entering the sump in the vicinity of the break. If the containment spray system activates, the drainage from these sprays also drains to the sump, but its entry would most likely occur at multiple locations. At first, water falling from a significant height onto the sump floor would spread out in a sheeting type of flow characterized as very shallow but fast-moving with a preference toward the sump (lowest elevation). After the spreading water has spread across the containment floor so that the sump pool begins to form, a hydraulic jump would begin to move back toward the source of the water until the source becomes fully engulfed by the pool. Pool formation hydraulics would be very dynamic and transient in nature and could move debris across the floor dramatically.

After the pool has formed, pool flow dynamics become less dynamic and less transient. When the ECCS switches over to the recirculation mode and the recirculation pumps begin to pump from the sump pool, the pool transitions to steady-state flows. Patterns formed in the pool are three-dimensional in nature and likely would have several features in common for any particular sump design. (If the pool is sufficiently shallow, the flow patterns may become more two-dimensional in nature.) Features of the pool would include accelerated flow through narrow passageways followed by decelerated flow, rotational flow (vortices), regions of relatively quiescent flow (sometimes referred to as inactive or dead zones), flow around and over obstacles, vertical mixing flows, and boundary layer flow.

A particular area of the pool would be characterized by bulk flow terms, such as the bulk flow velocity, but within this area, the localized flow may behave somewhat differently. For example, the flow around a particular piece of debris could be substantially different than the bulk flow velocity (either faster or slower). A particular piece of debris could move as a result of the local flow velocity, whereas the bulk flow velocity might not be sufficient for that movement. Hence, it is important to quantify the level of pool turbulence (or agitation) when predicting debris transport. Turbulence would be generated in the pool primarily by the various flows falling into the pool. Testing has effectively demonstrated that turbulence can keep debris suspended in the pool, enhance the transport of debris along the floor of the pool, and even cause additional degradation (or disintegration) of debris. Pool turbulence would vary throughout the pool, and the highest levels of turbulence would generally be underneath the break.

Debris Transport Processes

The transport processes that could be important for evaluating sump-pool debris transport can generally be grouped into debris entry processes, debris pool transport processes, debris entrapment processes, and debris transformation processes.

Debris would be carried into the containment sump area by either airborne flows or waterborne flows. During the violent blowdown portion of the accident scenario, RCS depressurization flows would carry debris into the sump area, where some of that debris would fall out of the airflow onto the sump floor, before the establishment of the sump pool. Upon completion of the blowdown, little, if any, additional debris would be borne by airflows to the sump. Following the brief blowdown period, drainage from condensate and containment spray (if activated) would wash debris that had deposited in the upper reaches of the containment (anywhere above the sump) down to the sump level. Thus, the entry of the debris into the sump would be time-dependent—some early blowdown-deposited debris and then somewhat continuous transport because of the containment sprays. Some debris would be subjected only to steady-state pool water flows, and some debris would be subjected to pool formation water flows, as well. The condensate drainage could transport some debris, but it would be much less than the spray drainage transport. Liquid-borne debris would generally enter the sump pool with the water flow.

Pool debris transport would involve several distinct debris-transport processes that all have been observed during debris transport testing discussed in Section 5.2. During the pool formation phase, the sheeting type of flow (discussed above) effectively transports debris previously deposited onto the sump floor with the spreading of the water flow. Depending on the relative location of the recirculation sump to the incoming flow (predominantly the break flow), the sheeting flow debris transport could move debris toward or away from the recirculation sump.

When the pool becomes sufficiently established to suspend debris that suspended debris would simply move along with the water flow. Fine debris, such as individual fibers or light particles (e.g., calcium silicate), would essentially remain suspended at relatively low levels of pool turbulence, throughout the entire accident scenario. Ultimately, most of this fine, suspended debris would be filtered from the pool by the recirculation sump screens.² Larger debris could be suspended in the more turbulent regions of the sump pool (e.g., under the break) or before it was completely water saturated. Debris not completely water saturated would contain some air that would give it buoyancy.

Truly buoyant debris, such as some of the forms of insulations, would float on the pool surface unless the pool turbulence was sufficient to pull the debris beneath the surface. Truly buoyant debris typically would float on the surface and move either toward the recirculation sump screen or into a quiescent or rotational region of flow. Buoyant debris over a submerged sump screen generally would orbit in a rotational flow established above the sump or it could accumulate against a sump screen that was not completely submerged.

When insulation debris enters the sump pool, it could be dry or fully or partially saturated with water depending on its exposure to moisture (e.g., fibrous debris). If the debris was not fully saturated (i.e., contains trapped air), then the debris could still be buoyant, whereas it would readily sink when it was fully saturated. The time required for water to saturate a piece of debris depends on the type of insulation and the size of the piece of debris; it also is very dependent on the temperature of the water. The space between the fibers of fibrous debris usually fills with water rapidly when the water is hot

²Some of this debris likely would pass through the sump screens and subsequently return to the sump pool unless it was trapped within the ECCS or RCS.

(sump-pool temperatures) but fills slowly when the water is cold (room temperature).

Nonbuoyant debris, such as saturated fibrous debris, would settle to the floor of the pool, except in regions of high turbulence. If local flow velocities were sufficiently high, sunken debris would transport along the floor with the water flow. This transport involves tumbling and sliding motions. The separate-effects test data provide the flow velocities needed to start debris in motion (referred to as "incipient motion") and the flow velocities needed to cause the debris to transport in bulk motion.⁵⁻⁴ Note that significant turbulence would cause debris to transport along the floor at lower bulk flow velocities than if there was no turbulence.

Debris moving across the sump pool floor could encounter an obstacle that stops further forward motion. These obstacles include equipment and curbs placed in front of the recirculation sump to trap debris. Typical equipment obstacles are the supports for equipment located at sump level. These supports are frequently large raised concrete pads. Debris trapped against one of these obstacles could be lifted over the obstacle when the flow velocities are sufficiently fast. The separate-effects test data also provide these lift velocities. This lifting action also applies to debris that would arrive at the base of the recirculation sump screen, where that debris could be lifted (or rolled) up onto the screen.

When the debris transport process is complete, debris would transport either to the recirculation sump screens or become trapped along the way. Some debris could become entangled on equipment, where it could remain, independent of flow velocity. For example, this could happen during the initial formation of the pool, where the rapid flow sheeting might force debris underneath a cable or a conduit. As another example, debris could become entangled in a chain-link gate or fence that sometimes is found in a containment. As previously noted, debris could become trapped behind an obstacle when local flow velocities were not sufficient to lift it over or around the obstacle. Some debris would simply move into a location where the local flow was insufficient to transport the debris further, such as in quiescent flow regions associated with rotational flow or a compartment off of the main flow. When flow decelerates and slows with a widening flow cross section, the debris could simply stop at some point. In some cases, trapped debris can become re-entrained into the main flow. For example, pieces of debris once trapped on the

floor inside a vortex have been observed to occasionally be forced by localized flow turbulence back into the faster flow of the vortex and thereby re-entrained into the main flow.

Debris that reaches the sump screen would remain on the screen if the approach velocity of the water were sufficiently fast, as would normally be the case. The separate-effects tests measured this velocity, which is referred to as the screen-retention velocity, for a few types of debris. When the approach velocity was marginal in the integrated tests, pieces of debris were observed to drift away from the screen after arriving at the base of the screen.

Debris has been observed to undergo transformation under some conditions, i.e., the agglomeration of small debris into larger debris or the disintegration (also referred to as erosion) of larger debris into finer debris. In general, agglomeration would make debris less transportable and disintegration would make debris more transportable. A form of agglomeration was observed during the integrated debris-transport tests in which small LDFG debris that accumulated on the floor in quiescent regions, such as the center of a vortex, tended to mat together. This mat then moved as though it was one piece of large debris. Such matting would increase the retention of debris at such locations; however, it likely would break apart easily if the mat subsequently was forced back into more dynamic flow.

Disintegration is the most important form of debris transformation because this process forms very fine debris that remained suspended in the water even at relatively low levels of turbulence, hence transporting to the sump screens virtually completely. For LDFG debris, this disintegration was observed in the integrated tank tests and during the Vattenfall tests,⁵⁻⁵ which noted that "larger pieces of insulation material would disintegrate into fibers and fines" when subjected to falling recirculating water. Calcium silicate also was observed to disintegrate, more so than the LDFG debris. The rate of debris disintegration would depend mostly on the turbulence to which the debris was subjected. Most of the disintegration likely would occur to debris thrashing around in the turbulence associated with the break flow plummeting into the sump pool. It is possible that higher temperatures and/or chemical decomposition could enhance disintegration. A concern here would be the breakdown during long-term pumping of the binder that holds fibers or particles together,

thereby releasing these fibers and particles from the larger debris. (See Section 2.5.)

5.1.4 Debris Characteristics

Transport of debris in a sump pool is strongly dependent on the characteristics of the debris formed. First, these characteristics include the type and the size of the debris. There are several kinds of insulation material in use in PWR containments. These are generally grouped as fibrous insulation, RMI insulation, and particulate insulation (e.g., calcium silicate). In addition, there are other types of debris, such as failed coatings, dust, and miscellaneous operational materials (Section 2). Pieces of debris would be varied in size; for example, fibrous debris would range from individual fibers to nearly intact pillows. Debris from failed coatings would range from very small particles to substantially large chips. Debris transport depends greatly on the type and size of the debris.

Each type of debris has its own set of physical properties, including properties that determine whether the debris would sink in a sump pool. The debris buoyancy would depend on the density of each piece of debris:

- the density of each constituent of the debris (e.g., the solid density of an individual fiber),
- the density of the insulation as fabricated or as installed, which for fibrous insulation includes the air space between the fibers,
- the density of a piece of insulation debris, which could differ significantly from the as-fabricated density, and
- the density of the debris after it becomes saturated with water.

In addition, the time required for a piece of debris to saturate with water could be important because this would determine how long and how far the debris could float before sinking to the floor. An intact pillow of fibrous insulation could retain sufficient air for the pillow to transport all the way to the recirculation sump screen. The debris settling velocity (the rate at which debris settles vertically in water) could become important if the pool were sufficiently deep.

The flow velocities needed to initiate specific debris transport motions are also debris transport characteristics. These motions include tumbling/sliding motion across the floor, lifting the debris over an obstacle, and retaining the debris on the sump screen when it arrives there. These

velocities have been measured for selected debris types and sizes and for both incipient and bulk motion. The lift velocity also depends on the height of the obstacle.

The characteristics associated with debris disintegration are also important because the by-product of the disintegration usually would be very fine debris that remains suspended and therefore transports readily to the sump screen. These properties are much more difficult to characterize, but chemical stability in the sump pool should be considered. For example, would the binding decompose during long-term submergence in the sump pool and would this decomposition depend on pool acidity? Both fibrous and particulate insulation debris are known to disintegrate to some extent, but data needed to quantify this disintegration is not readily available. For example, calcium silicate insulation debris disintegrates rapidly in water, leaving a fine particulate in suspension. The rate of disintegration is affected by the temperature of the water and agitation. The accumulation of calcium silicate debris along with fibrous debris on a screen is known to create a substantial head loss.

5.2 Debris Transport in Pooled Water Testing

The NRC, US industry, and international organizations have conducted numerous tests to examine experimentally different aspects of the transport of insulation and other debris in pooled water. The types of insulation tested have included fibrous insulations (mostly LDFG), RMI, particulate insulations, foam insulations, and a fire-barrier material known as Marinite. The non-insulation debris tested has included inorganic zinc paint particles and flakes, iron oxide rust chips, iron oxide particles, and Koolphen K vapor barrier foil paper. The results of these experiments provide qualitative insights and quantitative information relevant to considerations of debris transport in PWR containment sump pools.

5.2.1 Alden Research Laboratory Buoyancy and Transport Testing on Fibrous Insulation Debris

In the early 1980s, sponsored by the NRC, the Alden Research Laboratory (ARL) conducted buoyancy, transport, and head loss experiments on reactor insulations,⁵⁻⁶ primarily fibrous insulation. Three types of thermal insulation pillows with mineral wool and fiberglass cores were tested in an undamaged state, with their covers opened, and

with their insulation cores in broken-up and shredded conditions. A sample of closed-cell (foam glass) insulation and an intact RMI cassette also were tested for transport and buoyancy. The buoyancy and transport aspects and findings of the experiments are summarized below. (Head loss is addressed in Section 7.)

Objective

The objective of the experiments was to provide data to help assess the potential effect of dislodged fibrous insulation on ECCS sump performance. The experiments were configured to determine the buoyancy, transport, and head loss characteristics of the following types of insulation pillows.

- Type 1: Mineral wool enclosed in a Mylar-coated asbestos cover
- Type 2: HDFG insulation covered with silicone glass cloth on one side and stainless-steel mesh on the other
- Type 3: HDFG insulation covered with fiberglass cloth

A sample of closed-cell insulation and an intact RMI cassette also were tested for transport and buoyancy.

The experiments related to buoyancy and transport were to determine:

- The buoyancy characteristic of the fibrous insulation (this amounted to timing how long the insulation would float while sprayed with a fine mist of water), and
- The flow velocity at which sunken insulation would move and the manner by which transported insulation would collect on a vertical screen.

Methodology

Types of Insulation Pillows Considered

Three types of insulation pillows were tested, and their compositions are listed below. All pillows were 2 ft by 2 ft by 4 in. thick. These pillows were basically made of a 4-in. thickness of insulating material enclosed in a core. The cores were closed with staples and fastened with tie rods going through the insulation.

At the time of the experiments (1983), Type 1 insulation was in use at some operating nuclear plants, but plants under construction were not planning to use this type of insulation. The insulation used in the tests was layered, 4-in. thick, 6-lb mineral wool or refractory mineral fibers (two

2-in. layers in the material tested). The covering was Uniroyal #6555 asbestos cloth coated with a ½-mil Mylar film with stainless-steel staple seams. It should be noted that a small sample of mineral wool obtained from Maine-Yankee was included in the tests and that the mineral wool in the Maine-Yankee sample was manufactured by a different company than the mineral wool in all other samples used in the experiments.

Type 2 insulation was an oil-resistant insulation pillow. The core insulation was four-layer fiberglass Filomat-D – 1 in. (high-density, short-fiber E glass in needed pack). The cover includes an inner stainless-steel knitted mesh and outer silicone glass cloth (Alpha Maritex Product #2619). The blankets were closed with stainless-steel staples.

Type 3 pillows involve the same core insulation as Type 2 but with the cover a different 18-ounce fiberglass cloth (Alpha Maritex Product #7371). The blanket seams were fastened with stainless-steel staples.

Buoyancy Tests

The objective of these tests was to determine how long insulation pillows in undamaged, opened, and broken-up conditions would float. To approximate the conditions in the containment building following a LOCA, the insulation was sprayed continuously with a fine mist. Also, because preliminary tests indicated that the time needed for the insulation to sink decreased significantly with increased water temperature, the tests were performed with water temperatures between 120°F and 140°F, which is conservatively less than the containment pool temperature that would exist early in a LOCA.

The tests were carried out in a large tank roughly 15 ft x 5 ft x 9 ft tall filled with approximately 5 ft of water and separated vertically into three equal-sized compartments (5 ft by 5 ft in plan). A recirculating system with a 15-hp oil heater (boiler) was used to bring the tank water to the desired temperature and maintain it there. Conventional shower heads adjusted to fine spray and located about 3 ft above the water surface were used to spray the insulation. The top of the tank was covered with a plastic sheet to minimize heat loss, and as a result, the air above the water surface was saturated with water vapor.

In the buoyancy experiments, samples of insulation pillows were gently placed on the water surface and maintained under the spray. The time needed for the samples to sink was measured.

In addition to the fibrous insulation pillows, closed-cell insulation was tested for buoyancy. A small sample was deposited on the surface of water with the water at approximately 120°F, and its behavior was noted. The sample appeared to float indefinitely.

Transportation Tests

The objective of these tests was to determine the conditions under which insulation material would be transported by the flow to the sump screen and in what manner it would collect on the screen.

For floating insulation pillows, investigations were directed at corroborating transport to the screen at the water surface velocity and noting the conditions under which the pillows would flip vertically against the screen.

For sunken insulation, the flow velocity needed to initiate transport was measured, and the way the material collected on the screen was noted.

Tests were performed with insulation pillows in the following forms.

- Floating whole pillows
- Sunken whole pillows
- Sunken pillows with covers removed (but placed in the flume) and insulation layers separated
- Differently sized (6-in. square to 12-in. x 24-in.) full-thickness sunken pillow pieces with covers
- Sunken 4-in. x 4-in. x 1-in. and 4-in. x 1-in. x 1-in. pillow fragments without covers
- Sunken pillows in shreds (no cover material)
- Sunken individual shreds

Most of the transportation tests were conducted in a flume 6 ft wide by 6 ft deep and approximately 40 ft long equipped with a recirculation flow system. A screen similar to those used in containment sumps was erected across the flume, and a grating in front of the screen served as a trash rack. A water depth of 2 ft 8 in. was used with the equivalent insulation volume of two 2-ft x 2-ft x 4-in. pillows. The insulation pillows were dropped in the water 25 ft upstream of the screens, where the velocity distribution across the flume was approximately uniform. Flow velocities were measured using a laboratory current meter. Velocities were measured about 6 in. above the sunken insulation.

Turbulence generators were added to the flume for a few tests using 4-in. x 4-in. x 1-in. fragments of insulation pillows and pillow shreds. These turbulence generators were made with piles of cinder blocks extending nearly to the water surface and blocking part of the flow area. These piles of cinder blocks were intended to somewhat represent obstructions that might be present on a containment floor.

Tests with small single fragments of insulation material (4-in. x 4-in. x 1-in. shreds) were performed in a smaller 1-ft-wide flume with a 7-in. water depth. The flow velocity to initiate motion of the individual fragments (one at a time) was measured with a miniature propeller velocity meter.

In addition to the tests described above, the flow velocity needed to initiate the motion of an intact RMI cassette was measured. The sample was deposited on the bottom of the 6-ft flume with a water depth of 2 ft 8 in. Flow velocity was increased gradually until movement was observed.

Key Findings

The buoyancy tests revealed the following.

- In general, the time needed for both mineral wool and fiberglass insulation to sink is less at higher water temperatures.
- Most mineral wool does not readily absorb water and can remain afloat for several days. A notable exception to this was that the mineral wool received from Maine-Yankee, which sank in several hours in 50°F water and in 10 to 20 min in 120°F water.
- Fiberglass insulation readily absorbs water, particularly hot water, and sinks rapidly (from 20 to 60 min in 50°F water and from 20 to 30 s in 120°F water).
- Undamaged fiberglass pillows of Type 3 (and possibly also of Type 2) can trap air inside their covers and remain afloat for several days.
- Based on the observed sinking rates, it may be concluded that mineral wool pillows and some undamaged fiberglass pillows (those that trap air inside their covers) will remain afloat after activation of the containment recirculation system (approximately 20 min after the beginning of the LOCA). Those floating pillows will be transported readily to the sump screens. Damaged fiberglass insulation pillows will sink before activation of the recirculation system and will move only if the water velocity exceeds the incipient transport velocity associated with the pillows.

- RMI cassettes (at least of the type tested) sink immediately, and closed-cell foam insulation floats indefinitely. (The RMI cassette investigated measured 8 in. x 8 in. x 3 in. and had six sheets of reflective metal. The closed-cell insulation was a 6-in. x 4-in. x 2-in. parallelepiped of foamed glass.)

The transportation tests revealed the following.

- Floating insulation does move at the water surface velocity.
- Water velocities needed to initiate motion of sunken insulation are on the order of 0.2 ft/s for individual shreds, 0.5 to 0.7 ft/s for individual small pieces (up to 4 in. on a side), and 0.9 to 1.5 ft/s for individual large pieces (up to 2 ft on a side).
- Whole sunken fibrous pillows require flow velocities of 1.1 ft/s for Type 1 (mineral wool) and 1.6 to 2.4 ft/s for Types 2 and 3 (fiberglass) to flip vertically onto a screen.
- Floating pillows require a water velocity in excess of 2.3 ft/s to flip vertically against a screen.
- Sunken fragments of insulation pillows tend to congregate near the bottom of a vertical screen if there are no turbulence-generating structures (piles of cinder blocks in the flume experiments) in front of the screen. Depending on the water depth, unblocked space remains near the top of the screen. With a turbulence-generating structure a few feet in front of the screen, some insulation fragments get lifted and collect higher on the screen.
- Insulation shreds tend to remain waterborne and collect over the entire area of a screen.
- After reaching a screen, mineral wool fragments tend to lose their shape and turn into pulp. This contrasts with fiberglass fragments, which retain their shape and integrity.
- Intact RMI cassettes (or at least cassettes like the one tested) require a flow velocity of 2.6 ft/s to start and keep moving.

Limitations

Several references were made in the test report to the covers of fibrous insulation pillows being in place or removed. However, no mention of any buoyancy or transportability characteristics of the covers themselves could be found.

Different insulations than the specific ones tested in this study could have different characteristics. The

test results presented here are therefore only applicable for the specific insulations described.

No mention could be found as to whether the insulation tested had been pretreated (e.g., heated) or not.

5.2.2 Pennsylvania Power and Light Debris Transport Tests

In 1994, Pennsylvania Power and Light Company (PP&L) sponsored tests conducted at ARL to investigate issues relating to plugging of suppression pool suction strainers in BWR power plants.⁵⁻⁷ These tests, which commonly are referred to as the PP&L tests, were conducted in two parts.

- Transport tests—performed to quantify the transport velocities and turbulence levels (vertical mixing) required to keep materials waterborne where they could contribute to strainer plugging.
- Head loss tests—performed to investigate strainer head loss as a result of an accumulation of LDFG insulation debris with and without particulate present.

The transport tests are summarized here. Although these tests were conducted with BWR suppression pools in mind, they also provide meaningful information on the effects of vertical mixing on debris transport in PWR containment pools.

Transport Test Objectives

The transport tests were conducted to investigate the transport characteristics of various materials found in Susquehanna Steam Electric Station Units 1 and 2. The tests, which were conducted in a flume, were designed to investigate whether the flow patterns that would exist in a suppression pool could keep the materials suspended. The flume was configured to somewhat resemble a suppression pool with flow induced by ECCS recirculation and water returning to the pool via the downcomer vents. The tests provide information as to what types of material could be expected to settle to a suppression pool floor, where they would not be available to contribute to strainer plugging.

The transport of material over a weir also was investigated. Tests were conducted to quantify the flow rates required to draw the different debris types over a weir acting as a barrier to debris transport. These data were useful in assessing whether debris would remain on the drywell floor or be drawn over the drywell downcomer weir by recirculating water

flow spilling out of the broken pipe in a LOCA scenario. The data are applicable to considerations of debris transport over curbs in PWR containments.

The materials tested in the flume included LDFG insulation debris, inorganic zinc paint particles and flakes, iron oxide rust chips, iron oxide particulate, RMI, and Koolphen K vapor barrier foil paper. LDFG fibers and LDFG clumps of the following descriptions were tested.

- LDFG fibers—LDFG insulation debris of a light, loose, well-aerated texture with an average density of approximately 2.08 kg/m^3 (0.13 lbm/ft^3) usually consisting of a loose cluster of individual fibers.
- LDFG clumps—LDFG insulation debris torn from a blanket and aerated by a jet blast to an average density of approximately 20.8 kg/m^3 (1.3 lbm/ft^3). Clumps retain some of the structure of the original blanket where the binder keeps individual fibers consolidated at a lower density than the original blanket.

Test Apparatus

The flume had a 22-in.-wide, 16-in.-deep, rectangular cross section and was 18-ft long. It had one glass side to allow debris movement to be observed. Water was introduced at one end of the flume and passed through flow straighteners before it entered the test section. The influence of turbulence from return flow to a suppression pool through downcomers was investigated by discharging jets downward into the flume beneath the water surface. The downward jets were introduced through three 1-in. pipes distributed along the flume length. The jets imparted a known amount of mixing energy to the lateral flow, which was quantified as a power per unit volume (W/m^3).

In the tests involving a weir, the 12-in high weir was placed at the outlet end of the flume. Modeling similitude was addressed (i.e., the differences were studied between the linear weir in the flume and the circular weirs of BWR downcomer vents).

Key Findings

Material transport was observed in the flume, specifically whether debris settled at a given flow velocity and mixing energy. It was found that heavier debris, such as paint flakes, rust chips and RMI, settled readily. On the other hand, sludge was observed to remain largely waterborne. The LDFG fibers remained waterborne with very little flow mixing. The degree of mixing necessary to keep the

LDFG clumps waterborne was sizeable but not greater than the mixing that could be expected in a BWR suppression pool during ECCS recirculation.

For the weir tests, whether debris was carried over the weir depended on the speed of the flow through the flume.

Limitations

The quantitative information obtained for these tests relating mixing energy to debris transport is applicable in general to portions of a PWR containment sump pool away from the extreme turbulence of the pipe break flow plummeting into the pool.

5.2.3 Alden Research Laboratory Suppression Pool Debris Sedimentation Testing

The NRC sponsored tests, which were conducted by ARL, to investigate debris sedimentation in a BWR suppression pool. Although these tests apply specifically to the resolution of BWR suction strainer clogging issue, the debris settling data could have relevance to debris settling in a PWR sump pool, specifically in the portion of the pool where the debris transitions from the higher turbulent mixing near the pipe break into the calmer portions of the pool. Hence, these tests are summarized here.

After a postulated LOCA, the BWR suppression pool would experience a range of turbulence conditions, specifically, a high level of turbulence immediately following the LOCA, a transition period, and then a longer-term relatively quiescent period after primary system depressurization is completed. During the period of high turbulence, debris transported from the drywell to the suppression pool would undergo mixing and, potentially, fragmentation. In addition, any debris previously located on the suppression pool floor likely would be resuspended. During the quiescent period, debris would gradually settle to the suppression pool floor. These phenomena govern the transport of debris within the suppression pool, thereby determining the type, quantity, and form of debris deposited onto the strainers.

To study these debris behaviors, a test apparatus was designed that would simulate a Mark I suppression pool on a reduced scale. The fibrous debris sedimentation tests are discussed in Section 5.2.3.1, and the RMI debris sedimentation tests are discussed in Section 5.2.3.2.

5.2.3.1 Fibrous Debris Sedimentation Testing

Test Objective

The overall purpose of the suppression pool tests was to provide insights into debris transport within a suppression pool following a LOCA.⁵⁻⁸ However, the underlying processes are too complex to be addressed by a single set of experiments. Based on scoping studies and discussions with experts in related fields, the phenomena selected for further study were:

- debris transport and sedimentation within the suppression pool during the high-energy phase that would immediately follow a medium loss of coolant accident (MLOCA) and
- debris transport and sedimentation within the suppression pool during the post-high-energy phase.

The high-energy downcomer oscillations for a LLOCA would be driven initially by condensation oscillations for a relatively short period of time (about 30 s) and then be followed by chugging for the remainder of the blowdown phase. Because the condensation phase would be relatively short and more difficult to simulate experimentally, the tests focused on the chugging phase.

The primary focus was to obtain debris-settling-velocity data to support analytical evaluations, specifically analyses applicable to the potential for strainer blockage in the BWR reference plant analysis.⁵⁻⁹ Because the insulation used to insulate primary system piping in the reference plant consisted predominantly of LDFG mats, the debris beds formed on the reference plant strainers were expected to consist primarily of accumulated fragments of LDFG insulation with particulate debris embedded within its fibers. Therefore, LDFG debris and particulate debris with the characteristics of suppression pool sludge were used in these tests.

Test Apparatus and Instrumentation

A water tank designed to simulate a segment of a Mark I BWR suppression pool was constructed of steel with the appropriate lower curvature. The tank sidewalls of the segment were made of Plexiglas to provide complete visibility of the debris in motion. Turbulent chugging associated with steam-water oscillations (condensation oscillations) during depressurization of the primary system was simulated in these tests by including four 10-in. (0.25-m) diameter downcomers fitted with pistons. One of the downcomers was constructed of

Plexiglas to facilitate visualization of debris transport. The test apparatus is shown in Figure 5-1.

The geometric scale of the tank was 1 to 2.4, and the radius of the test tank was 13.5 ft (4.11 m). The spacing between the downcomers and their clearance with respect to the floor were also scaled. The front and back walls were spaced one-half the distance to the next pair of downcomers in either direction. Hence, the water volume of the tank per downcomer was scaled to the volume per downcomer of a typical BWR Mark I suppression pool.

The pool dynamic conditions associated with the high-energy phase of a MLOCA are usually referred to as “chugging.” Chugging occurs when water reenters the downcomers as a result of decreasing steam flow, thereby condensing steam. The build up of noncondensable gases would subsequently push the water from the downcomers until sufficient noncondensable gasses escapes the downcomers to initiate another cycle. Energy input to the suppression pool during chugging was based on data obtained by General Electric (GE) in a full-scale test of a Mark I containment at their full-scale test facility (FSTF).⁵⁻¹⁰ Two types of chugging behavior were observed in test data for a MLOCA.

- Type 1, where the neighboring downcomers oscillated in phase, i.e., oscillations were synchronized.
- Type 2, where the oscillations were relatively unsynchronized.

Because Type 1 chugging was deemed more prototypical of MLOCA, only Type 1 chugging was studied in these tests. All downcomer pistons oscillated in phase to simulate Type 1 chugging. For several Type 1 chugs, the FSTF tests provided pressure measurements within a downcomer. Because GE did not measure the actual kinetic energy imparted to the suppression pool during each chug directly, an analytical model was devised to deduce the energy from the measured chugging pressures. This model was then used to estimate both the chugging period of the downcomer oscillation and its amplitude of two-phase level movement. Because the dynamics of chugging changed continuously during primary system depressurization, the period and amplitude were estimated for the initial, middle, and later stages of chugging. Further, these estimates were modified to reflect scaling considerations.

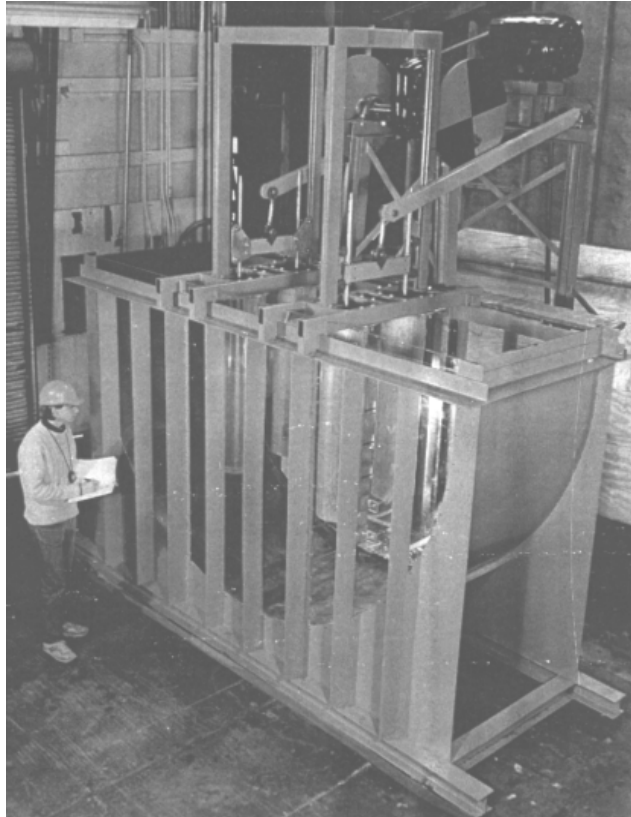


Figure 5-1 Suppression Pool Sedimentation Test Apparatus

The test facility included a series of sampling ports to allow concentrations of sampling debris at five equally spaced vertical locations at the center of the tank. The samples were filtered, dried, and weighed so that the concentrations could be expressed as the mass of debris per unit mass of water. A debris classification system was devised that classified pieces of debris into seven groups.

Test Data

Fourteen parametric tests were conducted to examine a variety of test conditions. The test parameters included

- the type, form, and quantity of insulation debris tested;
- the quantity of sludge tested; and
- the period and amplitude of the downcomer piston chugging.

Within the ranges of tested parameters, the data exhibited the following trends.

- Both the fibrous and particulate debris remained fully mixed in the tank during simulated chugging at all energies tested,

resulting in uniform vertical concentration profiles.

- Turbulence-resuspended debris initially deposited onto the suppression pool floor during simulated chugging at all energies tested.
- Fibrous debris underwent further fragmentation into smaller sizes, including individual fibers, at all energies tested. In general, the fragmentation occurred near the downcomers where the fibrous debris was subjected to cyclic shear forces from the downward jet and ingestion into the downcomer.
- Visual observations suggested that turbulence decays within a few minutes after termination of chugging simulation, thus enabling post-high-energy-phase debris settling. In the post-high-energy phase, the vertical concentration profiles were slightly nonuniform. The ranges of settling velocities in calm pools (terminal velocity) are listed in Figure 5-2 for each debris size classification. The terminal settling velocity for fibrous debris is shown in Figure 5-3 as a function of debris weight.

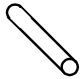

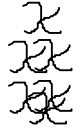



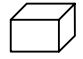
Class No.	Description	Settling Characteristics	Settling Velocity in Calm Pools	Strainer Filtration Efficiency
1	 Very small pieces of fiberglass material, "microscopic" fines which appear to be cylinders of varying L/D.	Drag equations for cylinders are well known, should be able to calculate fall velocity of a tumbling cylinder in still water.	1-3.5 mm/s Based on Cal. for 0.5 - 2.54 cm long fibers	Unknown
2	 Single flexible strand of fiberglass, essentially acts as a suspended strand.	Difficult to calculate drag forces due to changing orientation of flexible strand.	Same as above	Nearly 1.0
3	 Multiple attached or interwoven strands that exhibit considerable flexibility and which due to random orientations induced by turbulence drag could result in low fall velocities.	This category is suggested since this class of fibrous debris would likely be most susceptible to re-entrainment in the recirculation phase if turbulence and/or wave velocity interaction becomes significant.	0.04 ft/s - 0.06 ft/s (measured)	1.0 (measured)
4	 Formation of fibers into clusters which have more rigidity and which react to drag forces more as a semi-rigid body.	This category might be represented by the smallest debris size characterized by PCI air blast experiments.	0.08 - 0.13 ft/s (measured)	1.0 (measured)
5	 Clumps of fibrous debris which have been noted to sink. Generated by different methods by various experimenters.	This category was characterized by the PCI air test experiments as comprising the largest two sizes in a three size distribution.	0.13 - 0.18 ft/s (measured)	1.0 (measured)
6	 Larger clumps of fibers. Forms an intermediate between Classes 5 and 7.	Few of the pieces generated in PCI air blast tests consisted of these debris types.	0.16 - 0.19 ft/s (measured)	1.0 (measured)
7	 Precut pieces (i.e. .25" by .25") to simulate small debris. Other manual/mechanical methods to produce test debris.	Dry form geometry known, will ingest water, should be able to scope fall velocities in still water assuming various geometries.	³ 0.25 ft/s (calculated)	1.0 (estimated)

Figure 5-2 Fibrous Debris Classifications

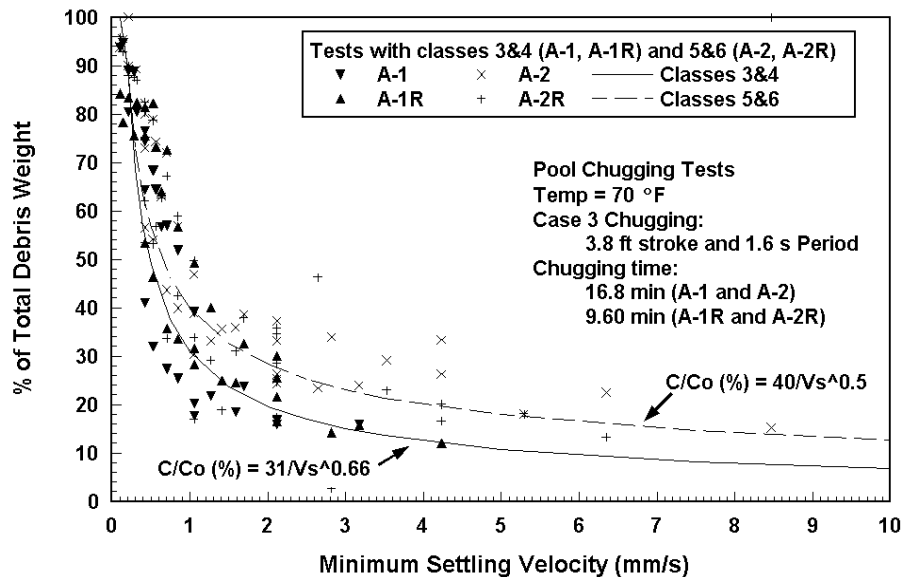


Figure 5-3 Fibrous Debris Terminal Settling Velocities

- Measured concentrations showed that fibrous debris settled slower than the sludge and that the settling behavior of each material is independent of the presence of the other material.

These results were deemed equally valid for other phases of accident progression and other sizes of LOCAs. These tests showed that the assumption of considering uniform debris concentration during strainer calculations is reasonable. However, it must be noted that the continuous operation of the recirculation ECC and the RHR systems in an actual BWR would add additional turbulence to the pool and that this type of turbulence was not considered in these tests. Therefore, applying these data to an actual plant analysis requires engineering judgment.

5.2.3.2 Reflective Metal Insulation Debris Sedimentation Testing

The potential for RMI debris transport within a suppression pool to an ECCS pump suction strainer was experimentally demonstrated. RMI debris that was transported from a BWR drywell into a suppression pool would undergo mixing during the period of high turbulence. Debris would settle to the suppression pool floor during the quiescent period. These phenomena govern the transport of debris within the suppression pool, thereby determining the quantity of RMI debris deposited onto the strainers.

Test Objective

The RMI test objective was similar to that of the fibrous debris sedimentation tests.⁵⁻¹¹ The overall purpose of the RMI suppression pool tests was to provide insights into RMI debris transport within a suppression pool following a LOCA. RMI debris transport and sedimentation within the suppression pool were studied both during the high-energy phase that would immediately follow a MLOCA and during the post-high-energy phase. A primary focus was to obtain debris-settling-velocity data to support analytical evaluations.

Test Apparatus and Instrumentation

The test apparatus used in the RMI debris testing was the same as the apparatus used in the fibrous debris testing described above. The RMI debris used in these tests was debris generated by the SIEMENS large-pipe-break debris-generation test.⁵⁻¹¹

Test Data

Still-water debris-settling tests were performed on individual pieces of RMI debris with representatives from each of six size groupings. Each piece was placed individually in the suppression pool test tank, and its time to settle a known distance was measured. For all sizes less than 6 in., the mean settling velocity was about 0.12 m/s (0.4 ft/s). The large 6-in. pieces settled about 20% slower than the smaller pieces.

Chugging energy and RMI debris size were varied to determine their effect on RMI debris suspension. Figure 5-4 is a photo of 6-in. pieces of debris in suspension during chugging. Approximate settling times after the simulated chugging ended were recorded for various sizes of RMI shreds.

Approximately 2/3 of the RMI pieces remained suspended at the higher energy levels, whereas ~1/2 of the pieces remained suspended during the lower energy chugging phase. The effect of residual turbulence on settling times was significant for the small RMI debris. After chugging, the turbulence decayed away, allowing settling to occur. In the turbulent pool after chugging stopped, the larger RMI debris (2- to 6-in. category) settled up to two times faster than the smaller RMI debris (0.25- to 0.5-in. category). All RMI debris settled within 2 min after chugging ceased. The settling time after simulated chugging ended was independent of chugging energy. The concentration or density of debris pieces did not affect settling rates within the range of concentrations tested. However, for concentrations larger than about 2 g/ft³, inter-action between RMI shreds on the floor of the tank somewhat inhibited re-entrainment during simulated chugging. Note that because suppression-pool ECCS flow recirculation was not simulated in these tests, these results do not consider the effects of recirculation on material settling or possible resuspension.

5.2.4 Alden Research Laboratory Reflective Metallic Insulation Materials Transport Testing

The ARL RMI testing was sponsored by the NRC to support the resolution of Unresolved Safety Issue A-43, "Containment Emergency Sump Performance." ARL investigated the transport characteristics of RMI assemblies and parts thereof in flowing water.⁵⁻¹² The investigation is summarized in the following paragraphs.



Figure 5-4 Typical Large (6-in.) RMI Debris in Suspension During Chugging

Objective

The study was aimed at determining

- the flow velocities needed to initiate the motion of sunken pieces of RMI, either entire jackets or components thereof and either basically undamaged or crumpled;
- the effects of interaction between multiple pieces of RMI or between RMI pieces and flow boundaries; and
- the screen blockage modes, i.e., the ways in which pieces of RMI would collect on and block a vertical PWR sump screen.

Methodology

The pieces of RMI tested were either components of a 36-in. long insulation assembly for a 10-in. pipe furnished by the Diamond Power Specialty Company or sheets of stainless-steel foil of different thicknesses. The tests were conducted in a 6-ft wide, 6-ft deep, and 40-ft long flume. Water was introduced at one end of the flume behind a flow-straightening plate and was maintained at a depth of 32 in. At the downstream end of the flume, a screen and trash rack similar to those used around recirculating sumps were erected vertically across the full width. The screen was made of 1/16-in. wire with a 1/4-in. mesh directly behind a standard 1-in. floor grating with its more closely spaced bars oriented horizontally.

The samples of RMI were placed in the flume approximately 20 ft upstream of the trash rack and screen. Flow velocity then was gradually increased, and the velocity at which a sample started to move was recorded. If a sample stopped, and judgment was made that it would not move further, flow velocity was increased until further movement was observed. The minimum flow velocity that caused movement all the way to the screen was recorded as the transport velocity for a sample.

Key Findings

Transport Velocities

- As-fabricated RMI units required water velocities of 1.0 ft/s or more to move.
- Single sheets of thin stainless-steel foil used in RMI (0.0025 and 0.0040 in. thick) can be transported by water flow velocities as low as 0.2 to 0.5 ft/s. Single sheets of thicker foil (0.008 in.) require higher velocities for transport of about 0.4 to 0.8 ft/s.
- Crumpled foils tend to transport at lower velocities than flat foils.
- Transport velocity tends to increase with material thickness except for easily flexible foils, where the thickness dependence is smaller.
- In all cases, the velocity of motion of the sample is much lower than that of the flow.

Transport Modes

- Transport at lower velocities occurs when the foil sheet is flexible enough that a corner or edge can be bent up by the flow, thereby increasing the frontal area and therefore the drag. The resulting motion is one of intermittent folding, tumbling, and rolling.
- Rigid pieces tend to be transported by sliding along the bottom. Rigidity can result from greater thickness (0.008 in. and above) or small size (less than about 12 in. x 12 in. for 0.0025-in. foil). Higher flow velocities typically are needed for transport of rigid pieces than for transport of flexible pieces.
- Even with high flow velocities (about 2 ft/s) and large water depths (60 in. but velocity of only 1.6 ft/s), the samples were never observed to become waterborne.
- The vertical sides of the flume were observed to hinder the transport of samples. Samples contacting a wall were often pushed and folded against it, needing higher flow velocities to dislodge.
- When several pieces of foil were released simultaneously, their interaction during transport often caused the pieces to jam and become immobilized. High flow velocities (up to 1.8 ft/s) then were required to break up the jams and resume the transport.

Blockage Modes

- Most foils readily flip vertically against the screen upon arriving there. Whether originally crumpled or not, the foils become flattened against the screen by the water force. An exception here is thicker foil (0.008 in.), which remains crumpled. The more flexible foils often become folded on the screen, blocking less than their surface area. The large 0.008-in.-thick foils, which exhibited rigidity relative to their transport mode but whose dimensions were larger than the water depth, often folded on the screen with a portion being caught under the trash rack.
- Because insulation specimens never became waterborne, they never blocked the screen above their width or length. Blockage up to the diagonal height was never observed, but this may be because the water depth was less than that height.
- When several foil pieces were released simultaneously, significant overlap was observed on the screen so that even if the total foil area was larger than the screen area (1.6 to 2.2 times), the screen was never blocked fully (only up to about 80% of the area was blocked).

Limitations

- All the tests, except one for waterborne transport mode checking, were done with a water depth of 32 in. This depth was used to allow comparison with earlier studies; however, the depth could have an effect on the blockage modes because the characteristic dimensions of the pieces of RMI debris were less than the depth of the water.
- The flume width was only 6 ft. It is possible that sidewall effects could be present in the observed blockage modes. Because the sidewalls were observed to hinder transport, screen sections near the walls could have had a reduced probability of becoming blocked.

5.2.5 University of New Mexico Separate Effects Debris Transport Testing

LANL and the University of New Mexico (UNM) conducted debris-transport experiments in the UNM Open-Channel Hydrology Laboratory.^{5-4,5-13} The experiments were sponsored by the NRC Office of Regulatory Research as part of a research program supporting resolution of GSI-191. Measurements were made of the fundamental transport properties of various types of thermal insulation and other debris that could be generated as a consequence of a LOCA involving a PWR. The experiments and the results obtained are summarized below.

Objectives

The overall purpose of the debris-transport experiments was to provide data to aid in assessing the potential effect of dislodged insulation and other debris on ECCS recirculation through the emergency sump. The specific objectives of the experiments were to measure the following properties for several types of insulation and other debris.

- Settling velocity—the terminal velocity of a material as it falls through water under the influence of gravity
- Flow velocity at incipient motion (tumbling or sliding) of sunken material—the minimum flow velocity required to initiate tumbling of the smaller pieces (within a given size class) or the pieces with special shapes that provide higher drag coefficients
- Flow velocity at bulk motion of sunken material—the flow velocity required to induce tumbling of a given class of debris
- Flow velocity required to convey material over a curb
- Flow velocity required for retaining debris on a screen after it's deposited there.

- The dissolution and erosion of debris, specifically calcium silicate insulation debris.

Methodology

The debris transport experiments used two flumes, one smaller than the other. The smaller flume had a 10-ft-long, 1-ft-wide, and 1.5-ft-high test section and a maximum water depth of 1 ft. The larger flume had a 20-ft-long, 3-ft wide, 4-ft-high, test section. The larger flume was used in the majority of the experiments. The smaller flume was used to study the transport of calcium silicate debris and paint chips because

- (1) it was easier to clean debris from the smaller flume than from the larger flume and
- (2) smaller debris was easier to see in the narrower test section of the smaller flume.

The advantage of the larger flume was its capacity to accommodate larger scale turbulent flow structure and larger test specimens (e.g., intact RMI cassettes).

Both of the flumes had structures to condition the inlet flow such that a uniform unidirectional flow resulted in their test sections. To investigate the influence of turbulent flow structure on debris transport, the inlet flow conditioning structures in the large flume were removed in some experiments. The flow velocity in the flume was taken to be that associated with the measured volumetric flow of the pump spread uniformly over the flow section of the flume.

In some experiments, boards were placed on the floor of the flume across the width of the test section and directly in front of the screen to form a curb. The curbs were either 2 in. or 6 in. high and 2 in. long in the direction of flow. Photographs and diagrams of the larger flume used for the majority of the debris transport tests are shown in Figures 5-5 through 5-7.

A 34-in. long, 10-in. diameter graduated, transparent pipe stood on end, blanked off at the bottom, and filled with water served as a settling column for measurements of debris settling velocity.

The types of debris tested included LDFG, RMI, and calcium silicate insulations, Marinite fire-barrier material, and paint chips. Three makes of LDFG insulation were investigated: Nukon®, Thermal-Wrap, and Kaowool. Two types of RMI insulation were investigated: aluminum and stainless-steel RMI. The transport characteristics of epoxy-based paint chips ranging in size from 1/8 in. square to

1/2 in. x 1 in. were investigated. The chips had a median thickness of 15 mil. It may be important to note that the paint chips used in the transport tests may not have been prototypical of those that might be found in a containment pool;³ however, these tests provide insights into their transport characteristics. Photos of typical samples of LDFG, RMI, and paint chip debris are shown in Figures 5-8 through 5-10, respectively.

Key Findings

The transport data from the separate-effects tests are summarized in Table 5-1; flow dampening was used in the tests and illustrated in a series of bar charts. Characteristics ranged from the buoyant behavior of silicone to that of Marinite board, which readily sank. Figure 5-11 shows a comparison of terminal settling velocities for a variety of insulation debris types and paint chips. It should be noted that sizes and forms of debris different from the debris tested might not fit within these ranges; for example, individual fibers of LDFG tend to settle very slowly if at all.

The transport of debris moving along a floor was characterized by the flow velocity required to move the debris across the floor, which is referred to as the tumbling velocity, and the velocity required to cause the debris to jump an obstruction (curb), which is referred to as the lift velocity. These velocities were measured for onset of movement, i.e., incipient motion, and for bulk or mass movement of debris. The bulk and incipient tumbling velocities are compared in Figure 5-12, and the incipient lift and tumbling velocities are compared in Figure 5-13. Again, these data are for conditions of uniform flow velocities and low levels of flow turbulence. When lift velocities over a curb were measured, the curbs were free of other debris⁴. For most debris, the velocity differences between incipient and bulk motion were not substantial; that is, after the debris started to show movement (incipient), a relatively modest increase in velocity induced bulk movement of debris.

³Because of the wide variety of paint chemical compositions and wear conditions (new, aged, irradiated, etc.) and paint failure mechanisms (dimpled, curled, flaked, powdered, etc.), a spectrum of paint chips sizes, shapes, and compositions could be involved in a LOCA scenario, i.e., a prototypical paint chip sample is difficult to define.

⁴The effect of debris accumulation upstream the curb on the lift velocity was not investigated. It is likely that debris would lift over the curb more easily if accumulated debris first forms a sort of ramp upstream the curb.



Figure 5-5 Photo of Large UNM Flume Test Apparatus

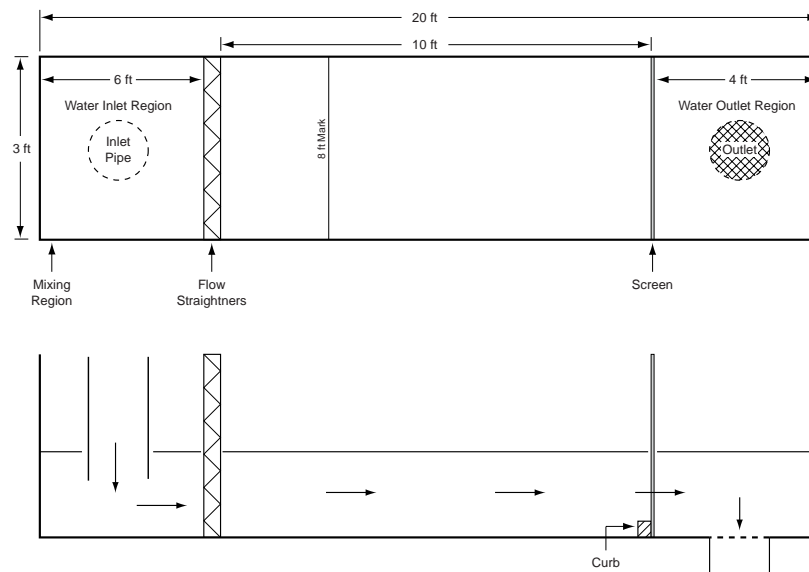


Figure 5-6 Diagram of Large UNM Flume Test Apparatus



Figure 5-7 Photo of Large UNM Flume Inlet Flow Conditioning Apparatus



Figure 5-8 Typical Test Sample of LDFG Insulation Debris



Figure 5-9 Typical Test Sample of Aluminum RMI Insulation Debris



Figure 5-10 Typical Test Sample of Paint-Chip Debris

Table 5-1 Summary Data for Diffused Flow Entry Inlet Conditions

Debris Type	Terminal Settling Velocity ft/s	Tumbling Velocities ft/s		2-in. Curb Lift Velocity ft/s		6-in. Curb Lift Velocity ft/s		Screen Retention Velocity ft/s
		Incipient	Bulk	Incipient	Bulk	Incipient	Bulk	
Calcium silicate	0.13 to 0.17	0.25	0.35	No Data	No Data	No Data	No Data	No Data
Paint Chip	0.08 to 0.19	0.40	0.45	0.50	> 0.55	No Data	No Data	No Data
Al RMI	0.08 to 0.21	0.20	0.25	0.30	No Data	0.37	No Data	0.11
SS RMI	0.23 to 0.58	0.28	0.30	0.84	No Data	> 1.0	No Data	0.12
Nukon	0.13 to 0.41	0.12	0.16	0.25	No Data	0.28	0.34	0.05
Thermal-Wrap	0.08 to 0.22	0.12	0.16	0.25	0.25	0.30	No Data	0.04
Kawool	0.15 to 0.30	0.12	0.16	0.25	0.25	0.41	0.41	No Data
Marinite Board	0.44 to 0.63	0.77	0.99	No Data	No Data	No Data	No Data	No Data
Silicone Foam	Always Floats	N/A	N/A	N/A	N/A	N/A	N/A	N/A

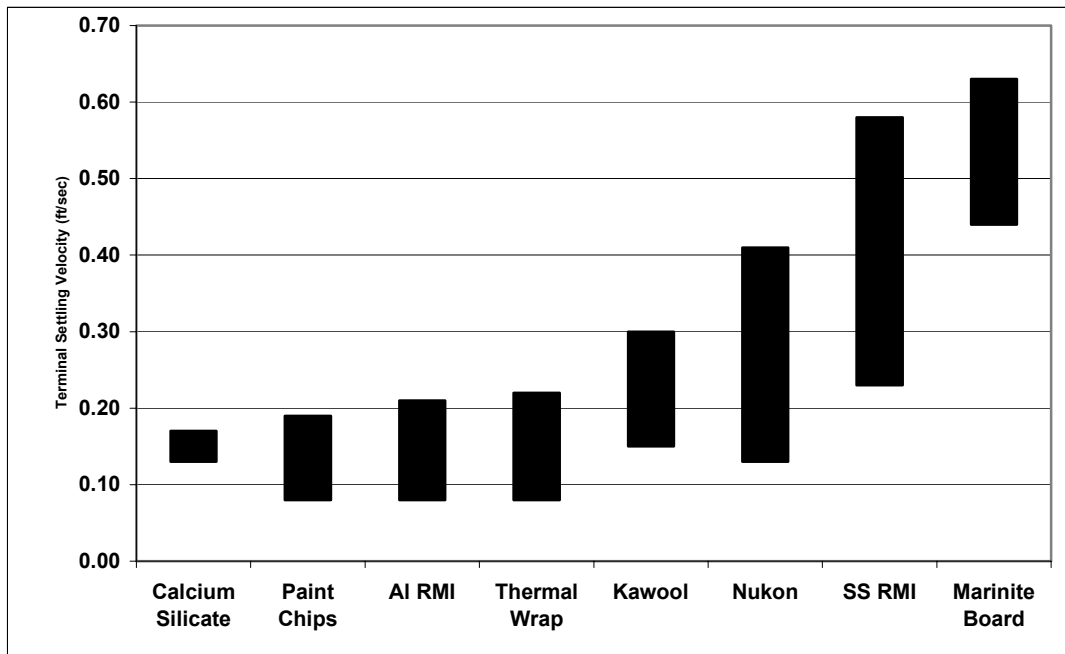


Figure 5-11 Comparison of Terminal Settling Velocities

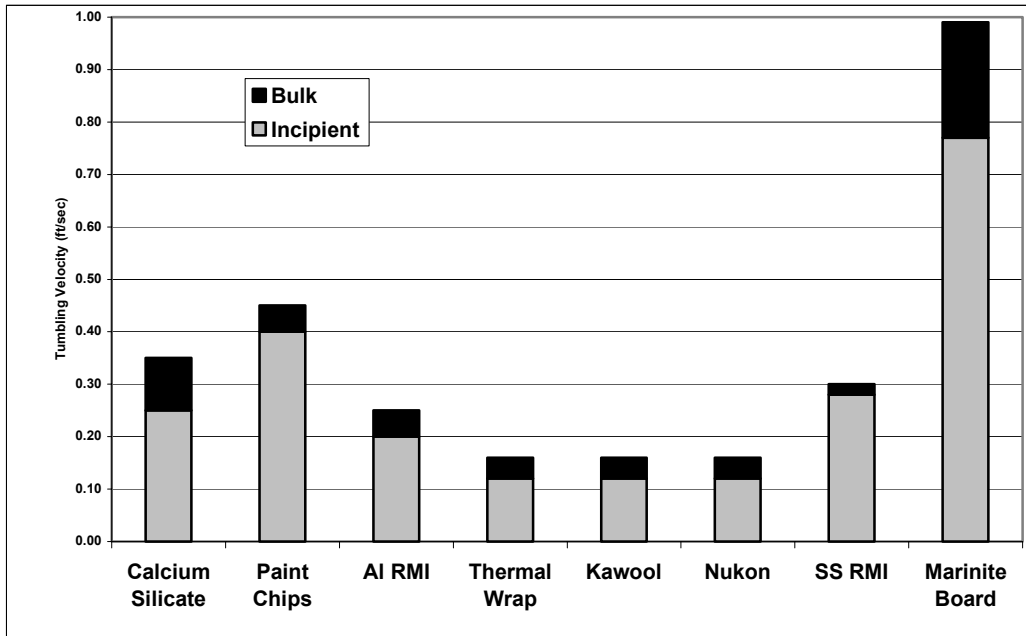


Figure 5-12 Comparison of Incipient and Bulk Tumbling Velocities

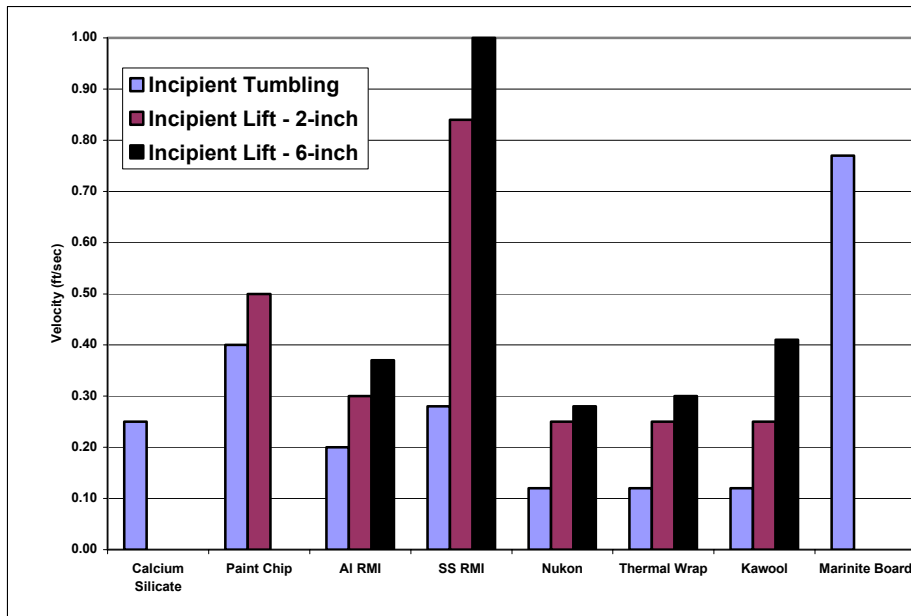


Figure 5-13 Comparison of Incipient Lift Velocities to Incipient Tumbling Velocities

The flow velocity needed to keep a piece of debris on the screen was less than the velocity needed to initiate transport of the debris on the screen. After debris arrives at the screen, it generally can be expected to stay on the screen.

The disintegration characteristics of calcium silicate insulation were investigated. Experiments were performed in which single fragments of calcium silicate were weighed and then dropped into three different water baths. One bath was maintained at ambient temperature (approximately 20°C), a second was maintained at elevated temperature (approximately 80°C), and a third was maintained at elevated temperature with occasional stirring. The fragments were subjected to these conditions for 20 min, after which the water was drained and the residue was dried and weighed. In the ambient-temperature bath, 18% of the calcium silicate separated from the original sample and went into suspension. Although not ascertained through weighing, stirring the water (after the 20 min of the test had passed) seemed to have little effect on the disintegration. In the 80°C bath, 46% of the calcium silicate separated from the original sample and went into suspension. Clearly, hot water furthered disintegration. In the 80°C bath with occasional stirring, 76% of the original sample disintegrated into suspension. Clearly, stirring furthered disintegration in the case of hot water.

Pieces of Marinite were submerged in boiling water for 30 min to investigate the tendency of the material to disintegrate. The Marinite became soft and rubbery on the surface but did not disintegrate. Small amounts of material could be pulled from the surface but not especially easily. As such, it was conjectured that the levels of agitation that might develop in a containment pool would not cause Marinite material to disintegrate.

The transport properties of silicone foam insulation were also investigated. The foam was found to be entirely resistant to sinking. In the flume, foam insulation fragments floated on the surface and moved with the flow.

Limitations

The debris transport tests had few limitations, discussed in the following paragraphs.

Most of the experimental data taken applies to flow fields where the turbulence has been damped out and the flows are uniform. Some data were taken where the dampeners were removed from the tests to qualitatively determine the effect of turbulence on

debris transport and turbulence was shown to enhance debris transport. However, no method was identified to quantitatively evaluate the effect of turbulence in an actual PWR sump pool.

The paint chip samples used in the transport tests were not taken from a PWR containment, and the samples were not pretreated in such a way to make them representative of actual containment paint. Actual paint likely would have aged and perhaps have been irradiated. There are many types of paints used in containment and under a variety of environmental conditions. The data matrix (Table 5-1) was not filled completely.

The effect of debris accumulation upstream the curb on the debris lift velocity was not investigated.

5.2.6 University of New Mexico Integrated Debris Transport Testing

Experiments were conducted to examine insulation-debris transport under flow conditions and geometric configurations typical of those found in PWRs.⁵⁻³ These experiments, which were sponsored by the NRC as part of a comprehensive research program to support the resolution of Generic Safety Issue (GSI) 191, were conducted by LANL at the Open-Channel Hydrology Laboratory operated by the University of New Mexico. The integrated testing was performed using a large tank with provisions to simulate a variety of PWR containment/sump features. The test program was designed to explore the effect of various containment internal structures on debris transport and from that draw inferences on the features of containment that could affect debris transport significantly. These tests were not planned to be “scaled” tests; instead, the focus was to simulate the sequential progression of various phases of accident progression and examine the overall effect on debris transport. The integrated phenomena included debris transport during the fill-up phase (i.e., while the sump and tank were being filled) and after steady-state conditions were achieved (i.e., water flow from the break is equal to the flow out the sump).

The integrated debris transport tests provide data to support the development and/or validation of appropriate analytical simulation models designed to evaluate debris transport in a PWR containment sump on a plant-specific basis. For example, the tests developed data that could be used to benchmark computational fluid dynamics (CFD)-based simulations supporting estimates of debris

transport in water pools formed on PWR containment floors. The insights gained from these tests specifically include the relative importance of the various debris transport mechanisms and containment geometry features, such as the important features of the containment layout and sump positioning that affect debris transport and accumulation on the sump screen. The physical processes and phenomena to which the observations pertain include flow patterns and flow turbulence, debris floatation, gravitational debris settling, the transport of debris along the pool floor, debris entrapment mechanisms, re-entrainment or retention of trapped debris, and disintegration of debris within the pool. The debris used in the test program included primarily fiberglass and RMI debris of different sizes and shapes. The debris was of sufficiently small size not to be affected by the scaling issues.

Objectives

The experimental program was designed primarily to complement concurrent CFD calculations by providing three-dimensional data for validating the CFD results. The experiments had three objectives.

- Provide debris-transport data and velocity field data that can be used to validate CFD calculations pertaining to three-dimensional transport phenomena in water pools formed on PWR containment floors.
- Identify features of containment layout and sump positioning that could affect debris transport to the sump and debris accumulation on the sump screen.
- Provide insights for developing a simple method (or criteria) that could be used for each plant-specific configuration to conservatively attest to its safety. Such methods potentially could be used in lieu of complex analyses (e.g., CFD), and may consist of performing small-scale experiments and/or one-dimensional (1-D) flow calculations, similar to those suggested in Ref. 5-14.

Setup

The tests were conducted in a steel tank that was 13 ft in diameter, and 2.5 ft deep, and open at the top, as shown in Figure 5-14. The floor of the tank was covered with high-strength concrete and leveled. The floor and the tank inner surfaces were coated with epoxy paint typical of PWRs. An outlet box designed to simulate a PWR containment recirculation sump was installed as shown in Figure 5-15 to drain water from the tank. The outlet box is 30 in. long, 14.5 in. wide, and 20 in. deep

with a volume of 5.3 ft³ (approximately 40 gal.). Water was pumped at variable speeds into the test tank from a below-floor reservoir by an overhead pipe and, in some tests, through a coarse diffuser designed to reduce inlet flow turbulence. The tank was drained at the outlet box after water flowed through the outlet screen that was used to collect debris transported to the outlet box. Debris collected on the outlet screen (both horizontal and vertical orientation were investigated) provided quantitative measurements of (a) the amount of debris that reached the sump screen and (b) the location of the remaining debris on the tank floor. Qualitative velocity mapping included local velocity measurements during steady state.

Structures were placed in the tanks that were designed to simulate the floor features of a typical PWR containment sump and to simulate this type of variability in PWR containment sump geometries. The location of the inlet pipe, one of the primary test parameters, was varied during the course of testing, resulting in three test configurations, A, B, and C, as shown in Figures 5-16, 5-17, and 5-18, respectively. In the latter tests, the interior walls nearest to the outlet box were removed to simulate an exposed sump condition, resulting in Configuration D as shown in Figure 5-19. In Configuration A, the inlet pipe was located well away from the outlet box, and the inlet pipe in Configuration D was located near the outlet box, thereby effectively simulating a remote sump and a fully exposed sump, respectively.

Methodology

The tests conducted during the course of the test program were broadly divided into three categories according to their purpose. The first category examined debris transport in the tank as it filled with water for a variety of insulation debris types and surrogate tracer particles. In these fill-up tests, debris was placed on the floor of the tank before the tank was filled. The second category of tests was designed to provide insights into the short-term transport of LDFG insulation debris. These tests were carried out over a period of 30 min and measured the fraction of debris that reached the outlet in that time. Several parameters were varied in the conduct of these tests that allowed test-to-test comparisons in which a single specific variable was altered. The third group of tests was carried out over an extended period (up to 6 h) to study the longer-term transport of LDFG debris in a configuration of the tank that tended to keep the debris stirred up (i.e., where the tank outlet was not far from the falling water stream entering the tank).



Figure 5-14 Steel Tank Used in Integrated Testing



Figure 5-15 Integrated Test Tank Outlet Box

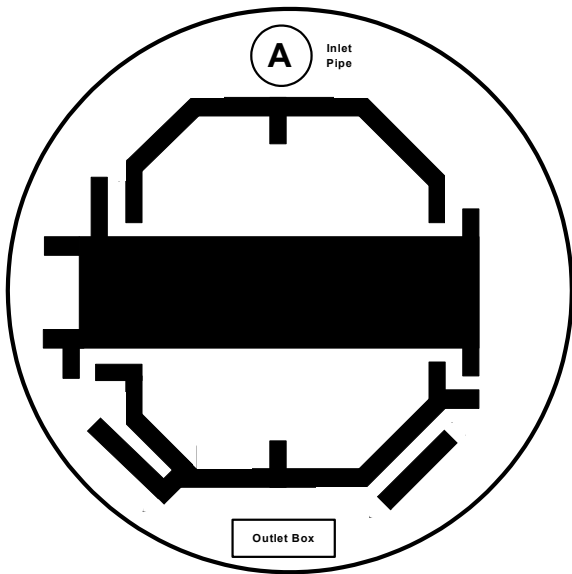


Figure 5-16 Test Configuration A

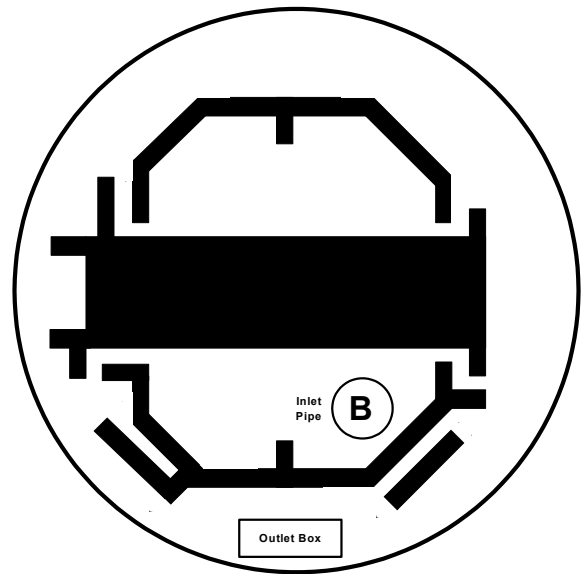


Figure 5-17 Test Configuration B

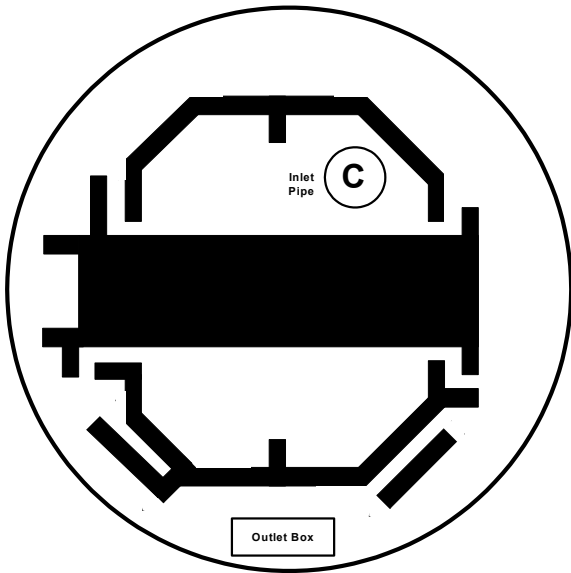


Figure 5-18 Test Configuration C

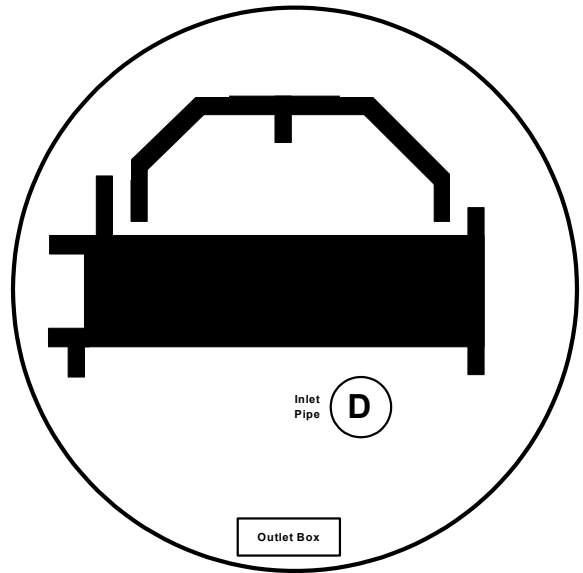


Figure 5-19 Test Configuration D

Of particular interest was the transport of fine debris. These longer-term tests provided time-dependent transport data. Data from selected tests were compared with CFD simulations of those tests to provide both further insights into the test results and insights into the ability of a CFD code to predict the complex flow patterns of the test. These simulations are addressed in Section 5.3.6.

Key Findings

The integrated debris-transport test program provided data for various combinations of inlet conditions, four geometrical configurations, two screen configurations, and different debris types. The conditions of the tests establish quiescent, turbulent, and rotational flow regimes within each test. Two phases of debris transport were examined: (1) debris transport during the period when the sump is filling with water and then (2) debris transport after the pool has filled. Important insights, observations, and findings from the test program include the following.

- Debris transport depended greatly on the buoyancy of each piece of debris. Fragments of buoyant foam insulation confirmed that truly buoyant debris simply floated across the top of the water surface until it reached either a quiescent region, where it remained, or the outlet screen. Neutrally or near neutrally buoyant debris stayed suspended in the pool even when the water was relatively quiescent. The most notable neutrally buoyant debris was the individual fiber or small clumps of fibers from fibrous insulation, which did not settle any place in the tank within the time frame of the tests. In the absence of significant pool agitation, nonbuoyant debris sank to the bottom of the pool, where its transport was a result of tumbling and sliding across the floor when the flow velocities were sufficiently high. Floor-level obstacles, such as a shallow barrier placed across the annulus, affected floor debris transport.
- Debris transport occurred in two phases:
 - (a) the fill-up transport phase, which is analogous to the pre-ECCS switchover containment sump fill-up phase, and
 - (b) the steady-state transport phase, which is representative of post-switchover conditions.

Debris placed initially on the tank floor before pump flow began underwent transport associated with the initial fast-moving flows as the tank began to fill, as well as undergoing steady-state pool transport after the tank

reached steady state (and all intermediate flow conditions). In contrast, debris introduced after the steady-state pool was established was subjected simply to steady-state pool transport. Depending on the test configuration, the spreading of the fill-up transport phase inlet flow demonstrated the ability to push debris away from the outlet screen or toward the screen, thereby either reducing or enhancing the debris-transport fraction. The fill-up flows also pushed debris into relatively quiescent inner compartments, where the debris tended to remain for the duration of the test.

- Pool turbulence associated with the inlet flow kept most small debris, including RMI debris, near the inlet in suspension and rather well mixed and further degraded fragile insulation fragments. The effect of the turbulence lessens with distance from the inlet, and all but the finer (nonbuoyant) debris settled to the sump floor before reaching the sump as the turbulence subsided. The distance required for the turbulence to dampen was dependent on the test configuration. With the inlet near the outlet screen, the turbulence of the inlet flow affects the accumulation of debris on the screen. In addition to keeping debris in suspension near the screen, turbulence could remove accumulated debris from the screen. Debris could be returned to the screen repeatedly, thereby increasing the residence time of the debris within the turbulence and enhancing further disintegration of the debris.
- Several of the containment features and structures represented in the integrated tests offered the potential for debris entrapment because of the rather complex flow patterns that these features established in the pool. Entrapped debris was observed in quiescent regions, such as inner compartments not associated with the inlet location, regions offset from the main flow, the centers of rotational flow (vortices) formed by flow-path expansion, and behind floor barriers. Debris stopped behind a barrier was likely to remain there unless the flow velocities and turbulence were sufficient to lift it over the barrier.
- LDFG insulation debris was found to undergo significant additional fragmentation when it was subjected to the intense, thrashing flow agitation associated with the inlet flow plummeting into the pool. Disintegration appeared to increase when the experiments did not use a flow diffuser and the insulation debris was added to the tank very close to the inlet. Such disintegration affects debris transport and

head loss because it results in the generation of additional fine debris that remains suspended even at low levels of pool turbulence. In addition to LDFG, calcium silicate insulation would undergo substantial disintegration. In the separate-effects tests, calcium silicate fragments were found to dissolve, resulting in a fibrous residue that can be transported easily. The chemical environment may accelerate this disintegration further.

- The beds of LDFG debris that formed on the outlet screen generally consisted of the accumulation of fine fibrous debris that normally remained suspended in the pool and of small pieces of debris that accumulated at the bottom of the screen and then occasionally “rolled up” onto the screen. Although the relative contributions of the two processes could not be determined explicitly, observations suggested that the quantities of accumulated fine, suspended debris were substantially greater than the quantities of debris transported across the floor. Because the fine debris remained suspended and reasonably well mixed in the tank pool, it tended to form a uniform layer across the entire cross section of the screen (that was under water), but the occasional roll-up pieces of debris contributed to its lumpiness. The approach velocities in the integrated tank tests (about 0.11 to 0.14 ft/s) were normally high enough to move pieces of LDFG along the floor to the outlet screen but were generally not high enough to lift a piece of LDFG from the floor to positions higher on the screen. Pulsations associated with flow turbulence occasionally provided the needed boost to lift a piece of debris onto the screen. If sufficient debris were to accumulate at the bottom of the screen to clog the bottom portion of the screen, the approach flow could be redirected upward at the floor level; this redirection could enhance debris lifting.
- RMI debris-transport tests indicated that the most important aspect of evaluating RMI debris transport is probably the transport during the fill-up phase, when the transport velocities associated with the fast-spreading flows can effectively push substantial RMI debris in the direction of the flow. Both stainless-steel RMI and aluminum RMI debris was pushed readily either toward the outlet screen or away from it, depending on the test configuration. After the tank became sufficiently flooded to slow water flows, the RMI did not substantially transport at the tank velocities normally tested. Pieces of RMI debris that were dropped into an

established steady-state pool sometimes floated a significant distance before sinking because air was trapped within the debris.

- Tests of an intact RMI cassette and an insulation pillow showed the ability for fill-up phase flows to transport these types of debris toward a sump screen. These components moved much more easily when dry than when saturated with water. After they were saturated, only the fill-up-phase flow velocities were fast enough in the integrated tests to move these intact items. In a PWR plant scenario, these items could be transported some distance during the fill-up phase until they become saturated or the pool level deepens sufficiently to slow the fill-up flow velocity. These types of debris have potential to block pathways connecting internal compartments.
- Comparisons of pool velocity measurements and debris movement data with CFD predictions provided a qualitative confirmation that CFD codes are suitable for providing the framework for modeling and analyzing debris transport.

The primary use of the data generated from the integrated test program should be the insights gained regarding the transport of debris and the accumulation of debris onto a sump screen. These insights should be valuable in the development of analytical debris-transport models. However, the actual transport fractions should not be applied directly to plant-specific analyses because there is no apparent means of scaling those transport fractions from the test geometry to an actual plant. (See Section 5.4.) Further, the flow velocities of the actual plant could be substantially different from the velocities of the integrated tests. Rather, the models must apply the debris transport phenomenology in conjunction with the separate effects debris transport data to all of the individual plant features for each specific plant. Another potential use of the integrated test data would be to use the data to benchmark a specific debris transport model (e.g., a CFD-based simulation), that is, show that the model can predict the measured transport fractions of the integrated tests.

5.2.7 Bremen Polytechnic Testing of KAEFER Insulation Systems

Extensive buoyancy, transport, and head loss tests were conducted on KAEFER insulation systems by Bremen Polytechnic, Department of Naval Architecture and Ocean Engineering, Laboratory for Ship Hydromechanics/Ocean Engineering.⁵⁻¹⁵ There

is excellent photographic documentation of these tests in the identified reference. The buoyancy and transport aspects and the results of the experiments are summarized below. The head loss aspects and the results of the tests are not addressed here.

Objective

The objective of the buoyancy tests was to measure the time taken for a material to submerge and the additional time taken for a submerged material to sink. The objective of the transport tests was to determine the flow velocity needed to first initiate movement of a sunken material, the velocity needed to maintain motion of the material, and the velocity needed to flip the material up against a vertical screen.

Methodology

KAEFER Insulation Systems Tested

A representative collection of KAEFER insulation samples was tested. All of the samples had been conditioned by heating at 350°C for a minimum of 15 h. Mattresses of fibrous insulation and cassettes of steel-encapsulated fibrous insulation of rectangular and circular cross section were tested. Base insulation materials of fiberglass and mineral wool were investigated, as were RMI cassettes and cassettes of steel-encapsulated silica. Three sample types/sizes were tested:

- As-fabricated: 700 mm x 700 mm, 100 mm thick (mattress or cassette)
- Fragments: As-fabricated samples cut in half transversely to expose the base insulation material
- Shreds: Base insulation material cut randomly into smaller pieces no larger than 50 mm square

Figure 5-20 shows the samples of KAEFER insulation systems tested.

Test Setup

A 1-m-square, 0.8-m-deep tank was used in the buoyancy tests. The water in the tank was maintained at a temperature of 49°C (120°F). Two differing chemical conditions of the water in the tank were established. They are identified in Table 5-2.

De-ionized water was sprayed onto the insulation samples continuously during the buoyancy tests. The spray water was not heated.

A 14-m long, 1.4-m wide flume with a water depth of 0.800 m was used to carry out the transport tests.

Key Findings

The key findings of the buoyancy tests performed on KAEFER insulation systems are identified below. (Note that “remained afloat” means the material was still floating after at least 2 h.)

- All as-fabricated mattresses sank quickly (18.2 to 45.5 s).
- Mattress fragments sank quicker than as-fabricated mattresses (14.7 to 23.3 s).
- Mattress shreds sank in several seconds.
- As-fabricated cassettes with fibrous base insulation remained afloat.
- As-fabricated cassettes with silica base insulation remained afloat.
- Some as-fabricated RMI cassettes sank (18 to 37 min) and some remained afloat.
- Cassette fragments with fiberglass base insulation remained afloat. This is inconsistent with the findings above—that mattress insulation material sinks quickly. The inconsistency is thought to be related to differences associated with the conditioning (heating) of the samples. Although all samples were heated for the same time at the same temperature, it was noticed that the base fiberglass insulation in cassettes had a much darker color than the fiberglass insulation in mattresses. The suspicion is that the darker color is indicative of changed material properties, including buoyancy characteristics.
- Fiberglass shreds removed from cassettes also remained float.
- Cassette fragments with mineral wool base insulation sank within a few minutes.
- Some cassette fragments with silica base insulation sank (9 to 52 min) and some remained afloat.
- RMI cassette fragments sank in several minutes.
- Only insignificant variations with water pH were seen.

Illustrative photographs of the buoyancy tests are included in the Bremen report of the buoyancy tests. Figure 5-21 is an example.

The key findings of the transport tests performed on the KAEFER insulation systems follow.

- As-fabricated mattresses began to show movement at flow velocities between 0.15 and 0.33 m/s.



Figure 5-20 Samples of KAEFER Insulation Systems Tested

Table 5-2 Water Chemical Conditions in KAEFER Insulation Buoyancy Tests		
Chemical	pH 7.0	pH 9.2
Boric acid	1800 ppm	1800 ppm
Sodium	84 ppm	2400 ppm



Figure 5-21 Bremen Buoyancy Test Illustration

- Mattress fragments began to move at velocities between 0.19 and 0.27 m/s.
- Fibrous insulation shreds began to move at velocities between 0.06 and 0.26 m/s.
- As-fabricated cassettes with fibrous base insulation began to move at flow velocities between 0.04 and 0.15 m/s.
- Cassette fragments with fibrous base insulation showed movement between 0.19 and 0.48 m/s.
- Fragments of cassettes having silica base insulation and RMI cassettes showed movement at flow velocities between 0.38 and 0.54 m/s.
- The velocity required to maintain the motion of a sample down the flume was typically slightly higher than the velocity first noticed to cause motion. The velocity required to flip material up against a vertical screen was slightly higher still.

Limitations

There is substantial spread in the data reported on the flow velocity needed to move seemingly very similar KAEFER insulation samples. The differences are not explained in the test report.

5.2.8 Alden Research Laboratory Testing of Owens-Corning Fiberglass (NUKON) Insulation

Alden Research Laboratory conducted transport and head loss experiments on nonencapsulated NUKON® insulation manufactured by Owens-Corning Fiberglass Corporation.⁵⁻¹⁶ NUKON® is a LDFG thermal insulation widely used in nuclear power plants. The transport aspects and results of the experiments are summarized below. The head loss aspects and results are discussed in Section 7.

Objective

The transport tests were aimed at determining the flow velocity needed to initiate motion of sunken NUKON® insulation fragments of various sizes.

Methodology

The tests were conducted in a 2-ft wide, 2-ft deep, 20-ft long flume. Water was introduced at one end of the flume behind a flow-straightening screen; it exited at the other end over a gate of adjustable height. The gate was far enough downstream from the test section to ensure a lack of velocity-profile disturbance.

The samples of insulation of various sizes first were sunk (which required prolonged squeezing under water) and then were placed at the bottom of the flume. Flow was initiated, and the flow velocity at which sustained motion of the samples occurred was recorded. Velocity was measured approximately 3 in. above the bottom of the flume. The water depth was 1.5 ft.

Key Findings

Table 5-3 lists the flow velocities needed to initiate motion of NUKON samples varying in size from shreds to 12 in. x 12 in. x 2 in.

The velocities needed to initiate motion of the insulation samples were rather independent of sample size, although a trend toward higher velocities for larger sample sizes can be detected.

Limitations

The test report did not discuss pretreatment of debris samples before they were introduced into the water. The report did state that prolonged squeezing of the samples under water was required to induce the samples to sink. More recent testing pretreated samples in heated water for a significant period to removed trapped air before introducing them into the test. Possible residual air trapped in the debris samples of these tests could have compromised the test results.

5.2.9 STUK Metallic Insulation Transport and Clogging Tests

A set of experiments investigating the transport characteristics and strainer-clogging potential of a specific type of RMI debris was carried out in the Imatran Voima Oy (IVO) Power Plant Laboratory for

the Finnish Centre for Radiation and Nuclear Safety (STUK).⁵⁻¹⁷ The following summary of the experiments is adapted from the reference cited above.

Summary

A series of experiments was conducted to quantify the transport characteristics and strainer-clogging potential of RMI debris. The experiments investigated DARMET insulation, the brand of metallic insulation that has been installed in Finnish BWRs. As the size and shape distribution of LOCA-generated metallic insulation debris is undefined, the study was conducted in a parametric manner, assuming that size can vary from 0.01 to 1 m and concentrating on fairly flat pieces. Most of the pieces investigated were square or rectangular, although triangular pieces and strips also were tested.

The experiments addressed settling, transport in both horizontal and vertical circulating flow fields, and strainer head loss caused by both metal foil pieces alone and foil pieces mixed with fibrous mineral wool debris. The effect of foils on the back-flushing of a clogged strainer also was investigated. The major findings related to settling and transport are summarized below. (Valuable observations of how RMI foils build up on a sump screen and measurements of related head loss were documented in the experiments.) These observations are presented in Section 7, “Debris Head Loss.”

- Metallic foils of all shapes tended to float. Foils had to be submerged and agitated to remove air bubbles before they would sink.

Sample Size (in.)	Flow Velocity Needed to Initiate Motion (ft/s)
12 x 12 x 1/2	0.35
12 x 12 x 2	0.36
6 x 6 x 1/2	0.34
6 x 6 x 2	0.37
3 x 3 x 1/2	0.30
3 x 3 x 2	0.36
1 x 3 x 1/2	0.28
1 x 3 x 2	0.26
1/2 x 1/2 x 1/8 (shred)	0.30

- Settling velocities ranging from 0.03 to 0.4 m/s were measured. Swinging/gliding, tumbling, and screw-like settling motions were observed. Settling with horizontal swinging/gliding was the most stable and took the most time. Only the largest pieces, > 0.6 m, folded significantly during settling because of the rigidity of the dimpled foil. Pieces that descended in horizontal orientations did so at velocities ranging from 0.04 to 0.08 m/s. Size had little effect on settling velocity.
- In horizontally circulating flow, crumpled pieces of metallic insulation moved readily at flow velocities between 0.1 and 0.2 m/s. Smaller, flatter foils required higher velocities to move than larger, crumpled foils.
- In a vertically rising flow, metallic insulation foils became waterborne if the upward flow velocity exceeded the settling velocity of the foil. In a vertically circulating flow, foil pieces exhibited circulatory motion within the flow field and remained water borne. Foil pieces settled at the threshold velocity above which foil circulation was sustained.
- From a settled condition, foils dispersed and became waterborne as the flow rate was increased.

5.3 Debris Transport in Pooled Water Analyses

The NRC has performed analyses investigating the transport of insulation and other debris in PWR containment sump pools, BWR drywell floor pools, and BWR suppression pools. The results of these analyses provide qualitative insights and quantitative information relevant to considerations of debris transport in PWR containment pools.

5.3.1 Phenomena Identification and Ranking Tables

5.3.1.1 Boiling-Water Reactor Phenomena Identification and Ranking Table

The NRC sponsored the formation of a PIRTs panel of recognized experts with broad-based knowledge and experience to identify and rank the phenomena and processes associated with the transport of break-generated debris through a BWR containment drywell following the initiation of one or more accident sequences.⁵⁻² The primary objective of the BWR PIRT was to support the drywell debris transport study (DDTS); the pool-transport portion of the study is discussed in Section 5.3.2. The PIRT process was designed to enhance the DDTS

analysis by identifying processes and phenomena that would dominate the debris transport behavior. Further, these processes and phenomena were prioritized with respect to their contributions to the reactor phenomenological response to the accident scenario. The PIRT panel also evaluated the plans for experimental research, the experimental results, and the analytical results. Their final report was updated to reflect the final results of the DDTS. Debris transport in the BWR drywell floor has similarities to debris transport in a PWR sump pool: both pools would be relatively shallow, both have water falling into the pool from break overflow and containment spray drainage, and both can have turbulent or quiescent modes of debris transport, depending on scenario conditions. The phenomena ranked as having the highest importance with respect to debris transport within a BWR drywell floor pool are listed in Table 5-4.

5.3.1.2 Pressurized-Water Reactor Phenomena Ranking and Identification Table

Like the BWR PIRTs discussed in Section 5.3.1.1, the NRC sponsored the formation of a PIRT panel of recognized experts with broad-based knowledge and experience to identify and rank the phenomena and processes associated with the transport of debris in PWR containments following the initiation of one or more accident sequences.^{5-1,5-18} The PWR PIRT has been used to support decision-making regarding analytical, experimental, and modeling efforts related to debris transport within PWR containments. The scope of the PWR PIRT was discussed in Section 4.3.2.2, which discussed the airborne and washdown transport aspects of the PIRT.

The panel identified a primary evaluation criterion for judging the relative importance of the phenomena and processes important to PWR containment debris transport. Each phenomenon or process identified by the panel was ranked relative to its importance with respect to the transportation of debris to the sump entrance. Highly ranked phenomena and processes were judged to have a dominant impact with respect to the primary evaluation criterion. The important processes relating to debris transport in a PWR sump pool are listed and described in Table 5-5.

It is important to note that the processes and phenomena ranked as highly important by the PIRT panel sometimes differed from the processes and phenomena that appeared to dominate transport in the experiments or analyses, because the PIRT assessments were done before the research was

Table 5-4 Highly Ranked Phenomena from BWR Drywell Floor Pool Debris Transport PIRT Table	
Processes and/or Phenomena	Description
Pool Formation	Creation of a pool of water on the drywell floor sufficiently deep to allow overflow into wetwell transfer piping due to the accumulation of water from all sources higher in the drywell.
Pool Overflow	Transport of water from the pool on drywell floor into wetwell vent pipes.
Pool Flow Dynamics	Multi-dimensional flow patterns and velocities within the pool of water on the drywell floor; includes free-surface (vertical) velocity profile and turbulent mixing (circulation) flows.
Pool Debris Transport	Relocation of debris in the pool of water on the drywell floor toward wetwell vent pipe entrances.
Debris Settling	Downward relocation (sedimentation) of debris within the pool of water on the drywell floor under the force of gravity.

Table 5-5 Highly Ranked Processes and Phenomena for the Debris Transport in a PWR Containment Sump Pool	
Processes and/or Phenomena	Description
Pool Formation	Creation of a pool of water on the containment floor sufficiently deep to allow overflow into sump due to the accumulation of water from all sources higher in the containment.
Pool Agitation	Agitation of the pool by liquid streams falling or draining from above.
Pool Flow Dynamics	Multidimensional flow patterns and velocities within the pool of water on the containment floor; including increasing pool height, circulating flows, and turbulent mixing flows.
Film Entry Transport	Introduction of debris into the pool on the containment floor as draining films containing debris enter the pool.
Liquid Entry Transport	Introduction of debris into the pool on the containment floor as draining liquid streams containing debris enter the pool.
Pool Debris Disintegration	Breakup of relatively large pieces of debris into smaller particles that can be reentrained into the flow stream caused by the impact of falling liquid streams from the break, fan coolers, and liquid draining off surfaces.
Pool Debris Settling	Downward relocation (sedimentation) of debris within the pool of water on the containment floor under the force of gravity.
Pool Debris Reentrainment	Movement of debris residing off the basement floor and into higher elevations of the pool.
Pool Debris Transport	Relocation of debris in the pool of water on the containment floor toward sump entrances.
Sump-Induced Flow	Following sump activation, a directed flow is established toward the sump.
Sump-Induced Overflow	Transport of suspended debris over the sump curb and to the trash rack/debris screen. In addition to the sump curb, the buildup of ramp-like debris beds at the base of the curb must be considered for their impact on flow patterns and debris transport.

performed. One such process was sheeting flow dynamics (the spreading of water on the containment floor before the pool is formed) with associated sheeting debris transport, which the PIRT panel ranked as having low or medium importance. However, the data from the integrated tank tests indicated that debris transport caused by sheeting flow could be very important. Thus, evaluating the importance of a process or phenomena should not be based solely on the PIRT evaluation.

5.3.2 Boiling-Water Reactor Drywell Floor Pool Debris Transport Study

In September 1996, the NRC initiated a study, the DDTS, to investigate the transport and capture characteristics of debris in BWR drywells using a bounding analysis approach.⁵⁻¹⁹ The focus of the DDTS was to provide a description of the important phenomena and plant features that control and/or dominate debris transport and the relative importance of each phenomenon as a function of the debris size. Further, these analyses were to demonstrate calculational methodologies that can be applied to plant-specific debris transport estimates. It should be noted that the DDTS focused almost entirely on the transport of LDFG insulation debris. The debris-transport processes studied included the processes involved in the transport of debris during the reactor blowdown phase by way of entrainment in steam/gas flows, during the post-blowdown phase by water flowing out of the break and/or containment sprays, and in the pool of water that would form on the drywell floor. The overall study and the airborne and washdown debris-transport processes were discussed in Section 4.3.3.2 of this report. The drywell floor pool aspects are discussed here.

Substantial quantities of insulation debris could land on the drywell floor during the primary system depressurization or be washed down to the drywell floor from drywell structures after being captured during depressurization. From here, the debris could then be transported from the floor into the vent downcomers. Therefore, determining the potential for debris to remain captured on the floor was a necessary step in the overall debris transport study. This determination was made based on simulating the drywell floor pool for a variety of conditions using a commercially available CFD code.⁵⁻²⁰ The primary objective of this analysis was to evaluate the potential for fibrous debris to settle in drywell pools and to estimate fractions of debris that would be transported to the suppression pool.

The study considered Mark I, II, and III designs for variations in pool depth and entrance conditions to the pools.

The CFD results needed to be benchmarked to prototypical experimental data to correlate pool turbulence levels with conditions that allowed debris to settle. This was accomplished by simulating the ARL PP&L flume tests⁵⁻⁷ with the CFD code and then correlating the code-predicted turbulence level for a given test with the test results showing whether fibrous debris actually settled in that test. The maximum levels of turbulence that allowed debris to settle were determined and applied to the drywell floor pool simulation results. Two maximum levels were determined, one for small debris and one for large debris.

The results of each of the drywell floor pool simulations consisted of graphical pictures (available in the reference⁵⁻²⁰) showing pool flow behavior, such as two- and three-dimensional color pictures of flow velocities and flow turbulence in the form of specific kinetic energy. These turbulence levels then were compared with the maximum levels for debris settling determined by the code calibration. If pool turbulence were higher than a maximum level, debris likely would not settle. On the basis of this graphical data, engineering judgment was applied to determine the likelihood for debris settling for each pool configuration. With noted design-specific exceptions, drywell floor pools formed by recirculation break flows are considered likely to transport the majority of insulation debris into the vent downcomers and pools formed by the containment sprays are likely to retain debris.

The BWR pool debris-transport methodology also is generally applicable to specific aspects of PWR sump pools because the debris transport in the BWR drywell floor has similarities to debris transport in a PWR sump pool. However, the drywell floor pools studied in the DDTS and the PWR sump pools have differences that would affect debris transport. In the DDTS, the potential for debris transport tended to be either the debris transported or it did not. When the break flow plummeted into the drywell floor pool at full throttle, the resulting turbulence levels were clearly high enough that, from a conservative standpoint, all of the debris would remain sufficiently suspended to transport into the downcomer vents. When the break flows were throttled back so that water flows to the drywell floor pool came mostly from the containment sprays, pool turbulence was low enough that it appeared that most of the debris

would settle and hence not transport with the overflow into the vent downcomers. Because the overflow was not at the floor level, floor debris transport was not as important because no mechanism was identified to reentrain the debris near the vents.

In a PWR sump pool, the pool turbulence level would be expected to be much less uniform because of the geometry of the sump. With the break located inside an interior compartment (e.g., steam generator compartment), most of the pool turbulence could be contained within the compartment, leaving the bulk of the sump annulus rather quiescent. If the break were in the annulus, then more of the annulus would be highly turbulent but not the inner compartments. In a PWR sump pool, the evaluation of pool turbulence will be much more plant- and accident-specific.

5.3.3 Boiling-Water Reactor Suppression-Pool Debris-Transport Analysis

In September 1993, the NRC initiated a detailed reference-plant study using a BWR/4 reactor with a Mark I containment.⁵⁻⁹ The reference plant was a Mark I design with a relatively small suppression pool, leading to comparatively faster strainer flow velocities than other BWR plants. In addition, more than 99% of the primary system piping was insulated with steel-jacketed fiberglass insulation. The primary objective of the study was to determine the likelihood that a postulated break in the primary system piping of the reference BWR plant could result in the blockage of an ECCS strainer and the loss of pump NPSH. The analyses involved both deterministic and probabilistic techniques. The deterministic analyses focused on models to simulate phenomena governing debris generation, drywell and wetwell debris transport, and strainer head loss. The probabilistic analyses focused on evaluating the likelihood of core damage related to strainer blockage based on LLOCA-initiators. The BLOCKAGE computer program^{5-21,5-22} was developed to calculate debris generation, debris transport, fiber/particulate debris-bed head losses, and impact on the available NPSH. The suppression pool debris transport analysis of that study is discussed here.

A model was developed to estimate the quantity of insulation debris, after it is in the suppression pool that would transport to an ECCS suction strainer. In addition, the suppression-pool model addressed the transport of sludge particles within the pool to a strainer. The transport of debris within the suppression pool to the ECCS suction strainers is

complicated by a variety of effects. Models for these effects were broken into two main phases with an interim transition phase. During the blowdown phase, pool dynamics would be governed by the extremely dynamic primary system depressurization. The LOCA-induced pool turbulence, such as condensation oscillations and chugging within the downcomers, would re-suspend debris initially settled to the pool floor (i.e., sludge), uniformly distribute the debris throughout the suppression pool, and further break up pieces of debris. During the relatively quiescent washdown phase, gravitational settling would be important as debris could settle to the suppression pool floor once again. Analytical models were developed that were based on and benchmarked to the experimental data collected for strainer head losses and suppression-pool sedimentation. These time-dependent models were programmed into the BLOCKAGE code, which was used to predict debris quantities that would accumulate on the strainers by type and size.

The BLOCKAGE code (Version 2.5) included models for transient debris bed formation and used the fiber/particulate head loss correlation (known as the NUREG/CR-6224 head loss correlation) developed in the reference plant study. The correlation was validated for laminar, transient, and turbulent flow regimes through mixed beds. BLOCKAGE is an integrated calculational method with a graphical user interface (GUI) for evaluating the potential for loss of ECCS pump net positive suction head margin as a result of insulation and non-insulation debris buildup on suction strainers following a postulated LOCA in BWRs. BLOCKAGE incorporates the results of multi-year NRC-sponsored research documented in NUREG/CR-6224. It also provides a framework into which users can input plant-specific/insulation-specific information for performing analysis in accordance with Revision 2 of Regulatory Guide 1.82.

BLOCKAGE 2.5 allows the user to simulate debris generation and subsequent transport of multiple types of debris, including fibers, particles, and metals, using either a three-zone destruction model or a user-specified quantity of debris for transport. The debris transport from the drywell to the wetwell can be location- and time-dependent. The transport during the blowdown period caused by depressurization flows is treated separately from the transport during the washdown phase, which is a result of ECCS recirculation, containment spray, and steam condensate flows. Two sizes of pipe-

break scenarios are considered: large and medium LOCAs. The debris transport within the suppression pool, including the deposition of debris on the strainers and the debris concentration within the pool, is calculated separately for each discrete debris size and debris type. The suppression pool is treated as a single volume of water. Specifically, debris concentration does not vary with location in the pool. The user supplies several model parameters that are time-dependent: the calculational time step, the pump flow rates, the drywell debris-transport rates, the suppression pool temperature, and the suppression pool resuspension and settling rates. The BLOCKAGE code was subjected to rigorous coding verification to ensure that it performs as it was designed to perform. BLOCKAGE was validated against applicable experiments.

At the time that the BLOCKAGE code was developed, the approach velocities to existing plants' strainers were relatively uniform even with the accumulation of debris. Hence, code models were based on the assumptions of uniform approach velocity, uniform debris deposition, and constant surface area. More complex strainer designs were developed as part of the resolution of the strainer-clogging issue, such as the stacked-disk and star-shaped designs. Debris deposition on strainers of these designs starts as a uniform deposition on the entire screen area, but eventually, debris shifts to fill the inner screen regions, creating substantially nonuniform approach velocities and debris deposition. After the inner spaces are filled, approach velocities and deposition again approach uniformity. Hence, the BLOCKAGE code is appropriate to calculate head loss with small quantities of debris on the strainer (uniform deposition) and again when there are substantial quantities of debris on the strainer (gaps filled with debris) but not with quantities between.⁵ With small quantities of debris on the strainer, the entire strainer screen area would be used. With large quantities of debris, the circumscribed area would be appropriate. BLOCKAGE could be modified with a variable area that is a function of debris volume so that complex strainers could be modeled through the full range of debris deposition.

A typical suppression-pool transport analysis result is shown in Figure 5-22.

⁵The quantities of debris involved depend on the size and design of the suction strainer.

5.3.4 Pressurized-Water Reactor Volunteer Plant Pool Debris Transport Analysis

A volunteer PWR plant was chosen for detailed analysis with the primary objective of developing and demonstrating an effective methodology for estimating containment debris transport that could be used to assess the debris transport within PWR plants. This work is ongoing and is thus not available for this report. (The preliminary methodology of the airborne and washdown debris-transport analysis was discussed in Section 4.3.3.3.) Once completed, it is expected that the report for this study will further demonstrate analytical methodology for estimating debris transport within a sump pool.

5.3.5 Nuclear Regulatory Commission Review of Licensee Experimental Approach to Sump Blockage Potential

The Millstone Nuclear Power Station, Unit 2, (Millstone-2) licensee conducted experiments to investigate the vulnerability of the station's emergency recirculation sump to blockage by debris resulting from a LOCA.⁵⁻²³ The experiments employed a sub-scaled representation of the Millstone-2 containment floor. The test report describing the experiments was submitted to the NRC for review and comment. LANL assisted NRC in its review.

Objectives

The objective of the Millstone-2 licensee's experiments was to determine whether the emergency recirculation sump of the Millstone-2 containment is susceptible to blockage by insulation and other debris that might be generated in a LOCA.

The objective of the review performed by NRC was to provide the industry with feedback regarding the validity of such experiments in resolving GSI-191 concerns on a plant-specific basis.

Methodology

Licensee Experiments

The debris-transport experiments employed a downsized representation of the Millstone-2 containment floor and sump complete with a sample sump screen and a physically representative curb. Figure 5-23 shows the experimental configuration. The experiments were conducted in a walled-off sector of a 1300-gal. cylindrical tank.

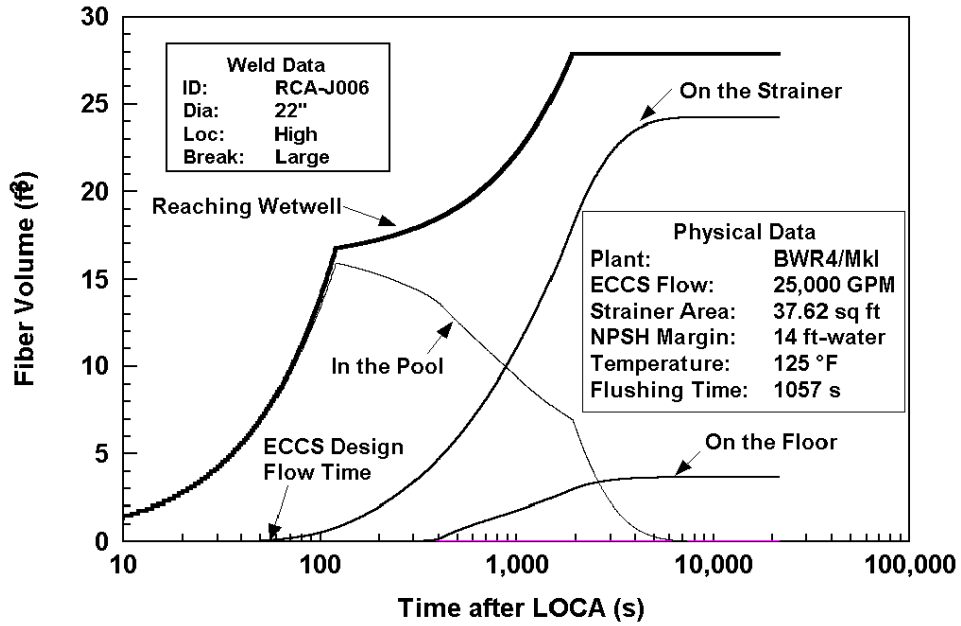


Figure 5-22 Typical Fibrous Debris Transport in the Suppression Pool

Millstone-2 Tank Test

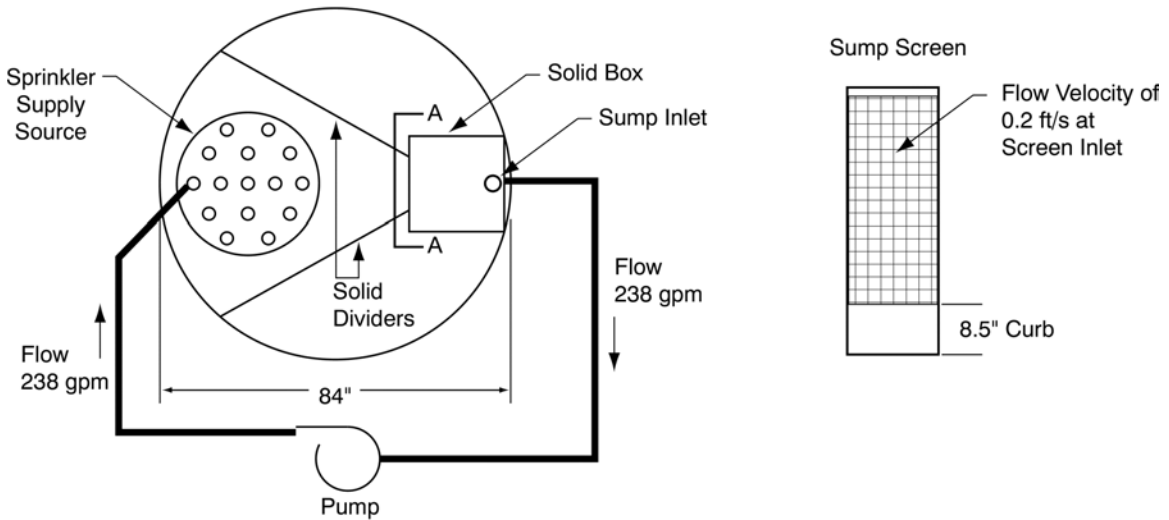


Figure 5-23 Configuration of Millstone-2 Debris-Transport Experiment

A box open to flow on one side and covered with screen on that side represented the sump. The screen area was 2.64 ft², and an 8.75-in. curb was placed in front of the screen. Water was circulated through a closed loop in the experiments. Suction was from the bottom of the sump box. Return flow was through a diffuser above the water surface such that the water fell into the tank. Flow rates were such that the flow velocity at the sump screen, assuming a uniform velocity over the whole screen, was between 0.2 and 0.25 ft/s. This compares favorably to the 0.2 ft/s at the actual Millstone-2 sump screen.

The tank was filled with water to a 55-in. height, and measured quantities of debris were added uniformly across the test sector of the tank. The debris was allowed to sink to the floor. The desired flow (~236 gpm) then was established, and the transport of the debris and its accumulation on the screen were observed. Paint chips (zinc and epoxy), LDFG shreds, and RMI fragments were investigated.

NRC Review

The NRC review of the licensee experiments focused on determining whether the water flows developed in the tests could be considered representative of what would exist on the floor of the Millstone-2 containment following a LOCA. CFD simulations of the experiments and of postulated pools on the Millstone-2 containment floor were used.

A CFD model of the licensee's experimental configuration was constructed. The flow rates explored in the experiments were established in the model. The velocities predicted near the floor of the tank were considered relative to the known transport velocity of the debris being tested and determinations were made as to the potential for debris transport. The transport determinations were compared with the transport observations made in the experiments.

A CFD model of the lower region of the Millstone-2 containment also was constructed. A break in the cold-leg piping 15 ft from the sump and 20 ft above the floor was represented. This reflects the position of the reactor coolant system piping nearest the sump. A recirculation flow rate characteristic of full ECCS design flow given a large LOCA was specified (10,480 gpm) and a characteristic pool depth of 55 in. was imposed. The flow velocities developed in the CFD calculation in the vicinity of the sump were considered with respect to their potential to transport debris. The inferred transport

potential was compared with the debris transport observed in the licensee experiments.

Results

Licensee Experiments

The experiments conducted by the licensee saw no debris transport. The conclusion was drawn that no potential exists for debris generated in a LOCA to block the emergency recirculation sump in the Millstone-2 containment.

NRC CFD Modeling of Licensee Experiments

The CFD simulation of the licensee's experiment showed that no transport of debris would occur in the experiment. This agrees with the licensee's findings in the experiments.

NRC CFD Modeling of Millstone-2 Lower Containment Pool

The CFD simulation of the pool that would develop on the floor of the Millstone-2 containment following a LOCA where the pipe break was near the sump, identified a large potential for debris transport to the sump. This contrasts with the conclusion drawn by the licensee from the results of their experiments that no potential for debris transport exists. The reason for this discrepancy is the way water was returned to the pool in the experiment versus the way water was returned to the pool in the CFD calculation. In the licensee's experiment, returning water passed through a fixture that sprayed the water over much of the surface of the test sector of the pool. The momentum of the spray streams was such that the spray streams penetrated only slightly into the pool. In the CFD calculation, returning water fell into the pool as a collected stream uninterrupted from a height of 20 ft. The momentum of the falling stream in the CFD calculation was such that the stream penetrated well into the pool. The effects of the CFD stream's greater penetration were larger velocities at the bottom of the pool and more mixing (higher turbulence) in the pool. Both of these effects aid debris transport.

Conclusions

The conclusion drawn by the NRC reviewers was that the experimental investigations performed by the licensee into the potential for debris transport to the emergency sump following a LOCA led to invalid conclusions. The reason for this was a problem of similitude. Specifically, the momentum that would carry into the containment pool with the water stream falling from an elevated pipe break (near in plan to the sump) was not accounted for in the experiments. Without this momentum accounted for, the velocity fields developed in the

experiments were not representative of what would develop in a pool on the containment floor of Millstone-2.

Presumably, the experiment could be modified to have the returning water plummet into the test sector of the pool, as it would fall into an actual Millstone-2 containment pool. Although there may be additional similitude (scaling) issues, debris-transport observations made with water entering the pool realistically would be credible.

The issue of continuously suspended debris (e.g., individual fibers) was apparently not addressed by the Millstone-2 licensee. When a break jet destroys LDFG insulation, some portion of the debris, perhaps a few percent of the ZOI insulation, would be in the form of fine fibers that would remain suspended in the sump pool. Virtually all of this debris would transport and accumulate on the sump screen. The tests should have used more realistic simulated debris (may be unnecessarily critical of licensee).

5.3.6 Computational Fluid Dynamic Simulations of UNM Integrated Debris-Transport Testing

The integrated debris transport experiments discussed in Section 5.2.6⁵⁻³ were complemented by computational fluid dynamic (CFD) calculations to demonstrate the ability of a CFD computer code to predict the complex flow patterns of the tests and to help visualize those flow patterns. CFD computer codes may well be used to support analyses of debris transport in PWR sump pools. The inherent difficulties associated with modeling a containment pool in any flow analyses are

- the complex three-dimensional non-uniform patterns of the flow with the sump pool;
- the complications associated with free-surface effects;
- the difficulties in resolving the momentum dissipation of the falling water stream(s) entering the pool, i.e., the localized circulative flows and related turbulence developed in the pool by falling streams;
- the complex influence of walls, curbs, etc.;
- the potentially complex influence of substantial quantities of larger debris within the pool, perhaps partially blocking flow channels;
- the directional influences of the flow being drawn from the pool through the sump; and
- the time variance of flow patterns.

The CFD simulations of the integrated debris-transport tests were performed using the FLOW-3D computer code. FLOW-3D⁵⁻²⁴ is a general-purpose software package for modeling the dynamic behavior of liquids and gases influenced by a wide variety of physical processes. The program was constructed for the treatment of time-dependent, multidimensional problems. FLOW-3D is applicable to almost any flow process.

The FLOW-3D model simulated the geometry of the test tank, including the internal wall structure, by scaling down the dimensions of the internal structures of a PWR plant layout provided in an AutoCAD drawing. (The test tank was one-tenth the size of the PWR containment.) The water was introduced into each simulation at a location that corresponded to the configuration of the test and at the mass flow rate specified for that test. The recirculation-cooling sump was simulated by a depression in the floor where water was removed from the simulation at the same rate as water was introduced. A variety of test configurations and flow rates was simulated.

The velocity pattern from a simulation is shown in Figure 5-24. As indicated by the right side of the figure bar, the velocities range from zero to 0.2 ft/s (0.06 m/s) and are indicated by shading; white indicates near-zero flow and black indicates near 0.2-ft/s or faster flow. (In the reference document, the flow patterns were in color and are easier to visualize.) The internal structures are indicated in the figure. The solid arrows indicate the general direction of flow. The water was introduced into one of the interior compartments that represented a steam generator enclosure (indicated by the circle). The simulated recirculation sump was located near the bottom of the diagram.

The CFD computer code simulations were compared qualitatively with experimental measurements of flow velocities and general observations of the pool flow patterns. The comparison clearly indicated that the simulation captured the significant features of the pool flow and the predicted flow velocities were comparable with the measured velocities.

5.4 Summary of Approaches to Modeling Containment Pool Transport

Two approaches to modeling the transport of debris in a containment pool are found in the literature. One is experimental in nature; the other is computational.

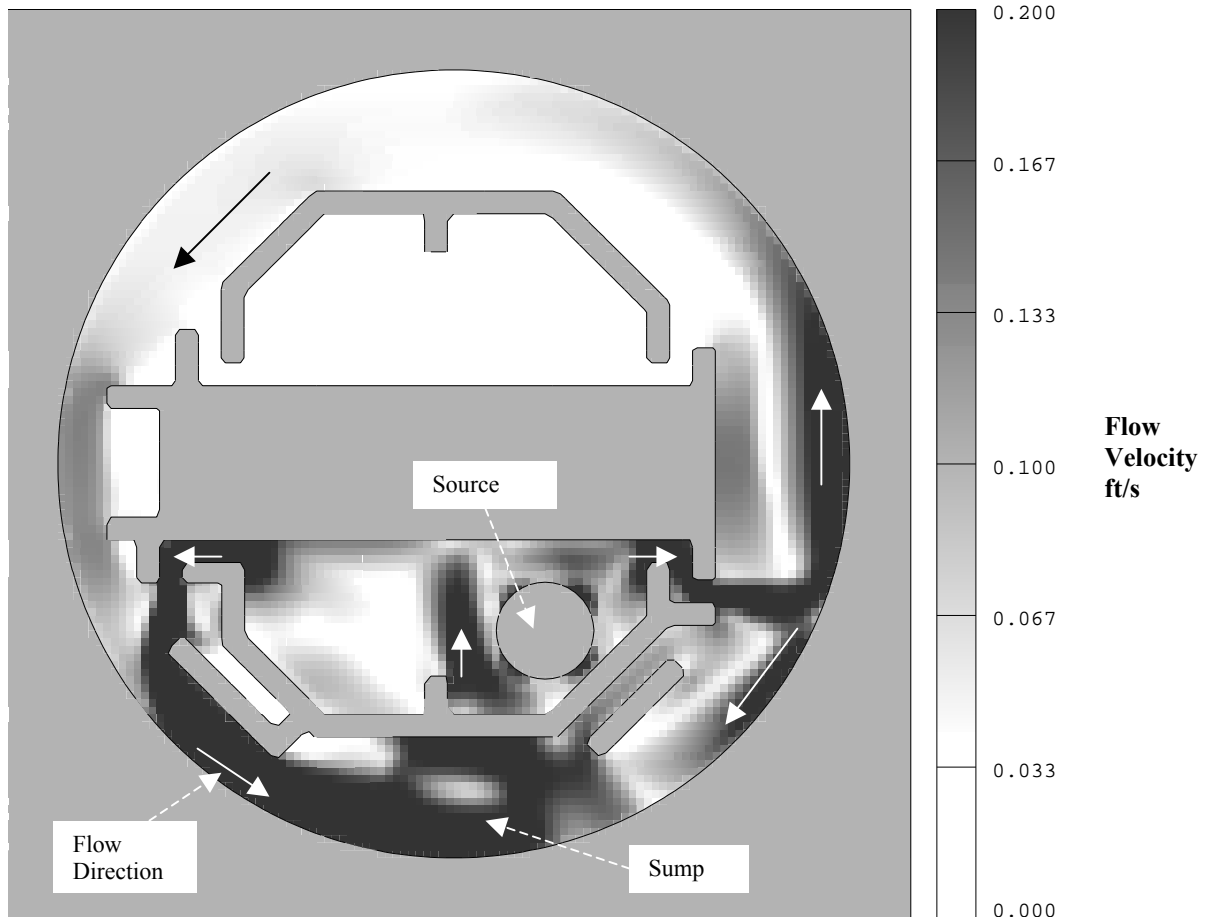


Figure 5-24 Sample CFD Prediction of Flow Velocities for One Test Configuration

The experimental approach to modeling debris transport in a particular containment sump pool involves building a scaled representation of the floor of the containment, complete with all the walls, curbs, equipment, etc. that would determine the flow patterns in the pool. Defendable similitude between the physical containment and the model must exist here; however, a defendable similitude would be difficult to develop. The rationale for scaling the water flow differs substantially from the rationale for scaling debris transport, but both processes must be scaled simultaneously. Appropriate inertial-force scaling, which governs water flow, requires that flow velocities be reduced with the square root of the length scale. Appropriate viscous force scaling, which governs debris transport, requires that flow velocities be increased proportional to the length scale. It may be that water-flow and debris-transport characteristics cannot be satisfied simultaneously in a scaled experiment. Although illustrative experiments of containment pool modeling are

documented, no defendable scale modeling of debris-transport potential in a specific containment has been accomplished to date. Critical testing considerations include recirculation flow rate, debris size, the height of the pipe break above the floor, the preparation of the debris (size distribution and pretreatment to remove trapped air), and introduction of the debris into the test. The potential for debris disintegration within the pool must be investigated.

The computational approach to modeling debris transport in a containment pool involves performing CFD calculations. Although commercially available CFD codes are clearly suited to predicting the flow patterns and velocity fields that would exist in a containment pool, the codes lack the ability to directly predict the transport of the various types of insulation and other debris that are present. This is because CFD codes do not have the capacity to resolve or account for the intricate transport characteristics of the different types, shapes, and

sizes of potential debris. As such, the flow-field predictions from a CFD containment pool calculation (e.g., velocities and turbulence levels) must be compared with experimentally determined debris transport characteristics to infer whether transport would occur. Illustrative CFD calculations of containment pool debris transport have been documented, but as with experimental containment pool modeling, no defensible complete CFD analysis of debris-transport potential in a specific containment has been accomplished to date.

Predicting the transport of insulation debris is a very complex process, perhaps too complex to generalize in any simple model. In addition, each plant has plant-specific features that would affect the transport of debris, and the transport process will necessarily vary with such parameters as the location of the break. Ideally, incorporating models for the various transport processes into CFD code might one day allow a code to perform the complete simulation. Such a CFD simulation then could take into account all the plant-specific aspects associated with debris transport. However, such computational capability does not yet exist. Meanwhile, the transport fractions measured in the integrated tests should provide some insights into plausible transport fractions for an actual plant. In addition, these tests, particularly the long-term LDFG transport tests, can serve as a potential means of benchmarking models developed to estimate debris transport.

5.5 Guidance

Certain accident specifics, plant features, debris characteristics, and physical phenomena are clearly important to consider in any analysis aimed at determining the potential for debris transport in a PWR containment pool. Based on the insights gained primarily from the integrated tests, the following guidance should prove helpful when developing a suitable plant- and accident-specific debris-transport model.

- Identify the accident scenario, including location, size, and possibly orientation of the pipe break and how water spilling from it would make its way to the containment floor. Determine whether the containment sprays would activate.
- Identify and conservatively estimate the sources of debris to the pool. This includes the type of debris (insulation or other type) and the size distribution of each type; when and where the debris enters the pool; and the transport

characteristics of the debris such as buoyancy, terminal settling velocity, tumbling, lift, and accumulation velocities.

- Evaluate the relocation of debris on the floor as the sump pool fills, specifically where the break overflow will push the debris initially deposited onto the floor. As the pool fills, most of the debris, if not all, will saturate relatively rapidly in hot water and sink to the floor, with the exception of the truly buoyant debris (e.g., Neoprene and some foam insulations) and the fine debris in suspension. A few pieces of debris may trap air and float for a while, but this is likely a smaller part of the total.
- Characterize the containment pool—determine the depth, flow patterns, flow velocities, turbulence levels, and locations of any quiescent regions in the pool after the directed flows associated with recirculation through the emergency sump develop. Also consider the effect that substantial debris, particularly larger pieces, could have on the sump pool characteristics (e.g., flow channel blockage).
- Specifically account for quantities of fine debris that would remain suspended in the pool long term even under relatively quiescent conditions. Such debris would include individual fibers⁶ (or small bunches of fibers) and particulate debris such as disintegrated calcium silicate. All amounts of these types of debris probably should be considered as directly transportable to the sump screens.
- Account for the quantities of fine debris generated by degradation of the larger pieces of debris by the pool turbulence associated with water plummeting into the pool. This must consider the location of the debris sources relative to the location of the plummeting water.
- Based on the characteristics of the containment and estimates of debris and the characteristics of that debris, conservatively estimate the quantities of debris likely to be entrapped in specific locations identified such as isolated compartments, offset from the main flow, the centers of vortices, and behind obstacles. This applies predominantly to sunken and floor transportable debris.

⁶As a point of reference, 15% to 25% of the LDFG insulation blankets destroyed in the air impact testing conducted at the Colorado Engineering Experiment Station (CEESI) was fine debris, i.e., debris so fine it either passed through a fine-debris retention screen or could be collected only by hosing down the interior test chamber walls.⁵⁻²⁵

- If the sump screen is not completely submerged in the pool, account for whether significant buoyant debris could float to the screen and contribute to screen head loss.

5.6 References

- 5-1. LA-UR-99-3371. B. E. Boyack et al., "PWR Debris Transport in Dry Ambient Containments—Phenomena Identification and Ranking Tables (PIRTS)," LA-UR-99-3371, Revision 2, December 14, 1999.
- 5-2. INEL/EXT-97-00894. G. Wilson et al., "BWR Drywell Debris Transport Phenomena Identification and Ranking Tables (PIRTS)," Final Report, INEL-EXT-97-00894, Lockheed Martin Idaho Technologies, Idaho Falls, ID, September 1997.
- 5-3. D. V. Rao, C. J. Shaffer, B. C. Letellier, A. K. Maji, and L. Bartlein, "GSI-191: Integrated Debris Transport Tests In Water Using Simulated Containment Floor Geometries," NUREG/CR-6773, December 2002.
- 5-4. D. V. Rao and B. C. Letellier, A. K. Maji, B. Marshall, "GSI-191: Separate-Effects Characterization of Debris Transport in Water," NUREG/CR-6882, August 2002.
- 5-5. Lars-Eric Bjerke and Mats Henriksson, "Modification of Sump Screens in Ringhals 2," International Working Group (IWG) on Sump Screen Clogging, Stockholm, May 10-11, 1999.
- 5-6. D. N. Brocard, "Buoyancy, Transport, and Head Loss of Fibrous Reactor Insulation," NUREG/CR-2982, Revision 1, July 1983.
- 5-7. K. W. Brinckman, "Results of Hydraulic Tests on ECCS Strainer Blockage and Material Transport in a BWR Suppression Pool," Revision 0, May 1994.
- 5-8. F. J. Souto and D. V. Rao, "Experimental Investigation of Sedimentation of LOCA-Generated Fibrous Debris and Sludge in BWR Suppression Pools," U. S. Nuclear Regulatory Commission, December 1995.
- 5-9. G. Zigler, J. Brideau, D. V. Rao, C. Shaffer, F. Souto, W. Thomas, "Parametric Study of the Potential for BWR ECCS Strainer Blockage Due to LOCA Generated Debris," NUREG/CR-6224, October 1995.
- 5-10. "Mark I Containment Full Scale Test Program," NEDE-24539-P, Final Report.
- 5-11. G. Zigler, et al., "Experimental Investigation of Head Loss and Sedimentation Characteristics of Reflective Metallic Insulation Debris," Letter Report to U.S. Nuclear Regulatory Commission, SEA-95-970-02-A:2, May 1996.
- 5-12. D. N. Brocard, "Transport and Screen Blockage Characteristics of Reflective Metallic Insulation Materials," NUREG/CR-3616, January 1984.
- 5-13. A. K. Maji, B. Marshall, D. V. Rao, B. C. Letellier, C. Shaffer, "Debris Transport Characteristics," LA-UR-00-4998, Los Alamos Technical Report, February 2001.
- 5-14. A. W. Serkiz, "Containment Emergency Sump Performance," U.S. Nuclear Regulatory Commission, NUREG-0897, Revision 1, October 1985.
- 5-15. "Buoyancy, Transport, and Head Loss Tests on KAEFER Insulation Systems According to USNRC Regulatory Guide 1.82," Bremen Polytechnic, Department of Naval Architecture and Ocean Engineering, Laboratory for Ship Hydromechanics / Ocean Engineering, July 1995.
- 5-16. D. N. Brocard, "Transport and Head Loss Tests of Owens-Corning NUKON Fiberglass Insulation", Alden Research Laboratory, Holden, Massachusetts, September 1983.
- 5-17. Juhani Hyvarinen and Olli Hongisto, "Metallic Insulation Transport and Strainer Clogging Tests," Finnish Centre for Radiation and Nuclear Safety, STUK-YTO-TR 73, June 1994.
- 5-18. B. E. Boyack, T. S. Andreychek, P. Griffith, F. E. Haskin, and J. Tills, "PWR Debris Transport in Ice Condenser Containments - Phenomena Identification and Ranking Tables (PIRTs)," LA-UR-99-5111, Revision 1, December 14, 1999.
- 5-19. D. V. Rao, C. Shaffer, and E. Haskin, "Drywell Debris Transport Study," U. S. Nuclear Regulatory Commission, NUREG/CR-6369, Volume 1, SEA97-3501-A:14, September 1999.
- 5-20. C. Shaffer, D. V. Rao, and J. Brideau, "Drywell Debris Transport Study: Computational Work," NUREG/CR-6369, Volume 3, SEA97-3501-A:17, September 1999.

- 5-21. D. V. Rao, W. Bernahl, J. Brideau, C. J. Shaffer, and F. Souto, "BLOCKAGE 2.5 User's Manual," NUREG/CR-6370, SEA96-3104-010-A:3, Inc., Prepared for U.S. Nuclear Regulatory Commission, December 1996.
- 5-22. C. J. Shaffer, W. Bernahl, J. Brideau, and D. V. Rao, "BLOCKAGE 2.5 Reference Manual," NUREG/CR-6371, SEA96-3104-010-A:4, Prepared for U.S. Nuclear Regulatory Commission, December 1996.
- 5-23. D. V. Rao and Luke Bartlein, "Technical Review of Licensee Technical Approach for Addressing Millstone II ECCS Sump Blockage by LOCA-Generated Debris," LA-UR-00-5158, Technical Report, Los Alamos National Laboratory, Los Alamos, New Mexico.
- 5-24. FLOW-3D, Version 8.0, 2/25/02, Windows Installation, Copyright 2002, Flow Sciences, Inc., Los Alamos, NM.
- 5-25. D. V. Rao, C. Shaffer, B. Carpenter, D. Cremer, J. Brideau, G. Hecker, M. Padmanabhan, and P. Stacey, "Drywell Debris Transport Study: Experimental Work," NUREG/CR-6369, Volume 2, SEA97-3501-A:15, September 1999.

6.0 DEBRIS ACCUMULATION

This section describes the potential accumulation of debris at critical locations within a PWR containment, where that debris accumulation could adversely affect the recirculation sump performance. It specifically describes what is currently known about how parameters such as insulation type and debris affect the spatial distribution that debris fragments assume on the surface of the screen. This information is gathered primarily from experimental observations of debris accumulation on simulated PWR sump screens.¹

LOCA-generated debris will have an adverse effect on recirculation sump performance if it either (a) covers the sump screen in sufficient quantity and over a sufficient surface area to impede flow or, (b) accumulates at a critical location for the flow of recirculation water along the containment floor such that the debris bed diverts water away from the sump.² In either case, debris first must be transported to a location of concern; debris transport processes are described in Sections 4 and 5 and are not discussed further here. However, after debris is transported to a location of concern, it must accumulate in sufficient quantity and in a configuration that impedes flow. The current knowledge on debris accumulation is summarized in this section.

6.1 Locations of Concern

The principal location of concern for debris accumulation is the surface of a recirculation sump screen. The physical configuration of the sump screen as well as its position and orientation in the pool of water that it services vary considerably among the U.S. PWRs. The features of sump-screen design and installation

that influence debris accumulation are summarized in Section 6.1.1.

Additional locations of concern are those in which the flow path for recirculating water passes through a narrow passageway or restriction in cross-sectional area. If debris were to accumulate at these locations (perhaps because of the presence of a trash rack or similar feature), water might be diverted away from the sump, thereby reducing the sump water level and associated hydraulic head. Examples of such locations are given in Section 6.1.2.

6.1.1 Sump Screens

Historically, the sump screen has been the principal location of concern for debris accumulation. For fully submerged screens, excessive accumulation of debris can cause the head loss across the debris bed to reduce the available NPSH to ECCS or containment spray pumps. For partially submerged screens, excessive debris accumulation can reduce the static head necessary to drive recirculation flow through the screen. Debris accumulation and head loss at this location are the primary focus of research supporting the resolution of USI A-43 and GSI-191.

Information regarding the configuration of containment recirculation sumps in U.S. PWRs was gathered by NEI and the U.S. NRC through initiatives supporting GSI-191 and GL-97-04, respectively. This information was reviewed by LANL to ascertain the type and range of design features that might affect debris accumulation and other factors that influence sump performance.⁶⁻¹ The results of this review clearly show that PWR sump designs span a wide range of geometries from horizontal screens below the floor elevation to vertical screens attached to elevated pedestals. Examples of various recirculation sump designs in U.S. PWRs are shown in Figure 6-1.

- Screen surface area: Values range from 11 ft² to 700 ft².
- Screen mesh size: A majority of plants have a sump-screen mesh size of 0.125 in. However, roughly 40% of U.S. PWRs have a screen mesh size larger than 0.125 in.

¹ Much of the debris accumulation data were obtained while conducting tests specifically designed to test either debris transport in water or to measure debris head loss across a screen or strainer.

² The knowledge associated with debris accumulation also applies to screens in the upper containment levels (e.g., fueling pool drain screens), but the potential blockage of such screens usually is treated as part of debris transport from the upper levels down to the sump pool (see Section 4).

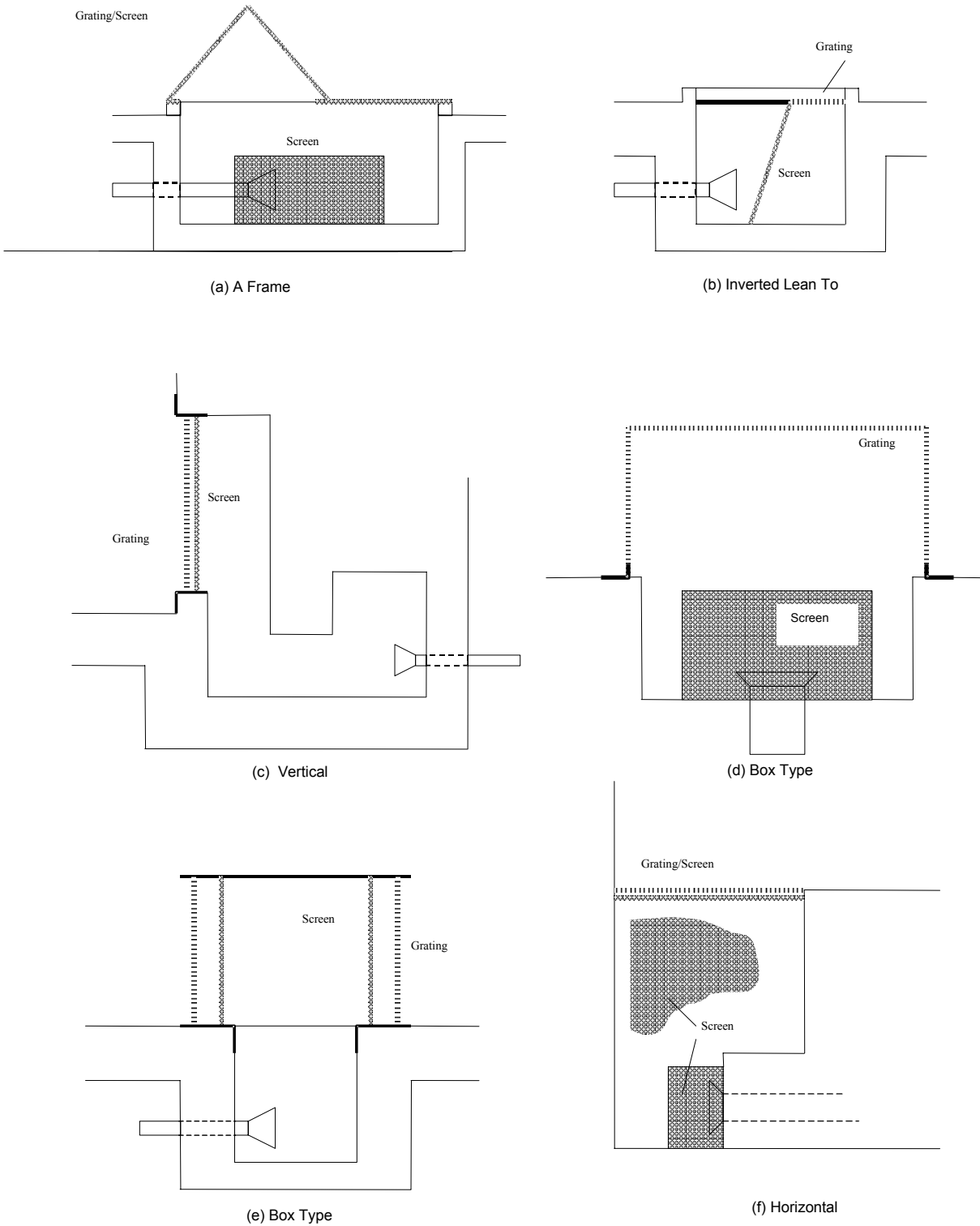


Figure 6-1 Examples of Various Recirculation Sump Configurations in PWRs

- Obstacles to water flow and/or debris transport:
 - Some plants employ curb-like features that would inhibit heavy debris from reaching the screen; many do not have a curb or any impediment to flow.
 - Most plants have trash racks in front of the screen to prevent large debris from reaching the screen.
- Level of submergence: For approximately 1/3 of the U.S. PWRs, the sump screens would not be submerged completely at the time that ECCS recirculation starts. Further, the sump screen for about 1/2 of these PWRs would not be submerged completely even at the maximum pool height.

6.1.2 Containment Flow Restrictions

The location of the sump in a PWR containment can vary considerably from one plant to another. Further, the path along the containment floor that water must travel to reach the containment sump can vary, depending on the location of a postulated break. These two variables lead to the possibility of flow restrictions at locations distant from the sump where debris might accumulate and interfere with the distribution of water on the containment floor.

A simple example of such a configuration is shown in Figure 6-2. In this example, the accumulation of debris on trash racks that are mounted on openings between the main portion of the containment and an isolated room in which the sump is located would restrict flow to the sump. One effect of this flow restriction could be to lower the water level at the sump, thereby depriving the sump of an adequate recirculation suction volume or possibly reducing available NPSH. Other plant design features that could produce a similar effect are

- screen doors at the entrance to high-radiation areas,
- small-diameter “drainage” holes drilled through interior walls (e.g., crane wall), and
- narrow gaps between concrete foundation pads for heavy equipment and neighboring walls.

6.2 Accumulation Patterns

The geometric configuration of a debris bed formed at a location of concern strongly influences the extent to which it affects flow. In this context, the term “geometric configuration”

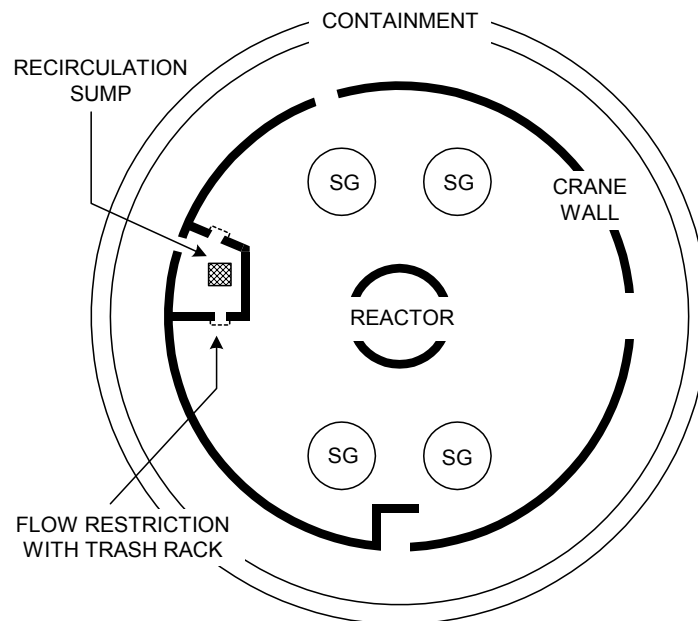


Figure 6-2 Example of a Containment Floor Flow Restriction that Might Result in Diversion of Flow From the Recirculation Sump

is meant to include qualitative and quantitative features of the bed, such as

- the fraction of surface area (sump screen) or cross-sectional area (flow restriction) covered by debris,
- the extent to which the debris bed is uniform in depth (perpendicular to the flow direction),
- the height of the debris bed off the floor (for vertical screens), and
- the porosity of debris material(s).

Variations in these features result in different accumulation patterns or debris bed profiles, which in turn affect water flow and/or head loss.

Qualitative insights were obtained from a number of experiments conducted with prototypic BWR recirculation suction strainers (both simple truncated-cone designs and the complex advanced designs) and, to some extent, experiments involving vertical PWR sump screens. The accumulation patterns depended strongly on the orientation of the screening surfaces, the flow conditions, and the type and size of the debris, specifically whether the debris was suspended or transported along the floor to the screen.

The data for a horizontally oriented PWR sump screen are very limited; these data include the horizontal screens in the integrated debris-transport tests (Section 5.2.6), the flat-plate screens in the closed-loop head loss tests, and certain horizontal portions of the BWR strainer designs (for example, the flat portion of a vertically mounted, truncated-cone strainer). For finer debris, the accumulation patterns tend toward uniformity, similar to those of the vertical screens. For coarser debris transported along the sump floor, the accumulation of debris has not been completely observed; however, it should be more uniform for a horizontal screen than for a vertical screen, where gravitational forces keep larger debris nearer the bottom of the screen.

Debris accumulation profiles on vertical sump screens have been reported in several experimental studies as described in Section 6.4.2. Additional relevant data is also available from experiments involving BWR ECCS suction strainers as summarized in Section 6.4.1. Three conclusions can be drawn from this collective body of experiments.

- Fine debris³ (e.g., shredded fiber, disintegrated calcium-silicate, and possibly small, crumpled fragments of RMI foil⁴) will arrive at the screen surface as a well-mixed suspension of material, and therefore deposit in a near-uniform pattern or will arrive at the screen by tumbling or rolling across the floor and then easily lift above the already deposited debris to spread across the screen.
- Moderate-sized pieces of debris⁵ represent debris that accumulates somewhat like the fine debris and somewhat like the large debris.
- Large or heavy pieces of debris⁶ will collect on a horizontal screen only if local water velocities are sufficient to transport the debris onto the screen surface. In the case of a horizontal screen mounted flush with the surface of the containment floor, this velocity is the same as that necessary to sustain lateral motion (as described in Section 5). For horizontal screens located above the floor elevation,⁷ large debris may still deposit on the surface if local velocities exceed the values necessary to “lift” debris above the curb (if present) or pedestal supporting the screen. The values of water velocity needed to lift debris above 2- and 6-in. obstacles were measured in debris-transport tests conducted by the NRC,^{6,2} which are discussed in Section 5.2.5.

³ Fine debris includes debris so fine (e.g., individual fibers and particles) that it will remain in suspension at very low levels of turbulence, as well as debris that readily settles in hot water but also easily moves across the pool floor.

⁴ Aluminum RMI foils are relatively lightweight and have waterborne transport properties similar to those of shredded fiber. Stainless-steel RMI foils are heavier and require higher levels of turbulence or higher water velocities than aluminum foils to remain suspended.

⁵ When a fiber insulation is destroyed by a jet; for example, large pieces of relatively intact fibrous insulation are usually blown free of the blanket. Although they are irregular in shape, these pieces are frequently several inches to a side and can be represented suitably as a 4-in. square.

⁶ Truly large debris could consist of insulation pillows, blankets, cassettes or large portions thereof, and miscellaneous items such as metal items.

⁷ This conclusion also applies to screens located in a sump below the floor elevation if the level of turbulence within the sump is sufficient to lift debris above the base of the sump.

These profiles can be grouped broadly into four distinct classes as shown in Figure 6-3. After they are put in motion, very large pieces of insulation debris, such as intact fiber pillows or RMI cassettes, tend to “slide” along the floor until they contact the base of the screen. Fiber pillows or RMI cassettes tend to stay in these prone positions unless high screen-approach velocities develop [see part (a) of Figure 6-3]. With high screen-approach velocities, these large objects can “flip” onto the surface of the screen. If they flip, they can obstruct a significant fraction of the screen flow area, partially blocking a sump screen. The values of approach velocity required to flip a fiber pillow or RMI cassette are described in Section 6.4.2.

The accumulation profile typically observed with moderate-size fragments⁸ of insulation material is shown in part (b) of Figures 6-3 and 6-4. This pattern has been observed when sections of fiber matting or RMI foil accumulate against a vertical screen. Debris of this size and weight requires relatively high water velocities to keep it suspended in the flow stream. Therefore, it often is observed to arrive at the sump screen near the floor elevation and “pile up” near the base of the screen. Again, at high approach velocities, these fragments can “flip” or roll up to higher elevations on the screen. The values of approach velocity required to lift moderate-size fragments are described in Section 6.4.2.

Smaller pieces of RMI foil (i.e., shrapnel approximately 1 to 2 in. across) form a more coherent debris bed against a vertical screen than larger foil fragments. Because RMI foils (crumpled or flat) tend to transport along the bottom of a body of moving water, the foils initially arrive at a vertical screen near its base. If the screen approach velocity is sufficiently high, small pieces of RMI foils can gradually “climb” the surface of the debris bed and cover a significant fraction of the screen surface. However, the accumulation pattern typically has a shape that is thicker at the bottom than at the top, as shown in part (c) of Figures 6-3 and 6-4. Data collected to date and summarized in Section 6.4.2 suggest that RMI foil fragments would not completely cover a submerged

vertical screen unless the total volume of material was relatively large—i.e., roughly the volume needed to fill a triangular cross-section perpendicular to the screen.

A general observation from experiments concerning fluid transport of fine shreds of fiber and disintegrated fragments of calcium-silicate is that after this type of debris is in motion upstream of the screen, it tends to stay suspended. This is particularly true in turbulent flow streams. As a result, this form of debris tends to arrive at the sump screen as a flux of suspended material that contacts the entire exposed surface of the screen. This leads to a relatively uniform accumulation profile as illustrated in part (d) of Figures 6-3 and 6-4. This accumulation pattern can vary slightly in situations where the screen is partially submerged in the pool of water. In such cases, fine debris has been observed to deposit more heavily near the bottom of the screen, creating a pattern that resembles a mixture of the bottom-skewed and the uniform patterns shown in parts (c) and (d) of Figures 6-3 and 6-4.

Another example of uniform debris accumulation is shown in Figure 6-5, where relatively fine debris accumulated uniformly across the lower, submerged portion of the vertical test screen during integrated debris-transport testing, which is discussed in Section 5.2.6.⁶⁻⁴ A primary component of this debris accumulation was fibrous debris so fine that it remained suspended even at low levels of pool turbulence; therefore its arrival at the screen was extremely uniform.⁹ Adding a small quantity of particulate to even a thin layer of such debris accumulation has been found to result in substantial head loss across the screen.

Experiments performed to determine the accumulation profiles that a particular debris type would attain for various flow conditions are described in Section 6.4.2.

⁸ “Moderate size” is meant to represent sections of fiber matting roughly 4 in. x 4 in. x 1 in. in size or RMI foils roughly 4 in.² in area.

⁹ In one such test, the resulting debris accumulation created such a significant head loss across the screen that the test was aborted. This debris accumulation subsequently was dried and removed from the screen. A small quantity of sand that had contaminated the test apparatus was mixed with the fibers. The dried layer debris was thin and had the relative texture of paper.

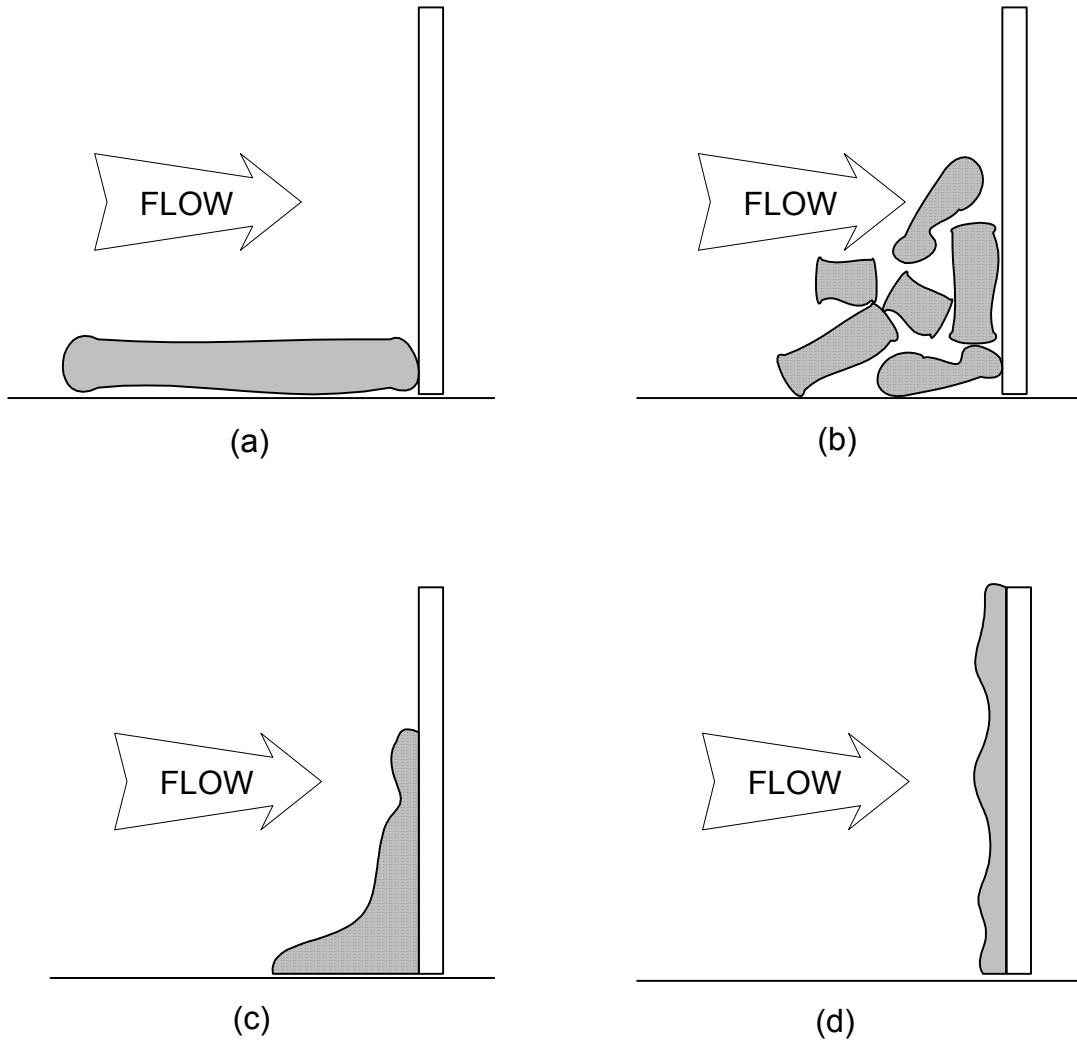


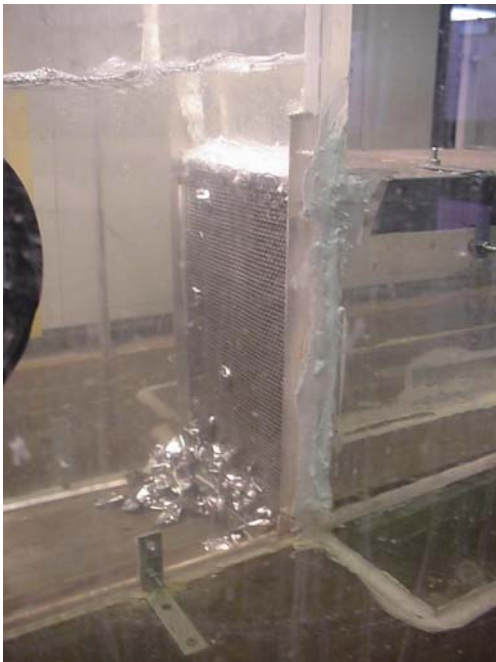
Figure 6-3 Debris Accumulation Profiles Observed in Linear Flume Experiments

[No photo available for intact pillow or cassette]



(a)

(b)



(c)



(d)

Figure 6-4 Photographs of Debris Accumulation on a 1-ft x 1-ft Vertical Screen in a Large Linear Flume [Ref. 6.3] (The photo shown in each frame corresponds to accumulation pattern shown in the same frame of Figure 6-3.)



Figure 6-5 Typical Buildup of Fine Fibrous Debris that Easily Remains Suspended

6.3 Parameters Affecting Debris Accumulation

The manner in which LOCA-generated debris accumulates at locations of concern is influenced by several parameters—each of which can vary considerably among plants of otherwise “similar” design features. Values for some of these parameters also can depend on the specific accident sequence for which flow through the recirculation sump is required to mitigate the accident.

6.3.1 Local Flow Field

The accumulation pattern that debris develops at a location of concern is influenced strongly by the characteristics of the local flow field (i.e., the level of turbulence and the flow velocity). Turbulence facilitates debris mixing into the flow stream and thereby promotes uniform deposition of material onto the surface of a debris screen, regardless of its orientation with respect to the bulk flow. In situations where the flow field is not turbulent, the screen approach velocity determines the hydraulic shear forces on the debris and therefore governs the extent to which individual debris fragments are distributed across the screen surface.

For horizontal screens, relatively small shear forces (i.e., low velocities) are needed to move debris across the surface of the screen. Small- and moderate-size debris fragments will move

laterally toward areas of low flow resistance (i.e., smaller bed thickness), thereby “self-adjusting” the debris bed and creating a near-uniform deposition profile.

The competition between gravitational and hydraulic shear forces can lead to nonuniform velocity profiles on vertical screens. Low velocity, combined with a high specific gravity of debris fragments, can cause debris to preferentially accumulate near the base of a vertical screen, leaving the upper portions of the screen relatively clean. However, at higher velocities, shear forces on debris can overcome gravitational sedimentation and “lift” or “flip” debris upward onto higher regions of the screen. The velocities needed to overcome the tendency for debris to settle at the bottom of a vertical screen have been determined experimentally as described in Section 6.4.2.

Changes in approach velocity with time also can affect debris accumulation. For geometric configurations in which persistent hydraulic forces are required to “hold” debris on a screen, a significant reduction in flow might allow debris to fall off the screen, changing the accumulation profile. This behavior has been observed in experimental simulations of debris accumulation on representative (vertical) sump screens when tests are terminated by turning off the pump that drives flow through a linear flume. The sharp reduction in flow typically causes the debris bed to expand. Subsequently, fragments of debris,

such as clumps of RMI foil or fibrous material, peel off the debris bed and fall to the floor in front of the screen. Some particulate material (if included in the debris mixture) is released from the bed and is resuspended in the flume water. If flow subsequently is increased to the initial rate by restarting the pump, a debris bed reforms, although not necessarily in a configuration similar to the one observed before the flow reduction. Detailed experimental studies of the effects of flow reduction on debris accumulation and retention on a vertical screen have not been performed. The comments above are based on qualitative observations made during debris transport and (initial) screen accumulation tests.

6.3.2. Local Geometry

Although large pieces of debris are not likely to be a significant concern for blockage for most PWR sump screens, accumulation of such debris at locations where recirculation water must pass through narrow passageways can initiate a sequence of events that diverts or impedes the flow of water to the sump. That is, accumulation of large debris at such locations provides a porous, but effective, medium for collecting smaller and smaller fragments of debris. This possibility is a potential concern at locations on the containment floor, for example, where the characteristic dimensions of openings in recirculation water flow area are comparable to (or smaller than) those of the largest debris constituents.

Local geometry also affects the performance of the recirculation sump screen. As indicated above, the orientation of a sump screen relative to the flow stream determines whether hydraulic shear forces beyond those needed to transport debris to the screen are required to distribute debris across the surface of the screen. Other geometric characteristics of a sump-screen design that are likely to influence the debris deposition pattern include

- the elevation of the screen relative to the containment floor (or base of the sump),
- the presence of a trash rack or other obstacle to remove large objects, and
- the screen surface area.

The specific effects of these characteristics on debris accumulation have not been studied experimentally.

The debris-capture efficiency of a screen is not strongly dependent on the size of the screen mesh over the narrow range of values typically found in U.S. PWRs.¹⁰ Debris collection efficiency typically is not measured as part of screen-accumulation and head loss experiments. However, observations of debris accumulation on a 1/4-in.-square mesh have not identified noteworthy differences from accumulation on a 1/8-in. mesh.^{6-2,6-3,6-4,6-5,6-6}

6.3.3 Submergence

Experiments designed to measure threshold velocities for incipient motion and bulk transport of debris in water (discussed in Section 5.2.5)⁶⁻² have shown that the results are not sensitive to the depth of water on the containment floor.¹¹ However, after debris arrives at the face of a vertical screen, the accumulation profile assumed by the debris is affected by the depth of the water.

Recent tests performed in the linear flume at UNM¹² suggest that the accumulation profiles on a partially submerged screen may differ from those on a totally submerged screen under otherwise identical conditions (i.e., debris type and flow patterns).⁶⁻³ This difference was observed initially in experiments performed in a linear flume after an adjustment was made to the construction of a simulated (vertical) sump screen to eliminate a screen bypass flow path along the upper perimeter of the screen. During initial shake-out tests, water was observed to spill over the top of the screen through a narrow gap along the upper perimeter of the square screen, thereby allowing a fraction of the total flume flow to bypass the screen surface. Under

¹⁰ There are a few exceptions where the mesh size is substantially larger. For these exceptionally large mesh sizes, there are essentially no data available regarding debris accumulation. Finer debris may essentially just pass through the screen.

¹¹ Experiments performed to date have all involved measurement of debris-transport properties for completely submerged debris. Similar statements currently cannot be made for very shallow pools of water where debris motion might be directly impacted by the free surface.

¹² The UNM experiments related to debris accumulation are ongoing at this writing; hence, only preliminary observations are included here. The UNM test report is expected to include a summary of the debris accumulation data from these tests.

these conditions, debris accumulation profiles against the screen tended to be skewed toward the bottom of the vertical screen. When this gap was sealed and all water was forced to pass through the screen to exit the flume, the accumulation profile for easily transportable forms of debris (e.g., small fiber fragments) became uniform. This observation led to the qualitative conclusion that the accumulation profile on a partially submerged screen might differ from that on a fully submerged screen. However, this conclusion could not be tested rigorously in the UNM flume because of the limitations in the vertical scaling of the flume cross section.

Other observations made from the UNM experiments are listed below.

- Debris that is readily suspended in the flow stream (i.e., small fiber or calcium-silicate fragments and particulate matter) is deposited uniformly across the exposed screen surface area when the screen is fully submerged. Hydraulic forces draw all suspended material to the screen, where it collects randomly. The deposition pattern self-corrects for asymmetries in the debris-bed depth when flow (and suspended debris) is diverted toward regions of lower flow resistance (i.e., blocked with less debris.)
- The accumulation pattern (below the surface of the pool and for the same debris material) on a partially submerged screen can appear to be slightly skewed toward the bottom of the screen. This pattern does not appear immediately but develops as debris accumulates in the following manner. Initially, suspended debris deposits on the face of the screen in a near-uniform pattern. The pressure drop across the screen caused by the thin debris bed is manifested as a difference (decrease) in water level across the screen. As debris accumulates on the screen, the axial velocity profile in front of the screen changes. The velocity of the water near the base of the screen decreases, and the velocity of the water near the pool surface increases. This shift in the axial velocity profile allows some debris to settle toward the base of the screen, thereby increasing the concentration of debris near the bottom the flume relative to the top of the flume. Slowly, the debris accumulation profile appears to grow more

heavily toward the base of the screen than toward the surface of the pool.

Similar experiments have not been performed for other forms of debris, such as RMI foils. However, as described in Section 6.4.2, such debris tends to accumulate in bottom-skewed profiles even on fully submerged screens.

6.3.4 Debris Characteristics

From the discussion provided in Section 6.2, the type and size of debris that approaches a sump screen clearly affects its accumulation profile. The data described in Section 6.4 clearly indicate differences in the accumulation of fibrous, calcium-silicate, and RMI debris on vertical screens. In contrast, little difference in the accumulation pattern would be expected if these types of debris collected on a horizontal screen close to or below the elevation of the containment floor.

6.4 Test Data

Section 5 describes numerous experiments that have been performed to evaluate the hydrodynamic conditions required to move debris of various types from their position of arrival on the containment floor to the recirculation sump. Many of these experiments also provide valuable insights on debris accumulation on a sump screen. These insights and quantitative criteria for attaining the debris accumulation patterns described above are summarized in Section 6.4.2. However, before these experiments are discussed, it is instructive to review relevant information obtained from BWR strainer performance tests.

6.4.1 BWR Strainer Tests

The BWROG and various ECCS recirculation suction strainer vendors performed numerous experiments to characterize the accumulation and head loss associated with LOCA-generated debris for replacement strainer designs thoroughly. Although the local flow conditions and strainer configurations differ considerably from a PWR recirculation sump screen, certain qualitative observations made from these experiments are worth noting.

A common BWR replacement strainer design is the “stacked-disk strainer.” This design consists of a central perforated tube that is sealed at one

end and mated to a flange at the other end for mounting to an ECCS recirculation suction pipe stub in the suppression pool. A series of perforated disks is welded to the outer circumference of the perforated tube, greatly increasing the effective surface area of the strainer without increasing its overall size. An example stacked-disk strainer design is shown in Figure 6-6.

Experiments performed to characterize debris accumulation and associated head loss through stacked-disk strainers were performed by several vendors and BWR utilities. The results of these tests provide useful information on the manner in which debris accumulates on the convoluted surface of this type of strainer design. Figures 6-7 and 6-8 show sample test results for increasing quantities of fibrous and RMI debris, respectively.¹³ The process of debris accumulation on a stacked-disk strainer is more complicated than that on a flat screen. In either case, the water flow always follows the path of least resistance. With a stacked-disk strainer, water flows through all of the screened surfaces and debris is deposited onto all of the screened surfaces, but the flow and deposition are skewed toward the screened surfaces of lesser resistance. Initially, the hydraulic resistance through a “clean” strainer is somewhat less along the surface of the central tube than along surface of the outer fins, resulting in somewhat more debris accumulation within the gaps between fins. As debris accumulates onto the disk-shaped surfaces inside the gaps, the flow moving somewhat parallel to these surfaces pushes the debris on these surface further into the gaps, thereby keeping a portion of the disk surface relatively clean of debris until the gaps are filled, as shown in the photographs on the left side of Figures 6-7 and 6-8. After the gaps are filled, the debris preferentially occurs on the disk rims until the accumulation becomes more circumferentially near uniform.

6.4.2 Test Results for Vertical PWR Sump Screen Configurations

Experiments conducted in a linear flume at ARL in support of USI A-43 studied the buoyancy, transport, and head loss properties of insulation materials of various sizes and compositions

(discussed in Sections 5.2.1 and 5.2.4).^{6-5,6-6} In addition to these properties, observations were recorded concerning the water velocity required for these materials to deposit on a vertical screen. The experiments were performed in a large linear flume; and the screen was manufactured with a metal mesh similar in size to that found on a typical PWR recirculation sump screen. The sizes of the insulation material spanned the full range from intact fiber pillows and RMI cassettes to small fragments of fiber and RMI foil.

The results of these experiments are summarized in the first two rows of Table 6-1. The results shown represent the velocity at which debris of a particular type and size would “flip up” or be lifted off the flume floor and adhere to the screen surface. For shredded fiber fragments, this velocity is relatively small (0.2 ft/s) and corresponds to the velocity required to induce incipient motion of the fragments in the flume. For larger pieces of debris, the lifting velocity was generally higher than that required to induce motion. For example, intact fiber pillows or RMI cassettes were observed to shuffle along the floor of the flume at velocities above approximately 1 ft/s. However, velocities approaching 2 ft/s were required to flip a pillow/cassette onto the screen surface. Investigators at Bremen Polytechnic in Germany observed similar results for intact insulation units manufactured by a different vendor, which are discussed in Section 5.2.7.⁶⁻⁷

The flow conditions required for debris to deposit on the upper portions of a vertical screen also can be inferred from measurements made of the velocity required to “lift” debris over a 2- or 6-in. curb. Such measurements were made in a large linear flume at UNM⁶⁻² as part of a debris-transport study (discussed in Section 5.2.5). The so-called “lifting” velocity for fiber fragments, moderate-size pieces of fiber matting, and RMI foils are listed in Table 6-1. The values of the lifting velocity are generally consistent with earlier measurements of the flip-up velocity. That is, debris can be lifted over a 6-in. curb (or be lifted onto a vertical screen) at relatively low velocities (i.e., less than 0.3 ft/s) if the flow field in the pool of water is turbulent. In laminar flow fields, the “lift” velocity increases only slightly for fiber fragments. Stainless-steel RMI debris was observed to remain near the base of the screen

¹³ Note: The strainers are installed in a vertical orientation in these photographs.

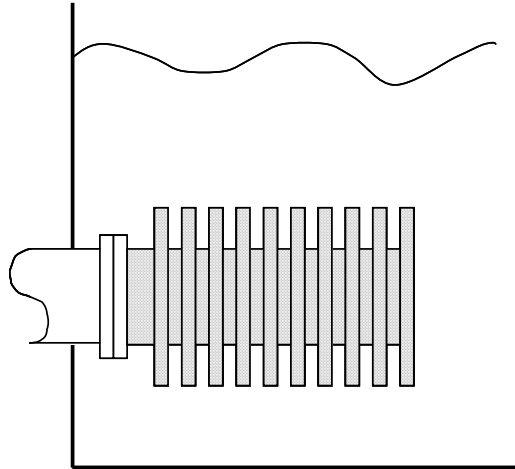
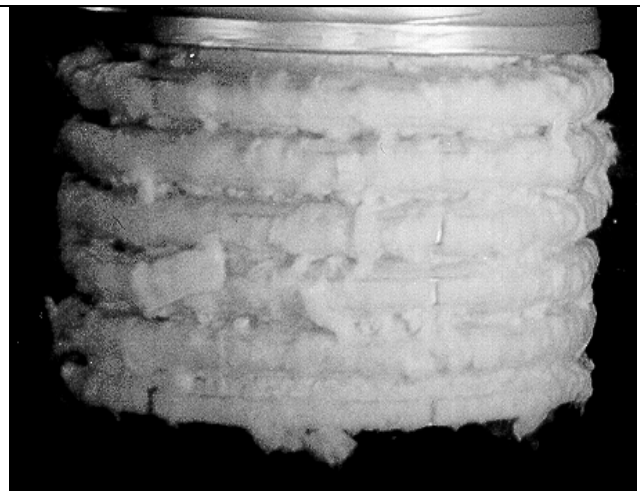


Figure 6-6 Example Installation of a BWR Stacked-Disk ECCS Recirculation Suction Strainer



Accumulation of a small amount of fiber between fins of a stacked-disk strainer



Larger quantities of fiber span the gaps and begin to form a coherent debris bed along the circumscribed area of the strainer.

Figure 6-7 Fibrous Debris Accumulation on a Stacked-Disk Strainer⁶⁻⁸

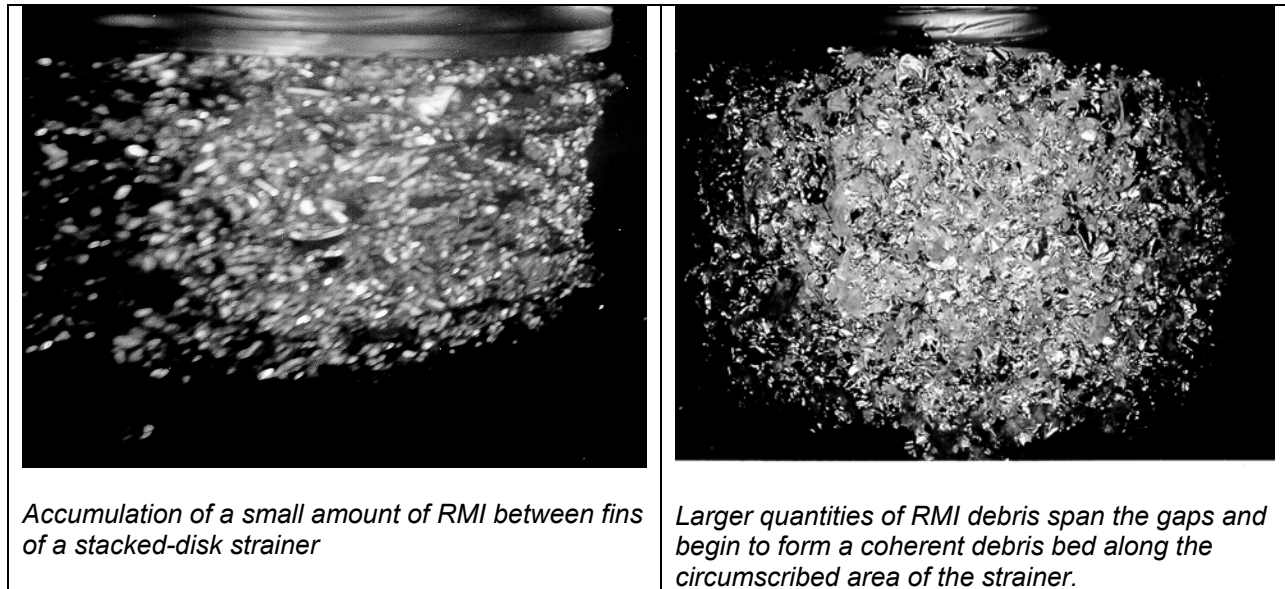


Figure 6-8 RMI Debris Accumulation on a Stacked-Disk Strainer⁶⁻⁸

Table 6-1 Minimum Screen Approach Velocity for Debris to “Flip Up” or be Hydraulically “Lifted” Onto a Sump Screen					
DATA SOURCE	Velocity (ft/s)				
	Intact Fiber Pillows *	Fiber Fragments * #	Shredded Fiber *	Intact RMI Cassettes	SS RMI foils
U.S. NRC (1983) ⁶⁻⁵	1.1–2.4	0.5–0.7 (turbulent)	0.2 (turbulent)	—	—
U.S. NRC (1984) ⁶⁻⁶	—	—	—	> 1.0	1.8–2.0 **
Bremen Polytech. (1995) ⁶⁻⁷	0.9–1.3	0.7–1.1 (laminar)	0.9–1.2 (laminar)	Tested by flipping on screen not observed	1.9 **
U.S. NRC (2001) ⁶⁻²	—	0.30–0.47 (laminar) 0.25–0.39 (turbulent)	0.28–0.34 (laminar) 0.25–0.30 (turbulent)	—	No lift (laminar) 0.30 (turbulent)

*Fibrous material varied among tests, but included fiberglass and mineral wool.

**Although SS foil fragments were observed to “lift” and flip onto the vertical screen at these velocities, the debris mass remained primarily near the bottom of the screen. Brocard reports maximum flow blockage in such cases was 60-70% of the screen area.⁶⁻⁶

#Fragment size typically 4-in. x 4-in. pieces of fiber matting.

at velocities greater than 1 ft/s when the flow stream was laminar.

A significant limitation of the studies listed in Table 6-1 is that none of them involved a sufficiently large quantity of debris fragments to allow observations to be made regarding the accumulation pattern that would result at water velocities above the “lifting” threshold. Experiments underway at UNM are examining this topic.⁶⁻³ These experiments examine debris bed patterns on a vertical screen for moderate- and small-size debris fragments of fiber, RMI foils, and calcium-silicate.

The preliminary results of the UNM tests generally confirm the use of data for debris lifting velocity to characterize the flow conditions needed to generate a uniform debris bed profile or (in the case of RMI foil), the bottom-skewed profile shown in part (c) of Figure 6-3. Three specific observations were made from these tests.

- Shredded fiber and disintegrated calcium-silicate developed a near-uniform debris bed at velocities exceeding approximately 0.5 ft/s¹⁴ when the screen was fully submerged. The debris-bed pattern shifted toward the bottom-skewed shape when the screen was partially submerged.
- Crumpled stainless-steel RMI foils (~2 in. in size) accumulated in a bottom-skewed pattern at velocities less than 1 ft/s. Individual foils that arrive at the base of the screen “climbed” on top of foils that arrived earlier and gradually formed a debris bed that was triangular in cross-section.
- Very small particles of calcium-silicate and suspended fibers collected on the screen in a uniform pattern at velocities as low as 0.2 ft/s. A significant fraction of larger calcium-silicate debris (e.g., clumps of particulate and binding fiber) either settled to the floor of the flume before reaching the screen or collected as a mass near the base of the screen at velocities as high as 0.9 ft/s.

6.5 References

- 6-1 Rao, D. V., B.C. Letellier, K.W. Ross, L.S. Bartlein and M.T. Leonard, “GSI-191 Technical Assessment: Summary and Analysis of U.S. Pressurized Water Reactor Industry Survey Responses and Responses to GL 97-04,” NUREG/CR-6762, Vol. 2, LA-UR-01-1800, August 2001.
- 6-2 Rao, D. V., B.C. Letellier, A.K. Maji, B. Marshall, “GSI-191: Separate-Effects Characterization of Debris Transport in Water,” NUREG/CR-6772, LA-UR-01-6882, August 2002.
- 6-3 Leonard, M.T., D.V. Rao, A.K. Maji, A. Ghosh, “GSI-191: Experimental Studies of LOCA-Generated Debris Accumulation and Head Loss with Emphasis on the Effects of Calcium Silicate Insulation,” Los Alamos National Laboratory, LA-UR-03-0471, January 2003.
- 6-4 Rao, D. V., C.J. Shaffer, B.C. Letellier, A.K. Maji and L. Bartlein, “GSI-191: Integrated Debris Transport Tests In Water Using Simulated Containment Floor Geometries,” NUREG/CR-6773, September 2002.
- 6-5 Brocard, D. N., “Buoyancy, Transport and Head Loss of Fibrous Reactor Insulation,” NUREG/CR-2982, SAND82-7205 (Rev. 1), July 1983.
- 6-6 Brocard, D. N., “Transport and Screen Blockage Characteristics of Reflective Metal Insulation Materials,” NUREG/CR-3616, SAND83-7471, January 1984.
- 6-7 Kastner, S., “Buoyancy, Transport and Head Loss Tests of KAEFER Insulation Systems according to USNRC Regulatory Guide 1.82,” Bremen Polytechnic, July 1995.
- 6-8 Zigler, G, “Test Evaluation Report for Test TPP-VL0400-005: LaSalle Strainer Fiber and RMI Debris Tests,” ITS Corporation, June 1998.

¹⁴This might not be the lower limit of velocity required to attain a uniform debris bed. Additional testing (underway) will evaluate accumulation patterns at lower velocities.

7.0 DEBRIS HEAD LOSS

This chapter discusses information related to estimating the pressure drop (or head loss) across the ECCS strainer or sump screen as a result of debris build-up. This subject was previously addressed in a knowledge base report⁷⁻¹ published by the Committee on the Safety of Nuclear Installations (CSNI) specifically Section 4 of that report, entitled "Strainer Pressure Drop." This report summarizes the head loss data and technical developments achieved since that report was published in conjunction with key aspects of the CSNI report. In that sense, this section could be viewed as an update to Section 4 of the CSNI report; even through the two reports have different sponsorship.

Attempts to resolve two major uncertainties listed in the previous CSNI document were specifically addressed herein. These uncertainties were:

1. A proven, accurate, and repeatable methodology for predicting the head loss caused by mixed beds is not yet fully developed. Although the U.S. NRC methodology performs well for flat strainers, its application to specialty strainers has not been established.
2. Different test methodologies, setup design, and test debris preparation may contribute significantly to pressure drop. No systematic evaluation has been performed to discuss desirability of each test methodology *vis-à-vis* other methods.

This section summarizes the present understanding of the underlying phenomena and their effect on the head loss and reviews the experimental and analytical options available for strainer design and performance evaluation. Although the knowledge base that can be used for such calculations has grown over the last decade, data are still incomplete for several combinations of materials present in U.S. and European nuclear power plants (e.g., asbestos or other micro-porous materials). Therefore, this section makes several recommendations on the need to obtain further head loss data or for analysis of existing data.

Section 7.1 identifies the underlying phenomena that affect head loss across the debris bed and provides phenomenological discussions related

to their importance. Section 7.2 presents a summary of the test design approaches adopted by various researchers and their relative advantages. Section 7.3 provides analytical approaches for estimating pressure drop. Section 7.4 discusses ongoing research on outstanding issues.

7.1 Factors Affecting Debris-Bed Build-Up and Head Loss

Head loss across the debris bed depends to a great extent on the debris bed constituents and their morphology. Debris beds of the most likely importance can be divided broadly into the following groups: (a) fibrous debris beds, (b) mixed fibrous and particulate debris beds, (c) beds formed by fragments of RMI, and (d) mixed RMI and fibrous debris beds.

7.1.1 Fibrous Debris Beds

The accumulation of fibrous debris on the strainer resembles flow through a porous medium (Figure 7-1). Typically, the flow to a strainer would deposit the fibrous shreds on the strainer surfaces such that the fibers generally lay across the strainer penetrations (i.e., somewhat perpendicular to the flow). The subsequent drag caused by the fibers would create a pressure differential across the bed of debris. As the pressure drop across fibrous beds increases, such beds have been observed to compress, leading to progressively higher head losses. Furthermore, it has been observed that compressed beds do not completely regain their original state when the water flow is terminated. In most cases, the experimental data obtained for fibrous beds can be explained using conventional porous-media head loss correlations.⁷⁻² The insights discussed in the following paragraphs were gained through close examination of the test data.

Head loss across a debris bed increases linearly with velocity in the viscous region and increases to the square of the velocity in the turbulent region.¹ Any model used to predict head loss across the strainer should take both these factors into consideration (unless the model is

¹A combination of these asymptotes can be used to describe the head loss behavior for velocities that lie in the transitional region.

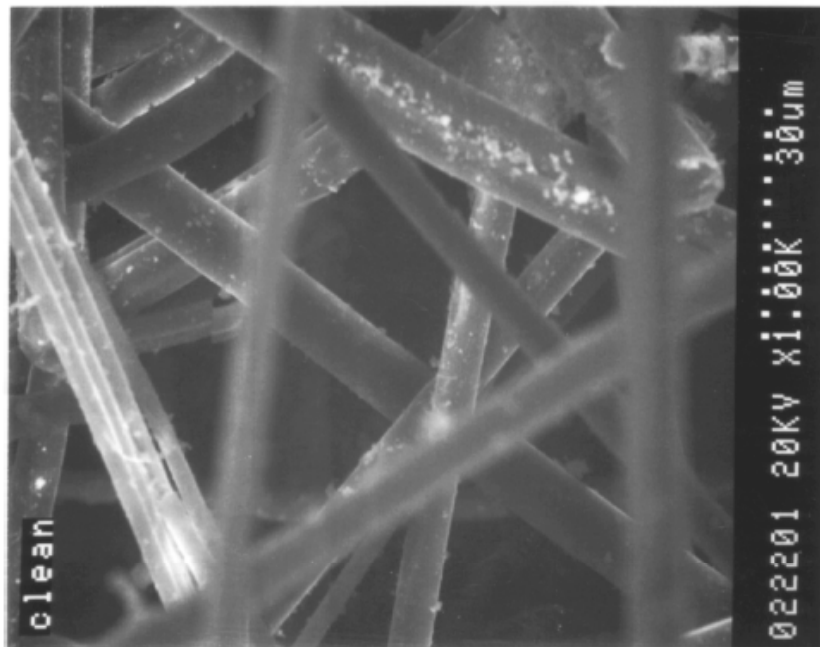


Figure 7-1(a) High-Resolution Scanning Electron Microscope Image of Fibrous Debris

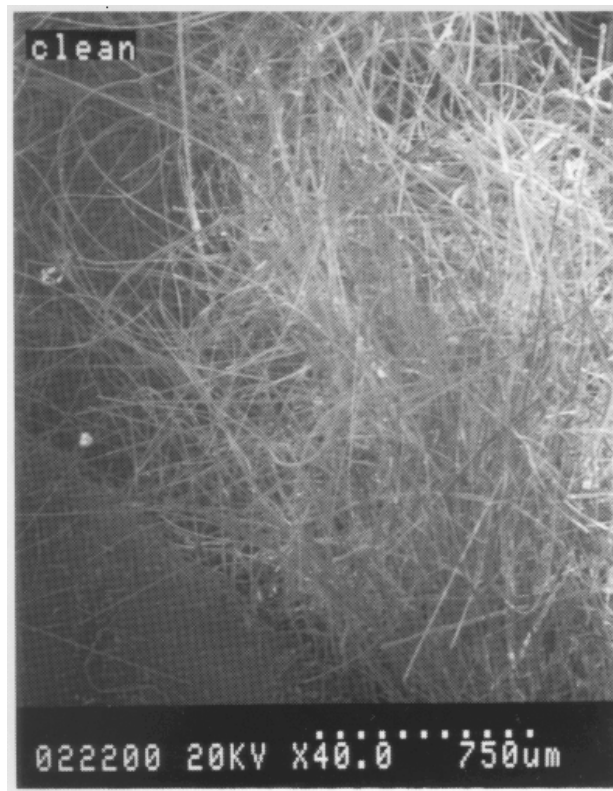


Figure 7-1(b) Low-Resolution Scanning Electron Microscope Image of Fibrous Debris

developed for a specific velocity range and is not intended to be applied outside that range). Reference 7-2 provides a method for including viscous and turbulent head loss regimes into a single correlation.

Head loss across the strainer is dependent on the quantity of the fibrous debris trapped on the strainer surface. A convenient measure for the quantity of fibrous debris trapped on the strainer is the debris bed thickness based on the as-fabricated density of the insulation, i.e. defined as the mass of fibrous debris per unit of strainer area divided by the as-fabricated density. This thickness has been generally referred to as the "theoretical" thickness. Typically, head loss varies linearly with bed thickness for beds that are uniform or nearly uniform. Deviation from this linear behavior has been seen where debris has accumulated in a non-uniform manner on the strainer surface, specifically such behavior has been observed at lower bed thicknesses, where clumps of fibrous debris have been observed to deposit non-uniformly on the strainer surface.² The non-uniformity also may lead to lower filtration efficiencies for entrapment of non-fibrous debris passing through the strainer. As a result, the pressure drop for non-uniform beds would be lower than that predicted by extrapolating data obtained for uniform beds. This is an important issue that should be taken into account when evaluating specialized strainers designed to collect debris in a non-uniform manner (e.g., a star strainer).

The size distribution of the fibrous debris is another factor that significantly influences head loss. Fibrous debris reaching the strainer may vary in size from individual fibers to shreds or clumps to large pieces of torn blankets. Experiments conducted before the Barsebäck-2 incident (incident described in Section 9.1) typically used larger debris fragments or regularly cut pieces of the fibrous blankets.⁷⁻³ The Barsebäck-2 incident and investigations since then have demonstrated that finer debris fragments are more likely to reach the strainer than the larger debris. As a result, considerable attention was given to studying the head loss characteristics of finer debris, which is much

more likely transport to the strainer surface. Comparison of the pre- and post-Barsebäck-2 experimental database would suggest that, in general, finer debris forms more uniform and compact beds, which are more resistant to flow than non-uniform or loose beds. Because finer shreds have generally lost their original blanket structure, the finer debris is more compressible than large pieces of debris. Based on this observation, it can be concluded that considerable attention should be paid to ensure that the size classifications of debris used in the experiments are representative of the debris expected to reach the strainer following a LOCA. Ultimately, engineering judgment must be relied upon to arrive at the debris size classifications used in the experiments. This judgment should be based partially on the following considerations: (a) the debris-size class is influenced strongly by the type of insulation, the mode of encapsulation, and the duration of its exposure to harsh environments (i.e., its age) and (b) debris disintegration would occur not only during its generation but also during its transport (e.g., thrashing due to pool turbulence). These factors should be considered when designing new experiments or evaluating the applicability of a particular set of experimental data.

Additional factors that influence head loss include fibrous material type (e.g., mineral wool vs fiberglass) and water temperature. Typically, higher water temperatures result in lower pressure drops that are caused primarily by corresponding decreases in the water viscosity. Analyses have successfully handled this effect by simply accounting for the temperature dependency in viscosity in the respective head loss correlations. Similarly, the differences in materials can typically be handled by accounting for differences in the material properties of the insulation and the individual fibers. A consistent approach to handling both these factors is described in Appendix B and in Reference 7-2. Particular attention should be paid to ensure that type(s) of debris used in the experiments and analyses are representative of the debris expected to reach the strainer. Head loss estimates should also consider debris generated from the destruction of the jacketing or encapsulation materials used to install the insulation (e.g., fiberglass cloth).

Finally, the effects of water chemistry (pH) on head loss have been studied for fibrous insulations. The data thus far indicate that this

² At very low thicknesses, the debris bed may resemble a partially blocked strainer, where only a small fraction of the flow passes through the debris layer and the remaining flow passes through the open area.

effect is minimal for the fiberglass insulations commonly installed in U.S. nuclear power plants (i.e., Nukon, Thermal Wrap, and Kaowool). However, most tests were conducted over a shorter interval and did not examine pH in conjunction with the higher temperatures typically expected for PWRs (e.g., 50–70°C). Some European investigators concluded that pH could dissolve some of the chemical coatings applied to the fibers, leading to their degradation and the formation of even more compact beds.³

7.1.2 Mixed Particulate and Fiber Beds

The Perry incident first demonstrated (and it was later confirmed by the Limerick incident) that fibrous debris beds would filter the particulate debris passing them, leading to the formation of very compact beds, and that such beds induce high head losses^{7-4,7-5} (both incidents are described in Section 9.2). Before the Perry incident, the majority of the investigations focused on measuring head loss for pure fiber beds. However, since then the focus shifted from pure fiber beds to debris beds formed of fibrous and particulate mixtures. The particulate mixtures examined typically included corrosion products, paint chips, organic sludge, concrete dust, and fragments of non-fibrous insulation (e.g., calcium-silicate). Attempts have been made to characterize the characteristics of the debris (e.g., size distributions) and to use appropriate material to simulate LOCA-generated debris in experiments and the appropriate characteristics in analyses. Subsequent experiments have shown that the addition of particulate debris would increase the pressure drop substantially.⁷⁻² This data clearly demonstrated that the head loss could increase by a factor of 100 as the particle-to-fiber mass ratio goes from zero to about 20. This is discussed further in Section 7.3.1.1 and in Reference 7-2.

The experiments also established that for a fixed amount of particulate debris, pressure differentials across the bed are significantly higher for smaller, rather than larger, quantities of fibrous material. This effect, which often is referred to as the thin-bed effect, has been studied extensively. Closer examination of the bed morphology reveals that thin beds closely resemble granular beds (rather than fibrous

beds) and that higher head loss is a direct result of bed morphology.

This effect is illustrated in Figure 7-2, which shows head losses vs fiber volume for fixed quantities of particulate, as predicted using the NUREG/CR-6224 head loss correlation. In Figure 7-2, the thin-bed peaks (near the center of the figure) reflect the higher head losses associated with the thin layer fiber supporting a granular bed of particulates. Note that head losses for mixed beds only exceed those of the thin beds at the excessively large volumes of fiber (at the right side of the figure). Even if a plant has large quantities of fibers that could lead to potentially thick mixed beds of debris, the initial bed formation would begin with a thin layer of fibers that could cause a thin bed head loss relatively early into the accident.

A significant number of experiments have been carried out to measure the head loss effects of mixed particulate and fibrous debris beds. The particulate debris of primary importance to many of the investigators was suppression-pool sludge. Fewer investigators focused on obtaining experimental data for debris other than sludge. The key findings are discussed in the following paragraphs.

Sludge

Corrosion products, primarily, along with dirt, dust, and other residues commonly found in U.S. BWR suppression pools are referred to as the BWR sludge or sludge. Surveys of U.S. BWR pools found that significant quantities of sludge are present in the suppression pools. Similar surveys of the European BWR suppression pools suggest that quantities of sludge are minimal in European pools. As a result, the majority of the head loss data for sludge and fiber combinations was obtained in the U.S.

The head loss effects of sludge were found to depend on the size distribution of the sludge. The U.S. NRC and BWROG established a consensus position on the sludge size distribution for use in experiments. It was based on the survey of U.S. BWR suppression pools. The base of U.S. knowledge on fiber and sludge head loss behavior is summarized in NUREG/CR-6224⁷⁻² for flat-plate-strainer geometries and the BWROG URG for large-scale strainers of different designs. Additional proprietary data exist for advanced strainers, such as GE stacked-disk strainers and ABB strainers (described in Sections 8.2.1.2 and 8.2.1.3). It

³ Personal communications from M. Henricksson, Vattenfall.

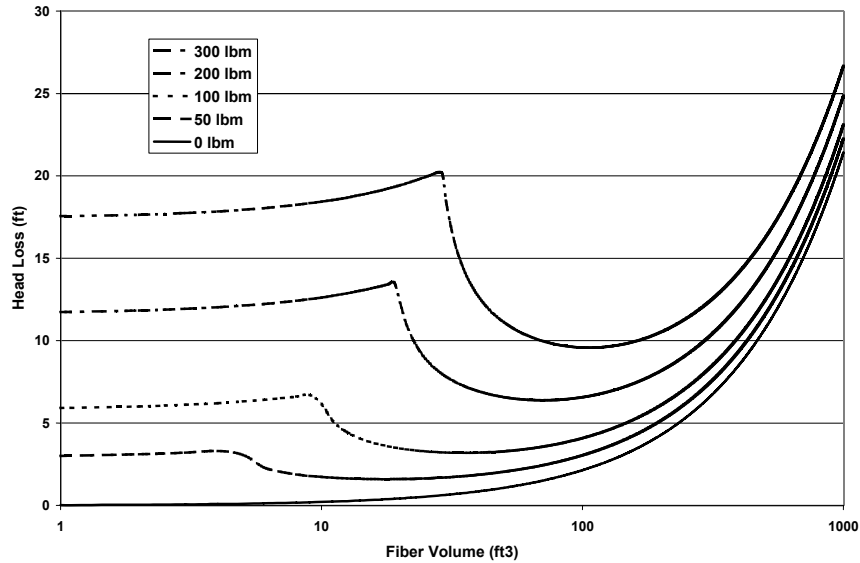


Figure 7-2 Head Losses vs Fiber Volume for Fixed Quantities of Particulate

(Predictions assumed LDFG insulation debris, dirt particulate, 200°F, 100 ft² of screen area, and 5,000 GPM flow.)

has been shown repeatedly that NUREG/CR-6224 provides a reasonable upper bound estimate for head loss caused by fiber and sludge mixtures.

Miscellaneous Debris

It was recognized that miscellaneous forms of particulate debris could also accumulate in a fibrous debris bed on a strainer along with the dominant form of particulate. ARL first reported head loss data for miscellaneous debris combinations.⁷⁻²⁷ In these NRC-sponsored experiments, head loss was measured for fiber, paint chips, and rust flakes. No correlations were developed for that data. The most comprehensive database for miscellaneous debris is reported by the BWROG using a gravity-driven head loss setup. BWROG quantified the head loss effects of corrosion products, paint chips, rust flakes, sand, cement dust, zinc filler, and calcium-silicate. The measured data were summarized in the BWROG URG.⁷⁻¹⁰

Calcium-Silicate

The head loss behavior of calcium-silicate debris materials has been investigated in various facilities, including the tests conducted by Vattenfall Development Corporation,⁷⁻¹⁹ the BWROG,⁷⁻¹⁰ and ITS Corp.⁷⁻²⁸ The publicly available data on the head loss as a result of mixtures of fiberglass and calcium-silicate insulation debris materials from these

experiments is summarized in Table 7-1. The tests were conducted at water temperatures between 60 and 70°F.

The assessment of the publicly available data on the head loss behavior of mixtures of calcium-silicate and fiberglass insulation debris materials indicates that calcium silicate in a fibrous debris bed affects the pressure differential across that bed in the same manner as the corrosion products, however that effect under certain conditions is stronger for the calcium silicate particulate.⁴ Another way to look at this effect is that when predicting a debris bed head loss, if the calcium silicate is treated as a simple particulate, it can cause a serious under-prediction of the head loss under certain conditions.

Further this effect appears to be dependent on the theoretical fibrous-debris-bed thickness. For a relatively thick fibrous bed, the effect could be relatively small, however for a relatively thin fiber bed, the effect of calcium-silicate debris materials can be substantial. In fact, for the same fiber loading and flow conditions, the head loss with calcium-silicate may increase the head loss without calcium-silicate by a factor of about 50 when the theoretical fiber bed is about 0.5 in.

⁴ Calcium silicate in a member of a type of insulation referred to as micro-porous or particulate insulations (Section 2). Other members of that insulation type would behave in a similar manner.

Table 7-1 Head Loss Test Data for Mixtures of Calcium-Silicate and Fiberglass Insulation Debris

Test	Screen Area (ft ²)	Flow Rate (gpm)	Fiber Mass in Tank (lbm)	Cal-Sil Mass in Tank (lbm)	Head Loss (ft-water)	Ref.
0	0.08	5	0.066	0	8.7	7-19
4	0.08	5	0.015	0.003	12.5	7-19
7	0.08	5	0.033	0.033	7.4	7-19
9	0.08	5	0	0.013	10.5	7-19
11	0.08	5	0.004	0.004	9.0	7-19
13	0.08	5	0.013	0.002	14.3	7-19
16	0.08	5	0.024	0.024	11.8	7-19
20	4.7	200	0	0.09	0.8	7-28
21	4.7	200	0.6	0.09	12	7-28
22	4.7	200	6	0.09	3.8	7-28
29	4.7	200	0.6	0	0.9	7-28
18*	18	5000	12	0	16.7	7-10
19**	18	5000	12	5	33.3	7-10

*Test 29 included 1.8 lb of corrosion products in the tank.

**Tests 18 and 19 also included 180 lb of corrosion products in the tank.

Based on these results, it may be possible that the head loss resulting from mixtures of fiberglass and calcium-silicate debris materials can be estimated by the NUREG/CR-6224⁷⁻² head loss correlation in combination with a bump-up factor⁵ that is a function of the theoretical fibrous-debris-bed thickness, however, further analysis is required to support this conclusion.

In contrast to other types of particulate, the test data indicate that calcium-silicate debris materials cause a head loss even without fibrous insulation debris present in the bed. Calcium silicate insulation contains its own fibrous material, however these fibers tend to be very fine and therefore pass more easily through strainers than does the fibers from fibrous insulations. Corrosion products would simple

⁵ As originally proposed by the BWROG,⁷⁻¹⁰ the bump-up factor was the ratio of the head loss due to fiber, corrosion products, and miscellaneous debris to the head loss of the fiber and corrosion products without the miscellaneous debris (at a specified velocity). In other words, it became a method for accounting the addition of particulates other than corrosion products under conditions where corrosion products were the main source of particulate (BWR conditions). In this discussion, the bump-up factor represents the relative increase in head loss due to calcium-silicate when corrosion products are not present (PWR conditions). When using a bump-up factor method, the bump-up factor must be defined along with the data for a complete understanding of that data.

pass through the strainer if a material like fiber were not present to filter the particles from the flow.

Experiments are ongoing at the University of New Mexico (UNM)⁷⁻³¹ under U.S. NRC sponsorship to study the head loss effects of calcium-silicate. Data from these studies confirm the following trends.

- The addition of calcium-silicate significantly increases head loss and a bed formed of calcium-silicate and fibrous debris is compressible and compact.
- The head loss effects of calcium-silicate in combination with fibrous debris are sensitive to the operating temperature of the flowing water, i.e., higher temperatures typically induced higher head losses from what appears to be a chemical softening of calcium-silicate.
- Calcium-silicate can induce significant head losses by itself, without the simultaneous presence of the fibrous debris.
- The NUREG/CR-6224 correlation will need considerable modification if it is to be used to predict calcium-silicate head loss estimates.

7.1.3 Reflective Metallic Insulation

The head loss caused by RMI fragments has been studied experimentally by various U.S. and European investigators.^{7-6,7-7,7-8,7-9} Review of these experiments suggested that the head loss

caused by RMI fragments is extremely sensitive to the type, shape, and size of the fragments used in the testing program because these properties of RMI debris effect the bed structure, i.e., the pressure differential across a bed of RMI debris is strongly dependent upon the structure of that bed.

LOCA generated RMI debris would likely consists of pieces ranging from small and deformed shreds, to large sheets of foil with varying degrees of damage, to relatively intact cassettes. The relative damage to RMI insulation would depend upon its relative location to the LOCA jet, i.e., the higher the jet pressure, the more damage would occur (referred to Section 3.3.3). Insulation exposed to high jet pressures would look more like that shown in Figure 3-8. At lower pressures, the debris would contain more of the larger pieces as illustrated by Figure 3-19 showing data from the BWROG tests. Although a spectrum of debris would be generated, the spectrum of sizes on the strainer would be skewed towards the smaller sizes because the smaller pieces would transport to the strainer or sump screen substantially easier than would the larger pieces. It takes, for example, a relatively fast flow of water to move an intact RMI cassette along the floor of the sump.

Whereas research performed in Finland tended to focus on larger RMI foils accumulating on the strainer, recent research in the U.S. focused on the smaller debris. Early U.S. research focused on damaged cassettes producing large foils. These different research focuses tended to produce differing results and perhaps conclusions that were more appropriate for the respective classifications of debris. The smaller debris would transport easier to the strainer, causing more debris accumulation, and would accumulate in a random pattern. Alternately, larger relatively flat foils, assuming the pieces could transport to the strainer, could conceivably accumulate in a somewhat organized and stacked arrangement resulting in higher postulated head losses than would be caused by the random small piece debris bed. Thus, RMI debris head loss considerations are dependent upon the conditions of debris generation and debris transport.

U.S. Research on Large Foils of RMI

Experiments performed as part of USI A-43 postulated that damaged RMI cassettes would

release large (primarily) undamaged foils that then would be transported and accumulate on the sump screen.⁷⁻³ However, the focus of the testing was measuring the water velocity required to flip the foils onto the screen, assuming the foils could be transported to the base of the screen. It was assumed that after the foils accumulated on the screen, the foils would partially block the flow. Very little experimental data were collected on the head loss implications; instead, the emphasis was on the square footage of transported debris versus the screen open area.

U.S. Research on Small Pieces of RMI

Experiments performed as part of BWR strainer-blockage research used small pieces of simulated stainless steel and aluminum RMI. Based on actual collected LOCA steam/water jet generated RMI debris, simulated debris was hand manufactured to resemble the actual debris by cutting RMI foils from an insulation cassette into small sheets and then artificially damaging the foils. This process resulted in pieces of RMI debris referred to as 'crumpled' debris. (Further descriptions of the debris and the head loss data are provided in the later sections.) These experiments demonstrated that RMI fragments typically form loose beds that induce low head losses. Figure 7-3 is a picture of RMI debris accumulation on a strainer. Visual examination of the RMI debris beds suggests that crumpled RMI fragments accumulated with their major cross-sections aligned generally perpendicular to the flow direction. It is also apparent that crumpled debris beds tended to be relatively uniform and typically have high porosity. The beds formed of smaller debris tended to be more compact than the beds formed of the larger debris; the most compact debris bed was observed when fragments ranging in size from ½ in. to 4 in. were allowed to accumulate randomly on the strainer surface. Finally, aluminum RMI debris tended to form more compact and compressible beds than did stainless steel RMI debris. As a result, aluminum beds resulted in approximately 25% more head loss than the stainless steel debris beds for a fixed number of foils. Head loss data for crumpled RMI debris were obtained in the U.S. by (a) the NRC,⁷⁻⁹ (b) the BWROG;^{7-10, 7-14} (c) Performance Contracting Inc.;⁷⁻¹¹ (d) GE;⁷⁻¹² and (e) the LaSalle nuclear power plant.⁷⁻¹³

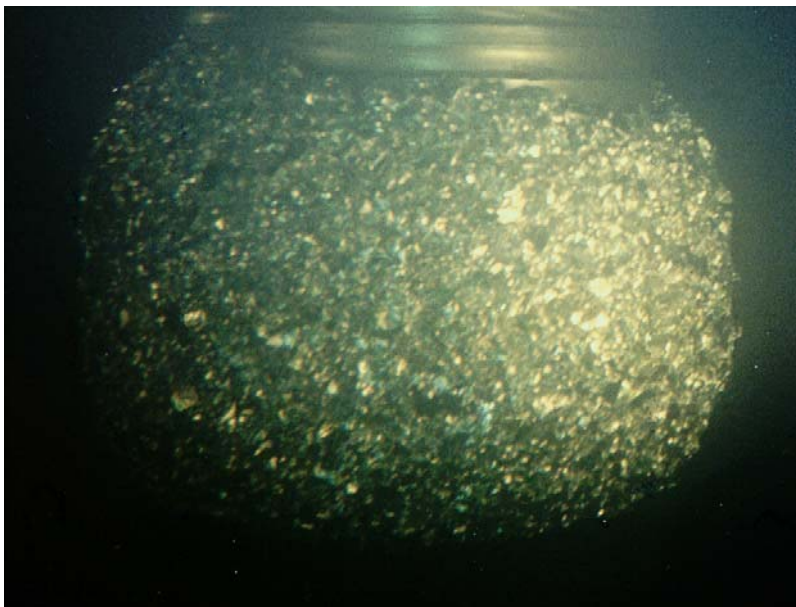


Figure 7-3 Aluminum RMI Accumulation on a Stacked Disk Strainer⁷⁻¹³

Flat Pieces of RMI

To measure head loss, Finnish researchers used regularly cut pieces of RMI foils that had 1-mm deep dimples and some curvature to the foils.^{7-6,7-15} At the time these head loss experiments were conducted, RMI debris had not been adequately characterized; all that was known was that irregularly sized and shaped debris would be produced and this was based on one HDR test. Not being able to reproduce “prototypic” debris, the researchers resorted to parametric studies. Note that the 1-mm deep dimples in the foils were manufactured into the foils to space the foils in the insulation cassettes, hence these dimples also maintained spacing in the foil debris, as well. Although no observations regarding bed structure were made in the original tests, a later investigation provided considerable insights into how bed structure may impact head loss.⁷⁻¹⁶

The understanding of the Finnish researchers was that flat pieces of RMI debris would tend to land flat on the surface of real strainers, thereby building up a bed resembling a disordered deck of cards. The more crumpled the debris, the more space there would be inside the debris bed. In such a model, the flow between the layers of foil can be simulated as flow through channels; hence, pressure changes can be predicted using standard flow channel models (e.g., head loss is proportional to the length

divided by hydraulic diameter). Other researcher insights on pure RMI include:

- RMI debris bed head losses are controlled by bed geometry much more than by characteristics of the individual debris elements; and the geometry in turn is controlled by how the debris arrives onto the screen.
- The larger the batch of debris approaching the filter at a given time, the smaller the head loss, i.e., the accumulation density affects the interstitial spacing in the debris bed so that a higher accumulation density leads to more interstitial space. During testing, the accumulation density can affect the edge effect.
- Accounting for edge effects is important even when testing prototypical strainers.

These data also are described in the following sections and have not been used in the U.S. strainer-design analyses.

7.1.4 Mixed Fiber and RMI Debris Beds

Mixed-fiber and crumpled RMI debris beds have been studied for head loss implications both in the presence of particulate debris and without particulate debris. A typical post head loss debris bed (after removal from the test apparatus) containing RMI pieces, LDFG,

and prototypical BWR sludge is shown in Figure 7-4(a) and a typical RMI/LDFG debris accumulation on a strainer is shown in Figure 7-4(b). The head loss data showed wide scatter. In most cases, the RMI head loss tests demonstrated that the introduction of crumpled RMI debris, in combination with fibrous debris and sludge, does not cause significantly different head losses than those observed with only fiber and sludge loadings. In fact, the most significant finding of the U.S. NRC tests was that under certain circumstances when RMI debris was mixed with fibrous debris and sludge, the head losses appeared to decrease as compared with similar conditions without RMI debris. However, in a few cases (e.g., the BWROG tests), it was noted that the head loss caused by RMI and fibrous debris mixtures was slightly higher than the head losses at the same fiber loading but without RMI. However, in all cases, the head loss caused by RMI debris in conjunction with fibrous (and other debris) was found to be bounded by adding the head loss caused by the individual constituents of the debris bed. As a result, U.S. NRC concluded that head loss impacts of a mixed RMI and fiber debris bed should preferably be based on measurements, or alternately can be calculated as an algebraic sum of fiber and RMI components after accurately accounting for the strainer geometry. However, it should be noted that these types of tests have not been repeated using particulate insulation debris (e.g., calcium silicate) instead of or in addition to the sludge debris actually used.

Finnish investigators also obtained head loss data for flat RMI pieces in conjunction with fibrous debris. They concluded that due to synergistic effects head loss caused by the mixed beds would actually be higher than the sum of individual contributions.^{7-8, 7-16}

7.2 Review of Experimental Programs

Head loss experiments were conducted by the following investigative organizations located in Europe and the U.S.⁶ and were reviewed in this report.

⁶Some experimental investigations were conducted in Canada but their results were not shared in public forums and hence were not included in this review.

- United States Nuclear Regulatory Commission (U.S. NRC)^{7-2,7-3,7-9}
- Pennsylvania Power and Light Co. (PP&L)⁷⁻¹⁷
- Performance Contracting, Inc. (PCI)⁷⁻¹¹
- Finnish Center for Radiation and Nuclear Safety (STUK)^{7-6,7-15,7-16}
- Vattenfall Development Co., Sweden (Vattenfall)^{7-18,7-19,7-20}
- Kernkraftwerk, Leibstadt, AG (KKL)⁷⁻²¹
- ABB Atom/Combustion Engineering (ABB) (proprietary to the company)
- Boiling Water Reactor Owner's Group (BWROG)⁷⁻¹⁰
- Fitzpatrick Nuclear Power Station (USA)
- General Electric Nuclear Energy Company (GE) (USA)⁷⁻¹²
- Continuum Dynamics, Inc. (CDI) (USA)⁷⁻²²
- Millstone Nuclear Power Plant (USA)⁷⁻²²
- Zion Nuclear Power Plant (USA)⁷⁻²³
- LaSalle County Nuclear Generation Station (USA)⁷⁻¹³
- Mark III BWR Owners Group (USA)⁷⁻²⁴

With the exception of a few investigators (e.g., Mark III BWR Owners Group, Millstone, and Zion), strainer-head loss measurements were made with no regard for debris transport or the inherent coupling that exists between debris transport and debris build-up. Instead, most tests presupposed that the quantity of debris that might be deposited on the strainers could be determined through other means, such as the assumption that debris would be distributed among operating strainers in proportion to their relative flow rates. Furthermore, the experiments sought to create conditions that assured uniform bed formation on the strainers.

The experimental approaches varied considerably, depending on what information was sought. The test setups used by these organizations can be divided broadly into four categories.

1. Horizontal flat-plate strainer setup arranged in a closed-loop test section
2. Vertical flat-plate strainer setup arranged in flumes
3. Prototype strainer modular testing
4. Semi-scale strainer testing

A review of the experimental approaches suggested that the approaches chosen have varied considerably, depending on the



Figure 7-4(a) RMI/Fiber/Sludge Post Head Loss Test Debris Bed

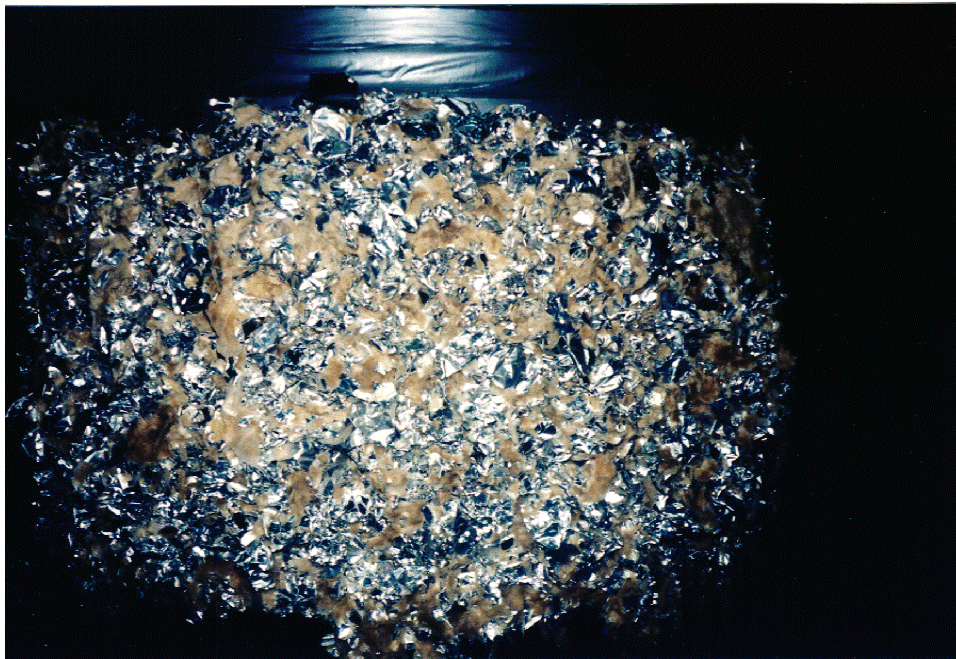


Figure 7-4(b) RMI and Fiber Accumulation on a Strainer

objectives of the experimenter, which varied from obtaining prototype test data that can be used directly in the plant-specific analyses to collecting separate-effects test data that can be used to develop a differential head loss model, which in turn can be used in the plant-specific analyses. Correspondingly, test geometries and test procedures have varied significantly. These differences have been known to contribute significantly to the test data variability, as elaborated below.

- *Differences in the test setup and geometry can introduce significant variability in the test data.* An example is that head loss measured across prototype strainers (e.g., a stacked-disk strainer or the ABB/CE strainers) at small debris loadings⁷ was found to be significantly different from that measured across flat-plate strainers (or semi-conical strainers) at the same debris loading. The difference is more pronounced for certain combinations of debris types and flow velocities. Typically, this difference is attributed to the fact that debris build-up on the special-shape strainers is unique and non-uniform. As a result, prototype strainers tended to exhibit nonlinear relationships between head loss and debris loading, which is in stark contrast to the linear relationship observed for flat-plate strainers. These differences in the data trends led some experimenters to conclude that flat-plate strainer data could not be used to predict the head loss caused by special strainer shapes.

Even among flat-plate strainer experiments, the data variability is significant between the NRC/ARL tests, which used closed-loop systems equipped with pumps, and the CDI/BWROG gravity-head loss tests. Here the differences can be attributed to differences in the bed compression and bed formation.

- *Differences in test procedures may add to some of the data variability.* Experiments have shown that differences in (1) the time sequence in which different debris species accumulate on the strainer and (2) the concentration at which debris approach the strainer affects head loss considerably.

These differences were found to affect bed morphology and uniformity.

This observed variability in the head loss measurements has led to confusion regarding the acceptability and applicability of test-data usage in the plant-specific analyses. In particular, it often has led to debate, without a consensus outcome, on what is the most appropriate approach for assessing strainer pressure drop performance. This uncertainty was reflected in the CSNI report. But as the research matured, common frameworks for addressing the variability has emerged, and this section takes a critical look at options available for performing tests and their relative merits.

7.2.1 Flat-Plate Strainers

Before the 1990s, the ECCS designs used conventional suction strainers (e.g., truncated-cone strainers, cylindrical strainers) and rectangular sump screens. The earliest experimenters (USI A-43) used small, perforated strainer plates to experimentally simulate the head loss performance of these regularly shaped strainers with the understanding that debris build-up on conventional strainers would be fairly uniform and that at a differential scale, the flat-plate would be a reasonable approximation for the curved strainer surface. Figure 7-5 illustrates how a portion of the debris bed on a strainer would behave in a manner similar to debris in a test loop, assuming both have a like thickness and composition. The validity of this assumption depends somewhat on the thickness of the debris bed. For a thin bed, the assumption is certainly valid, but for a thick bed, the curvature of the strainer may have to be considered because there would be more debris per unit area in a curved bed than in a flat bed of the same strainer area due to the curvature. However, this consideration has generally been less significant than other experimental uncertainties. Thus, flat-plate strainers present the simplest similitude for the conventional suction strainers/sump screens. The only scaling issue considered to be important relates to the dimensions of the test screen perforations relative to actual strainer perforations. (BWR strainers commonly used plate strainers compared with PWR sump screens that use wire-mesh screens.)

⁷Expressed in terms of debris mass per square-foot of the strainer area or, alternately, in terms of theoretical thickness.

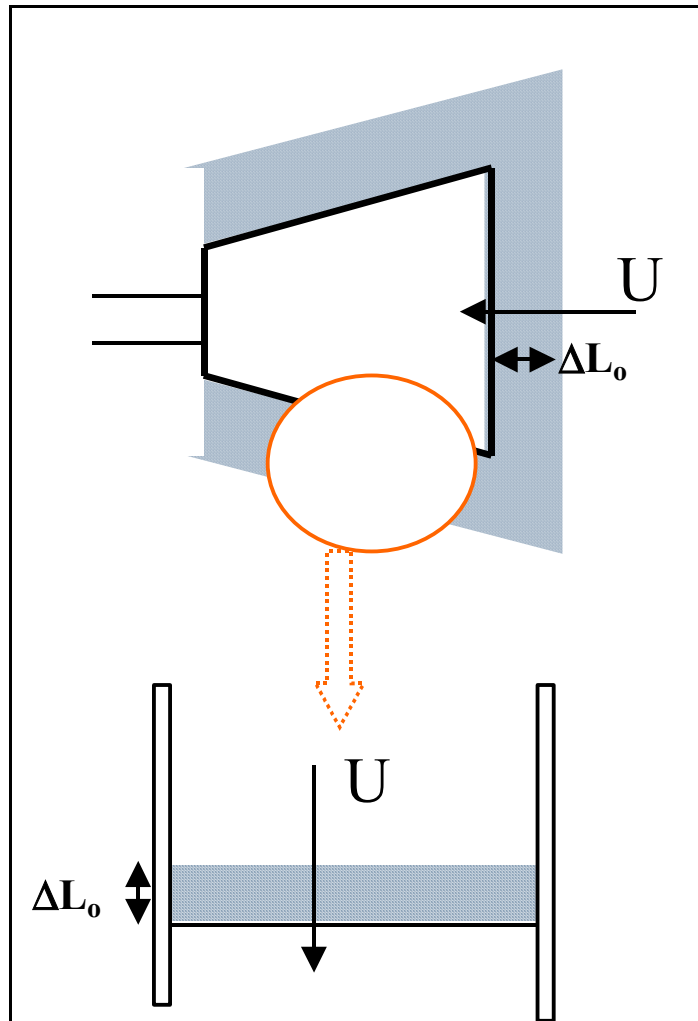


Figure 7-5 Equivalency Between a Truncated Cone Strainer Debris Accumulation and Flat-Plate Strainer Simulation

A typical example of a flat-plate-strainer test setup is presented in Figure 7-6. This test setup was originally used in the U.S. NRC tests that supported the resolution of USI A-43. Several insulation and strainer vendors, PCI and Transco, and nuclear power plant owners also used this same setup. In this setup, a 1-ft-diameter perforated plate, with a representative diameter for the perforation holes, was arranged horizontally in a closed loop equipped with the necessary instrumentation. A large-capacity pump capable of maintaining sufficiently high velocities circulated water through the test loop. Debris was introduced at the top of the setup and allowed to settle down on the strainer face and the corresponding head loss was measured.

The primary advantages of this type of testing are as follows.

1. Because the volume of water present in the test setup is small, it is possible to conduct the tests at elevated water temperatures and appropriate water pH and to quantify the effect of water temperature and pH on head loss.
2. The low surface area of the piping and equipment also means that it is easier to clean the test setup between tests.
3. Because the test setups typically use small strainer plates, the quantity of debris to be used in each test is small. This reduces the costs of experiments.

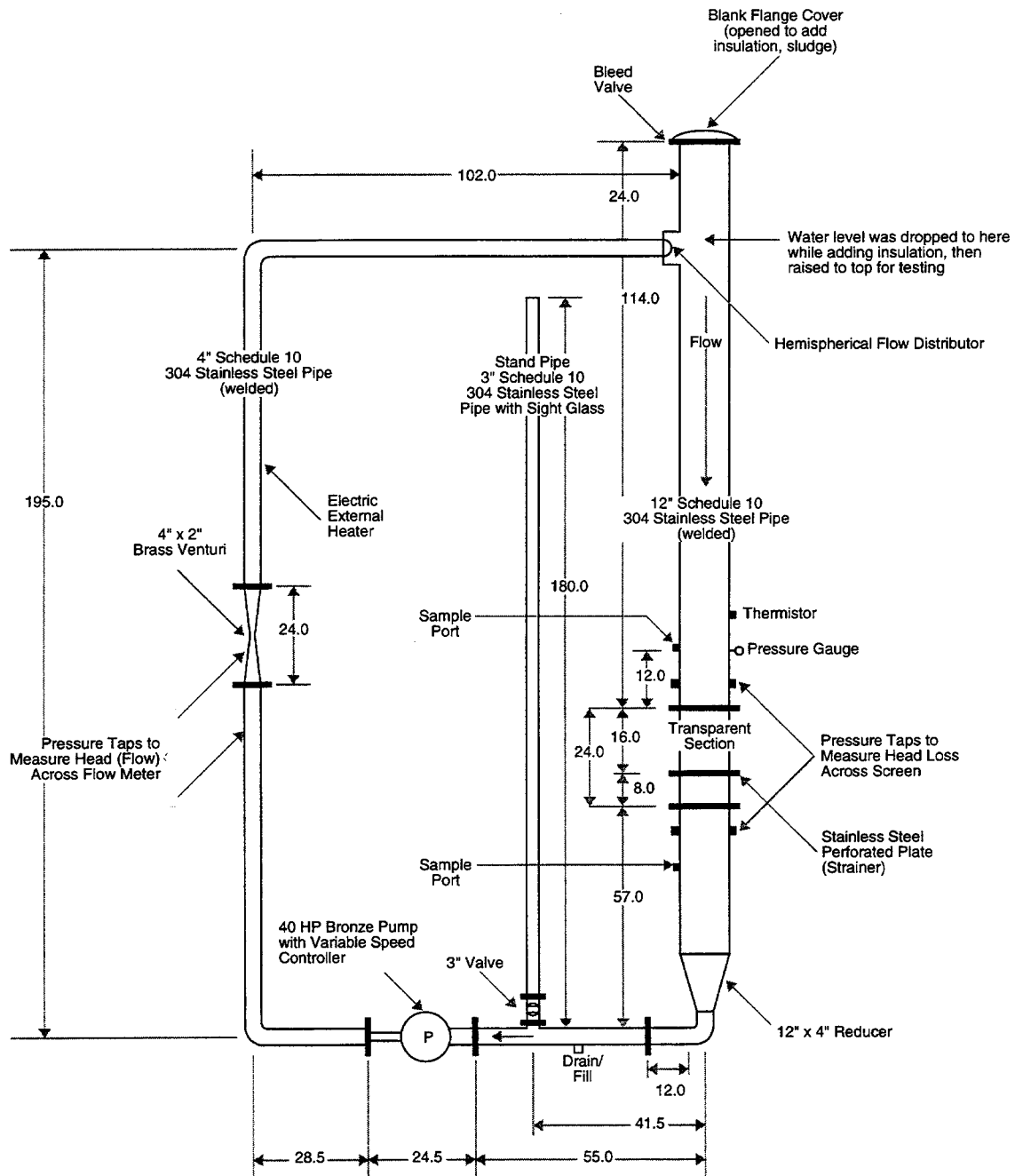


Figure 7-6 Vertical Flat-Plate-Straener Head Loss Facility at Alden Research Laboratory⁸

⁸ Such a facility is also operational at the University of New Mexico where head loss testing is ongoing at this time.

4. The experimenter can access the strainer easily after testing is completed and retrieve the debris bed without disturbing it. This allows the option to measure the actual quantity of debris, especially the sludge-like fine debris, deposited on the strainer surface *vis-à-vis* the quantity added to the loop and to examine the bed morphology analytically. This information can be used to develop a direct relationship between the bed morphology, the quantity of debris on the strainer, and the resulting head loss.

There are four major drawbacks for this particular design:

1. The debris introduction is artificial and non-representative. The experimenter drops the debris at the top of the setup and allows it to be deposited on the strainer under the combined influence of gravity and fluid drag. If performed improperly, this could result in some non-uniformity, which has a potential to render the test data non-conservative. It is strongly recommended that test procedures be developed to ensure that the debris build-up would be uniform. Introduction of debris over a long period of time and uniformly across the flow cross section seems to overcome this drawback.
2. The presence of the wall around the strainer has a potential to create peripheral gaps between the debris and the wall (because of the irregular shape of the debris). If these gaps are sufficiently large, a significant portion of the flow may pass around the debris bed instead of through it. This is an inherent shortcoming of these tests; as noted by STUK investigators, if close attention is not paid to this issue, it could lead to non-conservative test data. This concern appears to be significant for large irregularly shaped debris, such as RMI. For smaller debris, this concern may not be critical, but nevertheless should be evaluated and either eliminated (if possible) or minimized. In general, if the characteristic dimension of the largest debris is much smaller than the test filter dimensions, then the peripheral gap effect will not invalidate the test results.
3. Some of the finer debris (e.g., sludge) may settle out in the loop where the flow velocities are expected to be low. Concentration measurements should be used to ensure that finer debris is not

settling out in the loop. Furthermore, the loop should be designed to ensure that the flow velocities in the horizontal sections are sufficiently large to rule out extensive deposition of finer debris.

4. It is not possible to obtain single-pass-through filtration data from this closed-loop system. If information regarding the filtration efficiency of debris bed is important, then other alternatives to this setup should be sought.

Important Considerations for Future Experimenters

Although the flat-plate-strainer similitude was known to possess several shortcomings, it has long been thought that this approach would result in “conservative” head loss measurements for most debris types of interest.⁹ The acceptability of this approach has gained considerably from the fact that these tests are easy to design and conduct. Furthermore, because these tests are cheaper, it is possible to repeat them extensively and also to perform several exploratory tests to identify controlling test conditions that should be captured in the larger scale experiments. As a result, many investigators have used this test setup and reported experimental data for a variety of insulations and fluid velocities. Also, much of these test data formed the basis for several regulatory decisions both in the U.S. and Europe. In any case, the use of the flat-plate head loss data in conjunction with prototype strainer testing has proven to be an effective method of evaluating strainer head loss.

These tests are ideally suited for the following purposes:

1. *To perform separate-effects tests.* These tests explore the effect of each individual test parameter (either separately or in select combinations) on the head loss. Such an understanding would help the experimenter (a) to assess the need for conducting larger-scale tests and (b) to optimize the number of tests to be conducted in the larger scale tests.

⁹If proper procedures are followed, the setup allows for uniform distribution of debris on the strainer surface and thus results in higher head losses than the plant strainers.

2. *To augment larger-scale test data.* For example, consider that an experimenter obtained head loss data for fibrous debris bed formed on a stacked-disk strainer. The vendor now would like to quantify the effect of adding a small quantity of calcium-silicate on the head loss. The closed-loop flat-plate-strainer test setup can be used to measure the bump-up in the head loss (caused by addition of calcium-silicate) and use that information to scale the large-scale test data proportionally. Several past investigators have used this approach to augment strainer data and account for the effect of small quantities of miscellaneous debris (e.g., paint-chips, calcium-silicate, and asbestos). However, it should be noted that (a) the fluid velocity through the bed in complex strainers varies considerably and (b) the bump-up factor also varies with fluid velocity. Therefore, data from a flat-plate strainer, when used to augment larger scale head loss data, should be used judiciously.
3. *To judge performance of regularly shaped strainers.* The flat-plate strainers are a fairly adequate representation of truncated-cone and cylindrical strainers, especially at low debris loads. However, at higher debris loads, the debris build-up on the cylindrical strainers tends to resemble an ellipsoid. Application of flat-plate strainer data at higher debris loads may result in conservative conclusions.
4. *To develop head loss models.* If head loss models that can effectively predict head loss caused by debris buildup on advanced strainer designs can be developed and validated for use with advanced designs, it would streamline the process of tailor-making the strainers for each plant application. Section 7.3.2 provides an approach for how a head loss model developed based on flat-plate strainers can be used to predict the head loss caused by stacked-disk strainers.

Recently, there has been considerable debate among experimenters regarding the benefits of using flat-plate-strainer test setups and the acceptability of the conclusions reached from flat-plate strainer test programs. There has been some evidence presented by STUK investigators that the inherent geometrical features of the flat-plate-strainer test setups and the commonly used test procedures could

have a potential to make the test data non-conservative for some debris types. The specific debris of concern is large RMI, either with or without fiber, although similar concerns may exist for other debris types. There also have been concerns that the application of flat-plate-strainer test data to evaluate the head loss performance of advanced strainer designs is complex and impractical.

Known Variations in the Geometry

Several investigators used the closed-loop test setup shown in Figure 7-6. Primary examples are (a) U.S. NRC tests for head loss data for fiberglass, sludge, and RMI debris, (b) U.S. vendor tests for measuring the head loss effect of calcium-silicate debris, (c) Bremen Polytechnic tests for head loss data related to KAEFER insulation materials, and (d) KKB Bericht head loss tests. The Swiss investigators and Vattenfall research reportedly modified this experimental setup considerably by to improve the means by which debris accumulated on the strainer plate. Figure 7-7(a) presents a schematic of the test setup used in the KKL tests. In these tests, the flat-plate strainer piece was installed horizontally on the open end of the pump suction line. The pump suction line and the strainer were located in an open tank. The pump takes suction from the tank through the flat-plate strainer and returns the filtered water to the same tank, thus forming a closed loop. The debris was added to the tank and allowed to accumulate on the strainer surface gradually. A mixer was used to ensure that debris would not settle out in the tank.

This design modification retained the advantages of the closed-loop testing (small water volume, small surface area for deposition of sludge-like debris, etc.) and thus still provides an option to conduct tests at elevated temperatures and pH. It is possible that beds formed on the strainer would be more prototypical at the smaller debris loadings. However, at higher debris loadings, it is possible that bed build-up could be affected significantly by the tank turbulence, perhaps thereby affecting bed uniformity at the periphery of the bed. Nevertheless, prospective investigators should evaluate this variation and use it as necessary.

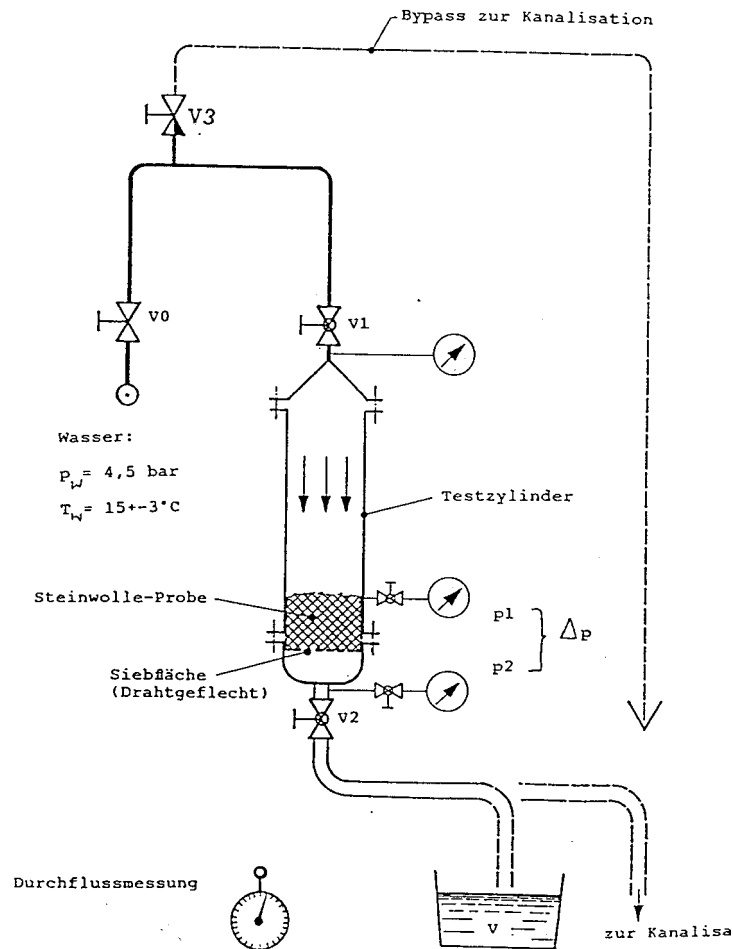


Figure 7-7(a) Flat-Plate-Strainer Head Loss Facility Used in KKL Testing

The BWROG developed an alternative approach that did not involve a pump and had one-through flows. This setup, referred to as the gravity head loss test setup, relied on the static head of water above the strainer to drive flow through the debris bed. As shown in Figure 7-7(b), this apparatus consists of a 16-ft-long, 6-in.-diameter clear plastic tube. The bottom of the tube had a sealed perforated plate to simulate a strainer and the top end was open. Water mixed with debris was introduced to the pipe, and sufficient time was allowed for debris to settle. In theory, because the debris is well mixed with water, the settling process would result in formation of a uniform bed on the strainer surface. Immediately below the strainer plate was a “quick-release” hinged sealing plate that was

opened quickly to induce water flow through the pipe. A pressure transducer monitored the water level as a function of time. This data was used to derive head loss and fluid velocity data. However, this approach had several deficiencies, among them are the following:

- (a) The test setup did not compress the bed before the head loss was measured.
- (b) There was no assurance that the debris beds were uniformly formed, especially when the experiments involved sludge.

This setup consistently resulted in lower head loss measurements. These deficiencies lead the U.S. NRC to conclude that the use of the test data by itself in the plant analyses was not

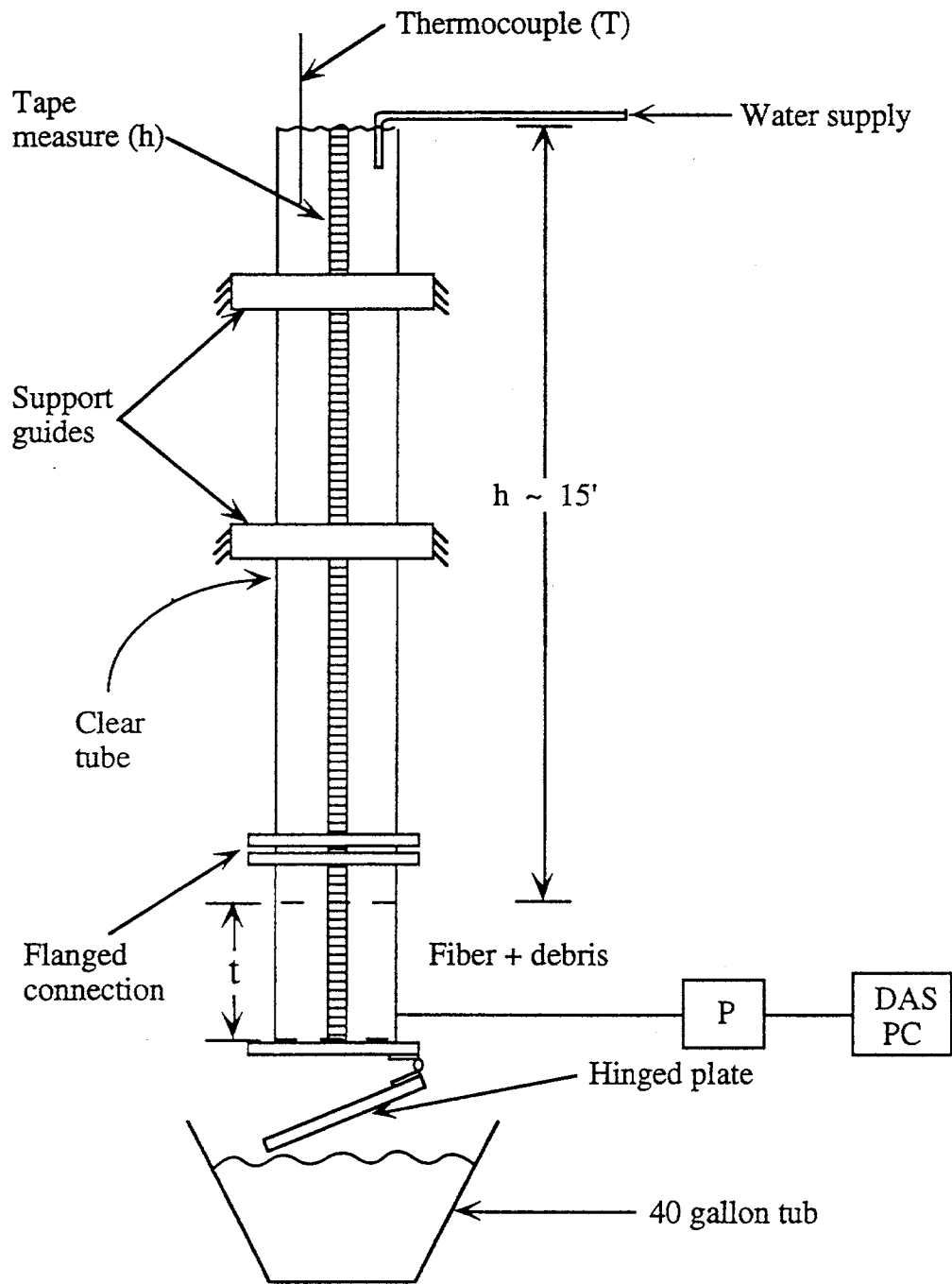


Figure 7-7(b) Gravity Head Loss Test Setup Used in the BWROG Tests

acceptable, therefore only limited use of the test data was allowed. Future investigators are strongly advised against using this setup.

7.2.2 Flat-Plate Strainers in Flumes

Starting in the 1980s (e.g., the USI A-43 study), vertical perforated flat-plate strainers located in the horizontal flumes were used to simulate PWR sump screens. Flume transport experiments have shown that debris tends under certain conditions to accumulate non-uniformly on the PWR sump screens, preferentially near the floor. The flume test setups were designed especially to study this type of debris build-up and its effect on head loss. In general, this setup retains the primary advantages of the closed-loop setups described above, and attempts to simulate the unique pattern of debris build-up on the PWR screens at the same time.

Figure 7-8(a) presents a schematic of the test setup used in the early NRC tests. In these tests, a horizontal flume several feet long was used to simulate water flow on the PWR containment floor approaching the sumps. Water enters on the right side of the flume at a pre-selected flow rate and flows through a perforated plate designed to reduce the flow perturbations. Debris introduced downstream of the perforated plate will be transported by the flow to the vertical flat-plate sump screen located near the far end of the flume. The head loss effect of debris build-up was then easily measured. Figure 7-8(b) is a photograph of large foil debris accumulation against the strainer/screen surface.

The primary advantages of this test setup are as follows:

1. This setup provides a more realistic representation, compared with the vertical setup described above, of debris build-up on vertical screens and its potential effect on head loss. Some of the past tests have shown that heavier debris (e.g., stainless-steel RMI and paint chips) would result in relatively small pressure differentials across the screen, due primarily to the observed non-uniformity in the debris bed.
2. This setup can be used to evaluate experimentally the effect of key geometrical features of the sump (e.g., curbs and multiple screens) on the head loss caused

by accumulation of a specific quantity of debris.

3. If sized appropriately, this setup retains most of the advantages listed above for the flat-plate strainer. For example, the setup could be designed to provide high-temperature and high-pH environmental conditions.
4. External means could be used to create prototypical flow patterns closer to the screen to ensure that the debris accumulation is representative of debris build-up on an actual plant sump screen.

The primary disadvantages of this setup are as follows:

1. This setup retains most of the disadvantages of the flat-plate strainers. For example, the presence of the wall around the screen has a potential to create peripheral gaps between the debris bed and the wall.
2. Although the setup presents an illusion that the debris build-up is prototypical, the debris build-up on the screen would not necessarily be representative of actual plant conditions. The debris build-up is a function both of gravity and the flow patterns closer to the screen. It is not necessarily true that a vertical screen arranged in an arbitrary flume would automatically provide the prototypical conditions expected to occur in a plant.

Important Considerations for Future Experimenters

Although the flume setup has been used for simulating the debris build-up on a PWR sump screen and the resulting head loss, the results should not be applied without careful comparison of the flume flow patterns with those of the real plant. The following factors should be considered while designing the tests:

Inflow Conditions. Implicitly, the flume setup attempts to quantify the combined effect of (a) transport and accumulation of debris on the sump screen as a result of flow patterns in the close vicinity and (b) head loss resulting from such a build-up. Therefore, measured head loss should be used in the analysis only if the analyst is reasonably certain that flow patterns close to the screen are indeed representative of the actual plant conditions. It appears that calmer (or longer) flumes provide a reasonable representation of the remote sumps, where

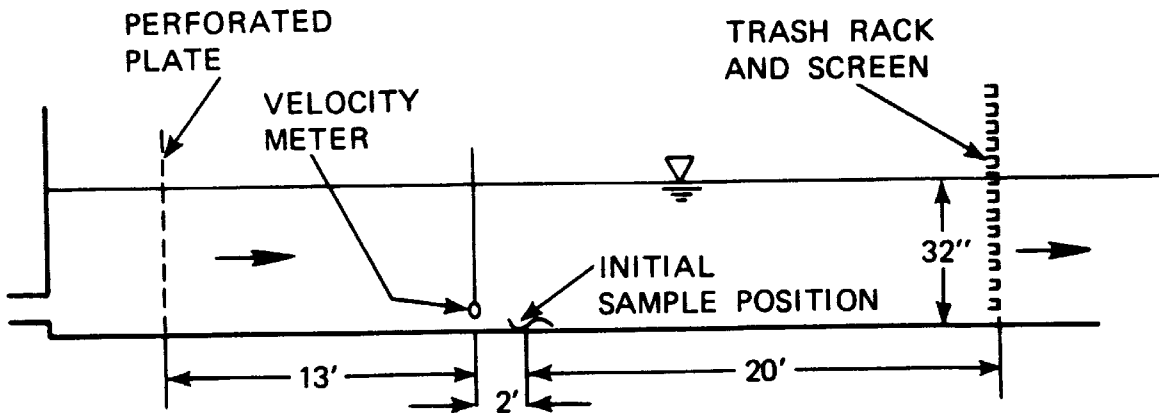


Figure 7-8(a) Schematic of the Horizontal Flume Used in the NRC-Sponsored ARL-Conducted PWR Sump Screen Tests¹⁰

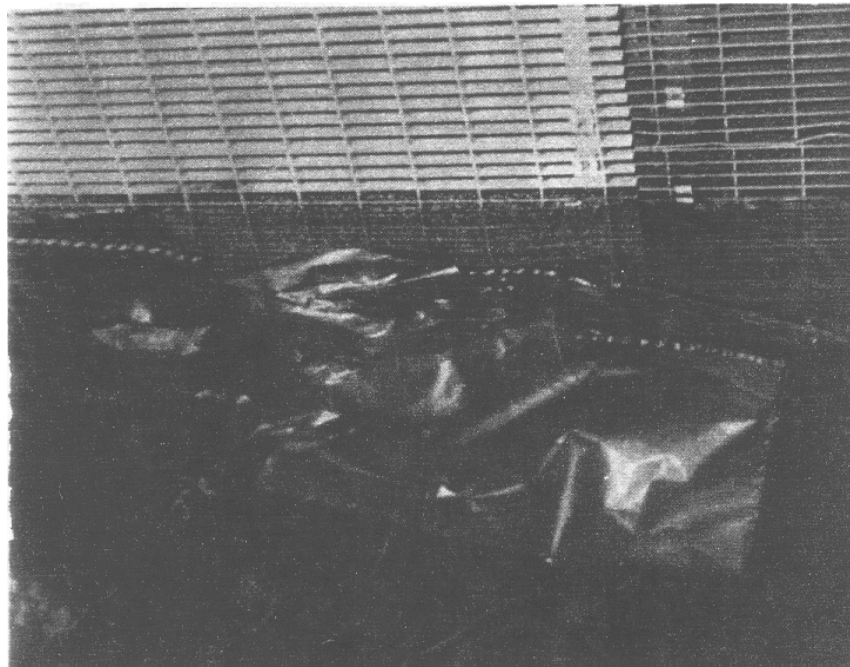


Figure 7-8(b) Picture of Large RMI Foil Accumulation on the Vertical Screen

¹⁰ Such a facility is also operational at the University of New Mexico where head loss testing is ongoing at this time.

either the sump is located away from the postulated break locations or the sump is shielded from the turbulence created by the break flow patterns and containment spray drainage. For other cases, it must be carefully considered whether the flume can capture the flow patterns adequately. Some experimenters have used external means (e.g., water injection or mixers) to create conditions that provide a conservative representation of the conditions that might exist closer to the sump.

Geometrical Features. The head loss measured has been reported to be strongly dependent on the physical features of the sump screen (e.g., screen orientation) and the structures located in the close proximity (e.g., debris curbs). The experimenters should model these features carefully to judge their effectiveness.

Known Variations in the Geometry

Several variations to the setup shown in Figure 7-8(a) have been considered. In the CDI test setup shown in Figure 7-9(a) for the Zion and Millstone Unit 2 nuclear power plants was significantly different. The setup used in the KKB tests, shown in Figure 7-9(b), was somewhat similar to Figure 7-8(a). The CDI setup, a pie-shaped flume was used to simulate gradually accelerating flow as it approached the sump screen. The sump was basically a solid box with its left side open for flume flow into the sump; the bottom opening allows for connection to the pump. The open side of the sump was fitted with a representative sample of the actual sump screen from the Millstone Unit 2 plant. The sump screen was placed on a full-scale-height curb.

The flume experiments were closed-loop in nature. Several small pumps were used to circulate water through the test setup. These pumps took suction from the bottom of the sump and delivered it to a diffuser mounted above the tank. The diffuser was chosen to simulate water falling from the steam generator compartment into the water pool formed on the containment floor.

In the CDI tests, the tank and the flume were filled to 55-in. high (full-scale height), and pre-measured volumes of the debris were added uniformly across the pie-shaped flume cross-section. The debris was allowed to settle to the flume floor, and the pumps were turned on to the desired flow. Observations of the transport of the

debris on the floor and their accumulation on the screen were made. The experimenters also measured the head loss resulting from debris accumulation.

7.2.3 Prototype Module Strainer Testing

The replacement strainers installed or being considered for installation at the U.S. and European nuclear plants rely on complicated structural features to maximize the strainer surface area. Some use planar surfaces to maximize the available surface area within a selected spatial envelope to enhance the strainer's capacity to accommodate a large quantity of debris while simultaneously minimizing the hydrodynamic load impacts. Other design concepts intentionally introduce non-uniform flow distribution across the strainer's surface with the intent of directing the debris to accumulate preferentially in selected areas of the strainer. A feature of the nonlinear flow is that flow can be somewhat parallel to some of the strainer's complex surfaces, such that the flow tends to sweep debris from these surfaces into the strainer's debris traps, thereby keeping some of the strainer's surfaces relatively free of debris until the debris traps fill. Emerging PWR strainer designs may intend to take advantage of the preferential accumulation of debris toward the lower parts of the sump screen. Many vendors have recognized that it is impractical to simulate the head loss performance of such strainers using flat-plate strainers in the arrangements discussed above.

An alternative was to use a full-scale or near-full-scale strainer modules in the experiments and investigate debris build-up and head loss. Early examples of individual-module tests were (a) the PP&L-sponsored tests conducted at the Alden Research Laboratory, Inc. (ARL) and (b) the metallic insulation transport and strainer-clogging testing reported by STUK (see Figure 7-10). Since then, almost all of the strainer vendors and some of the plants have used this type of testing, either during strainer development or as part of strainer qualification before the strainer is installed at a plant. It generally is believed that individual-module testing is a *necessary and sufficient* experimental approach—*necessary* because, without the module tests, it is not possible to obtain directly applicable test data, and *sufficient* because the experimental approach sufficiently

Millstone 2 Tank Test

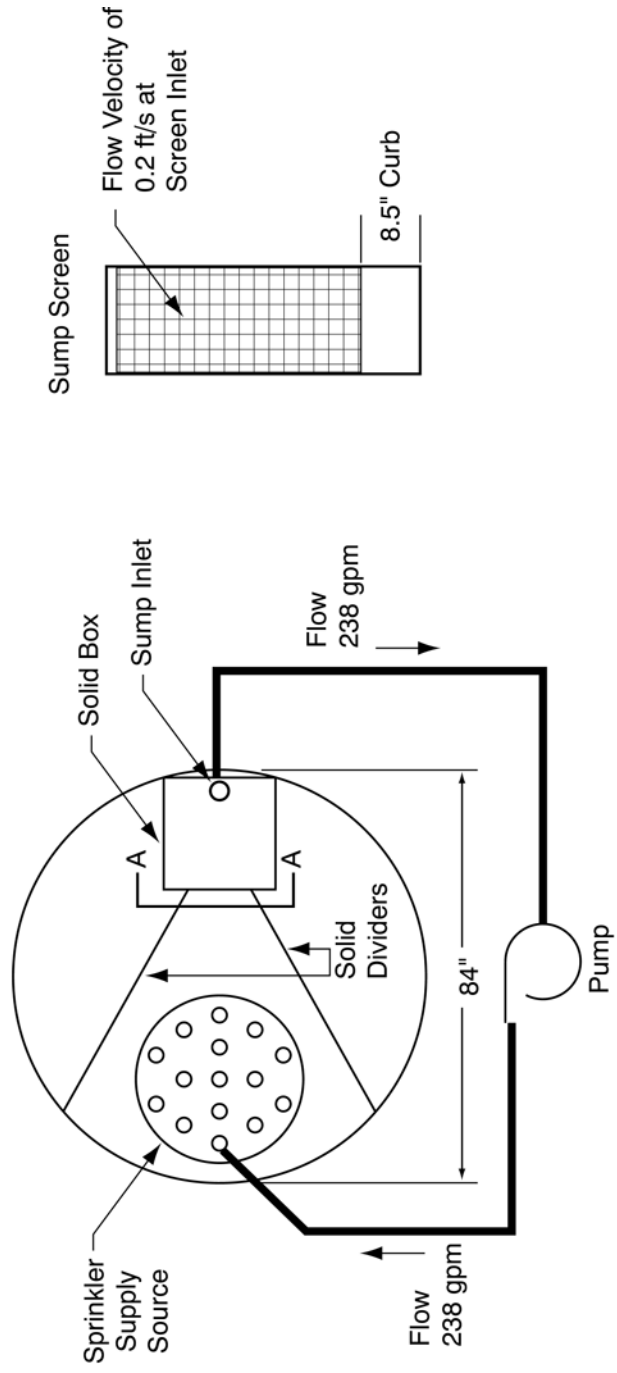


Figure 7-9(a) Flume Test Setup Used in the CDI Experiments for Millstone 2

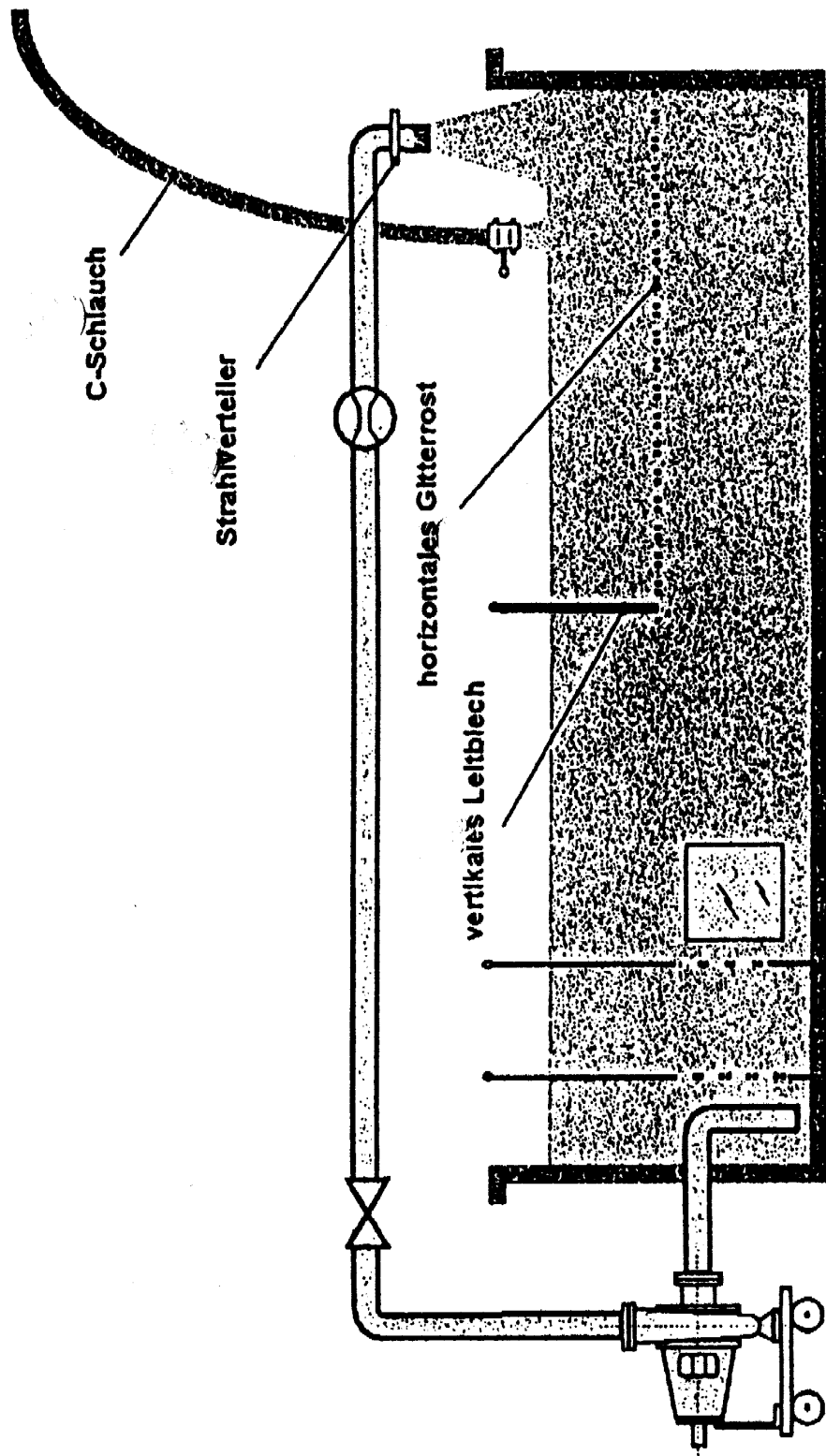


Figure 7-9(b) Test Setup Used for Transport and Head Loss Measurement in the KKB Plant-Specific Tests

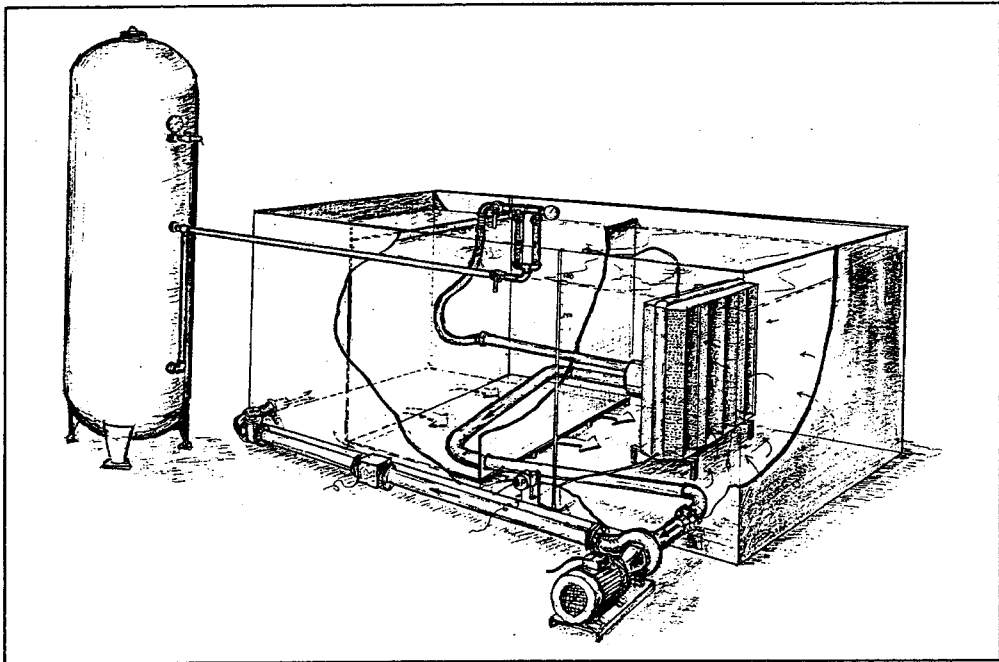
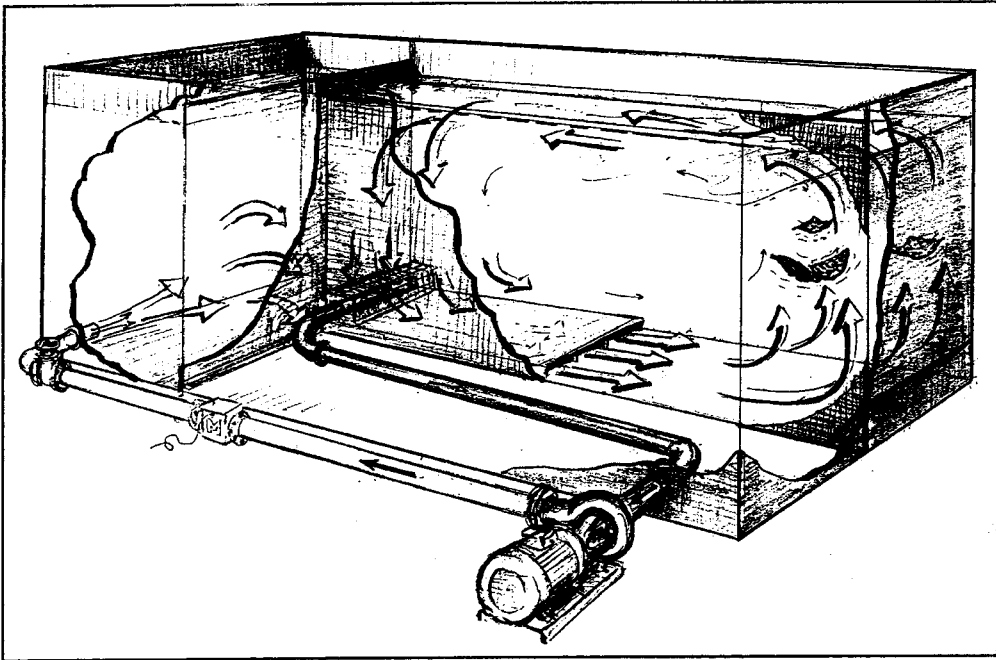


Figure 7-10 STUK RMI Head Loss Test Setup for Prototype Strainers

captures all the controlling phenomena. Although there are merits to this argument, it should be recognized that even prototype testing is associated with several non-prototypical conditions that have to be compensated for in the plant-specific analyses.

In the prototype tests, a strainer module (nearly 1:1 scale¹¹) is used to measure and relate head loss across the strainer to the quantity of debris accumulated on the strainer and the flow rate through the strainer. The special emphasis of this type of testing is to assess the effect of special strainer design features (e.g., crevices or cavities) on the debris build-up and the associated head loss across the strainer.

This type of prototype testing was carried out by the following strainer developers/vendors:

- Performance Contracting, Inc., (U.S.)
- Vattenfall Utveckling, (Europe)
- ABB Nuclear Services (Europe),
- ABB/Combustion Engineering (U.S.),
- BWROG/General Electric Nuclear Services (U.S.),
- Enercon/Mark III BWROG (U.S.),

The following plant owners took part in strainer qualification before installation.

- Vattenfall Utveckling (Europe)
- LaSalle County Electric Station (U.S.)
- Limerick Generating Station (U.S.)

The following regulatory agencies used this approach while developing guidance.

- Finnish Center for Radiation and Nuclear Safety (STUK)
- Swedish Nuclear Power Inspectorate (SKI)
- U.S. Nuclear Regulatory Commission (BWROG/SER)

Figure 7-11 presents a schematic representation of the test setup used in the BWROG prototype testing, which is similar in concept to the setup used by STUK (see Figure 7-10). Typically, the strainer module is located in a large tank of water. Water flow through the strainer module is

maintained by recirculation pumps, which take suction through the strainer and discharge it to the tank. In some test setups, water discharge locations are located strategically to maximize turbulence in the tank such that the potential for debris settling in the tank is minimal. Other test setups use mechanical or manual means to ensure that almost all of the debris added to the tank would reach the strainer, and the minimal debris, if any, would settle out in the tank. Head loss across the strainer is monitored using a pressure transducer located downstream of the pipe flange connected to the strainer. Figure 7-12 plots head loss as a function of the strainer load measured in these tests.

There are a few variations to the test setup. In the STUK tests, the strainer surface area was oriented vertically. A similar approach was also reportedly used in the Vattenfall tests involving wall-mount-type strainer modules. The other Vattenfall tests located the strainer vertically on the floor. These finer differences may not have influenced the test data because the test objects were small compared with the pool size and the pool turbulence was sufficient to ensure that debris deposition was uniform. However, future investigators should pay close attention to such details.

Adding a predetermined quantity of debris to the tank commences a typical test.¹² The debris would be transported to the strainer gradually, as water is being circulated through the strainer. The transient response of the pressure transducers was tracked to determine the onset of steady state. In most cases, several pool turnovers were necessary to reach steady state. Even an hour into the test, it could be seen that a noticeable fraction of the debris would still remain either entrained in the strong eddies or settled out in the localized regions of the tank where flow turbulence was low. Some investigators used manual means to guide the remaining debris towards the screen. After the steady-state head loss was measured, investigators did one of the following.

¹¹If the tests are not close to full-scale, non-prototypic edge effects could affect the head loss data in a manner similar but potentially different from the flat-plate peripheral gap effect.

¹²Most U.S. tests added sludge first to the test tank and circulated water through the tank at relatively high velocities to ensure that it is well mixed with the water. Other debris was then added to the tank, sequentially as necessary.

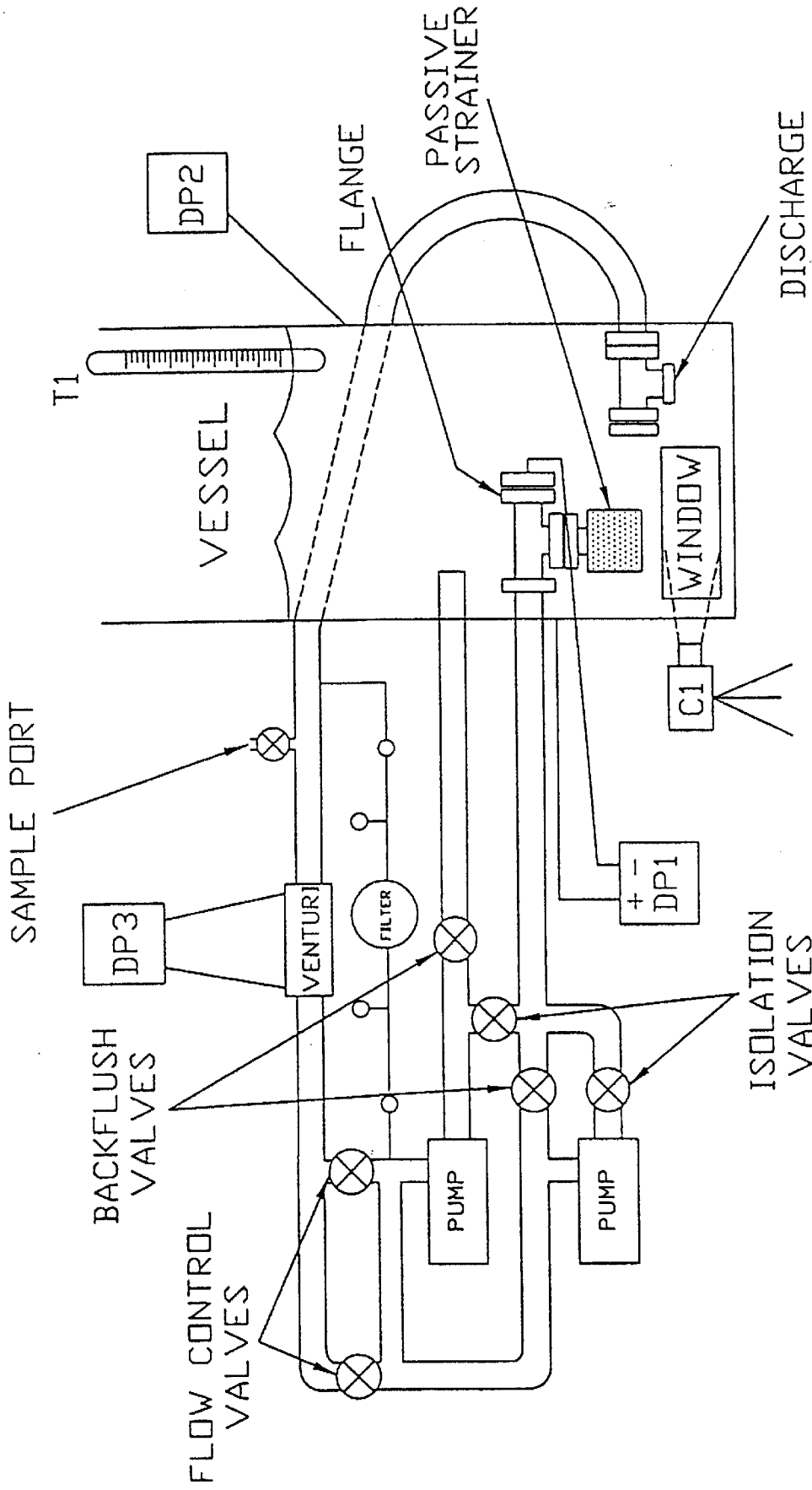


Figure 7-11 BWROG Prototype Strainer Module Test Setup

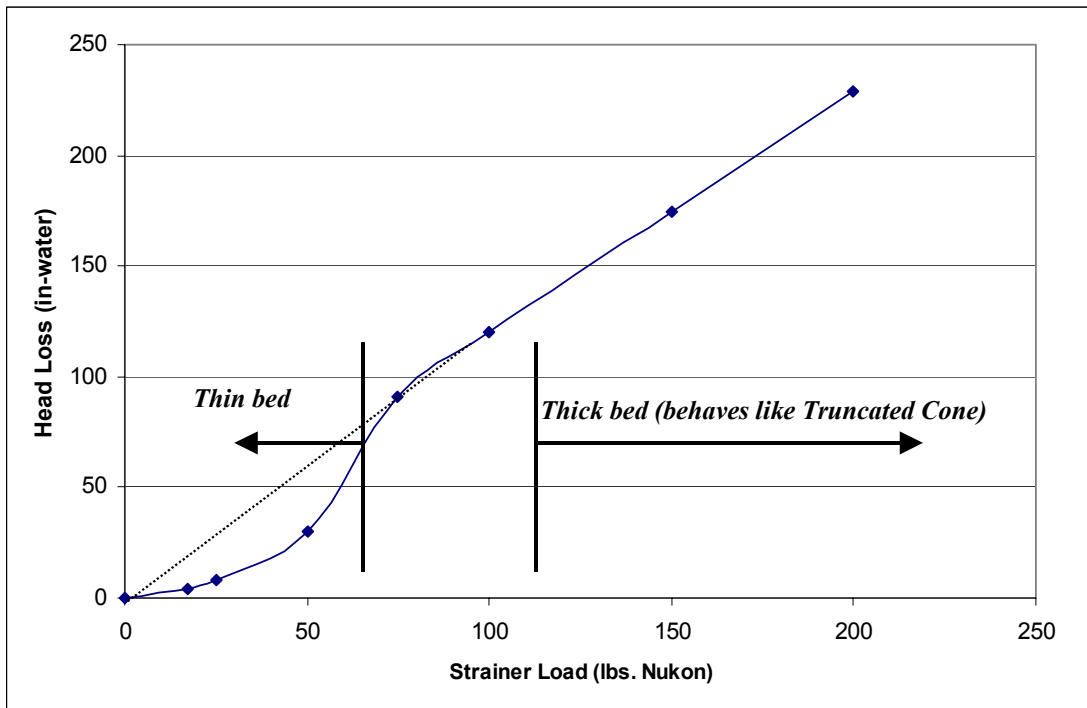


Figure 7-12 Measured Head Loss as Function of Strainer Debris Loading for Specialty Strainers

1. Terminated the test and moved on to the next test, which involved repeating the test at different debris loadings.
2. Added additional debris to the tank and repeated the entire test procedure to measure head loss at a higher debris loading.
3. Varied the flow through the strainer over a pre-set limit to measure head loss at different flow rates.

The primary advantages of prototype module testing are:

1. Prototype-strainer-module testing is the only option available for measuring and correlating clean-strainer head losses for many of the advanced designs. Some of these strainers incorporate advanced flow-control devices (e.g., vanes, ribs, channels, etc.) to distribute the flow more uniformly across the entire strainer surface area. Although several attempts have been made by various vendors to compute clean-

strainer head losses theoretically, they could not be used in the plant-specific analyses due to the large uncertainties.

2. Prototype-strainer-module testing is the only option available for examining how the debris would build up on the strainer surface and the effect it would have on the head loss. It also sheds light on how debris is distributed on the strainer surface at low and moderate loadings.
3. Because the strainer models used are actual size, the test data would not have to be corrected for non-prototypical aspects such as the bypass flow.

The primary shortcomings of prototype tests are listed below.

1. Because of the large water volume, the conduct of these tests is limited to ambient temperatures rather than the elevated suppression-pool/sump water temperatures. Non-prototypical temperatures must be corrected for. In some cases, correcting for

temperature effects is straightforward (e.g., compensate for the viscosity effect). However, there are special cases in which temperature correction is difficult. For example, it is not easy to correct for temperature effects if the strainer design is such that the circumscribed velocity is in the turbulent range and the plate velocity is in the laminar region. Similarly, if the debris type has special chemical reactions at elevated temperatures, a simple viscosity correction is not sufficient.

2. Large volumes of water and large surface areas also limit the number of tests that can be conducted, because it costs more to clean the test facility between each test and it costs more to refurbish insulation. In practical terms, this may have a serious effect because it limits how much understanding one can gain from such tests. This also forced past investigators to optimize the test conduct such that a single test could be used to derive head loss data for several operating conditions. This factor alone contributed to significant variability in the reported data.
3. It is almost impossible to measure precisely what fraction of the debris dropped in the tank actually reached the strainer surface. Past experience has shown that debris has a tendency to settle out in the corners of the tank. One could argue that the quantity of debris that settles out is very small compared to the quantity accumulated on the strainer.
4. The test program (at least in the traditional way that the results are applied in the plant-specific analyses) presupposes that the quantity of debris expected to accumulate on each strainer module and the sequence in which the debris accumulates are known, and that this sequence can be reproduced in the testing. This assumption can introduce uncertainties in the use of the test results because the debris arrival sequence derived from analyses would also be uncertain.
5. The flow patterns and turbulence levels encountered in the tank tests may not resemble the actual plant conditions, and thus conclusions drawn from the prototype testing regarding saturation quantities may not be accurate.
6. Repeatability testing should be conducted. Past repeatability of prototype strainer module tests has indicated substantial uncertainty in the head loss data for some

test conditions that should be factored into plant-specific analyses whenever such conditions are indicated by testing.

7. The transient head loss traces obtained from these tests are not expected to be representative of the actual plant application. One reason for this is that the pool turnover time in the prototype tests is significantly different from that in a plant. Even if the pool turnover time is the same, there is no assurance that the debris accumulation rate in the prototype tests would be representative of that in the plant. This point is particularly important for licensees that opt to take credit for ECCS throttling as part of their analyses.
8. Past experience has shown that reaching a true steady state head loss would take several hours to days, depending on the type of insulation and the flow velocities. Many tests were terminated when the head loss traces became fairly flat and the majority of the debris in the tank had accumulated on the strainer. Limited long-term testing (over days) has indicated that head loss increases slowly. This long-term behavior was believed (but not verified) to be due to debris bed decomposition that leads to more compact beds. Future investigators will have to deal with these considerations, as well. Therefore, it is important to note that this deficiency exists and correct for it through either the use of separate-effects testing or other defensible means (e.g., BWROG URG description).

Important Considerations for Future Experimenters

As previously discussed, the prototype-module tests are a necessary set of tests that must be conducted as part of the design or qualification process. However, it is questionable whether they are a sufficient set of tests. Evidently, the best option for experimenters appears to be (a) to conduct an abbreviated set of prototype-module tests to extract a sufficient amount of information, (b) augment that information using test data from the separate-effects tests, and (c) apply the data judiciously in the plant-specific analyses. Careful attention should be paid to the fact that although prototype-module tests appear to be "prototype tests," they have numerous non-prototypical features that must be addressed in the plant analyses.

During planning for prototype tests, attention should be paid to the insights gained from past experience, listed below:

1. Many vendors have recognized that the special strainers are not a “one-size-fits-all” type of standardized strainer. Instead, the concept is to use similarly designed strainer modules of various sizes and quantities as necessary for each plant. The technical method adopted by the vendors has been to use the prototype test data to develop a correlation, either empirical or semi-theoretical, and use it in the plant-specific analyses. For this method to be successful, particular attention should be paid to the process used to select the dimensions of the strainer being tested, the experimental parameter range (i.e., debris loading range and flow rate range) over which testing is being carried out, and the form of the correlation used to relate head loss to debris loading and flow rate. The correlation development should sufficiently address the factors discussed in Section 7.3.2 (i.e. special shapes of the strainers and as a result variations in the approach velocity).
2. The experimental results suggest that head loss across the specialty strainer is a nonlinear function of debris loading. Figure 7-12 presents an approximate representation of measured head loss as a function of strainer debris loading for a typical stacked-disk strainer. Specialty strainers are designed such that they would have a gap or crevice where debris would initially accumulate preferentially when the debris loading is light. The debris accumulated in these gaps would be subjected to lower fluid velocities and hence would result in lower head loss. After these gaps are filled, debris would start to accumulate on the circumscribed surface of the strainer, which resembles a regular-shaped strainer (cylindrical in the case of a stacked-disk strainer). In view of this complex relationship between head loss and debris loading, special attention should be paid to collecting head loss data over a wide range of debris loadings and to judging the applicability of test data to a plant application carefully.
3. The prototype module should be designed to ensure that it accurately represents the internal flow control devices (e.g., ribs and vanes). Testing has shown that these

geometrical features primarily control head loss across the clean strainer.

4. The measured head losses are a strong function of the sequence over which debris is introduced. There is considerable evidence that the introduction of RMI first, followed by fibrous debris, would maximize the head loss. In those tests, it appeared that RMI would fill up the interstitial gaps and cause fiber to accumulate on the strainer circumscribed surface. This mode of accumulation was found to result in the largest head loss compared with the other alternatives (e.g., fiber is added first followed by RMI or fiber and RMI are added together). However, this issue is only important if the test (and the plant application) involves significant quantities of both RMI and fibrous debris.

Known Variations in the Geometry

All prototype modular strainer tests used setups very similar to those shown in Figures 7-10 and 7-11. A few differences exist in the details of the test setup. In particular, the methods used to create the turbulence necessary to ensure that debris would not settle out in the test tank varied considerably. Other differences are related to the orientation of the strainer assembly and the test procedures. However, these variations most likely would not have a significant effect on the head loss.

7.2.4 Semi-Scale Installed Strainer Testing

As discussed above, the prototype modular tests de-emphasize the debris transport aspect by ensuring that all the debris would stay in suspension and ultimately reach the strainer. Application of the test data in the plant-specific analyses would require that the analyst have prior knowledge of the quantity and type of debris that would accumulate on each strainer module. A majority of the licensees relied on simplifying assumptions (e.g., equal distribution of debris on all strainers) to estimate the quantity of debris that might accumulate on each strainer. Other licensees have sought experimental means for predicting debris deposition by conducting semi-scaled, as-installed strainer tests. Figure 7-13 provides a schematic of the test setup used in the quarter-scale tests conducted by Grand Gulf generating station. These plants installed quarter-scale strainers, replicated to the exact details, in the quarter-scale suppression pool equipped with

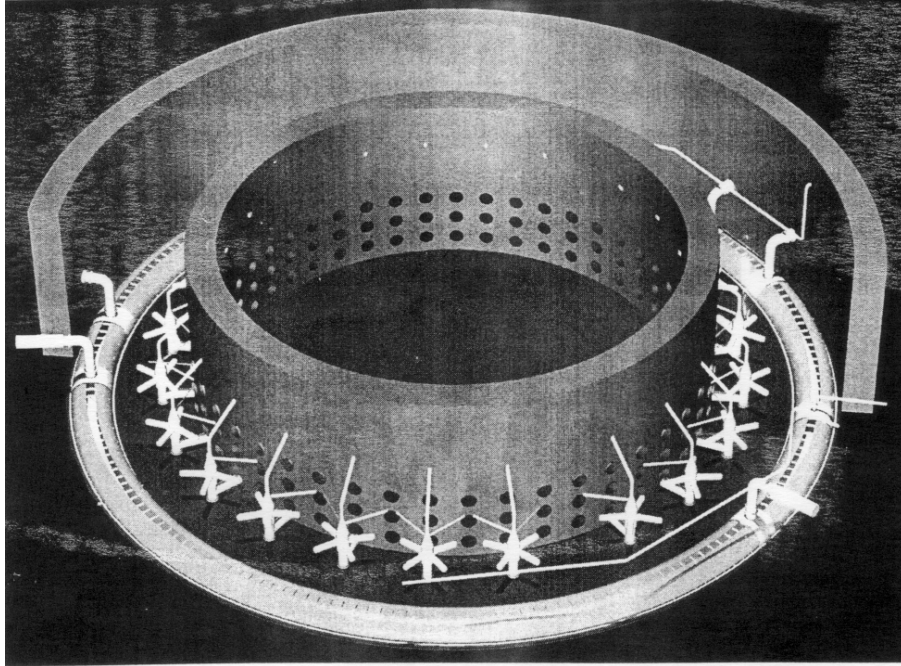


Figure 7-13 Semi-Scale Test Facility Used in Grand Gulf Quarter-Scale Testing

quarter-scale pumps and other geometrical features. The concept was to study debris build-up on strainers when they are subjected to prototype conditions. These plants also examined the head loss performance characteristics of individual modules simultaneously. Figure 7-14 shows the geometrical details of the individual modules tested. This comparison was used to draw conclusions regarding the applicability of individual module test data in the plant-specific analyses and the issues that should be factored into plant-specific analyses. These tests provide valuable insights on how to use individual module test data in the plant-specific analyses, at least for some debris types.

7.3 Analysis of Test Data

7.3.1 United States Nuclear Regulatory Commission Characterization of Head Loss Data

7.3.1.1 Fiberglass and Particulate Debris

The U.S. NRC characterization of head loss caused by fibrous and particulate debris is described in detail in Appendix A of the CSNI knowledge-base report⁷⁻¹ and Appendix B of NUREG/CR-6224.⁷⁻² This correlation was

validated by comparing its predictions for head loss with experimental data from the following sources:

1. NRC experimental data obtained as part of BWR study (NUREG/CR-6224)⁷⁻²
2. PP&L head loss data base
3. PCI head loss data base
4. NUREG/CR-2982 head loss data base
5. Vattenfall Development Co. data base
6. BWROG head loss data base for truncated-cone strainers
7. BWROG head loss data from gravity-head loss tests

As shown in Appendix A of the CSNI knowledge-base report,⁷⁻¹ the correlation predictions were within $\pm 25\%$ of the test data. NUREG/CR-6224, Appendix B,⁷⁻² provides the limitations of the correlation, as well as some of the assumptions associated with its applications. This experimental correlation was incorporated into the Blockage computer code.^{7-25,7-26}

7.3.1.2 Reflective Metallic Insulation

Conclusions regarding RMI head loss are based on a review of the following sources of experimental data.

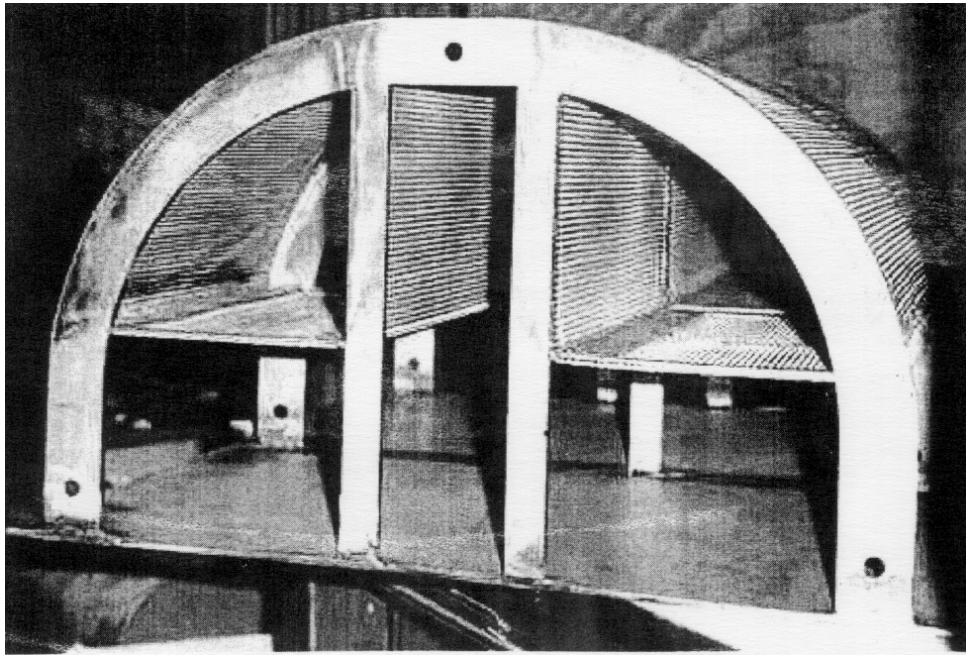


Figure 7-14 Prototype Strainer Module Test Setup Used in Grand Gulf Prototype Tests

- **NRC/ARL Test Data:** ARL conducted a series of tests under U.S. NRC sponsorship to examine the head loss resulting from the accumulation of RMI, fibrous and sludge debris. These tests used a small section of an ECCS strainer (a diameter of 1 ft) assembled in a vertical test section. The RMI debris was obtained directly from the steam blast tests. The results of the test program, along with a description of the test facility, were provided in References 7-8 and 7-9.
- **BWROG/URG Test Data:** The BWROG conducted a series of tests at the Electric Power Research Institute (EPRI) Non Destructive Evaluation (NDE) center in Charlotte, North Carolina, employing full-scale strainers to measure the head loss resulting from the accumulation of RMI, fibrous, and sludge debris. Of particular interest are the tests conducted using a truncated-cone strainer. In these tests, the RMI debris was fabricated manually—basically crumpled to look very similar to the RMI debris used in the ARL tests. The results of the test program were provided in the BWROG URG, Volume 2.⁷⁻¹⁰
- **LaSalle Test Data:** In 1998, ComEd sponsored a series of plant-specific tests to

study the head loss resulting from 1.5-mil aluminum RMI and Nukon fiberglass insulation. These experiments were conducted using the same test facility as the BWROG. The strainer used in the experiments was a stacked-disk strainer.⁷⁻¹³

- **STUK-94 Test Data:** The STUK experiments were conducted on a large strainer immersed in water (see Figure 7-10). Debris was simulated by “flat” metallic insulation inner foils cut into pieces of various sizes, ranging from 2 to 130 cm.^{7-6,7-16}

Review of this data suggests that head loss caused by RMI debris is very sensitive to the shape of the debris used in the experiments. Much of the RMI debris used in U.S. testing is crumpled pieces of 2.5-mil-thick stainless steel foils (except for the LaSalle data, which used aluminum foils). An example of RMI debris generated by steam break flow is shown in Figure 3-8. Visual examination of the beds suggests that crumpled RMI fragments accumulate with their major cross-section aligned perpendicular to the flow direction. It is also apparent that crumpled debris beds tended to be relatively uniform (volumetrically and planar) and typically have much larger porosity.

The beds formed of smaller debris tended to be more compact than the beds formed of the larger debris; the most compact debris bed was observed when fragments ranging in size from ½ in. to 4 in. were allowed to accumulate randomly on the strainer surface. Head loss data for such beds is reported by the following research organizations:

- NRC Test Data obtained at ARL^{7-8,7-9}
 - BWROG Test Data⁷⁻¹⁰
 - GE Test Data (Proprietary)⁷⁻¹²
 - LaSalle Test Data⁷⁻¹³
 - PCI Test Data⁷⁻¹¹
 - KEFER Test Data
- Finnish investigators used regularly cut, flat RMI pieces to simulate debris in the head loss tests. The rationale for use of flat pieces were:

1. The debris generation process could include the destruction of an RMI cassette where a significant portion of the cassette insulation becomes large relative flat pieces of foil.
2. Although RMI debris may be crumpled initially, it would be flattened as the debris is transported through the drywell and the wetwell.
3. The flatter RMI pieces typically would result in higher head losses and therefore provide a conservative alternative to the crumpled pieces.

The beds formed of flat RMI pieces behave fundamentally differently from the beds formed of crumpled pieces. The dimples, the bowing (either due to damage or initial curvature) of the relatively flat foils, and a certain randomness of accumulation would separate the adjacent foils in flat-foil debris beds resulting relatively compact beds of RMI debris. The pressure-drop characteristics of flat RMI debris are described by the STUK investigators.^{7-6,7-16}

Based on these analytical observations, LANL reasoned that the head loss across RMI beds is a function of debris loading (the ratio of foil surface area to strainer surface area), flow velocity through the debris, and the type, shape, and size of the debris. Figure 7-15 is an idealized view of flow through an RMI bed formed of debris size L, and an inter-foil distance of K_t.¹³

¹³ A realistic RMI debris, that would include crumpled pieces as well as flat foils, would be much more chaotic than the idealized diagram indicates. The

For such a flow configuration, head loss can be estimated to be

$$\Delta P \propto \frac{S_V(1-\epsilon)}{\epsilon^2} \rho U^2 N \propto \frac{L^2}{K_t^2} U^2 (A_{foil} / A_{str})$$

using the following variables.¹⁴

- Inter-foil channel gap thickness (K_t)
- Fluid velocity (U)
- Characteristic foil dimension (L)
- Foil specific surface area (S_v)
- Number of foil layers in bed (N)
- Foil surface area (A_{foil})
- Strainer surface area for deposition (A_{strainer})
- Fluid density (ρ)

For debris beds consisting of smaller debris (typically 2- to 4-in. sized pieces of debris), the head loss relationship was refined based on the experimental data.

$$\Delta H = \frac{1.56 \times 10^{-5}}{K_t^2} U^2 (A_{foil} / A_{str})$$

where

- ΔH is the head loss across the RMI bed (ft-water),
- U is the water velocity through the bed (ft/s),
- A_{foil} is the surface area of the RMI foils (ft² - nominal),
- A_{str} is the strainer cross-sectional area (ft²), and
- K_t is the inter-foil gap thickness (ft).

The inter-foil thickness was deduced from the experimental head loss data for different debris types. Nominal values for K_t are summarized in Table 7-2.

idealized approach was applied to the chaotic bed with the non-idealized geometry integrated into the variable K_t. Thus, k_t represents an effective gap width, which had to be deduced from test data rather than simply measured.

¹⁴As a potential alternative, it should be noted that the Finnish researchers (Reference 7-16) correlated data based on the linear ratio of L/K_t, rather than its square. The researchers claim a good correlation for their RMI debris in a tube experiment once the edge effects were considered.

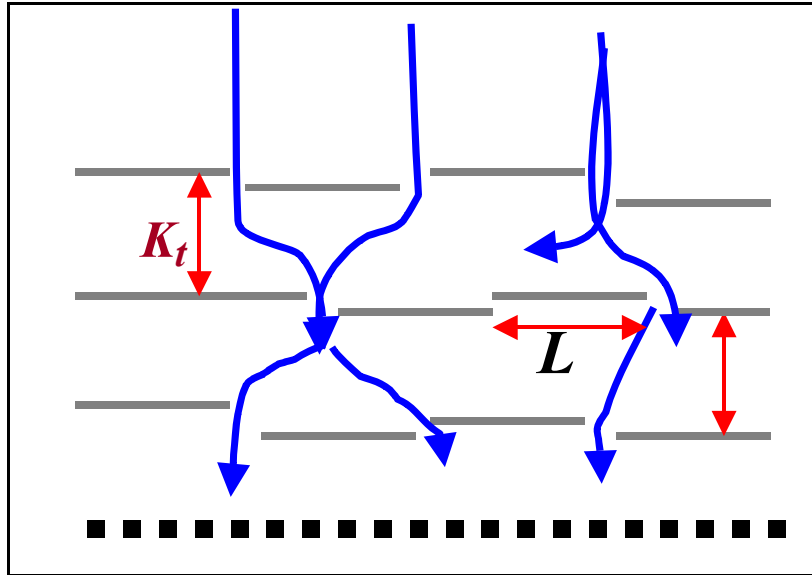


Figure 7-15 Idealized View of Flow Through an RMI Bed

Foil Type and Bed Type	Basis	K_t (ft)
2.5-mil S/S (NRC large pieces)	ARL test report provided measured values	0.014
2.5-mil S/S (NRC small pieces)	ARL test report provided measured values	0.010
1.5-mil Al (debris bed)	ComEd test report	0.008
1.5-mil Al (debris bed)	ComEd test report	0.006
2.5-mil S/S (STUK flat pieces)	Deduced from STUK 1994 test report*	0.007
2.5-mil S/S (1-mm dimple)	Deduced from STUK 1994 test report**	0.003

*This deduction explained in this subsection under subtitle "STUK-1994 Test Data."
 **The ARL tests were conducted at the same time as the BWROG test program described herein was being undertaken. The objective was not to develop a head loss correlation; but to independently verify insights provided by the BWROG test program using large strainers. These tests were envisioned from the beginning to be "separate-effects" tests.

For certain insulation types and head losses, the K_t values were observed to change with the head loss as the beds became compressed. Such changes in K_t values were accounted for in some of the evaluations reported below.

U.S. Nuclear Regulatory Commission/Alden Research Laboratory Tests

In 1996, NRC sponsored a series of tests at ARL to measure the head loss caused by the accumulation of RMI debris on a BWR strainer, with and without the simultaneous presence of fibrous insulation and sludge.¹⁵ These tests use

¹⁵The ARL tests were conducted at the same time as the BWROG test program described herein was

the vertical head loss test facility shown in Figure 7-6.

The RMI debris used in the testing was generated directly from the steam-blast tests conducted by NRC at Karlstein, Germany⁷⁻⁸ (debris shown in Figures 3-8). For debris fragments smaller than about 4-in., the debris beds were very uniform. Figure 7-16 provides a comparison of the correlation, immediately

being undertaken. The objective was not to develop a head loss correlation; but to independently verify insights provided by the BWROG test program using large strainers. These tests were envisioned from the beginning to be "separate-effects" tests.

above, (identified as Equation K.5a in the figure) with the test data obtained for RMI debris. As evident from this figure, the NRC correlation provides a reasonably conservative estimate for the test debris and test conditions, highlighted by the fact that only a single data point is above the correlation but that data point is still within the uncertainty band. Note that ARL deduced the values for the variable K_t from head loss data that are reported in Table 7-2 and these values were used in the correlation to develop the curve shown in Figure 7-16.

Boiling Water Reactor Owners' Group Tests

As part of BWR strainer blockage resolution research, the BWROG performed a series of tests to measure the head loss caused by RMI debris on "prototypical" pre-NRCB 96-03 ECCS strainers (i.e., truncated-cone strainers) and the replacement strainers (e.g., stacked-disk strainers). In these experiments, RMI debris was added to a large, turbulent pool of water and allowed to approach and accumulate on a full-scale strainer. The accumulation occurred over a period of about 1 h in some experiments, with the pressure drop gradually increasing until a plateau in the data was reached. The measured head loss was then tabulated as a function of the flow through the strainer and the amount of debris added to the pool. Visual examination confirmed that in many cases, a majority of the RMI debris added to the pool actually reached the strainer, resulting in the formation of relatively thick RMI debris beds. In Tests T3 through T6, the RMI debris loading varied between 7 ft²-foil/ft²-strainer to 40 ft²-foil/ft²-strainer, and the beds were fairly uniform. The debris used in these tests closely resembled (at least visually) the NRC/ARL debris (refer to Figure 3-8). The resultant head losses are plotted in Figure 7-17 as head loss normalized to circumscribed thickness vs the approach velocity. Also shown in Figure 7-17 are the head loss predictions obtained using the NRC correlation presented and discussed above. The agreement between the head loss data and the correlation is well within the experimental uncertainties and the correlation error margin. Once again, K_t values were deduced from the head loss data and these values were used in the correlation to develop the curve shown in Figure 7-17.

The BWROG also obtained head loss data for stacked-disk strainers and star strainers.

However, all those data were obtained for low debris loadings. Hence, no effort was made to compare the NRC head loss correlation with the data for these special-shaped strainers. Similarly, the BWROG database included head loss data for mixed beds consisting of RMI and fibrous debris. The NRC regulatory position was found to bound all such data.

LaSalle Tests

In 1998, ComEd sponsored a series of plant-specific tests⁷⁻¹³ to study the head loss resulting from 1.5-mil aluminum RMI and Nukon fiberglass insulation. These experiments were conducted using the same test facility that was used for the BWROG tests and the strainer tested was a stacked-disk strainer. Table 7-3 provides the geometric details of the strainer used in the testing.

Six tests were conducted in which the flow rates varied between 2000 and 5000 gpm and the RMI debris loading reached as high as 2250 ft² of foil (or a value of 144 $A_{\text{foil}}/A_{\text{circ}}$). In all tests, the RMI fragments used were crumpled pieces with a dominant length scale less than 2 in., so very compact beds would be expected. The measured head loss was tabulated as a function of the flow rate through the strainer and the quantity of insulation debris added to the pool. The report contained references to visual observations regarding the fraction of the debris that actually reached the strainer in each test. It also provided pictorial evidence of debris-bed build-up on the strainer, both for RMI and mixed beds.

Tests 2 and 4 examined pure RMI debris build-up on the strainer surface. In Test 2, RMI debris was added incrementally over a long duration (the test lasted 7.5 h). In both of these tests, a total of 2250 ft² of RMI foil was added to the pool and allowed to accumulate on the strainer. In Test 4, all of the RMI debris was added instantaneously and then allowed to accumulate on the strainer. From the head loss traces, it appears that accumulation occurred over a period of about the first 3 h, with head loss reaching the steady-state value near the end of the test. The head loss data measured in Tests 2 and 4 are presented in Figure 7-18. Figure 7-18 also provides a comparison of the head loss predictions obtained using the LANL RMI head loss correlation with the test data from

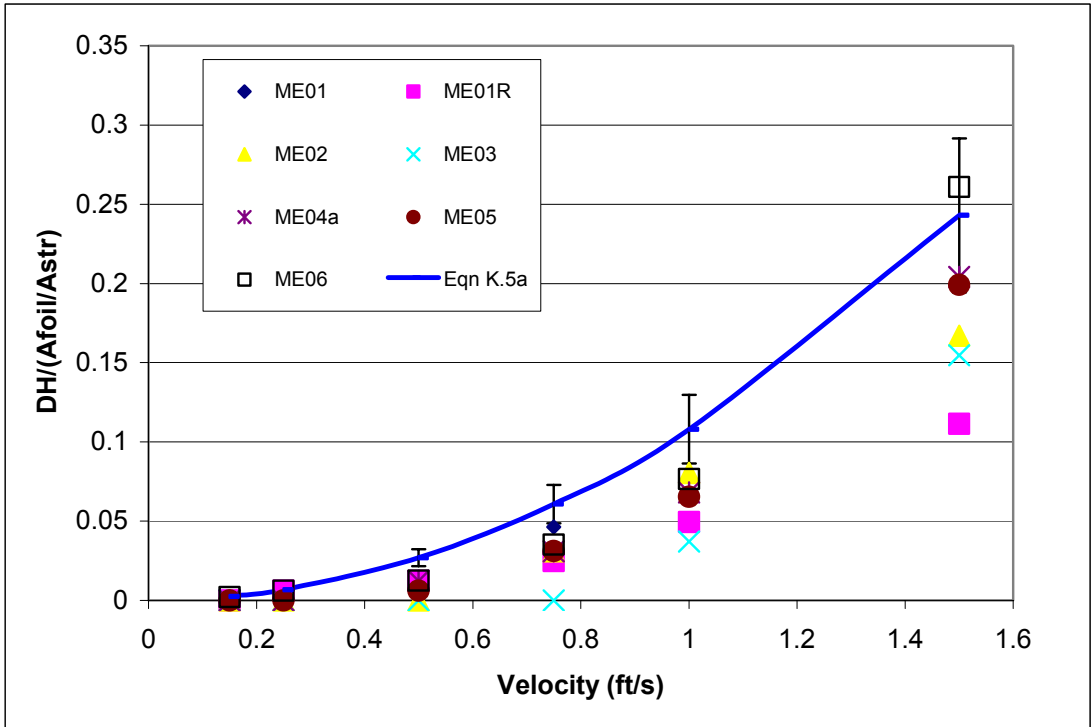


Figure 7-16 Comparison of NRC/ARL Test Data with LANL Correlation

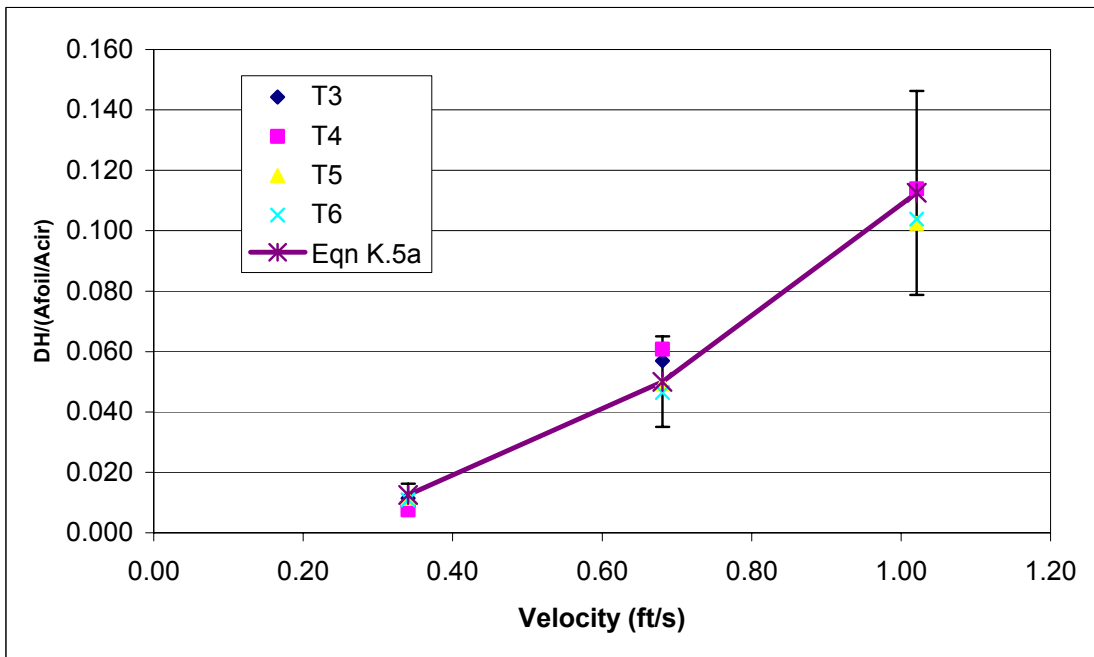


Figure 7-17 Comparison of BWROG Test Data for Truncated Cone Strainer with LANL RMI Correlation

Table 7-3 Geometric Details of the Portion of the Strainer Tested in the LaSalle Test Program	
Strainer Geometry Details (Half Strainer Effective)	
Number of Discs	6
Number of Gaps	6
Inner Diameter (in)	26
Outer Diameter (in)	34
Disc thickness (in)	1.5
Gap Thickness (in)	2
Length of Strainer (in)	21
Derived Geometry Variables (Half Strainer Effective)	
Total Flow Area (ft ²)	48.6
BWROG Circumscribed Area (ft ²)	15.6
Circumscribed Area + Area of Discs (ft ²)	21.9
Gap Volume (ft ³)	2.6

Tests 2 and 4. The correlation predictions were within $\pm 30\%$ of the test data. The correlation predictions were consistently less than Test 2 data and consistently higher than Test 4 data. Note that the K_t values used to generate the predictions shown in Figure 7-18 were reported in Reference 7-13 by the investigators.

STUK-1994 Test Data

In 1994, the Finnish Nuclear Authority (STUK) performed a series of tests to measure the head loss caused by the accumulation of RMI debris.^{7-6,7-15,7-16} In these tests, relatively flat pieces of RMI foil were used to simulate debris. Figure 7-19 provides a comparison of LANL RMI predictions with STUK head loss data. The comparison benefited from the compression data provided by the STUK investigators. The comparison shows that the predicted head losses are comparable ($\pm 30\%$) to correlation predictions. However, the following limitations of the correlation apply (when applied to the debris beds similar to the debris used in the STUK experiments):

1. The comparison shown in Figure 7-19 was based on test data obtained for small fragments (or pieces).
2. The K_t values used in the comparison were deduced from interpretation of data presented in Reference 7-16. In this reference, the investigators measured and reported debris bed thickness as a function of the head loss across the bed. This data was used to derive a value for K_t (provided

in Table 7-2) by inserting the test data into the LANL head loss correlation and solving for K_t .

Although the correlation appears to perform well in predicting head loss caused by the small flat pieces of debris used in the STUK experiments, the original investigators expressed reservations regarding the applicability of the correlation. So it is recommended that this correlation be used cautiously when applied to flat pieces.

7.3.2 Analysis of Non-Flat-Plate Strainer Data

The purpose of this section is to demonstrate the means by which the NUREG/CR-6224 correlation⁷⁻² can be adapted for non-flat-plate strainers (e.g., stacked-disk strainers). The NUREG/CR-6224 head loss correlation was developed based on experimental data obtained for flat-plate and truncated-cone strainers. The stacked-disk strainers are a type of passive strainer now used extensively in the U.S. BWR nuclear power plants. This section:

1. Establishes that flat-plate-strainer data, if applied correctly, can adequately predict the head loss performance of more complex strainers and
2. Highlights a list of parameters that should be considered carefully while evaluating the performance of advanced strainer designs (e.g., gap volume vs debris volume and circumscribed area vs plate area).

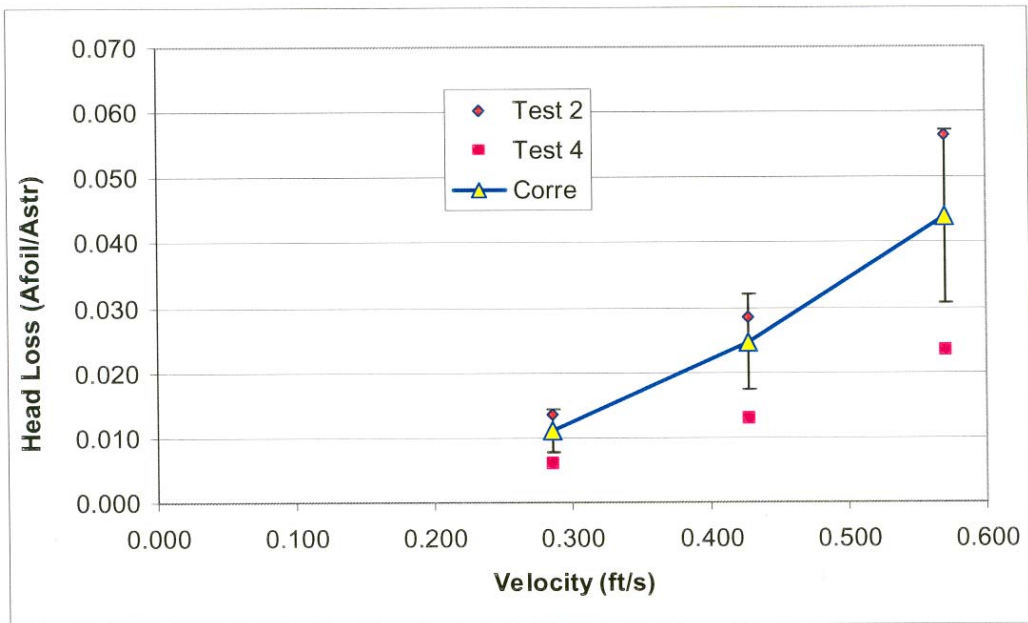


Figure 7-18 Comparison of LANL RMI Correlation Predictions for Truncated Cone Strainer with the Experimental Data Obtained from LaSalle Tests

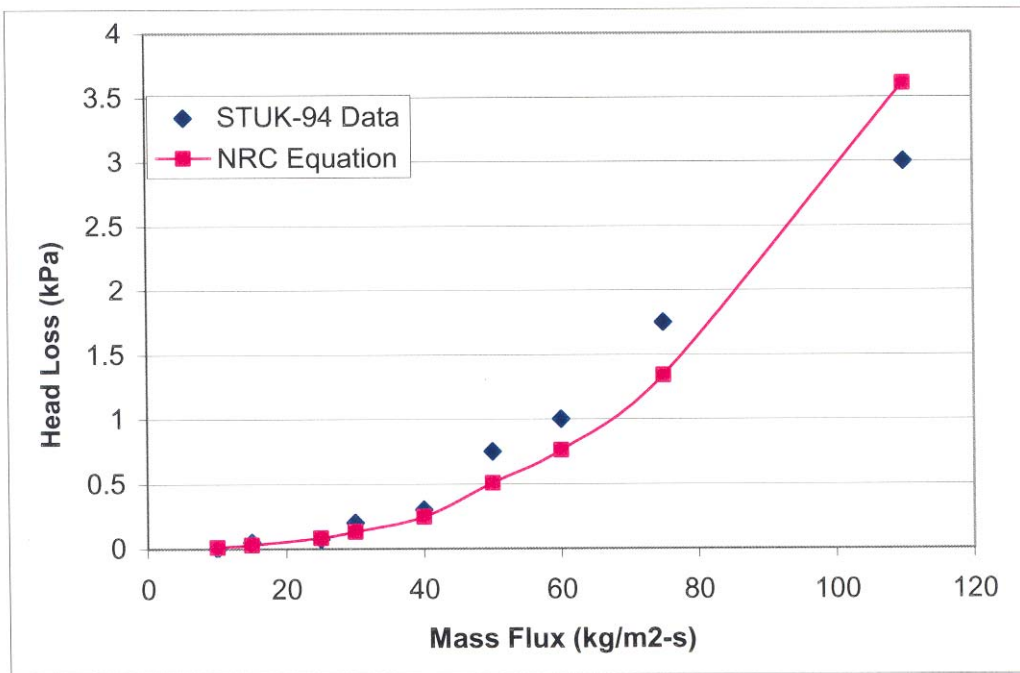


Figure 7-19 Comparison of LANL RMI Predictions with the STUK Head Loss Data

7.3.2.1 Phenomena of Debris Build-Up on Stacked-Disk Strainers

The basic idea of stacked-disk strainers is to maximize the perforated plate area for a given projected size of the strainer.¹⁶ The head loss caused by these strainers is controlled significantly by such factors as the gap volume, the plate surface area, and the change in deposition area with debris loading. The importance of these factors can be understood by considering the schematic presented in Figure 7-20, which illustrates the debris build-up on a stacked-disk strainer.

Initially, the debris would accumulate on the strainer plate surface nearly uniformly. At this extreme, the strainer surface area available for deposition would be very close to the total perforated plate area. Thus, models should be able to predict head loss at this stage by treating the strainer as a flat plate with a flow area equal to the total plate area. The flow velocity and bed thickness would be

$$V_{\text{thin-bed}} = Q \text{ (ft}^3\text{/s)}/A_{\text{plate}}$$

$$t_{\text{thin-bed}} = M_{\text{fiber}}/(\rho_f \cdot A_{\text{plate}})$$

The resulting head loss can be calculated using the NUREG/CR-6224 correlation or a similar correlation based on a flat-plate strainer by computing the bed thickness assuming that debris builds up on the entire plate area and by computing the fluid velocity based on the plate area.

The other extreme condition would be when large volumes of debris have accumulated such that the gap volumes were completely filled with the remaining debris deposited on the circumscribed area of the strainer. For the portion of the debris that accumulates on the circumscribed area, the NUREG/CR-6224 correlation can be used with the flow velocity and bed thickness evaluated using the circumscribed area instead of the plate area. For moderate loads, an interpolation scheme that gradually decreases the flow area can be sought; for example, an effective strainer area versus accumulated debris volume can be deduced from test data that covers the full range of debris loadings.

¹⁶ This is essentially the space occupied by the strainer but is also referred to as the circumscribed size.

One of the key parameters necessary to apply this criterion is the compressibility of fibrous debris beds. NRC measurements have shown that beds tend to be highly compressible when they are subjected to a large head loss across the bed. NUREG/CR-6224 provided the following relationship that can be used to calculate the compressed density of the bed debris as a function of the pressure drop across the bed:⁷⁻²

$$\rho_f = \rho_{fo} 1.3(\Delta H/\Delta L_o)^{0.38}$$

where

ρ_f is the density of fiber in the debris bed (lbm/ft³),

ρ_{fo} is the density of fiber insulation (as fabricated) (lbm/ft³),

ΔH is the head loss across the debris bed (ft-water),

ΔL_o is the theoretical thickness of the fibrous debris bed (i.e., thickness based on the as-fabricated density) (in),

The following section provides the head loss equations used to perform these calculations.

7.3.2.2 Application of the NUREG/CR-6224 Correlation to the PCI Strainer

The following methodology was used to calculate head loss across the debris bed for different debris loadings. The general head loss equation used is

$$\frac{\Delta P}{\Delta L} = 4.16 \times 10^{-5} \left[\begin{array}{l} 3.5 S_v^2 (1 - \epsilon)^{1.5} \\ \left[1 + 57 (1 - \epsilon)^3 \right] \mu V + \\ \frac{0.66 S_v (1 - \epsilon)}{\epsilon} \rho V^2 \end{array} \right]$$

where

ΔP is the pressure drop resulting from flow across the bed (ft-water),

ΔL is the thickness of the fibrous bed (in.),

μ is the fluid dynamic viscosity (lbm/s-ft),

ρ is the fluid density (lbm/ft³),

V is the fluid velocity (ft/s),

ϵ is the bed porosity, and

S_v is the specific surface area (ft²/ft³)

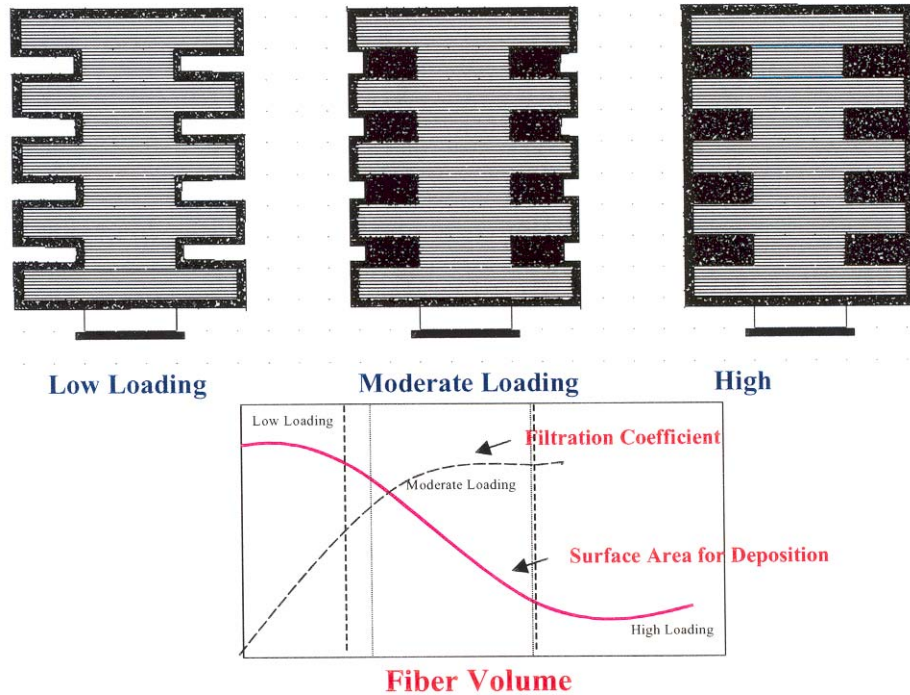


Figure 7-20 Schematic Representation of Debris Build-Up on a Stacked-Disk Strainer

Thin-Bed Approximation ($V_f/V_{gap}^{17} < 0.30$)

For thin beds, the whole plate surface area provides the location for debris deposition. In this case,

$$\begin{aligned} \Delta L_o(\text{in}) &= (12 \cdot M_{\text{fiber}})/(\rho_{fo} \cdot A_{\text{plate}}) , \\ \Delta L &= \rho \Delta L_o (\rho_{fo}/\rho_f) , \\ V \text{ (ft/s)} &= V_{\text{plate}} \equiv Q(\text{ft}^3/\text{s})/A_{\text{plate}} , \text{ and} \\ \rho_f/\rho_{fo} &= 1.3(\Delta H/\Delta L_o)^{0.38} . \end{aligned}$$

Intermediate-Bed Approximation ($1.0 > V_f/V_{gap} > 0.30$)

For intermediate loadings, the area available for deposition gradually decreases and the velocity within the bed gradually increases. An approximate formula¹⁸ for evaluating head loss is

$$\begin{aligned} \Delta L_o(\text{in}) &= (12 \cdot M_{\text{fiber}})/(\rho_{fo} \cdot A_{\text{plate}}) , \\ \Delta L &= \Delta L_o (\rho_{fo}/\rho_f) \\ V \text{ (ft/s)} &= V_{\text{plate}} (1 - (V_f/V_{gap} - 0.3)) + V_{\text{circ}} \\ &\quad (V_f/V_{gap} - 0.3) , \\ V_{\text{plate}} &= Q(\text{ft}^3/\text{s})/A_{\text{plate}} , \end{aligned}$$

$$\begin{aligned} V_{\text{circ}} &= Q(\text{ft}^3/\text{s})/A_{\text{circ}} , \text{ and} \\ \rho_f/\rho_{fo} &= 1.3(\Delta H/\Delta L_o)^{0.38} . \end{aligned}$$

This relation simply provides a means for calculating head loss using a volume-averaged velocity through the bed.

Thick-Bed Approximation ($V_f/V_{gap} > 1.0$)

Head loss from a thick bed is a sum of head loss resulting from a fully loaded strainer and a calculated contribution from the circumscribed portion using the following closure relationships:

$$\begin{aligned} \Delta L_o(\text{in}) &= (12 \cdot M_{\text{fiber}})/(\rho_{fo} \cdot A_{\text{circ}}) , \\ \Delta L &= \Delta L_o (\rho_{fo}/\rho_f) , \\ V \text{ (ft/s)} &= V_{\text{circ}} \equiv Q(\text{ft}^3/\text{s})/A_{\text{circ}} , \text{ and} \\ \rho_f/\rho_{fo} &= 1.3(\Delta H/\Delta L_o)^{0.38} . \end{aligned}$$

Although these equations appear complex, they can be solved easily. The results of the comparison are presented in Figures 7-21 and 7-22. As shown in these figures, the NUREG/CR-6224⁷⁻² correlation can predict the head loss data for PCI strainers fairly accurately (within $\pm 25\%$).

¹⁷ V_f/V_{gap} is the ratio of the total volume of debris to volume of debris located within the gaps.

¹⁸ The approximate formula applies to the PCI strainer design tested.

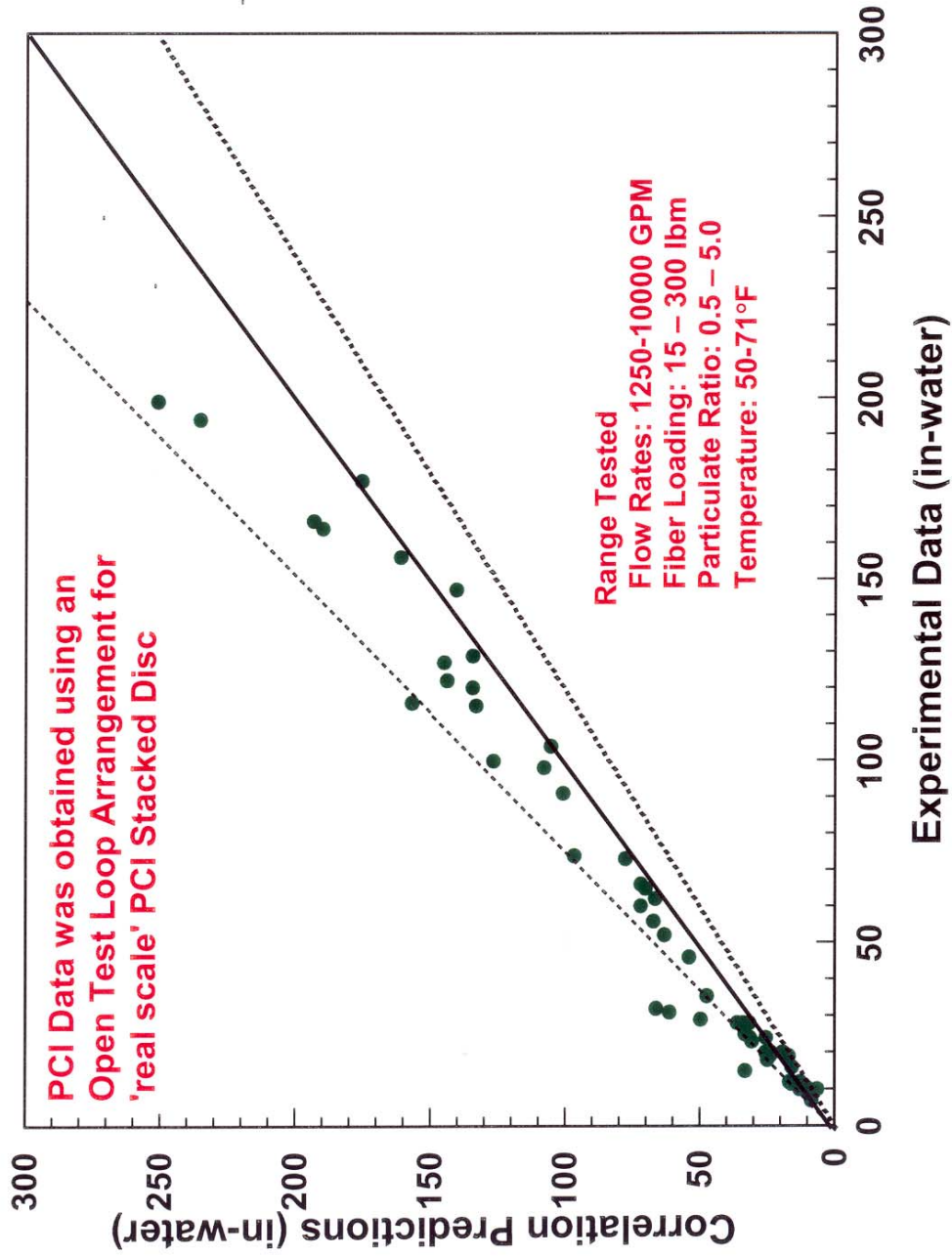


Figure 7-21 Point-By-Point Comparison of Correlation Predictions with PCI Head Loss Data

Comparison of PCI Stacked Disc Strainer Head Loss Data with NUREG/CR-6224 Correlation

$$A_{norm} = (A_e - A_c) / (A_s - A_c)$$

$$V_{norm} = V_d / V_{gap}$$

A_e = effective surface area for application
of NUREG/CR-6224

A_c = circumscribed area of the strainer

A_s = actual surface area of the perforated plate

V_d = theoretical volume of Nukon

V_g = gap volume

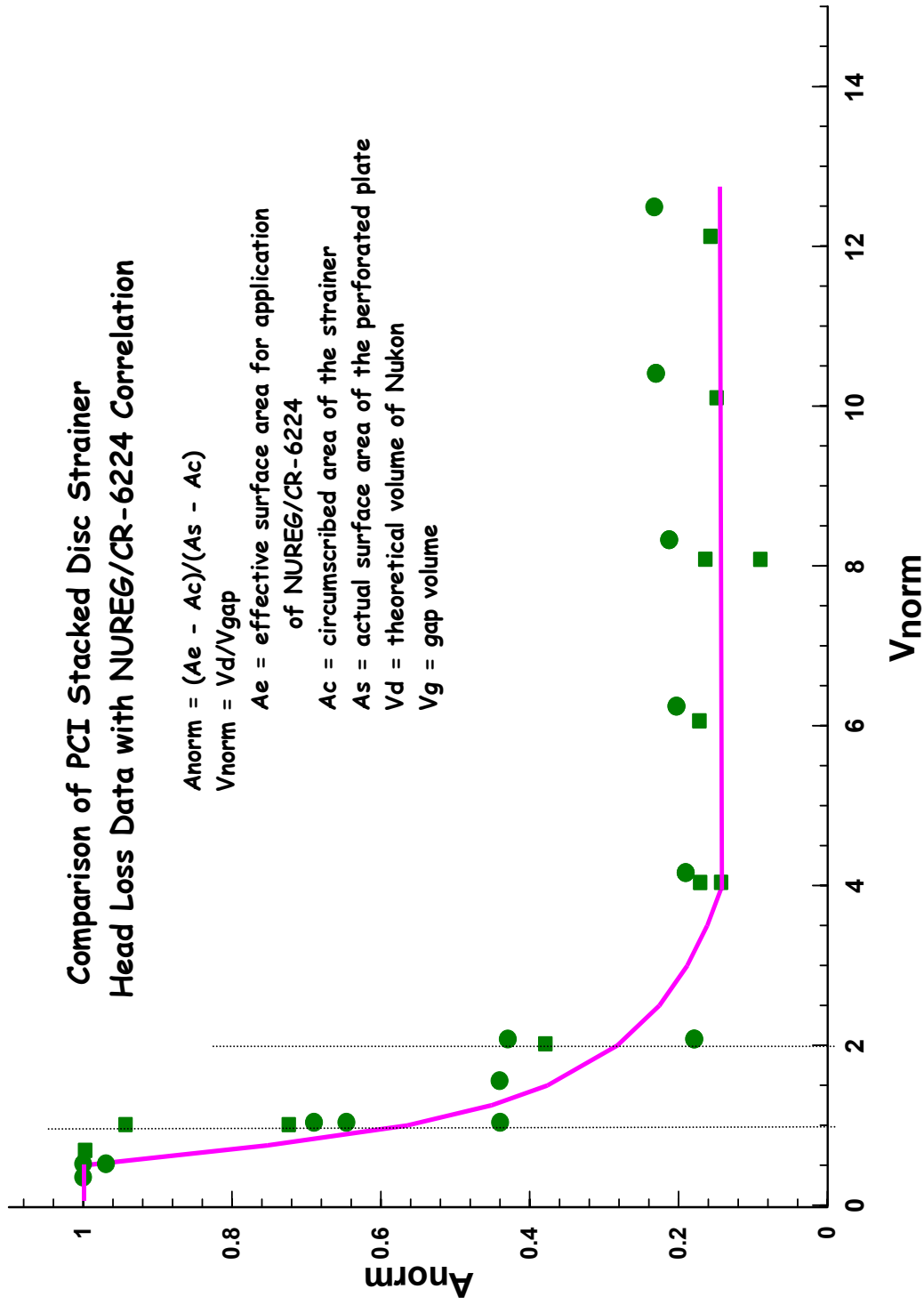


Figure 7-22 Dimensionless Representation of Stacked-Disk Strainer Effective Area as a Function of Debris Volume

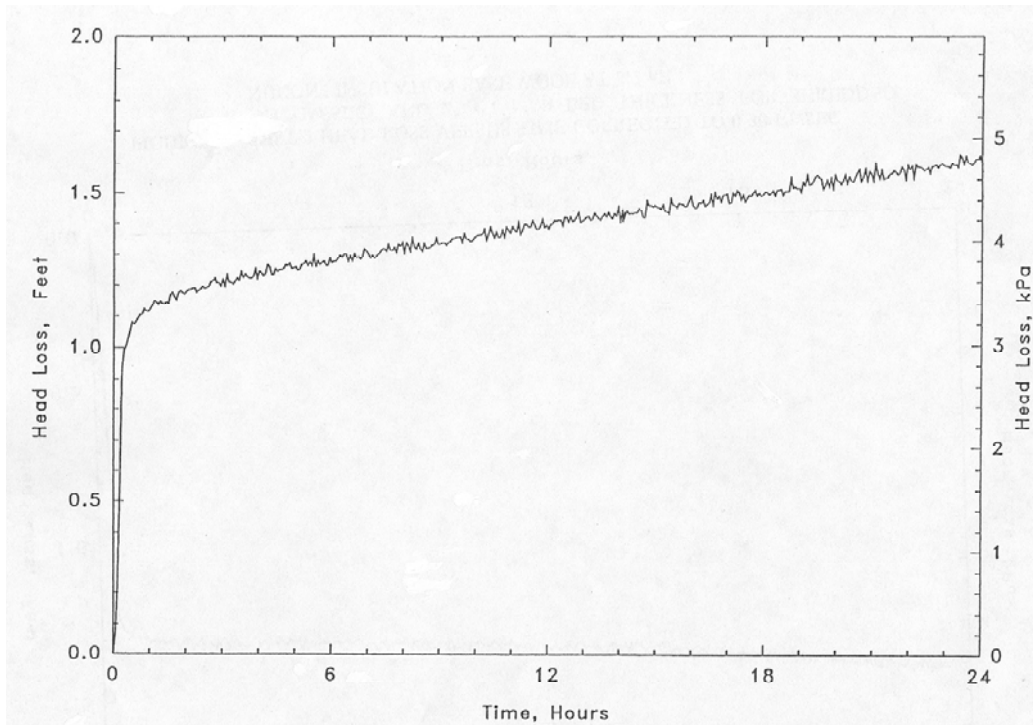


Figure 7-23 Example of Long Term Head Loss for a NUKON™ Debris Bed

Figure 7-21 presents a point-by-point comparison of the NUREG/CR-6224 model predictions with the experimental data. All the points were within $\pm 25\%$ bounds, indicating good agreement between the correlation and the test data. This agreement confirms that accurately accounting for the change in the effective flow area can be used to adequately simulate the head loss caused by deposition of debris on a stacked-disk strainer. Figure 7-22 presents a plot of the effective strainer area as a function of the volume of debris being deposited. This curve can be used to compute the effective strainer area and can be used directly in conjunction with the NUREG/CR-6224 head loss correlation.

7.4 Ongoing Research on Outstanding Issues

At the publication of this report, continuing NRC-sponsored research will provide additional data regarding specific issues currently not completely understood. These issues have to do with the long-term stability of a fibrous debris bed, head loss data for

calcium silicate debris, and the accumulation and head loss data for vertically oriented sump screens.

7.4.1 Long-Term Fibrous Debris Bed Stability

Head loss test procedures have generally continued the measurement of the pressure drop across the debris bed, following the establishment of that bed, until the head loss became relatively stable. The time required to reach 'steady-state' has generally been on the order of tens of minutes.

Occasionally tests were continued for a few hours. But some limited long-term testing has been conducted where the tests were continued for several days to examine the long-term effects of acidity on the debris bed. These tests have been described in an ARL Test Report⁷⁻²⁹ and in a paper presented to the 1999 OECD/NEA Workshop on Sump Screen Clogging.⁷⁻³⁰

The concern of the long term testing was whether or not the structure of a fibrous debris bed remained stable in the long term.

Although the long term testing was not extensive enough to conclusively determine the long-term debris bed behavior, it appeared that fiberglass in debris beds is subject to dissolution in alkaline solutions. Further, the binder could lose its attachment to the fibers and the bed matrix could break down, so that the bed would become denser. The primary parameters affecting increased long-term head loss appear to be water acidity level and temperature. In the limited testing, the head loss was shown to increase gradually (approximately linear with time) until the test was terminated. The length of the long-term tests ranged from 1 to about 11 days. An example of long-term head loss is shown in Figure 7-23.

NRC sponsored research is being conducted by the Civil Engineering Department of the University of New Mexico. This research is studying the chemistry associated with a PWR sump pool and the results of this research could provide insights into this issue.

7.4.2 Calcium Silicate Debris Head Loss

As discussed in Section 7.1.2, experiments at the University of New Mexico (UNM)⁷⁻³¹ under U.S. NRC sponsorship are being conducted to study the head loss effects of calcium-silicate. This data when available will indicate trends in the head loss associated with calcium silicate debris and provide definitive data that can be used to support head loss correlations.

7.4.3 Vertically Oriented Screens

Experiments at the University of New Mexico (UNM)⁷⁻³¹ under U.S. NRC sponsorship are also being conducted to study the debris accumulation and associated head loss for vertically oriented sump screens. For instance, the test data when available will show trends regarding conditions where the debris will accumulate uniformly and where the debris will deposit preferentially towards the bottom of the screen. Limited head loss data was also accumulated for a vertical screen.

7.5 References

- 7-1. NEA/CSNI/R (95) 11, "Knowledge Base for Emergency Core Cooling System Recirculation Reliability," Prepared by U.S. Nuclear Regulatory Commission for the Principal Working Group 1 (PWG-1), International Task Group, Committee on the Safety of Nuclear Installations, Organization for Economic Cooperation and development (OECD) Nuclear Energy Agency (NEA), Restricted, February 1996.
- 7-2. NUREG/CR-6224, G. Zigler, J. Bridaeu, D. V. Rao, C. Shaffer, F. Souto, W. Thomas, "Parametric Study of the Potential for BWR ECCS Strainer Blockage Due to LOCA Generated Debris," Final Report, U.S. Nuclear Regulatory Commission, October 1995.
- 7-3. NUREG-0897, Revision 1, A. W. Serkiz, "Containment Emergency Sump Performance," U. S. Nuclear Regulatory Commission, October 1985.
- 7-4. Bulletin 93-02, Supplement 1, "Debris Plugging of Emergency Core Cooling Suction Strainers," NRC Bulletin to Licensees, February 18, 1994.
- 7-5. Bulletin 95-02, "Unexpected Clogging of a Residual Heat Removal (RHR) Pump Strainer While Operating in Suppression Pool Cooling Mode," NRC Bulletin to BWR Licensees, October 17, 1995.
- 7-6. STUK-YTO-TR-73, Juhani Hyvärinen and Olli Hongisto, "Metallic Insulation Transport and Strainer Clogging Tests," Finnish Centre for Radiation and Nuclear Safety, June 1994.
- 7-7. MIJIT, Johan Trybom, "Metallic Insulation Jet Impact Tests (MIJIT)," Vattenfall GEK 77/95, June 1995.
- 7-8. SEA-95-970-01-A:2, G. Zigler, et al., "Experimental Investigation of Head Loss and Sedimentation Characteristics of Reflective Metallic Insulation Debris," Letter Report to U. S. Nuclear Regulatory Commission, May 1996.
- 7-9. 92-96/M787F, A. B. Johnson, et al., "Head Loss of Reflective Metallic Insulation Debris with and without

- Fibrous Insulation Debris and Sludge for BWR Suction Strainers,” Alden Research Laboratory, Inc., May 1996.
- 7-10. NEDO-32686, Rev. 0, “Utility Resolution Guidance for ECCS Suction Strainer Blockage,” BWROG, November 1996.
- 7-11. PCI-97, R. A. Biasca, “Summary Report on Performance of Performance Contracting, Inc.’s Sure-Flow™ Suction Strainer with Various Mixes of Simulate Post-LOCA Debris,” Revision 1, September 1997
- 7-12. NEDC-32721P, Rev. 0, GE Licensing Topical Report, “Application Methodology for GE Stacked Disk ECCS Suction Strainer,” General Electric Nuclear Energy, Proprietary information. Not publicly available. March 1997.
- 7-13. LaSalle-98, “Test Evaluation Report for Test TPP-VL0400-005: LaSalle Strainer Fiber and RMI Debris Tests,” Duke Engineering & Services, TPP-VL04 00 – 006, June 6, 1998.
- 7-14. NRC-SER-URG, “Safety Evaluation by the Office of Nuclear Reactor Regulation Related to NRC Bulletin 96-03 Boiling Water Reactor Owners Group Topical Report NEDO-32686, ‘Utility Resolution Guidance for ECCS Suction Strainer Blockage,’” Docket No. PROJ0691, August 20, 1998.
- 7-15. MRI-1194-TRR1, “Comparison of Test Results on Metallic Reflective Insulation as performed by the Finnish Centre for Radiation and Nuclear Safety (STUK) and the Materials and Configurations used in Boiling Water Reactor Plants in the United States,” Transco Products Inc. Document, Revision 1, Proprietary information. Not publicly available. November 30, 1994.
- 7-16. OECD/NEA/CSNI PWG-1, Juhani Hyvärinen and Nina Lahtinen, “On the Mechanics of Metallic Insulation Pressure Drop Generation,” Finnish Centre for Radiation and Nuclear Safety (STUK), July 1994.
- 7-17. EC-059-1006, Rev. 0, K. W. Brinkman and P. W. Brady, “Results of Hydraulic Tests on ECCS Strainer Blockage and Material Transport in a BWR Suppression Pool,” Pennsylvania Power and Light Company, May 1994.
- 7-18. IWG, Lars-Eric Bjerke and Mats Henriksson, “Modification of Sump Screens in Ringhals 2,” International Working Group (IWG) on Sump Screen Clogging, Stockholm, May 10-11, 1999.
- 7-19. Wilde G., Strainer Test with Fiber Insulation and reactor Tank Insulation, Results from Small Model, Vattenfall Development Corp., June 1993.
- 7-20. Research and Experiment in Support of Back Fitting Measures at the Swedish BWRs. Mats E. Henriksson, Vattenfall Utveckling AB, January, 1994.
- 7-21. Kernkraftwerk, Leibstadt, AG, Swiss Federal Nuclear Safety Inspectorate, “KKL-Specific ECCS Strainer Plugging Analysis According to Regulatory Guide 1.82, Rev. 1, for a Loss of Coolant Accident,” BET/93/031, April 1993.
- 7-22. Continuum Dynamics Inc., Debris Transport and Head Loss Test Report for the Millstone Unit II Sump, Revision 0.
- 7-23. Zion Nuclear Power Station, Units 1 and 2 Response to Request for Additional Information Concerning Containment Coatings, NRC Docket Nos. 50-295 and 50-304. September 5, 1997.
- 7-24. Mark-III ECCS Suction Strainer. Slide presentation by Enercon Services, Inc. Entergy Operations, Inc. and FirstEnergy Corp. to International Working Group Meeting, Rockville, MD, October 1999.
- 7-25. NUREG/CR-6370, D. V. Rao, W. Bernahl, J. Brideau, C. Shaffer, F. Souto, “BLOCKAGE 2.5 User’s Manual,” SEA96-3104-010-A:3, December 1996.
- 7-26. NUREG/CR-6371, C. Shaffer, W. Bernahl, J. Brideau, and D. V. Rao, “BLOCKAGE 2.5 Reference Manual,” SEA96-3104-A:4, December 1996.
- 7-27. 32-94/M216F, F. J. Weber, et al., “Hydraulic Evaluation of ECCS Strainer Blockage by Insulation and Other

Debris," Alden Research Laboratory, Inc., March 1994.

- 7-28. Zigler, G. and F. Souto, "Characterization of ECCS Suction Strainer Head Loss Due to Mixed Fibrous and Calcium Silicate Insulation Debris," Innovative Technology Solutions Corporation (ITS), Publicly Released, May 1999.
- 7-29. 72-92/M670F, James B. Nystrom, "Extended Head Loss Testing in Alkaline Water of Thermal Insulation used in Nuclear Containments," Alden Research Laboratory, Inc., May 1992.
- 7-30. Hart-99, Gordon Hart, "Tests for Long Term Head Loss Across Fiberglass Insulation Debris Using Warm, Alkaline Water," Paper presented to the OECD/NEA Workshop on Sump Screen Clogging, Stockholm, May 10-11, 1999.
- 7-31. Leonard, M.T., D.V. Rao, A.K. Maji, A. Ghosh, "GSI: Experimental Studies of LOCA-Generated Debris Accumulation and Head Loss with Emphasis on the Effects of Calcium Silicate Insulation," Los Alamos National Laboratory, LA-UR-03-0471, to be published in 2003.

8.0 RESOLUTION OPTIONS

Based on the recognition that debris clogging of the ECCS strainers is a significant safety concern, plant owner groups and vendors proposed a broad range of solutions to address this issue. This section provides a summary of some of the prominent solutions and how they were implemented in selected U.S. nuclear plants. This section does not provide all the information necessary to evaluate each solution comprehensively, because such information is in most cases protected by the proprietary nature of the vendor designs. Instead, this section provides an overview of solution options and important considerations.

The following subsection describes the replacement strainers explored for application in U.S. BWR plants. Although some or many of the hardware designs described below may be appropriate for implementation in U.S. PWR plants, none have been installed at any of the operating U.S. PWRs. It should also be noted that some strainer designs originated from European research and that several of the designs, both European and U.S. designs, are protected by proprietary constraints.

8.1 Overview of Resolution Options

BWR experience demonstrates that there are three general strategies for resolving the strainer clogging issue:

1. Remove (or replace) problematic insulation from the containment,
2. Install replacement strainers that can handle anticipated debris loads without exceeding the NPSH margin, or
3. A combination of items 1 and 2.⁸⁻¹

The replacement strainer options researched by the various investigators fall into four categories:

1. Installation of large capacity passive strainers with sufficient capacity to ensure that debris loadings equivalent to a scenario calculated in accordance with Section C.2.2 of RG 1.82, Rev. 2, do not cause a loss of NPSH for the ECCS,
2. Installation of a self-cleaning strainer that automatically prevents strainer clogging by providing continuous cleaning of the strainer surface with a scraper blade, brush, or other mechanism,

3. Installation of a backflush system that relies on operator action to remove debris from the surface of the strainer to prevent it from clogging, and
4. Installation of in-line (or inside ECCS suction piping) suction strainers located outside the suppression pool (or the containment) that can be realigned and flushed whenever the differential pressure exceeds the pump NPSH-margin.¹

Option 1 had the advantages of being completely passive so that operator intervention was not required and it did not require an interruption of ECCS flow. Licensees choosing Option 1 for resolution were required to establish new programs or modify existing programs to ensure that the potential for debris generated and transported to the strainer surface does not at any time exceed the assumptions used in estimating the amounts of debris for sizing of the strainers, in accordance with RG 1.82.

Option 2, like Option 1, would not rely on operator action nor interrupt ECCS flow but instead relies on an active component to keep the strainer surface clean that would be fully exposed to LOCA effects in the suppression pool. Therefore, appropriate measures must be taken to ensure its operability.

With the selection of Options 3 and 4, extensive measures had to be taken to:

1. Maximize the amount of time before clogging could occur,
2. Ensure that instrumentation and alarms indicate strainer differential pressure increases,
3. Institute operator training on recognition and mitigation of a strainer clogging event, and
4. Implement surveillance to ensure operability of the strainer instrumentation and backflush system.

The strainer designs explored experimentally in the U.S. (i.e., BWROG) included several concepts for passive strainer designs, passive strainers with backflush capability, and one self-cleaning strainer.⁸⁻¹

¹ The NRC suggested the first three of these options in NRCB 96-03⁸⁻² (discussed in Section 1.1).

In addition, the BWROG carried out engineering studies to examine the feasibility of adopting European solutions to the U.S. BWR plants. Based these studies, the BWROG concluded that replacing the existing strainers with large-capacity passive strainers is the preferred option for BWR implementation. Furthermore, it was recommended that backflush should be considered for installation as a “defense-in-depth” option, but not as a front-line option. Similarly, BWROG concluded that although a self-cleaning strainer installation was a feasible option, licensees would have to resolve significant design, qualification, and surveillance issues with the NRC on a plant-specific basis. Thus the BWROG all but ruled out all options other than installation of large replacement passive strainers that would reliably mitigate the adverse impacts of debris accumulation and maintain sufficient NPSH margin throughout an accident.

Installation of passive strainers that can handle anticipated debris loads consistent with BWROG guidance was not practical for all the plants due to additional constraints related to hydrodynamic loads. In those cases, plants installed the largest passive strainers acceptable in conjunction with the other options, including:

1. The replacement of problematic insulation with insulation determined to be less likely to generate or transport debris to the strainer, and
2. The revision of the NPSH calculation to include containment over pressure and/or eliminate conservatism in piping head loss calculations.

8.2 Replacement Strainer Designs

This section focuses on various strainer options installed in U.S. BWRs and draws inferences regarding their applicability to U.S. PWRs.²

² At the time of this report, one U.S. PWR implemented a partial solution to address concerns related to debris buildup and NPSH. The hardware changes made at this plant included increasing the sump screen area and possible redesign of parts of the sump. Reportedly, a series of experiments were performed in support of the strainer design and installation. The details of the design and the associated testing and qualification program were not available for review; therefore, a summary of this design is not included herein.

8.2.1 Passive Strainer Designs Installed in U.S. Nuclear Power Plants

The BWROG research into passive strainer design was limited in scope, focusing primarily on evaluating the feasibility of certain concepts, such as the star strainer and stacked disk strainer. This research program and the results are summarized in the BWROG URG.⁸⁻¹ Figure 8-1 presents a schematic representation of the test setup used in the BWROG prototype testing. Typically, the strainer module is located in a large tank of water. Water flow through the strainer module is maintained by recirculation pumps, which take suction through the strainer and discharges back into the tank. In some test setups, water discharge locations are located strategically to maximize turbulence in the tank, such that the potential for debris settling in the tank is minimal.³ Other test setups use either mechanical or manual means to ensure that most of the debris added to the tank would reach the strainer, and that minimal, if any, debris would settle out in the tank. Head loss across the strainer is monitored using a pressure transducer located downstream of the pipe flange connected to the strainer.

The experimental results suggest that head loss across the passive strainers modules (i.e., the advanced designs described below) is a non-linear function of debris loading. Figure 8-2 shows a representation of measured head loss as a function of strainer debris loading for a stacked disk strainer. The advanced passive strainers are designed such that they would have a gap or crevice where debris would initially accumulate preferentially when debris loading is small. The debris accumulated in these gaps would be subjected to lower fluid velocities, and hence would lead to lower head loss. Further, when the flow moves somewhat parallel to portions of the strainer surfaces, debris on these surface is pushed further into the gaps, thereby keeping a portion of the disk surface relatively clean of debris until the gaps are filled. After these gaps are filled, debris would start to accumulate on the circumscribed surface of the strainer, which resembles a regular shaped strainer (cylindrical in the case of stacked-disk strainers). In view of this complex

³ The quantity of debris on the strainer was usually based on the quantity of debris introduced into the test tank, therefore the quantity of debris not collected on the strainer needed to be negligible.

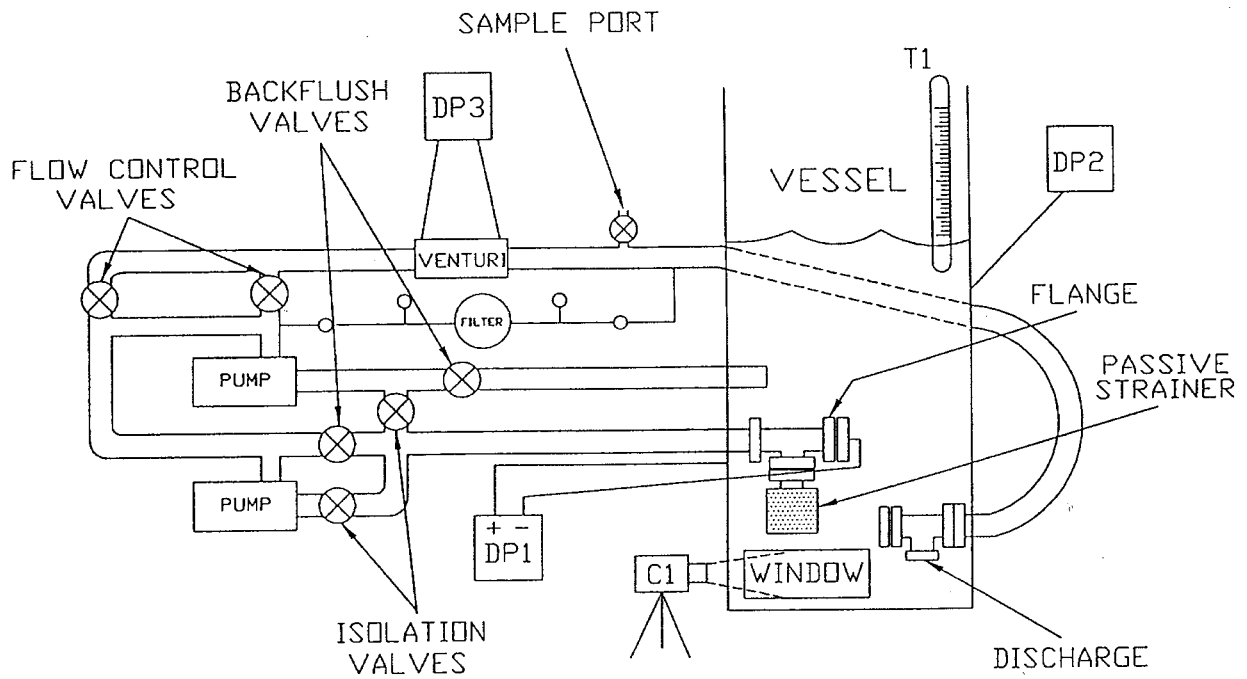


Figure 8-1 BWROG Prototype Module Test Program

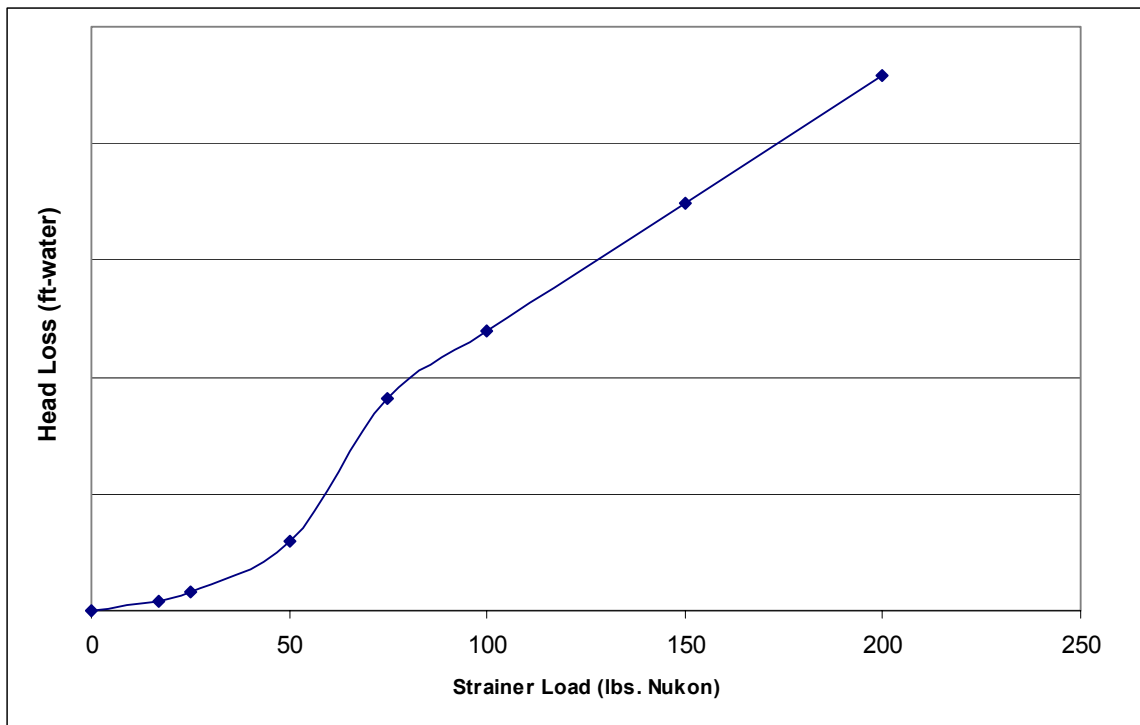


Figure 8-2 Measured Head Loss as a Function of Strainer Debris Loading for Typical Advanced Passive Strainers

relationship between the head loss and debris loading, special attention should be paid to collecting head loss data over a wide range of debris loading and carefully judging the applicability of test data to a given plant.

The primary design concept in all passive strainers is to maximize the strainer surface area (i.e., area of the perforated surface through which water flows into the strainer) while minimizing the space required for the strainer.⁴ These design concepts were further refined or reengineered as required by strainer vendors to suit specific plant needs. The vendors in support of particular strainer designs undertook separate testing and engineering studies. Ultimately, four types of passive strainer designs were installed at U.S. BWRs. Although these designs differ significantly from each other, the designs had one common feature in that they all rely on cavities, troughs, or traps where debris can collect on the strainer surface without significantly increasing head loss across the strainers.

8.2.1.1 PCI Stacked-Disk Strainers

PCI developed and tested prototype stacked-disk strainers, and designed, fabricated and installed advanced passive stacked-disk strainers for installation at several U.S. BWRs.^{8-3,8-4,8-5} The PCI strainer concept, referred to commercially under the trademark Sure-Flow, consists of a stack of coaxial, perforated metal plate disks that are welded to a common perforated internal core tube. The design maximizes the strainer surface area while keeping the volume occupied by the strainer to a minimum. Innovative Technology Solutions Corporation (ITS) provided the head loss performance modeling and sizing solutions for industry implementation⁸⁻⁶ based on NUREG/CR-6224 methodology.⁸⁻⁷ Figure 8-3 is a photograph of the PCI strainers installed at a BWR. Among the design features of the PCI strainer is the internal core tube designed to ensure relatively uniform approach flow⁵. The core tube is shown in Figure 8-4. Several

⁴Minimizing circumscribed area was of benefit to BWRs because of issues related to hydrodynamic loads and also because compact strainers were needed to fit into the suppression pools.

⁵The core tube provides structural support and also makes the approach flow more uniform.

prototypes of the PCI stacked-disk strainers were tested for head loss measurements at the EPRI NDE Center test facility and other test facilities. PCI reports provide a description of the test program and the results.^{8-3,8-4,8-5}

The hydraulic performance of PCI strainers was also tested by the BWROG⁸⁻¹ and as part of qualification testing by Commonwealth Edison.⁸⁻⁸

PCI Sure-Flow Strainer Design and Testing Program

PCI fabricated and tested prototypes over a period of nine months to evaluate the head loss performance of the Sure-Flow strainers. The hydraulic performance testing was conducted at the EPRI test facility using the test setup designed and operated as part of the BWROG testing program. One prototype, referred to as Stacked-Disk #1 in the URG, was a 40%-scale prototype with six disks, five troughs between the disks, a 13-in. core tube, a 30-in. outside diameter, and was 2.5 ft long. A larger prototype, referred to as Stacked-Disk #2, was a 4-ft-long strainer with a core tube diameter of 26 in. and a stack outer diameter of 40 in. Both the BWROG and PCI tested the head loss performance of these strainers. An engineering correlation of the test data was proposed by PCI for limited applications.

The Sure-Flow strainer is not a standardized strainer, i.e., one size does not fit all. Instead, the PCI concept is to use similarly designed strainer modules of various sizes and quantities as necessary for each plant. A plant would first determine the anticipated debris loading and the strainer design criteria applicable to that plant. PCI and its contractors would determine the size and number of stacked-disk modules necessary to meet the design criteria. For this approach to be successful, the PCI team needed a model that accurately predicted the head loss performance of a generic PCI Sure-Flow strainer. ITS Corp. adapted the head loss model used in the NUREG/CR-6224⁸⁻⁷ study for use with the stacked-disk strainer geometry,⁸⁻⁶ and developed a proprietary computer code named HLOSS to automate head loss calculations performed for each plant. The overall technical approach for using the NUREG/CR-6224 correlation to predict PCI Sure-Flow strainer performance was validated by comparing correlation predictions with head loss data.



Figure 8-3 PCI Stacked-Disk Strainer Being Installed at Pilgrim Nuclear Power Plant



Figure 8-4 The Core Tube Used in the PCI Stacked-Disk Strainers

NRC Review of the PCI Strainer Program

Because the PCI test data and the ITS head loss models were used by many licensees, the NRC contractor LANL performed an in-depth review of the PCI head loss data and evaluated the adequacy of the head loss models. The results of this review are summarized in the LANL technical evaluation report (TER) "Technical Review of Selected Reports on Performance Contracting, Inc. Sure-Flow

Strainer™ Test Data."⁸⁻⁹ In general, it was concluded that the test program used by PCI for verifying the hydraulic performance of the prototype strainer is acceptable.

Documentation

The PCI head loss data is documented in the PCI report "Summary Report on Performance of Performance Contracting, Inc.'s Sure-Flow™ Suction Strainer with Various Mixes of Simulated

Post-LOCA Debris.”⁸⁻³ The results of this review are summarized in the LANL TER entitled “Technical Review of Selected Reports on Performance Contracting, Inc. Sure-Flow Strainer™ Test Data.”⁸⁻⁹

8.2.1.2 General Electric Stacked-Disk Strainers

GE supplied an advanced passive stacked-disk strainer to the nuclear industry that was designed to alleviate the strainer blockage problem. The GE design (information regarding the design is proprietary) offered an improvement over the conventional stacked-disk strainers tested by the BWROG. A relatively large cavity volume accommodates larger volumes of insulation debris without a substantial increase in the head loss. Each GE strainer is designed specifically to suit a particular plant application to meet specific requirements for estimated debris and hydrodynamic loadings. The design details of the strainer and the hydraulic performance characteristics of the strainer were provided to NRC for review by GE in a proprietary GE Licensing Topical Report (LTR).⁸⁻¹⁰ The NRC review of the GE strainer performance and important conclusions are summarized in a LANL TER (not publicly available).⁸⁻¹¹ GE strainers were installed at Duane Arnold, Hatch (Unit 1), Oyster Creek, River Bend, Cooper, Fermi (Unit 2), Susquehanna (Units 1 and 2), Nine Mile Point (Unit 2), and Browns Ferry (Unit 2 and 3).

GE Program

GE fabricated a prototype strainer and tested its hydraulic performance at the EPRI NDE Center. The facility and testing procedures were the same as those used in the BWROG test program. The tests involved both fibrous debris and RMI debris. In each test, predetermined quantities of fibrous debris, corrosion products, and RMI debris were added to the test tank and kept in suspension by pumped-flow recirculating flow patterns. Sufficient time was allowed for debris to accumulate on the strainer surface, and then the head loss was measured at varying flow velocities. The objective was to examine the effect of velocity on debris bed compression without the results being affected by filtration. The actual quantity of debris deposited on the strainer surfaces was not directly measured but deduced from the quantity of debris added to the

pool. (A similar approach was followed in all BWROG tests.)

NRC Review of the GE Program

The NRC reviewed⁸⁻¹¹ GE’s “Application Methodology for GE Stacked-Disk ECCS Suction Strainer-1,”⁸⁻¹⁰ and associated documents. In addition, the NRC sponsored two sets of confirmatory analyses to evaluate the GE head loss methodology. In the first analysis, the NRC examined:

1. The actual range of experimental parameters explored in the GE tests and compared the parameters with those of the proposed plant applications, and
2. The process used to develop the correlation and the generic acceptability of the correlation.

The second set of calculations compared GE test data with the predictions of a modified version of NUREG/CR-6224 correlation.

Based on the NRC review, the NRC staff concluded that the test program used by GE for verifying the hydraulic performance of the prototype strainer is acceptable for BWR applications. However, the staff had concerns regarding the validity and use of this correlation for plants outside those reviewed.

Documentation

The GE methodology is documented in the GE’s “Application Methodology for GE Stacked-Disk ECCS Suction Strainer” (proprietary).⁸⁻¹⁰ The NRC review of the GE methodology for determining head loss across GE stacked-disk strainers is documented in a LANL TER entitled, “Technical Review of GE LTR NEDC-32721P: Application Methodology for GE Stacked-Disk ECCS Suction Strainer” (proprietary corporate information).⁸⁻¹¹

8.2.1.3 ABB Combustion Engineering Strainers

The ABB strainers use another approach to extend the screen area and thus reduce the approach velocity at the plate. The original strainer design is based on concepts developed in Europe; however, later developments were undertaken in U.S. The design was tested and demonstrated by ABB at the EPRI facility.⁸⁻¹² The ABB strainers were installed at Peach Bottom (Units 2 and 3) and Limerick (Units 1 and 2). The NRC did not specifically review the

testing program for the ABB strainers; however, the NRC did review plant specific evaluations where ABB strainers were employed. ABB designs are protected as proprietary information.

Documentation

LANL review of ABB strainer performance and related issues are summarized in the Limerick audit report entitled, "On-Site Audit of the Limerick Nuclear Power Plant Emergency Core Cooling System Strainer Blockage Resolution."⁸⁻¹³

8.2.1.4 Mark III Strainers

The Mark-III BWR owners sponsored a research program to design and qualify a strainer best suited for Mark III containments. This design takes advantage of the Mark III containment layout. The strainers are very large and are located on the floor of the suppression pool. Figure 7-14 is a photograph of an individual strainer module from the quarter-scale test facility. Several (up to 50) of these full-scale strainer modules are joined together to form the strainer in the plant. Figure 7-13 shows an assembled strainer. The resulting strainers have surface areas in excess of 6000 ft². These strainers were tested at the quarter-scale test facility. NRC review comments on the testing program and the application of the test results in the plant submittals are summarized in the Mark III Grand Gulf Nuclear Station (GGNS) Audit Report and LANL TER.⁸⁻¹⁴ GGNS replaced its existing truncated cone strainers that had a net surface area of 170 ft² with large-capacity passive strainers having a combined area of 6253 ft² (~37 fold increase). Strainers of this design were also installed at Perry and Clinton.

GGNS also conducted extensive quarter-scale pool transport and head loss testing for their replacement strainer design and small-scale testing for a segment of the design. The NRC staff audited the GGNS strainer clogging issue resolution in August 1999 and evaluated the application of quarter-scale testing to the GGNS plant analysis. The replacement strainers, designed by Enercon Services, Inc., were combined into a large single strainer that circumscribes the suppression pool near the floor, as illustrated in Figure 7-13. This strainer serves as a common header for all six ECCS pumps so that any combination of operating systems can draw recirculation water through the same large screen area. The primary concern regarding their test program was the

estimation of the combined effects of fibrous debris (Kaowool and fiberglass) and particulate debris consisting primarily of calcium silicate.

Grand Gulf Quarter-Scale Test Program

GGNS sponsored a research program to study head loss performance of their replacement strainer. A quarter-scale strainer was built and installed in the Mark-III quarter-scale test facility. Geometric, operational, and debris loading parameters were all scaled to the GGNS plant values. The flow velocity and debris bed thickness were monitored in the tests to ensure that the measured head loss caused by the debris buildup could be used directly in the plant NPSH analysis.

NRC Review of Grand Gulf Quarter-Scale Test Program

The staff compared the scaled test parameters to those of the plant and determined that the quarter-scale testing adequately simulated important flow parameters. In particular, the licensee ensured that the approach velocity at the strainer surface was the same as the approach velocity in the plant, and the debris loadings per unit area of the strainer in the tests were the same or greater than those expected in the plant. There are two geometrical differences between the quarter-scale test setup and the plant:

1. The quarter-scale tests used a significantly lower number of strainer sections compared to the plant, and
2. The construction of these strainer segments was different with respect to specifics, such as the number of ribs and the plate thickness.

These differences mean that clean-strainer head losses measured in the quarter-scale test setup were not directly scalable to the GGNS plant application. However, the licensee performed detailed analyses to correct for these differences.

All of the tests were conducted at 75°F whereas the suppression pool temperatures were expected to reach approximately 185°F. The licensee used the test results directly in their NPSH margin evaluation; however, this was conservative because testing at the lower test temperature resulted in higher head losses, due to viscous effects, than would have occurred if the testing had been performed at the temperatures expected to result following a LOCA. The clean-strainer head loss for the quarter-scale geometry was about 3 in. of water at the conditions representing runout ECCS flow.

The licensee sponsored five tests directly applicable to GGNS. The NRC staff drew the following conclusions regarding the GGNS quarter-scale testing program and its results:

- The licensee test program was extensive with great attention to detail.
- Data repeatability was acceptable. Head loss variations of 2-ft water or less were measured for repeatability tests and the plant has sufficient margin to account for these uncertainties.
- The head loss tests indicate that some of the tests might not have reached steady state before termination. The licensee accounted for this apparent shortcoming by extrapolating to a steady value.
- Debris bed combinations of Kaowool and calcium silicate resulted in high head losses, even though the approach velocity was relatively slow (0.016 ft/s). This finding was significant, because such data was previously not available. It should also be noted that the licensee continued selected testing after the staff completed their review to better understand head loss implications of calcium silicate insulation debris.

Documentation

A review of the GGNS strainer testing is found in a LANL TER, titled "On-Site Audit of the Grand Gulf Nuclear Station Emergency Core Cooling System Strainer-Blockage Resolution."⁸⁻¹⁴

8.2.2 Active Strainer Designs

8.2.2.1 BWROG Research into Active Strainer Concepts

BWROG test program performed two series of tests into active strainer concepts; these concepts were the passive strainer with backflush capability concept, and the self-cleaning strainer concept. For backflush strainers, tests were conducted to evaluate the maximum fiber and corrosion product capacity until backflush needs to be operated, the effect of thin fiber beds, the feasibility of backflushing, and the effect of RMI on backflush. Tested debris included prototypical fibrous insulation, RMI, simulated corrosion products, and miscellaneous debris. The self-cleaning strainer was tested to evaluate its ability to maintain a clean strainer surface area under various debris loadings at design flow rates and its start up capability after a period at a minimum flow condition. Utility Resolution Guidance for ECCS

Strainer Blockage, General Electric Nuclear Energy Company, Class 1, Nov. 1996,⁸⁻¹ describes these strainer design concepts and their associated test programs.

The summarized results for backflushing are as follows.

- The truncated core strainer was successfully backflushed under all conditions. Typically fibrous insulation can be easily backflushed, but when it is mixed with suppression pool sludge or other particulate debris removal became difficult. Also, the removed material tended to accumulate on the strainer again as the flow was reinitiated and at a rate faster than the first time.
- Although some relief was obtained for the 60-point star and the stack-disk strainer designs tested, debris was not adequately removed at flow rates up to the maximum backflushing 5000-gpm flow when fibrous insulation was used.
- With the exception of some RMI debris wedged into the internal portions of the stars of the 60-point strainer, the RMI debris by itself was successfully removed by shutting off pump suction flow (i.e., no backflush required).

The summarized results for self-cleaning strainer testing are:

- The active front portion of the strainer was kept clean for all debris types and loadings tested at the design flow rate of 5000-gpm. The head loss across the strainer was found to be essentially constant at a given flow rate and independent of the debris loading.
- It is possible that sufficient debris can accumulate on the active portion of the strainer under a low-flow start-up condition to prevent subsequent plow/brush rotation at design flow rates.
- Although the strainer maintained a clean front surface, the head loss across the clean strainer and the torque generated by the turbine were higher than expected. This result required that considerable additional engineering would be needed prior to installation. It is also possible that installation and operation may be difficult to qualify when subjected to hydrodynamic loads.
- Foreign materials, such as anti-contamination clothing and booties, tended

to become lodged in between the plow and the strainer surface. They are then difficult to dislodge.

Installation of active strainers at U.S. Nuclear Power Plants was not undertaken because:

- Operability testing and inspection of active components were deemed very resource intensive, especially for BWRs where strainers are located in the suppression pool, and
- Design and sizing of the strainers is complicated by the fact that all such analyses must make important assumptions regarding the rate at which the debris arrives at the strainer and the time available for operator action.

8.3 Overview of U.S. BWR Plant Implementation

From the beginning, it was recognized by both the NRC and the BWROG that none of the passive strainer designs are standardized designs (i.e., a one-size strainer fits all strainer applications). Further, it was recognized that additional analyses would have to play an important role in sizing the strainer. As a result, considerable effort was devoted in the BWROG URG to provide detailed guidance on performing plant-specific analyses to estimate the potential for debris loads on the ECCS suction strainers following a LOCA, taking into consideration the guidance provided in the RG 1.82, Rev. 2.

Every operating U.S. BWR plant replaced their existing LPCI and LPCS pump suction strainers (typically conical type strainers). The industry addressed the requirements of NRC Bulletin 96-03⁸⁻² by installing large capacity passive strainers in each plant (i.e., NRC Option 1) with sufficient capacity. There were, however, a few plants that installed the replacement strainer before the BWROG URG and the URG SER were issued. The supporting analyses for these plants deviated in some cases significantly from the approved URG methodologies.

8.3.1 NRC Review of U.S. Plant Implementation

The NRC closely followed plant implementations through active participation in the industry meetings, review of plant-specific submittals, and by performing onsite audits of four nuclear power plants. Participation in industry meetings

facilitated the exchange of information with the BWROG and individual licensees, and provided a means for the NRC to clarify specific elements of the regulatory guidance (e.g., the thin-bed head loss issue). The participation also helped the NRC staff to keep abreast of the methods used by the licensees and of uncertainties in some of the assumptions in sizing strainers.

Plant-specific submittals were provided by some licensees as part of licensing amendment requests, consistent with the requirements of 10 CFR 50.59 and 10 CFR 50.90. Most of the licensing amendments were related to licensee intent to use higher containment overpressure credit in the NPSH calculations.

Prior to the completion of the NRC staff's review of the URG, some submittals were provided for NRC review during the strainer sizing and design phase to minimize the replacement project risk. A list of plants that provided replacement strainer details for NRC review is as follows: Browns Ferry (Units 2 and 3), Brunswick (Units 1 and 2), Cooper, Hatch (Units 1 and 2), Hope Creek (Units 1 and 2), LaSalle (Units 1 and 2), Limerick (Units 1 and 2), Peach Bottom (Units 2 and 3), Pilgrim (Unit 1), and Quad Cities (Units 1 and 2).

The strainer areas (plant totals) installed at the operating BWR plants are listed in Table 8-1 along with their respective strainer vendors.⁸⁻¹⁹ As evident, the replacement strainers are in general very large compared to pre-NRCB 96-03 strainers. Only four sites installed strainers with areas less than 1100 ft² and these four sites use primarily RMI and have little fibrous insulation in containment. The flow velocities at the plate for the replacement strainers ranged between about 0.001 ft/s and 0.1 ft/s.

Based on their review of each plant submittal, the NRC concluded that the industry had addressed the requirements of NRC Bulletin 96-03 by installing large capacity passive strainers in each plant (i.e., NRC Option 1). The strainers had sufficient capacity to accommodate the debris loads postulated to reach the strainer following a worst-case large break LOCA. The NRC found that in most cases the licensees had voluntarily used conservative assumptions in sizing and designing the replacement strainers. This voluntary conservatism was in addition to conservatism built-in to the URG guidance.

Plant	Reactor Design	Containment Design	Total Area per Plant (ft²)	Strainer Vendor
Browns Ferry 2 & 3	BWR/4	Mark I	1192	GE
Brunswick 1 & 2	BWR/4	Mark I	1575	PCI
Clinton	BWR/6	Mark III	6057	Enercon
Cooper	BWR/4	Mark I	2164	GE
Dresden 2 & 3	BWR/3	Mark I	475	PCI
Duane Arnold	BWR/4	Mark I	1359	GE
Fitzpatrick	BWR/4	Mark I	2928	PCI
Fermi 2	BWR/4	Mark I	2322	GE
Grand Gulf	BWR/6	Mark III	6253	Enercon
Hatch 1 & 2	BWR/4	Mark I	1110	GE
Hope Creek	BWR/4	Mark I	3788	PCI
LaSalle 1 & 2	BWR/5	Mark II	500	PCI
Limerick 1 & 2	BWR/4	Mark I	2715	ABB
Monticello	BWR/3	Mark I	1224	PCI
Nine Mile Point 1	BWR/2	Mark I	1286	PCI
Nine Mile Point 2	BWR/4	Mark II	1412	GE
Oyster Creek	BWR/2	Mark I	1425	GE
Peach Bottom 2 & 3	BWR/4	Mark I	3550	ABB
Perry	BWR/6	Mark III	5326	Enercon
Pilgrim	BWR/3	Mark I	1340	PCI
Quad Cities 1 & 2	BWR/3	Mark I	832	PCI
River Bend	BWR/6	Mark III	2424	GE
Susquehanna 1 & 2	BWR/4	Mark II	1340	GE
Vermont Yankee	BWR/4	Mark I	2488	PCI
WNP 2	BWR/5	Mark II	825	PCI

8.3.2 Onsite Plant Audits

Four BWR plants were chosen for a detailed onsite audit by the NRC staff: Limerick (BWR/4 Mark II), Dresden (BWR/3 Mark I), Duane Arnold (BWR/4 Mark I), and Grand Gulf (BWR/6 Mark III). The primary objective of these audits was to independently confirm the adequacy of the strainer sizes and to independently evaluate the performance of the replacement strainers under LOCA conditions. In addition, the audit reviewed the supporting documentation to identify any concerns regarding licensee strainer design criteria and strainer performance analyses. In particular, the review of licensee strainer design analyses did the following:

1. Evaluated how the licensee estimated the quantity of debris used for sizing the strainer, that is, determined if the methodologies used for selecting the breaks were consistent with RG 1.82, Rev. 2, and

provided reasonable estimates for debris generation and transport.

2. Evaluated the licensee's proposed strainer design criteria and strainer performance.

During the plant audit, the NRC staff undertook a detailed review of the documentation provided by the licensee and performed several independent calculations, as necessary. The types of analyses performed by the staff during the audit included:

1. Debris Generation Calculations. Wherever possible or necessary, the NRC staff used reactor piping layout drawings to independently map the ZOI and estimate the quantity of debris contained within the ZOI.
2. Debris Loading Evaluations. In each case, the staff independently calculated the debris loads expected on the strainer following a LOCA and how these loadings compared with the licensee estimates. The comparison provided a measure of the

margin-of-conservatism in the licensee calculations.

3. Strainer Head Loss and NPSH Evaluations. NRC staff used the BLOCKAGE computer code to estimate head losses corresponding to various postulated ECCS responses (e.g., single-failure criterion). These head loss estimates were compared with the licensee estimates to draw conclusions regarding strainer performance.

- "On-Site Audit of the Dresden Nuclear Power Plant Emergency Core Cooling System Strainer Blockage Resolution."⁸⁻¹⁵
- "On-Site Audit of the Limerick Nuclear Power Plant Emergency Core Cooling System Strainer Blockage Resolution."⁸⁻¹³
- "On-Site Audit of the Duane Arnold Energy Center Emergency Core Cooling System Strainer Blockage Resolution."⁸⁻¹⁶

In addition, NRC staff paid close attention to judge the effectiveness of the licensee FME program. The results of the technical analyses are summarized in the audit reports. These TERs were:

- "On-Site Audit of the Grand Gulf Nuclear Station Emergency Core Cooling System Strainer-Blockage Resolution."⁸⁻¹⁴

Table 8-2 provides a brief summary of the issue resolution for the audited plants. The screen areas provided in the table again demonstrate the large sizes of the resolution strainers, especially when compared to their respective pre-NRCB 96-03 strainers.

Table 8-2 Issue Resolution Summary for Audited Plants

Plant	Design	Insulation Types Located in the Drywell	Plant Resolution	Resolution Basis	NRC Audit Findings
Grand Gulf Nuclear Station	BWR/6 Mark III	RMI Kaowool Calcium-Silicate Fiberglass	Increased existing strainer surface area from 170 ft ² to 6253 ft ² by installing passive large-capacity suction strainers.	Licensee based analyses on URG supported by ¼ scale testing.	Licensee conservatively estimated debris generation, transport, and strainer head loss. NRC estimated head losses substantially less than licensee estimate.
Limerick	BWR/4 Mark II	NUKON Min-K RMI**	Increased existing strainer surface area from 269 ft ² to 2715 ft ² by installing passive large-capacity suction strainers.	Licensee based analyses on URG. Head loss estimate less than 4-ft water and NPSH margin of 12-ft water.	Licensee conservatively estimated debris generation, transport, and strainer head loss. NRC estimated head loss less than 2-ft water.
Duane Arnold	BWR/4 Mark I	NUKON* Calcium-Silicate** RMI** Lead Wool**	Increased existing strainer surface area from 38 ft ² to 1359 ft ² by installing passive large-capacity suction strainers.	Licensee based analyses on URG and GE head loss correlation.	Licensee used NRC-approved methods to estimate debris generation and transport, and estimated conservative strainer head loss.
Dresden	BWR/3 Mark I	RMI NUKON Calcium-Silicate Asbestos** Amaflex**	Increased existing strainer surface area from 18.8 ft ² to 475 ft ² by installing passive large-capacity suction strainers.	Licensee based analyses on URG and plant specific alternate methods.	NRC determined licensee strainers adequately sized, although inconsistencies and deviations from URG found in licensee analyses.

* Majority of total insulation of this type.

** Insulation screened out of analysis due to location, e.g., inside biological shield.

8.4 Special Considerations for PWR Resolution Options

No special strainer designs have emerged to date in the U.S. for implementation in the PWRs⁶. This section provides some of the considerations, other than the head loss considerations described above, that should be addressed. Data for this subsection has been provided by the Finnish utilities Imatran Voima Oy (IVO) and Teollisuuden Voima Oy (TVO), the Electric Power Research Institute (EPRI), Performance Contracting Inc (PCI) and Transco Products Inc (TPI). This section was adopted from the CSNI Knowledgebase Report.⁸⁻¹⁷

8.4.1 Flow Path Blocking

Clogging or blocking of water pathways that connect locations where water is discharged into the containment and where the sump is located could prevent the free flow of water to the sump. This in turn could significantly alter the water level at the sump and the overall water inventory available for mitigating an accident. Such blockage could also significantly alter flow patterns in or around the sump, with implications to debris transport.

Flow path blocking becomes possible if there are debris interceptors, such as perforated plates, screens, gratings, entryways with grated doors, etc., along the flow path. Such structures can collect insulation debris and other materials behind the obstructing surface. Based on existing data and analyses, flow-path clogging, if it were to occur, would appear more likely at the earlier phases of a large or intermediate LOCA. During this phase, water and steam discharged from the break flows at high velocities through these pathways and would likely transport large pieces of debris (e.g., partially torn insulation blankets or damaged and stripped RMI cassettes) and subsequently depositing significant quantities of debris onto the debris interceptors.

The database for performing flow path clogging evaluations is very limited. In general, the risk of flow path clogging emerges due to the release of larger pieces of insulation blankets, pieces of

metallic insulation cassettes, and as-fabricated fibrous insulation pillows, all of which could float during early stages of the accident. The eventual risk depends on the structure of the pathways and the nature of the insulation employed, which vary considerably from plant to plant. Debris transport data from NRC sponsored tests at University of New Mexico and previously at Alden Research Laboratory provide some of the data on flow conditions required for the transport of larger debris and the potential for them to flip up onto obstructions (discussed in Sections 5 and 6).

8.4.2 Strainer Penetration

The purpose of an ECCS suction strainer or a sump screen is to prevent foreign materials from entering sensitive coolant systems. However, some amount of material (fibers, particulates, small metal shreds from metallic insulation, etc.) could potentially penetrate a strainer, particularly during the early stages of an accident, before sufficient debris accumulates on the strainer to effectively filter the smaller debris. If back-flushing or other types of strainer cleaning were to be employed then the cleaned screen would once again be more susceptible to debris penetration as a result of that operation (again note that U.S. BWRs did not select this option). This issue is especially important for current U.S. PWRs because the current sump screen clearances (i.e., mesh spacing) vary considerably, from 1/16-in. to 1-in. All U.S. BWR strainers now have clearances of 1/8-in. or smaller and there is standardization due to GE design control.

This concern can be attested to by the anecdotal information from the Marviken blowdown experiments, which were carried out in a canceled prototype BWR. In these experiments, there was a containment spray to which water was pumped from the containment sumps. The sump screens had 8-mm by 8-mm square holes (relatively large). At the time, the plant used primarily mineral wool insulation. During the first experiments, the insulation debris that passed through the screens clogged the spray nozzles. The experimenters also observed considerable quantities of the debris in the pump casings and other locations in the piping, such as in the valves.

The significance of strainer penetration depends on the types of materials that are present and on

⁶ As previously discussed, although sump screen modifications were made at one PWR, these modifications did not involve installation of any specialized strainer designs.

their potential influence on other system components, such as pumps (e.g., damage to pump seals), nozzles (e.g., clogging), or the reactor core, where blockages may also form, subsequently threatening fuel integrity by impairing heat transfer. All these are greatly affected by the properties of the individual particles, which vary substantially among the types of insulation and other materials present in the containment.

The Finnish and Swedish utilities have produced some experimental results on how fibrous insulation debris penetrates a perforated plate.⁸⁻¹⁷ These data are shown in Tables 8-3 and 8-4. In the U.S., the BWROG also obtained some data on the debris penetration of a perforated plate.⁸⁻¹

The debris that passes through the strainer proceeds through all components of ECCS or CS systems, that is, through valves, pumps, heat exchangers, and spray nozzles, into the reactor core, and back into the containment. Safety concerns predominantly relate to clogging, but as far as pumps are concerned, there may also be potential for problems with shaft seals, particularly leakage and heatup, which could lead to pump shaft seizure. The survey conducted so far has revealed no data on the possibilities or phenomenology of clogging phenomena in heat exchangers, or reactor internals, excluding the spray nozzles and fuel bundles. Whether a potential for problems exists is completely dependent on the setup of the individual application.

The components that have received attention, spray nozzles and fuel bundles, are discussed in more detail below. Although another component, valves/nozzles in the HPSI lines, received attention, no experimental data is available.

8.4.2.1 Spray Nozzles

Two data points have been reported, one an experiment with nozzles and the other an anecdote of large-scale blowdown experiments.

Tests were performed to determine the potential for NUKON glass fibers to clog a spray nozzle.⁸⁻¹⁷ The test apparatus consisted of a small tank, a centrifugal pump, piping and two 3/8-in. (9.5-mm) containment spray nozzles. NUKON blanket parts (glass wool, woven jacket,

nylon looped Velcro and stainless steel hooked Velcro) were cut into pieces ranging from 1 in. to 3 in. (2.5 to 7.5 cm) on a side, placed in the tank, and allowed to pass through the pump to the nozzles. The circulation rate was maintained as close as possible to the nominal nozzle flow rate.

The following general observations were made:

1. "Soft" pieces (without steel) were disintegrated into fine slurry in the pump and as such never caused clogging of the nozzles.
2. The stainless steel hooks and canvas clothing pieces passed through the pump without disintegrating and jammed into the nozzle.
3. When a piece of steel jammed in the nozzle, other components of the fine slurry would buildup behind the jammed steel and cause the nozzle to clog (i.e., caused a noticeable flow reduction and impaired the formation of the nozzle spray cone).

Susceptibility to nozzle clogging would depend on the size of the nozzle (i.e., a smaller nozzle would clog easier than would a larger nozzle) and on the particle density. Even, with a relatively large sized nozzle, clogging can be initiated by millimeter-scale pieces of debris (debris not completely disintegrated while passing through a pump), although such pieces alone may not overly impair the nozzle function. Such debris could subsequently collect finer debris, thereby causing complete or nearly complete blockage of that nozzle. Such clogging phenomenon would likely occur with any combination of fibrous material and other stiff debris (e.g., metallic debris).

8.4.2.2 Fuel Bundles

Four different mechanisms seem to exist that might cause clogging of the core from the debris or other ingredients present in the coolant: thermal adherence to hot surfaces, chemical adherence, hydraulic accumulation, and enrichment due to boiling. The first knowledgebase report⁸⁻¹⁷ provides detailed discussions on the effect of debris accumulation on the fuel bundles. Examples of accumulation include fibrous debris accumulation on the fuel bundle spacer grids, between the spacer grids and the rods, and on fuel assembly inlet debris screen, if present.

Table 8-3 Fiber Penetration, 4-mm Perforated Plate ⁸⁻¹⁷		
Concentration Per Volume of Water	Total Mass Passed Through Per Strainer Area	Remarks
Mineral Wool (Rockwool) 37 g/m ³ 150 g/m ³	16 g/m ² 24 g/m ²	See Notes 1 & 2
Glass Fibers/Rockwool Mixture, 1:1 by weight 37 g/m ³ 150 g/m ³	5 g/m ² 20 g/m ²	See Notes 1 & 2
<p>Note 1: The "Total Mass" is the total mass of material that the experimenters determined to have passed through the strainer. In the reported experiments,⁸⁻¹⁸ a fibrous bed formed on the strainer within three to five min. The experimenters report that no penetration occurs after that.</p> <p>Note 2: The uncertainties in this data are very large, up to a factor of 3 (that is, the mass passed per area may be 3 times larger). Other experiments have yielded even larger penetrations, over 2 kg/m².</p>		

Table 8-4 Fiber Penetration, 4-mm Perforated Plate ⁸⁻¹⁷						
Batch Size (kg/ m ²)	Final Coverage (kg/m ²)	Period (min)	Mass Passed (g/m ²)	Penetration Rate* (g/m ² min)	Note	
Rockwool, Fresh						
0.83	0.83	35	48	1.4	3	
0.83	1.66	30	0	0.0		
1.0	1.0	90	14	0.16	4	
Rockwool, Resin-Free						
0.33	0.33	95	250	2.6		
0.33	0.66	75	190	2.5		
0.33	1.0	60	170	2.8		
1.0	2.0	70	470	6.7		
1.0	3.0	100	610	6.1		
2.0	5.0	25	770	3.1		
0.0	5.0	70	250	3.6		
Totals		495	2710			
Glass Wool, Thermally Aged						
2.0	2.0	25	20	0.8		
2.0	4.0	30	0	0.0		
<p>Remarks:</p> <p>* Penetration rate is an average figure, obtained by dividing total passed mass by the period of observation. Instantaneous penetration measurements were attempted but no results are reported.</p> <p>Note 3: A strainer segment at 20 kg/m²s mass flux was to produce data on this and the next row.</p> <p>Note 4: A 1:2 strainer model at 8 kg/m²s mass flux was used to generate this row and the rest of the data.</p>						

8.4.3 LOCA Jet and Missile Considerations

The threats posed by postulated pipe breaks and other pressure boundary failures on the sump screens should be examined as part of sump screen redesign. The safety concern is that either due to LOCA jet impingement or due to missile impaction, the sump screen would be structurally damaged leading to partial or total loss of screening capability. A loss of screening capability would likely result in substantial debris, including potentially large pieces of debris, bypassing the screen.

Research performed so far indicates that LOCA jet impacts can easily cause substantial damage on finer mesh screens. Similarly, research indicates that hard insulations (i.e., reflective metallic insulations and encapsulated mass-type insulations) can become 'hard' missiles and could inflict severe damage on the components located in their proximity. Most of this data is in the form of anecdotal evidence and limited studies performed as part of the BWR resolution.⁷

8.4.4 Feasibility and Efficiency of Backflushing

Several European and U.S. experiments were carried out to examine feasibility and efficiency of backflushing. Two types of backflushing techniques were used: (1) compressed air injection and (2) water flow reversal. In both cases to carry out the backflushing procedure, it was necessary to terminate suction from the strainer and restart the flow after the backflushing process was completed. Head loss was measured both before and after the backflushing to examine efficiency of the backflush procedure. The experimental observations can be summarized as follows:

- Strainer clogging due to reflective metallic insulation debris was effectively mitigated by backflushing. Typically the RMI fragments tended to fall off when the flow was terminated. The few left over pieces were easily backflushed. Soon after completing the backflush procedure, the pressure differential was nearly zero but it steadily

increased again as the freed debris gradually accumulated back onto the strainer subsequently reaching the original differential pressure.

- Backflushing was also effective for removing fibrous debris from the strainers. In this case, fibrous debris fell off in chunks and some of this debris did not accumulate back onto the strainers; thus efficiency of backflushing was high for fibrous debris.
- Backflushing systems were not very effective where beds of mixed fibrous and RMI or fibrous and particulate debris were present. Particularly, backflushing of an essentially vertical surface (e.g., that in existing PWR sumps) was not very effective for mixed debris beds. This is due to the fact that only a small fraction of the strainer surface through which flow exits is cleared of debris. In the case of an air-based backflush system, the clearing occurred at the top of the strainer and in the case of water-based system, the clearing occurred where the majority of the water exited the screen. It was also observed that the debris tended to accumulate once again on the strainer surface, and this accumulated debris caused a higher head loss than did the original bed.

8.4.5 Debris Induced Mechanical Structural Loadings

The pressure differential caused by a bed of debris that has accumulated on a sump screen or suction strainer (including the flow resistance of the clean screen or strainer) would induce a mechanical strain on the structure. Should the sump screen or suction strainer fail mechanically, its function could be compromised, perhaps increasing the overall resistance to flow, or perhaps allowing debris to bypass the screen. For example, after the suction strainers at the Perry plant became clogged with fibers and corrosion products, the strainers were found upon inspection to be deformed, apparently from excessive differential pressure (Section 9.2). Appropriate engineering evaluations should be performed to ensure that these structures are strong enough to stand up to the increased mechanical loads of debris accumulation.

⁷ This issue was not a concern for BWR plants with the strainers located in the suppression pool where the strainers are protected from this type of damage.

8.5 References

- 8-1. NEDO-32686, Rev. 0, Utility Resolution Guidance for ECCS Strainer Blockage, General Electric Nuclear Energy Company, Class 1, Nov. 1996.
- 8-2. Bulletin 96-03, "Potential Plugging of Emergency Core Cooling Suction Strainers by Debris in Boiling-Water Reactors," NRC Bulletin to BWR Licensees, May 6, 1996.
- 8-3. PCI-97, Summary Report on Performance of Performance Contracting, Inc., Sure-Flow Suction Strainer with Various Mixes of Simulated Post-LOCA Debris, Revision 1., R. A. Biasca, Performance Contracting, Inc., Sept. 1997.
- 8-4. PCI-NPD-CE03, Tests Conducted at the Fairbanks Morse Pump Company to Determine Head Loss Performance of PCI Bare Sure-Flow Strainer, Tech. Doc. No.: June 1997.
- 8-5. CDI-96-22, Results of ECCS Sure-Flow Strainer Testing for Performance Contracting, Inc., Rev. 0, AE Kaufman, Continuum Dynamics, Inc., Technical Note No. 96-22, Dec 1996.
- 8-6. ITS-97, Comparison of Head Loss Model Based on NUREG/CR-6224 with PCI Full-Scale Strainer Test Data, P. Mast and F. Souto, Innovative Technology Solutions Corporation, Presented to U.S. Nuclear Regulatory Commission, Rockville, Md., Feb. 1997.
- 8-7. NUREG/CR-6224, G. Zigler, J. Bridaeu, D. V. Rao, C. Shaffer, F. Souto, W. Thomas, "Parametric Study of the Potential for BWR ECCS Strainer Blockage Due to LOCA Generated Debris," Final Report, U. S. Nuclear Regulatory Commission, October 1995.
- 8-8. LaSalle-98, "Test Evaluation Report for Test TPP-VL0400-005: LaSalle Strainer Fiber and RMI Debris Tests," Duke Engineering & Services, TPP-VL04 00 – 006, June 6, 1998.
- 8-9. LA-UR-00-5159, D. V. Rao, "Technical Review of Selected Reports on Performance Contracting, Inc. Sure-Flow Strainer™ Test Data," Prepared for U.S. Nuclear regulatory Commission, April 27, 2000.
- 8-10. GE Licensing Topical Report, "Application Methodology for GE Stacked Disk ECCS Suction Strainer," NEDC-32721P, Revision 0, General Electric Nuclear Energy, Proprietary information. Not publicly available. March 1997.
- 8-11. LA-CP-99-7, D. V. Rao, "Technical Review of GE LTR NEDC-32721P: Application Methodology for GE Stacked-Disk ECCS Suction Strainer," NRC Technical Evaluation Report, RP12-TER-98-02, Proprietary information. Not publicly available. December 23, 1998.
- 8-12. Continuum Dynamics, Inc., Tech. Report 97-04, "Data Report for ABB Model A&B Strainers with Fiber and Corrosion Products," June 1997.
- 8-13. LA-UR-00-426, D. V. Rao and Bruce Letellier, "On-Site Audit of the Limerick Nuclear Power Plant Emergency Core Cooling System Strainer Blockage Resolution," Los Alamos Technical Evaluation Report, January 21, 2000.
- 8-14. LA-CP-00-18, Bruce Letellier, and D. V. Rao, "On-Site Audit of the Grand Gulf Nuclear Station Emergency Core Cooling System Strainer-Blockage Resolution," Los Alamos Technical Evaluation Report, January 3, 2000.
- 8-15. LA-UR-01-738, D. V. Rao and Bruce Letellier, "On-Site Audit of the Dresden Nuclear Power Plant Emergency Core Cooling System Strainer Blockage Resolution," Los Alamos Technical Evaluation Report, Undated.
- 8-16. LA-CP-99-346, D. V. Rao and B. Letellier, "On-Site Audit of the Duane Arnold Energy Center Emergency Core Cooling System Strainer Blockage Resolution," December 1999.
- 8-17. NEA/CSNI/R (95) 11, "Knowledge Base for Emergency Core Cooling System Recirculation Reliability," Prepared by U.S. Nuclear Regulatory Commission for the Principal Working Group 1 (PWG-1), International Task Group, Committee on the Safety of Nuclear Installations, Organization for Economic Cooperation and development (OECD) Nuclear Energy Agency (NEA), February 1996.

- 8-18 Vattenfall Utveckling, "TVO 1&2-323-Strainers Penetration," Report VU-S 93:B11, June 1993.
- 8-19 NRC Memorandum to Gary M. Holahan, Director, Division of Systems Safety and Analysis, Office of Nuclear Reactor Regulation, from Robert B. Elliott, Reactor Systems Engineer, Balance of Plant Section, Plant Systems Branch, Division of Systems Safety and Analysis, Office of Nuclear Reactor Regulation, subject: Completion of Staff Reviews of NRC Bulletin 96-03, "Potential Plugging of Emergency Core Cooling Suction Strainers by Debris in Boiling-Water Reactors," and NRC Bulletin 95-02, "Unexpected Clogging of a Residual Heat Removal (RHR) Pump Strainer While Operating in Suppression Pool Cooling Mode" (TAC Number MA0704), October 18, 2001.

9.0 SIGNIFICANT EVENTS

This section describes operational events that have occurred at both PWR and BWR nuclear power plants that relate to the issue of sump-screen or suction-strainer blockage. These events are described in the general order of their relative severity, starting with operational events that have rendered systems inoperable with regard to the systems' ability to complete their safety mission. Two of these events resulted in the generation of insulation debris by jet flow from a LOCA caused by the unintentional opening of safety relief valves (SRVs). (See Section 9.1) Other events have involved the accumulation of sufficient operational debris to effectively block a strainer or screen or to plug a valve. (See Section 9.2.) Some event reports simply noted debris found in the containment (Section 9.3) and inadequate maintenance that would likely cause potential sources of debris within the containment (Section 9.4). Related event reports identified inadequacies in a sump screen where debris potentially could bypass the screen and enter the respective system. (See Section 9.5.)

9.1 LOCA Debris Generation Events

The two LOCA events that generated insulation debris both involved the unintentional opening of SRVs; these occurred at:

1. the German reactor Gundremmingen-1 (KRB-1) in 1977,⁹⁻¹ where the 14 SRVs of the primary circuit opened during a transient and,
2. the Barsebäck-2 nuclear power plant on July 28, 1992,⁹⁻¹ during a reactor restart procedure after the annual refueling outage.

Both of these reactors were BWR reactors with similarities to US reactors. These events are compared in Table 9-1 and summarized below.

Incident at Gundremmingen Unit 1

An event occurred at the German BWR reactor Gundremmingen-1 (KRB-1) in 1977 in which the 14 SRVs of the primary circuit opened during a transient. The SRVs were located inside the containment at a pipe attached to the main steam line between the reactor pressure vessel and the high-pressure turbine. The valves blew directly into the surrounding containment, where

the pipes had been insulated with fiberglass insulation reinforced with wire mesh and jacketed with sheet zinc. The piping insulation was extensively damaged.

After the incident, approximately 450 m³ (16,000 ft³) of water was found in the sump, of which about 240 m³ (8500 ft³) originated from the coolant circuit, with the rest delivered by the containment spray system. This water transported a substantial quantity of insulation debris into the control drive mechanism compartment directly below the SRVs. The floor was covered with flocks of insulation material. No larger parts of the insulation, such as sheet metals or textiles, were transported there. A thick layer of fiberglass insulation debris was found at strainers installed in front of ducts leading from this compartment into the sump. Because recirculation from the sump was not required, the layer of insulation debris on the strainers had no further consequences. Therefore, it is not known whether recirculation from the sump was possible. No details regarding debris quantities generated and transported were made available for further analysis. Nevertheless, the potential for clogging recirculation strainers with insulation debris generated by an operational incident was clearly demonstrated.

Incident at Barsebäck Unit 2

An event occurred at the Barsebäck-2 BWR nuclear power plant on July 28, 1992, during a reactor restart procedure after the annual refueling outage. The reactor power was below 2% of nominal power when an SRV opened inadvertently because of a leaking pilot valve. The main valve opened when the reactor pressure had reached 3.0 MPa (435 psia). The steam was released as a jet directly into the containment. The containment is basically an upright cylinder with the drywell in the upper part and the wetwell directly beneath. Vertical pressure relief pipes connect the drywell and wetwell and their openings (covered by gratings) are flush with the drywell floor. Because the containment was isolated when the drywell became pressurized, the water in the blowdown pipes from the drywell into the wetwell was forced from the pipes, allowing steam/air to flow through the pipes into the suppression pool.

Year	Plant (Type)	Event Initiator	Debris	Consequence	Reference
1977	Gundremmingen Unit 1 (BWR)	Unintentional opening of 14 SRVs.	Fiberglass insulation debris.	Potential clogging of recirculation strainers.	NEA/CSNI/R (95) 11 ⁹⁻¹
1992	Barsebäck Unit 2 (BWR)	Unintentional opening of a safety valve.	Metal-jacketed mineral wool insulation debris.	Clogged two of five spray-system suction strainers with loss of containment sprays at 1 h.	NEA/CSNI/R (95) 11 ⁹⁻¹ IN-92-71 ⁹⁻² IN-93-02 (S1) ⁹⁻³

The containment vessel spraying system and the ECCS were started automatically.

About 200 kg (440 lb) of fibrous insulation debris was generated, and about 50% of this debris subsequently reached the wetwell, resulting in a large pressure loss at the strainers about 70 min after the beginning of the event. Gratings in the drywell did not hold back the insulation material effectively. The insulation debris was distributed within the drywell following the event approximately as follows.

- 50% on the framework with the debris mainly concentrated in three areas: inside the drywell “gutter,” near the outer containment wall, and on or near the grid plates over the blowdown pipes
- 20% on the wall next to the affected pipe, from which most of the insulation originated, and on the components around the safety valve
- 10% on the wall opposite the affected pipe
- 12% on the walls above the grating lying above the safety valve
- 8% on the grating above the safety valve

The debris was transported by steam and airflow generated by the blowdown and by water from the containment spray system. It could not be determined how the transport developed with respect to time and whether the blowdown or washdown processes transported the major part of the debris found in the wetwell.

The generation and transport of large amounts of fibrous debris by the simple erroneous opening of a safety valve were observed. The debris transport included the short-term transport caused by the steam and air blast and the longer term debris washdown transport associated with the operation of the containment spray system. The extent of damage and of transport appeared remarkably large given the small leak size and low reactor pressure. The

significance of inertial impaction as a deposition mechanism was apparent upon examining the locations of debris deposited near the break.

9.2 Events Rendering a System Inoperable

In operating PWR and BWR nuclear power plants, events have occurred that resulted in a particular system being rendered inoperable; i.e., the ability of that system to perform its safety-related mission was in considerable doubt. These events include the accumulation of debris on a strainer or a screen that caused excessive head loss and events in which debris entered a system and thereby adversely affected the operability of a component of that system. These events, which occurred at PWR and BWR nuclear plants within the U.S., are compared in Table 9-2 and summarized below.

Grand Gulf

The Grand Gulf Nuclear Station experienced strainer-blockage events on March 18, 1988, and July 2, 1989.⁹⁻⁴ Both events occurred during testing of the RHR pumps. Pump suction pressures fell below the in-service inspection acceptance criteria. The licensee determined that a clogged strainer that takes suction from the suppression pool caused the low suction pressure.

Trojan

Debris and problems with the sump screen were found at the Trojan plant on several occasions.⁹⁻⁵

1. On July 8, 1989, the licensee of the Trojan plant discovered numerous items in the containment sump.
2. On July 14, 1989, after the containment was supposedly ready to be closed for operation, an NRC inspector and the licensee found additional debris.

Table 9-2 Events Rendering a System Inoperable					
Year	Plant (Type)	Event Initiator	Debris	Consequence	Reference
1988	Grand Gulf (BWR Mark III)	Inspection	Plastic wrap and other debris.	Clogged RHR strainers.	IN-93-34 ⁹⁻⁴
1989	Grand Gulf (BWR Mark III)	Inspection	Plastic wrap and other debris.	Debris could potentially block ECCS strainers during LOCA.	IN-93-34 ⁹⁻⁴
1989	Trojan (PWR Dry)	Inspection	Numerous debris items found in the sump. Sections of screen missing, damaged, or did not agree with drawings. Welding rod jammed in RHR pump impeller.	Debris blocked one pump and could potentially have blocked other ECCS strainers during LOCA.	IN-89-77 ⁹⁻⁵
1992	H. B. Robinson (PWR Dry)	Mode 4 hot shutdown operations surveillance testing of safety injection pumps.	Small piece of plastic blocked in-line orifice. Plastic used in a modification of RHR system.	Pumps rendered inoperable and loss of recirculation flow.	IN-92-85 ⁹⁻⁶
1992	Perry (BWR Mark III)	Inspection	Operational debris and a coating of fine dirt. Water samples found fibrous material and corrosion products.	Clogged and deformed strainers.	IN-93-02 ⁹⁻⁷ IN-93-34 ⁹⁻⁴
1992	Point Beach Unit 2 (PWR Dry)	Quarterly test of containment spray pumps.	Foam rubber plug.	Debris blocked pump impeller suction. One train of SI piping rendered inoperable in recirculation mode.	IN-92-85 ⁹⁻⁶
1993	Perry (BWR Mark III)	Several SRVs were manually lifted and RHR used for suppression pool cooling.	Glass fibers (from temporary cooling filters), corrosion products, dirt, and misc. debris.	Clogged and deformed strainers	IN-93-02 ⁹⁻⁷ IN-93-34 ⁹⁻⁴
1994	Palisades (PWR Dry)	Inspection	Plastic material.	HPSI and CS system pumps declared inoperable.	IN-95-06 ⁹⁻⁸
1994	Quad Cities Unit 1 (BWR Mark I)	Post-maintenance test.	Plastic bag and other miscellaneous operational debris.	Plugged valve on RHR torus cooling system. Pump fouled by metallic debris wrapped around a vane.	IN-94-57 ⁹⁻⁹
1995	Limerick Unit 1 (BWR Mark II)	Unexpected opening of SRV at 100% power.	Polymeric fibers and sludge.	RHR Loop A suction strainer (suppression pool cooling mode) covered by thin mat of fibers and sludge. Loop B to a lesser extent. Cavitation indicated on Loop A.	IN-95-47 ⁹⁻¹⁰ NRCB-95-02 ⁹⁻¹¹

3. On July 17, 1989, the top sump screen and portions of the inner sump screen were found to be missing.
4. On July 19, 1989, the NRC identified additional missing and damaged inner sump screens.
5. Debris had been found in the Trojan sump previously during a 1988 outage.
6. In 1980, a welding rod between the impeller and the casing ring jammed an RHR pump, clearly demonstrating the safety significance of loose debris in the containment emergency sump.

H. B. Robinson

On August 23, 1992, personnel at the H. B. Robinson plant were performing an operational surveillance test of the Train-B safety injection (SI) pump while the reactor was in Mode 4 hot shutdown.⁹⁻⁶ The recirculation flow in this test was 20% lower than it had been when last measured on July 12, 1992. The licensee retested this pump on August 24, 1992, and found no recirculation flow. Then, the licensee also tested the Train-A SI pump and found its recirculation flow 10% lower than last measured. Subsequently, the licensee declared both pumps inoperable and took the reactor to cold shutdown. On August 25, 1992, the licensee removed a single piece of plastic about the size of a nickel from the in-line orifice. The licensee previously had declared the Train-B SI pump inoperable after a quarterly in-service inspection surveillance test measured a recirculation flow of about 3 gpm rather than the required 35 gpm. On July 9, 1992, the licensee had found debris obstructing the in-line orifice. The licensee had subsequently flushed the Train-B SI pump, verified the recirculation flows as acceptable, and returned the unit to service believing that all debris had been removed. However, on August 24, 1992, the licensee found no recirculation flow.

Perry

Two ECCS suction-strainer clogging events occurred at the Perry plant.⁹⁻⁴ On May 22, 1992, debris was found on the suppression pool floor and on the RHR suction strainers during a refueling outage inspection. The debris consisted of general maintenance-type material and a coating of fine dirt that covered most of the surface of the strainers and the pool floor. After cleaning the strainers, it became evident that both the Train-A and Train-B RHR strainers were deformed, apparently from excessive

differential pressure. After the licensee cleaned the suppression pool and replaced the strainers, another event occurred at the plant in March 1993, where several SRVs were lifted manually and the RHR was used to cool the suppression pool. The strainers subsequently were inspected and were again coated with debris. A test of the Train-B RHR strainer in the as-found condition was terminated when the pump suction pressure dropped to 0. The debris on the strainers consisted of glass fibers (temporary drywell cooling filters inadvertently dropped into the suppression pool), corrosion products, and other materials filtered from the pool water by the glass fibers adhering to the strainer surfaces.⁹⁻¹² Fibrous material acted as a filter for suspended particles, a phenomenon not previously recognized. This event suggested that the filtering of small particles, such as suppression pool corrosion products (sludge), by the fibrous debris would result in significantly increased pressure drop across the strainers.

Point Beach Unit 2

On September 28, 1992, during a quarterly test of the containment spray pumps and valves, the licensee noted that the discharge pressure for the Train-A train pump was zero and that the pump was making an abnormal noise.⁹⁻⁶ The test was stopped and the pump was declared inoperable. Upon disassembly of the pump, a foam-rubber plug was found to be blocking the impeller suction.

Palisades

On April 28, 1994, with the reactor in cold shutdown, the licensee determined that plastic material used inside containment could block the containment sump screens after a design-basis accident.⁹⁻⁸ The licensee declared the high-pressure safety injection pumps and the containment spray pumps inoperable.

Quad Cities Unit 1

On July 14, 1994, during a post-maintenance test of RHR Loop A, test data indicated that the RHR torus cooling/test return valve was plugged.⁹⁻⁹ The shredded remains of a plastic bag were found within the anti-cavitation trim. The majority of the material was found lodged on the suction side of the valve trim. After the July 14 event, the licensee observed reduced flow from the RHR Loop C pump. Upon further investigation, the licensee found a 10-cm-diameter wire-brush wheel and a piece of metal wrapped around a vane of the pump.

Limerick Unit 1

On September 11, 1995, an event occurred at the Limerick Generating Station, Unit 1 in which an SRV opened on Unit 1 while it was at 100% power.⁹⁻¹⁰ Before the SRV opened, Limerick had been running Loop A of the RHR in suppression-pool cooling mode. The operators initiated a manual scram in response to the SRV opening and a second loop (Loop B) of suppression pool cooling. Approximately 30 min later, fluctuating motor current and flow were observed on Loop A. The cause was believed to be cavitation, and Loop A was secured. Following the event, inspection by a diver revealed a thin mat of material covering the strainer of Loop A. The mat consisted of fibrous material and sludge. The Loop B strainer had a similar covering but to a lesser extent. Limerick subsequently removed about 635 kg of debris from the pool. Similar to the Perry events, the mat of fibers on the strainer surface converted the strainer into a filter, collecting sludge and other material on the strainer surface.

9.3 Debris-Found-in-Containment Events

In operating PWR and BWR nuclear power plants, events have occurred in which debris was found inside the containment, and that debris had the potential to impair the operability of a safety system. These events are listed in Table 9-3 and summarized below.¹ The debris included fibrous material, sludge, dirt, paint chips, and miscellaneous operational materials. Even if the debris was not considered sufficient to render a system inoperable, it could still contribute to screen blockage following a LOCA.

Haddam Neck

In July 1975, six 55-gal. drums of sludge with varying amounts of debris were removed from the ECCS sump.⁹⁻¹³ In 1996, five 55-gal. drums of sludge were removed from the ECCS sump that included the following miscellaneous debris: plastic sheeting, nuts, bolts, tie wraps, and pencils. Discrepancies in the sump-screen sizing, screen fit-up, and method of attachment also were discovered.

¹The list is not comprehensive; i.e., inspection reports have noted other less significant discoveries of minor sources of debris that are not reported here.⁹⁻¹³

Surry Units 1 and 2

On June 16, 1988, following a recirculation flow verification test, loose parts and debris were found in the containment sump, the recirculation pumps, and the suction piping.⁹⁻⁵ Some of the items were large enough to have caused enough pump damage or flow degradation to render the system inoperable. In addition, some of the sump screens were found to have gaps, which could have allowed additional loose material to enter the sump. One screen section was found to be missing.

Diablo Canyon Units 1 and 2

In 1989, debris was found in the sumps of both Unit 1 and Unit 2.⁹⁻⁵ Further, the sump screens were not configured in accordance with the FSAR drawing, and plant inspection requirements were not sufficient or detailed enough to assure adequate inspections.

McGuire Unit 1

Loose material discovered in upper containment before entry into Mode 4.⁹⁻¹³

North Anna

As part of the steam-generator replacement program, personnel removed the mirror insulation from the SGs and discovered that most of the unqualified silicon aluminum paint covering the SGs had come loose from the exterior surfaces and was being supported only by the insulation jacketing.⁹⁻⁴ The pieces of paint ranged in size from dust particles to sheets 0.61 m (2 ft) wide. The same paint also had been used on the pressurizer and was also loose. The quantity of this coating in containment was significant—estimated at 1,087 m² (11,700 ft²). Paint fragments potentially could have reached the containment sump during a design-basis accident in which a pipe breach could have exposed the failed coating.

Spanish PWR

An inspection of the containment sumps during an outage surveillance found water in the sump that was unusually dirty.⁹⁻¹⁴ The water was a result of acceptable leakage during a functional testing of a three-way valve connecting the ECCS borated tanks with the containment sumps. After the water was removed, three of the four sumps had debris in the bottom below the suction pipe for the ECCS. A closer examination of the ECCS suction lines revealed

Table 9-3 Events With Debris Found Inside Containment

Year	Plant (Type)	Event Initiator	Debris	Consequence	Reference
1975	Haddam Neck (PWR Dry)	Inspection	Six 55-gal. drums of sludge with varying amounts of other debris removed from ECCS sump.	Debris potentially could block ECCS strainers during a LOCA.	GL-98-04 ⁹⁻¹³
1988	Surry Units 1 and 2 (PWR Sub)	Inspection	Construction materials and debris found in the sump, in cone strainer of recirculation spray system, and in recirculation pumps.	Materials could have rendered system inoperable.	GL-98-04 ⁹⁻¹³ IN-89-77 ⁹⁻⁵
1989	Diablo Canyon Units 1 and 2 (PWR Dry)	Inspection	Debris found in sumps.	Debris could potentially block ECCS strainers during LOCA.	GL-98-04 ⁹⁻¹³ IN-89-77 ⁹⁻⁵
1990	McGuire Unit 1 (PWR Ice)	Inspection	Loose material discovered in upper containment.	Material not likely to have made ECCS inoperable but debris could contribute to potential ECCS strainer blockage.	GL-98-04 ⁹⁻¹³
1993	North Anna (PWR Sub)	Steam Generator Replacement	Most of the unqualified silicon aluminum paint had come loose from SG and pressurizer and supported only by insulation jacketing.	Paint fragments potentially could reach sump during a LOCA.	IN-93-34 ⁹⁻⁴
1993	Spanish Plant (PWR)	Inspection	Unspecified debris (believed debris had been there since commission-ing), dirty sump water, and flow blockage.	ECCS lines taking suction from the sumps were partially blocked.	IN-96-10 ⁹⁻¹⁴
1994	Browns Ferry Unit 2 (BWR Mark I)	Inspection	Cloth-like material.	Partial strainer blockage, potential for 25% blockage	IN-95-06 ⁹⁻⁸
1994	LaSalle Unit 1 (BWR Mark II)	Inspection	Assortment of operational debris and sludge.	Potentially contribute to strainer blockage.	IN-94-57 ⁹⁻⁹
1994	River Bend (BWR Mark III)	Inspection	Miscellaneous operational debris and sediments. Plastic bag removed from RHR suction strainer.	Potentially contribute to strainer blockage.	IN-94-57 ⁹⁻⁹
1996	Haddam Neck (PWR Dry)	Outage Maintenance	Five 55-gal. drums of sludge with varying amounts of other debris removed from ECCS sump.	Debris could potentially block ECCS strainers during a LOCA.	GL-98-04 ⁹⁻¹³
1996	LaSalle Unit 2 (BWR Mark II)	Outage suppression pool cleaning.	Miscellaneous operational debris and sludge.	Suppression pool debris could potentially block ECCS strainers during a LOCA.	IN-96-59 ⁹⁻¹⁵
1996	Millstone Unit 3 (PWR Sub)	Inspection	Pieces of Arcor protective coating and mussel shell fragments. Construction debris found in recirculation spray system suction lines.	Potential failure of recirculation spray heat exchangers to perform specified safety function because of debris.	GL-98-04 ⁹⁻¹³ IN-97-13 ⁹⁻¹⁶

Year	Plant (Type)	Event Initiator	Debris	Consequence	Reference
1996	Nine Mile Point Unit 2 (BWR Mark II)	Inspection	Miscellaneous operational debris, including foam rubber, plastic bags, Tygon tubing, and hard hats.	Suppression pool debris potentially could block ECCS strainers during a LOCA.	IN-96-59 ⁹⁻¹⁵
1996	Vogtle Unit 2 (PWR Dry)	Inspection	Loose debris identified inside containment.	Debris could potentially block ECCS strainers during LOCA.	GL-98-04 ⁹⁻¹³
1996	Zion Unit 2 (PWR Dry)	Inspection	Extensive failure of protective coatings. Unqualified coatings identified. Miscellaneous debris found throughout containment.	Debris could potentially block ECCS strainers during LOCA.	IN-97-13 ⁹⁻¹⁶
	Calvert Cliffs Units 1 and 2 (PWR Dry)	Inspection	Unit 2 sump contained 11.3 kg (25 lb) of dirt, weld slag, pebbles, etc. Unit 1 had less than 1 lb debris.	Debris could contribute to potential ECCS strainer blockage.	GL-98-04 ⁹⁻¹³
	D. C. Cook Units 1 and 2 (PWR Ice)	Inspection	Fibrous material found in containments.	Debris potentially could block ECCS strainers during LOCA.	GL-98-04 ⁹⁻¹³

that two of the four ECCS lines taking suction from the sumps were partially blocked by debris and one of those lines had almost half of its flow area blocked. It is believed that the debris had been there since the plant was commissioned, thereby demonstrating a significant failure of the surveillance program.

Browns Ferry Unit 2

On October 10, 1994, divers discovered numerous pieces of cloth-like material on the bottom of the torus and on the ECCS strainers.⁹⁻⁸ The pieces were typically 25 cm² (4 in.²) in size, but smaller pieces were found, as well. The material was pieces of absorbent paper towels that are sometimes used inside the containment for maintenance and cleaning purposes. One of the two strainers was found with about 15% of its surface covered with debris. If all of the material had been drawn onto the strainers, about 25% of the strainer surface area would have been blocked.

LaSalle Unit 1

On April 26 and May 11, 1994, while in a refueling outage, two dives were made into the Mark II design suppression pool to clean the ECCS suction strainers of a small amount of debris, which caused less than 1% clogging.⁹⁻⁹ The divers found and removed an assortment of operational debris that included a hard hat, a

pair of anti-contamination coveralls, four lengths of Tygon tubing ranging in length from about 6 m (20 ft) to 15.2 m (50 ft), three nuts, a 4.6-m (15-ft) length of duct tape, four lengths of 1.9-cm (3.4-in.) hose ranging in length from about 8 m (20 ft) to 46 m (150 ft), a length of wood measuring 5 cm by 10 cm (2 in. by 4 in.), and a flashlight. The divers also noted that sediment had formed on the floor of the suppression pool ranging in thickness from 0.3 cm to 5 cm (1/8 to 2 in.). An analysis of a sample of the sediment showed a filterable solid that consisted of over 99% iron oxide with trace amounts of nickel, copper, and chrome. The licensee concluded that the sample contained normal system corrosion products.

River Bend

On June 13, 1994, a refueling outage inspection of the ECCS suction strainers and the Mark III design suppression pool discovered 16 foreign objects.⁹⁻⁹ One of these objects, a plastic bag, was removed from an RHR system suction strainer. The other objects removed from the pool included a hammer, a grinder wheel, a slugging wrench, a socket, a hose clamp, a bolt, a nut, a step-off pad, two ink pens, an antenna, a scaffold knuckle, a short length of rope, and used tape. The licensee also found sediment in the suppression pool.

LaSalle Unit 2

The licensee reported on October 16, 1996, that a significant amount of foreign material had been found under a layer of rust-particle sludge during the first thorough cleaning the suppression pool.⁹⁻¹⁵ Foreign material also was found in several downcomers that included a rubber mat, a sheet of gasket material, a nylon bag, and sludge.

Millstone Unit 3

On July 25, 1996, the licensee reported that about 20 pieces of Arcor were found in the Train-A recirculation spray heat exchangers.^{9-13, 9-16} Arcor is a coating material that was applied to the inside surfaces of the service water system piping. The Arcor chips were apparently swept into the recirculation spray heat exchanger channel during testing. The licensee also found 40 to 50 mussel shell fragments in the heat exchangers. The Arcor chips and mussel fragments were relatively small (on the order of 1 in.²) The licensee determined that the debris could have prevented the heat exchangers from performing their specified safety function. In addition, construction debris was discovered in all four containment recirculation spray system (RSS) suction lines. In addition, gaps were found in the RSS sump cover plates.

Nine Mile Point Unit 2

On October 17, 1996, the licensee reported that a significant amount of debris was found during inspection of the drywell vent downcomers to the suppression pool.⁹⁻¹⁵ Almost all of the debris was found in 17 of the downcomers. Some of the debris was floating on the water inside the downcomers and consisted of foam rubber cleanliness covers, plastic bags, Tygon tubing, and hard hats. Cleanliness covers were installed over the openings into seven of the downcomers located directly under the reactor vessel. The suppression pool had been cleaned during the previous refueling outage.

Vogtle Unit 2

In 1996, NRC inspectors identified loose debris in readily accessible areas inside the containment that had the potential to block emergency sump screens during accident conditions.⁹⁻¹³ An evaluation by the licensee concluded that the RHR pump would not have had adequate NPSH because of the debris.

Zion Unit 2

In November 1996, the licensee found that 40% to 50% of the concrete floor coatings showed extensive failure as a result of mechanical damage and wear, and that about 5% of the coating associated with the concrete wall and liner plate was degraded.⁹⁻¹⁶ Unqualified coatings had been applied to various surfaces, including instrument racks, struts, charcoal filter housings, valve bodies, and piping. Although adhesion tests showed acceptable adhesion strength in most of the locations tested, one test conducted on an unqualified coating system did not satisfy the acceptance criteria. Documentation was not found for over-coating (i.e., touch-up work) that had been applied to many of the liner plates and concrete wall surfaces.

Calvert Cliffs Units 1 and 2

An inspection of the Unit 2 sump found 11.3 kg (25 lb) of debris that consisted of dirt, weld slag, pebbles, etc.⁹⁻¹³ An inspection of the Unit 1 sump found less than 1 lb of debris. The debris had the potential to cause minor damage to the ECCS pumps.

D. C. Cook Units 1 and 2

Enough fibrous material was found in both Unit 1 and Unit 2 containments to potentially cause excessive blockage of the recirculation sump screens during the recirculation phase of a LOCA.⁹⁻¹³

9.4 Inadequate Maintenance Leading to Potential Sources of Debris

In operating PWR and BWR nuclear power plants, events have occurred in which inadequate maintenance conditions inside containments could potentially form significant sources of debris. These events are listed in Table 9-4 and summarized below.² In general, these events involved unqualified protective coatings and materials.

North Anna Units 1 and 2

In 1984, unqualified paint was identified on galvanized ductwork.⁹⁻¹³

²The list is not comprehensive; i.e., inspection reports have noted other less significant discoveries of inadequate maintenance potentially leading to sources of debris that are not reported here.⁹⁻¹³

Table 9-4 Events of Inadequate Maintenance Potentially Leading to Sources of Debris					
Year	Plant (Type)	Event Initiator	Debris	Consequence	Reference
1984	North Anna Units 1 and 2 (PWR Sub)	Inspection	Unqualified coatings identified	Debris could potentially block ECCS strainers during LOCA.	GL-98-04 ⁹⁻¹³
1988	Susquehanna Unit 2 (BWR Mark II)	Inspection	Extensive delamination of aluminum foil jacketing fiberglass insulation.	Debris could potentially block ECCS strainers during LOCA.	IN-88-28 ⁹⁻¹⁷
1993	Sequoyah Units 1 and 2 (PWR Ice)	Inspection	Unqualified coatings identified	Debris could potentially block ECCS strainers during LOCA.	GL-98-04 ⁹⁻¹³ IN-97-13 ⁹⁻¹⁶
1994	Browns Ferry Units 1, 2, & 3 (BWR Mark I)	Inspection	Unqualified coatings identified	Debris could contribute to potential ECCS strainer blockage.	GL-98-04 ⁹⁻¹³
1995	Indian Point Unit 2 (PWR Dry)	Inspection	Failure of protective coatings. Unqualified coatings identified.	Debris could potentially block ECCS strainers during LOCA.	IN-97-13 ⁹⁻¹⁶ GL-98-04 ⁹⁻¹³
1997	Clinton (BWR Mark III)	Inspection	Unqualified coatings identified	Debris could potentially block ECCS strainers during LOCA.	GL-98-04 ⁹⁻¹³
1997	Millstone Unit 1 (BWR Mark I)	Inspection	Unqualified coatings identified	Debris could potentially block ECCS strainers during LOCA.	GL-98-04 ⁹⁻¹³ IN-88-28 ⁹⁻¹⁷
1997	Sequoyah Units 1 (PWR Ice)	Inspection	Oil cloth introduced into containment.	Potential to block one or both refueling drains.	GL-98-04 ⁹⁻¹³

Susquehanna Unit 2

On March 14, 1988, during a refueling outage inspection, the licensee observed and reported extensive delamination of the aluminum foil coating on the surface of the fiberglass insulation used on valve bodies and pipe hangers and in other areas that are awkward or difficult to insulate.⁹⁻¹⁷ The licensee was concerned that this deterioration of drywell insulation could form debris that potentially could block the ECCS strainers during a LOCA. The licensee estimated that 50% of up to 5000 ft² of this insulation had undergone some degradation. The aluminum foil covering was 1-mil thick and was bonded to the outer covering of Alpha Maritex fiberglass cloth that covered Temp-Mat insulation.

Sequoyah Units 1 and 2

On October 18, 1993, the licensee reported unidentified coatings were used on the exterior surfaces of reactor coolant pump motor support structures.^{9-13, 9-16} These structures are all

located within the containment sump “zone-of-influence” at both units. The design-basis limit for unqualified coatings inside the containment had been exceeded. Then, during a shutdown on March 22, 1997, an oil cloth was introduced into containment. If it had come free, it could have blocked one or both refueling drains so that water in the upper containment might not have flowed freely to the lower level of containment, where the sump is located.

Browns Ferry Units 1, 2, and 3

Unqualified coatings were identified on the T-quenchers in the suppression pool.⁹⁻¹³

Indian Point Unit 2

On March 10, 1995, the licensee reported that paint was peeling from the containment floor. The paint had been applied improperly.⁹⁻¹⁶ The factors contributing to the delamination of the paint were: (1) the paint thickness exceeded the manufacturer’s specifications by up to twice the allowed thickness; (2) there was excessive paint

shrinkage caused by use of too much paint thinner; (3) the surface had not been cleaned and prepared properly before the paint was applied; and (4) appropriate inspection and documentation requirements were not implemented.

Clinton

On July 15, 1997, the licensee reported that a significant quantity of degraded protective coating was removed from the containment.⁹⁻¹³ Significant degradation occurred in the wetwell, and some degradation occurred in the drywell. The licensee stated that because of the indeterminate condition of these degraded coatings, reasonable assurance could not be given that the coatings would not disbond from their substrates enough to clog the ECCS suction strainers during accident conditions.

Millstone Unit 1

On April 16, 1997, the licensee reported that most of coating work inside the suppression pool torus was unqualified. The licensee stated that a number of different coating materials had been used inside the torus, but the locations and extent of various coating systems were unclear. The operability of the low-pressure coolant injection and core spray systems could be affected.⁹⁻¹³

9.5 Sump-Screen Inadequacies

In operating PWR and BWR nuclear power plants, events have occurred in which defects in the integrity of the sump screens were found. These defects could have caused a potential failure to adequately filter the ECCS water source that could result in degradation and eventual loss of ECCS function as a result of damaged pumps or clogged flow pathways. These events are listed in Table 9-5 and summarized below.³

Milestone Unit 1

In 1988, when the criteria of RG 1.82 Revision 1 were applied to plant safety analyses, it was determined that the existing suction strainers were too small.⁹⁻¹³ Strainers were replaced with larger strainers.

³The list is not comprehensive; i.e., inspection reports have noted other, less significant discoveries of sump screen inadequacies that are not reported here.⁹⁻¹³

Three Mile Island Unit 1

In 1990, holes were discovered in the top of the sump screen cage that were attributed to a modification of the sump access hatches.⁹⁻¹³ These breaches represented a potential failure to adequately filter the ECCS water source that could result in degradation and eventual loss of ECCS function as a result of damaged pumps or clogged flow pathways.

Arkansas Nuclear One Unit 1

On October 1, 1993, personnel found several breaches in the integrity of the containment sump.⁹⁻¹⁸ These breaches included the following:

1. 22 semicircular holes (scuppers) approximately 15.2 cm (6 in.) in diameter at the base of the sump curb (shown in original drawings).
2. Four conduit penetrations in the sump screen, totaling approximately 930 cm² (1 ft²).
3. A small conduit penetration in the sump curb, approximately 2.5 cm (1 in.) in diameter.
4. Two defects in the screen mesh covering the sump.
 - a. An L-shaped cut approximately 30.5 cm by 35.6 cm (12 in. by 14 in.).
 - b. A straight cut approximately 30.5 cm (12 in.) long.
5. Drain headers ranging in size from approximately 5.1 cm to 25.4 cm (2 in. by 10 in.) that lacked protective screen material.

These breaches represented a potential failure to adequately filter the ECCS water source, which could result in degradation and eventual loss of ECCS function as a result of damaged pumps or clogged flow pathways.

Arkansas Nuclear One Unit 2

In 1993, seven unscreened holes were discovered in masonry grout below the screen assembly of ECCS sump.⁹⁻¹⁸ These breaches represented a potential failure to adequately filter the ECCS water source, which could result in degradation and possible eventual loss of both trains of HPSI and containment spray.

San Onofre Unit 1

In 1993, an irregular annular gap was found that surrounded a low-temperature overpressure discharge line that penetrated a horizontal steel

Table 9-5 Events Where Inadequacies Found in Sump Screens					
Year	Plant (Type)	Event Initiator	Screen Condition	Consequence	Reference
1988	Millstone Unit 1 (BWR Mark I)	Safety Analysis	Existing suction strainers too small when criteria of RG 1.82, Rev. 1 applied.	Potential screen blockage due to accumulation of debris.	GL-98-04 ⁹⁻¹³
1990	Three Mile Island Unit 1 (PWR Dry)	Inspection	Modification of sump access hatches left holes in top of sump screen cage.	Potential debris bypass of the sump screens and subsequent potential damage to pumps or clogged spray nozzles.	GL-98-04 ⁹⁻¹³
1993	Arkansas Nuclear One Unit 1 (PWR Dry)	Inspection	Several breaches found in sump screens.	Potential debris bypass of the sump screens and subsequent potential degradation or even loss of ECCS function.	IN-89-77 Sup. 1 ⁹⁻¹⁸
1993	Arkansas Nuclear One Unit 2 (PWR Dry)	Inspection	Seven unscreened holes found in masonry grout below screen assembly of ECCS sump.	Potential debris bypass of the sump screens and subsequent potential degradation of both trains of HPSI and containment spray.	GL-98-04 ⁹⁻¹³ IN-89-77 Sup. 1 ⁹⁻¹⁸
1993	San Onofre Units 1 and 2	Inspection	Irregular annular gap surrounding low-temperature over-pressure discharge line penetrating horizontal steel cover plate.	Potential debris bypass of the sump screens and subsequent potential degradation or even loss of ECCS function.	GL-98-04 ⁹⁻¹³
1993	Vermont Yankee (BWR Mark I)	Safety Analysis	LPCS suction strainers smaller than assumed in NPSH calculations. Existing NPSH calculations invalid.	Potential loss of NPSH margin on LPCS during accident conditions.	GL-98-04 ⁹⁻¹³
1994	South Texas Units 1 and 2 (PWR Dry)	Inspection	Sump-screen openings from initial construction discovered.	Potential debris bypass of the sump screens and subsequent potential degradation of ECCS function.	GL-98-04 ⁹⁻¹³
1996	Watts Bar Unit 1 (PWR Ice)	Inspection	Containment sump trash-screen door found open with plant in Mode 4 and ECCS required to be operable.	Potential impairment of sump screen function.	GL-98-04 ⁹⁻¹³
1996	Millstone Unit 2 (PWR Dry)	Inspection	Containment sump screens incorrectly constructed.	Debris larger than analyzed could pass through screens.	GL-98-04 ⁹⁻¹³

cover plate. The discharge line was an 8-in. (20.3-cm) diameter pipe, and the gap was approximately 6 in. (15.2 cm) wide, resulting in an area of approximately 1.8 ft² (0.18 m²) that would not filter debris. This gap represented a potential failure to adequately filter the ECCS water source, which that could result in degradation and eventual loss of ECCS function as a result of damaged pumps or clogged flow pathways.⁹⁻¹³

Vermont Yankee

In 1993, the LPCS suction strainers were found to be smaller than was assumed for the NPSH calculations, rendering those calculations invalid.⁹⁻¹³ These NPSH calculations were performed in 1986 following an insulation changeout. The strainers were replaced with larger strainers.

South Texas Units 1 and 2

In 1994, sump-screen openings from initial construction were discovered.⁹⁻¹³ A frame plate was warped at the floor, creating several openings approximately 1.6 cm (5/8 in.) wide. Additional gaps 0.6 cm (1/4 in.) wide were found.

Watts Bar Unit 1

In 1996, the operator observed that the containment sump screen door was open during Mode 4 operation when the ECCS was required to be operable.⁹⁻¹³

Millstone Unit 2

In 1996, it was discovered that the containment sump screens were constructed incorrectly and that debris larger than the size assumed in previous analyses could pass through the ECCS.⁹⁻¹³

9.6 References

- 9-1 NEA/CSNI/R (95) 11, "Knowledge Base for Emergency Core Cooling System Recirculation Reliability," Prepared by U.S. Nuclear Regulatory Commission for the Principal Working Group 1 (PWG-1), International Task Group, Committee on the Safety of Nuclear Installations, Organization for Economic Cooperation and development (OECD) Nuclear Energy Agency (NEA), February 1996.
- 9-2 IN-92-71, "Partial Blockage of Suppression Pool Strainers at a Foreign BWR," NRC Information Notice, September 30, 1992.
- 9-3 Bulletin 93-02, Supplement 1, "Debris Plugging of Emergency Core Cooling Suction Strainers," NRC Bulletin to Licensees, February 18, 1994.
- 9-4 IN-93-34, "Potential for Loss of Emergency Cooling Function Due to a Combination of Operational and Post-LOCA Debris in Containment," NRC Information Notice, April 26, 1993.
- 9-5 IN-89-77, "Debris in Containment Emergency Sumps and Incorrect Screen Configurations," NRC Information Notice, November 21, 1989.
- 9-6 IN-92-85, "Potential Failures of Emergency Core Cooling Systems Caused by Foreign Material Blockage," NRC Information Notice, December 23, 1992.
- 9-7 Bulletin 93-02, "Debris Plugging of Emergency Core Cooling Suction Strainers," NRC Bulletin to Licensees, May 11, 1993.
- 9-8 IN-95-06, "Potential Blockage of Safety-Related Strainers by Material Brought inside Containment," NRC Information Notice, January 25, 1995.
- 9-9 IN-94-57, "Debris in Containment and the Residual Heat Removal System," NRC Information Notice, August 12, 1994.
- 9-10 IN-95-47, "Unexpected Opening of a Safety/Relief Valve and Complications Involving Suppression Pool Cooling Strainer Blockage," NRC Information Notice, Revision 1, November 30, 1995.
- 9-11 NRCB 95-02, "Unexpected Clogging of a Residual Heat Removal (RHR) Pump Strainer While Operating in Suppression Pool Cooling Mode," NRC Bulletin to BWR Licensees, October 17, 1995.
- 9-12 IN-93-34, Supplement 1, "Potential for Loss of Emergency Cooling Function Due to a Combination of Operational and Post-LOCA Debris in Containment," NRC Information Notice, May 6, 1993.
- 9-13 GL-98-04, "Potential for Degradation of the Emergency Core Cooling System and the Containment Spray System After Loss-of-Coolant Accident Because of Construction and Protective Coating

- Deficiencies and Foreign Material in Containment," NRC Generic Letter to All Holders of Operating Licenses for Nuclear Power Plants, July 14, 1998.
- 9-14 IN-96-10, "Potential Blockage by Debris of Safety System Piping Which is not Used During Normal Operation or Tested During Surveillances," NRC Information Notice, February 13, 1996.
- 9-15 IN-96-59, "Potential Degradation of Post Loss-of-Coolant Recirculation Capability as a Result of Debris," NRC Information Notice, October 30, 1996.
- 9-16 IN-97-13, "Deficient Conditions Associated with Protective Coatings at Nuclear Power Plants," NRC Information Notice, March 24, 1997.
- 9-17 IN-88-28, "Potential for Loss of Post-LOCA Recirculation Capability Due to Insulation Debris Blockage," NRC Information Notice, May 19, 1988.
- 9-18 IN-89-77, Supplement 1, "Debris in Containment Emergency Sumps and Incorrect Screen," NRC Information Notice, December 3, 1993.

10.0 SUMMARY AND CONCLUSIONS

10.1 Summary of Knowledge Base

In the event of a LOCA within the containment of a LWR, piping thermal insulation and other materials in the vicinity of the break will be dislodged by the pipe break and ensuing steam/water-jet impingement. A fraction of this fragmented and dislodged insulation and other materials, such as paint chips, paint particulates, and concrete dust, will be transported to the containment floor by the steam/water flows induced by the break and the containment sprays. Some of this debris eventually will be transported to and accumulated on the recirculation pump suction sump screens in PWR containments or the pump suction strainers in BWR containments. Debris accumulation on the sump screens or strainers could challenge the plant's capability to provide adequate, long-term cooling water to the ECCS and the CSS pumps.

This report describes the different analytical and experimental approaches that have been used to assess the aspects of sump and strainer blockage and identify the strengths, limitations, important parameters and plant features, and appropriateness of the different approaches. The report also discusses significant U.S. NRC regulatory actions regarding resolution of the issue. The report is designed to serve as a reference for plant-specific analyses with regard to whether the sump or strainer would perform its function without preventing the operation of the ECCS pumps.

This report is intended primarily for analyzing the PWR sump-screen clogging issue because the BWR issue had been resolved at the time this report was written. Nevertheless, the report also will be valuable in the review of any additional analyses for BWR plants, as well. A majority of the strainer-blockage research to date was conducted specifically for the resolution of the BWR issue; however, most of this research is also directly applicable to the resolution of the PWR issue. Therefore, both BWR and PWR research and analytical approaches are discussed and the applicability of that research, i.e., PWR vs BWR, is stated.

Section 1 of this report provides background information regarding the PWR containment-sump and the BWR suction-strainer debris-clogging issues. This background information includes a brief historical overview of the resolution of the BWR issue with a lead-in to the PWR issue, a description of the safety concern relative to PWRs, the criteria for evaluating sump failure, descriptions of postulated accidents, descriptions of the relevant plant features that influence accident progression, and a discussion of the regulatory considerations.

The purpose of the sump screen, and the associated trash rack, is to prevent debris that may damage or clog components downstream of the sump from entering the ECCS and RCS. Actual sump designs vary significantly among PWR containments, but all share similar geometric features. Sump screens can be grouped according to their submergence, i.e., many sump screens would be submerged completely in the containment sump pool when the ECCS switched over to recirculation, but others would be submerged only partially. Debris accumulation on a completely submerged sump screen would create a pressure drop across that screen that potentially could cause a loss of NPSH margin. Debris accumulation on a partially submerged sump screen would also create a pressure drop across the submerged portion of the screen, but this pressure drop would cause the downstream water level to drop below the upstream water level. If the pressure drop were severe enough, the flow to the pump would be insufficient to supply the pump. The maximum hydrostatic head across a partially submerged sump screen would be approximately half the height of the sump pool. Debris accumulation potentially could block the flow of water to the sump screen at locations other than the screen itself, such as at narrow flow pathways or floor drains from the upper levels or the refueling pool drains. Such blockage could lower the water level in the sump pool, thereby decreasing the hydrostatic head upstream of the screen. All such considerations are plant-specific.

The knowledge base report is organized in the same order that an evaluation of the potential of sump screen blockage would be performed. These steps are as follows.

- The identification of sources of potential debris (Section 2).
- The potential generation of insulation debris by the effluences from a postulated LOCA (Section 3).
- The potential transport of the LOCA-generated debris to the containment sump pool (Section 4).
- The potential transport of debris within the sump pool to the recirculation sump screen (Section 5).
- The potential accumulation of the debris on the sump screen, specifically, the uniformity and composition of the bed of debris (Section 6).
- The potential head loss associated with the accumulated debris (Section 7).

The knowledge base report also summarizes the resolution options that were available to the BWR plant licensees to resolve the BWR suction-strainer-clogging issue (Section 8). This section also discusses the advanced features of the new replacement strainers that were implemented into the BWR plants so that the strainers can accumulate the potential debris loading without the associated debris-bed head loss becoming excessive. This new technology is available for the resolution of the PWR sump-screen clogging issue as well.

A number of events have occurred at plants, both in the U.S. and abroad, that are relevant to the PWR sump-screen clogging issue (Section 9). Two events occurred in which insulation debris was generated as a result of a LOCA. A number of events have occurred in which debris rendered a system inoperable, debris was found in the containment, inadequate maintenance could have led to potential sources of debris, and inadequacies in a sump screen were discovered.

Key aspects of these knowledge base subjects are discussed in the following paragraphs.

Debris Sources

Sources of debris that could contribute to the potential clogging of a strainer or sump screen include LOCA-generated debris, exposure-generated debris, and operational debris. All of these sources of debris should be considered. The break effluent following a LOCA could generate substantial quantities of debris within

the containment, mostly in the vicinity of the break. The majority of the destruction to materials near the break would occur within the region usually designated as the zone of influence (ZOI). The size of the ZOI, which usually is considered spherical but could be conical, depends on the type of material, i.e., the region of destruction extends further out for some materials than for others. However, some debris could be generated well beyond the ZOI. As the containment pressurizes, equipment covers, loose coatings, etc., could be blown free to become debris, but the debris generated within the ZOI would likely be the largest source of transportable debris. Sources of debris within the ZOI generally include insulation materials and their respective jacketing, fire-barrier materials, surface coatings, and the erosion of concrete. The dominant source of debris within the ZOI would be destroyed or damaged insulation. There are several types of insulation materials, as well as manufacturers of insulation, and each has unique destruction and transport characteristics. The types of insulation include fibrous insulations, RMI, particulate insulations, and foam insulations.

When the primary system depressurization completes, the materials inside the containment would be subject to high temperatures and humidity resulting from depressurization. In addition, the containment sprays, if activated, would impact and wet surfaces throughout the containment continuously. Prolonged exposure to the LOCA environment, both during depressurization and afterward, could cause some materials to fail, thereby generating additional debris. One concern is that protective coatings within containments would have the potential to detach from the surfaces where they had been applied as a result of prolonged exposure to a LOCA environment. Qualified protective coatings are expected to be capable of adhering to their substrate during a design-basis LOCA (except coatings directly impacted by the break jet), unless those coatings have received extensive irradiation. Coatings, even qualified coatings, that have been subjected to irradiation of 10^9 rads, even when they were applied properly, exhibited profound blistering, leading to disbondment of a near-surface coating layer when exposed to the elevated temperatures and moisture conditions within the range of design-basis LOCA conditions. Not all coatings inside the containment are qualified, and therefore, the amount of unqualified

coatings must be controlled because the unqualified coatings are assumed to detach from their substrates during a design-basis LOCA. Besides coating systems, the LOCA environment, especially with the containment sprays operating, could cause failure of the adhesive used to permanently attach tags or labels to walls and equipment. Exposure to the LOCA environment likely would cause oxidation of unpainted metallic surfaces that could generate transportable particulate debris. In addition to generating certain types of debris, exposure to the LOCA environment can degrade previously generated debris further.

Operational debris is debris formed from the operational erosion of containment materials or from materials that normally would not be left inside the containment during operation. Examples of operational debris that has been found inside containments include dirt and dust, rust, cloth and plastic products, tools, and temporary air filters. Good general housekeeping programs are needed to limit such debris.

Debris Generation

The hydrodynamic forces created during a postulated LOCA in a PWR would damage or destroy surrounding insulation, creating debris that subsequently could transport to the containment sump. Analysis has indicated dynamic (shock) forces and mechanical erosion caused by impingement of the steam/water jet emerging from the broken pipe on neighboring pipe insulation, equipment coatings, and other structures would be the dominant mechanisms for LOCA-generated debris. The blast effects of a shock wave expanding away from an RCS pipe break would cause the initial insulation destruction (unless the break opened slowly enough to preclude the development of a shock wave); however, the strength of the shock wave would decay rapidly as the wave expanded away from the break plane. After the shock wave passes, shear forces and consequential erosion of piping insulation, paint, coatings, and other materials in the wake of the break jet result in additional debris generation.

Unobstructed, the shock wave would expand away from the break in a spherical pattern, and the steam/water jet would expand away from the break plane in the shape of a cone. However, for typical candidate break locations in a typical

PWR containment, the piping congestion, containment structures, and other obstacles would reflect expansion waves and redirect the jet flow, thereby breaking up the jet and possibly dissipating some of its energy. In addition, the broken pipes also could be in motion following the break, and the effluences from the two broken ends could impinge on each other. The resulting expansion of the jet most likely would be rather complex, and as varied as the piping configurations within the plants and the types of break and flow conditions. The pressure distribution within an unobstructed conical jet has been characterized experimentally and analytically with reasonable accuracy but not for a complex obstructed break flow pattern. ANSI/ANS-58.2-1988 describes an analytical method for evaluating the geometry of a freely expanding jet from its initial jet core to the equilibration with ambient conditions, including the intermediate radial isentropic expansion. The generation of debris also would be complex and varied. The generation of insulation debris depends on the location and orientation of the insulation relative to the break, the type of insulation, and whether the insulation is protected by a jacket or installed with banding, as well. For example, an insulation jacket with its seam oriented more toward the jet flow would be much more easily separated than if its seam were oriented on the opposite side of the pipe from the jet.

Analytical methods have been devised to characterize a three-dimensional region of insulation damage, which is referred to as the ZOI. These methods attempt to correlate the energy contained in the steam/water jet to a region in space within which jet pressure would be large enough to cause damage to various types of insulation material. The volume of insulation that would be damaged depends on the size of the ZOI, and the severity of damage to the insulation would decrease as the jet pressure dissipates. Depending on the specific modeling assumptions, the shape of the ZOI could be either conical or spherical.

The minimum (threshold) jet pressure that would cause damage to a particular insulation, referred to as the damage pressure, has been determined experimentally for a number of insulation types and methods of installation. The damage pressure also depends on whether the insulation is jacketed, the type of jacket (and bands), and the orientation of the jacket seams.

The insulation jacket may provide some protection to the insulation, which would be reflected by an increase in the pressure needed to cause damage. The orientation of the jacket seam relative to the jet has been found to profoundly affect the damage pressure in some cases. Another method for expressing the threshold for damage is to correlate the distance from the break to where the jet stagnation pressure drops below the damage pressure. (This distance would actually be a three-dimensional envelope.) The thermodynamic state of the break effluent, i.e., steam, steam/water, or water, has been found to have an important effect on the rate at which jet pressure decays with distance from the break plane and the extent to which the jet expands in the radial direction. The threshold distance (envelope) represents the maximum distance away from the break plane at which an insulation blanket or cassette has been observed in controlled experiments to be damaged, i.e., eroded, fragmented, or dislodged. Inside this distance, the insulation closest to the jet generally would be more damaged, whereas the insulation nearer the edge of the pressure envelope would be less damaged. Beyond this distance, the insulation would remain intact and undamaged. In reality, the damage to insulation within the ZOI could be rather chaotic because the jet would impact insulation at a variety of seam and pipe orientations. Insulation closer to the jet but with its jacket seam opposite the jet might survive, whereas insulation further out was destroyed because its seam was oriented toward the jet. Because the distance to the threshold damage pressure is dependent on the size of the break, the threshold distance frequently is correlated in terms of the diameter of the break, i.e., the distance divided by the break or pipe diameter, expressed as the number of L/D.

Debris generation testing generally has been unobstructed; i.e., the break jet expanded uniformly in two dimensions, axial and radial, without impacting a significant obstacle. The unobstructed geometry provided the means of measuring and/or analytically estimating jet pressures accurately enough to determine the damage pressure for the test specimen. During a series of tests, a test specimen (of the insulation type being tested) would be placed at an increasing distance until a test specimen was not damaged, thus bracketing the threshold damage distance. When debris-generation

testing was conducted using two-phase steam/water break-flow jets, the damage pressures were somewhat lower than when the tests were conducted using air jets.

Rather than attempting to model the complex jet deflections and pipe motions, which would be different for each break scenario, the analytical approach generally used to simulate typical obstructed jet expansion is to assume a spherical expansion of the jet from the break location in an attempt to account for the effects of jet deflections and pipe motion. This approach transforms the total energy within the idealized conical jet model into an equivalent sphere surrounding the break location. The volume (break-size- and fluid-dependent) within a particular conical isobar of the idealized jet model is used to determine the radius of the equivalent sphere, where the isobar corresponds to the threshold damage pressure for the insulation of interest. After the radius of the equivalent sphere for a particular break and insulation type is determined, the analysis must determine the quantities of insulation located within this volume (ZOI), which represents the volume of damaged insulation or insulation debris. Computer programs have been developed using the equivalent-sphere method to systematically assess the insulation inside the ZOI for all potential break locations within containment. The systematic analysis provides a spectrum of potential insulation debris volumes by insulation type, which can be used to determine a screen size capable of handling the potential debris load to the recirculation sump screens.

The extent of damage to the ZOI insulation, i.e., the characteristics of the debris, is also very important. This damage would range from debris that consisted of individual fibers, particles, or small metallic shreds to nearly intact insulation blankets still attached to piping. The finer debris would be much more transportable to the recirculation sump screens than the coarser debris. Here, the equivalent sphere volume may be subdivided into a number of discrete intervals (spherical shells) in which the extent of damage for each interval becomes less severe from the center outward. The insulation in the inner interval likely would be nearly completely degraded into finer debris, whereas the outer interval would be only partially damaged. The integration of the damage over the intervals would provide an estimate of the

debris-size distribution that would be used by the transport calculations. These estimates should be based on available debris-generation data. For example, when an LDFG insulation blanket was completely destroyed during NRC-sponsored air-jet debris-transport tests, from 15 to 25% of the original blanket insulation mass was debris in the form of very fine and very transportable fibrous debris. The transport characteristics of debris are extremely dependent on the debris-size distribution, and the transport of each size grouping or type should be analyzed separately.

Debris Transport to Containment Sump Pool

The transport of insulation debris within the containment from the locations of origin down to the containment sump pool would be first a result of the effluences from a high-energy pipe break that would not only destroy insulation near the break, but also would transport that debris throughout the containment (airborne debris transport). If the break effluences were to pressurize the containment sufficiently to activate the CSS to suppress further pressurization, the transport of insulation debris also would be driven by the drainage of the spray water from the spray heads to the recirculation sump (washdown debris transport). The transport of debris within a PWR would be influenced both by the spectrum of physical processes and phenomena and by the features of a particular containment design. Because of the violent nature of flows following a LOCA, insulation destruction and subsequent debris transport are rather chaotic processes.

Many important debris-transport parameters will be dependent on the postulated accident scenario. Both the LOCA break size and its location influence the debris transport by determining the flow dynamics within the containment, the timing of the accident sequence, the activation of the containment sprays, and the pumping flow rate from the sump. A number of features in nuclear power plant containments, including engineered safety features and associated plant operating procedures, would affect the transport of insulation debris significantly. In PWR containments, break effluences would tend to flow generally up toward the large free volume of the containment dome, carrying debris with the flow and thus generally away from the ECCS sump screens. Entrained debris would be

deposited inertially, in part, on gratings, piping, beams, ice condenser banks (in ice condenser plants), etc. Debris would settle gravitationally from the upper dome atmosphere as flow velocities and turbulence dissipated. If it were not for the containment sprays washing the debris back down toward the recirculation sump, the debris carried aloft likely would remain in the higher reaches of the containment. The complete range of thermal-hydraulic and physical processes affect the transport of insulation debris. The dominant debris-capture mechanism in rapidly moving flow likely would be inertial capture, but in slower flows, the dominant process likely would be gravitational settling.

After the airborne debris is dispersed throughout the containment, the subsequent washdown of that debris to the recirculation sump would be determined primarily by the design of the containment spray system including the drainage of the sprayed water. First, the spray droplets would tend to sweep any remaining airborne debris out of the containment atmosphere. Then the falling droplets would wash substantial portions of the debris off surfaces; structures, equipment, walls, floors, etc. As the drainage water worked its way downward, entrained debris would move along with the flow.

The locations where spray drainage enters the sump pool relative to the location of the recirculation sump are important. Debris transport within the sump pool depends upon a number of plant features, including the lower compartment geometry, that define the shape and depth of the sump pool, such as the open floor area, ledges, structures, and obstacles within the pool. In addition, the relative locations of the sump, LOCA break, and drainage paths from the upper reaches of the compartment to the sump pool are important in determining pool turbulence, which in turn determines whether debris can settle in the pool.

Transport of debris is strongly dependent on the characteristics of the debris formed, and several distinct types of insulation are used in PWR plants. These characteristics include the types of debris (insulation type, coatings, dust, etc.) and the size distribution and form of the debris. Each type of debris has its own set of physical properties, such as density; buoyancy when dry,

partially wet, or fully saturated; and settling velocities in water.

The U.S. NRC, U.S. industry, and international organizations have conducted tests and analyses to examine different aspects of airborne and washdown debris transport within nuclear power plant containments and developed methodologies for performing analyses to estimate the transport of debris. Although much of this information was obtained specifically to support the resolution of the BWR strainer-blockage issue, that information is directly applicable to the PWR sump screen blockage issue, for the most part.

Analytical work has demonstrated clearly that available computer codes do not have the capability to realistically simulate debris transport except for limited transport conditions. Specifically, the aerosol transport models of these codes do not usually have inertial impaction models that can be applied universally to containments. An exception would be the transport of small debris at relatively slow flow velocities, where the debris deposition was primarily a result of gravitational settling. There are computer codes, such as the MELCOR code, that can characterize thermal-hydraulic conditions within the containment. Alternative methods have been devised to estimate airborne and washdown debris by decomposing the problem such that the individual parts of the overall transport problem can be resolved by adapting experimental data tempered with engineering judgment. This approach works best where there are relatively few flow pathways and substantial inertial capture along those pathways by structures such as gratings or by sharp bends in the flow.

Debris Transport in Containment Sump Pool

Debris transported to the containment sump, by airborne transport (entrained in the break flow) or by containment spray washdown transport, would reside in the water pool that would accumulate in the sump. The transport of debris within a PWR containment sump pool would be influenced by a variety of physical processes and phenomena and by the features of a particular containment design. Many aspects of a PWR accident scenario are important in estimating debris transport in the containment floor sump pool; these include: the break location, orientation, and flow rate, the

containment spray drainage locations and flow rates, the recirculation sump location, flow rate, and the activation time, and the sump pool geometric shape, depth, and temperature. Fundamental to analyzing the potential for debris transport in a containment pool are the types, sizes, and quantities of debris that could be in the pool as well as where and when the debris entered the pool.

The transport of debris within the sump pool would occur in two very different phases. The first pool transport phase would occur as the sump pool forms where debris that was deposited onto the sump floor during and shortly after RCS depressurization before sump-pool formation (and also before ECCS switchover to the recirculation mode) would be transported with the fill-up water flows. During the fill-up phase, debris on the floor would transport as the initially shallow and fast flowing water spreads out across the sump floor. In this mode, debris could be transported a substantial distance from its initial deposition location; the transport could either move debris toward the recirculation sump or away from the recirculation sump. The second pool transport phase generally covers the period after the ECCS has switched over to recirculation where the pool flow conditions are at or near quasi-steady state.

The complex movement of water through the sump pool would be unique for each postulated accident sequence and for each plant. The geometry of the sump pool affects the complexity of the water movement and that geometry is plant-specific. Pool turbulence affects whether or not debris can settle and whether it will further disintegrate. Pool turbulence depends upon the entrance of water into the pool; here the plummeting of break overflow water would be the primary source of turbulence. The turbulence therefore depends upon the location, orientation, and elevation of the break, and on the surrounding congestion of piping and equipment below the break. It is known that pool turbulence can affect the further disintegration of certain types of debris; disintegration due to turbulence has been observed for LDFG and calcium silicate debris. This type of disintegration, essentially an erosion process, forms very fine debris that remains suspended in the water even at relatively low levels of turbulence, hence virtually complete transport to the sump screens.

Water from containment spray drainage would enter the sump pool at multiple locations and the drainage pattern would be very plant specific. The locations of the incoming water relative to the location of the recirculation sump would be especially important. The relative locations determine the flow patterns, which in turn determine whether or not or how many significant quiescent regions would exist in the pool. Debris within these quiescent regions could well remain in those regions. If the incoming water entered the sump pool well away from the recirculation sump inlet, then the water flow could sweep a majority of the pool, thereby enhancing debris transport. Conversely, the incoming water could be near the recirculation inlet, so that much of the sump pool was relatively quiescent. The depth of the pool strongly affects debris transport primarily because the depth affects flow velocities and turbulence. The temperature of the water affects the water density and viscosity, the rate at which water penetrates dry insulation debris, and could affect debris disintegration rates.

Geometric features such as compartmentalization, free flowing annuli, flow restrictions, and obstacles all affect the patterns of flow. There would be areas of relative high flow velocity and areas of relatively slow or quiescent flow velocities. Debris would readily transport in the high velocity areas but not in the low velocity areas. Further, the shape of the sump pool would contribute to the creation of rotational flows (vortices) where debris can be trapped within the vortex. The flow would accelerate through narrow pathways, such as an entrance into an interior compartment, and then decelerate beyond the entrance as the flow expands. Debris that did not transport to the sump screen would have been effectively trapped within a quiescent region, such as an inner compartment that does not receive significant flow; effectively trapped inside a vortex; or stopped behind an obstacle. Obstacles to debris transport on the floor of the sump pool include the variety of equipment located there and curbs deliberately placed along the floor in front of the sump screen to retard the transport of debris to the sump screen. These obstacles could stop tumbling debris from reaching the screen unless the local flow velocities were sufficient to lift the piece of debris over or around the obstacle.

The analysis of debris transport test results has identified many processes and phenomena that could significantly affect the transport of debris within the sump pool. The processes include both the bulk flow processes and the localized processes such as pulses of turbulence. Local flow turbulence can cause a piece of debris to move whereas the bulk flow velocity might not be sufficient for that movement. Testing has effectively demonstrated that turbulence can keep debris suspended in the pool, enhance the transport of debris along the floor of the pool, and cause additional disintegration of the debris.

Once the pool becomes sufficiently established to suspend debris, that suspended debris would simply move along with the water flow. Fine debris, such as individual fibers or light particles (e.g. calcium silicate), would essentially remain suspended even at relatively low levels of pool turbulence. Ultimately, most of this fine suspended debris would likely be filtered from the pool by the recirculation sump screens. Larger debris could be suspended in the more turbulent regions of the sump pool or before the debris was completely saturated with water. Debris not completely water saturated would contain some air that could give the debris buoyancy. Truly buoyant debris, such as some of the form insulations, would float on the pool surface unless the pool turbulence was sufficient to pull the debris beneath the surface. When insulation debris enters the sump pool, the debris could be dry, or fully or partially saturated with water depending upon its exposure to moisture. If the debris was not fully saturated, then the trapped air could make the debris buoyant, whereas it would readily sink when fully saturated. The time required for water to saturate a piece of debris is very dependent on the temperature of the water.

Non-buoyant debris, such as saturated fibrous debris, would settle to floor of the pool, except in regions of high turbulence. If the local flow velocities were sufficiently high, sunken debris would transport along the floor with the water flow. This transport involves tumbling and sliding motions. The separate effects test data provides the flow velocities needed to start debris in motion, referred to as incipient motion, and the flow velocities needed to cause the debris to transport in bulk motion. Note that significant turbulence would cause debris to transport along the floor at lower bulk flow velocities than if there was no turbulence.

Debris moving across the sump pool floor could encounter an obstacle that stops further forward motion. Debris trapped against one of these obstacles could be lifted over the obstacle when the flow velocities were sufficiently fast. The separate effects test data also provides these lift velocities.

The NRC, U.S. industry, and international organizations have conducted both tests and analyses to examine different aspects regarding the transport of insulation and other debris in pooled water. The results of these experiments provide qualitative insights and quantitative information relevant to considerations of debris transport in PWR containment pools. The NRC has performed analyses investigating the transport of insulation and other debris in PWR containment sump pools and BWR drywell floor pools and BWR suppression pools. The results of these analyses provide qualitative insights and quantitative information relevant to considerations of debris transport in PWR containment pools.

Two approaches to modeling the transport of debris in a containment pool are found in the literature. One is experimental in nature; the other is computational. The experimental approach to modeling debris transport in a particular containment sump pool involves building a scaled representation of the floor of the containment complete with all the walls, curbs, equipment, etc., that would determine the flow patterns in the pool. Defensible similitude between the physical containment and the model must exist here, however a defensible similitude will be difficult to develop. The rationale for scaling the water flow differs substantially from the scaling rationale for scaling debris transport, but both processes must be scaled simultaneously. Appropriate inertial force scaling, governing water flow, requires that flow velocities be reduced with the square root of the length scale. Appropriate viscous force scaling, governing debris transport, requires that flow velocities be increased proportional to the length scale. It may be that water flow and debris transport characteristics cannot be simultaneously satisfied in a scaled experiment. While illustrative experiments of containment pool modeling are documented, no defensible scale modeling of debris transport potential in a specific containment has been accomplished to date. Critical testing considerations include

recirculation flow rate, debris size, the height of the pipe break above the floor, the preparation of the debris (size distribution and pretreatment to remove trapped air), and introduction of the debris into the test. The potential for debris disintegration within the pool must be investigated.

The computational approach to modeling debris transport in a containment pool involves performing CFD calculations. While commercially available CFD codes are clearly suited to predicting the flow patterns and velocity fields that would exist in a containment pool, the codes lack the ability to directly predict the transport of the various types of insulation and other debris that could be present there. This is because CFD codes do not have the capacity to resolve or account for the intricate transport characteristics of the different types, shapes, and sizes of potential debris. As such, the flow field predictions from a CFD containment pool calculation (e.g., velocities and turbulence levels) have to be compared with experimentally determined debris transport characteristics to infer whether or not transport would occur. Illustrative CFD calculations of containment pool debris transport have been documented, but as with experimental containment pool modeling, no defensible complete CFD analysis of debris transport potential in a specific containment has been accomplished to date.

Debris Accumulation

LOCA-generated debris will have an adverse effect on recirculation sump performance if it accumulates in sufficient quantity and in a configuration that impedes flow. Although the principal location of concern for debris accumulation is the surface of a recirculation sump screen, debris accumulation also can apply to other locations in the containment; such as a critical location for the flow of recirculation water along the containment floor where an accumulation of debris could impede water flow to the sump, or screens in the upper containment levels at floor or refueling pool drains. The physical configuration of the sump screen, as well as its position and orientation in the pool of water it services, vary considerably among the U.S. PWRs. Recirculation sump screens can be classified as either fully submerged or partially submerged, and as horizontal, vertical, or sloped. For fully submerged screens, excessive accumulation of

debris can cause the head loss across the debris bed to reduce available NPSH to ECCS or CSS pumps. For partially submerged screens, excessive debris accumulation can reduce the static head necessary to drive recirculation flow through the screen.

The geometric configuration of a debris bed formed at a location of concern strongly influences the extent to which it affects flow. The geometric configuration includes such features of the bed as the fraction of sump screen area covered by debris, the uniformity of the bed covering the screen, the height of the debris bed off the floor (for vertical screens), and the bed composition (i.e., porosity). Variations in these features result in different accumulation patterns or debris bed profiles, which in turn affect resistance to water flow. The manner in which LOCA-generated debris accumulates is influenced by plant-specific and accident-specific parameters, including those that determine the characteristics of the local flow field, i.e., level of turbulence and flow velocity. Turbulence facilitates debris mixing into the flow stream, and thereby promotes uniformity in the deposition. At low turbulence levels, gravitational settling leads to non-uniform accumulation profiles on vertical screens. At higher velocities, shear forces on debris can lift or flip debris upward onto higher regions of the screen. The following experimentally observed qualitative insights apply to simulated PWR screens. When fine debris (e.g., individual fibers, smaller clumps of fibers, and calcium silicate particles) arrives at the screen in a well-mixed suspension, it deposits nearly uniformly across the screen. Small debris (e.g., clumps of fibrous or calcium silicate debris or crumpled RMI debris) that arrives at a PWR screen by tumbling or rolling across the pool floor may form a pile of debris at the bottom of a vertical screen, or if the flow velocities are sufficient, the debris may be lifted above the already deposited debris to spread across the screen. At the other extreme, non-buoyant large or heavy pieces of debris (e.g., insulation pillows, blankets, or cassettes or large portions thereof) will collect on a screen only if local water velocities are sufficient to transport the debris across the pool floor and then lift or flip it onto the screen surface. The accumulation behavior of the moderate sized (in-between the small and the large) pieces of debris (e.g., an irregular shaped piece of fibrous insulation a few inches to a side) represents a mixture of smaller and larger debris

behavior. Qualitatively, the debris capture efficiency of a screen is not strongly dependent on the size of the screen mesh for the meshes tested (i.e., 1/8 to 1/4 mesh), which are typical of screens found in U.S. PWRs. (A few exceptions have larger mesh sizes.)

Experiments have provided valuable qualitative insights on debris accumulation on BWR suction strainers and these insights are also applicable to PWR sump screens. To resolve the BWR suction strainer issue, tests were conducted on both the original cone shaped strainers and the replacement strainer designs where the most common BWR replacement strainer design is the so-called stacked-disk strainer. The cone strainers effectively accumulated debris in a manner similar to a flat plate strainer (unless the accumulation is excessive). The process of debris accumulation on a stacked disk strainer is more complicated than for a flat screen but the stacked disk process increased the debris accumulation capability of the strainer. With water flow following the path of least resistance, debris is deposited onto all of the screened surfaces of a stacked disk strainer but the flow and deposition is skewed towards the screened surfaces of lesser resistance. As debris accumulates onto the disk-shaped surfaces inside the gaps, the flow moving somewhat parallel to these surfaces pushes the debris on these surfaces further into the gaps, essentially keeping a portion of the disk surface relatively clean of debris until the gaps are filled. After the gaps filled, the debris preferentially occurs on the disk rims until the accumulation becomes circumferentially more uniform. The BWR stacked disk strainer technology potentially could be applied to possible PWR screen replacements.

Qualitative observations made during debris transport and screen accumulation tests have illustrated that a significant reduction in flow might allow debris to expand, fall off or shift on the screen, thereby changing the accumulation profile. If flow is subsequently restored, the debris bed re-forms, however the bed configuration may be substantially different from those formed before the reduction in flow.

Debris Head Loss

The accumulation of debris onto a PWR sump screen or a BWR suction strainer would cause a head loss that could compromise long-term

recirculation ECCS and CSS. Head loss across the debris bed depends on the debris bed composition, i.e., its constituents and its morphology. The spectrum of possible debris bed compositions is as varied as the types of insulation and other materials in the containment and as varied as the conditions of the accident scenario. The debris bed compositions can be broadly divided into the following groups: (a) fibrous debris beds, (b) mixed fibrous and particulate debris beds, (c) beds formed by fragments of reflective metallic insulation, and (d) mixed RMI and fibrous debris beds. Note that beds can also contain miscellaneous other materials, such as shreds of insulation jacketing or miscellaneous operation debris.

The fibrous shreds filtered from the water flow by the screens tend to overlay the mesh holes of the screen and as the accumulation builds, the flow through the resulting fibrous bed resembles flow through a porous media. Note that a smaller quantity of individual fibers can slip through the holes of the screen. Head loss is caused as water accelerates past the cylindrical fibers oriented somewhat normal to the screen surface. Then the resulting pressure drop across the bed compresses the bed leading to progressively higher head losses.

Experimental head loss data obtained for fibrous beds has been adequately explained using conventional porous media head loss correlations. Head loss across a debris bed increases linearly with velocity in the viscous region and to the square of the velocity in the turbulent region; a combination of these two terms can explain the transition between the viscous and the turbulent flows. A correlation developed by the NRC, referred to as the NUREG/CR-6224 correlation, has performed well in predicting the head losses associated with fiber debris beds. Head loss across the strainer is dependent on the thickness of the fiber bed (i.e., the volume of fiber debris divided by the screen area for a uniform bed) trapped on the strainer surface, the uniformity of the bed, and the diameters of the fibers, the density of the fibers, and the water temperature (i.e., water density and viscosity). The pressure drop across a non-uniform bed would be lower than that predicted by assuming uniformity. Non-uniformity can happen when debris is deposited in larger shreds and most likely happens when the bed starts to form. As the formation continues, the bed tends towards more

uniformity. Very fine debris tends to form very uniform debris beds. Higher water temperatures result in lower pressure drops primarily due to the corresponding decrease in the water viscosity. One concern still not completely understood is whether or not the effects of water chemistry (pH) could alter the bed composition and thereby affect the head loss. Some investigators concluded that pH could dissolve some of the chemical coatings/binders applied on the fibers leading to their degradation and formation of even more compact beds, however most testing was not conducted for a long enough time for the water chemistry effect to be tested.

Fibrous debris accumulation on a screen will filter particulate from the passing flow forming a debris bed consisting of a mixture of fibers and particulate that is substantially more compact resulting in much higher head losses than fiber alone. The filtered particulate could include corrosion products, paint chips, organic sludge, concrete dust and fragments of non-fibrous insulation (e.g., calcium silicate). This behavior has been experimentally verified and measured for some potential bed compositions. Debris beds consisting of relatively thin layers of fibrous debris (as thin as 1/8-in. or possibly less) and substantial quantities of particulate lead to relatively high head losses. This effect, referred to the thin-bed effect, has been experimentally verified. The morphology of a thin bed closely resembles granular beds, rather than fibrous beds. Debris beds formed with calcium silicate, or other particulate insulations, have a substantially higher associated head loss than if the particulate were simple dust or dirt. The calcium silicate morphology is not completely understood and its effect is still being investigated experimentally but its effect on head loss may be due to small fibers and binder in the insulation with the particulate.

In plants that have nearly all RMI insulation, either stainless steel or aluminum RMI, the debris bed could consist almost entirely of fragments of RMI insulation debris. The head loss associated with these RMI fragments would be highly sensitive to type, shape and size of the accumulated fragments. The fragments could range from relatively intact cassettes to sheets of foil to crumpled pieces or shreds of foil (both large and small). If the water approach velocity were fast enough to transport large foils (or even cassettes) to the sump screen and then flip the

foils onto the screen, the foils would partially block the screen essentially by reducing the screen area available to flow. Experiments using simulated crumpled debris demonstrated that RMI fragments, typically, form loose beds that induce low head losses. These crumpled debris beds tended to be relatively uniform and typically have a much larger porosity than the fibrous debris beds. Compactness and porosity depend upon the general size of the RMI fragments, i.e., the smaller fragments beds are more compact, less porous, and result in higher head losses. Aluminum RMI debris tended to form more compact beds than the stainless steel debris. The extent of crumpling exhibited by RMI fragments apparently depends upon the orientation of the steam/water jet impacting the RMI cassette; hence some flat-not-crumpled pieces of foil, as well as, crumpled pieces. In addition, it has been postulated that crumpled foils could be compressed during transport, effectively transforming the debris into flattened debris that could increase the resulting head losses.

Mixed fiber and RMI debris beds have been studied by various U.S. and European investigators for head loss implication both with and without the presence of particulate debris. The head loss data shows a wide scatter in results. In most cases, the RMI head loss tests demonstrated that introduction of crumpled RMI debris, in combination with fibrous debris and sludge, does not cause significantly different head losses than those observed with only fiber and sludge loadings. In fact, the most significant finding of NRC tests was that under certain circumstances when RMI debris was mixed with fibrous debris and sludge, the head losses appeared to decrease as compared to similar conditions without RMI debris. However, in a few cases, the head loss caused by RMI and fibrous debris mixtures was slightly higher than the head losses at the same fiber loading but without RMI. It was concluded that generally the head loss caused by RMI debris, in conjunction with fibrous (and other) debris, would be bounded by adding the head loss caused by the individual constituents of the debris bed, (e.g., the RMI head loss without fibers plus the fiber/particulate head loss without RMI). However, the European investigators observed that its validity needs to be established for each application.

Analytical methods have been developed to estimate the head loss associated with a variety of debris beds. For fibrous/particulate debris beds, the NUREG/CR-6224 correlation that was developed by the NRC based on experimental data, for flat-plate strainers and truncated cone strainers, has been successfully validated against a variety of experimental data and for a variety, but not all, debris bed compositions. Appendix B of the NUREG/CR-6224 report characterizes the head loss caused by fibrous and particulate debris in detail including the assumptions and limitations of the correlation. The correlation predictions were generally within +25% of the test data. (Note that there is substantial data variability between the arrays of test data attributable to debris bed formation, test procedures, etc, even data for flat-plate strainer experiments.) The NUREG/CR-6224 head loss correlation was incorporated into the NRC-developed BLOCKAGE computer code that evaluates the head loss associated with BWR suction strainers.

The NUREG/CR-6224 head loss correlation has been applied piecemeal to the non-uniform debris buildup associated with the special-shape strainers (e.g., stacked disk strainers), where the head loss has a non-linear relationship with the debris loading; the correlation was applied to the light initial debris loading and the heavier circumferential debris loading that were approximately uniform, by assuming a different effective screen area for the two conditions. Applicable test data was important to proper evaluation of the capability of these strainer designs. While the BLOCKAGE code was developed for the truncated cone strainers in use at that time, the code could be modified to accommodate the advanced strainers.

A correlation was developed for reflective metallic insulation based on debris loading (ratio of foil surface area-to-strainer surface area), the flow velocity, and the type/size of the debris. This correlation was also verified using experimental data.

Resolution Options

BWR experience demonstrated that the options for resolving the strainer clogging issue were to replace problematic insulations in the containment, or install replacement strainers capable of handling the anticipated debris loads (or both). The replacement strainer options

included: (1) the installation of large capacity passive strainers; (2) the installation of self-cleaning strainers; (3) the installation of backflush systems; and (4) the installation of in-line suction strainers outside suppression pool that can be realigned and flushed. Licensees of U.S. BWR plants chose to replace their strainers with large capacity passive strainers due to the advantages of these strainers not having active components and not requiring operator intervention.

A number of replacement strainers were designed, tested, and installed in U.S. BWR plants. The primary design concept in all passive strainers was to maximize the strainer surface area while minimizing physical size of the strainer. Four types of passive strainer designs were ultimately installed at one or more U.S. BWRs. There were (1) the PCI stacked disk strainers, (2) the General Electric stacked disk strainers, (3) the ABB Combustion Engineering star shaped strainers, and (4) the Mark III strainer designs. But the most prominent strainer designs were of the stacked disk design. Although these designs differ significantly from each other, the designs had one common feature in that the designs all relied on crevices (troughs, or traps) where debris can collect on the strainer surface while keeping a portion of the screen area relatively free of debris, thereby not significantly increasing the head loss across the strainers. Each of these design concepts was further refined or reengineered as required to suit a particular plant need and each design was tested to determine its capability to collect debris. The constraints related to hydrodynamics loads were factored into the plant-specific designs. In some cases, these loads limited the size of the strainer, thereby requiring the plant to take additional actions, such as the replacement of problematic insulation to help facilitate the solution.

The experimental results demonstrated that head loss across the advanced passive strainers modules is a non-linear function of debris loading. As debris accumulates on one of these strainers, the debris is preferentially forced into the gaps or crevices, thereby leaving some screen area relatively free of debris, until the gaps become filled. After the gaps filled, the debris preferentially occurs on the disk rims until the accumulation becomes circumferentially

(cylindrically shaped in the case of stacked disk strainer) more uniform.

Special sump screen designs for implementation in the PWR plants have yet to emerge in the U.S. However, the BWR advanced strainer design technology should be applicable to the design of PWR screen replacements, as well. The basic concepts of enlarging the screen area and incorporating debris traps (e.g., the stacked disk strainers) are as applicable to PWR sump screens as the concepts were to BWR pump suction strainers. It is conceivable that a BWR stacked disk suction strainer could be simply installed in a PWR sump in some situations.

The design of replacement sump screens should also consider the water approach pathways to the recirculation sumps, the screen mesh size, and protection from damage due to LOCA jet impingement and missile impactation. Debris blockages along the water approach pathways could reduce the availability of the water to the sump screen, resulting in a lowering in the water level at the screen. The type and size of debris passing through the sump screen is determined by the size of the screen mesh, particularly in the early stages of the accident before a bed of debris forms. Debris passing through the screen has the potential to clog or damage components throughout the ECCS and/or CCS systems (e.g., a spray nozzle). The impingement of a LOCA jet onto finer mesh screens or the impact of fragments of hard insulation (e.g., RMI) could cause substantial damage potentially threatening the integrity of the screen.

Event History

Operational events have occurred at both PWR and BWR nuclear power plants that relate to the issue of sump screen or suction strainer blockage. Two of these events resulted in the generation of insulation debris by jet flow from a LOCA caused by the unintentional opening of safety relief valves (SRVs). These occurred at:

1. the German reactor Gundremmingen-1 (KRB-1) in 1977 where the 14 safety relief valves of the primary circuit opened during a transient and
2. the Barsebäck-2 nuclear power plant on July 28, 1992 during a reactor restart procedure after the annual refueling outage.

Both of these reactors were BWR reactors with similarities to U.S. reactors. Perhaps the most notable event was the Barsebäck-2 LOCA where the reactor power was below 2% of nominal and the reactor pressure had reached 3.0 MPa (435 psia) when a safety relief valve inadvertently opened. The steam was released as a jet of steam directly into the containment. Subsequently, the containment pressure cleared the vertical pressure relief pipes connecting the drywell to the wetwell allowing steam/air flow to the suppression pool and the containment vessel spraying system and the ECCS were automatically started. About 200 kg (440 lb) of fibrous insulation debris was generated and about 50% of this debris subsequently reached the wetwell resulting in a large pressure loss at the strainers about 70 min after the beginning of the event. The debris was transported by steam and airflow generated by the blowdown, and by water from the containment spray system. The extent of damage and the transport of large amounts of fibrous debris due to the simple erroneous opening of a safety valve appeared remarkably large, given the small leak size and low reactor pressure.

Other events have occurred in operating PWR and BWR nuclear power plants that resulted in a particular system being rendered inoperable or at high risk of not operating. These included events where the accumulation of debris on a strainer or a screen caused excessive head loss and events where debris entered a system and thereby adversely affected the operability of a component of that system. Perhaps the most notable of these events were the two ECCS strainer-clogging events that occurred at the BWR Perry plant. Debris was found during a refueling outage inspection and again later when several safety relief valves were manually lifted and the RHR system was used to cool the suppression pool. These events involved the clogging and deformation of the pump suction strainers due to glass fibers from temporary drywell cooling filters inadvertently dropped into the suppression pool, corrosion products (sludge), fine dirt, and other materials. Fibrous material acted as a filter for suspended particles, a phenomenon not previously recognized, strongly suggesting that the filtering of small particles by the fibrous debris would result in significantly increased pressure drop across the strainers.

Events have occurred in operating PWR and BWR nuclear power plants where debris was found inside the containment and that debris had the potential to impair the operability of a safety system. The debris included fibrous material, sludge, dirt, paint chips, and miscellaneous operational materials. Even if the debris was not considered sufficient to render a system inoperable, the debris could still contribute to screen blockage following a LOCA. Events have occurred where inadequate maintenance conditions inside containments had the potential of forming sources of debris. In general, these events involved unqualified protective coatings and materials. Events have occurred where defects in the integrity of the sump screens were found. These defects could have caused a potential failure to adequately filter the ECCS water source that could result in degradation and eventual loss of ECCS function as a result of damaged pumps or clogged flow pathways.

10.2 Conclusions

As a result of years researching the BWR suction strainer and PWR sump screen clogging issues, a substantial base of knowledge has been amassed that covers all aspects of the issues, from the generation of debris to the head loss associated with a debris bed on a strainer or screen. A majority of the research (testing and analysis) was done to support the suction strainer clogging issue for BWR plants; however, most of this research is directly applicable to PWRs, as well. The spectrum of physical processes and phenomena that affect debris generation, transport, and strainer/screen head loss are the same for PWR sump screens as for BWR suction strainers.

Although the physical processes and phenomena associated with the resolution of the sump screen clogging issue are generally the same for all PWR plants, the actual resolution will be very specific to each plant. With few exceptions, each plant has unique distributions of insulation (types and locations) and other potential debris materials, unique geometric features affecting debris generation and transport, unique recirculation sump designs, and unique flow and NPSH requirements. This is true even among plants of similar containment design. The exceptions might be multiple units of essentially the same plant, e.g., the three units at Palo Verde, but even here the actual

make up of insulation within each of the plants may have evolved separately from the others. Only plant-specific analyses can determine such aspects of the resolution.

While the base of knowledge covers the breadth of the PWR sump screen clogging issue, gaps exist in the completeness of the knowledge base. For example, the research tended to focus on fibrous insulation debris, specifically low-density fiberglass insulation (LDFG) debris. This focus was partially the result of the initial analyses of strainer event blockages that involved LDFG debris but it was also due to the relative importance of fiberglass to the issue. Research has also considered other types of insulation debris but to a lesser extent, notably experimental RMI debris research, but the potential for fibrous insulation debris to clog a strainer has generally been found to be substantially greater for fibrous debris than the potential for RMI debris. Further other types of fibrous debris were not researched as thoroughly as was LDFG, for example, HDFG or mineral wool fibrous debris. These other types of fibrous debris are as important to the resolution of the issue as LDFG but less data was amassed for these types, hence gaps exist in the completeness of debris transport research data but not in the overall understanding. Other examples of database gaps include:

1. full-range size distributions for LOCA generated debris as a function of the jet pressure so that a size distribution can be integrated (less conservatively) over the volume of the ZOI, thereby determining the overall size distribution for the debris generated,¹ and
2. data for the lifting of debris over an obstacle once significant debris has already accumulated upstream of the obstacle, thereby reducing the effectiveness of the obstacle to trap debris.²

Even with gaps in the knowledge base, a general understanding has been gained regarding nearly all aspects of the clogging issue. The spectrum of physical processes and phenomena all affect debris generation, debris transport, and strainer/screen head loss, but

¹ As noted in Section 3.3.3, current debris size distribution data is limited.

² As noted in Section 5.2.5, current measurements of debris lifting velocities were made using a clean curb.

research has generally determined the processes/phenomena that have the most influence, i.e., which processes/phenomena that definitely must be considered in a plant-specific analysis. Besides experimental data, the knowledge base includes methodologies and analyses that provide guidance that will support plant-specific analyses.

The knowledge base includes key concepts and insights to ensure the important aspects are addressed in the plant-specific analyses. Examples include the role of damage pressures in determining the potential quantities of insulation debris and that two-phase jets appear to generate more and finer debris than does an air jet, the importance of properly defining debris size classifications for transport analyses, (note that size classifications have varied through the years of research), the importance of tracking the finest debris as a separate class, and the importance of estimating the further degradation of debris as it is transported (especially within the sump pool), the importance of accounting for pool turbulence and the establishment of the initial pool flow when estimating pool debris transport, and the composition of the debris bed when estimating head losses across the debris bed, particularly when the bed contains fibers and calcium silicate.

There are a few areas where the basic understanding of a particular process is not fully understood; future research may provide additional data for some processes. For example, it is known that sump pool turbulence will further degrade fibrous debris, creating more of the very fine debris, perhaps substantial quantities, that remains suspended, but no data exist to provide a means of quantifying the degradation. Another example is that it has been postulated that chemical changes within the debris bed could alter the composition in the longer term due to changes in the acidity level in the sump pool. Altering the debris bed composition would alter the associated head loss; if the bed compacted, the head loss could well increase. The plant-specific resolutions may require that additional data be taken for insulation components that were not specifically covered in the current knowledge base, for example, the damage pressure for insulation jacketed or oriented differently than any of the current data. Despite the gaps in the base of knowledge, this knowledge base should provide a valuable resource for the sump screen issue resolution.